toxins

Ciguatoxins

Edited by

Panagiota Katikou and Marie-Yasmine Dechraoui Bottein

Printed Edition of the Special Issue Published in *Toxins*

www.mdpi.com/journal/toxins

MDPI

Ciguatoxins

Ciguatoxins

Editors

Panagiota Katikou
Marie-Yasmine Dechraoui Bottein

MDPI • Basel • Beijing • Wuhan • Barcelona • Belgrade • Manchester • Tokyo • Cluj • Tianjin

Editors

Panagiota Katikou
Ministry of Rural
Development and Food
Greece

Marie-Yasmine Dechraoui Bottein
CNRS
France

Editorial Office
MDPI
St. Alban-Anlage 66
4052 Basel, Switzerland

This is a reprint of articles from the Special Issue published online in the open access journal *Toxins* (ISSN 2072-6651) (available at: https://www.mdpi.com/journal/toxins/special_issues/Ciguatoxin).

For citation purposes, cite each article independently as indicated on the article page online and as indicated below:

LastName, A.A.; LastName, B.B.; LastName, C.C. Article Title. *Journal Name* **Year**, *Volume Number*, Page Range.

ISBN 978-3-0365-6428-9 (Hbk)
ISBN 978-3-0365-6429-6 (PDF)

Contents

toxins

MDPI

Communication

Liquid Chromatography Coupled to High-Resolution Mass Spectrometry for the Confirmation of Caribbean Ciguatoxin-1 as the Main Toxin Responsible for Ciguatera Poisoning Caused by Fish from European Atlantic Coasts

Pablo Estevez [1], Manoella Sibat [2], José Manuel Leão-Martins [1], Pedro Reis Costa [3], Ana Gago-Martínez [1,*] and Philipp Hess [2,*]

1 Biomedical Research Center (CINBIO), Department of Analytical and Food Chemistry, University of Vigo, Campus Universitario de Vigo, 36310 Vigo, Spain; paestevez@uvigo.es (P.E.); leao@uvigo.es (J.M.L.-M.)
2 Ifremer, DYNECO, Laboratoire Phycotoxines, Rue de l'Île d'Yeu, 44311 Nantes, France; manoella.sibat@ifremer.fr
3 IPMA—Portuguese Institute of the Sea and Atmosphere, Av. Brasília, 1449-006 Lisbon, Portugal; prcosta@ipma.pt
* Correspondence: anagago@uvigo.es (A.G.-M.); philipp.hess@ifremer.fr (P.H.); Tel.: +34-647-343417 (A.G.-M.); +33-2-4037-4257 (P.H.)

Received: 31 March 2020; Accepted: 18 April 2020; Published: 21 April 2020

Abstract: Ciguatera poisoning (CP) is a common seafood intoxication mainly caused by the consumption of fish contaminated by ciguatoxins. Recent studies showed that Caribbean ciguatoxin-1 (C-CTX1) is the main toxin causing CP through fish caught in the Northeast Atlantic, e.g., Canary Islands (Spain) and Madeira (Portugal). The use of liquid chromatography coupled to tandem mass spectrometry (LC-MS/MS) combined with neuroblastoma cell assay (N2a) allowed the initial confirmation of the presence of C-CTX1 in contaminated fish samples from the abovementioned areas, nevertheless the lack of commercially available reference materials for these particular ciguatoxin (CTX) analogues has been a major limitation to progress research. The EuroCigua project allowed the preparation of C-CTX1 laboratory reference material (LRM) from fish species (*Seriola fasciata*) from the Madeira archipelago (Portugal). This reference material was used to implement a liquid chromatography coupled to high-resolution mass spectrometry (LC-HRMS) for the detection of C-CTX1, acquisition of full-scan as well as collision-induced mass spectra of this particular analogue. Fragmentation pathways were proposed based on fragments obtained. The optimized LC-HRMS method was then applied to confirm C-CTX1 in fish (*Bodianus scrofa*) caught in the Selvagens Islands (Portugal).

Keywords: ciguatoxins; HRMS; Q-TOF; ciguatera poisoning; C-CTX1; fragmentation pathways

Key Contribution: LC-Q-TOF-MS in full-scan MS and MS/MS mode permitted successful acquisition of C-CTX1 spectra. Fragmentation pathways are presented. C-CTX1 was confirmed in a barred hogfish (*Bodianus scrofa*) from the Selvagens Islands (Portugal).

1. Introduction

Ciguatera poisoning (CP) is a food intoxication mainly related to the consumption of fish contaminated with ciguatoxins (CTXs) [1]. Ciguatoxins (CTXs) are lipophilic cyclic polyethers, which are stable to temperature and accumulate in seafood. CP is endemic in temperate waters of the Pacific Ocean and Caribbean Sea and was recently detected in the Northeast Atlantic [2–6].

A main difficulty in advancing CP research is the lack of reference materials of these toxins and the numerous toxic analogues present in the toxic samples [7,8]. This lack of reference materials limits progress in method development and identification of CTX analogues responsible for the CP. Liquid chromatography coupled to tandem mass spectrometry (LC-MS/MS) is considered the most adequate approach for CTX detection, not only due to the ability for the separation of the different analogues involved in the contamination but also for their sensitive detection by monitoring their mass-to-charge ratio. Several LC-MS/MS methods have been developed for CTX analysis [4,9–11]. Research on Caribbean CTXs and in particular on Caribbean ciguatoxin-1 (C-CTX1) as the main toxin responsible for CP in the Caribbean Sea and the Northeast Atlantic has been limited [12,13]. Despite this limitation, efforts have been recently made to implement LC-MS/MS methods for the detection of CTXs, particularly in the areas of concern [14,15]. Alternative approaches such as the combination of neuroblastoma cell assay (N2a) with LC-MS/MS have also been used as a powerful tool for the confirmation of C-CTX1 and different C-CTX congeners [16].

The potential for confirmation provided by high-resolution mass spectrometry (HRMS) makes this approach necessary, in particular when the availability of reference materials is limited. Nevertheless, the lack of sensitivity is a challenge that compromises its applicability as concentrations of CTXs are typically low. The complexity of the matrix and the difficulty in the ionization of CTXs also jeopardizes the applicability of LC-HRMS for the detection of CTXs. Despite this, the applicability of HRMS has been demonstrated in particular for CTX1B and CTX3C as the main toxins responsible of CP in the Pacific Ocean, the fragmentation pathways have been identified, increasing the knowledge on how these complex toxins fragment in the mass spectrometer [17–19]. Recent studies published by Kryuchkov et al. [20] reported strategies for the structure elucidation of Caribbean ciguatoxin analogues (C-CTX3 and C-CTX4).

This study responds to one of the objectives included in the EUROCIGUA project, which focused on the risk characterization of ciguatera food poisoning in Europe, and it is partially funded by the European Food Safety Authority (EFSA). One of the objectives of the project is the confirmation by HRMS of the CTX analogues previously detected by LC-MS/MS in fish samples from selected areas in the EU. To accomplish this objective, an LC-HRMS method was developed to obtain C-CTX1 fragmentation pathways, which will allow the characterization of the C-CTX1 molecule. The method was subsequently applied to confirm the presence of C-CTX1 in a contaminated fish sample from the Northeast Atlantic (Selvagens Islands, Madeira archipelago, Portugal), previously identified by LC-MS/MS.

2. Results and Discussion

2.1. LC-HRMS Analysis in Full-Scan MS Mode of C-CTX1

A laboratory reference material (LRM) of C-CTX1 isolated from amberjack, *Seriola fasciata*, was analyzed by LC-HRMS. The use of aqueous methanol as mobile phase was dismissed due to the formation of highly stable $[M + Na]^+$ and the difficulty in its fragmentation. For this reason, the LC and ion source conditions proposed by [15] for C-CTX1 confirmation monitoring water losses and specific fragments in the presence of aqueous acetonitrile were followed.

LC-HRMS in full-scan MS acquisition mode detected C-CTX1 at a retention time of 7.8 min with an ion pattern where the predominant ion was the first water loss *m/z* 1123.6184 (−4.5 ppm) $[M + H - H_2O]^+$ followed by the sodium adduct *m/z* 1163.6106 (−1.6 ppm) $[M + Na]^+$. The protonated molecule $[M + H]^+$ as well as ammonium $[M + NH_4]^+$ and potassium adducts $[M + K]^+$ were present but with a lower intensity and with higher mass differences (>10 ppm) (Figure 1A). The assigned positive HRMS ion species and their corresponding mass errors (ppm) are presented in Figure 1A.

2.2. LC-HRMS Analysis in Targeted MS/MS Mode of C-CTX1

C-CTX1 fragmentation pathways were proposed based on HRMS/MS spectra in positive targeted MS/MS mode with a range of six collision energies (from 20 to 70 eV). In HRMS spectra (Figure 1A), the protonated ion $[M + H]^+$ was not the predominant ion cluster; so due to its high intensity, the first water loss *m/z* 1123.6200 $[M + H - H_2O]^+$ was selected as precursor ion to be fragmented.

MS/MS spectra of C-CTX1 selecting *m/z* 1123.6200 $[M+H-H_2O]^+$ were characterized by the detection of successive water losses at *m/z* 1105.6094 $[M+H-2H_2O]^+$, *m/z* 1087.5989 $[M + H - 3H_2O]^+$, and *m/z* 1069.5883 $[M + H - 4H_2O]^+$ (Figure 1B and Figure S1, Table S1). As with CTX3C and CTX1B [17], the opening of the G- and H- rings allowed the formation of the ion at *m/z* 563.3220 followed by water losses at *m/z* 545.3115, *m/z* 527.3009, and *m/z* 509.2903, these fragments were also detected in [20] (Figure 1B and Figure S1, Table S1). Fragmentation in K-, L-, M-, and N-rings gave rise to several fragments with water losses at *m/z* 253.1439 and *m/z* 235.1333 as reported in [20] and *m/z* 181.1229 as well as the fragment *m/z* 147.1021 followed by the loss of a $-CH_2$ group *m/z* 133.0865. A-, B-, C-, and D- rings were also prone to fragmentation showing ions with water losses and the loss of a $-CH_2$ group at *m/z* 209.1178, *m/z* 191.1072, *m/z* 153.0916, *m/z* 103.0759, *m/z* 89.0603, and *m/z* 59.0497 (Figure 1B and Figure S1, Table S1). LC-HRMS allowed to confirm the exact mass as well as the fragmentation pathway of C-CTX1 fragments previously detected in LC-LRMS [15,21].

These results confirmed that the C-CTX1 molecular ion with theoretical *m/z* 1141.6306 $[M + H]^+$ tends to be fragmented in the source compromising its detection. Therefore, the first water loss *m/z* 1123.6200 $[M + H - H_2O]^+$ is the highest intense ion formed in C-CTX1 ionization when using acetonitrile with aqueous ammonium formate and formic acid as mobile phase. This is in agreement with previous studies where C-CTX1 first water loss is selected as precursor ion in SRM (selected reaction monitoring) or MRM (multiple reaction monitoring) mode [4,15].

2.3. Analysis of a Naturally Contaminated Sample from Selvagens Islands (Madeira Archipelago, Portugal)

Barred hogfish (*Bodianus scrofa*) from Selvagens Islands (Madeira, Portugal) was extracted and purified following the conditions described by [15]. The presence of C-CTX1 was confirmed by LC-HRMS under the conditions described in this work. C-CTX1 was detected at the same retention time as the C-CTX1 LRM (7.8 min) (Figure S2). Ion pattern confirmed the detection of C-CTX1 with the first water loss *m/z* 1123.6214 (+1.2 ppm) $[M + H - H_2O]^+$ and the sodium adduct at *m/z* 1163.6138 (+1.1 ppm) $[M + Na]^+$ (Figure S3). Despite the detection of C-CTX1 by LC-HRMS and the good mass accuracy obtained in full-scan MS mode, sensitivity was not enough to obtain MS/MS spectra.

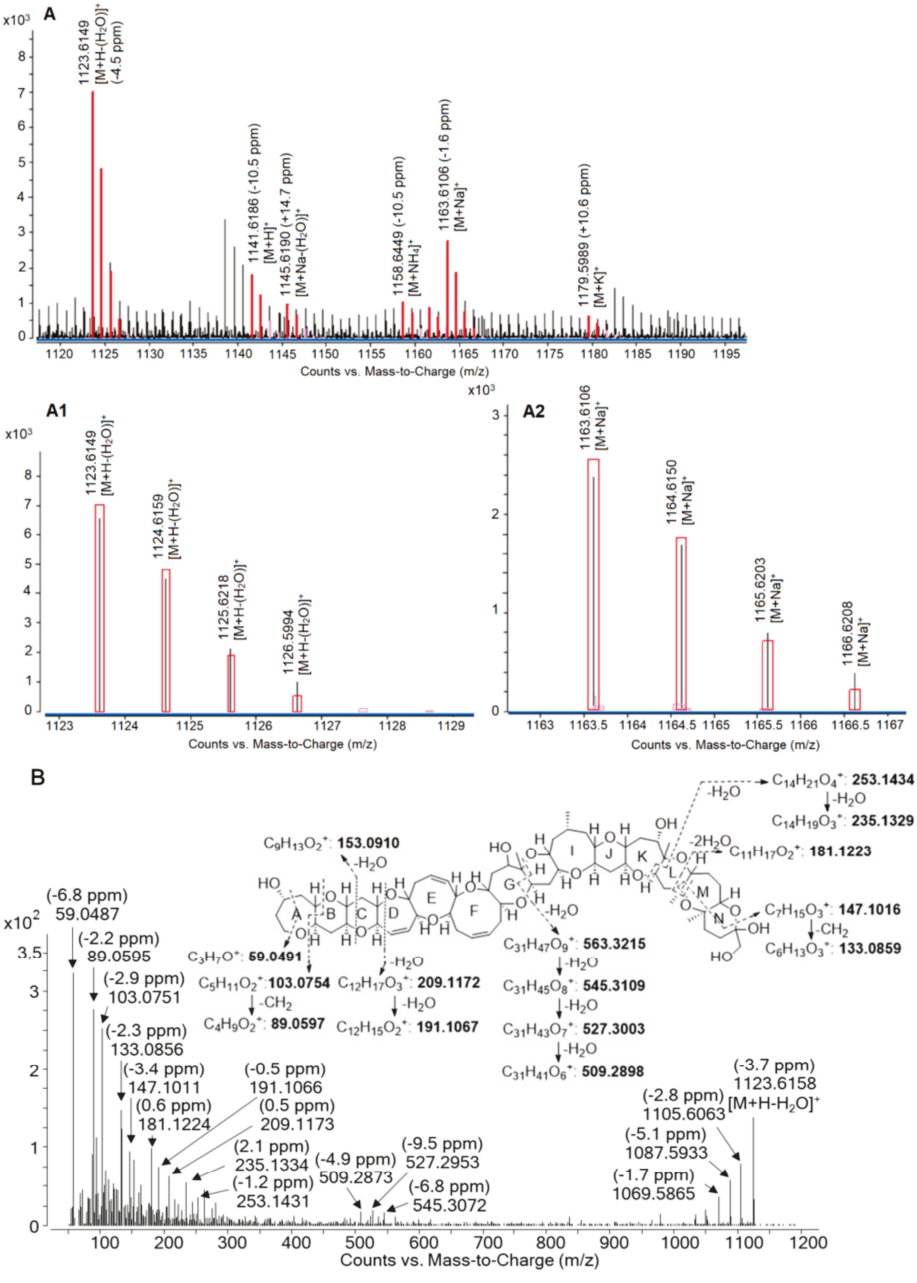

Figure 1. (**A**) Positive electrospray ionization (ESI^+) full-scan MS spectra of Caribbean ciguatoxin-1 (C-CTX1) laboratory reference material (LRM) (estimated to 123 ng/mL); (**A1**) zoom of C-CTX1 *m/z* 1123.6149 $[M + H - H_2O]^+$; (**A2**) zoom of C-CTX1 *m/z* 1163.6106 $[M + Na]^+$ (rectangles in red represent the theoretical isotope abundance and spacing of C-CTX1). (**B**) ESI^+ targeted MS/MS spectra of C-CTX1 LRM (estimated to 123 ng/mL) selecting C-CTX1 *m/z* 1123.6200 $[M + H - H_2O]^+$ at an average collision energy of 30, 50, and 70 eV.

3. Conclusions

The results obtained in this study show the potential of LC-HRMS for the confirmation of the presence of C-CTX1 in fish from the European Atlantic coasts. C-CTX1 full-scan MS and MS/MS spectra were successfully obtained and fragmentation pathways showed a similar fragmentation pattern compared to CTX3C and CTX1B, with fragmentation, not only in the ends of the molecule but also in the G- and H- rings. The confirmation of C-CTX1 by LC-HRMS is in agreement with previous studies carried out by combination of N2a and LC-MS/MS in which C-CTX1 had been confirmed as the main compound responsible for the CTX contamination in EU Atlantic Coasts. The relevance of the results obtained in this study are justified not only by the accomplishment of an important objective of the EUROCIGUA project in which the authors of this work are involved, but also for having contributed to the characterization of CP in areas where this contamination is being considered an emerging issue.

4. Materials and Methods

4.1. Reference Materials and Samples

C-CTX1 LRM (estimated to 123 ng/mL) purified from amberjack *S. fasciata* from Madeira archipelago (Portugal) was prepared at the University of Vigo, in the framework of the Specific Grant 4 of the project EuroCigua (the preparation of these materials is fully described on a manuscript in preparation, by Gago Martínez and coauthors). C-CTX1 in the LRM was identified by comparison with authentic C-CTX1 kindly provided by Robert W. Dickey (previously, U.S. Food and Drug Administration) via Ronald Manger (Fred Hutchinson Cancer Research Center, Seattle, WA, USA).

Barred hogfish (*B. scrofa)* was captured in the marine protected area of Selvagens Islands (Madeira, Portugal) under the EUROCIGUA framework agreement in September 2018. A portion of flesh tissue was dissected and stored raw at −20 °C until use.

4.2. Reagents

Acetone, water, methanol, hexane, diethyl ether, and ethyl acetate used for sample preparation were HPLC grade (Merck KGaA, Darmstadt, Germany).

Water, acetonitrile, formic acid, and ammonium formate used to prepare mobile phases were of LC-MS grade. All these chemicals were purchased from Sigma Aldrich (Saint Quentin Fallavier, France).

4.3. Sample Pretreatment

Barred hogfish was extracted and purified following the conditions proposed by [15].

4.4. LC-HRMS and HRMS/MS (Q-TOF 6550 iFunnel)

LC-HRMS analyses were carried out using a UHPLC system 1290 Infinity II (Agilent Technologies, Santa Clara, CA, USA) coupled to a HRMS quadrupole/time-of-flight (Q-TOF) mass spectrometer, i.e., Q-TOF 6550 iFunnel (Agilent Technologies, Santa Clara, CA, USA). Chromatographic separation was performed using a Kinetex C18 column (100 Å, 1.7 μm, 100 × 2.1 mm, Phenomenex, Le Pecq, France) at 40 °C with 5 mM ammonium formate and 0.1% formic acid in water (A) and acetonitrile (B). The flow rate was set at 0.4 mL/min and the injection volume was 5 μL. Gradient of mobile phase was carried out as follows: 35% B was kept for 1 min increasing to 80% B in 15 min, 95% of B in 16 min keeping for 5 min, and returning to the initial conditions in 0.1 min equilibrating the column for 4.9 min prior to the next injection.

LC-HRMS analyses were carried out in full-scan and targeted MS/MS mode in positive ionization. Full-scan analysis operated at a mass resolution of 40,000 full width at half maximum (FWHM) over a mass-to-charge ratio (*m/z*) ranging from 800 to 1200 with a scan rate of 1 spectrum/s. Targeted MS/MS was performed in a collision induced dissociation (CID) cell at 45,000 FWHM over the scan rage from

m/z 50 to 1200 with a scan rate of 10 spectra/s and a scan rate of 3 spectra/s applying three different collision energies in order to have a good fragmentation pathway. A reference mass of *m/z* 922.0099 (hexakisphosphazine) was continuously monitored during the entire run. Acquisition was controlled by MassHunter software (Agilent technologies, CA, USA). Raw data were processed with Agilent MassHunter Qualitative Analysis software (version B.07.00, service pack 1) using the Find by Formula (FbF) algorithm screening with a Personal Compound Database and Library (PDCL) created by the Phycotoxins Laboratory (IFREMER, Nantes, France).

Source conditions were as follows: gas temperature, 250 °C; gas flow, 16 L/min; nebulizer, 15 psi; sheath gas temperature, 400 °C; sheath gas flow, 12 L/min; capillary voltage, 5000 V, and nozzle voltage, 1000 V. The instrument was calibrated, using the Agilent tuning mix, in positive ionization mode before each analysis.

Supplementary Materials: The following are available online at http://www.mdpi.com/2072-6651/12/4/267/s1, Figure S1. ESI^+ Targeted MS/MS spectra of C-CTX1 LRM (123 ng/mL approx.) selecting C-CTX1 *m/z* 1123.6200 $[M+H-H_2O]^+$ at an average collision energy of 20, 40 and 60 eV; Figure S2. LC-HRMS chromatogram of (A) C-CTX1 LRM (123 ng/mL approx.) at 7.8 min; (B) C-CTX1 detected at 7.8 min in a naturally contaminated sample of barred hogfish (*Bodianus scrofa)* from Selvagens Islands (Portugal); Figure S3. (A) ESI^+ Full scan MS spectra of Barred hogfish (*Bodianus scrofa)* from Selvagens Islands (Portugal); (A.1) Zoom of C-CTX1 *m/z* 1123.6214 $[M+H-H_2O]^+$; (A.2) Zoom of C-CTX1 *m/z* 1163.6138 $[M+Na]^+$;Table S1. Accurate mono-isotopic masses (theoretical and measured) of C-CTX1 after ESI^+ Targeted MS/MS analysis selecting $[M+H-(H_2O)]^+$ at *m/z* 1123.6200 with an averaged collision energy of 20, 40 and 60 eV (A) and 30, 50 and 70 eV (B).

Author Contributions: Conceptualization, P.E., M.S., A.G.-M., and P.H.; methodology, P.E. and M.S.; investigation, P.E. and M.S.; resources, P.R.C., A.G.-M., and P.H.; data curation, P.E. and M.S.; writing—original draft preparation, P.E., M.S., A.G.-M., and P.H.; writing—review and editing, M.S., P.R.C., J.M.L.-M., A.G.-M., and P.H.; supervision, J.M.L.-M., A.G.-M., and P.H.; project administration, A.G.-M. and P.H.; funding acquisition, P.R.C., A.G.-M., and P.H. All authors have read and agreed to the published version of the manuscript.

Funding: The financial support was received through the project EUROCIGUA: "Risk Characterization of Ciguatera Fish Poisoning in Europe" GP/EFSA/AFSCO/2015/03, co-funded by the European Food Safety Authority (EFSA). Pablo Estevez (P.E.) acknowledges financial support from the Xunta de Galicia (Regional Government, Spain) under grant ED481A-2018/207.

Acknowledgments: Thanks to all technicians of Regional Fisheries Management—Madeira Government, Divisão de Serviços de Investigação - Direção Regional de Pescas (DSI-DRP), to Natural Park of Madeira and to Nature's Wardens of Selvagens Islands for their efforts and contribution obtaining fish samples. C-CTX1 standard was kindly provided by Robert W. Dickey (previously, U.S. Food and Drug Administration) via Ronald Manger (Fred Hutchinson Cancer Research Center, Seattle, WA, USA).

Conflicts of Interest: The authors declare no conflict of interest.

References

1. Yasumoto, T.; Murata, M. Marine toxins. *Chem. Rev.* **1993**, *93*, 1897–1909. [CrossRef]
2. Oshiro, N.; Yogi, K.; Asato, S.; Sasaki, T.; Tamanaha, K.; Hirama, M.; Yasumoto, T.; Inafuku, Y. Ciguatera incidence and fish toxicity in Okinawa, Japan. *Toxicon* **2010**, *56*, 656–661. [CrossRef] [PubMed]
3. Otero, P.; Pérez, S.; Alfonso, A.; Vale, C.; Rodríguez, P.; Gouveia, N.N.; Gouveia, N.; Delgado, J.; Vale, P.; Hirama, M.; et al. First Toxin Profile of Ciguateric Fish in Madeira Arquipelago (Europe). *Anal. Chem.* **2010**, *82*, 6032–6039. [CrossRef] [PubMed]
4. Abraham, A.; Jester, E.L.E.; Granade, H.R.; Plakas, S.M.; Dickey, R.W. Caribbean ciguatoxin profile in raw and cooked fish implicated in ciguatera. *Food Chem.* **2012**, *131*, 192–198. [CrossRef]
5. Costa, P.R.; Estevez, P.; Castro, D.; Soliño, L.; Gouveia, N.; Santos, C.; Rodrigues, S.M.; Leao, J.M.; Gago-Martínez, A. New Insights into the Occurrence and Toxin Profile of Ciguatoxins in Selvagens Islands (Madeira, Portugal). *Toxins (Basel)* **2018**, *10*, 524. [CrossRef]
6. Estevez, P.; Castro, D.; Pequeño-Valtierra, A.; Giraldez, J.; Gago-Martinez, A. Emerging Marine Biotoxins in Seafood from European Coasts: Incidence and Analytical Challenges. *Foods* **2019**, *8*, 149. [CrossRef]
7. Kato, T.; Yasumoto, T. Quantification of Representative Ciguatoxins in the Pacific Using Quantitative Nuclear Magnetic Resonance Spectroscopy. *Mar. Drugs* **2017**, *15*, 309. [CrossRef]
8. Ikehara, T.; Kuniyoshi, K.; Oshiro, N.; Yasumoto, T. Biooxidation of Ciguatoxins Leads to Species-Specific Toxin Profiles. *Toxins (Basel)* **2017**, *9*, 205. [CrossRef]

9. Yogi, K.; Oshiro, N.; Inafuku, Y.; Hirama, M.; Yasumoto, T. Detailed LC-MS/MS Analysis of Ciguatoxins Revealing Distinct Regional and Species Characteristics in Fish and Causative Alga from the Pacific. *Anal. Chem.* **2011**, *83*, 8886–8891. [CrossRef]
10. Murray, J.S.; Boundy, M.J.; Selwood, A.I.; Harwood, D.T. Development of an LC–MS/MS method to simultaneously monitor maitotoxins and selected ciguatoxins in algal cultures and P-CTX-1B in fish. *Harmful Algae* **2018**, *80*, 80–87. [CrossRef]
11. Lewis, R.J.; Jones, A.; Vernoux, J.-P. HPLC/Tandem Electrospray Mass Spectrometry for the Determination of Sub-ppb Levels of Pacific and Caribbean Ciguatoxins in Crude Extracts of Fish. *Anal. Chem.* **1999**, *71*, 247–250. [CrossRef]
12. Vernoux, J.P.; Lewis, R.J. Isolation and characterisation of Caribbean ciguatoxins from the horse-eye jack (Caranx latus). *Toxicon* **1997**, *35*, 889–900. [CrossRef]
13. Lewis, R.J.; Vernoux, J.-P.; Brereton, I.M. Structure of Caribbean Ciguatoxin Isolated from Caranx latus. *J. Am. Chem. Soc.* **1998**, *120*, 5914–5920. [CrossRef]
14. Moreiras, G.; Leão, J.M.; Gago-Martínez, A. Design of Experiments for the Optimization of Electrospray Ionization in the LC-MS/MS Analysis of Ciguatoxins. *J. Mass Spectrom.* **2018**, *53*, 1059–1060. [CrossRef]
15. Estevez, P.; Castro, D.; Leao, J.M.; Yasumoto, T.; Dickey, R.; Gago-Martinez, A. Implementation of liquid chromatography tandem mass spectrometry for the analysis of ciguatera fish poisoning in contaminated fish samples from Atlantic coasts. *Food Chem.* **2019**, *280*, 8–14. [CrossRef]
16. Estevez, P.; Castro, D.; Pequeño-Valtierra, A.; Leao, J.M.; Vilariño, O.; Diogène, J.; Gago-Martínez, A. An Attempt to Characterize the Ciguatoxin Profile in Seriola fasciata Causing Ciguatera Fish Poisoning in Macaronesia. *Toxins (Basel)* **2019**, *11*, 221. [CrossRef]
17. Sibat, M.; Herrenknecht, C.; Darius, H.T.; Roué, M.; Chinain, M.; Hess, P. Detection of pacific ciguatoxins using liquid chromatography coupled to either low or high resolution mass spectrometry (LC-MS/MS). *J. Chromatogr. A* **2018**, *1571*, 16–28. [CrossRef]
18. Suzuki, T.; Ha, D.V.; Uesugi, A.; Uchida, H. Analytical challenges to ciguatoxins. *Curr. Opin. Food Sci.* **2017**, *18*, 37–42. [CrossRef]
19. Ha, D.V.; Uesugi, A.; Uchida, H.; Ky, P.X.; Minh, D.Q.; Watanabe, R.; Matsushima, R.; Oikawa, H.; Nagai, S.; Iwataki, M.; et al. Identification of Causative Ciguatoxins in Red Snappers Lutjanus bohar Implicated in Ciguatera Fish Poisonings in Vietnam. *Toxins (Basel)* **2018**, *10*, 420. [CrossRef]
20. Kryuchkov, F.; Robertson, A.; Miles, C.O.; Mudge, E.M.; Uhlig, S. LC–HRMS and Chemical Derivatization Strategies for the Structure Elucidation of Caribbean Ciguatoxins: Identification of C-CTX-3 and -4. *Mar. Drugs* **2020**, *18*, 182. [CrossRef]
21. Estevez, P.; Leao, J.M.; Yasumoto, T.; Dickey, R.W.; Gago-Martinez, A. Caribbean Ciguatoxin-1 stability under strongly acidic conditions: Characterisation of a new C-CTX1 methoxy congener. *Food Addit. Contam. Part A* **2020**, *37*, 519–529. [CrossRef] [PubMed]

toxins

MDPI

Article

Use of Mass Spectrometry to Determine the Diversity of Toxins Produced by *Gambierdiscus* and *Fukuyoa* Species from Balearic Islands and Crete (Mediterranean Sea) and the Canary Islands (Northeast Atlantic)

Pablo Estevez [1], Manoëlla Sibat [2], José Manuel Leão-Martins [1], Angels Tudó [3], Maria Rambla-Alegre [3], Katerina Aligizaki [4], Jorge Diogène [3,*], Ana Gago-Martinez [1,*] and Philipp Hess [2,*]

1 Biomedical Research Center (CINBIO), Department of Analytical and Food Chemistry, Campus Universitario de Vigo, University of Vigo, 36310 Vigo, Spain; paestevez@uvigo.es (P.E.); leao@uvigo.es (J.M.L.-M.)
2 Laboratoire Phycotoxines, Ifremer, Rue de l'Île d'Yeu 44311 Nantes, France; manoella.sibat@ifremer.fr
3 Marine and Continental Waters programme, Ctra. Poble Nou, km. 5.5, IRTA, Sant Carles de la Ràpita, 43540 Tarragona, Spain; angels.tudo@irta.cat (A.T.); maria.rambla@irta.cat (M.R.-A.)
4 Laboratory Unit on Harmful Marine Microalgae, Biology Department, Aristotle University of Thessaloniki, 54124 Thessaloniki, Greece; aligiza@auth.gr
* Correspondence: jorge.diogene@irta.cat (J.D.); anagago@uvigo.es (A.G.-M.); philipp.hess@ifremer.fr (P.H.); Tel.: +34-97-774-3381 (J.D.); +34-64-734-3417 (A.G.-M.); +332-4037-4257 (P.H.)

Received: 25 March 2020; Accepted: 4 May 2020; Published: 7 May 2020

Abstract: Over the last decade, knowledge has significantly increased on the taxonomic identity and distribution of dinoflagellates of the genera *Gambierdiscus* and *Fukuyoa*. Additionally, a number of hitherto unknown bioactive metabolites have been described, while the role of these compounds in ciguatera poisoning (CP) remains to be clarified. Ciguatoxins and maitotoxins are very toxic compounds produced by these dinoflagellates and have been described since the 1980s. Ciguatoxins are generally described as the main contributors to this food intoxication. Recent reports of CP in temperate waters of the Canary Islands (Spain) and the Madeira archipelago (Portugal) triggered the need for isolation and cultivation of dinoflagellates from these areas, and their taxonomic and toxicological characterization. Maitotoxins, and specifically maitotoxin-4, has been described as one of the most toxic compounds produced by these dinoflagellates (e.g., *G. excentricus*) in the Canary Islands. Thus, characterization of toxin profiles of *Gambierdiscus* species from adjacent regions appears critical. The combination of liquid chromatography coupled to either low- or high-resolution mass spectrometry allowed for characterization of several strains of *Gambierdiscus* and *Fukuyoa* from the Mediterranean Sea and the Canary Islands. Maitotoxin-3, two analogues tentatively identified as gambieric acid C and D, a putative gambierone analogue and a putative gambieroxide were detected in all *G. australes* strains from Menorca and Mallorca (Balearic Islands, Spain) while only maitotoxin-3 was present in an *F. paulensis* strain of the same region. An unidentified *Gambierdiscus* species (*Gambierdiscus* sp.2) from Crete (Greece) showed a different toxin profile, detecting both maitotoxin-3 and gambierone, while the availability of a *G. excentricus* strain from the Canary Islands (Spain) confirmed the presence of maitotoxin-4 in this species. Overall, this study shows that toxin profiles not only appear to be species-specific but probably also specific to larger geographic regions.

Keywords: maitotoxins; ciguatoxins; *Gambierdiscus*; *Fukuyoa*; LC-MS/MS; HRMS; QToF; ciguatera poisoning

Key Contribution: Metabolites were identified in several *Gambierdiscus* strains from the Balearic Islands, Greece and the Canaries. High-resolution mass spectrometry confirmed the presence of 44-methyl gambierone (MTX3) and did not detect maitotoxin-1 (MTX1), desulfo-MTX1 and didehydro-desulfo-MTX1 above the detection limit in Mediterranean strains of *G. australes*.

1. Introduction

Ciguatera Poisoning (CP) is described as a food intoxication endemic in tropical and subtropical areas of the world. The poisoning is caused by the consumption of fish or shellfish that accumulate toxic compounds produced by benthic dinoflagellates of the genus *Gambierdiscus* and *Fukuyoa* [1]. The two main toxin groups produced by these dinoflagellates are ciguatoxins (CTXs) and maitotoxins (MTXs) [2].

CTXs are considered the main toxins responsible for CP as their lipophilic character allows for intestinal absorption and accumulation. They are cyclic polyether compounds of around 1100 Da being classified as Pacific (P-CTXs), Caribbean (C-CTXs) and Indian (I-CTXs) ciguatoxins. Different CTX analogues from these groups have been detected in fish tissue associated to a CP case, while only a few P-CTXs were detected in *Gambierdiscus* extracts from the Pacific Ocean [3–7].

MTXs are water soluble cyclic polyethers containing one or two sulfate ester groups; these groups are responsible for the intermediate polarity of MTXs, and their low intestinal absorption casts doubts as to their involvement in CP [8]. Six MTX analogues have currently been identified: maitotoxin-1 (MTX1), maitotoxin-2 (MTX2), maitotoxin-3 (MTX3), maitotoxin-4 (MTX4), desulfo-MTX1 and didehydro-demethyl-desulfo-MTX1, all of which were isolated from different strains of *Gambierdiscus* [9–12].

MTX1 is the most toxic marine compound and the largest natural non-biopolymer toxin consisting on a ladder-shaped cyclic polyether compound containing two sulfate groups [9]. MTX2 was isolated from an Australian *Gambierdiscus* strain from Queensland [10]. Its structure has not yet been elucidated and it showed a lower potency than MTX1 by intraperitoneal injection in mice. MTX3 (44-methylgambierone) was first characterized by [10], but it was not until recently that its structure had been elucidated by its isolation from *G. belizeanus* and *G. australes*, being identified as a gambierone homologue [13–15]. MTX3, which is about one third the molecular weight of MTX1, showed a biological activity similar to CTX3C but with much lower potency, indicating that despite being grouped in the MTX group, this compound exhibits CTX-like activity rather than MTX-like activity [13]. MTX4 was recently isolated from *G. excentricus* extracts from the Canary Islands (Spain) [11]. Its structure is not yet elucidated but it has ion clusters and molecular mass in a similar range as MTX1, as well as sulfate esters; it was reported to exhibit a similar toxic effect of MTX1 in neuroblastoma cells detecting a high cytotoxicity and Ca^{2+} influx [11]. Other large but mono-sulfated MTXs were recently elucidated by their isolation from *Gambierdiscus* spp. from the Caribbean Sea, i.e., desulfo-MTX1 from *G. belizeanus* and didehydro-demethyl-desulfo-MTX1 from *G. ribotype-2*, showing the wide variety of MTXs that seem to be produced by these dinoflagellates [12] (Table 1). Furthermore, *Gambierdiscus* and *Fukuyoa* have shown to produce non-structurally related cyclic polyether compounds such as gambierol, gambieric acids, gambieroxide and gambierone [15–18].

Table 1. List of the maitotoxins isolated from dinoflagellates of the genus *Gambierdiscus* and *Fukuyoa.*

MTX Congener	Chemical Formula	Monoisotopic Mass (Da)	Reference
MTX1	$C_{164}H_{258}O_{68}S_2$	3379.6171 for the free acid form	[9]
MTX2	Unknown	3298 for the mono-sodium salt	[10]
MTX3	$C_{52}H_{78}O_{19}S$	1038.4858 for the free acid form	[13,14]
MTX4	Unknown	3292.486 for the free acid form	[11]
desulfo-MTX1	$C_{164}H_{258}O_{65}S$	3299.6603 for the free acid form	[12]
didehydro-demethyl-desulfo-MTX1	$C_{163}H_{254}O_{65}S$	3283.6290 for the free acid form	[12]

Most of these compounds can be classified depending on their mechanism of action into two groups: (i) MTX-like compounds, associated with a massive Ca^{2+} influx causing a rapid cell death, including MTX1, MTX2 and MTX4; and (ii) CTX-like compounds, which create a disequilibrium in the voltage-gated sodium channels (VGSCs), including all CTXs, and with much lower potency, MTX3 and gambierone [13].

A wide variety of *Gambierdiscus* species are present in regions considered endemic for CP (the Pacific Ocean or the Caribbean Sea) [19]. These dinoflagellates have also been detected in CP-emerging regions such as the Canary Islands (Spain) and Madeira archipelago (Portugal), as well as in the Mediterranean Sea, from which no CP cases have been reported until now [20]. *Gambierdiscus excentricus* was the first *Gambierdiscus* species detected in the Canary Islands [21], but its detection led to further research that concluded with the detection of a large number of *Gambierdiscus* species (*G. australes*, *G. caribaeus*, *G. carolinianus*, *G. excentricus*, *G. silvae* and *Gambierdiscus* ribotype3) suggesting that the Canary Islands would be a "hot spot" for these dinoflagellates [22]. On the other hand, the only available data from the Selvagem Islands (Madeira, Portugal) is the detection of numerous strains of *G. australes*, which test positive in the Neuro2a cell-based toxicity assay (N2a), suggesting they contain CTX- and MTX-like compounds [23]. In the Mediterranean Sea, the presence of *Gambierdiscus* was first reported in 2003 (*Gambierdiscus* sp.) in Crete (Greece), while to our knowledge only one study in 2016 attempted to characterize a strain of *F. paulensis* from Formentera (Balearic Islands, Spain) by LC-MS, however, the trace levels of toxic compounds present did not allow for conclusive results about the compounds produced [24,25].

As part of the ongoing EuroCigua project [26], *G. australes* and *F. paulensis* were isolated from Menorca and Mallorca (Balearic Islands, Spain), *Gambierdiscus* sp.2 from Crete (Greece), as well as *G. excentricus* from La Gomera (Canary Islands, Spain), showing CTX and MTX-activity. The aim of the present study was to describe the diversity of toxins produced by a selection of these strains of *Gambierdiscus* and *Fukuyoa* species using liquid chromatography coupled to low- and high-resolution mass spectrometry (LC-MS/MS and LC-HRMS). While LC-MS/MS was used for a rapid screening of the toxic compounds potentially present, allowing for the estimation of their concentrations, the purpose of LC-HRMS was the confirmation and structural characterization of the toxic compounds previously identified by LC-MS/MS.

2. Results

2.1. LC-MS/MS Analysis

In an attempt to separate MTXs and gambierones from CTXs, liquid/liquid partitioning of the crude extracts was carried out between MeOH:H_2O (3:2) and dichloromethane. The methanol-soluble fraction (MSF) and the dichloromethane-soluble fraction (DSF) of each crude extract of dinoflagellate cell pellets were analyzed by LC-MS/MS monitoring MTXs, as well as gambierone (Table 2). A Multiple Reaction Monitoring (MRM) method in negative ionization mode screened for six MTXs (MTX1, MTX2, MTX3, MTX4, desulfo-MTX1 and didehydro-demethyl-desulfo-MTX1), as well as gambierone. The ESI^- MRM method was based on monitoring a qualitative transition from the (pseudo-)molecular ion to the hydrogenated sulfate anion *m/z* 96.9 $[HOSO_3]^-$ at high collision energy, which is typical

of these compounds, and for quantitation based on monitoring the pseudo-molecular ion itself $[M-2H]^{2-}$/$[M-2H]^{2-}$ for MTX1, MTX4, desulfo-MTX1 and didehydro-demethyl-desulfo-MTX1. This was due to the single-charged ion of these compounds being outside the mass range of the mass spectrometer (50–2800 Da), whereas $[M-H]^-$/ $[M-H]^-$ was selected for MTX3 and gambierone. Due to the absence of MTX2 MS/MS fragmentation data, the double-charged $[M-2H]^{2-}$/$[HOSO_3]^-$ and triple-charged $[M-3H]^{3-}$/$[HOSO_3]^-$ molecular anions to the sulfate anion *m/z* 96.9 $[HOSO_3]^-$ were selected as MRM transitions for this compound, assuming similar MS/MS fragmentation behavior of MTX1 and MTX2 [27].

The identification of MTX1, MTX3, gambierone and MTX4 was carried out by comparing retention times as well as ion ratios with the reference materials available (Table S8). On the other hand, the lack of structural information and reference material of MTX2 limited its identification. Therefore, the absence of this compound was reported as not detected above the limit of detection of any ion transition monitored. The lack of reference material of desulfo-MTX1 and didehydro-demethyl-desulfo-MTX1 also limited its identification, with the approach followed being the same as that described for MTX2. However, the accurate mass of these compounds was available, only hampering its identification in LC-HRMS by the uncertainty of the limit of detection of our method for these compounds.

44-methyl-gambierone (MTX3) was identified in all samples of *G. australes* from Menorca and Mallorca (Balearic Islands, Spain), detecting both quantitative *m/z* 1037.6 $[M-H]^-$/ *m/z* 1037.6 $[M-H]^-$ and qualitative *m/z* 1037.6 $[M-H]^-$/ *m/z* 96.9 $[HOSO_3]^-$ MRM ion transitions in negative ionization mode. MTX3 concentrations in *G. australes* strains ranged from 344 to 1661 pg MTX1 equivalent/cell (eq./cell) taking into account the total amount detected in the sum of MSF + DSF. *Gambierdiscus* sp.2 from Crete (Greece) contained significantly less MTX3 (4.3 pg MTX1 eq./cell). The recovery of MTX3 in the MSF ranged between 66.7% and 84.1% for *G. australes* for the Balearic and Crete strains (Table 2). MTX3 was also present in one *F. paulensis* from Menorca (Balearic Islands, Spain) at a concentration of 10.5 pg MTX1 eq./cell. In this case, however, the recovery of MTX3 in the MSF was only 17.7% (Table 2). This difference compared to the recovery observed in the MTX3 detected in *G. australes* must be explored; at this stage, we can only presume a matrix effect during the partitioning step. Gambierone was only identified in the one *Gambierdiscus* strain from Crete, albeit at a significant concentration of 776 pg MTX1 eq./cell for the sum of MSF + DSF. The recovery of gambierone in the MSF was 92.2% (Table 2).

A putative gambierone analogue, with an earlier retention time than gambierone on the C_{18} column, was detected in all *G. australes* from Menorca and Mallorca (Balearic Islands, Spain) at concentrations ranging from 148.6 to 523.4 pg MTX1 eq./cell and an average recovery of the putative gambierone analogue in the MSF of 99.7% (Table 2). Negative ionization mode detected both quantitative *m/z* 1023.5 $[M-H]^-$/ *m/z* 1023.5 $[M-H]^-$ and qualitative ion transitions *m/z* 1023.5 $[M-H]^-$/m/z 96.9 $[HOSO_3]^-$ with the same ion ratios as gambierone. This compound was not present in the other three strains of *Gambierdiscus*.

Further confirmation of MTX3, gambierone and the putative gambierone analogue was carried out in positive ionization mode and not only in MRM, but also in full scan and enhanced product ion modes, confirming the presence of MTX3 and gambierone due to the detection of their common fragment *m/z* 803 as well as their specific fragments *m/z* 233 and *m/z* 219, respectively. This was already reported by Boente-Juncal et al. [13], and a common fragment with *m/z* 109 was assigned to the fragmentation of the side chain in the last ring (Figures S1 and S2). The putative gambierone analogue did not show any common or specific gambierone fragments but showed a fragmentation pattern similar to these compounds, including water losses and sulfate loss followed by water losses (Figures S1 and S2).

MTX4 was confirmed in a strain of *G. excentricus* from La Gomera (Canary Islands, Spain). Retention time as well as MRM ion ratios transitions *m/z* 1646.2 $[M-2H]^{2-}$/*m/z* 1646.2 $[M-2H]^{2-}$ and *m/z* 1646.2 $[M-2H]^{2-}$/*m/z* 96.9 $[HOSO_3]^-$ were consistent with those obtained in the MTX4 reference material. The recovery of MTX4 from the DSF to the MSF was 99.3% (See Table 2).

Table 2. Results obtained after the liquid chromatography mass spectrometry (LC-MS/MS) analysis of the dinoflagellate extracts using a triple-stage quadrupole instrument. Results are expressed in pg MTX1 eq./cell: equivalent/cell; MSF: Methanol Soluble Fraction; DSF: Dichloromethane Soluble Fraction; Σ: sum, n.d.: not detected.

Species	Strain Code	Location	pg MTX1 eq./Cell (% of TOTAL)															
			MTX1	MTX2	MTX3			MTX4			desulfo-MTX1	didehydro-demethyl-desulfo-MTX1	Gambierone			P-Gambierone Analogue		
					MSF (%)	DSF (%)	Σ	MSF (%)	DSF (%)	Σ			MSF (%)	DSF (%)	Σ	MSF (%)	DSF (%)	Σ
G. australes	IRTA-SMM-17-189	Torret, Menorca, Balearic Islands, Spain	n.d.	n.d.	241 (70.2)	102 (29.8)	344.0		n.d.		n.d.	n.d.		n.d.		148 (99.7)	0.4 (0.3)	149
G. australes	IRTA-SMM-17-162	St. Adeodat, Menorca, Balearic Islands, Spain	n.d.	n.d.	575 (79.9)	150 (20.1)	720		n.d.		n.d.	n.d.		n.d.		275 (99.6)	1.0 (0.4)	276
G. australes	IRTA-SMM-17-164	St. Adeodat, Menorca, Balearic Islands, Spain	n.d.	n.d.	1108 (66.7)	553 (33.3)	1661		n.d.		n.d.	n.d.		n.d.		522 (99.8)	1.2 (0.2)	523
G. australes	IRTA-SMM-17-271	Macarella, Menorca, Balearic Islands, Spain	n.d.	n.d.	1107 (83.7)	215 (16.3)	1322		n.d.		n.d.	n.d.		n.d.		408 (99.9)	0.4 (0.1)	409
F. paulensis	IRTA-SMM-17-209	Sacaleta, Menorca, Balearic Islands, Spain	n.d.	n.d.	1.8 (17.7)	8.6 (82.3)	10.5		n.d.		n.d.	n.d.		n.d.			n.d.	
G. australes	IRTA-SMM-17-253	Anguila, Mallorca, Balearic Islands, Spain	n.d.	n.d.	781 (72.3)	300 (27.7)	1081		n.d.		n.d.	n.d.		n.d.		229 (99.8)	0.5 (0.2)	229
G. australes	IRTA-SMM-17-244	Camp de Mar, Mallorca, Balearic Islands, Spain	n.d.	n.d.	403 (84.1)	75.9 (15.9)	479		n.d.		n.d.	n.d.		n.d.		173 (99.6)	0.7 (0.4)	174
Gambierdiscus sp.2	0010G-CR-CCAUTH	Kolimpari, Crete, Greece	n.d.	n.d.	3.0 (70.1)	1.3 (29.9)	4.3		n.d.		n.d.	n.d.	716 (92.2)	60.3 (7.8)	775.9		n.d.	
G. excentricus	IRTA-SMM-17-407	Playa de vueltas, La Gomera, Canary Islands, Spain	n.d.	n.d.		n.d.		36.8 (99.3)	0.3 (0.7)	37.1	n.d.	n.d.		n.d.			n.d.	

MTX1, MTX2, desulfo-MTX1 and didehydro-demethyl-desulfo-MTX1 were not detected in any *Gambierdiscus* or *Fukuyoa* samples from the Mediterranean Sea and the *G. excentricus* from Canary Islands (Spain), neither in the MSF nor in the DSF.

2.2. LC-HRMS/MS Analysis

The presence of the compounds previously identified and quantified by LC-MS/MS was confirmed by LC-HRMS. Mass spectral detection was performed in full scan and targeted MS/MS mode in negative (ESI^-) and positive (ESI^+) ionization mode. Both DSF and MSF of dinoflagellate extracts were analyzed in ESI^- and ESI^+ full scan mode, and screening with an in-house database allowed for identification of several compounds based on their characteristics reported in the literature.

MTX3 was confirmed in all *G. australes* in both ESI^- and ESI^+ full scan mode at 7.6 min. Negative ionization mode showed the detection of a single ion corresponding to the deprotonated molecule $[M-H]^-$ with Δppm < 1 ppm in all samples of this species (Figure 1A1, Table S1). At the same retention time, positive ionization mode showed a prominent ion corresponding to the molecular ion $[M+H]^+$ and also pseudo-molecular ions $[M+H-H_2O]^+$, $[M+NH_4]^+$, $[M+Na]^+$ with Δppm < 3.7 ppm in all ions of these samples (Figure 1A) (See Table S1).

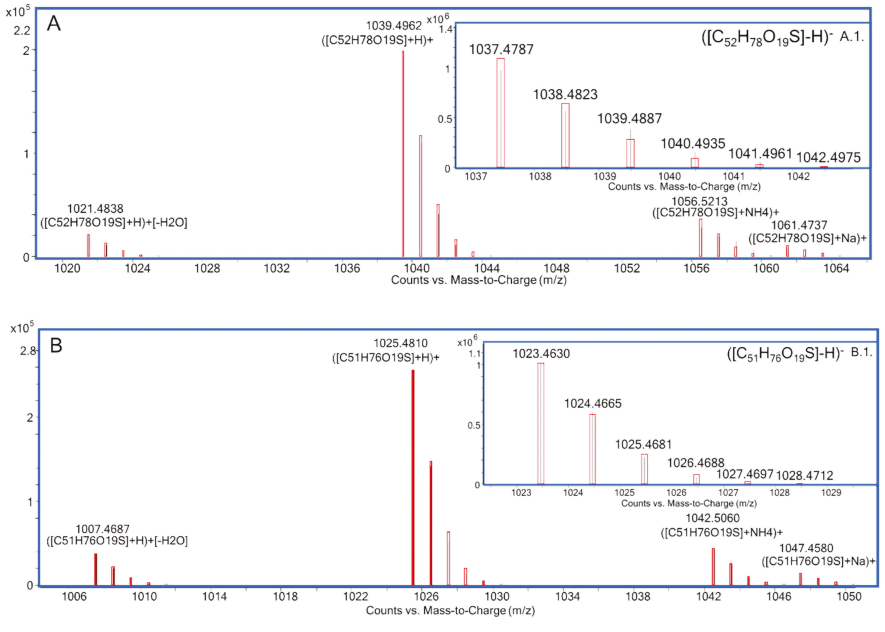

Figure 1. LC-HRMS analysis in MS full scan mode of: MTX3 detected in *G. australes*, (**A**) ESI^+ mode, (**A1**) ESI^- mode; gambierone detected in *Gambierdiscus* sp.2, (**B**) ESI^+ mode, (**B1**) ESI^- mode.

The molecular ion $[M-H]^-$ of MTX3 was also detected in *F. paulensis* and *Gambierdiscus* sp.2 in ESI^- ionization mode at 7.6 min with a Δppm < 1.9 ppm, whereas the lower sensitivity of the ESI^+ ionization mode for this compound only allowed the detection of the molecular ion $[M+H]^+$ with Δppm < 2.2 ppm and traces of the first water loss $[M+H-H_2O]^+$ (Δppm < 8 ppm) (See Table S1).

Gambierone was identified at 7.4 min in the *Gambierdiscus* sp.2 from Crete (Greece) showing a similar ion pattern as the one detected for MTX3 in both ESI^- and ESI^+ full scan mode. Negative ionization mode showed the detection of a single ion matching the deprotonated molecule $[M-H]^-$ *m/z* 1023.4630 (Δppm = +0.1 ppm) (Figure 1B1, Table S2). Positive ionization mode showed, at the same retention time, a prominent ion corresponding to the molecular ion $[M+H]^+$ *m/z* 1025.4810 (Δppm =

+3.5 ppm) and also the pseudo-molecular ions $[M+H\text{-}H_2O]^+$ *m/z* 1007.4687 (Δppm = +1.8), $[M+NH_4]^+$ *m/z* 1042.5060 (Δppm = +1.9) and $[M+Na]^+$ *m/z* 1047.4580 (Δppm = −1.3) (Figure 1B, Table S2).

MTX3 and gambierone were further confirmed in targeted MS/MS in both ESI^- and ESI^+ mode. ESI^--targeted MS/MS selected the deprotonated molecule $[M\text{-}H]^-$ applying 30 eV, 50 eV and 70 eV, detecting the hydrogen-sulfate fragment $[HOSO_3]^-$ in both compounds (Figures 2A and 2B). An ion representing a water loss $[M\text{-}H\text{-}H_2O]^-$ was also detected in low abundance, as well as the fragments specific for MTX3, *m/z* 977.4535 (Δppm = −4.0 ppm) and *m/z* 959.4428 (Δppm = −4.2 ppm), and those specific for gambierone, *m/z* 963.4392 (Δppm = −2.6 ppm) and *m/z* 945.4302 (Δppm = −1.0 ppm). Fragmentation pathways are also proposed on the basis of the observed fragments, including the two common fragments with theoretical *m/z* 899.3741 and *m/z* 839.3529, as well as water losses common to both MTX3 and gambierone (Figures 2A1 and 2B1) (Table 3).

Table 3. Accurate masses (measured and theoretical) of informative ions of MTX3 and gambierone in ESI^- mode and ESI^+ mode.

Ion	Molecular Formula	MTX3 m/z		Δ ppm	Molecular Formula	Gambierone m/z		Δ ppm
		Measured	Theoretical			Measured	Theoretical	
				ESI^-				
$[M\text{-}H]^-$	**$C_{52}H_{77}O_{19}S^-$**	**1037.4774**	1037.4785	−1.1	$C_{51}H_{75}O_{19}S^-$	1023.4612	1023.4629	−1.6
$[M\text{-}H\text{-}H_2O]^-$	$C_{52}H_{75}O_{18}S^-$	1019.4625	1019.4680	−5.3	$C_{51}H_{73}O_{18}S^-$	1005.4463	1005.4523	−6.0
	$C_{50}H_{73}O_{17}S^-$	977.4535	977.4574	−4.0	$C_{49}H_{71}O_{17}S^-$	963.4392	963.4417	−2.6
H_2O	$C_{50}H_{71}O_{16}S^-$	959.4428	959.4468	−4.2	$C_{49}H_{69}O_{16}S^-$	945.4302	945.4312	−1.0
	$C_{43}H_{63}O_{18}S^-$	899.3707	899.3741	−3.7	$C_{43}H_{63}O_{18}S^-$	899.3707	899.3741	−3.7
$-H_2O$	$C_{43}H_{61}O_{17}S^-$	881.3613	881.3635	−2.5	$C_{43}H_{61}O_{17}S^-$	881.3618	881.3635	−1.9
	$C_{41}H_{59}O_{16}S^-$	839.3501	839.3529	−3.4	$C_{41}H_{59}O_{16}S^-$	839.3517	839.3529	−1.5
$-H_2O$	$C_{41}H_{57}O_{15}S^-$	821.3362	821.3424	−7.5	$C_{41}H_{57}O_{15}S^-$	821.3306	821.3424	−14.3
$[HOSO_3]^-$	$HOSO_3^-$	96.9611	96.9601	10.3	$HOSO_3^-$	96.9615	96.9601	14.4
				ESI^+				
$[M+H]^+$	$C_{52}H_{79}O_{19}S^+$	1039.4911	1039.4931	−1.9	$C_{51}H_{77}O_{19}S^+$	1025.4749	1025.4774	−2.4
$[M+H\text{-}H_2O]^+$	$C_{52}H_{77}O_{18}S^+$	1021.4795	1021.4825	−2.9	$C_{51}H_{75}O_{18}S^+$	1007.4636	1007.4668	−3.2
$[M+H\text{-}2H_2O]^+$	$C_{52}H_{75}O_{17}S^+$	1003.4692	1003.4720	−2.8	$C_{51}H_{73}O_{17}S^+$	989.4528	989.4563	−3.5
$[M\text{-}SO_3+H]^+$	$C_{52}H_{79}O_{16}^+$	959.5333	959.5363	−3.1	$C_{51}H_{77}O_{16}^+$	945.5171	945.5206	−3.7
$[M\text{-}SO_3\text{-}H_2O+H]^+$	$C_{52}H_{77}O_{15}^+$	941.5232	941.5257	−2.7	$C_{51}H_{75}O_{15}^+$	927.5070	927.5100	−3.2
$[M\text{-}SO_3\text{-}2H_2O+H]^+$	$C_{52}H_{75}O_{14}^+$	923.5125	923.5152	−2.9	$C_{51}H_{73}O_{14}^+$	909.4968	909.4995	−3.0
$[M\text{-}SO_3\text{-}3H_2O+H]^+$	$C_{52}H_{73}O_{13}^+$	905.5022	905.5046	−2.7	$C_{51}H_{71}O_{13}^+$	891.4849	891.4889	−4.5
$[M\text{-}SO_3\text{-}4H_2O+H]^+$	$C_{52}H_{71}O_{12}^+$	887.4911	887.4940	−3.3	$C_{51}H_{69}O_{12}^+$	873.4743	873.4783	−4.6
$[M\text{-}SO_3\text{-}5H_2O+H]^+$	$C_{52}H_{69}O_{11}^+$	869.4812	869.4835	−2.6	$C_{51}H_{67}O_{11}^+$	855.4656	855.4678	−2.6
	$C_{43}H_{65}O_{18}S^+$	901.3854	901.3886	−3.6	$C_{43}H_{65}O_{18}S^+$	901.3884	901.3886	−0.2
$-H_2O$	$C_{43}H_{63}O_{17}S^+$	883.3756	883.3780	−2.7	$C_{43}H_{63}O_{17}S^+$	883.3744	883.3780	−4.1
$-OSO_3H$	$C_{43}H_{63}O_{14}^+$	803.4182	803.4212	−3.7	$C_{43}H_{63}O_{14}^+$	803.4173	803.4212	−4.9
	$C_{15}H_{21}O_2^+$	233.1533	233.1536	−1.3	$C_{14}H_{19}O_2^+$	219.1375	219.1380	−2.1
	$C_{15}H_{19}O^+$	215.1429	215.1430	−0.5	$C_7H_9O^+$	109.0644	109.0648	−3.6
	$C_8H_{11}O^+$	123.0800	123.0804	−3.2	$C_6H_9^+$	81.0697	81.0699	−2.2
	$C_7H_9O^+$	109.0645	109.0648	−2.8				
	$C_7H_{11}^+$	95.0852	95.0855	−3.2				
	$C_6H_9^+$	81.0696	81.0699	−3.7				

Positive mode ESI^+-targeted MS/MS of MTX3 and gambierone molecular ion $[M+H]^+$, *m/z* 1039.4931 and *m/z* 1025.4774, respectively, at an average CE of 20, 40 and 60 eV allowed for the unambiguously confirmation of both compounds. MTX3-targeted MS/MS spectra showed a series of: 1) water losses and sulfite loss plus water losses (Δppm < 4 ppm), 2) the ion with theoretical *m/z* 803.4212 also common to gambierone, and 3) the ions corresponding to those already reported in LC-MS/MS at *m/z* 233.1553 (Δppm = −1.3 ppm) and *m/z* 109.0645 (Δppm = −2.8 ppm), assigned to the fragmentation of MTX3 I-ring (Figure 3A) (Table 3).

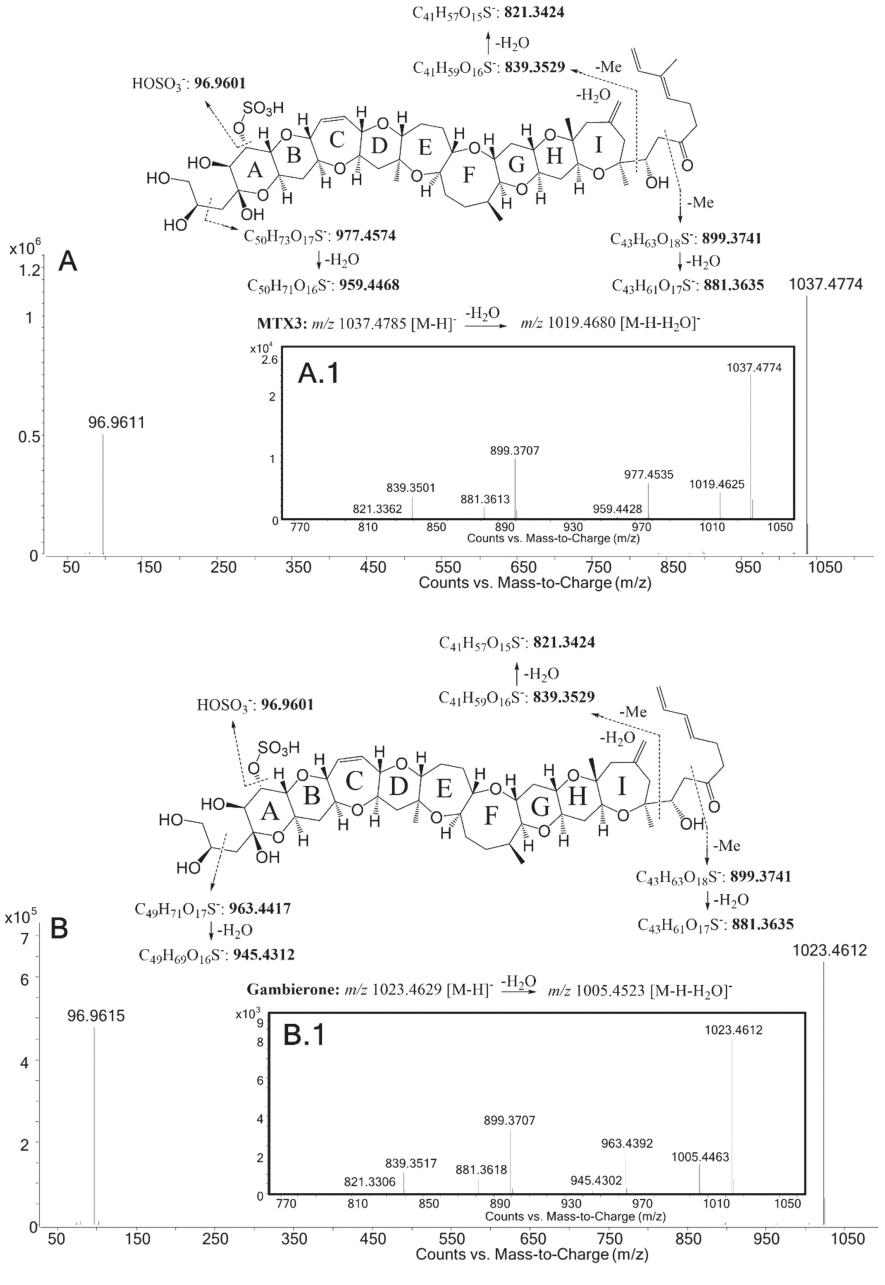

Figure 2. ESI-targeted HRMS/MS spectra of: MTX3 in *G. australes*: (**A**) average CE of 30 eV, 50 and 70 eV; (**A1**) zoom from *m/z* 770 to *m/z* 1050 at 70 eV, gambierone in *Gambierdiscus* sp.2; (**B**) average CE of 30 eV, 50 and 70 eV; (**B1**) zoom from *m/z* 770 to *m/z* 1050 at 70 eV.

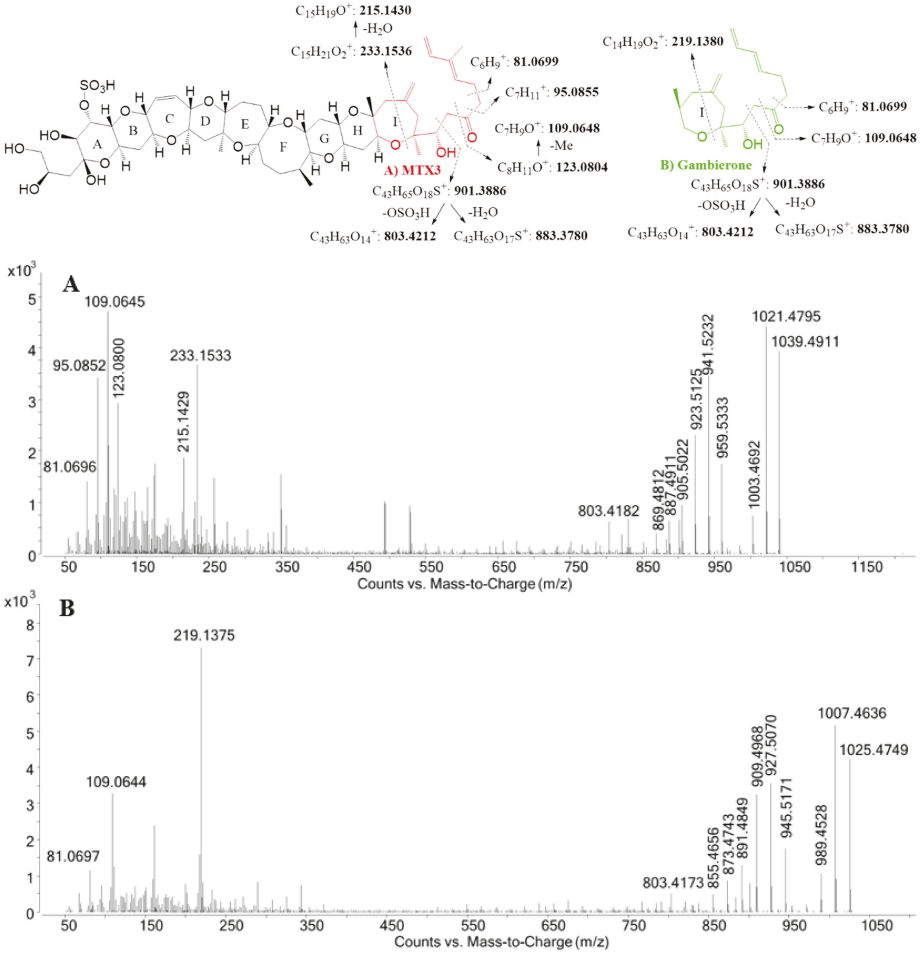

Figure 3. +ESI averaged 20 eV, 40 eV and 60 eV and targeted HRMS/MS spectra of: (**A**) MTX3 in *G. australes*, (**B**) gambierone in *Gambierdiscus.* sp.2.

The same fragmentation pattern was observed for gambierone with the detection of water losses and sulfite loss plus water losses (Δppm < 5 ppm), the ion with *m/z* 803.4173 (Δppm = −4.9 ppm), and the gambierone specific ions *m/z* 219.1375 (Δppm = −2.1 ppm) and *m/z* 109.0644 (Δppm = −3.6 ppm) (Figure 3B) (Table 3).

Due to the lack of the molecular formula of MTX4, its confirmation in the *G. excentricus* from the Canary Islands (Spain) could not be carried out by screening with the database. However, the availability of MTX4 reference material allowed for confirmation of this compound by comparing retention time (7.5 min), as well as further ESI$^-$-targeted MS/MS by selecting the $[M\text{-}2H]^{2-}$ and detection of the two fragment ions $[HOSO_3]^-$ and $[SO_3]^-$ (Figure 4).

The putative gambierone analogue detected by LC-MS/MS was identified by LC-HRMS ESI$^+$ full scan analysis using the algorithm Find-By-Molecular-Feature (FBF) to detect, at a retention time of 6.0 min, a prominent ion with *m/z* 1042.4911 assigned to $[M+NH_4]^+$ as well as $[M+H]^+$ *m/z* 1025.4632, $[M+Na]^+$ *m/z* 1047.4427 and $[M+K]^+$ *m/z* 1063.4108 (Figure S3). The mass differences (Δppm) for these ions were higher than 13, indicating that this compound is probably not a gambierone isomer (Table S3,

Figure S3). It was also observed that under the LC-HRMS conditions the ion pattern of this compound is different to both gambierone and the putative gambierone analogue in low- and high-resolution MS, where the prominent ion is the protonated molecule $[M+H]^+$. ESI^--targeted MS/MS of the $[M-H]^-$ of the putative gambierone revealed a hydrogenated sulfate anion loss typical of MTX-like compounds, whereas no specific or common fragments to gambierone or MTX3 were detected between *m/z* 770 and *m/z* 1010 (Figure S4). Positive ionization mode targeted MS/MS of the $[M+H]^+$ also revealed a similar fragmentation pattern as gambierone and MTX3 with sulfate loss plus water losses, however, large mass differences (Δppm > 20) were observed compared to gambierone and no fragments common to gambierone were detected (Table S4 and Figure S5).

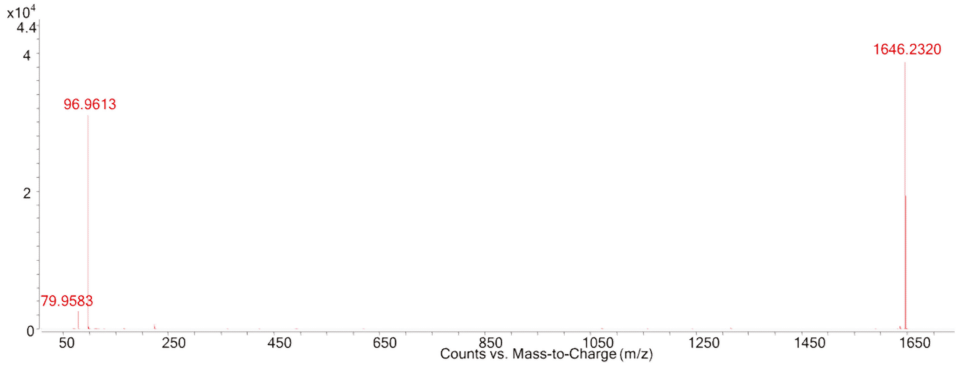

Figure 4. ESI^--targeted HRMS/MS spectra at 110 eV of MTX4 from *G. excentricus* extract.

The screening of raw data with the database of the ESI^- and ESI^+ full scan data also detected a putative gambieroxide at a retention time of 5.3 min in the MSF of all *G. australes* strains (Table S5). Negative ESI full scan mode allowed for detection of the deprotonated molecule $[M-H]^-$ of the putative gambieroxide with Δppm < 3 ppm (Figure S6). Positive ESI full scan acquisition showed a prominent ion at *m/z* 1212.6019 corresponding to $[M+NH_4]^+$ with Δppm = +3.0 ppm, and $[M+Na]^+$ was also detected at *m/z* 1217.5553 but with lower intensity and a Δppm = +1.2 ppm (Figure S7). Negative ESI-targeted MS/MS of $[M-H]^-$ *m/z* 1193.5572 of the putative gambieroxide only revealed a fragment at *m/z* 453.1964 which was not identified in the molecule [18], whereas ESI^+-targeted MS/MS of $[M+NH_4]^+$ *m/z* 1212.5983 showed a prominent fragment at *m/z* 1159.5493 corresponding to $[M+H-2H_2O]^+$ (−1.1 ppm) and followed by six water loss molecules. The lack of authentic gambieroxide MS/MS data or standard limited the confirmation of this compound (Figures S8 and S9).

As above mentioned, the DSF was also analyzed and compared with the corresponding compounds reported in the literature. Two compounds matching gambieric acid C and D were identified in both the ESI^+ and ESI^- MS full scan in *G. australes*. These compounds partially coeluted on the C_{18}-column with retention times of 8.895 min for the compound tentatively identified as gambieric acid C and 8.928 min for the compound tentatively identified as gambieric acid D.

For both putative gambieric acid C and D, the deprotonated molecular cluster $[M-H]^-$ was detected with Δppm < 2.5 ppm in all samples of *G. australes* (Figures 5A1 and 5B1) (See Tables S6 and S7). Positive ESI full scan mode showed at the same retention time three prominent ions corresponding to the molecular ion $[M+H]^+$ and also pseudo-molecular ions $[M+NH_4]^+$, $[M+Na]^+$ with Δppm < 5 ppm in all ions of these samples (Figures 5A and 5B, Tables S6 and S7).

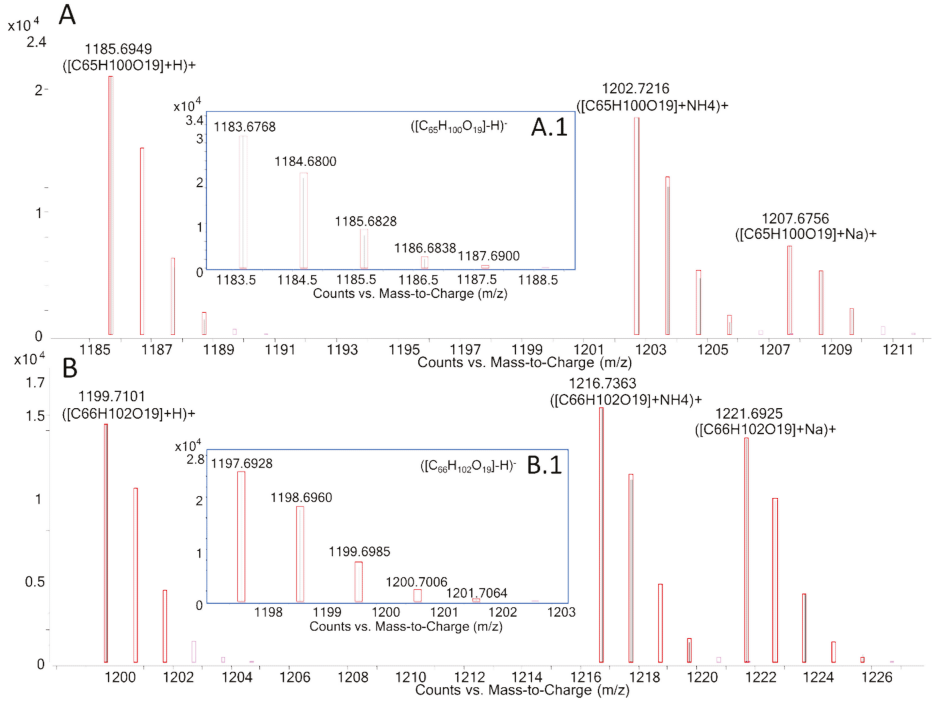

Figure 5. LC-HRMS full scan analysis of putative gambieric acid C, (**A**) ESI^+, (**A1**) ESI^-; putative gambieric acid D, (**B**) ESI^+, (**B1**) ESI^- in *G. australes* extract.

Positive ESI-targeted MS/MS selecting gambieric acid C and D $[M+H]^+$ *m/z* 1185.6932 and *m/z* 1199.7088 respectively, showing a common fragment with *m/z* 135.1174 assigned to the fragmentation of the side chain containing an ester group (Figure 6). Putative gambieric acid C spectra showed two prominent ions *m/z* 1039.6331 (Δppm = −2.0 ppm) and *m/z* 943.5394 (Δppm = −2.0 ppm), both followed by four water losses (Figure 6A). Putative gambieric acid D spectra showed a similar fragmentation pattern with the detection of *m/z* 1053.6477 (Δppm = −3.0 ppm) and *m/z* 957.5542 (Δppm = −2.9 ppm) both followed by water losses, with the most intense being the first water loss of both ions (Figure 6B).

ESI^--targeted MS/MS was also carried out by selecting the deprotonated molecular ions of putative gambieric acid C and D $[M-H]^-$, *m/z* 1183.6786 and *m/z* 1197.6943, respectively. Despite the difficulty in fragmentation of the molecules in this ionization mode and the low abundance of the fragments, both compounds showed a similar fragmentation pattern, detecting a single water loss molecule $[M-H-H_2O]^-$ *m/z* 1165.6633 (Δppm = −4.0 ppm) and *m/z* 1179.6758 (Δppm = −6.7 ppm), respectively, a fragment corresponding to cleavage on the alfa carbonyl group of the ester *m/z* 1055.6275 (Δppm = −3.6 ppm) and *m/z* 1069.6389 (Δppm = −7.5 ppm) and a common fragment with *m/z* 112.9852 (Figure S10).

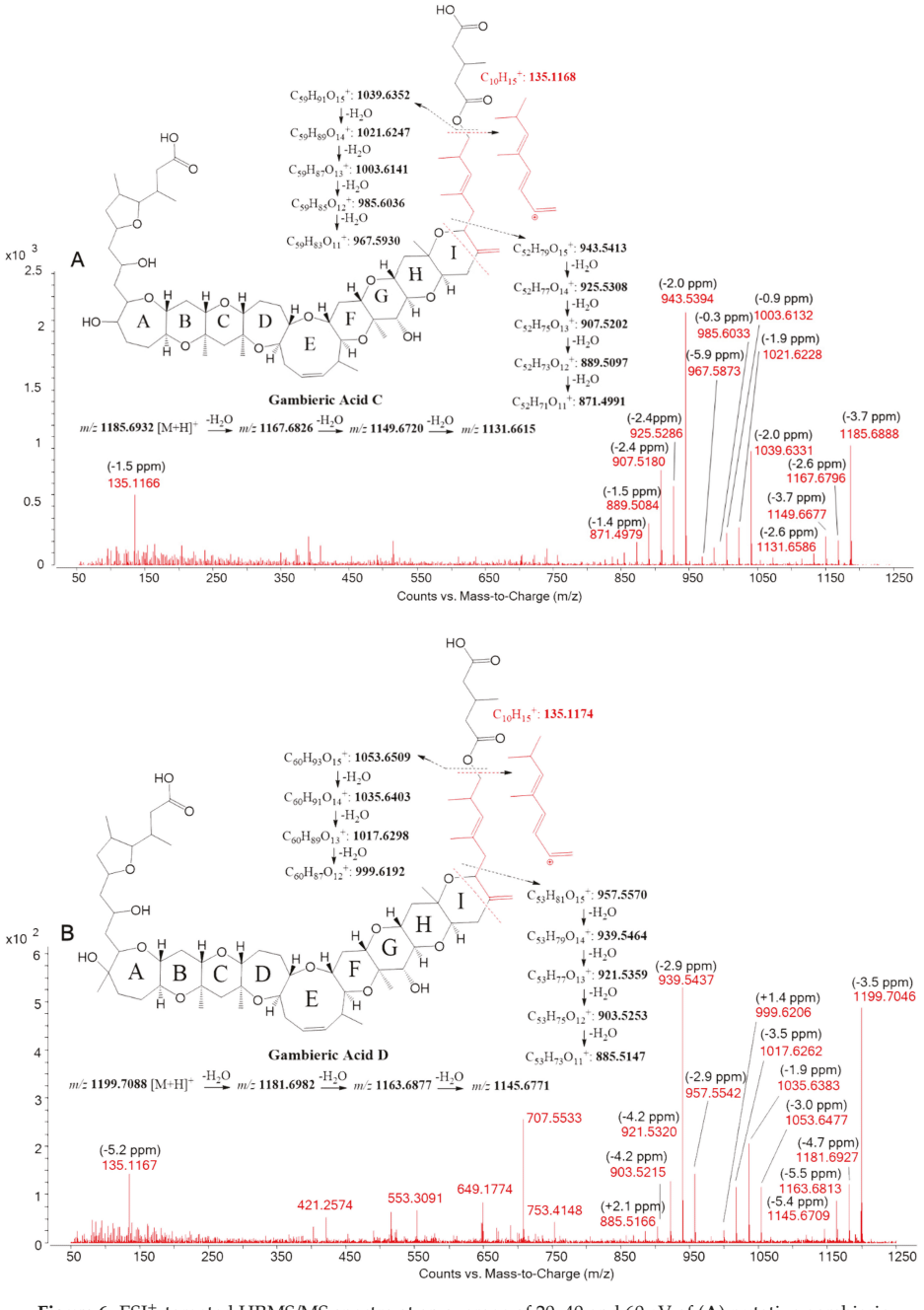

Figure 6. ESI$^+$-targeted HRMS/MS spectra at an average of 20, 40 and 60 eV of (**A**) putative gambieric acid C and (**B**) putative gambieric acid D; both detected in *G. australes*.

3. Discussion

The present study identified and quantified compounds by LC-MS/MS and further confirmed via LC-HRMS the presence of maitotoxins as well as gambierone and other cyclic polyether compounds in dinoflagellates of the genus *Gambierdiscus* and *Fukuyoa* from the Mediterranean Sea and one *G. excentricus* from the Eastern Atlantic (Canary Islands, Spain).

LC-MS/MS negative ionization in MRM mode allowed for the sensitive quantitation of various MTXs. The two mono-sulfated MTXs recently isolated from *Gambierdiscus* of the Caribbean Sea, desulfo-MTX1 and didehydro-demethyl-desulfo-MTX1, were also monitored, assuming that due to their similarities to MTX1 they would have a similar fragmentation pattern monitoring $[M-2H]^{2-}/[M-2H]^{2-}$ as a quantitative transition and $[M-2H]^{2-}/[HOSO_3]^-$ as qualitative transition. Quantitation of the different MTXs and gambierone was carried out using MTX1, the only commercially available maitotoxin. This quantitation may be most adequate for MTX4 which is a compound chemically similar to MTX1, not only in its molecular weight, but also in its fragmentation pattern. MTX3 (=44-methyl-gambierone) and gambierone, which are one-third the molecular weight of MTX1 and MTX4, were also quantified using this approach as they also contain a sulfate group and with results comparable to a commercially available analogue. This approach is traceable but results in somewhat increased uncertainty on any estimated concentration of these compounds.

Among the dinoflagellate species analyzed in this study, *G. australes* appears to be the species that produces the widest variety of hitherto reported *Gambierdiscus* metabolites: MTX3, putative gambieric acids C and D, a putative gambierone analogue and a putative gambieroxide. All *G. australes* strains analyzed were from the same geographical region, Mallorca and Menorca, which are located in the western Mediterranean (Balearic Islands, Spain). The detection of MTX3 in this species is in agreement with the strains of *G. australes* recently isolated from Raoul Island (New Zealand) [14]. No MTX1 was detected in any strain of *G. australes* from Balearic Islands while, in contrast, this compound was detected by LC-MS/MS with MTX3 in strains of the same species from Kochi (Japan) as well as Macaulay Island (New Zealand) [11,28].

The recovery of MTX3 from the DSF was 75% which indicates that the liquid/liquid partition using aqueous MeOH and dichloromethane must be further optimized to quantitatively separate MTX3 from CTXs. This partition behavior also shows that MTX3 has a somewhat lipophilic character which may result in MTX3 being absorbed and accumulated as CTXs in fish and the human digestive system. A recent study showed the accumulation of MTX1 in carnivorous fish tissues (liver and muscles of snappers) after exposure to *G. australes* [29]. While MTX3 clearly has much lower CTX-like activity compared to CTX3C [13], MTX3 was detected in much higher concentrations, estimated up to 1662 pg MTX1-equiv. $cell^{-1}$, suggesting that MTX3 should be monitored in fish muscle in order to explore its possible role in CP.

The absence of MTX1 and the detection of a putative gambierone analogue in all *G. australes* pointed out another possible difference in the toxin profiles of *G. australes* from the Mediterranean Sea and the Pacific Ocean. The use of LC-HRMS showed the ability to conclude that this compound, which initially seemed to be a gambierone isomer by full scan and MRM mode in LC-MS/MS, is not a gambierone isomer due to its high Δppm compared to authentic gambierone. Toxicity of purified fractions containing this compound should be evaluated to check its possible interest for the overall assessment of the toxicity of *G. australes*.

Putative gambieric acids C and D were detected in the DSF of all strains of *G. australes*, but not in any other species. Again, this suggests a strong lipophilic character and the potential to accumulate in fish flesh and potentially pass through the human intestinal barrier. Despite the lack of reference material for gambieric acids C and D to compare retention time, the HRMS ESI^- and ESI^+ full scan and targeted MS/MS analysis showed confident data to conclude that the compounds detected should match these potent antifungal compounds, initially isolated from *G. toxicus* from French Polynesia in 1992 [17,30], i.e., prior to this species being separated into several other species. Gambieric acid D was recently detected in the tissue of a shark involved in a CP in the Indian Ocean, suggesting the stability

of some of these compounds through the food web [4]. The toxicity of gambieric acids C and D and their role in CP is not clear, the only toxicological data is in mouse lymphoma cells L5178Y showing a moderately low toxic effect [17,30].

Despite the detection of a putative gambieroxide in the MSF of all strains of *G. australes* by LC-HRMS, its confirmation is not conclusive due to the lack of authentic gambieroxide to compare retention time as well as fragmentation in targeted MS/MS. Gambieroxide was first isolated from the *G. toxicus* GTP2 strain collected at Papeete in French Polynesia and has a structure similar to yessotoxin [18].

The only *F. paulensis* analyzed in this work was also from Menorca (Balearic Islands, Spain) and showed a low amount of MTX3, 10.5 pg MTX eq./cell, which may explain the poor recovery of 18% from the MSF, reinforcing the inadequacy of this liquid/liquid partition for this particular compound. MTX3 was also detected by LC-MS/MS in *F. paulensis* from Australia and New Zealand [31,32]. In the Western Mediterranean Sea (Formentera, Balearic Islands, Spain), a positive response was observed in the mouse bioassay (MBA) for both MSF and DSF of a *F. paulensis* and the inconclusive detection by LC-HRMS of gambieric acid A and 54-deoxy-CTX1B in trace levels [25].

Gambierdiscus sp.2 from Crete (Greece) showed a profile with low MTX3 concentration (4.2 pg MTX1-eq./cell) and gambierone at much higher concentration (776 pg MTX1-eq./cell). The biological activity of gambierone is similar to CTX3C but of lower potency (similar to MTX3) and since approximately 8% partitioned into the DSF, it should also be monitored in fish tissue from CP cases [15]. The presence of *Gambierdiscus* in Crete Island was first reported in 2003 by [24], while it was not until 2017 that a putative MTX3 was detected by LC-MS/MS in a *G. carolinianus* strain from this region [20].

The availability of a strain of *G. excentricus* from La Gomera (Canary Islands, Spain) allowed for confirmation that MTX4 is the main MTX present in this species as previously reported [11]. The liquid/liquid partitioning step appeared adequate for MTX4 as 99.3% of MTX4 were recovered in the MSF.

4. Conclusions

This study allowed for the characterization of the toxins produced by different species of dinoflagellates from the Mediterranean Sea. LC-MS/MS was used for a first and rapid screening, allowing a quantitative estimation of the toxins involved, while LC-HRMS allowed for their confirmation and characterization. Dinoflagellates from the Mediterranean Sea showed toxin profiles similar to those detected in CP endemic regions. Strains of *G. australes* from Mallorca and Menorca (Spain, Mediterranean Sea) produced MTX3, putative gambieric acid C and D, a putative gambierone analogue and putative gambieroxide, while MTX1 was absent in contrast to the same species from temperate waters of the Pacific Ocean. *F. paulensis* from the same region only produced MTX3, and the strain of *Gambierdiscus* sp.2 from Crete (Greece) produced MTX3 and gambierone. Further research needs to be carried out in order to evaluate the possible presence of CTXs in fish from the Mediterranean Sea, considering that the presence of these dinoflagellates is associated with the production and accumulation of CTXs through the marine food web.

5. Materials and Methods

5.1. Reference Toxins and Chemicals

Maitotoxin-1 (MTX1) standard used for the LC-MS analysis was obtained from Wako Chemicals USA, Inc. (Richmond, VA, USA). MTX1 standard was dissolved in MeOH:H_2O (1:1, v/v) being the stock solution 10 $\mu g \cdot mL^{-1}$. MTX4 qualitative laboratory reference material partially purified from *Gambierdiscus excentricus* was available from a previous study at the Phycotoxins Laboratory [11]. MTX3 and gambierone were identified as both compounds have identical retention times in our chromatography in both *G. australes* and *G. belizeanus*, the two species from which they have been originally isolated. MTX3 and gambierone qualitative laboratory reference material from *G. australes*

and *G. belizeanus* was available at the Phycotoxins Laboratory [11]. HPLC-grade methanol and dichloromethane for extraction were purchased from Sigma Aldrich (Saint Quentin Fallavier, France). Milli-Q water was supplied by a Milli-Q integral 3 system (Millipore, Saint-Quentin-Yvelines, France). Water, acetonitrile, formic acid and ammonium formate used to prepare mobile phases were of LC-MS grade. All these chemicals were purchased from Sigma Aldrich (Saint Quentin Fallavier, France).

In order to carry out the toxicity evaluation by Neuro-2a, CTX1B was provided by Dr. Lewis, University of Queensland and was stored in absolute methanol at −20 °C. Neuroblastoma murine cells were purchased in ATCC LGC standards (USA). Fetal bovine serum (FBS), L-glutamine solution, ouabain, veratridine, phosphate buffered saline (PBS), penicillin, streptomycin, RPMI-1640 medium, sodium pyruvate, thiazolyl blue tetrazolium bromide (MTT) were purchased from Merck KGaA (Darmstadt, Germany). Dimethyl sulfoxide (DMSO) and absolute methanol were purchased from Honeywell (Fürth, Germany) and from Chemlab (Zedelgem, Belgium), respectively. The incubator was purchased from Binder, Germany. The microplate reader KC4 was purchased from BIO-TEK Instruments, Inc.

5.2. Gambierdiscus and Fukuyoa Strains

All nine dinoflagellate extracts analyzed in this work were obtained from the collection of strains obtained in the EuroCigua project. All strains were cultivated at the IRTA laboratory (Tarragona, Spain) and the detailed information about these strains is shown in Table 4.

Table 4. Detailed information about the dinoflagellate extracts analyzed with the neuroblastoma cell-based assay.

Species	Strain Code	Location	Number of Cells Extracted	Volume of Culture (L)	CTX-like (fg CTX1B Equiv./Cell)
G. australes	IRTA-SMM-17-189	Torret, Menorca, Balearic Islands, Spain	17 134 000	20	83 ± 12 [a]
G. australes	IRTA-SMM-17-162	St. Adeodat, Menorca, Balearic Islands, Spain	27 811 000	20	101 ± 7.5
G. australes	IRTA-SMM-17-164	St. Adeodat, Menorca, Balearic Islands, Spain	4 257 000	20	>62.5 (NQ)
G. australes	IRTA-SMM-17-271	Macarella, Menorca, Balearic Islands, Spain	14 007 000	20	271 ± 29
F. paulensis	IRTA-SMM-17-209	Sacaleta, Menorca, Balearic Islands, Spain	6 964 000	20	16 ± 1.7 [a]
G. australes	IRTA-SMM-17-253	Anguila, Menorca, Balearic Islands, Spain	13 735 000	20	164 ± 16
G. australes	IRTA-SMM-17-244	Camp de Mar, Mallorca, Balearic Islands, Spain	4 121 000	5	155 ± 25
Gambierdiscus sp.2	0010G-CR-CCAUTH	Kolimpari, Crete, Greece	2 300 000	5	NQ
G. excentricus	IRTA-SMM-17-407	Playa de vueltas, La Gomera, Canary Islands, Spain	6 084 000	5	>794 (NQ)

NQ: not quantifiable; [a] CTX-like toxicity evaluated in [33].

Culturing, Harvesting, Toxin Extraction of Gambierdiscus and Fukuyoa, and N2a Assay

All strains were inoculated in 5 L of medium ES (Provasoli 1968, modified by Jorge Diogène) and salinity was adjusted to 36 in 8 L flat-bottom, round glass-flasks. Cultures were maintained in filtered air, and light turbulence (gentle bubbling) was supplied by an air-pump system. The initial concentration of dinoflagellates was between 25 and 50 cells/mL. Strains were incubated at 24 ± 0.5 °C. The illumination was provided by fluorescent tubes with photon irradiance of 100 µmol m^{-2} s^{-1} under a 12:12 h L:D photoperiod. When cultures arrived at the late-exponential phase (after 20 ± 3 days),

cultures were vigorously shaken and 15 mL aliquots were taken and fixed with Lugol's iodine solution (3%) to estimate the cell concentration (cell/mL). Subsequently, the remaining volume of each strain was filtered and collected through a 10 μm plankton net (Holmbladsvej, Denmark) in sterile 50 mL Falcon tubes and centrifuged at 4300 *g* for 20 min (Allegra X-15R, Beckman Coulter). Supernatants were discarded and micro-algal pellets of each strain were pooled in one 50 mL Falcon tube. Centrifugation was repeated and supernatants were discarded. Pellets were subsequently kept at –20 °C with absolute methanol (10 mL for 10^6 cells) until toxin extraction. To extract the toxin from micro-algal pellets, each pellet in methanol was sonicated using an ultrasonic cell disrupter (Watt ultrasonic processor VCX750, USA). The tip amplitude was set at 37% 3 sec on/3 sec off for 15 min. The sample was then centrifuged at 600 g for 5 min at 4 °C. Supernatant was then transferred to a glass vial. The procedure was repeated twice, one with methanol and another with aqueous methanol (50:50; v:v) (10 mL for 10^6cells) and these were pooled. After that, the pool was evaporated to dryness with a rotary evaporator (Büchi Syncore, Switzerland) or dried under N_2 gas (Turbovap, Caliper, Hopkinton, USA) at 40 °C and re-suspended in pure methanol. These extracts were filtered with PTFE filters (0.2 μm) and stored at −20 °C.

The Neuro-2a assay was performed according to Reverté et al., (2018) [23].

5.3. Sample Pretreatment

The methanol extract from the cell pellet extraction was evaporated to dryness under N_2 stream at 50 °C and CTX- and MTX-like compounds were partitioned as previously described [11]. Briefly, the residue from extraction was reconstituted in dichloromethane (50 mL/1 million cells) and partitioned twice with MeOH:H_2O (3:2, v/v) (25 mL/1 million cells). Both organic and aqueous layers were evaporated to dryness under N_2 stream at 50 °C and kept at −20 °C prior to the analysis. MTX-like compounds were supposed to partition into the MeOH:H_2O (3:2, v/v), whereas CTX-like compounds were supposed to partition into the dichloromethane layer. Dried residue from the aqueous methanol fraction was reconstituted in 0.5 mL of MeOH:H_2O (1:1, v/v), whereas the solid residue from the dichloromethane layer was reconstituted in 0.5 mL MeOH, with both being filtrated through 0.22 μm prior to the LC-MS analysis.

5.4. LC-MS Analysis

5.4.1. LC-MS/MS (API 4000 QTrap)

LC-MS/MS analysis to monitor specific MTX congeners and gambierone was performed using an LC system (UFLC XR Nexera, Shimadzu, Japan) coupled to a hybrid triple quadrupole/ion-trap mass spectrometer API 4000 QTrap (SCIEX, Redwood City, CA, USA) equipped with a turboV® ESI source. Maitotoxins and gambierone were separated using a reversed-phase C18 Kinetex column (100 Å, 2.6 μm, 50 × 2.1 mm, Phenomenex, Le Pecq, France) with water (A) and 95% acetonitrile/water (B), both containing 2 mM of ammonium formate and 50 mM of formic acid. The column oven and the sample tray temperatures were set at 40 °C and 4 °C, respectively. The flow rate was set at 0.4 mL min^{-1} and the injection volume was set to 5 μL. Separation was achieved using the following mobile phase gradient: from 10% to 95% B in 10 min, keep at 95% B for 2 min, return to 10% B in 0.1 min and equilibration for 3.9 min prior the next injection. The instrument control, data processing and analysis were conducted using Analyst software 1.6.3 (Sciex, Redwood city, CA, USA). LC-MS/MS analyses were carried out in negative ion acquisition mode, monitoring the transitions shown in Table S5 in Multiple Reaction Monitoring (MRM) mode with a dwell time of 80 ms Retention time of the different compounds with reference material available are shown in Table S8. Source conditions were curtain gas 25 psi, ionspray −4.5 kV, turbogas temperature of 500 °C, gas 1 and 2 set at 50 psi, and an entrance and declustering potential of −10 V and −210 V, respectively. Positive ion acquisition mode was also used in the analysis of MTX3 and gambierone. Source conditions were curtain gas 25 psi, ionspray

4.5 kV, turbogas temperature of 500 °C, gas 1 and 2 set at 50 psi, and an entrance and declustering potential of 10 V and 100 V, respectively.

The fragment ion monitored in negative ionization mode for all the MRM transition of the MTX-group of toxins was the hydrogenated sulfate anion *m/z* 96.9 $[HOSO_3]^-$ which was used as the confirmatory transition. Quantification of MTX1, MTX4, desulfo-MTX1 and didehydro-demethyl-desulfo-MTX1 was conducted using the MRM transition $[M-2H]^{2-}/[M-2H]^{2-}$ for MTX3 and gambierone $[M-H]^-/[M-H]^-$ (Table S8). Due to the lack of the appropriate standards for the quantitation of each compound, MTX3, MTX4 and gambierone were quantified against the MTX1 calibration curve, assuming equal molar response and applying the same LOD and LOQ calculated for MTX1.

The MTX1 standard calibration range for the LC-MS/MS analysis consisted of seven concentrations ranging from 0.2 to 10 μg mL^{-1} in MeOH:H_2O (1:1, v/v). Limit of detection (LOD) and quantification (LOQ) were determined with the ordinary least-squares regression data method [34,35]. The LOD was calculated as three times the standard deviation of the y-intercepts over the slope of the calibration curve; the LOQ was calculated as 10 times the standard deviation of the y-intercepts over the slope of the calibration curve [34,35]. Therefore, LOD and LOQ for the MTX1 MRM transition $[M-2H]^{2-}/[M-2H]^{2-}$ were 0.32 and 0.97 μg mL^{-1}, respectively.

5.4.2. LC-HRMS and HRMS/MS (Q-Tof 6550 iFunnel)

LC-HRMS analyses were carried out using a UHPLC system 1290 Infinity II (Agilent Technologies, Santa Clara, CA, USA) coupled to a HRMS time of flight mass spectrometer Q-Tof 6550 iFunnel (Agilent Technologies, Santa Clara, CA, USA). Chromatographic separation was performed using a Kinetex C18 column (100 Å, 1.7 μm, 100 × 2.1 mm, Phenomenex, Le Pecq, France) at 40 °C with water (A) and 95% acetonitrile (B) both containing 2 mM ammonium formate and 50 mM formic acid. The flow rate was 0.4 mL min^{-1} and the injection volume was 5 μL. Gradient of mobile phase was carried out as follows: 5% B was kept for 1 min, then increased to 100% B over 11 min, kept at 100% B for 2 min and returned to the initial conditions in 0.5 min and then equilibrated the column for 4.5 min prior to the next injection.

Source conditions were set as follows: gas temperature, 160 °C; gas flow, 11 L/min; nebulizer, 45 psi; sheath gas temperature, 250 °C; sheath gas flow, 11 L/min; capillary voltage, 4500 V and nozzle voltage, 500 V. The instrument was calibrated, using the Agilent tuning mix, in negative and positive ionization mode before each analysis.

LC-HRMS analyses were carried out in full scan and targeted MS/MS mode in positive and negative ionization mode in separate runs. Full scan analysis operated at a mass resolution of 40,000 Full width at Half Maximum (FWHM) over a mass-to-charge ratio (*m/z*) ranging from 100 to 3200 with a scan rate of 1 spectra/s. Targeted MS/MS was performed in a Collision Induced Dissociation (CID) cell at 45,000 FWHM over the scan rage from m/z 50 to 1700 with a scan rate of 10 spectra/s and a scan rate of 3 spectra/s applying three different collision energies in order to have a good fragmentation pathway. Two reference masses *m/z* 121.0509 (purine) and *m/z* 922.0099 (hexakisphosphazine) were continuously monitored during the entire run. Data acquisition was controlled by MassHunter software (Agilent technologies, CA, USA). Raw data were processed with Agilent MassHunter Qualitative Analysis software (version B.07.00, service pack 1) using the Find by Formula (FbF) algorithm screening with a Personal Compound Database and Library (PDCL) created by Phycotoxins laboratory (IFREMER, France).

Supplementary Materials: The following are available online at http://www.mdpi.com/2072-6651/12/5/305/s1, Figure S1. LC-MS/MS Full scan analysis of: A) MTX3 from *G. australes*; B) gambierone from *Gambierdiscus sp;* C) putative gambierone analogue from *G. australes*, Figure S2. LC-MS/MS spectra resulting from enhanced product ion scan at an average CE of 20, 40 and 60 eV of: A) MTX3 from *G. australes*; B) gambierone from *Gambierdiscus sp;* C) putative gambierone analogue from *G. australes,* Table S1. Accurate mass measurements using LC-HRMS full scan analysis in ESI^- and ESI^+ mode for MTX3, Table S2. Accurate mass measurements using LC-HRMS full scan analysis in ESI^- and ESI^+ mode for gambierone, Figure S3. Putative gambierone analogue detected in LC-HRMS

using the Find by Molecular Feature (FMF) algorithm in *G. australes* at 6.08 min, Table S3. *m/z* measured values for the putative gambierone analogue and Δ ppm calculated in base of gambierone theoretical values, Figure S4. ESI^--targeted MS/MS analysis of the putative gambierone analogue selecting $[M-H]^-$ ion in *G. australes* at 6.08 min. *m/z* measured values for the putative gambierone analogue and Δ ppm calculated in base of gambierone theoretical values, Figure S5. ESI^+-targeted MS/MS analysis of the putative gambierone analogue selecting $[M+H]^+$ ion in *G. australes* at 6.08 min, Table S4. Accurate mass measurements for the putative gambierone analogue and Δ ppm calculated in base of gambierone theoretical values, Table S5. Accurate mass measurements using LC-HRMS full scan analysis in ESI^- and ESI^+ mode for putative gambieroxide, Figure S6. ESI^- LC-HRMS full scan analysis of putative gambieroxide detected in *G. australes* at 5.32 min, Figure S7. ESI^+ LC-HRMS full scan analysis of putative gambieroxide detected in *G. australes* at 5.32 min, Figure S8. ESI^--targeted HRMS/MS spectrum of putative gambieroxide selecting $[M-H]^-$ ion in *G. australes* at a collision energy of 50 eV, Figure S9. ESI^+-targeted HRMS/MS spectrum of putative gambieroxide selecting $[M+H]^+$ ion in *G. australes* at a collision energy of 20 eV, Table S6. Accurate mass measurements using LC-HRMS full scan analysis in ESI^- and ESI^+ mode for putative gambieric acid C, Table S7. Accurate mass measurements using LC-HRMS full scan analysis in ESI^- and ESI^+ mode for putative gambieric acid D, Figure S10. ESI^--targeted MS/MS spectra at an average of 20, 40 and 60 eV of: A) gambieric acid C; B) gambieric acid D detected in *G. australes*, Table S8. MRM transitions monitored using the LC-MS API 4000 QTrap.

Author Contributions: Conceptualization, P.E., M.S., A.G.-M., J.D. and P.H.; methodology, P.E., M.S., A.T., M.R.-A.; investigation, P.E., A.T., M.R.-A., K.A. and M.S.; resources, A.G.-M., J.D. and P.H.; data curation, P.E., M.S.; writing—original draft preparation, P.E., MS. and P.H.; writing—review and editing, A.G.-M., J.M.L.-M., M.R.-A., J.D. and P.H.; supervision, J.M.L.-M., A.G.-M. and P.H.; project administration, A.G.-M. and P.H.; funding acquisition, A.G.-M., J.D. and P.H. All authors have read and agreed to the published version of the manuscript.

Funding: The authors acknowledge the financial support from the European Food Safety Authority (EFSA) through the EUROCIGUA project (GP/EFSA/AFSCO/2015/03). Pablo Estevez (P.E.) acknowledges the PhD fellowship from the Xunta de Galicia (Regional Government, Spain) under grant ED481A-2018/207. The authors also acknowledge support from CERCA Programme / Generalitat de Catalunya and A. Tudó acknowledges IRTA-URV-Santander for her Phd grant (2016 PMF-PIPF-74).

Acknowledgments: Authors acknowledge the support received form technical staff in the different institutions; special thanks also to Maria Rey for her contribution to the micrograph of *G. australes.*

Conflicts of Interest: The authors declare no conflict of interest. The funders had no role in the design of the study; in the collection, analyses, or interpretation of data; in the writing of the manuscript, or in the decision to publish the results.

References

1. Yasumoto, T. The chemistry and biological function of natural marine toxins. *Chem. Rec.* **2001**, *1*, 228–242. [CrossRef] [PubMed]
2. Yasumoto, T.; Murata, M. Marine toxins. *Chem. Rev.* **1993**, *93*, 1897–1909. [CrossRef]
3. Oshiro, N.; Yogi, K.; Asato, S.; Sasaki, T.; Tamanaha, K.; Hirama, M.; Yasumoto, T.; Inafuku, Y. Ciguatera incidence and fish toxicity in Okinawa, Japan. *Toxicon* **2010**, *56*, 656–661. [CrossRef] [PubMed]
4. Diogène, J.; Reverté, L.; Rambla-Alegre, M.; Del Río, V.; De La Iglesia, P.; Campàs, M.; Palacios, O.; Flores, C.; Caixach, J.; Ralijaona, C.; et al. Identification of ciguatoxins in a shark involved in a fatal food poisoning in the Indian Ocean. *Sci. Rep.* **2017**, *7*, 8240. [CrossRef] [PubMed]
5. Estevez, P.; Castro, D.; Valtierra, A.P.; Leão-Martins, J.M.; Vilariño, O.; Diogène, J.; Gago-Martínez, A. An Attempt to Characterize the Ciguatoxin Profile in Seriola fasciata Causing Ciguatera Fish Poisoning in Macaronesia. *Toxins* **2019**, *11*, 221. [CrossRef]
6. Murray, J.S.; Boundy, M.J.; Selwood, A.I.; Harwood, T. Development of an LC–MS/MS method to simultaneously monitor maitotoxins and selected ciguatoxins in algal cultures and P-CTX-1B in fish. *Harmful Algae* **2018**, *80*, 80–87. [CrossRef]
7. Abraham, A.; Jester, E.L.; Granade, H.R.; Plakas, S.M.; Dickey, R.W. Caribbean ciguatoxin profile in raw and cooked fish implicated in ciguatera. *Food Chem.* **2012**, *131*, 192–198. [CrossRef]
8. Murata, M.; Naoki, H.; Matsunaga, S.; Satake, M.; Yasumoto, T. Structure and Partial Stereochemical Assignments for Maitotoxin, the Most Toxic and Largest Natural Non-Biopolymer. *J. Am. Chem. Soc.* **1994**, *116*, 7098–7107. [CrossRef]
9. Murata, M.; Yasumoto, T. The structure elucidation and biological activities of high molecular weight algal toxins: Maitotoxin, prymnesins and zooxanthellatoxins. *Nat. Prod. Rep.* **2000**, *17*, 293–314. [CrossRef]
10. Holmes, M.J.; Lewis, R.J. Purification and characterisation of large and small maitotoxins from cultured *Gambierdiscus toxicus*. *Nat. Toxins* **1994**, *2*, 64–72. [CrossRef]

11. Pisapia, F.; Sibat, M.; Herrenknecht, C.; Lhaute, K.; Gaiani, G.; Ferron, P.-J.; Fessard, V.; Fraga, S.; Nascimento, S.M.; Litaker, R.W.; et al. Maitotoxin-4, a Novel MTX Analog Produced by *Gambierdiscus excentricus*. *Mar. Drugs* **2017**, *15*, 220. [CrossRef] [PubMed]
12. Mazzola, E.P.; Deeds, J.R.; Stutts, W.L.; Ridge, C.D.; Dickey, R.W.; White, K.D.; Williamson, R.T.; Martin, G.E. Elucidation and partial NMR assignment of monosulfated maitotoxins from the Caribbean. *Toxicon* **2019**, *164*, 44–50. [CrossRef] [PubMed]
13. Boente-Juncal, A.; Álvarez, M.; Antelo, Á.; Rodríguez, I.; Calabro, K.; Vale, C.; Thomas, O.P.; Botana, L.M. Structure Elucidation and Biological Evaluation of Maitotoxin-3, a Homologue of Gambierone, from *Gambierdiscus belizeanus*. *Toxins* **2019**, *11*, 79. [CrossRef] [PubMed]
14. Murray, J.S.; Selwood, A.; Harwood, D.T.; Van Ginkel, R.; Puddick, J.; Rhodes, L.L.; Rise, F.; Wilkins, A.L. 44-Methylgambierone, a new gambierone analogue isolated from *Gambierdiscus australes*. *Tetrahedron Lett.* **2019**, *60*, 621–625. [CrossRef]
15. Rodríguez, I.; Genta-Jouve, G.; Alfonso, C.; Calabro, K.; Alonso, E.; Sánchez, J.A.; Alfonso, A.; Thomas, O.P.; Botana, L.M. Gambierone, a Ladder-Shaped Polyether from the Dinoflagellate *Gambierdiscus belizeanus*. *Org. Lett.* **2015**, *17*, 2392–2395. [CrossRef]
16. Satake, M.; Murata, M.; Yasumoto, T. Gambierol: A new toxic polyether compound isolated from the marine dinoflagellate *Gambierdiscus toxicus*. *J. Am. Chem. Soc.* **1993**, *115*, 361–362. [CrossRef]
17. Nagai, H.; Torigoe, K.; Satake, M.; Murata, M.; Yasumoto, T.; Hirota, H. Gambieric acids: Unprecedented potent antifungal substances isolated from cultures of a marine dinoflagellate *Gambierdiscus toxicus*. *J. Am. Chem. Soc.* **1992**, *114*, 1102–1103. [CrossRef]
18. Watanabe, R.; Uchida, H.; Suzuki, T.; Matsushima, R.; Nagae, M.; Toyohara, Y.; Satake, M.; Oshima, Y.; Inoue, A.; Yasumoto, T. Gambieroxide, a novel epoxy polyether compound from the dinoflagellate *Gambierdiscus toxicus* GTP2 strain. *Tetrahedron* **2013**, *69*, 10299–10303. [CrossRef]
19. Litaker, R.W.; Vandersea, M.; Faust, M.A.; Kibler, S.; Nau, A.W.; Holland, W.C.; Chinain, M.; Holmes, M.J.; Tester, P.A. Global distribution of ciguatera causing dinoflagellates in the genus *Gambierdiscus*. *Toxicon* **2010**, *56*, 711–730. [CrossRef]
20. Pisapia, F.; Holland, W.C.; Hardison, D.R.; Litaker, R.W.; Fraga, S.; Nishimura, T.; Adachi, M.; Nguyen-Ngoc, L.; Séchet, V.; Amzil, Z.; et al. Toxicity screening of 13 *Gambierdiscus* strains using neuro-2a and erythrocyte lysis bioassays. *Harmful Algae* **2017**, *63*, 173–183. [CrossRef]
21. Fraga, S.; Rodríguez, F. Genus *Gambierdiscus* in the Canary Islands (NE Atlantic Ocean) with Description of *Gambierdiscus silvae* sp. nov., a New Potentially Toxic Epiphytic Benthic Dinoflagellate. *Protist* **2014**, *165*, 839–853. [CrossRef] [PubMed]
22. Rodríguez, F.; Fraga, S.; Ramilo, I.; Rial, P.; Figueroa, R.I.; Riobó, P.; Bravo, I. Canary Islands (NE Atlantic) as a biodiversity 'hotspot' of *Gambierdiscus*: Implications for future trends of ciguatera in the area. *Harmful Algae* **2017**, *67*, 131–143. [CrossRef] [PubMed]
23. Reverté, L.; Toldrà, A.; Andree, K.B.; Fraga, S.; De Falco, G.; Campàs, M.; Diogène, J. Assessment of cytotoxicity in ten strains of *Gambierdiscus* australes from Macaronesian Islands by neuro-2a cell-based assays. *Environ. Boil. Fishes* **2018**, *30*, 2447–2461. [CrossRef]
24. Aligizaki, K.; Nikolaidis, G. Morphological identification of two tropical dinoflagellates of the genera *Gambierdiscus* and *Sinophysis* in the Mediterranean Sea. *J. Biol. Res. Thessaloniki* **2008**, *9*, 75–82.
25. Laza-Martínez, A.; David, H.; Riobó, P.; Miguel, I.; Orive, E. Characterization of a Strain of *Fukuyoa paulensis* (Dinophyceae) from the Western Mediterranean Sea. *J. Eukaryot. Microbiol.* **2016**, *63*, 481–497. [CrossRef]
26. AECOSAN Website. Available online: http://www.aecosan.msssi.gob.es/AECOSAN/web/ciguatera/home/aecosan_home_ciguatera.htm (accessed on 25 March 2020).
27. Lewis, R.J.; Holmes, M.J.; Alewood, P.F.; Jones, A. Lonspray mass spectrometry of ciguatoxin-1, maitotoxin-2 and -3, and related marine polyether toxins. *Nat. Toxins* **1994**, *2*, 56–63. [CrossRef]
28. Rhodes, L.L.; Smith, K.F.; Murray, J.S.; Harwood, T.; Trnski, T.; Munday, R. The Epiphytic Genus *Gambierdiscus* (Dinophyceae) in the Kermadec Islands and Zealandia Regions of the Southwestern Pacific and the Associated Risk of Ciguatera Fish Poisoning. *Mar. Drugs* **2017**, *15*, 219. [CrossRef]
29. Kohli, G.S.; Papiol, G.G.; Rhodes, L.L.; Harwood, T.; Selwood, A.; Jerrett, A.R.; Murray, S.A.; Neilan, B.A. A feeding study to probe the uptake of Maitotoxin by snapper (*Pagrus auratus*). *Harmful Algae* **2014**, *37*, 125–132. [CrossRef]

30. Nagai, H.; Murata, M.; Torigoe, K.; Satake, M.; Yasumoto, T. Gambieric acids, new potent antifungal substances with unprecedented polyether structures from a marine dinoflagellate *Gambierdiscus toxicus*. *J. Org. Chem.* **1992**, *57*, 5448–5453. [CrossRef]
31. Munday, R.; Murray, J.S.; Rhodes, L.L.; Larsson, M.E.; Harwood, T. Ciguatoxins and Maitotoxins in Extracts of Sixteen *Gambierdiscus* Isolates and One *Fukuyoa* Isolate from the South Pacific and Their Toxicity to Mice by Intraperitoneal and Oral Administration. *Mar. Drugs* **2017**, *15*, 208. [CrossRef]
32. Larsson, M.E.; Harwood, T.D.; Lewis, R.J.; Himaya, S.W.A.; Doblin, M.A. Toxicological characterization of *Fukuyoa* paulensis (Dinophyceae) from temperate Australia. *Phycol. Res.* **2018**, *67*, 65–71. [CrossRef]
33. Tudó, À.; Toldrà, A.; Rey, M.; Todolí, I.; Andree, K.B.; Fernández-Tejedor, M.; Campàs, M.; Sureda, F.X.; Diogène, J. *Gambierdiscus* and *Fukuyoa* as potential indicators of ciguatera risk in the Balearic Islands. *Harmful Algae* **2020**, submitted.
34. Vial, J.; Jardy, A. Experimental Comparison of the Different Approaches To Estimate LOD and LOQ of an HPLC Method. *Anal. Chem.* **1999**, *71*, 2672–2677. [CrossRef]
35. Sanagi, M.M.; Ling, S.L.; Nasir, Z.; Hermawan, D.; Ibrahim, W.A.W.; Abu Naim, A. Comparison of Signal-to-Noise, Blank Determination, and Linear Regression Methods for the Estimation of Detection and Quantification Limits for Volatile Organic Compounds by Gas Chromatography. *J. AOAC Int.* **2009**, *92*, 1833–1838. [CrossRef] [PubMed]

toxins

MDPI

Article

Evaluation of Matrix Issues in the Applicability of the Neuro-2a Cell Based Assay on the Detection of CTX in Fish Samples

David Castro [1], Ronald Manger [2], Oscar Vilariño [1] and Ana Gago-Martínez [1,*]

[1] Biomedical Research Center (CINBIO), Department of Analytical and Food Chemistry, University of Vigo, Campus Universitario de Vigo, 36310 Vigo, Spain; dcastro@uvigo.es (D.C.); ovilarino@uvigo.es (O.V.)
[2] Fred Hutchinson Cancer Research Center (retired), Seattle, WA 98109, USA; rlmanger@yahoo.com
* Correspondence: anagago@uvigo.es; Tel.: +34-647-343-417

Received: 27 March 2020; Accepted: 7 May 2020; Published: 9 May 2020

Abstract: Ciguatoxins (CTXs) are a group of neurotoxins responsible for the syndrome ciguatera fish poisoning (CFP) as a result of the consumption of contaminated fish. The presence of these toxins has been detected around the Pacific, Caribbean and Indian coasts. Recent reports indicate the emergence of CFP in other geographic areas, in particular in European coasts, of the Canary Islands (Spain) and Madeira (Portugal). A neuroblastoma cell line of murine origin (N2a) has been applied to assay different groups of neurotoxins, acting on voltage-gated sodium channel (VGSC) of excitable cells, N2a-MTT. The great potential of N2a-MTT as a sensitive tool for the CTXs screening is clearly recognized, notably because it allows the detection of these toxins at levels below recommended as security levels. However, the complexity of the matrix is a critical point on the application of N2a-MTT, which needs to be evaluated. The aim of this work is to provide recommendations for an implemented N2a-MTT method for CTXs determination in fish that avoids matrix effects, particularly those related to high lipid content.

Keywords: ciguatoxins; neuroblastoma cell assay; matrix effect

Key Contribution: The methodology developed in this work facilitates the analysis of fish samples contaminated with CTXs trough the study of the MTDE required to avoid non-specific toxic effects allowing the increase of both sensitivity and reliability of N2a-MTT assay.

1. Introduction

Ciguatera poisoning (CP) is a non-bacterial food intoxication endemic in tropical and subtropical regions of the world and caused by the consumption of fish contaminated with ciguatoxins (CTXs) [1,2]. CTXs are ladder-like cyclic polyethers, lipophilic and are stable to pH and temperature; which are produced by fish metabolization of its algal precursors [3,4]. There is uncertainty about their algal precursors but different benthic dinoflagellates such as *Gambierdiscus* spp. [5–7] or *Fukuyoa* spp. [8] were identified as producers of CTX-like compounds [9,10]. CTXs are classified depending on the geographical region they appear as Pacific, Indian and Caribbean Ciguatoxins (P-CTXs, I-CTXs and C-CTXs) [11]. P-CTXs are widely distributed in the Pacific and some regions of the Indian Ocean, I-CTXs are not yet elucidated and seem to be present in the Indian Ocean and C-CTXs are detected in fish from the Caribbean Sea and have recently emerged in Macaronesia (Northeast Atlantic), specifically in the Canary Islands (Spain) and Madeira (Portugal) [12–14].

The US Food and Drug Administration (FDA) established a guidance level of 0.01 ng/g fish tissue for the most potent congener CTX1B and 0.1 ng/g for C-CTX1 [15]. On the other hand, there are no regulatory limits in Europe, where the European Food Safety Authority (EFSA) published a scientific

opinion about CTXs, where they highlighted the importance of developing analytical methods for CTXs evaluation, recommending in vitro assays for screening and liquid chromatography coupled with tandem mass spectrometry (LC–MS/MS) for confirmation [16].

Different strategies for in vitro assays have been developed for the monitoring purpose of CTXs, including pharmacological (i.e., receptor binding assay) [17–19], cytotoxicity [20–25], immunochemical approaches (ELISA) [26–28] or reporter gene assays [29,30]. The in vitro assay most widely applied in the CTXs screening is a cytotoxicity cell based assay using a neuroblastoma cell line of murine origin (N2a) and measuring the mitochondrial activity of viable cells by MTT colorimetric assay (N2a-MTT). N2a-MTT was originally developed by Manger et al. [21,22] and it is based on the CTXs mechanism of action in the voltage-gated sodium channels (VGSC) of excitable cells [17,18,31,32]. The specificity towards the effects of certain VGSC toxins, such as CTXs, is achieved by the pretreatment of cells with veratridine (V) and ouabain (O), cells untreated with both compounds are not sensitive to these types of specific toxins. Additionally, despite not being specific for CTXs alone, this procedure allows to distinguish between sodium channel-enhancing toxins, also called CTX-like compounds such as ciguatoxins and brevetoxins (PbTxs) and blocking toxins such as saxitoxin (STXs) and tetrodotoxin (TTXs) [33,34]. The main advantage compared to the traditional mouse bioassay (MBA), apart from animal welfare issues, is its higher sensitivity and ability to meet the US FDA guidance level.

Its importance is also found in the capacity of qualitatively and semi quantitatively estimating the total presence of CTX-like compounds in contaminated samples. Due to the lack of commercially available standards and reference materials its combination with sample fractionation and LC–MS/MS it is a useful approach in the identification of CTXs analogues.

Although N2a-MTT is a very sensitive tool to monitor CTX-like compounds its main disadvantage is that the specificity can be influenced by possible matrix effects contributing to non-specific toxic effects, interfering with CTXs detection and reducing the reliability of the assay. Therefore, since the exposure to excessive amount of matrix compounds (i.e., lipids) may be toxic to N2a cells, it is necessary to establish a maximum tissue dose equivalent (MTDE) [35]. However, the MTDE can potentially vary according to different characteristics such as fish species, origin and season of capture. N2a-MTT has been used for the discrimination of CTXs in a wide variety of biological matrices (i.e., dinoflagellates and blood, mussels) [35–38]. However, a few studies have documented the relationship between non-specific toxic effects in N2a and fish lipid content. The study by Caillaud et al. (2012) [35] is the first report that provided information about the maximal concentration of fish tissue equivalent that did not induce non-specific toxic effects in the analysis of species of amberjack and wahoo harvested in the Macaronesian region. However, this study did not provide information regarding interference of the matrix associated with different species or other factors. To help address these issues, previous studies highlighted the importance of using efficient sample pretreatment protocols as an important factor in modulating matrix interference [22,35–38].

The objective of this work was the evaluation and elimination of interfering matrix effects on the N2a-MTT assay, thereby contributing to an increased sensitivity and reliability of the method. For these studies several fish species widely consumed in the Canary Islands where this study was focused, were selected. The species selected also took into account an important nutritional parameter, fat content, as a potentially significant component for the observed matrix effect in N2a-MTT assays. The methodology and results obtained from this evaluation facilitate analysis of the MTDE required to avoid non-specific toxic effects and increase both sensitivity and reliability of this cell-based assay.

For VGSC-activating toxins, the reduction on cell viability in the presence of ouabain and veratridine (OV) shows a typical sigmoidal dose-response curve. Consequently, the effects of the matrix on CTXs analogues toxicity were also evaluated to exclude a possible response of interfering endogenous compounds on VGSCs.

2. Results and Discussion

To our knowledge this is the first study where the matrix effect of different fish species from Macaronesia (Eastern Atlantic) were evaluated with the objective of minimizing non-specific toxic effects. The control of these non-specific toxic effects would facilitate the reduction in the number of false positives or negatives and therefore increase the reliability of the assay.

Five different uncontaminated fish species prone to contain CTXs were extracted under the conditions described by (Estevez et al. 2019a) [39] and the non-specific toxic effects were evaluated in non-purified and purified by solid phase extraction (SPE) extracts (Table 1).

Table 1. Detailed information of the different fish species studied.

ID Sample	Species	Common Name	Total Lipids * (g/100 g)
NC1	*Pagrus pagrus*	Red porgy	<3% (0.7 g/100 g)
NC2	*Epinephelus marginatus*	Dusky grouper	<3% (1.0 g/100 g)
NC3	*Pomatomus saltatrix*	Bluefish	3–6% (4.2 g/100 g)
NC4	*Seriola dumerili*	Greater amberjack	3–6% (5.2 g/100 g)
NC5	*Acanthocybium solandri*	Wahoo	>6% (9.4 g/100 g)

* Data obtained from National Nutrient Database for Standard Reference (USDA) and F. M. Rueda et al., 2003. These values may change slightly depending on the season, age, sex, size or habitat.

Although there is not an established official classification, fish species used in this work were grouped depending on their total lipid content (% of lipid), being NC1 and NC2 considered as low-fat fish (<3% of lipid), NC3 and NC4 as semi-fat fish (between 3% and 6% of lipid) and NC5 as fat fish (>6% lipid content)

2.1. Matrix Effect in Non-Purified Sample Extracts

To determine matrix effects alone, non-purified fish extracts were analyzed without the addition of OV compounds. Non-purified fish extracts were analyzed at two equivalent tissue (TE) doses, 25 and 2.5 mg TE, in order to demonstrate the relation between lipid fish content and non-specific toxic effects (cell viability ≥ 90% of control).

When 25 mg TE of these fish extracts were added, NC1 and NC2 did not exhibit any cytotoxic effect whereas NC3, NC4 and NC5 showed a cytotoxic effect reducing cell viability to levels below 20%. Results show that the cytotoxic effects increase with the total fatty acids content and a 10-fold dilution (2.5 mg TE) was needed to avoid these non-specific toxic effects (Figure 1). Although sample dilution is a well-known alternative to reduce the matrix effect, this approach endangers the detection of potential CTX-like compounds when the sample has a low contamination.

Additionally, non-purified extracts were analyzed in a working range from 0.1 TE to 100 mg. At a dose > 50 mg TE, non-specific toxic effects can be observed for the low-fat fish (NC1 and NC2) (Figure 2). However, for semi- and fat fish (NC3, NC4 and NC5) these effects were observed for amounts > 10 mg TE. Consequently, in order to minimize matrix effect without compromise to sensitivity two alternatives were proposed: (1) incorporation of additional clean up step or (2) establishing a maximum tissue dose equivalent (MTDE) for different species.

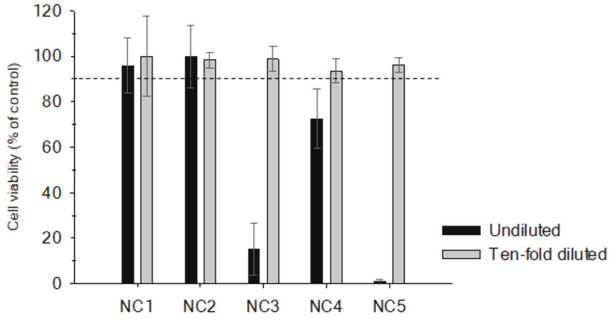

Figure 1. Cell viability after 16 h exposure to ciguatoxin (CTX)-negative fish extracts without the clean-up step: *Pagrus pagrus* (NC1); *Epinephelus marginatus* (NC2); *Pomatomus saltatrix* (NC3); *Seriola dumerili* (NC4) and *Acantocybium solandri* (NC5). Black bars show cell viability for a tissue equivalent dose of 25 mg and gray bars represent the ten-fold diluted fish extracts (2.5 mg two equivalent tissue (TE) dose). Dotted line represents 90% of cell viability, limit of non-specific toxic effects. Each extract was analyzed in triplicate and error bars represent assay variability.

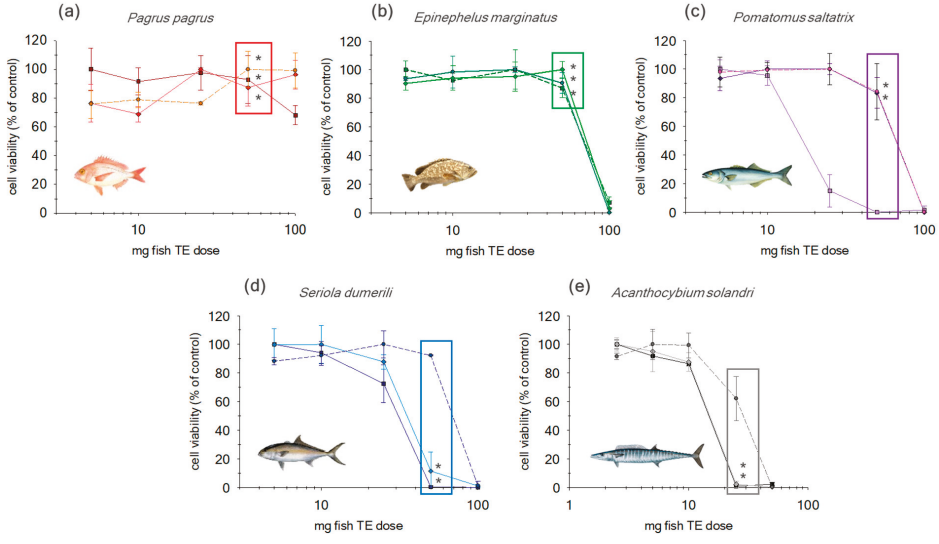

Figure 2. Viability assay in N2a cells exposed for 16 h to CTX-negative fish extracts obtained by different steps of purification for (**a**) *Pagrus pagrus* (NC1); (**b**) *Epinephelus marginatus* (NC2); (**c**) *Pomatomus saltatrix* (NC3); (**d**) *Seriola dumerili* (NC4) and (**e**) *Acantocybium solandri* (NC5) by: ■ No cleanup step, ♦ SPE-Florisil and • SPE-Florisil + C18. Data are expressed as mean ± SD (n = 3). The asterisks (boxed area) show homogenous groups when 50 mg of tissue equivalent was added (ANOVA, Bonferroni's HSD test, $p < 0.05$).

2.2. Evaluation of Additional Cleanup Steps

Previous studies highlighted the importance of using different clean-up procedures to selectively remove matrix interferences and increase the specificity of the assays [35,40–44]. Prior work carried out by the research team involved in this study was focused on the implementation of sample pretreatment to improve performance of the LC–MS/MS method for the analysis of CTXs (Estevez et al. 2019) [39]. In addition to optimization of the LC–MS/MS conditions, improvements of the sample pretreatment

were performed, in particular the purification step, to efficiently remove matrix effects and interfering compounds. The optimized sample pretreatment protocol includes a cleanup in two steps by solid phase extraction (SPE) with two different separation mechanisms and was the same used in the present study. As detailed in the previous study, the efficiency of these SPE steps has been evaluated in terms of overall CTX recovery of 72.7% [39].

2.2.1. SPE-Florisil

Purified fish extracts through SPE-Florisil were analyzed in a working range from 0.1 TE to 100 mg (Figure 2). Results showed that N2a cells did not exhibit non-specific toxic effects throughout the working range in NC1 fish extracts. At a dose > 50 mg TE, non-specific toxic effects can be observed for the low-fat fish (NC2). At a dose of 50 mg of TE of the lower lipid content fish species no significant differences in cell viability were observed compared to the non-purified extracts. For the semi-fat fish group, NC3 showed a similar response to the low-fat fish with non-specific toxic effects for tissue amounts > 50 mg. Contrary statistically significant differences were observed compared to extracts without cleanup for NC3 and NC4. For NC4, non-specific toxic effects were observed when 50 mg TE were added to the assay, with 25 mg TE being the adequate amount to avoid significant matrix effect. SPE Florisil showed a significate but minor improvement (around 15%) in the reduction of non-specific toxic effects for this particular fish species. Finally, for NC5 (fat fish) extracts, at 50 mg TE an important reduction on cell viability was observed for non-purified and purified extracts. Therefore, a maximum dose of 10 mg TE must be added in order to avoid non-specific toxic effects. Results show no significant effect over cell viability when a SPE-Florisil was applied.

2.2.2. SPE-Florisil + C18

An additional SPE C18 step was evaluated in the same working range (0.1–100 mg TE; Figure 2). NC1 and NC2 samples did not manifest any significant difference at 50 mg TE. Therefore, the introduction of an additional step of SPE C18 did not offer any improvement compared to SPE-Florisil.

A different performance was observed in NC3 and NC4 (semi-fat fish) after the incorporation of SPE-C18. By selecting 50 mg TE no significant effect was observed for NC3 compared to the SPE Florisil, showing non-specific toxic effects at a dose > 50 mg TE. In contrasts, in NC4 extract, the incorporation of an additional SPE-C18 allowed for an increase of the maximum dose from 25 to 50 mg TE.

Finally, in NC5 extracts, despite an observed significant reduction in matrix effect after SPE-C18 (35%) at 25 mg TE, this step did not adequately improve the interference removal.

As observed the efficiency of the different SPE treatments depended on the lipid content of the fish species. The low-fat fish (NC1 and NC2) slightly increased the maximum tissue dose equivalent, MTDE, on a 26% basis. When NC3 was analyzed incorporation of SPE-C18 offered no significant improvement with results obtained after the SPE-Florisil step alone. Nevertheless, the statistically significant differences between three treatments shows that employing both purification steps worked very well in order to remove non-specific toxic effects. NC5 (fat fish) was also considerably affected by the addition of further clean-up. In this case, incorporation of additional cleanup steps, including SPE C18, did not eliminate non-specific toxic effects when a dose of 50 mg TE was added; however, this additional step improved cell viability for the lower dose of 25 mg TE. No statistically significant improvement was observed after the SPE-Florisil step alone was utilized for the NC5 extract.

This approach was also followed to allow the potential evaluation of the same extracts analyzed by LC–MS/MS in order to confirm the toxicity of possible additional toxic compounds initially detected by the mass spectrometer [39,45].

2.3. Optimum Maximum Tissue Dose Equivalent (MTDE)

An alternative method to increase sensitivity while avoiding non-specific toxic effects is the establishment of a MTDE. Therefore, based upon results observed a MTDE was proposed for the

different fish species groups (low, semi and fat fish) as well as for steps of purification (no clean-up, SPE Florisil and SPE Florisil+C18; Figure 3).

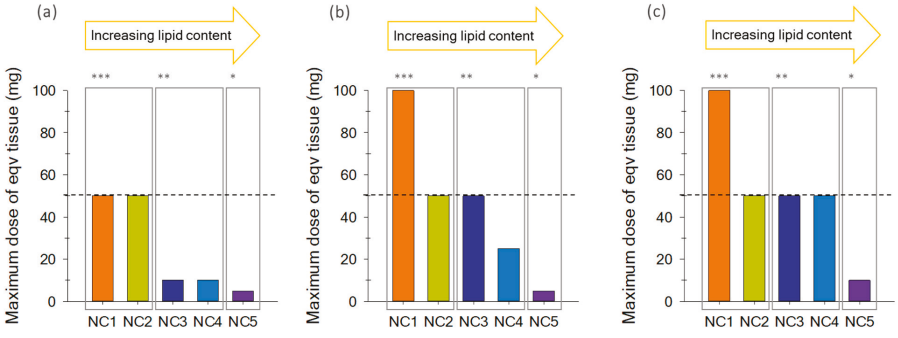

Figure 3. Graph bars shows MTDE for each species, framing * fat fish; ** semi-fat fish; *** low-fat fish. Results were obtained after 16 h exposure to CTX-negative fish extracts obtained by (**a**) Extraction procedure without cleanup step (**b**) SPE Florisil and (**c**) SPE Florisil + SPE-C18 step: *Pagrus pagrus* (orange); *Epinephelus marginatus* (yellow); *Pomatomus saltatrix* (dark blue); *Seriola dumerili* (blue) and *Acantocybium solandri* (purple). Dotted line represents a dose of 50 mg TE.

In the extracts without clean-up, the higher dose of equivalent tissue was established for the low-fat fish NC1 and NC2 (50 mg TE), whereas the lower dose equivalents were obtained for the fish species with the higher lipid content, NC5 (5 mg TE; Figure 3a). Intermediate interference was observed for the semi-fat species, NC3 and NC4, suggesting a MTDE of 10 mg TE.

The addition of Florisil SPE and further C18 steps significantly decreased the non-specific toxic effects for all the fish species, allowing to increase the amount of MTDE and therefore increasing the sensitivity of the assay (Figure 3b,c). For the most purified extracts, the same amount of a tissue equivalent was considered for low-fat and semi-fat fish (50 mg TE). In contrast with the unpurified extracts, the addition of further purification steps, such as SPE Florisil+C18, in order to remove interfering compounds of the matrix implies less dependence between METD and fish lipid content.

The results obtained demonstrated a good correlation between MTDE and lipid content, showing that matrix effects in N2a cells were probably related to interfering factors such as the fatty acids of the different fish species.

The MTDE was established for each type of fish species with different lipid content in order to avoid matrix effects and improve sensitivity. The sample pretreatment followed in this work allows us to propose an amount of 50 mg TE/well (217 mg TE/mL) of wet weight of equivalent tissue for low-fat fish and semi-fat fish as the MTDE. For fat fish 10 mg TE/well (43 mg TE/mL) was proposed.

The limits obtained for low- and semi-fat fish are higher than the proposed in the bibliography (50 mg eqv/mL proposed by Pawlowiez et al. (2013) [41]; A. Caillaud et al. (2012) [35] proposed 20 mg TE/mL to extracts of *Seriola* spp (semi-fat fish) and *Acanthocybium solandri* (fat fish). The results provided by A. Caillaud were obtained according to the protocol described by Lewis et al. (2013), in which no cleanup step was included. A similar result of 5 mg TE/well (22 mg/mL) was obtained in this work for fat fish (*Acanthocybium solandri*) in unpurified extract. The cleanup procedure used in this work, which includes two different SPE steps as described above, allowed increasing this MTDE until 10 mg TE/well (43 mg/mL) was achieved for the same species. Other authors, such as Botein Dechraoui, Tiedeken et al. (2005) [46], reported the use of 20 mg TE/mL in the analysis of a specimen of *Sphyraena barracuda* from Florida using an extraction protocol that includes a SPE silica gel column. The sample extraction procedures used in the different studies (with different purification levels) and the fish species analyzed in each case, could be the reason of the variability of the limits observed in the references cited. Results obtained in this work demonstrated that the variability in the MTDE could

be reduced when different species are analyzed including a cleanup procedure, in addition allowing higher assay sensitivity while avoiding matrix effects. However, exposures up to 2000 mg eqv/mL were achieved by Dickey (2008) [38] for more purified fish extracts.

2.4. Evaluation of the Toxicity of the Major CTX Analogues

Differences in the toxic potency of the three main CTXs responsible of CFP worldwide, C-CTX1, CTX1B and CTX3C, were evaluated in order to observe the different response in N2a cells. This study is the first time all three congeners were directly compared in the same study. In addition, we evaluated the matrix effect of C-CTX1 and CTX1B in the N2a assay with the objective of minimizing interference and being able to obtain an adequate and reliable semi-quantitative value.

2.4.1. CTX1B, CTX3C and C-CTX1 Toxic Potency in Neat Solution

CTX1B, CTX3C and C-CTX1 toxic potency were evaluated under the same conditions, 16 h of incubation time and a concentration range from 5 to 0.05 pg/well (pg in 10 µL of addition). Dose-response curves were obtained and differences in CTX1B, CTX3C and C-CTX1 toxicity was determined with the inhibitory concentration 50 (IC_{50}), which represents the pg of CTXs that produces a reduction of 50% in cell viability.

CTX1B was the most toxic analogue with an IC_{50} of 0.26 ± 0.07 pg/well (n = 4), followed by CTX3C with an IC_{50} of 0.03 ± 0.06 pg/well (n = 4) and the potency of C-CTX1 was the lowest with an IC_{50} of 0.44 ± 0.07 pg/well (n = 7; Table 2).

Table 2. IC_{50} of the different CTXs analogues evaluated.

CTX Analogue	IC_{50} ± σ (pg·well^{-1})	/Hill Slope/
CTX1B	0.26 ± 0.07	2.3 ± 0.48
CTX3C	0.43 ± 0.06	2.1 ± 0.49
C-CTX1	0.44 ± 0.07	2.4 ± 0.44

The three CTXs analogues exhibited a similar toxic response in the N2a assay, in descending toxicity order: CTX1B > CTX3C ≥ CCTX1, where sigmoidal curves fitted showed a slope equal to 2 for all toxins. This is in disagreement with the mouse bioassay (MBA), where CTX1B is ten-fold more toxic than C-CTX1 [38,47]. The use of ouabain and veratridine, in the N2a-MTT assay, which create an artificial environment, and the different expression level of critical ion channels (i.e., VGSCs or NMDA receptors) in N2a cells and mouse target cells could originate the discrepancies observed between N2a-MTT and MBA assay [24,47–51]. Moreover, a possible molecular transformation of the CTXs congeners caused by mouse metabolism or interaction of CTXs with blood could also be considered to explain the discrepancies in the relative toxic potency [24]. However, metabolic pathways for CTXs still need to be established, and the role of an organismal response in contrast to a singular cell line variant in vitro should also be considered.

2.4.2. CTX1B and C-CTX1 Effectiveness in the Presence of the Matrix

The toxin content (ng CTXs g^{-1} fish) in the analysis of different fish species is estimated by comparing the IC_{50} of the CTX pure standard with the IC_{50} of the sample. However, CTXs dose-response curves might be modified in presence of matrix in respect to those obtained from CTXs pure standards, suggesting shifts either in potency (IC_{50}-values) or in the effectiveness (slope values). Therefore, the assessment of the matrix influence could avoid an inadequate semi-quantitation of CTXs in naturally contaminated fish samples.

IC_{50} and slope values were calculated according to the dose-response curves using a sigmoid regression curve (4PL) with variable slopes. An estimation of the effect caused by the matrix over the

CTXs toxic potency was obtained through the dose-ratio (DR). The DR is defined as the relationship between LD_{50} obtained for CTXs in the presence of the matrix and the IC_{50} obtained for pure CTXs.

On the other hand, the slope determines how the reduction in cell viability occurs as the dose of CTXs is increased. Pöch et al. (1995) [52] proposed a mathematical approach to obtain slope-corrected DR (DR_{corr}): $\log DR_{corr} = (\log DR_{obs}) \cdot slope_{obs}$, where $slope_{obs}$ is the slope coefficient (in absolute value) of the dose-response curve with matrix and DR_{obs} is the DR-value obtained directly from IC_{50}s measured in both curves.

DR_{corr} were calculated when significant differences in slope of dose-response curves were determinate. Differences between both slopes and IC_{50}-values were evaluated using ANOVA, and applying a Bonferroni´s post hoc test, with a 95% confidence level.

In order to evaluate matrix influence in the CTXs semi quantitation, a standard addition experiment was carried out over non-contaminated fish extracts (*Pagrus pagrus*) without and with clean-up (SPE Florisil+C18). N2a cells were exposed to a fixed amount of matrix ranging from 0.25 to 0.0025 ng CTXs/g fish, using the concentration range of 5–0.05 pg/well. Therefore, in the absence of the matrix effect it would be expected to observe the same slope and IC_{50}-values in both cases.

The significant decrease of the C-CTX1 slope in the presence of the matrix is linked with a lower effectiveness (regardless of the level of purification; Figure 4). Therefore, DR-values obtained from those dose-response curves must be corrected using the approach proposed by Pöch et al. (1995) [52]. LD_{50} was corrected using the DR_{corr} according to the relation: $IC_{50(corr)} = IC_{50(STD\ pure)}\ DR_{corr}$.

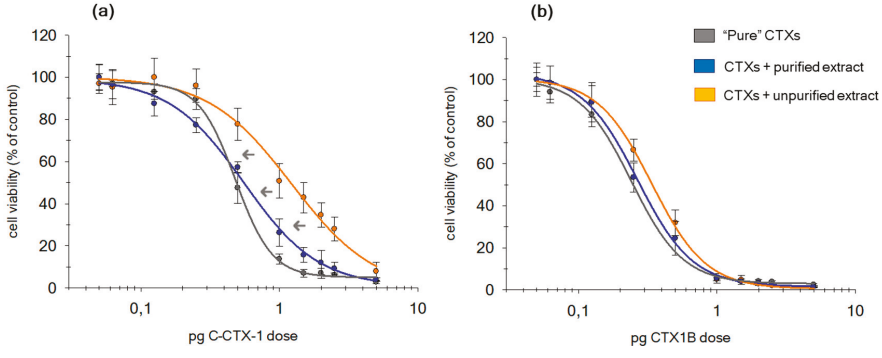

Figure 4. Dose-response curves of N2a cells in +OV conditions (cells with ouabain and veratridine treatment), exposed to an increasing dose of: (**a**) C-CTX1 and (**b**) CTX1B when 20 mg of fish TE, unpurified (orange curves) and purified (blue curves), was added to each well. Gray curves represent response of cells to both CTXs without matrix.

After applying the appropriate corrections, results did not manifest significant differences between C-CTX1 toxic potency when it was analyzed without a matrix and with a purified matrix. However, a significant decrease of the toxic potency of C-CTX1 was observed in the presence of an unpurified matrix, obtaining the lower $IC_{50(corr)}$ (Table 3). In this case, C-CTX1 was 3.6 times less toxic than without a matrix.

Table 3. IC_{50} and dose-ratios (DRs)-values of CCTX1 and CTX1B obtained from extracts with and without a cleanup step.

CTXs Type	Analysis Conditions	IC_{50} ± SD (pg·well^{-1})	ng CTXs·g^{-1} Fish ± SD	/Hill slope/ ± SD	DR ± SD	DR_{corr} ± SD	$IC_{50(corr)}$ ± SD	ng CTXs·g^{-1} $Fish_{corr}$ ± SD
CCTX1	No matrix	0.48 ± 0.04	0.024 ± 0.002	3.5 ± 0.5	-	-	-	0.024 ± 0.002
	Purified	0.56 ± 0.04	0.027 ± 0.002	1.6 ± 0.1	1.1 ± 0.1	1.3 ± 0.1	0.6 ± 0.1	0.031 ± 0.003
	Unpurified	1.3 ± 0.1	0.06 ± 0.01	1.5 ± 0.3	2.6 ± 0.2	3.6 ± 0.9	1.8 ± 0.2	0.12 ± 0.02
CTX1B	No matrix	0.26 ± 0.02	0.013 ± 0.001	2.4 ± 0.1	-	-	-	0.013 ± 0.001
	Purified	0.27 ± 0.02	0.013 ± 0.001	2.4 ± 0.2	1.0 ± 0.1	1.0 ± 0.2	0.27 ± 0.05	0.014 ± 0.003
	Unpurified	0.34 ± 0.02	0.017 ± 0.001	2.3 ± 0.4	1.3 ± 0.1	1.6 ± 0.3	0.4 ± 0.1	0.022 ± 0.006

Contrarily, CTX1B did not show differences in terms of effectiveness (Table 3). Comparison between toxic potency, with and without matrix, can be estimated with the IC_{50} obtained directly from the curves. CTX1B exhibited almost the same toxic potency without/with a clean-up matrix (Table 3). In the absence of a matrix, a IC_{50} of 0.26 ± 0.02 pg CTX1B/well was obtained while a IC_{50} of 0.27 ± 0.02 pg CTX1B/well, when a cleanup step was applied, was obtained. A significant difference was observed in the IC_{50}-values when a cleanup step was not applied, and a little diminution in the toxic potency was observed (1.6 times less toxic).

C-CTX1 and CTX1B effectiveness was clearly different in the presence of matrix. While C-CTX1 was influenced by the matrix reducing the reliability and accuracy of sample semi-quantitation, CTX1B was not affected. These differences might be due to the different affinity of the CTXs to the matrix, which will reduce their affinity to the VGSCs and consequently their effectiveness.

C-CTX1 and CTX1B toxic potency was influenced by the matrix, leading to an overestimation of the toxin content in contaminated samples (Table 3). Therefore, the removal of these compounds by incorporating a cleanup step allowed one to minimize this matrix effect and to obtain a better estimation of both CTXs, especially for CCTX1, which was the most affected.

Limit of detection (LOD) and limit of quantitation (LOQ), corresponding to the concentrations of CTXs necessary to inhibit the cell viability by 10% (IC_{90}) and 20% (IC_{80}), divided by mg of TE added to the assay (20 mg). The lower sensitivity of the method was obtained in the presence of the unpurified matrix for CCTX1 and CTX1B, but the first one was the most affected. In this case, LODs and LOQs were significantly improved when a clean-up step was included in the sample pretreatment (Table 4). Nevertheless, CTX1B LODs and LOQs were not affected significantly by the elimination of the matrix.

Table 4. LOD and LOQ of CCTX1 and CTX1B.

CTXs Type	Analysis Conditions	LOD		LOQ	
		IC_{10} ± SD (pg·well^{-1})	ng CTXs·g^{-1} Fish ± SD	IC_{20} ± SD (pg·well^{-1})	ng CTXs·g^{-1} Fish ± SD
CCTX1	No matrix	0.20 ± 0.02	0.010 ± 0,002	0.29 ± 0.03	0.014 ± 0.002
	Purified	0.12 ± 0.09	0.008 ± 0,001	0.23 ± 0.02	0.012 ± 0.001
	Unpurified	0.26 ± 0.02	0.013 ± 0,004	0.46 ± 0.09	0.023 ± 0.005
CTX1B	No matrix	0.12 ± 0.02	$0.007 \pm 9 \times 10^{-3}$	0.17 ± 0.02	$0.009 \pm 9 \times 10^{-3}$
	Purified	0.10 ± 0.01	$0.007 \pm 6 \times 10^{-3}$	0.14 ± 0.01	$0.008 \pm 3 \times 10^{-3}$
	Unpurified	0.13 ± 0.01	$0.005 \pm 5 \times 10^{-3}$	0.19 ± 0.01	$0.007 \pm 5 \times 10^{-3}$

Differences in the toxic effectiveness of both CTXs, in the absence and presence of matrix interfering compounds, was not critical when the N2a-MTT assay was used for screening purposes. On the other hand, significant errors might be obtained when applied to semi-quantitative estimation in samples contaminated with C-CTX1.

3. Conclusions

The N2a-MTT assay is considered as a suitable tool to monitor CTX-like compounds, although its applicability in fish samples might be compromised by the matrix effect. A good correlation between

MTDE and lipid content of the fish species was observed in this study. The inclusion of a cleanup step by solid phase extraction (SPE) allowed a significant increase of the MTDE for fat fish species and in particular for semi-fat species, the inclusion of this step also contributed to an improved sensitivity. Furthermore, this study also demonstrated that the toxic activity of CCTX1 is highly influenced by the presence of endogenous compounds, suggesting that the matrix compounds might reduce its affinity to the VGSCs. The inclusion of this SPE cleanup will also contribute to a better estimation of naturally incurred C-CTX1 in fish samples therefore increasing the reliability and accuracy of toxin semi-quantitation.

4. Materials and Methods

4.1. Standards and Reagents

CCTX1 standard solution (10 pg·μL^{-1}) was kindly supplied by Dr. Manger and Dr. Dickey from the Fred Hutchinson Cancer Research Center and the Marine Science institute of the University of Texas (USA), respectively. The CTX1B pure standard solution was kindly provided by professor Takeshi Yasumoto from the Japan food Research Laboratory (JFRL). The CTX3C standard was purchased from Wako Chemicals GmBH (Neuss, Germany).

Acetone, diethyl ether, methanol, water, hexane and ethyl acetate used for extraction and purification were of HPLC grade (Merck KGaA, Darmstadt, Germany). Water for preparation of ouabain and veratridine solutions was deionized and purified at 15 MΩ cm+ through a Milli-Q Gradient A10 system (Millipore, Spain). Water (J. T. Baker, Center Valley, PA, USA) for LC–MS analysis were of LC–MS grade. Methanol (Merck KGaA, Darmstadt, Germany) for diluted samples utilized in the N2a assay were of HPLC grade.

4.2. Sample Pretreatment for the N2a-MTT Assay (and HPLC–MS/MS)

Fish samples not containing CTX's were shipped to the IUSA for testing matrix effects using the N2a-MTT assay. Absence of CTX was confirmed by HPLC–MS/MS. Standard Operating Procedure (SOP) for sample pretreatment was carried out according to conditions initially proposed by Yogui et al. (2011) [53] and modified by Estevez et al. (2019) [39]. Briefly, 15 g of fish tissue were extracted by acetone at 3 mL/g tissue homogenate twice. Acetone was separated from the tissue by centrifugation and dried to an aqueous phase. This phase was extracted with diethyl ether at 1 mL/g fish tissue two times and organic phases were then dried by nitrogen. Residue was partitioned between 90% methanol and n-Hexane (at 0.3 mL 90% MeOH/g fish tissue). The hexane wash was discarded and the methanol phase was dried by nitrogen. Sample cleanup was done with Florisil and C18 solid phase extraction cartridges before analysis by LC–MS/MS. Sample extracts with and without cleanup step were analyzed by an N2a-MTT assay.

4.3. In Vitro N2a-MTT Assay

4.3.1. Maintenance of Culture

Neuro-2a (N2a) cell line was obtained from American Type Culture Collection (ATCC, CCL 131, Manassas, VA, USA) and cultured in T75 flask (Corning, NY, USA) in 30 mL of growth medium consisting on RPMI-1640 medium (R8758, Sigma, Irvine, UK) containing 1% (v/v), 100 mM sodium pyruvate (S8636, Sigma, Irvine, UK), 1% (v/v) 200 mM L-glutamine (G7513, Sigma, Irvine, UK) and 1% (v/v) penicillin-streptomycin solution formed by 5000 units and 5 mg/mL, respectively (P4458, Sigma, St. Louis, MO, USA). This medium was supplemented with 10% (v/v) fetal bovine serum (FBS, F2442, Sigma, St. Louis, MO, USA) to obtain a complete growth media (RPMI-10). The N2a cell line was maintained at 37 °C under 5% CO_2 in a humidified atmosphere and subcultured when a confluence > 80% was observed (four times per week for a split 1:5).

4.3.2. Cytotoxicity Cell Based assay (N2a-MTT Assay)

The N2a-MTT assay applied to the analysis of fish extracts was developed by Manger et al. (1993) [20] with some modifications. To evaluate the toxic activity of each fraction, prepared from different contaminated samples, cells were seeded into 96-well assay plates (Corning, NY, USA) at a density of 30,000 cells per well in 0.2 mL of growth medium supplemented with 5% (v/v) FBS (RPMI-5) and incubated for 24 h, at 37 °C in humidified atmosphere enriched with 5% CO_2.

Plates were divided into non-sensitized and sensitized sections. Cells from the sensitized section were exposed to 20 µL/well of a mixture of Ouabain (O3125, Sigma, St. Louis, MO, USA) and Veratridine (V5754, Sigma, St. Louis, MO, USA) (+OV section), prepared from the 10 mM ouabain and 1 mM veratridine stock solutions, in RPMI-C (growth medium without FBS), allowing a reduction of 20% of cell viability. A volume of 20 µL of PBS was added to wells of the non-sensitized cells (-OV section).

Extracts obtained from non-contaminated fish samples in the different steps of the sample pretreatment were evaporated under N_2 stream at 40 °C until dryness. Then these extracts were reconstituted in MeOH to obtain a concentration of 20 g TE/mL. Non-sensitized cells were exposed to a range of fish extract concentration, which varied from between 0.1 and 100 mg fish TE $well^{-1}$. Serial dilutions were prepared from the extracts of 20 g TE/mL in RPMI-C and 10 µL of each dilution was tested in replicates of 4 wells.

In order to evaluate the matrix effect in the CTXs semi quantification by the N2a-MTT assay, 15 g of a non-contaminated fish sample of *Pagrus pagrus* was extracted. A portion of the sample was collected after extraction and after purification step, then 20 mg TE from each extract was added by well for sensitized and non-sensitized sections by triplicate. Additionally, cells were exposed to CTXs using the concentration range of 5–0.05 pg/well. The CTXs content was equivalent to ranging from 0.25 to 0.0025 ng CTXs/g fish. Dose-response curves were obtained and IC_{50} values calculated.

Sensitivity of the N2a cells to the presence of CTXs compounds was calibrated with a standard solution of C-CTX1, CTX1B and CTX-3C that was serially diluted ten times (ranging from 50 to 0.5 ng mL^{-1}). Of each dilution 10 µL was tested in replicates of 4 wells in the presence of OV.

4.3.3. Measurement of Mitochondrial Activity

Following a 16 h incubation with samples, cell viability was assessed by colorimetric MTT (3-(4,5-dimethylthiazol-2-yl)-2,5-diphenyl tetrazolium bromide, Sigma, St. Louis, MO, USA). Briefly, the medium was removed from the wells and replaced by 60 µL of RPMI-5 containing 0.8 mg/mL of MTT. After 40 min at 37°, MTT medium was discarded and the resulting formazan crystals, produced from mitochondrial dehydrogenases of live cells, were solubilized by 100 µL of dimethyl sulfoxide (DMSO, D5879, Honeywell, Seelze, Germany). Absorbance was read with a spectrophotometer (Multiskan® FC Microplate Photometer, Thermo Fisher Scientific Oy, Ratastie, Finland) at 570 nm for testing and 630 nm for reference [54].

4.3.4. Analysis and statistical treatment of the data

Results of cell viability were obtained with SigmaPlot v.12.0 software and were expressed as a percentage relative to control wells. For those data that were fitted to a sigmoidal dose-response curve, the IC_{50} value (concentration of CTXs required to cause 50% reduction in cell viability) was calculated using a four parameters logistic function (4PL) with variable slope. From this equation, the limit of quantitation was calculated by IC_{80} (concentration of CTXs necessary to inhibit the cell viability by 20%). All data are expressed as the means ± SD for n replicates.

Author Contributions: Conceptualization, A.G.-M., O.V.; methodology, R.M., A.G.-M., O.V. and D.C.; experimental work D.C.; data analysis and interpretation, D.C., O.V., R.M. and A.G.-M.; supervision, A.G.-M.; project administration and resources, A.G.-M. All authors were involved in the writing, review and editing of the manuscript; final revision, A.G.-M. All authors have read and agreed to the published version of the manuscript.

Funding: This work has been partially financed through EUROCIGUA project: Risk characterization of Ciguatera Fish Poisoning in Europe, framework partnership agreement GP/EFSA/AFSCO/2015/03. D. Castro financial

support for the PhD studies was obtained through EUROCIGUA project: Risk characterization of Ciguatera Fish Poisoning in Europe, framework partnership agreement GP/EFSA/AFSCO/2015/03, cofounded by the European Food Safety Authority.

Acknowledgments: Robert Dickey (previously, U.S. Food and Drug Administration) via Ronald Manger (Fred Hutchinson Cancer Research Center, Seattle, USA) for kindly provided the standard of C-CTX1. Takeshi Yasumoto (Japan Food Research Laboratories) for kindly provided standards of Pacific Ciguatoxins.

Conflicts of Interest: The authors declare no conflict of interest.

References

1. Friedman, M.A.; Fleming, L.E.; Fernandez, M.; Bienfang, P.; Schrank, K.; Dickey, R.; Bottein, M.Y.; Backer, L.; Ayyar, R.; Weisman, R.; et al. Ciguatera fish poisoning: Treatment, prevention and management. *Mar. Drugs* **2008**, *6*, 456–479. [CrossRef]
2. Berdalet, E.; E Fleming, L.; Gowen, R.; Davidson, K.; Hess, P.; Backer, L.C.; Moore, S.K.; Hoagland, P.; Enevoldsen, H. Marine harmful algal blooms, human health and wellbeing: Challenges and opportunities in the 21st century. *J. Mar. Boil. Assoc. UK* **2015**, *96*, 61–91. [CrossRef]
3. Lehane, L.; Lewis, R.J. Ciguatera: Recent advances but the risk remains. *Int. J. Food Microbiol.* **2000**, *61*, 91–125. [CrossRef]
4. Fraga, S.; Rodríguez, F. Genus Gambierdiscus in the Canary Islands (NE Atlantic Ocean) with Description of Gambierdiscus silvae sp. nov., a New Potentially Toxic Epiphytic Benthic Dinoflagellate. *Protist* **2014**, *165*, 839–853. [CrossRef]
5. Nishimura, T.; Sato, S.; Tawong, W.; Sakanari, H.; Uehara, K.; Shah, M.R.; Suda, S.; Yasumoto, T.; Taira, Y.; Yamaguchi, H.; et al. Genetic Diversity and Distribution of the Ciguatera-Causing Dinoflagellate Gambierdiscus spp. (Dinophyceae) in Coastal Areas of Japan. *PLoS ONE* **2013**, *8*, e60882. [CrossRef] [PubMed]
6. Yasumoto, T.; Nakajima, I.; Bagnis, R.; Adachi, R. Finding of a dinoflagellate as a likely culprit of ciguatera. *Bull. Jpn. Soc. Sci. Fish* **1977**, *43*, 1021–1026. [CrossRef]
7. Gómez, F.; Qiu, D.; Lopes, R.; Lin, S. Fukuyoa paulensis gen. et sp. nov., a New Genus for the Globular Species of the Dinoflagellate Gambierdiscus (Dinophyceae). *PLoS ONE* **2015**, *10*, e0119676. [CrossRef] [PubMed]
8. Bienfang, P.; Trapido-Rosenthal, H.; Laws, E.A. Bioaccumulation/Biomagnifications in Food Chains. *Environ. Toxicol.* **2012**, 35–69. [CrossRef]
9. Holmes, M.J.; Lewis, R.J. Toxin-producing dinoflagellates. In *Perspectives in Molecular Toxicology*; Menez, A., Ed.; John Wiley & Sons: Hoboken, NJ, USA, 2002; pp. 39–65.
10. Litaker, R.W.; Vandersea, M.; Faust, M.A.; Kibler, S.; Nau, A.W.; Holland, W.C.; Chinain, M.; Holmes, M.J.; Tester, P.A. Global distribution of ciguatera causing dinoflagellates in the genus Gambierdiscus. *Toxicon* **2010**, *56*, 711–730. [CrossRef]
11. Vernoux, J.-P.; Lewis, R.J. Isolation and characterisation of Caribbean ciguatoxins from the horse-eye jack (Caranx latus). *Toxicon* **1997**, *35*, 889–900. [CrossRef]
12. Otero, P.; Pérez, S.; Alfonso, A.; Vale, C.; Rodrıguez, P.; Gouveia, N.N.; Gouveia, N.; Delgado, J.; Vale, P.; Hirama, M. First toxin profile of ciguateric fish in Madeira Archipelago (Europe). *Anal. Biochem.* **2010**, *82*, 6032–6039. [CrossRef] [PubMed]
13. Arellano, J.L.P.; Luzardo, O.P.; Brito, A.P.; Cabrera, M.H.; Zumbado, M.; Carranza, C.; Angel-Moreno, A.; Dickey, R.W.; Boada, L.D. Ciguatera Fish Poisoning, Canary Islands. *Emerg. Infect. Dis.* **2005**, *11*, 1981–1982. [CrossRef] [PubMed]
14. Lewis, R.J.; Vernoux, J.-P.; Brereton, I. Structure of Caribbean Ciguatoxin Isolated fromCaranx latus. *J. Am. Chem. Soc.* **1998**, *120*, 5914–5920. [CrossRef]
15. Dickey, R.W.; Plakas, S.M. Ciguatera: A public health perspective. *Toxicon* **2010**, *56*, 123–136. [CrossRef] [PubMed]
16. Chain, E.P.O.C.I.T.F. Scientific Opinion on marine biotoxins in shellfish - Emerging toxins: Ciguatoxin group. *EFSA J.* **2010**, *8*, 1627. [CrossRef]
17. Lombet, A.; Bidard, J.-N.; Lazdunski, M. Ciguatoxin and brevetoxins share a common receptor site on the neuronal voltage-dependent Na+ channel. *FEBS Lett.* **1987**, *219*, 355–359. [CrossRef]

18. Dechraoui, M.-Y.; Naar, J.; Pauillac, S.; Legrand, A.-M. Ciguatoxins and brevetoxins, neurotoxic polyether compounds active on sodium channels. *Toxicon* **1999**, *37*, 125–143. [CrossRef]
19. Van Dolah, F.M.; Finley, E.L.; Haynes, B.L.; Doucette, G.J.; Moeller, P.D.; Ramsdell, J.S. Development of rapid and sensitive high throughput pharmacologic assays for marine phycotoxins. *Nat. Toxins* **1994**, *2*, 189–196. [CrossRef]
20. Manger, R.; Leja, L.; Lee, S.; Hungerford, J.; Wekell, M. Tetrazolium-Based Cell Bioassay for Neurotoxins Active on Voltage-Sensitive Sodium Channels: Semiautomated Assay for Saxitoxins, Brevetoxins, and Ciguatoxins. *Anal. Biochem.* **1993**, *214*, 190–194. [CrossRef]
21. Manger, R.L.; Leja, L.S.; Lee, S.Y.; Hungerford, J.M.; Hokama, Y.; Dickey, R.W.; Granade, H.R.; Lewis, R.; Yasumoto, T.; Wekell, M.M. Detection of Sodium Channel Toxins: Directed Cytotoxicity Assays of Purified Ciguatoxins, Brevetoxins, Saxitoxins, and Seafood Extracts. *J. AOAC Int.* **1995**, *78*, 521–527. [CrossRef]
22. Fairey, E.R.; Bottein Dechraoui, M.Y.; Sheets, M.F.; Ramsdell, J.S. Modification of the cell based assay for brevetoxinsusing human cardiac voltage dependent sodium channels expressed in HEK-293 cells. *Biosens. Bioelectron.* **2001**, *16*, 579–586. [CrossRef]
23. Dechraoui, M.-Y.B.; Ramsdell, J.S. Type B brevetoxins show tissue selectivity for voltage-gated sodium channels: Comparison of brain, skeletal muscle and cardiac sodium channels. *Toxicon* **2003**, *41*, 919–927. [CrossRef]
24. Dechraoui, M.-Y.B.; Wang, Z.; Turquet, J.; Chinain, M.; Darius, H.T.; Cruchet, P.; Radwan, F.F.; Dickey, R.W.; Ramsdell, J.S. Biomonitoring of ciguatoxin exposure in mice using blood collection cards. *Toxicon* **2005**, *46*, 243–251. [CrossRef] [PubMed]
25. Dechraoui, M.-Y.B.; Wang, Z.; Ramsdell, J.S. Optimization of ciguatoxin extraction method from blood for Pacific ciguatoxin (P-CTX-1). *Toxicon* **2007**, *49*, 100–105. [CrossRef]
26. Pauillac, S.; Branaa, P.; Chinain, M.; Naar, J. The reversed micellar medium as a universal tool for the development of antibody-based assays to marine phycotoxins using small amount of toxic material. In *Harmful Algal Bloom*; Hallegraeff, G.M., Blackburn, S.I., Bolch, C.J., Lewis, R.J., Eds.; Intergovernmental Oceanographic Commission of UNESCO: Hobart, Tasmania, 2001; pp. 288–291.
27. Tsumuraya, T.; Fujii, I.; Inoue, M.; Tatami, A.; Miyazaki, K.; Hirama, M. Production of monoclonal antibodies for sandwich immunoassay detection of ciguatoxin 51-hydroxyCTX3C. *Toxicon* **2006**, *48*, 287–294. [CrossRef]
28. Campora, C.E.; Hokama, Y.; Ebesu, J.S. Comparative analysis of purified Pacific and Caribbean ciguatoxin congeners and related marine toxins using a modified elisa technique. *J. Clin. Lab. Anal.* **2006**, *20*, 121–125. [CrossRef]
29. Fairey, E.R.; Edmunds, J.G.; Ramsdell, J.S. A Cell-Based Assay for Brevetoxins, Saxitoxins, and Ciguatoxins Using a Stably Expressed c-fos–Luciferase Reporter Gene. *Anal. Biochem.* **1997**, *251*, 129–132. [CrossRef]
30. Fairey, E.R.; Ramsdell, J.S. Reporter gene assays for algal-derived toxins. *Nat. Toxins* **1999**, *7*, 415–421. [CrossRef]
31. A Catterall, W. Neurotoxins that Act on Voltage-Sensitive Sodium Channels in Excitable Membranes. *Annu. Rev. Pharmacol. Toxicol.* **1980**, *20*, 15–43. [CrossRef]
32. Wang, G.K. Voltage-gated sodium channels as primary targets of diverse lipid-soluble neurotoxins. *Cell. Signal.* **2003**, *15*, 151–159. [CrossRef]
33. Leão-Martins, J.M.; Lozano-Leon, A.; Giraldez, J.; Vilariño, O.; Gago-Martínez, A. Preliminary Results on the Evaluation of the Occurrence of Tetrodotoxin Associated to Marine Vibrio spp. in Bivalves from the Galician Rias (Northwest of Spain). *Mar. Drugs* **2018**, *16*, 81. [CrossRef] [PubMed]
34. Kogure, K.; Tamplin, M.L.; Simidu, U.; Colwell, R.R. A tissue culture assay for tetrodotoxin, saxitoxin and related toxins. *Toxicon* **1988**, *26*, 191–197. [CrossRef]
35. Caillaud, A.; Eixarch, H.; De La Iglesia, P.; Rodríguez, M.; Domínguez, L.; Andree, K.; Diogène, J. Towards the standardisation of the neuroblastoma (neuro-2a) cell-based assay for ciguatoxin-like toxicity detection in fish: Application to fish caught in the Canary Islands. *Food Addit. Contam. Part A* **2012**, *29*, 1000–1010. [CrossRef] [PubMed]
36. Bienfang, P.; Oben, B.; DeFelice, S.; Moeller, P.; Huncik, K.; Oben, P.; Toonen, R.; Daly-Engel, T.; Bowen, B. Ciguatera: The detection of neurotoxins in carnivorous reef fish from the coast of Cameroon, West Africa. *Afr. J. Mar. Sci.* **2008**, *30*, 533–540. [CrossRef]
37. Campora, C.E.; Dierking, J.; Tamaru, C.S.; Hokama, Y.; Vincent, D. Detection of ciguatoxin in fish tissue using sandwich ELISA and neuroblastoma cell bioassay. *J. Clin. Lab. Anal.* **2008**, *22*, 246–253. [CrossRef] [PubMed]

38. Dickey, R.W. Ciguatera toxins: Chemistry, toxicology and detection. In *Seafood and Freshwater Toxins: Pharmacology, Physiology, and Detection*; Botana, L.M., Ed.; CRC Press/Taylor & Francis: Boca Raton, FL, USA, 2008; pp. 479–500.
39. Estevez, P.; Castro, D.; Leão-Martins, J.M.; Yasumoto, T.; Dickey, R.; Gago-Martinez, A. Implementation of liquid chromatography tandem mass spectrometry for the analysis of ciguatera fish poisoning in contaminated fish samples from Atlantic coasts. *Food Chem.* **2019**, *280*, 8–14. [CrossRef]
40. Caillaud, A.; De La Iglesia, P.; Darius, H.T.; Pauillac, S.; Aligizaki, K.; Fraga, S.; Chinain, M.; Diogène, J. Update on Methodologies Available for Ciguatoxin Determination: Perspectives to Confront the Onset of Ciguatera Fish Poisoning in Europe [1]. *Mar. Drugs* **2010**, *8*, 1838–1907. [CrossRef]
41. Pawlowiez, R.; Darius, H.T.; Cruchet, P.; Rossi, F.; Caillaud, A.; Laurent, D.; Chinain, M. Evaluation of seafood toxicity in the Australes archipelago (French Polynesia) using the neuroblastoma cell-based assay. *Food Addit. Contam. Part A* **2013**, *30*, 567–586. [CrossRef]
42. Aballay-Gonzalez, A.; Ulloa, V.; Rivera, A.; Hernandez, V.; Silva, M.; Caprile, T.; Delgado-Rivera, L.; Astuya, A. Matrix effects on a cell-based assay used for the detection of paralytic shellfish toxins in bivalve shellfish samples. *Food Addit. Contam. Part A* **2016**, *33*, 869–875. [CrossRef]
43. Wong, C.K.; Hung, P.; Lee, K.L.; Kam, K.M. Solid-phase extraction clean-up of ciguatoxin-contaminated coral fish extracts for use in the mouse bioassay. *Food Addit. Contam. Part A* **2009**, *26*, 236–247. [CrossRef]
44. Loeffler, C.; Robertson, A.; Quintana, H.A.F.; Silander, M.C.; Smith, T.B.; Olsen, D. Ciguatoxin prevalence in 4 commercial fish species along an oceanic exposure gradient in the US Virgin Islands. *Environ. Toxicol. Chem.* **2018**, *37*, 1852–1863. [CrossRef] [PubMed]
45. Moreiras, G.; Leão, J.M.; Gago-Martínez, A. Design of experiments for the optimization of electrospray ionization in the LC-MS/MS analysis of ciguatoxins. *J. Mass Spectrom.* **2018**, *53*, 1059–1069. [CrossRef] [PubMed]
46. Dechraoui, M.-Y.B.; Tiedeken, J.A.; Persad, R.; Wang, Z.; Granade, H.R.; Dickey, R.W.; Ramsdell, J.S. Use of two detection methods to discriminate ciguatoxins from brevetoxins: Application to great barracuda from Florida Keys. *Toxicon* **2005**, *46*, 261–270. [CrossRef] [PubMed]
47. Lewis, R.J.; Hoy, A.W.W.; Sellin, M. Ciguatera and mannitol: In Vivo and In Vitro assessment in mice. *Toxicon* **1993**, *31*, 1039–1050. [CrossRef]
48. Lewis, R.J.; Holmes, M.J. Origin and transfer of toxins involved in ciguatera. *Comp. Biochem. Physiol. Part C Pharmacol. Toxicol. Endocrinol.* **1993**, *106*, 615–628. [CrossRef]
49. Bidard, J.N.; Vijverberg, H.P.; Frelin, C.; Chungue, E.; Legrand, A.M.; Bagnis, R.; Lazdunski, M. Ciguatoxin is a novel type of NaC channel toxin. *J. Biol. Chem.* **1984**, *259*, 8353–8357.
50. Lepage, K.T.; Dickey, R.W.; Gerwick, W.H.; Jester, E.L.; Murray, T.F. On the use of neuro-2a neuroblastoma cells versus intact neurons in primary culture for neurotoxicity studies. *Crit. Rev. Neurobiol.* **2005**, *17*, 27–50. [CrossRef]
51. Wu, J.J.; Mak, Y.L.; Murphy, M.B.; Lam, J.C.W.; Chan, W.H.; Wang, M.; Chan, L.L.; Lam, P.K.S. Validation of an accelerated solvent extraction liquid chromatography–tandem mass spectrometry method for Pacific ciguatoxin-1 in fish flesh and comparison with the mouse neuroblastoma assay. *Anal. Bioanal. Chem.* **2011**, *400*, 3165–3175. [CrossRef]
52. Pöch, G.; Pancheva, S.N. Calculating slope and ED50 of additive dose-response curves, and application of these tabulated parameter values. *J. Pharmacol. Toxicol. Methods* **1995**, *33*, 137–145. [CrossRef]
53. Yogi, K.; Oshiro, N.; Inafuku, Y.; Hirama, M.; Yasumoto, T. Detailed LC-MS/MS Analysis of Ciguatoxins Revealing Distinct Regional and Species Characteristics in Fish and Causative Alga from the Pacific. *Anal. Chem.* **2011**, *83*, 8886–8891. [CrossRef]
54. Mosmann, T. Rapid colorimetric assay for cellular growth and survival: Application to proliferation and cytotoxicity assays. *J. Immunol. Methods* **1983**, *65*, 55–63. [CrossRef]

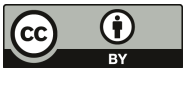

toxins

MDPI

Article

Assessment of Ciguatera and Other Phycotoxin-Related Risks in Anaho Bay (Nuku Hiva Island, French Polynesia): Molecular, Toxicological, and Chemical Analyses of Passive Samplers

Mélanie Roué [1,2,*], Kirsty F. Smith [3], Manoella Sibat [4], Jérôme Viallon [2], Kévin Henry [2], André Ung [2], Laura Biessy [3], Philipp Hess [4], Hélène Taiana Darius [2] and Mireille Chinain [2]

1 Institut de Recherche pour le Développement, UMR 241 EIO, 98702 Faa'a, Tahiti, French Polynesia
2 Institut Louis Malardé, UMR 241 EIO, 98713 Papeete, Tahiti, French Polynesia; jviallon@ilm.pf (J.V.); khenry@ilm.pf (K.H.); aung@ilm.pf (A.U.); tdarius@ilm.pf (H.T.D.); mchinain@ilm.pf (M.C.)
3 Cawthron Institute, Nelson 7042, New Zealand; kirsty.smith@cawthron.org.nz (K.F.S.); laura.biessy@cawthron.org.nz (L.B.)
4 Ifremer, DYNECO, 44000 Nantes, France; manoella.sibat@ifremer.fr (M.S.); philipp.hess@ifremer.fr (P.H.)
* Correspondence: melanie.roue@ird.fr; Tel.: +689-40-416-413

Received: 2 April 2020; Accepted: 1 May 2020; Published: 13 May 2020

Abstract: Ciguatera poisoning is a foodborne illness caused by the consumption of seafood contaminated with ciguatoxins (CTXs) produced by dinoflagellates from the genera *Gambierdiscus* and *Fukuyoa*. The suitability of Solid Phase Adsorption Toxin Tracking (SPATT) technology for the monitoring of dissolved CTXs in the marine environment has recently been demonstrated. To refine the use of this passive monitoring tool in ciguateric areas, the effects of deployment time and sampler format on the adsorption of CTXs by HP20 resin were assessed in Anaho Bay (Nuku Hiva Island, French Polynesia), a well-known ciguatera hotspot. Toxicity data assessed by means of the mouse neuroblastoma cell-based assay (CBA-N2a) showed that a 24 h deployment of 2.5 g of resin allowed concentrating quantifiable amounts of CTXs on SPATT samplers. The CTX levels varied with increasing deployment time, resin load, and surface area. In addition to CTXs, okadaic acid (OA) and dinophysistoxin-1 (DTX1) were also detected in SPATT extracts using liquid chromatography coupled to tandem mass spectrometry (LC-MS/MS), consistent with the presence of *Gambierdiscus* and *Prorocentrum* species in the environment, as assessed by quantitative polymerase chain reaction (qPCR) and high-throughput sequencing (HTS) metabarcoding analyses conducted on passive window screen (WS) artificial substrate samples. Although these preliminary findings await further confirmation in follow-up studies, they highlight the usefulness of SPATT samplers in the routine surveillance of CP risk on a temporal scale, and the monitoring of other phycotoxin-related risks in ciguatera-prone areas.

Keywords: ciguatera monitoring; *Gambierdiscus*; ciguatoxins; SPATT passive samplers; HP20 resin; CBA-N2a; LC-MS/MS; WS artificial substrate; qPCR; HTS metabarcoding

Key Contribution: SPATT technology allowed the detection of CTXs, OA, and DTX1 in samples from Anaho Bay, French Polynesia, consistent with concomitant reports of the occurrence of *Gambierdiscus* and *Prorocentrum* species in the area. The deployment of 44 cm^2 SPATT devices filled with 2.5 g of HP20 resin for 24 h allowed the highlighting of the circulation of dissolved CTXs in this well-known ciguatera hotspot. These preliminary results suggest that increasing both the deployment time and resin load could be useful when monitoring areas with a moderate-to-low CP risk.

1. Introduction

Harmful algal blooms (HABs) cause major sanitary, environmental, and economic problems in many aquatic environments worldwide [1]. Numerous countries thus maintain routine monitoring programs for the early detection of HAB events and the presence of associated toxins in order to mitigate the associated impacts. Most of these programs are based on the direct monitoring of potentially toxic microalgal and cyanobacterial species and qualitative/quantitative analyses of toxins accumulated in marine products intended for human consumption [2,3]. Since 2004, the Solid Phase Adsorption Toxin Tracking (SPATT) technique, which enables the passive sampling of dissolved toxins present in the water column associated with episodic HAB events, has increased in popularity as a complementary method [4]. Numerous laboratory- and field-based studies have demonstrated the ability of this technique to detect a large array of lipophilic and hydrophilic toxins produced by various microalgae and cyanobacteria, in both marine and freshwater environments [5,6]. SPATT samplers contain porous synthetic resins, and of the many adsorbent substrates tested to date, the DIAION® HP20 resin, an aromatic type adsorbent based on a cross-linked polystyrene matrix, appears to be the most versatile, and thus most used, substrate [6].

Ciguatera poisoning (CP) is a seafood-borne illness caused by the consumption of tropical marine seafood products (i.e., fish and invertebrate species) contaminated with ciguatoxins (CTXs) [7]. These polyether neurotoxins are produced by benthic dinoflagellates belonging to the genera *Gambierdiscus* and *Fukuyoa* [8]. Ciguatera is endemic to coral reef areas in the Caribbean Sea and Pacific and Indian Oceans [9]; however, its expansion into previously unaffected temperate regions has been documented since 2004 [10,11]. This rise of CP prevalence worldwide has prompted increased research efforts, most notably towards the improvement of current monitoring methods to predict and manage outbreaks. The suitability of SPATT samplers for the in situ monitoring of CTXs was recently assessed in a ciguatera hotspot in French Polynesia (Anaho Bay, Nuku Hiva Island, Marquesas archipelago) [12]. Previous studies in Anaho Bay have shown the recurrent presence of *Gambierdiscus* communities with the co-occurrence of at least five species and the predominance of *G. polynesiensis* [13–15], a species known to be a high producer of Pacific CTXs (P-CTXs) [16,17]. Moreover, P-CTXs were detected in fish [13], as well as in trochus [14] and sea urchins [15] collected from Anaho Bay. Finally, both trochus and sea urchin specimens were recently involved in atypical CP cases [15,18]. P-CTXs were successfully detected in methanol extracts of SPATT devices containing 10 g of HP20 resin, following a two-day deployment in Anaho Bay in July 2015 [12]. The presence of P-CTXs in these samplers was concomitant with the observation of *Gambierdiscus polynesiensis* populations [15], as well as the detection of P-CTXs in sea urchins [15]. These results confirmed the potential of SPATT technology as a passive environmental surveillance tool to support CP risk assessments and management programs, particularly in areas at high risk of ciguatera [12]. SPATT samplers—which are known for their relatively low cost as well as simplicity of preparation, deployment, transport, and storage [19]—appear well-suited for monitoring CTXs in remote and widely dispersed island locations, such as Nuku Hiva Island, and, more globally, other Pacific Islands Countries and Territories (PICTs), whose populations are the most vulnerable to CP [20].

The present work is a follow-up study to previous investigations conducted by Roué, et al. [12] in the Anaho Bay. To this end, two successive field experiments were conducted in the same study site using SPATT technology in an attempt to (i) follow the dissolved CTX trend in the environment over a 22 month period, and (ii) study the effects of different deployment times and device formats (i.e., resin load and surface of exposure) on the overall adsorption efficacy of SPATT samplers towards CTXs. Practically, SPATT devices of various surface areas, filled with 2.5 or 5 g of HP20 resin, were deployed in Anaho Bay in November 2016 and August 2018 for one, three, or six days. The levels of CTXs in methanol extracts were assessed using the mouse neuroblastoma cell-based assay (CBA-N2a), and the identity of congeners was determined using liquid chromatography coupled to tandem mass spectrometry (LC-MS/MS). In parallel, the abundance of specific *Gambierdiscus* species in Anaho Bay was assessed through quantitative polymerase chain reaction (qPCR) assays conducted on passive window screen (WS) artificial substrate samples. Finally, in order to further characterize the potential human

health risks associated with the consumption of marine products from Anaho Bay, the composition of benthic dinoflagellate assemblages and presence of related toxic compounds in this area were also assessed using the (i) high-throughput sequencing (HTS) metabarcoding of WS samples and (ii) LC-MS/MS based multi-toxin screening of SPATT samples, respectively.

2. Results

2.1. Molecular Analyses of Environmental Samples

Benthic/epiphytic dinoflagellate cells were collected from macroalgal substrates as well as WS artificial substrates during November 2016 and August 2018 field campaigns in Anaho Bay.

Microscopic observations revealed the presence of *Gambierdiscus*, *Ostreopsis*, and *Prorocentrum* cells on macroalgal substrates collected in November 2016, whereas only *Gambierdiscus* and *Ostreopsis* cells were observed in August 2018 (Table 1).

Semi-quantitative, species-specific qPCR assays were performed on WS samples to determine the *Gambierdiscus* spp. relative abundance and species distribution. A reduction in *Gambierdiscus* cell abundance was observed between November 2016 and August 2018, with *Gambierdiscus* cells no longer detected in the 2018 samples (Table 1). Among the five species detected in November 2016, *G. polynesiensis* was the dominant species, followed by *G. carpenteri* (Table 1).

Table 1. Dinoflagellate genera observed by light microscopy on macroalgal substrates and semi-quantitative polymerase chain reaction (qPCR) estimates of *Gambierdiscus* species composition identified from window screen (WS) samples, from Anaho Bay in November 2016 (n = 6 for each substrate) and August 2018 (n = 5 for each substrate).

Field Experiment	Dinoflagellate Genera Observed on Macroalgal Substrates	qPCR Analyses of Artificial WS Substrates	
		Cell Density of *Gambierdiscus* spp. [2]	*Gambierdiscus* Species Identification
November 2016 [1]	*Gambierdiscus* *Ostreopsis* *Prorocentrum*	~2900	*G. polynesiensis* (82%) *G. carpenteri* (17%) *G. caribaeus* (<1%) *G. pacificus* (<1%) *G. toxicus* (<1%)
August 2018	*Ostreopsis* *Gambierdiscus*	ND	ND

[1] Data from Darius, et al. [14]; [2] Density expressed in cells 150 cm^{-2}. ND = not detected.

In order to fully characterize the composition of benthic assemblages in *Gambierdiscus* and other HAB species, HTS metabarcoding analyses were carried out on artificial WS samples from August 2018. Sequencing targeting the large subunit ribosomal RNA (LSU) D1-D2 region generated between 27,069 and 97,610 Dinophyceae reads per sample after quality filtering, size trimming, and chimera detection (Table S1). Only 2% of the reads corresponded to *Gambierdiscus* species (Figure 1a), with four species identified: *G. polynesiensis* was the dominant species, representing 46% of *Gambierdiscus* reads, followed by *G. pacificus* (31%), *G. carpenteri* (22%), and *G. toxicus* (1%) (Figure 1b, Table S1). The most abundant Dinophyceae genus detected was *Ostreopsis*, representing nearly 48% of all Dinophyceae reads (Figure 1a), with three species identified: *O.* cf. *ovata*, *O.* cf. *lenticularis*, and *O.* cf. *rhodesiae* (Table S1).

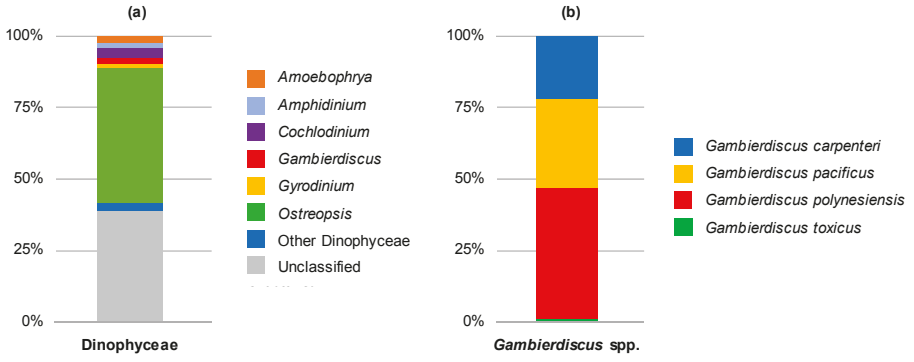

Figure 1. Relative abundances of (**a**) Dinophyceae reads at the genus level and (**b**) *Gambierdiscus* reads at the species level from window screen samples collected in Anaho Bay in August 2018 (n = 5). All the classified genera representing less than 1% of all Dinophyceae reads (Table S1) were identified as "other Dinophyceae".

In addition, other known toxin-producing genera were detected, e.g., *Amphidinium*, *Azadinium*, *Coolia*, *Dinophysis*, *Karenia*, and *Prorocentrum*, although the numbers of reads for these taxa were low (Table S1). Bayesian phylogenetic analyses showed that all taxa classifications using the custom dinoflagellate sequence databases were correct, although the short sequences (approximately 350 bp) were not able to resolve some deeper phylogenetic relationships (Figure S1). Some taxa were able to be classified to the species level, in particular, *Gambierdiscus* spp., while other groups could not be successfully resolved. For example, some *Ostreopsis* spp. and *Amphidinium* spp. were not able to be assigned to specific species (Figure S1) either because they represent undescribed species or species that are not present in the GenBank database. Therefore, some taxa have been assigned to the genus-level only, or "cf." has been used to indicate some uncertainty with the classification.

2.2. Evaluation of SPATT Samples Toxicity Using CBA-N2a

Regardless of the resin load (2.5 or 5 g of HP20 resin), deployment time (1, 3, or 6 days), or surface area (44 or 71 cm^2) of the SPATT devices deployed in Anaho Bay in November 2016 and August 2018, all methanol extracts were found to be toxic toward neuroblastoma (N2a) cells, with activity typical for CTXs: cytotoxic effects were observed in the presence of ouabain (O) and veratridine (V) (i.e., OV^+ conditions), whereas no cytotoxicity was detected in the absence of O and V (i.e., OV^- conditions) (Figure 2).

Mean half-maximal effective concentration (EC_{50}) values ranging from 614 ± 123 to 6319 ± 1237 pg of dry extract μL^{-1} were obtained. These raw EC_{50} values were then converted into quantities of resin (ng HP20 resin equiv. μL^{-1}) to be further compared with each other whatever the amount of resin used (i.e., 2.5 or 5 g), which ranged from 270 ± 51 to $1.5 \times 10^4 \pm 0.5 \times 10^4$ ng HP20 resin μL^{-1} (Table 2). Corresponding toxin contents were estimated at between 0.14 ± 0.04 and 7.0 ± 1.2 ng P-CTX3C equiv. g^{-1} HP20 resin (Table 2).

When the toxin contents were calculated according to the total quantity of resin per SPATT device, i.e., 2.5 or 5 g, these toxin contents varied from 0.34 ± 0.10 to 23.5 ± 3.2 ng P-CTX3C equiv. $SPATT^{-1}$ (Figure 3). The toxicity data indicated a significant decrease ($p < 0.0001$) in CTX levels in Anaho Bay in 2018 compared to 2016; indeed, the amounts of CTXs detected on SPATT devices from August 2018 were 10- to 34-fold lower than those from November 2016, for a deployment time of 24 h and resin loads of 5 and 2.5 g, respectively (Figure 3).

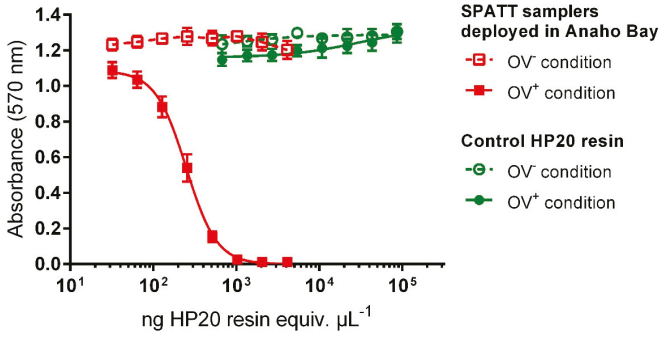

Figure 2. Dose–response curves for neuroblastoma (N2a) cells exposed, in the absence (OV^- condition) and presence (OV^+ condition) of ouabain and veratridine, to increasing concentrations of methanol extracts (expressed in pg dry extract μL^{-1} and then converted to ng HP20 resin equiv. μL^{-1}) from control HP20 resin or Solid Phase Adsorption Toxin Tracking (SPATT) devices (n = 3) filled with 2.5 g of HP20 resin and deployed for three days in Anaho Bay in November 2016. Data represent the means ± standard errors (SE) of values obtained from three independent neuroblastoma cell-based assays (CBA-N2a), each point run in triplicate.

Table 2. Mean half-maximal effective concentration (EC_{50}) values (CBA-N2a) and toxin content estimates for SPATT devices deployed in Anaho Bay in November 2016 and August 2018.

Field Experiment	Deployment Time (days)	Resin Load (g)	Surface of Exposure (cm^2)	EC_{50} [1] (ng HP20 Resin Equiv. μL^{-1})	Toxin Content (ng P-CTX3C Equiv. g^{-1} HP20 Resin)
November 2016	1	2.5	44	410 ± 78	4.6 ± 0.9
		5		486 ± 52	3.8 ± 0.4
	3	2.5		270 ± 51	7.0 ± 1.2
		5		381 ± 44	4.9 ± 0.6
August 2018	1	2.5	44	14,611 ± 4817	0.14 ± 0.04
		5		4937 ± 966	0.38 ± 0.08
	6	2.5	44	4589 ± 149	0.40 ± 0.01
			71	3661 ± 1391	0.54 ± 0.21
		5	44	2290 ± 410	0.82 ± 0.14
			71	1095 ± 95	1.7 ± 0.2

[1] Data represent the mean ± SE of values obtained from two or three different SPATT devices, each tested in two to three independent CBA-N2a experiments.

Concerning the effect of resin load, whatever the period of study, time of deployment, and surface of exposure, the use of 5 g of HP20 resin led to the adsorption of 1.4- to 6.2-fold higher levels of CTXs compared with a resin load of 2.5 g (Figure 3).

As for the deployment time, 44 cm^2 SPATT devices deployed for three and six days accumulated 1.3- to 1.5- and 2.1- to 2.3-fold more CTXs than the ones deployed for one day, respectively, with the highest increases with deployment duration being observed for resin loads of 2.5 g (Figure 3).

Finally, regarding the sampler surface (only tested in 2018), after six days of deployment, the amounts of CTXs contained in larger SPATT devices were found to be 1.7- and 2.1-fold higher than in smaller SPATT samplers for resin loads of 2.5 and 5 g, respectively (Figure 3).

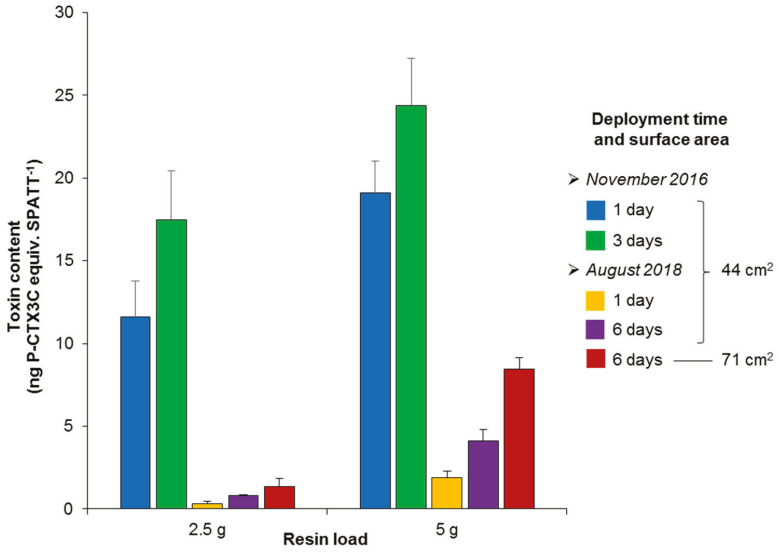

Figure 3. Toxin contents adsorbed on SPATT devices deployed in Anaho Bay in November 2016 and August 2018, based on the CBA-N2a data detailed in Table 1. Error bars represent SE.

2.3. Characterization of Toxins Adsorbed by HP20 Resin Using LC-MS/MS

All methanol extracts from SPATT devices deployed in Anaho Bay in November 2016 and August 2018 were analyzed using a LC-MS/MS based multi-toxin screening approach, leading to the detection of two groups of marine toxins. The presence of P-CTXs was confirmed in all samples, although at non-quantifiable concentrations (limit of quantification of P-CTX3C: 6 ng/mL). Two uncharacterized P-CTX3C isomers, consistently present in methanol extracts of TB92—a highly toxic strain of *Gambierdiscus polynesiensis* (Figure 4a)—were also detected in SPATT samples collected in November 2016 and August 2018 (Figure 4b,c), whereas P-CTX3B was found only in November 2016 samples (Figure 4b).

Among the other toxins sought, okadaic acid (OA) and dinophysistoxin-1 (DTX1) were also detected in all SPATT devices for OA, depending on the deployment time for DTX1 (Figure 5).

The toxin contents of OA per SPATT device ranged from 3.3 to 47.0 ng OA SPATT^{-1} (Table 3). For similar conditions, an increase in the time of exposure, resin load, or surface area led to 1.4- to 5.6-, 1.4- to 2.9-, or 1.4- to 1.9-fold higher levels of OA, respectively (Table 3). For a 24 h deployment time, a 3-fold decrease in OA contents was observed between November 2016 and August 2018.

Low toxin contents of DTX1 per SPATT device were detected, ranging from 2.0 to 6.9 ng DTX1 SPATT^{-1}, provided that SPATT devices were deployed for at least three days (Table 3). As observed for OA, the highest level of DTX1 was detected after six days of exposure in August 2018 using 71 cm^2 SPATT devices filled with 5 g of HP20 resin.

None of the other marine biotoxins sought (see Section 5.6 for details) were detected through LC-MS/MS multi-toxin screening analyses.

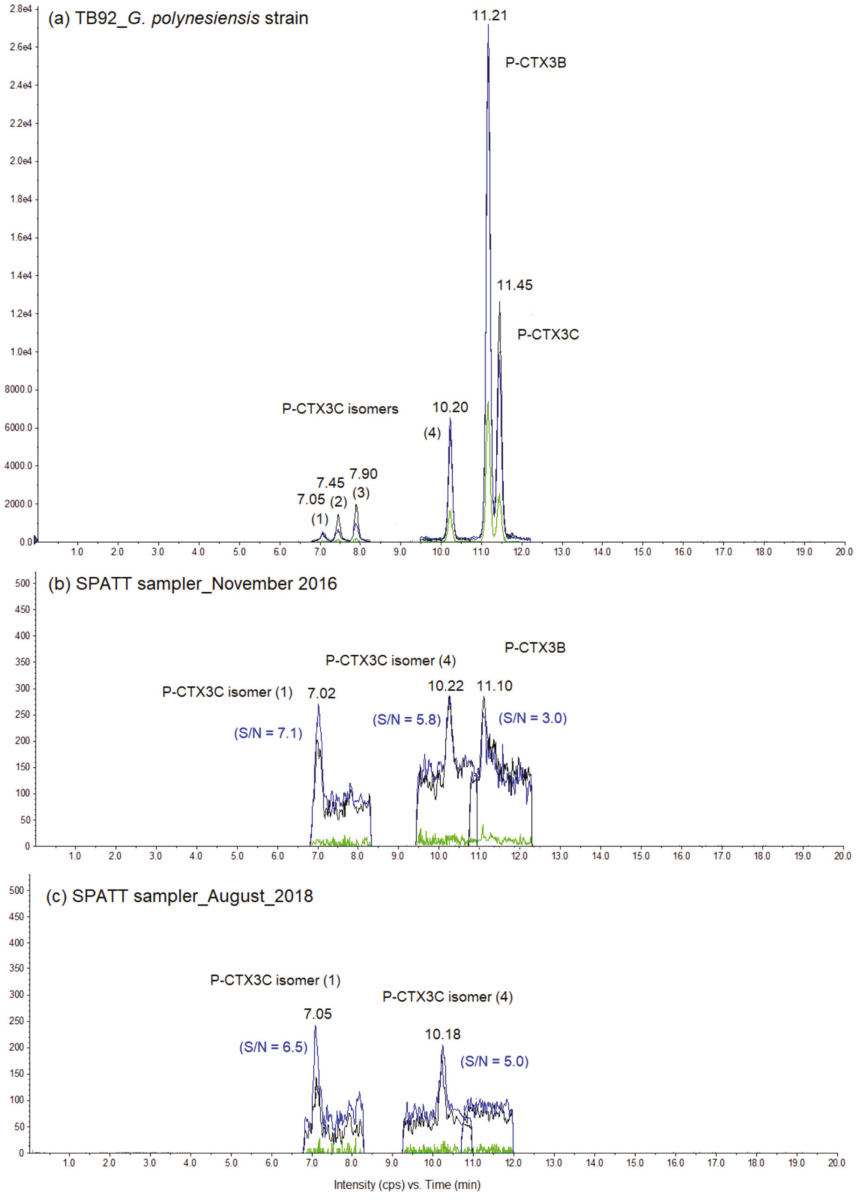

Figure 4. Liquid chromatography coupled to tandem mass spectrometry (LC-MS/MS) chromatograms of methanol extracts from (**a**) TB92-*Gambierdiscus polynesiensis* strain, and (**b**,**c**) SPATT devices filled with 5 g of HP20 resin and deployed for 24 h in Anaho Bay in November 2016 and August 2018, respectively. Chromatograms were acquired in positive scheduled multi-reaction mode (MRM) mode with a retention window of 90 sec, representing the MRM transitions of P-CTX3B/C at *m/z* 1023.5 > 1005.6 (in blue), 1040.6 > 1005.6 (in black), and 1023.6 > 125.1 (in green). The signal-to-noise (S/N) was calculated with three standard deviations for the *m/z* transition 1023.6 > 1005.6. The two potential P-CTX3C isomers were tentatively identified on the basis of two MRM transitions and the correct retention time of these isomers compared to that of the highly toxic *G. polynesiensis* strain TB92.

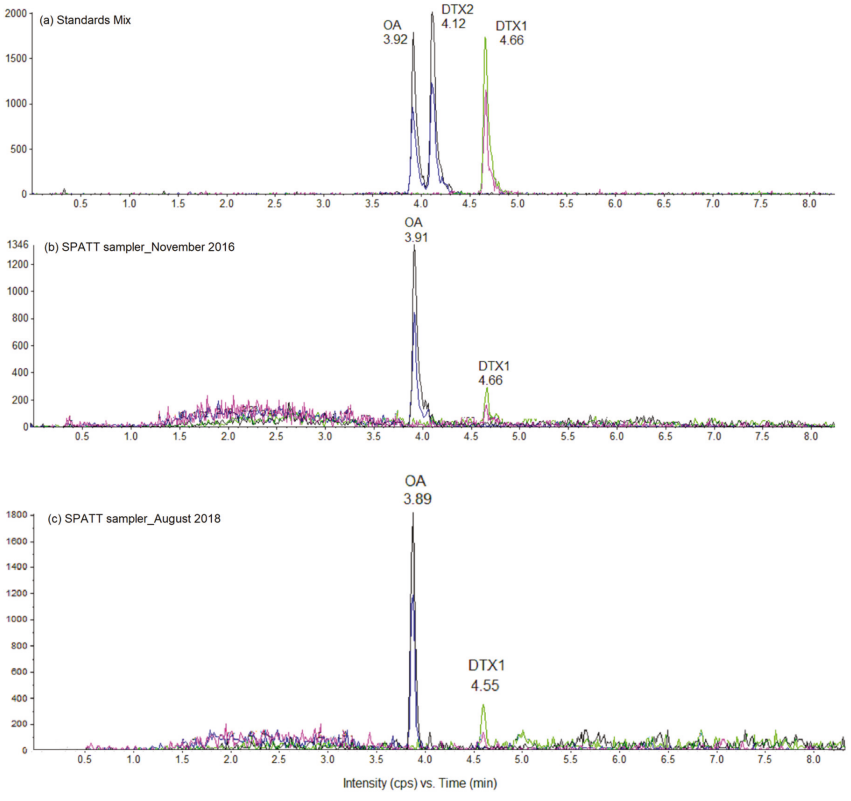

Figure 5. LC-MS/MS chromatograms of (**a**) okadaic acid (OA), dinophysistoxin-1 (DTX1), and dinophysistoxin-2 (DTX2) standards mix solution (NRC certified reference material); and (**b**,**c**) methanol extracts from SPATT devices filled with 5 g of HP20 resin and deployed in Anaho Bay for three days in November 2016 and for six days in August 2018, respectively. Chromatograms were acquired in negative MRM mode on *m/z* transitions 803.4 > 255.1 (black) and 803.4 > 113.5 (blue) for OA and its analog DTX2, as well as on *m/z* transitions 817.5 > 257.9 (green) and 817.5 > 112.9 (pink) for DTX1.

Table 3. Estimated OA and DTX1 contents in SPATT devices deployed in Anaho Bay in November 2016 and August 2018, based on LC-MS/MS data.

Field Experiment	Deployment Time (Days)	Resin Load (g)	Surface of Exposure (cm^2)	Toxin Content [1] (ng Toxin $SPATT^{-1}$) OA	DTX1
November 2016	1	2.5	44	9.0 ± 1.6	ND [2]
		5		21.3 ± 4.3	ND
	3	2.5		13.0 ± 1.3	ND
		5		37.0 ± 13.0	4.2 ± 1.6
August 2018	1	2.5	44	3.3 ± 0.1	ND
		5		6.2 ± 0.8	ND
	6	2.5	44	18.6 ± 0.2	2.1 ± 0.5
			71	25.4 ± 1.3	2.0 ± 0.1
		5	44	25.4 ± 6.4	3.1 ± 0.8
			71 [3]	47.0	7.0

[1] Data represent the mean ± SE of values obtained from two or three different SPATT devices and are expressed in ng of toxin per SPATT device; [2] ND: not detected; [3] Only one SPATT device was analyzed.

3. Discussion

3.1. Benthic Harmful Algae Populations and Toxin Profiles over Time in Anaho Bay

This study confirmed the ciguateric status of Anaho Bay. Indeed, the CBA-N2a toxicity data showed that dissolved CTXs previously detected on SPATT samplers deployed in the area in July 2015 [12] were still present in the water column at decreasing, yet quantifiable, amounts in November 2016 and August 2018. Molecular analyses of WS samples showed that *G. polynesiensis*, a species known to be highly toxic [16,17], was the dominant *Gambierdiscus* species both in November 2016 [14] and August 2018, although the abundance of total *Gambierdiscus* cells was low, especially in August 2018. The concentrations of CTXs detected on SPATT samplers after 24 h of deployment in August 2018 were significantly lower than in November 2016, consistent with the qPCR data for WS samples indicating a reduction in *Gambierdiscus* cells between November 2016 and August 2018. In addition, HTS metabarcoding analyses of environmental samples confirmed the very low abundance of *Gambierdiscus* in August 2018, in comparison with other dinoflagellate genera, in particular, *Ostreopsis*. Similarly, a two- to three-fold decrease in the levels of CTXs detected in locally sourced marine invertebrates was observed between November 2016 [14,15] and August 2018 (i.e., 0.15 and 0.19 ng P-CTX3C equiv. g^{-1} of tissue for sea urchins and trochus, respectively; unpublished data). Finally, the LC-MS/MS data showed that P-CTX3B, as well as two uncharacterized P-CTX3C isomers (tentative identification), were detected on SPATT devices deployed in November 2016, whereas only the two potential P-CTX3C analogs were present in the August 2018 samples. The detection of fewer CTX analogs in the SPATT devices in August 2018 vs. November 2016 could be due to the lower levels of total P-CTXs, as confirmed by the CBA-N2a results. As observed for trochus or sea urchin, the number of analogs detected decreased when the amount of total P-CTXs decreased [14,15]. Another explanation could be that uncharacterized P-CTX3C analogs are more stable in the water column and thus take longer to degrade than P-CTX3B; however, this hypothesis still needs to be confirmed.

The LC-MS/MS multi-toxin screening approach resulted in the detection of dissolved OA and DTX1 in Anaho Bay for the first time (in both November 2016 and August 2018). This result is consistent with the concomitant detection of *Prorocentrum* cells, by both microscopic observation and HTS metabarcoding analyses of environmental samples, although at very low abundance at the time of the field campaigns. Dinoflagellates of the genus *Prorocentrum* are potential producers of diarrheic shellfish poisoning (DSP) toxins [21]. Traces of *Dinophysis*, another potential producer of DSP toxins [21], were also detected in Anaho Bay in August 2018 using HTS metabarcoding. The low levels of OA and DTX1 (ng order) detected on the SPATT devices are consistent with the low number of reads detected for *Prorocentrum* (0.35%) and the very low number of reads detected for *Dinophysis* (0.03%). In bloom scenarios, much higher concentrations of OA-group toxins are typically detected in such SPATT devices, e.g., as was the case in France in 2016 [22]. The low concentrations of OA-group toxins are coherent with the low numbers of *Prorocentrum* cells in Anaho Bay, and it is not clear whether these were in decline, similarly to *Gambierdiscus* cells, or had been low over longer periods. In any case, the presence of OA and DTX1 in Anaho Bay may have contributed to the gastrointestinal symptoms reported by patients following the consumption of marine invertebrates from Anaho Bay [15,18], even though detectable amounts of these two toxins could not be positively confirmed in trochus and sea urchins analyzed one month after the poisoning occurred [14,15].

Conversely, neither palytoxin nor its analogs (i.e., ovatoxins) were found in SPATT samples by LC-MS/MS despite the high predominance of *Ostreospsis* spp. in Anaho Bay. This result is consistent with recent findings that both *O. lenticularis* [23] and *O.* cf. *ovata* (pers. comm., M. Chinain and D. Réveillon) strains from French Polynesia show no toxicity (as assessed by CBA-N2a and LC-MS/MS analyses), whereas strains of both species were found to be toxic in the Caribbean and Mediterranean regions [21,24]. However, the reporting of other potentially toxic HAB genera, such as *Amphidinium*, *Azadinium*, *Coolia*, *Karenia*, and *Ostreopsis* [21] in Anaho Bay emphasizes the importance of extending the environmental surveillance in this CP-endemic area to toxin groups other than CTXs.

Using the LC-MS/MS multi-toxin screening approach, several other biotoxin groups were screened for but were not detected, because of either the absence or low levels of the producing dinoflagellates in Anaho Bay. As an example, the non-detection of cyclic imines and azaspiracids is consistent with the very low number or absence of metabarcoding reads for the genera *Alexandrium*, *Azadinium*, *Karenia*, and *Vulcanodinium* (0% to 0.01% of the total Dinophyceae reads).

3.2. Effects of Deployment Time on the Efficacy of CTX Detection

To date, there is no consensus about the minimum/optimal deployment time of SPATT devices in the field and, as highlighted by Kudela [5], the deployment duration usually depends on the research or monitoring design of the programs. The present study provides some preliminary data about the potential of SPATT samplers to adsorb different amounts of CTXs under varying deployment times. In most of the field studies reported in the literature, SPATT samplers were deployed for one week [25–30], but sometimes for longer periods (up to one month) [31,32]. However, from a practical point of view, a deployment time of several days/weeks may be difficult or even impossible to implement, most notably in remote areas that are difficult to access, as is the case for Anaho Bay or many ciguatera-prone areas in PICTs. In the present study, using a highly sensitive detection method such as the CBA-N2a, the results showed that CTXs could be detected on SPATT samplers deployed in a long-standing ciguatera hotspot after only 24 h of deployment time. To the best of our knowledge, only one laboratory study has investigated the effect of different sorbent materials on SPATT adsorption efficiency [33], and two field studies have previously documented the successful monitoring of various toxin groups using limited deployment times; detectable amounts of OA, DTX1, yessotoxin (YTX), and pectenotoxins (PTXs) were found on HP20 SPATT devices deployed for only 3.5 h at Wedge point, New Zealand [4], while anatoxin-a and homoanatoxin-a were successfully detected on Strata-X^{TM} SPATT devices exposed for only 4 h in Waipoua River, New Zealand [34].

Most importantly, using longer deployment times—i.e., three and six days—led to the adsorption of higher levels of CTXs onto HP20 resin. However, the highest level of CTXs adsorbed per gram of HP20 resin (i.e., 7 ng P-CTX3C equiv. g^{-1} HP20 resin) was nearly 8-fold lower than the saturation rate previously determined under laboratory conditions by Roué, et al. [12] (i.e., 55 ng P-CTX3C equiv. g^{-1} HP20 resin for a deployment of 10 g of HP20 resin during 48 h in an in vitro culture of TB92, a highly toxic *G. polynesiensis* strain). These findings suggest that SPATT devices deployed in Anaho Bay could potentially have retained higher amounts of CTXs if they had been deployed for a longer period, provided the presence of higher concentrations of CTXs in the environment. Likewise, the results also showed an increase in OA adsorption with increasing deployment times but with maximum levels per gram of HP20 resin lower than those reported in other studies [22,29], suggesting the limit of saturation of the SPATT has not been reached in the field experiments.

The results from the present study showed that a time of exposure of at least three days was necessary to detect DTX1. A previous study had already demonstrated a linear increase in the quantities of several polyether biotoxins adsorbed by HP20 resin for at least the first eight days of exposure at Wedge point, New Zealand [4]. Taken together, all these observations are consistent with laboratory studies suggesting that HP20 resin is a slow accumulator of various toxins as compared with other adsorbent substrates (e.g., Sepabeads®, Oasis® HLB, or Strata-X resins) and is thus more appropriate for long exposure periods [33,35,36]. Consequently, when low concentrations of toxins are expected to circulate in the water column (i.e., in areas with low-to-moderate CP risk), using longer deployment times (i.e., ≥1 week) could prove useful for increasing the detectability of toxins. Similarly to other kinetic samplers, if the uptake kinetic of SPATT devices is faster than their offload kinetic, toxin adsorption would increase linearly under prolonged exposure [5]. However, this is not a general rule for all toxins; for example, a fast desorption rate of paralytic shellfish poisoning (PSP) toxins from SP700 resin was observed in toxin-free seawater, indicating that for these hydrophilic toxins, the field deployment of SPATT samplers should not exceed seven days to avoid toxin loss [37]. Furthermore, it should be noted that a longer deployment time is likely to increase biofouling on SPATT devices,

thus reducing water flow through the resin and toxin adsorption, although biofouling may play less of a role in tropical oligotrophic areas than in temperate eutrophic areas.

3.3. Effects of Resin Load on the Efficacy of CTX Detection

No consensus currently exists on the minimal/optimal resin load to use in SPATT samplers. In the literature, the resin loads tested in the different studies ranged from 0.3 g [22,33] to 10 g [12,27], although the amount most commonly used is between 3 and 5 g [4,25,28,30–32,36]. To the best of our knowledge, only one field-study by Zendong, et al. [22], conducted in the Mediterranean Sea, has compared the efficacy of SPATT devices to detect several lipophilic phycotoxins when filled with different resin loads (i.e., 0.3, 3, and 10 g of HP20 resin). The authors concluded that 3 g of resin offered the best compromise in terms of cost (lesser resin and solvent consumption), adsorption capacity, and efficacy (lesser potential for clogging) [22]. They noted that the 69 cm^2 exposure surface used in their study was insufficient to avoid the superimposition of resin particles for a 10 g resin load, leading to a decrease in toxin adsorption efficiency. The results obtained in the present study are thus consistent with previous findings by Zendong et al. [22], as SPATT devices filled with 5 g of HP20 resin always led to the adsorption of higher levels of P-CTXs, OA, and DTX1 per device than with 2.5 g. The same observation applies when larger devices were used, i.e., 71 vs 44 cm^2. These findings suggest that the contact surface between resin and seawater was relatively well optimized in the 44 cm^2 SPATT samplers filled with 2.5 g and that 71 cm^2 devices should be used for resin loads of 5 g in order to allow a better distribution of the resin (or higher surface/resin weight ratio) and thus a higher toxin adsorption.

4. Conclusions

This study provides preliminary data on the modular use of the SPATT technique (HP20 resin)—i.e., different deployment time, resin loads and surface areas—for the in situ monitoring of CTXs in CP-prone areas, as well as the survey of additional HAB-related toxin groups potentially present in ciguateric biotopes. In the Anaho ciguatera hotspot, the deployment of 44 cm^2 SPATT devices filled with 2.5 g of HP20 resin for only 24 h allowed the assessment of a decrease in CTX concentrations over a 22 month time period. The results obtained over longer deployment times led us to speculate that in areas where the ciguatera risk is unknown or considered low-to-moderate, increasing the amount of resin and time of deployment could help improve toxin detection, provided the surface of the device is optimized to avoid resin clogging. From a practical point of view, it is suggested that when the concentrations of dissolved toxins are potentially low, the deployment of 71 cm^2 SPATT samplers filled with 5 g of resin for at least one week could be considered.

More widely, both the design of the passive sampler (e.g., adsorbent substrate, resin load, and device surface) and deployment times should be adapted to the characteristics of the study site (e.g., the accessibility, hydrodynamics, trophic state, and diversity of HAB communities) and the targeted toxin(s) (e.g., lipophilic or hydrophilic toxins). Similarly to that of other environmental passive samplers, the calibration of SPATT samplers is problematic and is perhaps the single greatest issue in current efforts to achieve better acceptance of this technology in HAB monitoring and management programs [5]. While waiting for the inclusion of this useful tool in the context of routine monitoring programs, the use of SPATT technology in combination with classic monitoring techniques (e.g., microalgal cell enumeration/identification or the quantification of toxins in fish/shellfish) should be strongly encouraged, in order to gain better knowledge of the extent of toxin contamination of aquatic environments.

5. Materials and Methods

5.1. Environmental Analyses

The study site is located in Anaho Bay (Nuku Hiva Island, Marquesas archipelago, French Polynesia; 08°49.171’ S, 140°03.923’ W). Anaho Bay is a remote area, difficult to access from the main

island of Tahiti (i.e., several hours' travel by plane, 4 × 4 car, and boat) and field campaigns cannot be regularly conducted.

Environmental samples of phytobenthos were collected from Anaho Bay in November 2016 and August 2018, using both natural (i.e., macroalgae) and artificial (i.e., window screen, WS) substrate methods, as previously described by Darius et al. [14]. The presence of *Gambierdiscus*, *Ostreopsis*, and *Prorocentrum* cells was assessed microscopically in macroalgal samples.

Semi-quantitative, species-specific qPCR assays were performed on WS samples to assess the relative cell abundance and distribution of the following *Gambierdiscus* species: *G. polynesiensis*, *G. toxicus*, *G. pacificus*, *G. australes*, *G. caribaeus*, and *G. carpenteri*, which are currently reported in French Polynesia, as well as four additional species/phylotypes, i.e., *G. belizeanus*, *G. carolinianus*, *G. ruetzleri*, and *Gambierdiscus* ribotype 2. The qPCR assays were performed using the protocol previously described in Vandersea et al. [38] and Darius et al. [14], with a sensitivity of detection of the assays established at approximately 10 cells, i.e., ranging from ≈ 20 to 5000 gene copy numbers depending on the species targeted [38]. The same procedure was followed for the taxonomic identification at the species level of the eight clonal cultures of *Gambierdiscus* further established from field samples.

Additionally, the WS samples collected in August 2018 were further analyzed using HTS metabarcoding, using primers targeting the LSU D1-D2 region, as previously described by Smith et al. [39]. Briefly, samples were centrifuged, and DNA was extracted from the pellets using Qiagen DNeasy PowerSoil kits (Qiagen, Carlsbad, CA, USA). The primers (D1R-F and D3B-R) were modified to include Illumina™ overhang adaptors. Libraries were prepared using the Illumina™ two-step PCR amplicon library preparation method and sequenced using an Illumina™ MiSeq sequencer with 2 × 250 bp paired-end reads at Auckland Genomics (University of Auckland, Auckland, New Zealand). All data generated were quality checked using the following tools: FastQC, FastQscreen, and SolexaQA [40]. Further analyses were carried out in Mothur v1.37.6 [41] as described by Smith et al. [42]. Phylogenetic analyses were carried out in Geneious® using MrBayes 3.1.2 [43].

5.2. HP20 Resin and SPATT Device Preparation

Adsorbent styrene-divinylbenzene resin (Diaion® HP20, Supelco, USA) was activated overnight by stirring at a low speed in methanol (MeOH) at a 10:1 ratio (mL g^{-1}). The HP20 resin was then filtered under vacuum using a fritted funnel and, subsequently, thoroughly rinsed with de-ionized (MilliQ) water to remove any methanol residues. The hydrated resin was kept in MilliQ water at a 10:1 ratio (mL g^{-1}) at 4 °C until the preparation of the SPATT devices.

SPATT samplers consisted of two layers of 100 µm nylon mesh filled with HP20 resin (2.5 or 5 g wet weight) and clipped between either two PVC circular disks (7.5 cm in diameter, corresponding to a surface of 44 cm^2) or embroidery frames (9.5 cm diameter, corresponding to a surface of 71 cm^2). SPATT devices were set up shortly before the field experiments (i.e., less than 1 week before) and were kept in MilliQ water at 4 °C until in situ deployment.

5.3. Field Deployments of SPATT Devices

On-site, SPATT devices were placed in plastic grids to prevent damage from fish grazing and then maintained in a vertical position in the water column using weights and floats. The deployment occurred near dead coral blocks colonized by macroalgae likely to shelter benthic *Gambierdiscus* cells, in locations with a moderate current to allow the circulation of seawater through the HP20 resin. Two series of experiments were conducted: one in November 2016, where 44 cm^2 SPATT devices were filled with 2.5 and 5 g of HP20 resin and retrieved after one or three days of deployment (Table 1); and the second one in August 2018, where 44 and 71 cm^2 SPATT devices were filled with 2.5 and 5 g of HP20 resin and retrieved after one or six days of deployment (Table 1). Each condition was tested in triplicate (n = 30 SPATT devices). A total of 6 samplers could not be retrieved due to damage or loss. Following collection, SPATT devices were stored at 4 °C in natural seawater until toxin extraction.

5.4. Toxin Extraction from HP20 Resin

Each SPATT device was rinsed thoroughly with MilliQ water, in order to remove any cell debris or epiphytes possibly adhering to the nylon mesh, and then carefully dismantled to retrieve the HP20 resin. Using a fritted funnel under vacuum, the resin was washed thoroughly with MilliQ water in order to eliminate salt residues. Toxins were extracted from HP20 resin with MeOH in a 10:1 ratio ($mL \cdot g^{-1}$). The resulting methanol extracts were dried under vacuum at 40 °C using a rotary evaporator (Rotavapor RII, Büchi, Switzerland) and stored at 4 °C until CBA-N2a or LC-MS/MS analyses.

5.5. Neuroblastoma Cell-Based Assay

Methanol extracts were screened for the presence of CTXs using the CBA-N2a assay performed following the protocol previously described by Darius et al. [14]. The final concentrations for ouabain/veratridine treatment (OV^+ conditions) ranged from 85/8.5 to 100/10 μM in order to obtain 90–100% of cell viability against control cells without ouabain/veratridine treatment (OV^- conditions). Each sample was tested in two or three independent experiments, with each concentration run in triplicate per plate. Methanol extracts were tested using a serial dilution at 1:2 of eight concentrations ranging from 74 to 9524 or 186 to 23,809 pg dry extract μL^{-1} for SPATT devices deployed in November 2016 or August 2018, respectively.

Absorbance data were fitted to a sigmoidal dose–response curve (variable slope) based on the four-parameter logistic model (4PL), allowing the calculation of raw EC_{50} values expressed in pg dry extract μL^{-1} using the Prism v6.07 software (GraphPad, San Diego, CA, USA). For a more convenient presentation of our results, the CBA-N2a curves and EC_{50} of samples were further converted into ng HP20 resin equiv. μL^{-1}. The calibration of the assay was achieved using a P-CTX3C reference material sourced from the Institut Louis Malardé (Papeete, French Polynesia) and that had been quantified gravimetrically. The EC_{50} value obtained for P-CTX3C was 1.84 ± 0.31 fg μL^{-1} (n = 5). The toxin contents (T) of samples were estimated using the formula T = (P-CTX3C EC_{50} / sample EC_{50}) and expressed in ng P-CTX3C equiv. g^{-1} HP20 resin. The toxin content per SPATT device was also estimated using the following formula: T × 2.5 or 5 g and expressed in ng P-CTX3C equiv. $SPATT^{-1}$. A Mann–Whitney test was applied to the CBA-N2a data using the Prism v6.07 software (GraphPad, San Diego, CA, USA) in order to compare all the toxin contents obtained in November 2016 vs. August 2018.

The maximum concentration of dry extract (MCE) that does not induce non-specific cytotoxic effects on N2a cells was assessed using a methanol extract obtained from 10 g of non-exposed activated HP20 resin. MCE was found to be higher than 1×10^4 pg dry extract μL^{-1}, corresponding to 1×10^5 ng HP20 resin equiv. μL^{-1} (Figure 1). The limit of quantification (LOQ) was thus estimated to be at 0.02 ng P-CTX3C equiv. g^{-1} HP20 resin.

5.6. Liquid Chromatography Coupled with Tandem Mass Spectrometry Analyses

LC-MS/MS analyses were conducted on methanol extracts for the detection of several marine biotoxin groups.

5.6.1. Detection Method for P-CTXs

P-CTX analysis [44] was carried out using an LC system (UFLC Nexera, Shimadzu, Kyoto, Japan) coupled to a hybrid triple quadrupole/ion-trap mass spectrometer (API4000Qtrap, Sciex, Redwood City, CA, USA) equipped with a turbo spray® interface. A C_{18} Zorbax Eclipse Plus column (1.8 μm, 50 × 2.1 mm, Agilent Technologies, Santa Clara, CA, USA) was employed at 40 °C and eluted at 400 μL min^{-1} with a linear gradient. Eluent A was water and Eluent B was methanol, with both eluents containing 2 mM ammonium formate and 50 mM formic acid. The elution gradient ran from 78% to 88% B over 10 min and was held for 4 min before re-equilibration over 5 min.

Mass spectrometric detection was operated in positive mode and using scheduled Multiple Reaction Monitoring (MRM) with a detection window of 90 s, with *m/z* values of the transitions listed

in Table 4. MRM experiments were established using the following electrospray ionization (ESI) parameters: curtain gas (CG) set at 25, ion spray (IS) at 5500 V, a turbogas temperature (T) of 300 °C, gas 1 (GS1) set at 40, and gas 2 (GS2) set at 60 psi, with an entrance potential (EP) of 10 V.

Data processing and analysis were achieved with the Analyst software (Sciex, Redwood City, CA, USA). Quantification was performed from a linear calibration curve generated from the P-CTX3C standard (Wako chemicals GmbH, Neuss, Germany) using the MRM transition $[M + H]^+/[M + H - H_2O]^+$. The LOD and LOQ for P-CTX3C were 2 and 6 ng mL^{-1}, respectively. For the comparison of retention times, an extract of TB92, a highly toxic *G. polynesiensis* strain provided by the Institut Louis Malardé (Papeete, French Polynesia), was injected in the sequence.

5.6.2. Detection Method for OA and DTXs

OA and DTXs are part of our analytical method for lipophilic toxins, performed in negative ionization mode. This analytical method grouped OA, DTXs, and yessotoxins (YTXs) and was carried out on the same instrument system as described above.

Chromatographic separation was carried out on a C_{18} Kinetex (50 × 2.1 mm, 2.6 µm, Phenomenex, Le Pecq, France), using a mobile phase composed of (A) water and (B) 95% acetonitrile, both containing 2 mM ammonium formate and 50 mM formic acid at a flow rate of 400 µL min^{-1} and maintained at 40 °C. The elution gradient ran from 10% to 50% B over 2 min, to 95% B over the next 4 min and was held for 2 min before re-equilibration.

MRM experiments were carried out in negative mode and the *m/z* selected are listed in Table 4. The ESI parameters were set as follows: CG, 20; IS, −4500 V; T, 550 °C; GS1, 40 psi; GS2, 50 psi; and EP, −13 V. Quantification was performed from linear calibration curves generated from certified standards of OA, DTX2, DTX1, and YTX (National Research Council, Ottawa, ON, Canada). The LOD and LOQ for the standards available were determined with the ordinary least-squares regression data method [45,46] (Table 4).

Table 4. List of selected *m/z* for the MRM experiments.

Compound	Pseudo Molecular Ion	MRM Transitions (*m/z*)	DP (V)	CE (eV)	LOD (ng mL^{-1})	LOQ (ng mL^{-1})
P-CTX1B	$[M + NH_4]^+$	1128.6/1093.6	105	20		
		1128.6/1075.6 [1]	105	30		
		1128.6/95.1	105	90		
P-CTX3C & P-CTX3B	$[M + NH_4]^+$	1040.5/1005.6	105	30		
	$[M + H]^+$	1023.6/1005.6 [1]	105	20	2	6
		1023.6/125.1	105	50		
P-CTX4A & P-CTX4B	$[M + NH_4]^+$	1078.6/1043.6	105	30		
	$[M + H]^+$	1061.6/1043.6 [1]	105	20		
		1061.6/125.1	105	50		
2,3-diOH-P-CTX3C	$[M + NH_4]^+$	1074.6/1039.6	105	30		
	$[M + H]^+$	1057.6/1039.6 [1]	105	20		
		1057.6/125.1	105	50		
51-OH-P-CTX3C	$[M + NH_4]^+$	1056.6/1021.6 [1]	105	30		
	$[M + H]^+$	1039.6/1021.6	105	20		
		1039.6/1003.6	105	20		
M-*seco*-P-CTX3C	$[M + H]^+$	1041.6/1023.6 [1]	105	30		
		1041.6/1005.6	105	20		
		1041.6/125.1	105	50		
P-CTX2 & P-CTX3	$[M + NH_4]^+$	1112.6/1077.6	105	20		
		1112.6/1059.6 [1]	105	30		
		112.6/95.1	105	90		
2-OH-P-CTX3C & 3-OH-P-CTX3C	$[M + NH_4]^+$	1058.6/1023.6 [1]	105	30		
		1058.6/1005.6	105	20		
		1058.6/125.1	105	50		

Table 4. *Cont.*

Compound	Pseudo Molecular Ion	MRM Transitions (*m/z*)	DP (V)	CE (eV)	LOD (ng mL^{-1})	LOQ (ng mL^{-1})
OA	[M – H]$^-$	803.4/255.1 [1]	−170	−62	1	3
		803.4/113.1	−170	−92		
DTX2	[M – H]$^-$	803.4/255.1 [1]	−170	−62	1	3
		803.4/113.1	−170	−92		
DTX1	[M – H]$^-$	817.5/255.1 [1]	−170	−68	1	3
		817.5/113.1	−170	−92		
YTX	[M – H]$^-$	1141.4/1061.6 [1]	−120	−48	1	3
		1141.4/855.6	−120	−98		
Homo-YTX	[M – H]$^-$	1155.5/1075.6 [1]	−120	−48		
		1155.5/869.4	−120	−98		
45-OH YTX	[M – H]$^-$	1157.5/1077.5 [1]	−120	−48		
		1157.5/855.5	−120	−98		
45-OH homo YTX	[M – H]$^-$	1171.5/1091.5 [1]	−120	−48		
		1171.5/869.4	−120	−98		
COOH YTX	[M – H]$^-$	1173.5/1093.5 [1]	−120	−48		
		1173.5/855.5	−120	−98		
Homo COOH YTX	[M – H]$^-$	1187.5/1107.5 [1]	−120	−48		
		1187.5/869.4	−120	−98		

[1] MRM transition used for quantification in each method.

5.6.3. Detection Methods for Other Toxins

In addition, quantitative targeted analyses (MRM mode) were conducted following the methods previously described for some of the other major marine biotoxin groups: (i) lipophilic toxins, i.e., pectenotoxins (PTXs) and azaspiracids (AZAs) [47]; (ii) cyclic imines, i.e., gymnodimins (GYMs), spirolids (SPXs), and pinnatoxins (PnTXs) [47]; (iii) palytoxin-like toxins, i.e., palytoxin (PLTX), 42-hydroxy-palytoxin (42-OH-PLTX), and ovatoxins (OvTXa to OvTXh) [48]; (iv) maitotoxins (MTX1 to MTX4) [49]; and (v) cyanotoxins, i.e., microcystins (dm-MC-RR, MC-RR, MC-YR, MC-LR, dm-MC-LR, MC-LA, MC-LY, MC-LW, and MC-LF) and nodularin (NOD) [50].

Supplementary Materials: The following are available online at http://www.mdpi.com/2072-6651/12/5/321/s1, Table S1: Read number and classification levels at 98% identity for the large subunit ribosomal RNA gene region from each window screen sample collected from Anaho Bay (Nuku Hiva Island, French Polynesia) in August 2018. Figure S1: Phylogenetic analysis of large subunit ribosomal DNA (D1-D2 region) sequences obtained from the high-throughput sequencing metabarcoding using Bayesian analyses. Sequences in grey represent the consensus sequence from all reads of each taxonomic assignment. Values at nodes represent Bayesian posterior probability support. Scale bar is substitutions per site.

Author Contributions: Conceptualization, M.R. and M.C.; Data curation, M.R., K.F.S., M.S., P.H. and M.C.; Field experiments, M.R., K.H., A.U. and M.C.; Formal analysis, M.R., K.F.S., M.S., J.V. and L.B.; Funding acquisition, M.R. and M.C.; Methodology, M.R., K.F.S., M.S., J.V., K.H., A.U. and L.B.; Supervision, M.R.; Validation, M.R., K.F.S., P.H., H.T.D. and M.C.; Writing—original draft, M.R., K.F.S., M.S. and M.C.; Writing—review & editing, M.R., K.F.S., M.S., L.B., P.H., H.T.D. and M.C. All authors have read and agreed to the published version of the manuscript.

Funding: The present work was supported by funds from France and French Polynesia in the framework of the "CARISTO-Pf" (no. 7937/MSR/REC of 4 December 2015 and Arrêté no. HC/491/DIE/BPT of 30 March 2016) and "CYANOTOX" (no. AFD CPF 1440 01 N of 22 December 2016) research programs, and from the New Zealand Ministry for Business, Innovation and Employment (no. CAWX1801).

Acknowledgments: The authors wish to thank Clémence Gatti and Taina Revel from Institut Louis Malardé for their technical assistance in field experiments and qPCR analyses, respectively, as well as the two anonymous reviewers whose comments greatly helped improve the manuscript.

Conflicts of Interest: The authors declare no conflict of interest. The funders had no role in the design of the study; in the collection, analyses, or interpretation of data; in the writing of the manuscript; or in the decision to publish the results.

References

1. Kudela, R.M.; Berdalet, E.; Bernard, S.; Burford, M.; Fernand, L.; Lu, S.; Roy, S.; Tester, P.A.; Usup, G.; Magnien, R.; et al. *Harmful Algal Blooms: A Scientific Summary for Policy Makers*; International Society for the Study of Harmful Algae (ISSHA) and Intergovernmental Oceanographic Commission (IOC) of UNESCO: Paris, France, 2015.
2. Doucette, G.J.; Kudela, R.M. In situ and real-time identification of toxins and toxin-producing microorganisms in the environment. *Compr. Anal. Chem.* **2017**, *78*, 411–443. [CrossRef]
3. Abraham, A.; Rambla-Alegre, M. Marine toxins analysis for consumer protection. *Compr. Anal. Chem.* **2017**, *78*, 343–378. [CrossRef]
4. MacKenzie, L.; Beuzenberg, V.; Holland, P.; McNabb, P.; Selwood, A. Solid phase adsorption toxin tracking (SPATT): A new monitoring tool that simulates the biotoxin contamination of filter feeding bivalves. *Toxicon* **2004**, *44*, 901–918. [CrossRef] [PubMed]
5. Kudela, R.M. Passive sampling for freshwater and marine algal toxins. *Compr. Anal. Chem.* **2017**, *78*, 379–409. [CrossRef]
6. Roué, M.; Darius, H.; Chinain, M. Solid phase adsorption toxin tracking (SPATT) technology for the monitoring of aquatic toxins: A review. *Toxins* **2018**, *10*, 167. [CrossRef] [PubMed]
7. Soliño, L.; Costa, P.R. Global impact of ciguatoxins and ciguatera fish poisoning on fish, fisheries and consumers. *Environ. Res.* **2020**, *182*, 109111. [CrossRef]
8. Chinain, M.; Gatti, C.M.; Roué, M.; Darius, H.T. Ciguatera-causing dinoflagellates in the genera *Gambierdiscus* and *Fukuyoa*: Distribution, ecophysiology and toxicology. In *Dinoflagellates: Morphology, Life History and Ecological Significance*; Durvasula, S.R., Ed.; Nova Science Publishers: Hauppauge, NY, USA, 2020; in press.
9. Parsons, M.L.; Aligizaki, K.; Dechraoui Bottein, M.Y.; Fraga, S.; Morton, S.L.; Penna, A.; Rhodes, L. *Gambierdiscus* and *Ostreopsis*: Reassessment of the state of knowledge of their taxonomy, geography, ecophysiology, and toxicology. *Harmful Algae* **2012**, *14*, 107–129. [CrossRef]
10. Pérez-Arellano, J.-L.; Luzardo, O.P.; Pérez Brito, A.; Hernández Cabrera, M.; Zumbado, M.; Carranza, C.; Angel-Moreno, A.; Dickey, R.W.; Boada, L.D. Ciguatera fish poisoning, Canary Islands. *Emerg. Infect. Dis.* **2005**, *11*, 1981–1982. [CrossRef]
11. Otero, P.; Pérez, S.; Alfonso, A.; Vale, C.; Rodríguez, P.; Gouveia, N.N.; Gouveia, N.; Delgado, J.; Vale, P.; Hirama, M.; et al. First toxin profile of ciguateric fish in Madeira arquipelago (Europe). *Anal. Chem.* **2010**, *82*, 6032–6039. [CrossRef]
12. Roué, M.; Darius, H.T.; Viallon, J.; Ung, A.; Gatti, C.M.; Harwood, D.T.; Chinain, M. Application of solid phase adsorption toxin tracking (SPATT) devices for the field detection of *Gambierdiscus* toxins. *Harmful Algae* **2018**, *71*, 40–49. [CrossRef]
13. Darius, H.T.; Ponton, D.; Revel, T.; Cruchet, P.; Ung, A.; Tchou Fouc, M.; Chinain, M. Ciguatera risk assessment in two toxic sites of French Polynesia using the receptor-binding assay. *Toxicon* **2007**, *50*, 612–626. [CrossRef] [PubMed]
14. Darius, H.T.; Roué, M.; Sibat, M.; Viallon, J.; Gatti, C.M.; Vandersea, M.W.; Tester, P.A.; Litaker, R.W.; Amzil, Z.; Hess, P.; et al. *Tectus niloticus* (Tegulidae, Gastropod) as a novel vector of ciguatera poisoning: Detection of Pacific ciguatoxins in toxic samples from Nuku Hiva Island (French Polynesia). *Toxins* **2018**, *10*, 2. [CrossRef] [PubMed]
15. Darius, H.T.; Roué, M.; Sibat, M.; Viallon, J.; Gatti, C.M.; Vandersea, M.W.; Tester, P.A.; Litaker, R.W.; Amzil, Z.; Hess, P.; et al. Toxicological investigations on the sea urchin *Tripneustes gratilla* (Toxopneustidae, Echinoid) from Anaho Bay (Nuku Hiva, French Polynesia): Evidence for the presence of Pacific ciguatoxins. *Mar. Drugs* **2018**, *16*, 122. [CrossRef]
16. Chinain, M.; Darius, H.T.; Ung, A.; Cruchet, P.; Wang, Z.; Ponton, D.; Laurent, D.; Pauillac, S. Growth and toxin production in the ciguatera-causing dinoflagellate *Gambierdiscus polynesiensis* (Dinophyceae) in culture. *Toxicon* **2010**, *56*, 739–750. [CrossRef]
17. Longo, S.; Sibat, M.; Viallon, J.; Darius, H.T.; Hess, P.; Chinain, M. Intraspecific variability in the toxin production and toxin profiles of in vitro cultures of *Gambierdiscus polynesiensis* (Dinophyceae) from French Polynesia. *Toxins* **2019**, *11*, 735. [CrossRef]

18. Gatti, C.M.; Lonati, D.; Darius, H.T.; Zancan, A.; Roué, M.; Schicchi, A.; Locatelli, C.A.; Chinain, M. *Tectus niloticus* (Tegulidae, Gastropod) as a novel vector of ciguatera poisoning: Clinical characterization and follow-up of a mass poisoning event in Nuku Hiva Island (French Polynesia). *Toxins* **2018**, *10*, 102. [CrossRef]
19. MacKenzie, L.A. In situ passive solid-phase adsorption of micro-algal biotoxins as a monitoring tool. *Curr. Opin. Biotechnol.* **2010**, *21*, 326–331. [CrossRef]
20. Skinner, M.P.; Brewer, T.D.; Johnstone, R.; Fleming, L.E.; Lewis, R.J. Ciguatera fish poisoning in the Pacific Islands (1998 to 2008). *PLOS Negl. Trop. D* **2011**, *5*, e1416. [CrossRef]
21. Lassus, P.; Chomérat, N.; Hess, P.; Nézan, E. *Toxic and Harmful Microalgae of the World Ocean/Micro-Algues Toxiques et Nuisibles de L'océan Mondial*; IOC Manuals and Guides, 68; International Society for the Study of Harmful Algae (ISSHA) and Intergovernmental Oceanographic Commission (IOC) of UNESCO: Copenhagen, Denmark, 2016.
22. Zendong, Z.; Bertrand, S.; Herrenknecht, C.; Abadie, E.; Jauzein, C.; Lemée, R.; Gouriou, J.; Amzil, Z.; Hess, P. Passive sampling and high resolution mass spectrometry for chemical profiling of French coastal areas with a focus on marine biotoxins. *Environ. Sci. Technol.* **2016**, *50*, 8522–8529. [CrossRef]
23. Chomérat, N.; Bilien, G.; Derrien, A.; Henry, K.; Ung, A.; Viallon, J.; Darius, H.T.; Mahana iti Gatti, C.; Roué, M.; Hervé, F.; et al. *Ostreopsis lenticularis* Y. Fukuyo (Dinophyceae, Gonyaulacales) from French Polynesia (South Pacific Ocean): A revisit of its morphology, molecular phylogeny and toxicity. *Harmful Algae* **2019**, *84*, 95–111. [CrossRef]
24. Accoroni, S.; Totti, C. The toxic benthic dinoflagellates of the genus *Ostreopsis* in temperate areas: A review. *Adv. Oceanogr. Limnol.* **2016**, *7*, 1–15. [CrossRef]
25. Fux, E.; Bire, R.; Hess, P. Comparative accumulation and composition of lipophilic marine biotoxins in passive samplers and in mussels (*M. edulis*) on the West Coast of Ireland. *Harmful Algae* **2009**, *8*, 523–537. [CrossRef]
26. Pizarro, G.; Moroño, Á.; Paz, B.; Franco, M.J.; Pazos, Y.; Reguera, B. Evaluation of passive samplers as a monitoring tool for early warning of *Dinophysis* toxins in shellfish. *Mar. Drugs* **2013**, *11*, 3823–3845. [CrossRef] [PubMed]
27. García-Altares, M.; Casanova, A.; Bane, V.; Diogène, J.; Furey, A.; de la Iglesia, P. Confirmation of pinnatoxins and spirolides in shellfish and passive samplers from Catalonia (Spain) by liquid chromatography coupled with triple quadrupole and high-resolution hybrid tandem mass spectrometry. *Mar. Drugs* **2014**, *12*, 3706–3732. [CrossRef]
28. Gibble, C.M.; Kudela, R.M. Detection of persistent microcystin toxins at the land-sea interface in Monterey Bay, California. *Harmful Algae* **2014**, *39*, 146–153. [CrossRef]
29. Zendong, Z.; Kadiri, M.; Herrenknecht, C.; Nézan, E.; Mazzeo, A.; Hess, P. Algal toxin profiles in Nigerian coastal waters (Gulf of Guinea) using passive sampling and liquid chromatography coupled to mass spectrometry. *Toxicon* **2016**, *114*, 16–27. [CrossRef]
30. Hattenrath-Lehmann, T.K.; Lusty, M.W.; Wallace, R.B.; Haynes, B.; Wang, Z.; Broadwater, M.; Deeds, J.R.; Morton, S.L.; Hastback, W.; Porter, L.; et al. Evaluation of rapid, early warning approaches to track shellfish toxins associated with *Dinophysis* and *Alexandrium* blooms. *Mar. Drugs* **2018**, *16*, 28. [CrossRef]
31. McCarthy, M.; Bane, V.; García-Altares, M.; van Pelt, F.N.A.M.; Furey, A.; O'Halloran, J. Assessment of emerging biotoxins (pinnatoxin G and spirolides) at Europe's first marine reserve: Lough Hyne. *Toxicon* **2015**, *108*, 202–209. [CrossRef]
32. Li, F.-L.; Li, Z.-X.; Guo, M.-M.; Wu, H.-Y.; Zhang, T.-T.; Song, C.-H. Investigation of diarrhetic shellfish toxins in Lingshan Bay, Yellow Sea, China, using solid-phase adsorption toxin tracking (SPATT). *Food Addit. Contam. A* **2016**, *33*, 1367–1373. [CrossRef]
33. Zendong, Z.; Herrenknecht, C.; Abadie, E.; Brissard, C.; Tixier, C.; Mondeguer, F.; Séchet, V.; Amzil, Z.; Hess, P. Extended evaluation of polymeric and lipophilic sorbents for passive sampling of marine toxins. *Toxicon* **2014**, *91*, 57–68. [CrossRef]
34. Wood, S.A.; Holland, P.T.; MacKenzie, L. Development of solid phase adsorption toxin tracking (SPATT) for monitoring anatoxin-a and homoanatoxin-a in river water. *Chemosphere* **2011**, *82*, 888–894. [CrossRef] [PubMed]
35. Fux, E.; Marcaillou, C.; Mondeguer, F.; Bire, R.; Hess, P. Field and mesocosm trials on passive sampling for the study of adsorption and desorption behaviour of lipophilic toxins with a focus on OA and DTX1. *Harmful Algae* **2008**, *7*, 574–583. [CrossRef]

36. Lane, J.Q.; Roddam, C.M.; Langlois, G.W.; Kudela, R.M. Application of solid phase adsorption toxin tracking (SPATT) for field detection of the hydrophilic phycotoxins domoic acid and saxitoxin in coastal California. *Limnol. Oceanogr. Meth.* **2010**, *8*, 645–660. [CrossRef]
37. Rodríguez, P.; Alfonso, A.; Turrell, E.; Lacaze, J.-P.; Botana, L.M. Study of solid phase adsorption of paralytic shellfish poisoning toxins (PSP) onto different resins. *Harmful Algae* **2011**, *10*, 447–455. [CrossRef]
38. Vandersea, M.W.; Kibler, S.R.; Holland, W.C.; Tester, P.A.; Schultz, T.F.; Faust, M.A.; Holmes, M.J.; Chinain, M.; Wayne Litaker, R. Development of semi-quantitative PCR assays for the detection and enumeration of *Gambierdiscus* species (Gonyaulacales, Dinophyceae). *J. Phycol.* **2012**, *48*, 902–915. [CrossRef]
39. Smith, K.F.; Biessy, L.; Argyle, P.A.; Trnski, T.; Halafihi, T.; Rhodes, L.L. Molecular identification of *Gambierdiscus* and *Fukuyoa* (Dinophyceae) from environmental samples. *Mar. Drugs* **2017**, *15*, 243. [CrossRef]
40. Cox, M.P.; Peterson, D.A.; Biggs, P.J. SolexaQA: At-a-glance quality assessment of Illumina second-generation sequencing data. *BMC Bioinform.* **2010**, *11*, 485. [CrossRef]
41. Schloss, P.D.; Westcott, S.L.; Ryabin, T.; Hall, J.R.; Hartmann, M.; Hollister, E.B.; Lesniewski, R.A.; Oakley, B.B.; Parks, D.H.; Robinson, C.J.; et al. Introducing mothur: Open-source, platform-independent, community-supported software for describing and comparing microbial communities. *Appl. Environ. Microbiol.* **2009**, *75*, 7537–7541. [CrossRef]
42. Smith, K.F.; Kohli, G.S.; Murray, S.A.; Rhodes, L.L. Assessment of the metabarcoding approach for community analysis of benthic-epiphytic dinoflagellates using mock communities. *N. Z. J. Mar. Freshw. Res.* **2017**, *51*, 555–576. [CrossRef]
43. Huelsenbeck, J.P.; Ronquist, F. MRBAYES: Bayesian inference of phylogenetic trees. *Bioinformatics* **2001**, *17*, 754–755. [CrossRef]
44. Sibat, M.; Herrenknecht, C.; Darius, H.T.; Roué, M.; Chinain, M.; Hess, P. Detection of Pacific ciguatoxins using liquid chromatography coupled to either low or high resolution mass spectrometry (LC-MS/MS). *J. Chromatogr. A* **2018**, *1571*, 16–28. [CrossRef] [PubMed]
45. Vial, J.; Jardy, A. Experimental comparison of the different approaches to estimate LOD and LOQ of an HPLC method. *Anal. Chem.* **1999**, *71*, 2672–2677. [CrossRef]
46. Sanagi, M.M.; Ling, S.L.; Nasir, Z.; Hermawan, D.; Ibrahim, W.A.; Abu Naim, A. Comparison of signal-to-noise, blank determination, and linear regression methods for the estimation of detection and quantification limits for volatile organic compounds by gas chromatography. *J. AOAC Int.* **2009**, *92*, 1833–1838. [CrossRef]
47. Zendong, Z.; Sibat, M.; Herrenknecht, C.; Hess, P.; McCarron, P. Relative molar response of lipophilic marine algal toxins in liquid chromatography/electrospray ionization mass spectrometry. *Rapid Commun. Mass Spectrom.* **2017**, *31*, 1453–1461. [CrossRef]
48. Brissard, C.; Hervé, F.; Sibat, M.; Séchet, V.; Hess, P.; Amzil, Z.; Herrenknecht, C. Characterization of ovatoxin-h, a new ovatoxin analog, and evaluation of chromatographic columns for ovatoxin analysis and purification. *J. Chromatogr. A* **2015**, *1388*, 87–101. [CrossRef]
49. Pisapia, F.; Sibat, M.; Herrenknecht, C.; Lhaute, K.; Gaiani, G.; Ferron, P.-J.; Fessard, V.; Fraga, S.; Nascimento, S.M.; Litaker, R.W.; et al. Maitotoxin-4, a novel MTX analog produced by *Gambierdiscus excentricus*. *Mar. Drugs* **2017**, *15*, 220. [CrossRef]
50. Bormans, M.; Amzil, Z.; Mineaud, E.; Brient, L.; Savar, V.; Robert, E.; Lance, E. Demonstrated transfer of cyanobacteria and cyanotoxins along a freshwater-marine continuum in France. *Harmful Algae* **2019**, *87*, 101639. [CrossRef]

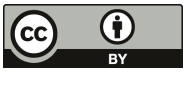

toxins

MDPI

Article

Further Advance of *Gambierdiscus* Species in the Canary Islands, with the First Report of *Gambierdiscus belizeanus*

Àngels Tudó [1], Greta Gaiani [1], Maria Rey Varela [1], Takeshi Tsumuraya [2], Karl B. Andree [1], Margarita Fernández-Tejedor [1], Mònica Campàs [1] and Jorge Diogène [1,*]

[1] Institut de Recerca i Tecnologies Agroalimentàries (IRTA), Ctra. Poble Nou Km 5.5, Sant Carles de la Ràpita, 43540 Tarragona, Spain; angie.ducaebre@gmail.com (À.T.); greta.gaiani@irta.cat (G.G.); maria.rey@irta.cat (M.R.V.); karl.andree@irta.cat (K.B.A.); margarita.fernandez@irta.cat (M.F.-T.); monica.campas@irta.cat (M.C.)

[2] Department of Biological Science, Graduate School of Science, Osaka Prefecture University, Osaka 599-8570, Japan; tsumu@b.s.osakafu-u.ac.jp

* Correspondence: jorge.diogene@irta.cat

Received: 22 September 2020; Accepted: 27 October 2020; Published: 31 October 2020

Abstract: Ciguatera Poisoning (CP) is a human food-borne poisoning that has been known since ancient times to be found mainly in tropical and subtropical areas, which occurs when fish or very rarely invertebrates contaminated with ciguatoxins (CTXs) are consumed. The genus of marine benthic dinoflagellates *Gambierdiscus* produces CTX precursors. The presence of *Gambierdiscus* species in a region is one indicator of CP risk. The Canary Islands (North Eastern Atlantic Ocean) is an area where CP cases have been reported since 2004. In the present study, samplings for *Gambierdiscus* cells were conducted in this area during 2016 and 2017. *Gambierdiscus* cells were isolated and identified as *G. australes*, *G. excentricus*, *G. caribaeus*, and *G. belizeanus* by molecular analysis. In this study, *G. belizeanus* is reported for the first time in the Canary Islands. *Gambierdiscus* isolates were cultured, and the CTX-like toxicity of forty-one strains was evaluated with the neuroblastoma cell-based assay (neuro-2a CBA). *G. excentricus* exhibited the highest CTX-like toxicity (9.5–2566.7 fg CTX1B equiv. cell^{-1}) followed by *G. australes* (1.7–452.6.2 fg CTX1B equiv. cell^{-1}). By contrast, the toxicity of *G. belizeanus* was low (5.6 fg CTX1B equiv. cell^{-1}), and *G. caribaeus* did not exhibit CTX-like toxicity. In addition, for the *G. belizeanus* strain, the production of CTXs was evaluated with a colorimetric immunoassay and an electrochemical immunosensor resulting in *G. belizeanus* producing two types of CTX congeners (CTX1B and CTX3C series congeners) and can contribute to CP in the Canary Islands.

Keywords: ciguatera; ciguatoxins (CTXs); *Gambierdiscus*; neuroblastoma cell-based assay (CBA); immunoassay; immunosensor

Key Contribution: *G. belizeanus* is reported for the first time in the Canary Islands (El Hierro). *G. belizeanus* produced CTX1B and CTX3C series of congeners. CTX-like toxicity of *G. australes*, *G. excentricus* and *G. caribaeus* was re-assessed.

1. Introduction

Gambierdiscus [1] species are marine benthic dinoflagellates that produce secondary metabolites such as ciguatoxins (CTXs) and maitotoxins (MTXs). CTXs are lipid-soluble polyethers [2], which are introduced in food webs when filter feeders and herbivorous organisms eat free-swimming microalgal cells, macroalgae, or substrates that are colonized by benthic dinoflagellates [3]. Then, CTXs are transferred, transformed, and bioaccumulated through the food webs. Humans can get poisoned after

the consumption of CTX-contaminated fish or very rarely some invertebrates (crustaceans, gastropods, echinoderms and bivalves) and suffer a disease known as Ciguatera Poisoning (CP) [4].

CTXs activate voltage-gated sodium channels (VGSCs) of cells, resulting in intracellular sodium increase and causing the repetitive firing of action potentials [5,6]. As a consequence, a few hours after the consumption of CTXs, gastrointestinal symptoms appear, typically followed by cardiac and neurological disorders. The neurological symptoms can last weeks, months, and even years [7]. The number of people who suffer from the disease is unknown, mainly due to the variability of symptoms, which leads to misdiagnoses and under-reporting. Annually, it is estimated that about 10,000–500,000 people suffer from the illness [8,9]. Even though CP is one of the most relevant poisonings worldwide, so far, there is no specific treatment [8]. CP was typical from tropical and subtropical regions, but during recent decades, CP cases have increased [10,11] and they have appeared in temperate zones through the importation of tropical ciguateric fish [12] or by the consumption of local ciguateric fish [13,14]. Climate change could change the geographical distribution of the dinoflagellates and the migration patterns of ciguateric fish and contribute to the geographical expansion of CP or increasing population densities of CTX-producing species in temperate areas [15,16]. In Europe, outside the boundaries of endemic areas in intertropical climates, new CP cases appeared in the North Eastern Atlantic Ocean after the consumption of fish from the Selvagens Islands (Portugal) and the Canary Islands (Spain) [17,18]. In the Canary Islands, CP is an illness of concern. In one decade (2008–2018), more than one hundred people have suffered from CP [19]. To prevent CP cases, the local authorities of this area have implemented the neuroblastoma cell-based assay (neuro-2a CBA) [20] to evaluate the possible presence of CTXs in the flesh of certain species of fish through the assessment of CTX-like toxicity [21].

It should be noted that only a few *Gambierdiscus* species have been confirmed to be CTXs producers [22,23], the toxin production is often very low, and not all the species produce the same quantities of toxins [22,24,25]. Therefore, the composition of species in the local areas could be an indicator of the level of risk to catch a ciguateric fish. One of the main factors to explain the latitudinal presence of *Gambierdiscus* species is the temperature [26], but other factors could be involved.

The Canary Islands are a transition zone between the oligotrophic waters associated with the Canary Current (CC), which is the subtropical gyre of the North Atlantic Ocean, and the eutrophic waters produced by the upwellings of deep cold waters with high nutrients along the African coast [27]. The east part of the Archipelago is semiarid; it is influenced by aeolian dust from the African continent and by the cold waters from the African upwelling system [28]. In contrast, the west is more humid, with more oceanic conditions and a minor influence of the African continent and the upwellings [28]. These conditions cause a longitudinal oceanographic east–west gradient of productivity (≈100 g of carbon m^{-2} yr^{-1}) and the sea surface temperature (SST) (1–2 °C), which could explain the geographical distribution of the *Gambierdiscus* species.

Regarding the presence of *Gambierdiscus* species, in the Canary Islands, *Gambierdiscus* sp. was reported in 2004 [29]. Afterwards, in 2011, *G. excentricus* was described as a new species [30]. After that, the new species *G. silvae* [31] and *G. excentricus* were considered endemic from the Canary Islands. During the last decades, several samplings in the islands showed the high biodiversity and the wide geographical distribution of the *Gambierdiscus* genus [32,33]. At present, six species have been recorded in the Canary Islands, *G. australes* [31], *G. belizeanus* (in the current study), *G. caribaeus* [33], *G. carolinianus* [33], *G. excentricus*, and *G. silvae* [31], and none of them is limited to the Canary Islands.

The present study reports for the first time *G. belizeanus* in the Canary Islands. Previously, *G. belizeanus* was reported in Belize in the West Atlantic Sea [34], in Cuba [35], Cancun, St. Barthelemy, St. Marteen, and St. Thomas [36,37] in the Caribbean Sea. Additionally, it was detected in the Saudi Arabia in the Red Sea [38] and in Australia [39], Malaysia [40], and Kiribati Island [41] in the Pacific Ocean. Referring to *G. belizeanus*, it is considered a low toxin producer [24,38]. Among *Gambierdiscus* species from the Canary Islands, the evaluation of CTX-like toxicity has revealed that *G. excentricus*

is one of the highest CTX-producing species within the genus *Gambierdiscus* and the most likely contributor to CP in the Atlantic Ocean [24,25,30].

Globally, it is not understood what triggers CP cases [4]. To fully understand the process of CP, to elucidate factors that may trigger CP, and to prevent the cases, it is necessary to identify and monitor the ciguateric fish but also to identify the CTX-producing species, their distribution, their physiology, and their toxicity.

The current study aimed to characterize the biodiversity and the geographical distribution of the *Gambierdiscus* genus in the seven most important islands of the Canary Islands Archipelago and to evaluate the potential CTX production of *Gambierdiscus* species to complement previous studies. For that purpose, samplings in the seven big islands of the Canary Archipelago were performed between October 2016 and October 2017. Isolates of *Gambierdiscus* cells were brought into culture. The molecular identification and morphological characterization of cultures contributed to the new report of *G. belizeanus* in the Archipelago. In addition, CTX-like toxicity was evaluated for forty-one strains of four species (*G. australes*, *G. belizeanus*, *G. caribaeus*, and *G. excentricus*) with the neuro-2a CBA, and the production of CTXs by the *G. belizeanus* strain was analyzed by a colorimetric immunoassay and an electrochemical immunosensor. New strategies within the microalgal field for future research of CP in the Canary Islands are further discussed.

2. Results and Discussion

2.1. Molecular Identification

Fifty-two strains including four species (*G. australes* (n = 32), *G. excentricus* (n = 18), *G. caribaeus* (n = 1) and *G. belizeanus* (n = 1)) were identified using sequences of the LSU D8-D10 rDNA region. The results of the BLAST analysis were well supported by the trees obtained using the Maximum Likelihood (ML) and the Bayesian Inference (BI) methods. Figure 1 shows the topology of the ML phylogenetic tree with bootstrap support values (bt) and the posterior probability (pp) of BI analysis displayed at branch nodes. Topography with the two phylogenetic trees was very similar. In both trees, the strains of this study are well defined within their respective clades for *G. australes*, *G. excentricus*, *G. caribaeus*, or *G. belizeanus* with bt/pp values of 96/1.00, 100/1.00, 98/0.92, and 96/1.00, respectively. Further, *G. pacificus* species were split into two clades. One sequence is grouped in the ML tree with *G. lewisii* with a high bootstrap value (>70). In contrast, in the BI tree, the clade of *G. lewisii* with *G. pacificus* appears, but it is less well supported (0.83 pp). The sequence of IRTA-SMM-17-421 was in the *G. belizeanus* cluster. This sequence exhibited 99% of similarity by BLAST with the isolate RS2-B6 of *G. belizeanus* (KY782638) from the Red Sea [38]. The genetic distance or pairwise distance (p-distance) between those two sequences was 0.011 substitutions per site. The strain IRTA-SMM-17-421 jointly with RS2-B6 has a deletion of 121 bp as described previously in Catania et al. [38], and this may indicate that it could be a ribosomal pseudogene. After excluding the deletion, the p-distance between IRTA-SMM-17-421 and *G. belizeanus* sequences ranged between 0.002 and 0.019 substitutions per site.

2.2. Morphological Characterization

The depth and width were measured in 50 cells for each species: *G. australes*, *G. excentricus*, *G. caribaeus* and *G. belizeanus* using the Calcofluor White stain method under light microscopy. Measurements for each species are shown in Table 1.

Cell morphology can vary depending on the culture conditions, growth phase, and different genotypes [32,42]. The morphological characterization showed that some cells of *G. australes* in the present work were smaller than the original description (76.0–93.0 μm of depth, 65.0–84.0 μm of width) in Chinain et al. [43]. However, overall, values are according to measurements presented in Bravo et al. [32], Litaker et al. [44], Rhodes et al. [23]. For *G. belizeanus*, the minimum measurements of depth in the present study are in accordance with the original description of 53–67 μm in Faust [34]; but, the minimum value for width (described in Faust as length), is lower than the first description

(54–63 µm of width). Moreover, the maximum value for depth and width are higher than the description of Faust [34]. *G. caribaeus* cells from the current study were bigger than the original description in Litaker et al. [44] and the cells of Bravo et al. [32]. In reference to *G. excentricus*, all measurements are in accordance with the original description Fraga et al. [30], and the values were similar to Bravo et al. [32] and Hoppenrath et al. [45].

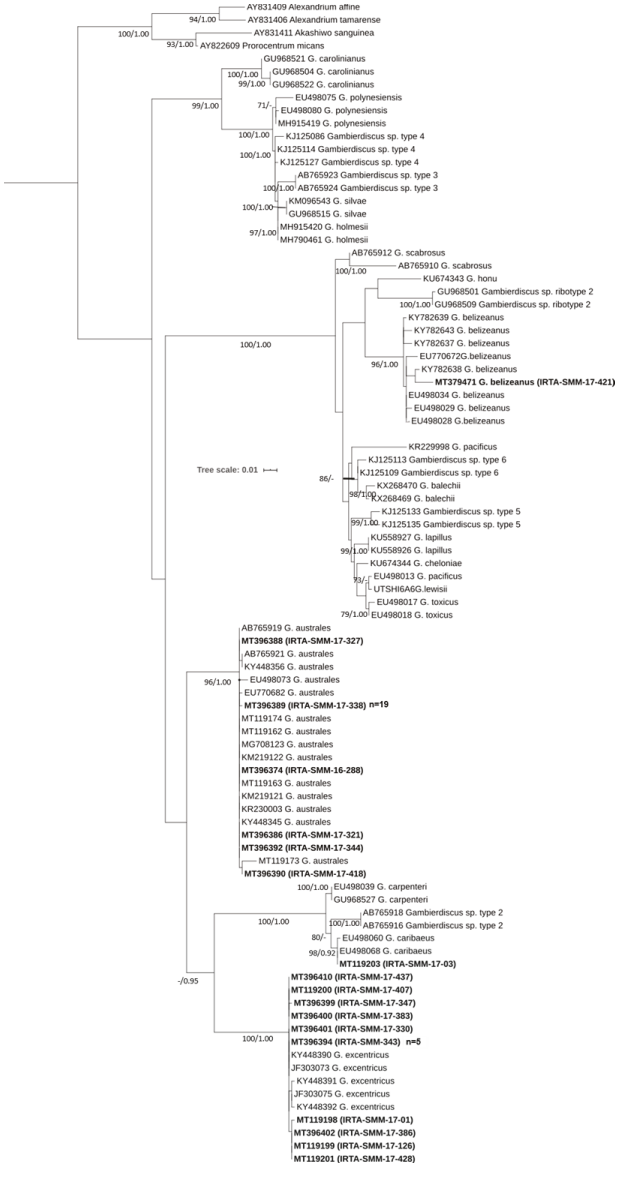

Figure 1. Phylogenetic tree of the LSU D8-D10 region (rDNA) using Maximum Likelihood analysis. Sequences in bold represent the strains of this study. The number of clones (*n*) with the same haplotypes is shown in parentheses. Values at nodes represent bootstrap values (≥70) and the Bayesian posterior probability (≥0.95) (bt/pp).

Table 1. Morphological sizes average of depth and width (±SD) of *Gambierdiscus* species of this study measured with light microscopy. The ranges of values are shown in parentheses.

Species	Depth (µm)	Width (µm)
G. australes	71.13 ± 7.06 (60.6–98.4)	65.40 ± 6.54 (53.4–82.1)
G. belizeanus	64.12 ± 5.28 (52.8–76.2)	59.64 ± 5.95 (46.5–76.0)
G. caribaeus	87.20 ± 11.19 (61.2–116.5)	86.45 ± 11.44 (63.17–119.7)
G. excentricus	90.25 ± 8.90 (72.2–109.7)	82.97 ± 9.06 (67.8–106.7)

Morphological Characterization of *G. belizeanus*

Cells were anterior–posteriorly compressed. The plate formula of *G. belizeanus* was Po, 4′, 0a, 6′′, 6c, ?s, 5′′′, 0p, 2′′′′ based on Fraga et al. [30]. The cells were heavily aerolated (Figure 2A–C). Limits of the thecae are well defined by intercalary bands. These two latter characteristics are typical of *G. belizeanus* [38,40,44]. The 2′ plate is rectangular (Figure 2A), and the 2′′′′ plate is pentagonal (Figure 2B). Figure 2D shows the apical pore plate (Po).

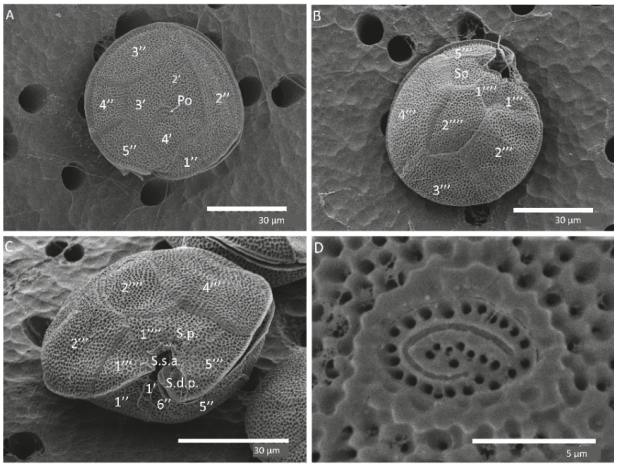

Figure 2. SEM images of *G. belizeanus* (IRTA-SMM-17-421): apical (**A**), antapical (**B**), ventral (**C**) views, detail of Po plate and pores (**D**).

2.3. Distribution of the Gambierdiscus Species in the Canary Islands

The observation of the samples under light microscopy showed that cells of *Gambierdiscus* spp. were found at 21 stations of the 53 stations sampled in the seven islands in 2016 and 2017. *Gambierdiscus* cells co-occurred with cells of the genera *Coolia*, *Ostreopsis*, *Prorocentrum*, *Amphidinium*, *Karenia* and *Trichodesmium*, among others. Details of the islands and the number of identifications for each station are shown in Figure 3. Overall, *G. australes* was the most abundant and it was present in all the islands. *G. excentricus* was the second most abundant. It was present in four islands Gran Canaria, Tenerife, La Gomera, and La Palma, excluding the eastern islands (Lanzarote and Fuerteventura) and the western island (El Hierro). *G. caribaeus* and *G. belizeanus* were identified in El Hierro.

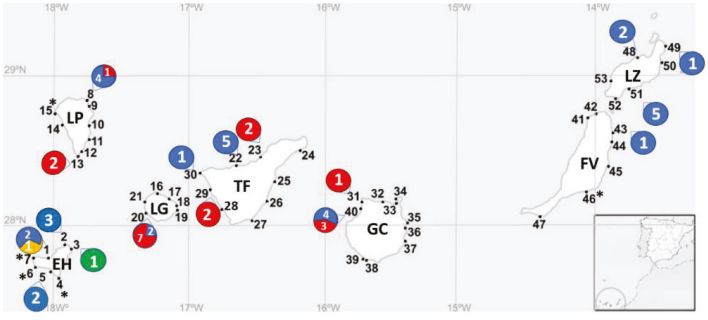

Figure 3. Distribution of each species in the stations of the Canary Islands during 2016–2017. Station numbers are represented in bold. The presence of *Gambierdiscus* species determined with molecular analysis is presented with a circle and includes the number strains identified for each species. The asterisk represents the presence of *Gambierdiscus* sp. Colors of circles are for *G. australes* (blue), *G. excentricus* (red), *G. caribaeus* (green), and *G. belizeanus* (yellow). EH (El Hierro), FV (Fuerteventura), GC (Gran Canaria), LG (La Gomera), LP (La Palma), LZ (Lanzarote), and TF (Tenerife).

Before 2004, the Canary Islands were considered outside of the geographical distribution of the *Gambierdiscus* genus, and the first reports of the genus were considered the result of a recent arrival in the islands [30]. The first reports of the *Gambierdiscus* genus in the Canary Islands were occasional, in one or two islands, and they were obtained from very few samples [30,31]. The finding of the new species *G. excentricus* and *G. silvae* in the Canary Islands, and the rapid increase in the number of species in consecutive samplings combined with the occurrence of CP cases in the islands [13] elicited the alarm to conduct urgent systematic and wide samplings in the area in order to understand the distribution and origin of the dinoflagellates and their potential contribution to CP cases. Rodríguez et al. [33] collected samples in numerous stations in La Graciosa (Chinijo Archipelago) in March 2015 and in the big islands excluding La Palma and La Gomera in September and October 2015. In the study of Rodríguez et al. [33], numerous isolates were identified, and *Gambierdiscus* cell abundances were determined in the sampling stations. The authors found a high richness of the *Gambierdiscus* genus in the Canary Islands, reporting five species: *G. excentricus*, *G. silvae*, *G. australes*, *G. caribaeus*, and *G. carolinianus*. This unexpected richness revealed a more likely ancient origin of the genus, which was contrary to what had been previously considered as a recent introduction [46]. In October 2017, Bravo and collaborators [32] performed systematic samplings in La Gomera and La Palma and complemented the geographical distribution of the *Gambierdiscus* species, among other issues. To date, samplings in the Canary Islands have been performed during very specific temporal scales, mainly in periods from October to September. In the current study, systematic samplings were performed in a higher number of stations, including new ones in the seven big islands. It is important to remark that a general bias in the identification process for the presence of species in a given area occurs since identification is a result of success growth under laboratory conditions. In Rodriguez et al. [33], this factor was partially avoided due to the identification of single cells in addition to the identification of cultured strains. The current study has contributed to a better understanding of the biodiversity of the genus in the Canary Islands, while providing a review and update of the geographical distribution of the species. A new contribution of the current work is the first report of *G. belizeanus* in the Canary Islands Archipelago (El Hierro) and *G. australes* in La Palma.

Gambierdiscus species have distinct lower and upper thermal limits and optimal temperatures for their growth [47]. Additionally, they are considered to have a high intraspecific variable response in growth depending on the temperature, salinity, and irradiance [47,48], and the response could be influenced by the geographical origin of the isolate [48]. Even so, biodiversity in the islands could follow a geographical pattern depending on the maximum and minimum temperatures on each island.

For instance, as mentioned before, the SST of the western part of the Archipelago is higher. Therefore, a priori, the west could be more suitable for the warmer tropical species. This phenomenon has already been observed in fish [49]. Overall, the range of SST during 1972–2012 in the Archipelago was 15.9 °C in March–April and 25.5 °C in August–October [50]. The optimal temperatures for *Gambierdiscus* species are between 20 and 28 °C, and the maximal growth temperatures usually are >25 °C (Tester et al., 2020). Hence, it is expected that high abundances and more diversity of *Gambierdiscus* species would be found during August–October.

The distributions of *G. australes* and *G. excentricus* observed in the current study were similar to those reported by Rodriguez et al. [33] and Bravo et al. [32]. Table 2 compiles the records of *Gambierdiscus* species in the Canary Archipelago from the literature together with the results of the current study. *G. australes* is present in all seven big islands. These data are consistent since *G. australes* is the *Gambierdiscus* species with the widest optimal temperature range: between 19 and 28 °C [26,51]. In the current study, its presence is not dominant in all the islands, being slightly less abundant in La Gomera. This observation is in accordance with the previous results of Bravo et al. [32] reported for this island, where *G. excentricus* was the dominant taxa followed by *G. silvae*, *G. caribaeus*, and *G. australes*. The second most dominant species in the islands is *G. excentricus*, although it is not reported in El Hierro. Physiological data have not been reported for *G. excentricus*, even though its distribution in the Canary Islands is coherent considering that El Hierro has the most tropical conditions and that *G. excentricus* is more commonly present in temperate areas [26,45,52]. *G. silvae* was recorded in the central islands: Tenerife, La Gomera, and Gran Canaria. Overall, the longitudinal distribution of *G. silvae* is quite broad, including the Caribbean Sea and the Atlantic Sea [33,52]. However, compared to other species, one *G. silvae* strain, originating from Caribbean Sea, showed a narrow range of tolerance to temperature, and the maximal temperature for growth was low (24.8 °C) [48]. This result should be contrasted with maximal temperature of other *G. silvae* strains, but these data are presently lacking. *G. carolinianus* is present only in Tenerife. In Kibler et al. [47], the responses to environmental factors among strains were highly variable, but globally, *G. carolinianus* was well adapted to low temperatures (15 °C). Additionally, optimal temperatures for growth were also low (21.8–27.9 °C) [48]. Finally, *G. caribaeus* was reported in La Gomera and El Hierro, while *G. belizeanus* was present only in El Hierro. Experimentally, strains of *G. belizeanus* and *G. caribaeus* exhibited a wide range of temperature tolerance [48], but their range of temperature for maximal growth is considered high, since their temperature ranges are 26.1–29.1 °C [48] and 25–31 °C [48,53], respectively. Thus, the geographical distribution of both species in the Canary Islands is in accordance with the high-temperature adaptation in the laboratory. Tenerife and La Gomera have the highest richness of *Gambierdiscus* species. Tenerife is the biggest island and, consequently, more different habitats could be available. Additionally, this location in the middle of the Archipelago provides intermediate conditions. However, there are some inconsistences when trying to explain the biodiversity in the islands according to temperatures. For instance, experimentally, *G. belizeanus* has an optimal temperature range similar to *G. caribaeus* reported in El Hierro and in La Gomera. In contrast, *G. belizeanus* has not been reported in La Gomera. This may indicate that the presence of species is not yet well recorded or that more important factors for *Gambierdiscus* species are still unidentified. For instance, the exposure of the station to wave action was an important factor influencing the variability of macroalgae in the Canary Islands [54]. Additionally, it is important to highlight that there is a high intraspecific variation in the physiologic response under laboratory conditions. In other words, the strains from the Canary Islands may differ from other strains tested in previous studies.

The prevalence of the *Gambierdiscus* isolates in the Canary Islands since 2004 shows a good adaptation of the genus to the conditions found in the Archipelago. During recent decades, oceans have suffered a warming trend, and the SST in the Canary Islands is projected to increase 0.25 °C decade^{-1} [56]. The SST between 1985–2018 in the Canary Islands did not surpass 26 °C [50], which is far from the lethal temperatures for *Gambierdiscus* species (≈31 °C) [47,57]. Globally, the abundances of *Gambierdiscus* in the Canary Islands could be higher during the next years influenced by rising temperatures. Nonetheless,

in the easternmost islands, the trend of the upwelling is not clear [56], and how upwelling could affect *Gambierdiscus* cell densities under the influence of the SST in the eastern islands is still to be studied.

Table 2. Literature review of the distribution of the species in the Canary Islands. EH (El Hierro), FV (Fuerteventura), GC (Gran Canaria), LG (La Gomera), LP (La Palma), LZ (Lanzarote), and TF (Tenerife).

Species	Islands	Date of Sampling (References)
G. australes	LZ, FV, GC	September–October 2015 [33] October 2016 (this study)
	EH	September–October 2015 [33] October 2017 (this study)
	TF	2013 [31] September–October 2015 [33] October 2017 (this study)
	LG	October 2017 ([33] and this study)
	LP	October 2017 (this study)
G. belizeanus	EH	October 2017 (This study)
G. caribaeus	EH	September–October 2015 [33] October 2015 [55] October 2017 (this study)
	LG	October 2017 [32]
G. carolinianus	TF	September–October 2015 [33]
G. excentricus	TF	March 2004 [30] 2013 [31] September–October 2015 [33] October 2017 (This study)
	LZ	September–October 2015 [33]
	FV	September–October 2015 [33]
	GC	September–October 2015 [33] April 2017, October 2017 (this study)
	LP	March 2004 [30] October 2017 ([33] and this study)
	LG	March 2004 [30] October 2017 ([33] and this study)
G. silvae	TF	2013 [31] September–October 2015 [33]
	GC	Winter 2010 [31]
	LG	October 2017 [32]

2.4. Evaluation of CTX-Like Toxicity with the Neuro-2a CBA

The evaluation of the CTX-like toxicity was conducted for 41 extracts from cultures harvested in late exponential-early stationary phase of the four *Gambierdiscus* species: *G. australes*, *G. excentricus*, *G. caribaeus* and *G. belizeanus*, using the neuro-2a CBA. Obtaining CTX purified standards from microalgae is a very difficult task, since the CTX production in microalgae is often very low. For this reason, the toxicological evaluation often is carried out with CTX standards purified from fish. It has been found that CTX4A, CTX4B, and CTX3C are produced by the alga, and they are oxidized to the analogs CTX1B, 52-epi-54-deoxyCTX1B, 54-deoxyCTX1B, 2-hydroxyCTX3C, and 2,3-dihydroxyCTX3C [58]. In the present study, the reference molecule standard was CTX1B [59], which is a CTX typically found in large carnivorous fish in the Pacific Ocean [59,60] and which has never been found in microalgae.

As expected, in each experiment, the standard CTX1B displayed a non-significant reduction of viability with O/V$^+$ treatment, whereas a typical sigmoid curve was exhibited in the O/V$^-$ treatment. The average of the maximum exposed concentration of cells without toxicity in the O/V$^-$ treatment for *G. australes*, *G. excentricus*, *G. belizeanus* and *G. caribaeus* ranged between 2–201, 0.2–50, 160 and 6800 cells mL^{-1}, respectively. The one-way ANOVA showed that differences of CTX-like toxicities among the *G. excentricus* and *G. australes* were significant (p-value < 0.01). Moreover, the one-way ANOVA test for the CTX-like toxicity for the islands between species was significant; differences were for Fuerteventura for *G. australes* and in la Palma for *G. excentricus*. For these islands only one strain was tested. If these islands were not considered in the analysis, then the one-way ANOVA was not significant. Table 3 shows the results of the CTX-like toxicity expressed as fg CTX1B equiv. cell^{-1}. The most toxic species was *G. excentricus* with a range of 9.5–2566.7 fg CTX1B equiv. cell^{-1}. The most toxic strain was IRTA-SMM-17-330 from La Palma. The second most toxic species was *G. australes* with a range of 1.7–452.6 fg cell^{-1}, followed by *G. belizeanus* which presented 5.6 ± 0.1 fg CTX1B equiv. cell^{-1}. *G. caribaeus* did not show toxicity at 6800 cells mL^{-1} with an LOD of 0.42 fg CTX1B equiv. cell^{-1}. Table S3 shows the neuro-2a cell viability and the CTX-like estimations obtained by the exposure to *Gambierdiscus* spp. extracts in O/V$^+$ and O/V$^-$ conditions.

Table 3. Ciguatoxin (CTX)-like toxicity of *Gambierdiscus* spp. using the neuro-2a CBA. CTX-like toxicity and the limit of detection (LOD) are expressed as fg CTX1B equiv. cell^{-1}. Ref: number of the station according to Figure 1, EH (El Hierro), FV (Fuerteventura), GC (Gran Canaria), LG (La Gomera), LP (La Palma), LZ (Lanzarote) and TF (Tenerife).

Strain Code	CTX-Like Toxicity	Island	Station	Strain Code	CTX-Like Toxicity	Island	Station
G. australes				*G. australes*			
IRTA-SMM-17-004	205.1 ± 34.5	LZ	48	IRTA-SMM-17-316	51.5 ± 6.9	TF	22
IRTA-SMM-17-006	127.7 ± 85.0	LZ	51	IRTA-SMM-17-307	37.3 ± 12.6	TF	30
IRTA-SMM-16-288	106.1 ± 75.3	LZ	51	IRTA-SMM-17-436	98.6 ± 25.4	LG	20
IRTA-SMM-16-290	46.1 ± 22.2	LZ	51	IRTA-SMM-17-393	44.6 ± 11.5	LG	20
IRTA-SMM-16-292	39.7 ± 10.5	LZ	49	IRTA-SMM-17-344	41.2 ± 0.1	LP	8
IRTA-SMM-16-286	33.6 ± 6.5	LZ	51	IRTA-SMM-17-335	29.1 ± 8.6	LP	8
IRTA-SMM-16-293	32.7 ± 10.0	LZ	51	IRTA-SMM-17-287	11.3 ± 2.3	LP	8
IRTA-SMM-17-007	15.8 ± 1.7	LZ	48	IRTA-SMM-17-288	5.7 ± 3.8	LP	8
IRTA-SMM-17-002	452.6 ± 23.2	FV	43	IRTA-SMM-17-389	226.3 ± 24.5	EH	1
IRTA-SMM-17-103	118.7 ± 30.3	GC	40	IRTA-SMM-17-324	160.4 ± 17.2	EH	5
IRTA-SMM-17-107	12.2 ± 2.1	GC	40	IRTA-SMM-17-418	68.3 ± 9.5	EH	2
IRTA-SMM-17-112	1.9 ± 0.6	GC	40	IRTA-SMM-17-321	31.9 ± 15.0	EH	5
IRTA-SMM-17-106	1.7 ± 0.1	GC	40	IRTA-SMM-17-425	27.8 ± 3.3	EH	2
IRTA-SMM-17-358	138.9 ± 17.7	TF	22	IRTA-SMM-17-327	7.2 ± 0.3	EH	2
IRTA-SMM-17-291	82.8 ± 22.2	TF	22				
G. belizeanus				*G. caribaeus*			
IRTA-SMM-17-421	5.6 ± 0.1	EH	1	IRTA-SMM-17-003	Neg. LOD < 0.42	EH	3
G. excentricus				*G. excentricus*			
IRTA-SMM-17-001	1149.3 ± 212.3	EH	1	IRTA-SMM-17-386	12.8 ± 2.8	TF	23
IRTA-SMM-17-126	226.7 ± 22.1	GC	40	IRTA-SMM-17-429	1525.9 ± 634.1	LG	20
IRTA-SMM-17-128	9.5 ± 2.6	GC	40	IRTA-SMM-17-432	962.1 ± 154.7	LG	20
IRTA-SMM-17-404	1257.64.8 ± 319.3	TF	29	IRTA-SMM-17-413	18.1 ± 5.7	LG	20
IRTA-SMM-17-405	1153.4 ± 238.8	TF	29	IRTA-SMM-17-330	2566.7 ± 333.3	LP	13

The differences of CTX-like toxicity among strains of *G. excentricus* (n = 10) and *G. australes* (n = 29) from different islands are shown in a boxplot in Figure 4.

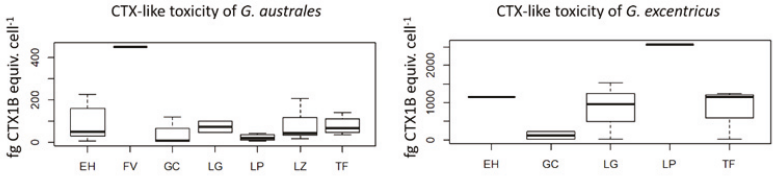

Figure 4. Distribution of CTX-like toxicity of *G. australes* and *G. excentricus* according to island of origin. EH (El Hierro), FV (Fuerteventura), GC (Gran Canaria), LG (La Gomera), LP (La Palma), LZ (Lanzarote) and TF (Tenerife).

In parallel to the identification attempts of the *Gambierdiscus* species in the Canary Islands and the determination of their geographical distribution, efforts to confirm if the local populations of *Gambierdiscus* produce CTXs and contribute to the CP of the Canary Islands have been made. Currently, although the CTX-like toxicity has been described for almost all species from the Canary Islands [24,25,61], the confirmation of the CTXs production in isolates from the Canary Islands has only been determined for *G. excentricus* by Paz et al. [62]. The production of CTXs seems to be very low and infrequent compared to the production of MTXs [22]. For instance, maitotoxin-4 (MTX4) was detected in strains of *G. excentricus* from Tenerife (VGO791 and VGO792) by Pisapia et al. [63] and from la Gomera (IRTA-SMM-17-407) by Estevez et al. [64]. In the evaluation of CTX-like toxicity by neuro-2a CBA of the crude extracts, other compounds can interfere, since the evaluated toxicity in neuro-2a CBA is a composite effect, and sometimes, other compounds can cause unspecific mortality [25]. In Estevez et al. [64], the toxic effect on neuro-2a cells of the methanolic crude extract of the *G. excentricus* (IRTA-SMM-17-407) was very high, making the identification/quantification of CTX-like toxicity impossible. This effect was likely due to the presence of MTX4, which was also described in the same paper, since MTXs have high toxicity to neuro-2a cells [65]. In neuro-2a CBA, the use of controls with and without ouabain and veratridine allow the discrimination of CTX-like toxicity. Nevertheless, high amounts of MTXs, for example, and eventually other compounds, could also mask the presence of CTXs.

Fraga and collaborators [30] observed that *G. excentricus* from the Canary Islands produces compounds with high CTX-like toxicity. Afterwards, Pisapia et al. [24] reported that *G. silvae* was 100-fold less toxic and *G. australes* was 1000-fold less toxic than *G. excentricus*. Thus, *G. excentricus* and *G. silvae* seemed to be the top producers of CTX-like toxicity in the Atlantic Ocean. Nonetheless, after Reverté et al. [61] and Rossignoli et al. [25], this statement is controversial. Both studies listed *G. australes* and *G. excentricus* as the most toxic species in the Canary Islands and not *G. silvae*. In particular, Rossignoli et al. [25] examined the CTX-like toxicity using the neuro-2a CBA for the isolates of the five species originating from the Canary Islands. In that study, the highest CTX-like activity was for *G. excentricus* (VGO1361) with 510 fg CTX1B equiv. cell^{-1} followed by *G. australes* (VGO1252) with 107 fg CTX1B equiv. cell^{-1}, *G. carolinianus* (VGO1197) with 101 fg CTX1B equiv. cell^{-1}, *G. caribaeus* (VGO1367), with 90 fg CTX1B equiv. cell^{-1} and *G. silvae* (VGO1378) with 77 fg CTX1B equiv. cell^{-1}. These results can be compared with our study because both studies used the same molecule of reference (CTX1B) and the same method for the toxicological evaluation.

Among the strains of the present work, *G. excentricus* exhibited the highest toxicity levels. These values are higher than those of Rossignoli et al. [25], being more similar to the levels measured by Fraga et al. [25] of 1100 fg CTX1B equiv. cell^{-1}. The second most toxic species was *G. australes*. The mean values of the current study were similar to the highest values of Rossignoli et al. [25] (31–107 fg CTX1B equiv. cell^{-1}) and globally lower than the values of Reverté et al. [61] (200 to 600 fg CTX1B equiv. cell^{-1}). The *G. caribaeus* strain (IRTA-SMM-17-03) did not exhibit CTX-like toxicity; this in accordance with Rossignoli et al. [25]. In fact, in previous studies, *G. caribaeus*, *G. belizeanus*, and *G. carolinianus* were classified as low CTX producers [25,37]. *G. caribaeus* showed no CTX-like toxicity

by CBA [66]. Referring to *G. belizeanus*, the CTX-like toxicity values of the current study are higher than the average of the toxicity for the *G. belizeanus* strains from the Red Sea of 0.038 fg of CTX1B equiv. cell^{-1} [38]. In the Red Sea, there is no confirmation of any CP cases [67], and *G. belizeanus* is the only *Gambierdiscus* species reported in that area. Even though only one isolate has been evaluated, its low toxicity, together with its restricted geographical distribution to El Hierro, suggests that the contribution of *G. belizeanus* to CP of the Canary Islands may be negligible, although more strains should be evaluated.

The literature shows that there is a high variation of CTX-like response between isolates within the same species [24,25,61]. This variation has been observed also in the current study. For *G. excentricus* and *G. australes*, the strains with the highest toxicity were 160 and 100-fold more toxic than the least toxic strain of the same species, respectively. This variability is higher than the obtained intraspecific values in Litaker et al. [37], Pisapia et al. [24], and Rossignoli et al. [25]. These differences may be related to the large number of strains that have been evaluated in the present study.

According to our results, the CTX-like toxicity levels have no clear pattern relating to the islands of origin. This is relevant because data of the fish from the official control program of ciguatera from the Canary Islands showed that ciguateric fish follow an east–west gradient. Toxic fish were more likely to be caught in Lanzarote (53%), followed by Fuerteventura (21%), Gran Canaria (18%), El Hierro (15%), Tenerife (14%), La Palma (5%), and La Gomera (2%) [21]. Sanchez-Henao et al. [21] suggested that the percentage of Lanzarote results must be considered with caution, since some samples were not accompanied by the total information and may not reflect the reality. Thus, the global tendency of ciguateric fish could be explained by the *Gambierdiscus* cell abundances from the samplings of Rodriguez et al. [33], which showed higher abundances in the east than in the west. However, for some fish species, the east–west gradient of CTX-like toxicity is not followed [21]. For instance, the major percentage of CTX positive groupers was found in El Hierro followed by Lanzarote and the other islands. As it has been mentioned before, the cell densities were lower in El Hierro than in Lanzarote and Fuerteventura. In addition, the presence of the most toxic species, *G. excentricus*, is not confirmed in El Hierro. Therefore, these results of ciguateric fish should be compared with cell abundances by seasonality and include temporal series for different years. Additional other factors could contribute to toxin production and bioaccumulation in fish, as well as the mobility of fish. After all, it is still early to establish a list of the riskiest areas for CP, as the relation between microalgae and fish are unknown in the Canary Islands, and further research should be undertaken.

2.5. Evaluation of the Presence of Two Series of CTX Congener Equivalents (CTX1B and CTX3C) in G. belizeanus with a Colorimetric Immunoassay and an Electrochemical Immunosensor

The role of the antibodies in the immunosensing tool is not to confirm the presence of individual CTXs congeners as in instrumental analysis techniques, but to screen the presence of compounds with wings structurally similar to those of the four CTX targets (CTX1B, 54-deoxyCTX1B, CTX3C, and 51-hydroxyCTX3C). Therefore, and because of the sandwich format of the assay, the analysis is indicating the presence of compounds structurally related to two series of CTXs congeners, although no evidence can be obtained about which specific CTXs congeners are present. It is important to mention that the strategy will detect only the CTXs recognized by the antibodies (the four major CTX congeners previously mentioned), but it is also important to highlight that the antibodies have been demonstrated to not cross-react with brevetoxin A, brevetoxin B, okadaic acid, and maitotoxins.

Analyses with the immunoassay and the immunosensor revealed the presence of the two series of CTXs congeners in the *G. belizeanus* extract. Immunoassay results when antibodies were used separately showed a higher concentration of 51-hydroxyCTX3C equiv. (0.28 ± 0.02 fg cell^{-1}) than of CTX1B equiv. (0.15 ± 0.03 fg cell^{-1}). As expected, the use of both antibodies simultaneously resulted in higher toxin content (0.40 ± 0.02 fg of CTX1B equiv. cell^{-1}). Similar results were obtained with the electrochemical immunosensor. The use of 10C9 antibody resulted in a higher concentration (0.17 ± 0.08 fg 51-hydroxyCTX3C equiv. cell^{-1}) than the one obtained with 3G8 (0.13 ± 0.03 fg of

CTX1B equiv. cell^{-1}). Again, the use of both antibodies together provided higher toxin content (0.35 ± 0.04 fg CTX1B equiv. cell^{-1}). Both immunochemical tools provide similar CTX quantifications of CTX congeners in *G. belizeanus* extract. The use of these techniques not only revealed the presence of CTXs, but also allowed the discrimination between two series of CTX congeners (CTX1B and CTX3C). When using the mAbs separately, results showed slightly higher contents for the CTX3C series than for the CTX1B series. In fact, 51-hydroxyCTX3C equiv. contents were similar to those obtained in a previous study for *G. caribaeus* IRTA-SMM-17-03 (0.13–0.21 fg cell^{-1}), *G. australes* IRTA-SMM-17-286 (0.16–0.37 fg cell^{-1}), and *G. excentricus* VGO791 (0.16–0.31 fg cell^{-1}), both originating from the Canary Islands [68]. Regarding CTX1B equiv. contents, the toxin contents in *G. belizeanus* were similar to those obtained for *G. caribaeus* IRTA-SMM-17-03 (0.13–0.24 fg cell^{-1}) and surprisingly, *G. excentricus* strains IRTA-SMM-17-01, IRTA-SMM-17-407 and IRTA-SMM-17-432 (0.09–0.19 fg cell^{-1}). It is important to note that CTX contents obtained with the immunochemical tools do not fully agree with those obtained with CBA. The reason is the different principle of recognition of both systems: whereas CBA is based on the toxic effect of a compound on the cell viability, the immunochemical tools are based on a structural recognition and affinity interaction between antibodies and their target molecules. Nevertheless, the analysis of microalgal extracts with different techniques provides complementary information and contributes toward improved characterization of the different *Gambierdiscus* species.

2.6. Future Research Strategies to Understand CP in the Canary Islands

During the last years, the official control of CTX-like toxicity evaluation of the harvested fish in the Canary Islands has been used as the first step to prevent CP cases [21,69]. The official control obliges all analyzed fish to be stored and frozen until CTX-like toxicity results are available, influencing its commercial value.

In order to prevent and to identify the future trends of CP in the Canary Islands, knowledge about the microalgal communities should be considered. The link between dinoflagellates and CP remains uncertain, and the key vectors of the transfer of CTXs into fish and eventually shellfish are still unclear. It is essential to identify the principal involved species. One of the first big steps in the microalgal field is the unequivocal identification of the species and the estimation of their abundance in the environmental samples. It is not clear whether only the genus *Gambierdiscus* can contribute to CP [22]. For example, *Coolia tropicalis* produces 44-methylgambierone (previously reported as MTX3) [70], which in human neuroblastoma cells (SH-SY5Y cell line) induces current sodium as the CTX3C but with lower potency [71]; additionally, neither of these toxins induce cell death in human cortical neurons when they were exposed at 20 nM concentration [72] Even so, a recent study considers it unlikely that 44-methylgambierone contributes to CP due to its low toxicity by mouse bioassay (MBA) [73]. It is necessary to clarify the toxin profiles of microalgae by instrumental analysis and analyze the toxicity of each compound to evaluate which species are low or high producers of CTX analogues. At present, there is a lack of knowledge of which compounds microalgae can produce and how these compounds interact with the food webs. Therefore, we need to identify these compounds in the microalgal, fish, and invertebrate matrixes and establish their interactions. Hence big gaps in the detection of fish and microalgal toxins still exist [74,75].

Another issue to be solved is related to the identification of *Gambierdiscus* species, which should be conducted to clarify the taxonomy and improve the molecular diagnoses. During the last years, there have been several attempts to identify *Gambierdiscus* species in environmental samples, and they have achieved good results [52,76,77], but they are not implemented in monitoring programs extensively.

The sampling method still requires standardization. Given that *Gambierdiscus* cells are found in a heterogeneous distribution, it is necessary to perform exhaustive geographical and temporal samplings using a standardized method. Artificial substrates have been used to sample benthic dinoflagellates such as *Gambierdiscus* spp., showing a reduction in the variability of densities of several samples collected at the same station [78]. However, when using artificial substrates, some ecological data are dismissed. For example, samplings in macroalgae substrates could aid in recognizing the

potential preference by *Gambierdiscus* for particular macroalgae species or species assemblages. A priori, macroalgae are more visible and easier to monitor. Hence, understanding the population dynamics of the preferred macroalgae for *Gambierdiscus* could be relevant to explain the trend of the dinoflagellates. Additionally, identifying the grazers of these macroalgae could help to understand the accumulation through the food web. Nevertheless, it has to be taken into account that free-living cells could contribute to CP [3].

Additionally, to understand the future trend of populations in local areas, it is essential to identify critical factors for such regional populations. To this end, experimental design in field, such as environmental, ecological, and anthropogenic activities that potentially can modulate the *Gambierdiscus* populations, should be considered. This field data should be combined with experimental/laboratory data. Other factors should be examined to understand, for instance, which variables affect the toxin content of cells.

3. Conclusions

The present study provides more data of *Gambierdiscus* species distribution and toxicity in the Canary Islands. The new report of *G. australes* in La Palma and the new finding of *G. belizeanus* in the Canary Islands (El Hierro) show that data in the geographical and temporal scale is still scarce. Similar to the previous studies, the evaluation of the CTX-like toxicity shows that *G. excentricus* and *G. australes* are the species which could more contributeto CP. These species are widely distributed in the Canary Islands. Further investigations are needed on the CTX-producing species, sampling methods, toxin profiles in microalgae and fish, relations between macroalgae, microalgae, and fish, and the accumulation of CTXs throughout the food webs. Until these issues are solved, it will be challenging to implement the best decisions to prevent CP at the local level of the Archipelago.

4. Methods

4.1. Reagents and Equipment

CTX1B standard solution was obtained from Prof. Richard J. Lewis (The Queensland University, Australia) [60] and calibrated (correction factor of 90%) in relation to the NMR-quantified CTX1B standard solution from Prof. Takeshi Yasumoto (Japan Food Research Laboratories, Japan). 51-OH-CTX3C standard solution was kindly provided by Prof. Takeshi Yasumoto (Japan Food Research Laboratories, Japan) and was used as a model for the series of CTX3C congeners. Neuroblastoma murine cells (neuro-2a) were purchased from ATCC LGC standards (USA). Poly-L-lysine, fetal bovine serum (FBS), L-glutamine solution, ouabain, veratridine, phosphate buffered saline (PBS), penicillin, streptomycin, RPMI-1640 medium, sodium pyruvate, thiazolyl blue tetrazolium bromide (MTT), *N*-(3-dimethylaminopropyl)-*N*′-ethylcarbodiimide hydrochloride (EDC), *N*-Hydroxysuccinimide (NHS), Tween 20, bovine serum album (BSA), poly horseradish peroxidase–streptavidin (polyHRP–streptavidin), and 3,3′,5,5′-tetramethylbenzidine (TMB) liquid substrate were supplied by Merck KGaA (Germany). Dimethyl sulfoxide (DMSO) and absolute methanol were purchased from Honeywell (Spain) and Chemlab (Spain), respectively. Taq Polymerase and Dynabeads M-270 Carboxylic Acid (2×109 beads mL^{-1}) were purchased from Invitrogen (Spain). QIAquick PCR Purification Kit was obtained from Qiagen (Germany). For the DNA amplification, a Mastercycler nexus gradient thermal cycler purchased from Eppendorf (Spain) was used. The 3G8, 10C9, and 8H4 monoclonal antibodies (mAbs) had been prepared by immunizing mice with keyhole limpet hemocyanin (KLH) conjugates of rationally designed synthetic haptens [79–85]. A microplate Reader KC4 (BIO-TEK Instruments, Inc., Vermont, VT, USA) was used to perform colorimetric measurements, and Gen5 software was used to collect and process the data. Arrays of eight screen-printed carbon electrodes (DRP-8 × 110), a boxed connector (DRP-CAST8X), and a magnetic support (DRP-MAGNET8X) were purchased from Dropsens S.L. (Spain). A PalmSens potentiostat (PalmSens, Houte, Netherlands) connected to an 8-channel multiplexer (MUX8) was used

to perform amperometric measurements. Data from potentiostat were collected and evaluated with PalmSens PC software (PalmSens, Houte, Netherlands).

4.2. Sampling Area and the Strategy

The Canary Islands are located in the north-east Atlantic Ocean (28.36715°–17.61396°) between 100 km and 600 km west of the north-west African coast. Samplings were performed in seven big islands during 2016 and 2017. Gran Canaria, Fuerteventura, and Lanzarote were sampled in October 2016 and La Palma, Tenerife, El Hierro, and La Gomera were sampled in October 2017. Additionally, samplings were carried out in Gran Canaria in April 2017. Sampling locations are shown on a map in Figure 5, and Table 4 shows the details. In total, 53 sampling stations were studied. In each station, the temperature, salinity, pH, oxygen saturation, and oxygen concentration were recorded with a multiparametric probe (YSI 556 MPS). The coordinates of the stations, date, and the environmental data are shown in Table S1. In each sampling station, two samples were obtained: epilithic (surface rasping of rocky substrates) and epiphytic (sampling of macrophytes). Samples were collected using a plastic bottle (Nalgene, HDPE, 1 L). For the first sample, the substrates were scratched using the bottleneck, and for the second, macroalgae were gently removed from their substrate and introduced into the bottle under the water. Then, the bottles were manually shaken, and each sample was filtered through a 300 µm nylon mesh to remove the detritus and the larger grazers. The filtered water was stored in a plastic bottle (Nalgene, HDPE, 125 mL).

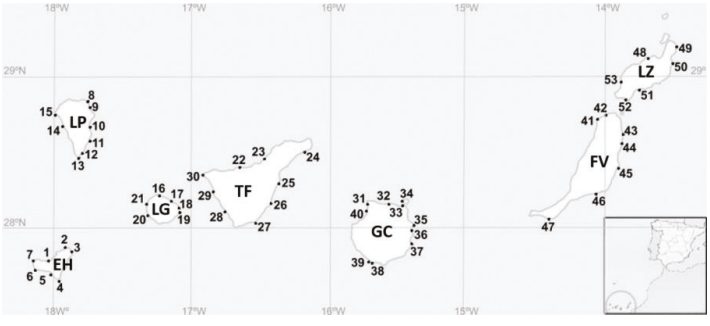

Figure 5. Sampling stations in the Canary Islands for the current study. Numbers correspond to locations described in Table 1. EH (El Hierro), FV (Fuerteventura), GC (Gran Canaria), LG (La Gomera), LP (La Palma), LZ (Lanzarote), and TF (Tenerife).

4.3. Isolation and Culturing

Samples were observed under a light microscope (Leica Microsystems GmbH, Germany) to isolate *Gambierdiscus* and *Fukuyoa* cells by the capillary method [86]. Each dinoflagellate cell was placed individually in one well of an untreated Nunc 24 well plate (Thermo Fisher Scientific) with 1 mL of modified ES medium [87]. The culture medium was constituted with seawater from L'Ametlla de Mar (Spain), Mediterranean Sea (40.8465°; 0.772432°), which was aged for two months in the dark and was filtered through an activated carbon filter of PTFE (Thermo Fisher Scientific) and after through a 0.22 µm cellulose acetate filter (Merck KGaA, Germany). The salinity was adjusted to 36 with Milli-Q water. After 2–3 weeks, fifty-two cultures achieved at least 20 cells mL^{-1} and cells were transferred to fresh medium for maintenance in 28 mL round-bottom glass tubes (Thermo Fisher Scientific). Cells were cultured at 24 ± 1 °C, with a photon irradiance of 100 µmol photons m^{-2} s^{-1} and 12:12 light:dark cycle. Light was provided by fluorescent tubes with white light. Irradiance was measured by QSL-2100 Radiometer (Biospherical Instruments, San Diego, CA, USA).

Table 4. Description of the sampling stations of the present study in the Canary Islands. Ref.: correspond to the locations in Figure 1. Details of the date, coordinates, and environmental data are compiled in Table S1.

Ref.	Island	Location	Ref.	Island	Location
1	El Hierro	Charco Azul	27	Tenerife	La Tejita
2	El Hierro	Charco Manso	28	Tenerife	La Caleta
3	El Hierro	Tamaduste	29	Tenerife	El Pto. de Santiago
4	El Hierro	La Restinga	30	Tenerife	Punta de Teno
5	El Hierro	Tacoron	31	Gran Canaria	Punta Sardina
6	El Hierro	Orchilla	32	Gran Canaria	El Puertillo, Bañaderos
7	El Hierro	Verodal	33	Gran Canaria	Las Canteras
8	La Palma	La Fajana	34	Gran Canaria	El Confital
9	La Palma	El Puerto Espíndola	35	Gran Canaria	Melenara
10	La Palma	Los Cancajos	36	Gran Canaria	Playa Tufia
11	La Palma	Salemera	37	Gran Canaria	Agüimes, Playa El Cabrón
12	La Palma	El Puerto de Trigo	38	Gran Canaria	Arguineguín El Pajar
13	La Palma	El Faro Fuencaliente	39	Gran Canaria	Arguineguín Sta. Águeda
14	La Palma	Tazacorte	40	Gran Canaria	Las Charcas de Agaete
15	La Palma	Puntagorda	41	Fuerteventura	Caleta del Río, El Cotillo
16	La Gomera	Vallehermoso	42	Fuerteventura	Majanicho
17	La Gomera	La Caleta	43	Fuerteventura	Playa Jabalito
18	La Gomera	Playa de Ávalos	44	Fuerteventura	Puerto Lajas
19	La Gomera	Playa de la Cueva	45	Fuerteventura	Puerto Caleta del Fuste
20	La Gomera	Playa de Vueltas	46	Fuerteventura	Gran Tarajal
21	La Gomera	Alojera	47	Fuerteventura	Morro Jable
22	Tenerife	Charca del Viento	48	Lanzarote	Caleta Caballo
23	Tenerife	Puerto del Sauzal	49	Lanzarote	Las Cocinitas
24	Tenerife	Playa las Teresitas	50	Lanzarote	Charco del Palo
25	Tenerife	El Puertito	51	Lanzarote	Puerto Calero
26	Tenerife	Punta de Abona	52	Lanzarote	Playa Mujeres
			53	Lanzarote	El Golfo

4.4. Molecular Identification

To identify the fifty-two cultures at the species level, the D8-D10 region of the LSU rDNA was used [43,44]. The cultures were transferred to 100 mL Erlenmeyer flasks at a final concentration of 50 cells mL^{-1}. Afterwards, 50 mL of culture were harvested at the exponential phase by centrifugation (4300 g, 20 min). The resulting cell pellet was processed for DNA extraction using the phenol/chloroform/isoamylalcohol extraction (PCI) protocol according to Toldrà et al. [88]. Genomic DNA was quantified and checked for its purity using a NanoDrop 2000 spectrophotometer (Thermo Fisher Scientific). The D8-D10 of the LSU region was amplified by PCR using the primers FD8 and RB [43]. Amplifications were carried out in a Mastercycler nexus gradient thermal cycler (Eppendorf, Spain) as it was described in Reverté et al. [61]. The similarity of sequences was checked by BLAST (National Centre of Biotechnology Information, NCBI) and deposited in GenBank. Sequences of >562 were aligned using MAFFT v.7 [89] with the G-INS-1 progressive method. The final alignment consisted of 42 seqs from the current study with 562 positions. The origin of the sequences and the date of collection are shown in Table S2. The phylogenetic relationships were inferred by Maximum Likelihood (ML) using RaxML v.8 [90] and by Bayesian inference (BI) using Mr. Bayes v.3.2.2 [91]. The model of evolutionary reconstruction for ML analysis was estimated using JModelTest 2.1.10 [92].

In the BI approach, two analyses were run in parallel, 10^6 generations, and four chains in each run. The parameters used for analysis were nst = mixed and rates = gamma. By default, 25% of the trees were discarded. The stability of the chains was checked using Tracer v.1.7.1 [93].

4.5. Morphological Characterization

Monoclonal cultures were cultivated and acclimated for a minimum of one year before experimentation to reduce the variability of the response that stress can produce [94]. The morphological characterization was conducted in 4 strains: IRTA-SMM-16-286 (*G. australes*) from Lanzarote, IRTA-SMM-17-407 (*G. excentricus*) from La Gomera, IRTA-SMM-17-03 (*G. caribaeus*),these three strains were reported in Gaiani et al. [68], and IRTA-SMM-17-421 (*G. belizeanus*) from El Hierro. A 5 mL aliquot of each culture at the late exponential phase was fixed with 3% Lugol's iodine solution. Then, the aliquots were stained using Calcofluor White M2R (Sigma Aldrich, Spain), according to Fritz and Triemer [95]. The thecae were described following the nomenclature proposed by Fraga et al. [30]. The depth (dorso-ventral axis) and the width (transdiameter lateral extremes of cingulum) of 50 individuals of each strain were measured using an epifluorescence microscope (LEICA DMLB and NIKON eclipse 80i) equipped with an Olympus camera (Olympus DP70). The software used for measurements was an Olympus DP controller (Olympus Corporation). Cell dimensions were expressed as mean ± standard deviation (SD). In addition, cells of *G. belizeanus* (IRTA-SMM-17-421) were observed by scanning electron microscopy (SEM). For that, 10 mL of cultures at the initial exponential growth phase were fixed with glutaraldehyde at a final concentration of 4% for 2 h at room temperature. After that, 3 mL of culture were collected with a syringe by applying a low pressure on a 5 µm Nuclepore Track-Etch Membrane (Thermo Fisher Scientific). Previously, the membrane had been coated with poly-L-lysine and held in a plastic filter mold of 13 mm diameter (PALL, life Science). The membrane with the cells was rinsed twice: once with seawater (autoclaved and filtered with active carbon 0.22 µm) and a second time with seawater/MilliQ water (50:50, v:v). Afterwards, dehydration was performed in a graded EtOH series of 30, 50, 70, 80, 90 and twice with 96%. Filters were transferred to vessels with absolute EtOH and sent to SEM facilities of the Institut de Ciències del Mar (ICM-CSIC). Then, filters were submitted to critical-point drying with liquid carbon dioxide in a BAL-TEC CPD030 unit (Leica Microsystems, Austria). Dried filters were mounted on stubs with colloidal silver and then sputter-coated with gold in a Q150R S (Quorum Technologies Ltd.). Cells were observed with a Hitachi S3500N scanning electron microscope (Hitachi High Technologies Co., Ltd., Japan) at an accelerating voltage of 5 kV.

4.6. Production of Microalgal Extracts for Toxin Evaluation

Forty-one cultures of *Gambierdiscus* were inoculated in 500 mL Fernbach at an initial concentration of 50 cells mL^{-1}. When cultures arrived at the late exponential-early stationary phase, aliquots of microalgal cultures were collected and fixed with 3% Lugol's iodine solution for cell counting under the light microscope. Then, cultures were harvested by centrifugation (4300 g, 20 min), obtaining between 1×10^5–1.6×10^6 cells of each strain. Cell pellets were kept with absolute methanol (1 mL of methanol for 1 x 10^{-6} cells) at −20 °C. For toxin extraction, each microalgal pellet was sonicated using an ultrasonic cell disrupter (Watt ultrasonic processor VCX750, USA) at 3 s on and 2 s off, 34% amplitude for 15 min. After that, the sample was centrifuged (600 g, 5 min), and the supernatant was removed and kept in a glass vial. Then, new absolute methanol was added to the cell pellet and the whole process of toxin extraction was repeated twice. Supernatants were pooled and evaporated under N_2 by Turbovap (Caliper, Hopkinton, MA, USA) at 40 °C. Dried extract was dissolved with methanol and kept at −20 °C until toxin evaluation.

4.7. Evaluation of CTX-Like Toxicity with the Neuroblastoma Cell-Based Assay

The CTX-like toxicity of forty-one cultures of *Gambierdiscus*, consisting of *G. australes* (n = 29), *G. excentricus* (n = 10), *G. caribaeus* (n = 1), and *G. belizeanus* (n = 1), was evaluated using the neuro-2a

CBA. This assay is used to detect compounds that target voltage-gated sodium channels (VGSCs). The assay uses ouabain, which blocks the Na^+/K^+-ATPase ion pump and inhibits the efflux of Na^+ [96] and veratridine, which activates the VGSC, enhancing the influx of Na^+ [97]. The neuro-2a CBA is based on the reduction of viability of the neuro-2a cells when the extract presents CTXs or molecules that activate VGSCs after the ouabain and veratridine treatment [98].

The neuro-2a CBA and the data analysis were conducted following the protocol described in Caillaud et al. [99]. CTX1B was the molecule of reference (standard) to quantify the CTX-like toxicity of the extracts, and a dose-response curve was obtained each day of experimentation. To be able to discriminate CTX-like toxicity from other types of toxicity, neuro-2a cells were exposed to extracts or standards with and without ouabain and veratridine. It was considered that samples contained CTX-compounds or other compounds that target VGSCs when toxicity was not observed in the O/V^- conditions but was observed in the O/V^+ conditions. In the cases that toxicity was observed in both conditions (O/V^- and O/V^+), it indicates the presence of a non-specific toxic compounds, other that target the VGSCs.

Concentrations of CTX1B ranged between 0.2 and 25 pg mL^{-1}, and concentrations of microalgal extracts ranged between 0.3 and 6000 cells equiv. mL^{-1}. The concentrations of microalgal extracts were chosen based on the toxic effect observed in the neuro-2a cells from previous screening experiments. After 24 h of exposure, the viability of the neuro-2a cells was assessed by the quantitative colorimetric MTT assay [98]. Data analysis was performed using SigmaPlot software 12.0 (Systat Software Inc., San Jose, CA, USA). Matrix effect was considered when significant toxicity appeared in the neuro-2a cells without O/V^-. Significant toxicity was described as the inhibition of more than 20% of the cell viability. The normality of the CTX-like toxicities was checked using the Shapiro-Wilk test. Then, a one-way ANOVA was used to test if significant differences in CTX-like toxicities occurred among *G. excentricus* and *G. australes*, and if significant differences occurred between the islands within these species. The statistical test and graphs were performed with R studio [100].

4.8. Evaluation of the Presence of Two Series of CTX Congeners (CTX1B and CTX3C) in G. belizeanus with a Colorimetric Immunoassay and an Electrochemical Immunosensor

The use of 3G8 and 10C9 mAbs in the screening of the *Gambierdiscus* extracts allowed the detection of two series of CTXs congeners (CTX1B and CTX3C) thanks to the high affinities of these capture antibodies for their CTX targets. In particular, 3G8 mAb binds to the left wing of CTX1B and 54-deoxyCTX1B [83], and 10C9 mAb binds to the left wing of CTX3C and 51-hydroxyCTX3C [81]. The 8H4 mAb, used as a reporter antibody, binds to the right wing of all the four congeners [101]. For this reason, quantifications are expressed in fg $cell^{-1}$ of CTX1B equiv. when only the 3G8 mAb was incubated with the microalgal extract and in fg $cell^{-1}$ of 51-hydroxyCTX3C equiv. in presence of only the 10C9 mAb. The use of separated mAbs allows the discrimination between the two series of CTX congeners. Therefore, when both antibodies are incubated with the extract, a global response is obtained, and thus quantifications can be provided either in fg $cell^{-1}$ of CTX1B equiv. or 51-hydroxyCTX3C equiv. In this work, the obtained quantifications when the two antibodies are incubated together are provided only in CTX1B equiv. for comparison with neuro-2a CBA results. Analyses of *G. belizeanus* extracts were performed as described in Gaiani et al. [68]. Briefly, magnetic beads (MBs) were activated with an EDC and NHS solution and incubated with 3G8 or 10C9 mAbs. In particular, 3G8 mAb binds against the left wing of CTX1B and 54-deoxyCTX1B. Instead, 10C9 mAb binds specifically to the left wing of CTX3C and 51-hydroxyCTX3C [83,85]. Figure 6 shows the structure of the four CTX congeners (CTX1B and CTX3C congeners) that the antibodies recognize. After the incubation, the mAb–MB conjugates were washed, placed into new tubes in a separate or mixed way, exposed to microalgal extract (previously evaporated and suspended in PBS–Tween) or CTX standard (CTX1B or 51-hydroxyCTX3C) for calibration purposes. Afterwards, a blocking step was performed with PBS–Tween–BSA. Then, the conjugates were incubated with biotin-8H4 mAb [101]. The 8H4 mAb binds to the right wing of CTX1B and 54-deoxyCTX1B and has cross-reactivity with

the right wing of CTX3C and 51-hydroxyCTX3C. Finally, immunocomplexes were incubated with polyHRP–streptavidin, washed, and re-suspended in PBS–Tween. The colorimetric immunoassay was performed incubating the immunocomplexes with TMB (HRP enzyme substrate) and reading the absorbance at 620 nm using an automated plate spectrophotometer. Measurements were performed in triplicate. The electrochemical immunosensor was performed placing the immunocomplexes on the working electrodes of an 8-electrode array, incubating with TMB, and measuring the reduction current using amperometry (−0.2 V (vs. Ag) for 5 s). Measurements were performed in quadruplicate.

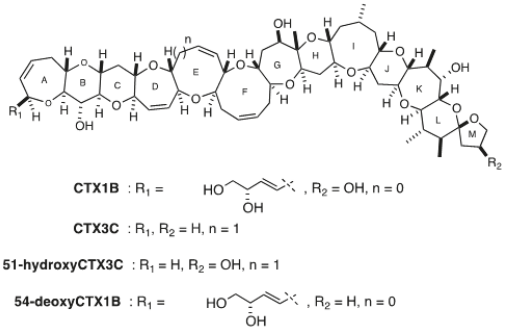

Figure 6. Structure of CTX1B and CTX3C congeners recognized by the antibodies used in this work.

Supplementary Materials: The following are available online at http://www.mdpi.com/2072-6651/12/11/692/s1, Table S1: supplementary material, Table S2: supplementary material, Table S3: Cell viability and CTX-like toxicity after the exposure of neuro-2a cells to *Gambierdiscus* spp. extracts with (O/V^{+}) and without (O/V^{-}) ouabain and veratridine treatment.

Author Contributions: À.T., G.G., M.C. and J.D., M.F.-T. and T.T. designed the experiments. À.T. and M.R.V. carried out the samplings, the microalgae isolation and scale up the cultures. À.T. and G.G. performed the experiments. À.T. and K.B.A. carried out the identification of isolates by molecular tools. À.T., M.R.V. and M.F.-T. characterized the species by light and electron microscope. À.T., M.C., J.D., G.G., M.R.V., K.B.A. and M.F.-T. analyzed and interpreted the data. À.T. wrote the paper. All authors contributed to editing the paper. All authors have read and agreed to the published version of the manuscript.

Funding: This research was funded bythe European Food Safety Authority (EFSA) through the EUROCIGUA project (GP/EFSA/AFSCO/2015/03) and the Ministerio de Ciencia, Innovación y Universidades (MICINN), the Agencia Estatal de Investigación (AEI) and the Fondo Europeo de Desarrollo Regional (FEDER) through the CIGUASENSING project (BIO2017-87946-C2-2-R). The authors also acknowledge support from CERCA Programme/Generalitat de Catalunya. A.T. and G.G. acknowledge IRTA-URV-Santander for her their respective PhD grants (2016 PMF-PIPF-74 and 2018 PMF-PIPF-19).

Acknowledgments: The authors gratefully acknowledge José Luis Costa and Vanessa Castán for their assistance in the samplings and Louis Caray his value work in the toxin extractions We would like to thank José Manuel Fortuño from Institut Ciències del Mar (CSIC) for his advices in scanning electronic microscopy.

Conflicts of Interest: The authors declare no conflict of interest.

References

1. Adachi, R.; Fukuyo, Y. The thecal structure of a marine toxic dinoflagellate *Gambierdiscus toxicus* gen. et spec. nov. collected in a ciguatera-endemic area. *Bull. Jpn. Soc. Sci. Fish.* **1979**, *45*, 67–71. [CrossRef]
2. Murata, M.; Ishibashi, Y.; Fukui, M.; Yasumoto, T.; Legrand, A.M. Structures and Configurations of Ciguatoxin from the Moray Eel *Gymnothorax javanicus* and Its Likely Precursor from the Dinoflagellate *Gambierdiscus toxicus*. *J. Am. Chem. Soc.* **1990**, *112*, 4380–4386. [CrossRef]
3. Parsons, M.L.; Settlemier, C.J.; Ballauer, J.M. An examination of the epiphytic nature of *Gambierdiscus toxicus*, a dinoflagellate involved in ciguatera fish poisoning. *Harmful Algae* **2011**, *10*, 598–605. [CrossRef] [PubMed]
4. FAO; WHO. *Report of the Expert Meeting on Ciguatera Poisoning*; Food Safety and Quality: Rome, Italy, 2020; ISBN 9789240006294.

5. Molgó, J.; Shimahara, T.; Legrand, A.M. Ciguatoxin, extracted from poisonous morays eels, causes sodium-dependent calcium mobilization in NG108-15 neuroblastoma × glioma hybrid cells. *Neurosci. Lett.* **1993**, *158*, 147–150. [CrossRef]
6. Nicholson, G.M.; Lewis, R.J. Ciguatoxins: Cyclic polyether modulators of voltage-gated ion channel function. *Mar. Drugs* **2006**, *4*, 82–118. [CrossRef]
7. Gillespie, N.C.; Lewis, R.J.; Pearn, J.H.; Bourke, A.T.; Holmes, M.J.; Bourke, J.B.; Shields, W.J. Ciguatera in Australia. Occurrence, clinical features, pathophysiology and management. *Med. J. Aust.* **1986**, *145*, 584–590. [CrossRef]
8. Friedman, M.A.; Fernandez, M.; Backer, L.C.; Dickey, R.W.; Bernstein, J.; Schrank, K.; Kibler, S.; Stephan, W.; Gribble, M.O.; Bienfang, P.; et al. An updated review of ciguatera fish poisoning: Clinical, epidemiological, environmental, and public health management. *Mar. Drugs* **2017**, *15*, 72. [CrossRef]
9. Skinner, M.P.; Brewer, T.D.; Johnstone, R.; Fleming, L.E.; Lewis, R.J. Ciguatera fish poisoning in the pacific islands (1998 to 2008). *PLoS Negl. Trop. Dis.* **2011**, *5*, 1–7. [CrossRef]
10. Llewellyn, L.E. Revisiting the association between sea surface temperature and the epidemiology of fish poisoning in the South Pacific: Reassessing the link between ciguatera and climate change. *Toxicon* **2010**, *56*, 691–697. [CrossRef]
11. Tester, P.A.; Feldman, R.L.; Nau, A.W.; Kibler, S.R.; Wayne Litaker, R. Ciguatera fish poisoning and sea surface temperatures in the Caribbean Sea and the West Indies. *Toxicon* **2010**, *56*, 698–710. [CrossRef]
12. Farrell, H.; Edwards, A.; Zammit, A. Four recent ciguatera fish poisoning incidents in New South Wales, Australia linked to imported fish. *Commun. Dis. Intell.* **2019**, *43*. [CrossRef]
13. Bravo, J.; Suarez, F.C.; Ramirez, A.S.; Acosta, F. Ciguatera, an Emerging Human Poisoning in Europe. *J. Aquac. Mar. Biol.* **2015**, *3*, 1–6.
14. Chinain, M.; Gatti, C.M.; Roué, M.; Darius, H.T. Ciguatera poisoning in French Polynesia: Insights into the novel trends of an ancient disease. *New Microbes New Infect.* **2019**, *31*, 100565. [CrossRef] [PubMed]
15. Nishimura, T.; Sato, S.; Tawong, W.; Sakanari, H.; Uehara, K.; Shah, M.M.R.; Suda, S.; Yasumoto, T.; Taira, Y.; Yamaguchi, H.; et al. Genetic Diversity and Distribution of the Ciguatera-Causing Dinoflagellate *Gambierdiscus* spp. (Dinophyceae) in Coastal Areas of Japan. *PLoS ONE* **2013**, *8*, e60882. [CrossRef] [PubMed]
16. Tester, P.A.; Vandersea, M.W.; Buckel, C.A.; Kibler, S.R.; Holland, W.C.; Davenport, E.D.; Clark, R.D.; Edwards, K.F.; Taylor, J.C.; Pluym, J.L.V.; et al. *Gambierdiscus* (Dinophyceae) species diversity in the flower garden banks national marine sanctuary, Northern Gulf of Mexico, USA. *Harmful Algae* **2013**, *29*, 1–9. [CrossRef]
17. Pérez-Arellano, J.L.; Luzardo, O.P.; Brito, A.P.; Cabrera, M.H.; Zumbado, M.; Carranza, C.; Angel-Moreno, A.; Dickey, R.W.; Boada, L.D. Ciguatera fish poisoning, Canary Islands. *Emerg. Infect. Dis.* **2005**, *11*, 1981–1982. [CrossRef]
18. Gouveia, N.N.; Vale, P.; Gouveia, N.; Delgado, J. Primeiro Registo da Ocorrência de Episódios do Tipo Ciguatérico no Arquipélago da Madeira. In *Algas Toxicas e Biotoxinas nas Águas da Península Ibérica*; IPIMAR: Lisboa, Portugal, 2010; pp. 152–157.
19. Falcón García, I. *Epidemiología de la Intoxicación Alimentaria por Ciguatoxinas en Canarias*; Hospital Universitario Nuestra Señora de Candelaria: Santa Cruz de Tenerife, Spain, 2018.
20. Caillaud, A.; Eixarch, H.; de la Iglesia, P.; Rodriguez, M.; Dominguez, L.; Andree, K.B.; Diogène, J. Towards the standardisation of the neuroblastoma (neuro-2a) cell-based assay for ciguatoxin-like toxicity detection in fish: Application to fish caught in the Canary Islands. *Food Addit. Contam. Part A Chem. Anal. Control. Expo. Risk Assess.* **2012**, *29*, 1000–1010. [CrossRef]
21. Sanchez-Henao, J.A.; García-Álvarez, N.; Fernández, A.; Saavedra, P.; Silva Sergent, F.; Padilla, D.; Acosta-Hernández, B.; Martel Suárez, M.; Diogène, J.; Real, F. Predictive score and probability of CTX-like toxicity in fish samples from the official control of ciguatera in the Canary Islands. *Sci. Total Environ.* **2019**, *673*, 576–584. [CrossRef]
22. Munday, R.; Murray, S.; Rhodes, L.; Larsson, M.; Harwood, D. Ciguatoxins and Maitotoxins in Extracts of Sixteen *Gambierdiscus* Isolates and One *Fukuyoa* Isolate from the South Pacific and Their Toxicity to Mice by Intraperitoneal and Oral Administration. *Mar. Drugs* **2017**, *15*, 208. [CrossRef]
23. Rhodes, L.; Harwood, T.; Smith, K.; Argyle, P.; Munday, R. Production of ciguatoxin and maitotoxin by strains of *Gambierdiscus australes*, *G. pacificus* and *G. polynesiensis* (Dinophyceae) isolated from Rarotonga, Cook Islands. *Harmful Algae* **2014**, *39*, 185–190. [CrossRef]

24. Pisapia, F.; Holland, W.C.; Hardison, D.R.; Litaker, R.W.; Fraga, S.; Nishimura, T.; Adachi, M.; Nguyen-Ngoc, L.; Séchet, V.; Amzil, Z.; et al. Toxicity screening of 13 *Gambierdiscus* strains using neuro-2a and erythrocyte lysis bioassays. *Harmful Algae* **2017**, *63*, 173–183. [CrossRef] [PubMed]
25. Rossignoli, A.E.; Tudó, A.; Bravo, I.; Díaz, P.A.; Diogène, J.; Riobó, P. Toxicity characterisation of *Gambierdiscus* species from the canary Islands. *Toxins (Basel)* **2020**, *12*, 134. [CrossRef] [PubMed]
26. Tester, P.A.; Litaker, R.W.; Berdalet, E. Climate change and harmful benthic microalgae. *Harmful Algae* **2020**, *91*, 101655. [CrossRef]
27. Navarro-Pérez, E.; Barton, E.D. Seasonal and interannual variability of the Canary Current. *Sci. Mar.* **2001**, *65*, 205–213. [CrossRef]
28. Davenport, R.; Neuer, S.; Helmke, P.; Perez-Marrero, J.; Llinas, O. Primary productivity in the northern Canary Islands region as inferred from SeaWiFS imagery. *Deep. Res. Part II Top. Stud. Oceanogr.* **2002**, *49*, 3481–3496. [CrossRef]
29. Fraga, S.; Riobó, P.; Diogène, J.; Paz, B.; Franco, J.M. Toxic and potenially toxic benthic dinoflagellates observed in Macaronesia (NE Atlantic Archipelago). In Proceedings of the Abstract Book of the 11th International Conference on Harmful Algae, Capetown, South Africa, 15–19 November 2004; p. 115.
30. Fraga, S.; Rodríguez, F.; Caillaud, A.; Diogène, J.; Raho, N.; Zapata, M. *Gambierdiscus excentricus* sp. nov. (Dinophyceae), a benthic toxic dinoflagellate from the Canary Islands (NE Atlantic Ocean). *Harmful Algae* **2011**, *11*, 10–22. [CrossRef]
31. Fraga, S.; Rodríguez, F. Genus *Gambierdiscus* in the Canary Islands (NE Atlantic Ocean) with Description of *Gambierdiscus silvae* sp. nov., a New Potentially Toxic Epiphytic Benthic Dinoflagellate. *Protist* **2014**, *165*, 839–853. [CrossRef]
32. Bravo, I.; Rodriguez, F.; Ramilo, I.; Rial, P.; Fraga, S. Ciguatera-causing dinoflagellate *Gambierdiscus* spp. (Dinophyceae) in a subtropical region of North Atlantic Ocean (Canary Islands): Morphological characterization and biogeography. *Toxins (Basel)* **2019**, *11*, 423. [CrossRef]
33. Rodríguez, F.; Fraga, S.; Ramilo, I.; Rial, P.; Figueroa, R.I.; Riobó, P.; Bravo, I. "Canary Islands (NE Atlantic) as a biodiversity 'hotspot' of *Gambierdiscus*: Implications for future trends of ciguatera in the area". *Harmful Algae* **2017**, *67*, 131–143.
34. Faust, M.A. Observation of sand-dwelling toxic dinoflagellates (Dinophyceae) from widely differing sites, including two new species. *J. Phycol.* **1995**, *31*, 996–1003. [CrossRef]
35. Díaz-Asencio, L.; Clausing, R.J.; Vandersea, M.; Chamero-Lago, D.; Gómez-Batista, M.; Hernández-Albernas, J.I.; Chomérat, N.; Rojas-Abrahantes, G.; Litaker, R.W.; Tester, P.; et al. Ciguatoxin occurrence in food-web components of a cuban coral reef ecosystem: Risk-assessment implications. *Toxins (Basel)* **2019**, *11*, 722. [CrossRef] [PubMed]
36. Richlen, M.L.; Morton, S.L.; Barber, P.H.; Lobel, P.S. Phylogeography, morphological variation and taxonomy of the toxic dinoflagellate *Gambierdiscus toxicus* (Dinophyceae). *Harmful Algae* **2008**, *7*, 614–629. [CrossRef]
37. Litaker, R.W.; Holland, W.C.; Hardison, D.R.; Pisapia, F.; Hess, P.; Kibler, S.R.; Tester, P.A. Ciguatoxicity of *Gambierdiscus* and *Fukuyoa* species from the Caribbean and Gulf of Mexico. *PLoS ONE* **2017**, *12*, 1–19. [CrossRef]
38. Catania, D.; Richlen, M.L.; Mak, Y.L.; Morton, S.L.; Laban, E.H.; Xu, Y.; Anderson, D.M.; Chan, L.L.; Berumen, M.L. The prevalence of benthic dinoflagellates associated with ciguatera fish poisoning in the central Red Sea. *Harmful Algae* **2017**, *68*, 206–216. [CrossRef] [PubMed]
39. Murray, S.; Momigliano, P.; Heimann, K.; Blair, D. Molecular phylogenetics and morphology of *Gambierdiscus yasumotoi* from tropical eastern Australia. *Harmful Algae* **2014**, *39*, 242–252. [CrossRef]
40. Leaw, C.P.; Lim, P.T.; Tan, T.H.; Tuan-Halim, T.N.; Cheng, K.W.; Ng, B.K.; Usup, G. First report of the benthic dinoflagellate, *Gambierdiscus belizeanus* (Gonyaulacales: Dinophyceae) for the east coast of Sabah, Malaysian Borneo. *Phycol. Res.* **2011**, *59*, 143–146. [CrossRef]
41. Xu, Y.; Richlen, M.L.; Morton, S.L.; Mak, Y.L.; Chan, L.L.; Tekiau, A.; Anderson, D.M. Distribution, abundance and diversity of *Gambierdiscus* spp. from a ciguatera-endemic area in Marakei, Republic of Kiribati. *Harmful Algae* **2014**, *34*, 56–68. [CrossRef]
42. Bravo, I.; Figueroa, R.I.; Fraga, S. Cellular and nuclear morphological variability within a single species of the toxigenic dinoflagellate genus *Gambierdiscus*: Relationship to life-cycle processes. *Harmful Algae* **2014**, *40*, 1–8. [CrossRef]
43. Chinain, M.; Faust, M.A.; Pauillac, S. Morphology and molecular analyses of three toxic species of *Gambierdiscus* (Dinophyceae): *G. pacificus*, sp nov., *G. australes*, sp nov., and *G. polynesiensis*, sp nov. *J. Phycol.* **1999**, *35*, 1282–1296. [CrossRef]

44. Litaker, R.W.; Vandersea, M.W.; Faust, M.A.; Kibler, S.R.; Chinain, M.; Holmes, M.J.; Holland, W.C.; Tester, P.A. Taxonomy of *Gambierdiscus* including four new species, *Gambierdiscus caribaeus*, *Gambierdiscus carolinianus*, *Gambierdiscus carpenteri* and *Gambierdiscus ruetzleri* (Gonyaulacales, Dinophyceae). *Phycologia* **2009**, *48*, 344–390. [CrossRef]
45. Hoppenrath, M.; Kretzschmar, A.L.; Kaufmann, M.J.; Murray, S.A. Morphological and molecular phylogenetic identification and record verification of *Gambierdiscus excentricus* (Dinophyceae) from Madeira Island (NE Atlantic Ocean). *Mar. Biodivers. Rec.* **2019**, *12*, 1–9. [CrossRef]
46. Aligizaki, K.; Nikolaidis, G.; Fraga, S. Is *Gambierdiscus* expanding to new areas? *Harmful Algae News* **2008**, *36*, 6–7.
47. Kibler, S.R.; Litaker, R.W.; Holland, W.C.; Vandersea, M.W.; Tester, P.A. Growth of eight *Gambierdiscus* (Dinophyceae) species: Effects of temperature, salinity and irradiance. *Harmful Algae* **2012**, *19*, 1–14. [CrossRef]
48. Xu, Y.; Richlen, M.L.; Liefer, J.D.; Robertson, A.; Kulis, D.; Smith, T.B.; Parsons, M.L.; Anderson, D.M. Influence of Environmental Variables on *Gambierdiscus* spp. (Dinophyceae) Growth and Distribution. *PLoS ONE* **2016**, *11*, e0153197. [CrossRef] [PubMed]
49. Espino, F.; Tuya, F.; Rosario, A.; Bosch, N.E.; Coca, J.; Gonz, A.J.; Rosario, F.; Otero-ferrer, F.J.; Moreno, Á.C.; Haroun, R. Geographical Range Extension of the Spotfin burrfish, *Chilomycterus reticulatus* (L. 1758), in the Canary Islands: A Response to Ocean Warming? *Diversity* **2019**, *11*, 230. [CrossRef]
50. PLOCAN Oceanic Platform of the Canary Islands (PLOCAN). Available online: http://obsplatforms.plocan.eu/climatology (accessed on 3 June 2020).
51. Yoshimatsu, T.; Yamaguchi, H.; Iwamoto, H.; Nishimura, T.; Adachi, M. Effects of temperature, salinity and their interaction on growth of Japanese *Gambierdiscus* spp. (Dinophyceae). *Harmful Algae* **2014**, *35*, 29–37. [CrossRef]
52. Litaker, R.W.; Tester, P.A.; Vandersea, M.W. Species-specific PCR assays for *Gambierdiscus excentricus* and *Gambierdiscus silvae* (Gonyaulacales, Dinophyceae). *J. Phycol.* **2019**, *55*, 730–732. [CrossRef]
53. Tawong, W.; Yoshimatsu, T.; Yamaguchi, H.; Adachi, M. Temperature and salinity effects and toxicity of <i>*Gambierdiscus caribaeus* (Dinophyceae) from Thailand. *Phycologia* **2016**, *55*, 274–278. [CrossRef]
54. Tuya, F.; Haroun, R.J. Spatial patterns and response to wave exposure of shallow water algal assemblages across the Canarian Archipelago: A multi-scaled approach. *Mar. Ecol. Prog. Ser.* **2006**, *311*, 15–28. [CrossRef]
55. Soler-Onis, E.; Fernández-Zabala, J.; Ojeda-Rodriguez, A.; Amorim, A. Bloom of *Gambierdiscus caribaeus* in the temperate-subtropical waters of El Hierro, Canary Islands (North East Atlantic). *Harmful Algae News* **2016**, *55*, 14–16.
56. Vélez-Belchí, P.; Gonzalez-Carballo, M.; Perez-Hernández, M.D.; Hernández-Guerra, A. Open ocean temperature and salinity trends. *Oceanogr. Biol. Featur. Canar. Curr. Large Mar. Ecosyst.* **2015**, *13*, 299–308.
57. Kibler, S.R.; Tester, P.A.; Kunkel, K.E.; Moore, S.K.; Litaker, R.W. Effects of ocean warming on growth and distribution of dinoflagellates associated with ciguatera fish poisoning in the Caribbean. *Ecol. Modell.* **2015**, *316*, 194–210. [CrossRef]
58. Ikehara, T.; Kuniyoshi, K.; Oshiro, N.; Yasumoto, T. Biooxidation of ciguatoxins leads to species-specific toxin profiles. *Toxins (Basel)* **2017**, *9*, 205. [CrossRef] [PubMed]
59. Yogi, K.; Sakugawa, S.; Oshiro, N.; Ikehara, T.; Sugiyama, K.; Yasumoto, T. Determination of toxins involved in ciguatera fish poisoning in the Pacific by LC/MS. *J. AOAC Int.* **2014**, *97*, 398–402. [CrossRef] [PubMed]
60. Lewis, R.J.; Sellin, M.; Poli, M.A.; Norton, R.S.; MacLeod, J.K.; Sheil, M.M. Purification and characterization of ciguatoxins from moray eel (*Lycodontis javanicus*, Muraenidae). *Toxicon* **1991**, *29*, 1115–1127. [CrossRef]
61. Reverté, L.; Toldrà, A.; Andree, K.B.; Fraga, S.; de Falco, G.; Campàs, M.; Diogène, J. Assessment of cytotoxicity in ten strains of *Gambierdiscus australes* from Macaronesian Islands by neuro-2a cell-based assays. *J. Appl. Phycol.* **2018**, *30*, 2447–2461. [CrossRef]
62. Paz, B.; Riobó, P.; Franco, J.M. Preliminary study for rapid determination of phycotoxins in microalgae whole cells using matrix-assisted laser desorption/ionization time-of-flight mass spectrometry. *Rapid Commun. Mass Spectrom.* **2011**, *25*, 3627–3639. [CrossRef]
63. Pisapia, F.; Sibat, M.L.; Herrenknecht, C.; Lhaute, K.; Gaiani, G.; Ferron, P.J.; Fessard, V.; Fraga, S.; Nascimento, S.M.; Litaker, R.W.; et al. Maitotoxin-4, a novel MTX analog produced by *Gambierdiscus* excentricus. *Mar. Drugs* **2017**, *15*, 220. [CrossRef]
64. Estevez, P.; Sibat, M.; Leao, J.M.; Tudó, A.; Rambla-Alegre, M.; Aligizak, K.; Gago-Martinez, A.; Diogène, J.; Hess, P. Use of Mass Spectrometry to determine the Diversity of Toxins Produced by *Gambierdiscus* and *Fukuyoa*

Species from Balearic Islands and Crete (Mediterranean Sea) and the Canary Islands (Northeast Atlantic). *Toxins (Basel)* **2020**, *12*, 305. [CrossRef]
65. Caillaud, A.; Yasumoto, T.; Diogène, J. Detection and quantification of maitotoxin-like compounds using a neuroblastoma (Neuro-2a) cell based assay. Application to the screening of maitotoxin-like compounds in Gambierdiscus spp. *Toxicon* **2010**, *56*, 36–44. [CrossRef]
66. Lewis, R.J.; Inserra, M.; Vetter, I.; Holland, W.C.; Hardison, D.R.; Tester, P.A.; Litaker, R.W. Rapid extraction and identification of maitotoxin and ciguatoxin-like toxins from Caribbean and pacific Gambierdiscus using a new functional bioassay. *PLoS ONE* **2016**, *11*, e0160006. [CrossRef] [PubMed]
67. De Haro, L.; Pommier, P.; Valli, M. Emergence of Imported Ciguatera in Europe: Report of 18 Cases at the Poison Control Centre of Marseille. *J. Toxicol. Clin. Toxicol.* **2003**, *41*, 927–930. [CrossRef] [PubMed]
68. Gaiani, G.; Leonardo, S.; Tudó, À.; Toldrà, A.; Rey, M.; Andree, K.B.; Tsumuraya, T.; Hirama, M.; Diogène, J.; O'Sullivan, C.K.; et al. Rapid extraction of ciguatoxins from *Gambierdiscus* and *Fukuyoa* and detection with immunosensing tools. *Ecotoxicol. Environ. Saf.* **2020**, *204*, 111004. [CrossRef]
69. Sanchez-Henao, A.; García-álvarez, N.; Silva, F.; Estévez, P.; Gago-martínez, A.; Martín, F.; Ramos-sosa, M.; Fernández, A.; Diogène, J.; Real, F. Presence of CTXs in moray eels and dusky groupers in the marine environment of the Canary Islands. *Aquat. Toxicol.* **2020**, *221*, 105427. [CrossRef] [PubMed]
70. Tibiriçá, C.E.J.A.; Sibat, M.; Fernandes, L.F.; Bilien, G.; Chomérat, N.; Hess, P.; Mafra, L.L., Jr. Diversity and Toxicity of the Genus *Coolia* Meunier in Brazil, and Detection of 44-methyl Gambierone in *Coolia tropicalis*. *Toxins* **2020**, *12*, 327. [CrossRef] [PubMed]
71. Rodríguez, I.; Genta-Jouve, G.; Alfonso, C.; Calabro, K.; Alonso, E.; Sánchez, J.A.; Alfonso, A.; Thomas, O.P.; Botana, L.M. Gambierone, a Ladder-Shaped Polyether from the Dinoflagellate *Gambierdiscus belizeanus*. *Org. Lett.* **2015**, *17*, 2392–2395. [CrossRef]
72. Boente-Juncal, A.; Álvarez, M.; Antelo, Á.; Rodríguez, I.; Calabro, K.; Vale, C.; Thomas, O.P.; Botana, L.M. Structure elucidation and biological evaluation of maitotoxin-3, a homologue of gambierone, from *Gambierdiscus belizeanus*. *Toxins (Basel)* **2019**, *11*, 79. [CrossRef]
73. Murray, J.S.; Nishimura, T.; Finch, S.C.; Rhodes, L.L.; Puddick, J.; Harwood, D.T.; Larsson, M.E.; Doblin, M.A.; Leung, P.; Yan, M.; et al. The role of 44-methylgambierone in ciguatera fish poisoning: Acute toxicity, production by marine microalgae and its potential as a biomarker for *Gambierdiscus* spp. *Harmful Algae* **2020**, *97*, 101853. [CrossRef]
74. Reverté, L.; Soliño, L.; Carnicer, O.; Diogène, J.; Campàs, M. Alternative methods for the detection of emerging marine toxins: Biosensors, biochemical assays and cell-based assays. *Mar. Drugs* **2014**, *12*, 5719–5963. [CrossRef]
75. Caillaud, A.; De La Iglesia, P.; Darius, H.T.; Pauillac, S.; Aligizaki, K.; Fraga, S.; Chinain, M.; Diogène, J. Update on methodologies available for ciguatoxin determination: Perspectives to confront the onset of ciguatera fish poisoning in Europe. *Mar. Drugs* **2010**, *8*, 1838–1907. [CrossRef]
76. Kretzschmar, A.L.; Verma, A.; Kohli, G.; Murray, S. Development of a quantitative PCR assay for the detection and enumeration of a potentially ciguatoxin-producing dinoflagellate, *Gambierdiscus lapillus* (Gonyaulacales, Dinophyceae). *PLoS ONE* **2019**, *14*, 1–18. [CrossRef]
77. Smith, K.F.; Biessy, L.; Argyle, P.A.; Trnski, T.; Halafihi, T.; Rhodes, L.L. Molecular identification of *Gambierdiscus* and *Fukuyoa* (Dinophyceae) from environmental samples. *Mar. Drugs* **2017**, *15*, 243. [CrossRef] [PubMed]
78. Fernández-Zabala, J.; Tuya, F.; Amorim, A.; Soler-Onís, E. Benthic dinoflagellates: Testing the reliability of the artificial substrate method in the Macaronesian region. *Harmful Algae* **2019**, *87*, 101634. [CrossRef] [PubMed]
79. Nagumo, Y.; Oguri, H.; Tsumoto, K.; Shindo, Y.; Hirama, M.; Tsumuraya, T.; Fujii, I.; Tomioka, Y.; Mizugaki, M.; Kumagai, I. Phage-display selection of antibodies to the left end of CTX3C using synthetic fragments. *J. Immunol. Methods* **2004**, *289*, 137–146. [CrossRef]
80. Nagumo, Y.; Oguri, H.; Shindo, Y.; Sasaki, S.-Y.; Oishi, T.; Hirama, M.; Tomioka, Y.; Mizugaki, M.; Tsumuraya, T. Concise synthesis of ciguatoxin ABC-ring fragments and surface plasmon resonance study of the interaction of their BSA conjugates with monoclonal antibodies. *Bioorg. Med. Chem. Lett.* **2001**, *11*, 2037–2040. [CrossRef]
81. Oguri, H.; Hirama, M.; Tsumuraya, T.; Fujii, I.; Maruyama, M.; Uehara, H.; Nagumo, Y. Synthesis-based approach toward direct sandwich immunoassay for ciguatoxin CTX3C. *J. Am. Chem. Soc.* **2003**, *125*, 7608–7612. [CrossRef]
82. Oguri, H.; Tanaka, S.-I.; Hishiyama, S.; Oishi, T.; Hirama, M.; Tumuraya, T.; Tomioka, Y.; Mizugaki, M. Designed hapten aimed at anti-ciguatoxin monoclonal antibody: Synthesis, immunization and discrimination of the C2 configuration. *Syntesis* **1999**, *S1*, 1431–1436. [CrossRef]

83. Tsumuraya, T.; Takeuchi, K.; Yamashita, S.; Fujii, I.; Hirama, M. Development of a monoclonal antibody against the left wing of ciguatoxin CTX1B: Thiol strategy and detection using a sandwich ELISA. *Toxicon* **2012**, *60*, 348–357. [CrossRef]
84. Tsumuraya, T.; Fujii, I.; Hirama, M. Production of monoclonal antibodies for sandwich immunoassay detection of Pacific ciguatoxins. *Toxicon* **2010**, *56*, 797–803. [CrossRef]
85. Tsumuraya, T.; Fujii, I.; Inoue, M.; Tatami, A.; Miyazaki, K.; Hirama, M. Production of monoclonal antibodies for sandwich immunoassay detection of ciguatoxin 51-hydroxyCTX3C. *Toxicon* **2006**, *48*, 287–294. [CrossRef]
86. Hoshaw, R.W.; Rosowski, J.R. *Handbook of Phycological Methods: Culture Methods and Growth Measurements*; Stein, J.R., Ed.; Cambridge University Press: London, UK; New York, NY, USA, 1973; p. 448.
87. Provasoli, L. Media and prospects of the cultivation of marine algae. In *Culure and Collection of Algae Proceedings*; Japanese Society of Plant Physiology: Hakone, Japan, 1968; pp. 63–75.
88. Toldrà, A.; Andree, K.B.; Fernández-Tejedor, M.; Diogène, J.; Campàs, M. Dual quantitative PCR assay for identification and enumeration of *Karlodinium veneficum* and *Karlodinium armiger* combined with a simple and rapid DNA extraction method. *J. Appl. Phycol.* **2018**, *30*, 2435–2445. [CrossRef]
89. Rozewicki, J.; Li, S.; Amada, K.M.; Standley, D.M.; Katoh, K. MAFFT-DASH: Integrated protein sequence and structural alignment. *Nucleic Acids Res.* **2019**, *47*, W5–W10. [CrossRef]
90. Stamatakis, A. RAxML version 8: A tool for phylogenetic analysis and post-analysis of large phylogenies. *Bioinformatics* **2014**, *30*, 1312–1313. [CrossRef] [PubMed]
91. Huelsenbeck, J.P.; Ronquist, F. MRBAYES: Bayesian inference of phylogenetic trees. *Bioinformatics* **2001**, *17*, 754–755. [CrossRef]
92. Darriba, D.; Taboada, G.L.; Doallo, R.; Posada, D. jModelTest 2: More models, new heuristics and high-performance computing Europe PMC Funders Group. *Nat. Methods* **2012**, *9*, 772. [CrossRef]
93. Rambaut, A.; Drummond, A.J.; Xie, D.; Baele, G.; Suchard, M.A. Posterior summarization in Bayesian phylogenetics using Tracer 1.7. *Syst. Biol.* **2018**, *67*, 901. [CrossRef] [PubMed]
94. Bomber, J.W.; Tindall, D.R.; Miller, D.M. Genetic variability in toxin potencies among seventeen clones of *Gambierdiscus toxicus* (Dinophyceae). *J. Phycol.* **1989**, *25*, 617–625. [CrossRef]
95. Fritz, L.; Triemer, R.E. A Rapid simple technique utilizing calcofluor white M2R for the visualization of dinofalgellate thecal plates. *J. Phycol.* **1985**, *21*, 662–664. [CrossRef]
96. Catterall, W.A.; Nirenberg, M. Sodium uptake associated with activation of action potential ionophores of cultured neuroblastoma and muscle cells. *Proc. Natl. Acad. Sci. USA* **1973**, *70*, 3759–3763. [CrossRef]
97. Catterall, W.A. Molecular Properties of Voltage-Sensitive Sodium Channels. In *New Insights into Cell and Membrane Transport Processes*; Springer: Boston, MA, USA, 1986; pp. 3–20.
98. Manger, R.L.; Leja, L.S.; Lee, S.Y.; Hungerforg, J.M.; Wekell, M.M. Tetrazolium-based cell bioassay for neurotoxins active on voltage-sensitive sodium channels: Semiautomated assay for saxitoxins, brevetoxins, and ciguatoxins. *Anal. Biochem.* **1993**, *214*, 190–194. [CrossRef]
99. Caillaud, A.; Cañete, E.; de la Iglesia, P.; Giménez, G.; Diogène, J. Cell-based assay coupled with chromatographic fractioning: A strategy for marine toxins detection in natural samples. *Toxicol. Vitr.* **2009**, *23*, 1591–1596. [CrossRef] [PubMed]
100. R Core Team. *R: A Language and Environment for Statistical Computing*; R Foundation for Statistical Computing: Vienna, Austria, 2017.
101. Tsumuraya, T.; Sato, T.; Hirama, M.; Fujii, I. Highly Sensitive and Practical Fluorescent Sandwich ELISA for Ciguatoxins. *Anal. Chem.* **2018**, *90*, 7318–7324. [CrossRef]

toxins

MDPI

Article

Stereoselective Synthesis of the I–L Fragment of the Pacific Ciguatoxins

J. Stephen Clark * and Michael Popadynec

School of Chemistry, Joseph Black Building, University of Glasgow, Glasgow G12 8QQ, UK; m.popadynec@live.co.uk

* Correspondence: stephen.clark@glasgow.ac.uk; Tel.: +44-(0)141-330-6296

Received: 30 October 2020; Accepted: 20 November 2020; Published: 24 November 2020

Abstract: The I–L ring system found in all the Pacific ciguatoxins has been prepared from a tricyclic precursor in a highly stereoselective manner. Subtle differences in the reactivity of the enones present in the seven- and eight-membered rings of the tricyclic ether starting material have been exploited to allow selective protection of the enone in the eight-membered ring. Subsequent distereoselective allylation of the seven-membered ring has been accomplished by a palladium-mediated Tsuji-Trost reaction. The K-ring methyl and hydroxyl groups have been installed in a highly stereoselective manner by sequential conjugate reduction and enolate oxidation reactions. Ring L has been constructed by a use of a novel relay ring-closing metathesis reaction to complete the tetracyclic framework, which possesses the functionality necessary for elaboration of rings I and L and the introduction of ring M.

Keywords: pacific ciguatoxins; natural product; polycyclic ether; ring-closing metathesis; Tsuji-Trost allylation

Key Contribution: A tetracyclic lactone that corresponds to the I–L fragment that is common to all of the Pacific ciguatoxins has been prepared form a readily available tricyclic bis-enone by a 10-step sequence that involves a novel strategy involving relay ring-closing metathesis.

1. Introduction

1.1. Structures and Bioactivities of the Ciguatoxins

The ciguatoxins are a family of large and structurally complex fused polycyclic ether natural products of marine origin. Although the ciguatoxins had been implicated as the causative agents of ciguatera poisoning in humans since the 1960s, it was not until the late 1980s that the first structures of members of the ciguatoxin family—P-CTX-1 and P-CTX-4B—were fully elucidated by Yasumoto et al. (Figure 1) [1,2]. Subsequently, more than 30 other ciguatoxins have been isolated from marine dinoflagellates or from fish and marine organisms that accumulate the toxins by predation. The ciguatoxins can be grouped as Pacific, Caribbean or Indian according the ocean or sea where samples containing each toxin were first collected [3–6]. Pacific ciguatoxins are the most numerous and well-characterised of the ciguatoxins and this group accounts for more than three quarters of the ciguatoxins that are known [4–6]. Four Caribbean ciguatoxins have been characterized—C-CTX-1 and C-CTX-2 are equilibrating lactols and C-CTX-3 and C-CTX-4 are diastereomers that arise by reduction of C-CTX-1/C-CTX-2 [7,8]. A further eight Caribbean ciguatoxins have been detected by mass spectrometry but have yet to be characterised and the structures of the six ciguatoxins—I-CTX-1–6—isolated from samples collected in the Indian Ocean have yet to be elucidated [6,9,10].

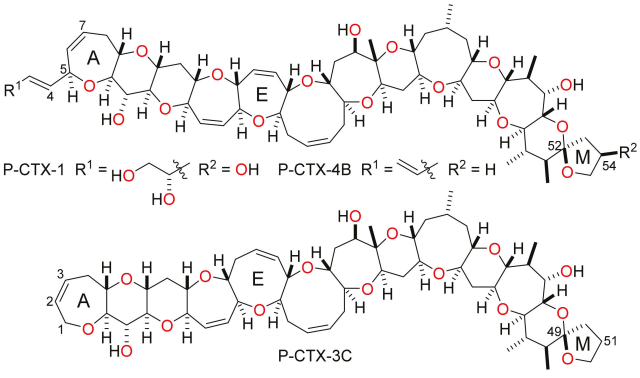

Figure 1. Representative Pacific ciguatoxins.

The Pacific ciguatoxins can be divided into two distinct structural sub-groups. The first is exemplified by P-CTX-1 and P-CTX-4B, and the second by P-CTX-3C (Figure 1) [3,5]. Natural products in the first group have a four-carbon chain attached to the A-ring (C-5) and a seven-membered E-ring. This group comprises more than a dozen congeners that have a variety of structural modifications such as a hydroxyl substituent at C-54, inverted configuration at C-52, a seco M-ring or oxidation at the C-4 and/or C-7 positions. The second and larger group is based on a P-CTX-3C skeleton. Compounds in this group have an expanded (eight-membered) E-ring and lack the A-ring side chain found in P-CTX-1 and related ciguatoxins. Variations on the P-CTX-3C structure include A-ring and M-ring seco compounds, a C-49-epi compound (P-CTX-3B) and oxidised analogues in which there is a hydroxyl group at the C-51 position, and/or the A-ring alkene is replaced by a C-2 carbonyl group, a C-2 hydroxyl group or a 1,2-diol.

The ciguatoxins are extremely potent neurotoxins and some of them have been shown to have LD_{50} values of 4 μg/kg or lower in mice. Ingestion of fish or seafood that is contaminated by ciguatoxins causes a type of food poisoning known as ciguatera that can result in the victim experiencing a myriad of unpleasant and sometimes severe neurological (both peripheral and central nervous system), cardiovascular and gastrointestinal symptoms [11]. It has been estimated that tens or even hundreds of thousands of people suffer from ciguatera poisoning each year. Symptoms can persist for many months or even years and, in extreme cases, ciguatera food poisoning can be fatal. The pharmacological effects of the ciguatoxins result primarily from their ability to cause persistent activation of voltage-gated sodium channels in nerve membranes and thereby prevent the nerve repolarisation that is essential for normal nerve function [12,13]. There is also evidence that the ciguatoxins can block voltage-gated potassium channels [14].

1.2. Total Syntheses of Pacific Ciguatoxins

The ciguatoxins are daunting targets for total synthesis because of their size, their stereochemical complexity, the large number of rings they possess and the high proportion of synthetically challenging medium-sized cyclic ethers in their trans-fused polycyclic structures. The synthetic challenges presented by the ciguatoxins combined with their potent neurotoxic activities makes them highly alluring synthetic targets and many research groups have performed methodological studies in which substantial fragments or smaller sub-units of various ciguatoxins have been constructed. However, despite a continuous stream of highly innovative synthetic work spanning more than two decades, the ciguatoxins have proved to be very difficult to synthesise. The only successes in this area have been achieved by Hirama et al., who reported the first total synthesis of a ciguatoxin—P-CTX-3C—in 2001 followed by the total syntheses of 51-hydroxy-P-CTX-3C and P-CTX-1 in 2006 [15–17], and by Isobe et al., who completed a total synthesis of P-CTX-1 in 2009 [18]. These elegant and impressive syntheses

are the only complete total syntheses of members of the ciguatoxin family of natural products to have been reported.

1.3. Proposed Synthetic Strategy and Previous Synthetic Work Concerning the Total Synthesis of P-CTX-3C and Related Ciguatoxins

We have been engaged in the development of new reactions, tactics and strategies for the rapid and efficient synthesis of fused polycyclic ether arrays for many years [19]. As part of this research program, we have invented and explored a variety of iterative and bidirectional strategies to assemble large fragments of fused polycyclic ether natural products of marine origin such as the brevetoxins, gambieric acids and ciguatoxins [20–23]. In our previous studies concerning the synthesis of P-CTX-3C, the A–E fragment of the natural product was assembled by a route in which ring-closing metathesis (RCM) reactions were used to construct the rings in an iterative manner [18]. We have also reported a novel bidirectional RCM approach to the synthesis of the tricyclic I–K fragment of P-CTX3-C from a simple monocyclic precursor and now present the results of studies concerning its elaboration to give an I–L fragment that can serve as an advanced intermediate for the preparation of the terminal fragment of any of the Pacific ciguatoxins [24].

Retrosynthesis of P-CTX-3C commences with disconnection through rings G and H to give two fragments—the hexacyclic A–F fragment **i** and the pentacyclic I–M fragment **ii**—that are of similar size and structural complexity (Figure 2). The focus of the synthetic work described herein was the I–M fragment **ii**. Disconnection of this pentacyclic system by removal of the methyl substituents in rings I and scission of the M-ring spiroacetal leads to the tetracyclic fragment **iii**. This intermediate contains an α,β-unsaturated ketone in ring I and an α,β-unsaturated lactone in ring L to enable introduction of the methyl substituents by conjugate addition in the case of ring I and sequential conjugate addition and enolate alkylation in the case of ring L.

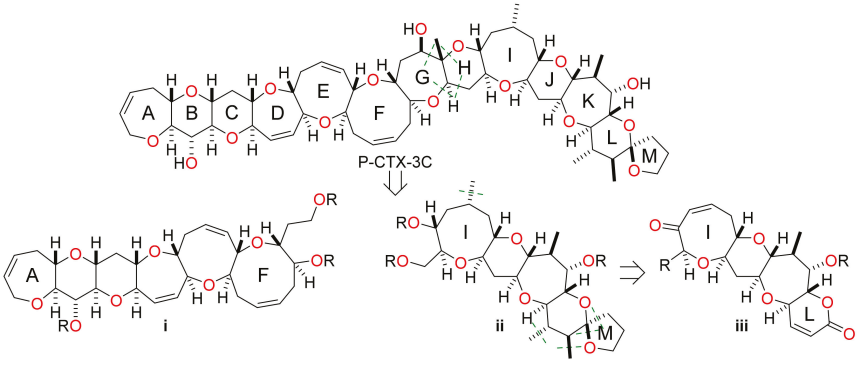

Figure 2. Retrosynthetic analysis of P-CTX-3C (**1**) to reveal the key A–F and I–L fragments.

In previous work concerning the synthesis of the I–M fragment of P-CTX-3C and related ciguatoxins, we have demonstrated that the tricyclic sub-unit **1** can be prepared from a simple tetrahydropyranyl precursor by double ring-closing metathesis (RCM) and that subsequent bidirectional functionalisation of the diketone **1** is possible by sequential double allyl enol carbonate formation and double palladium-mediated Tsuji-Trost allylation (Scheme 1) [24,25]. Although it was possible to direct the double Tsuji-Trost reaction of the substrate **2** to give just two of the four possible diastereomeric products by the choice of a suitable chiral ligand, we were unable to identify a catalyst that would deliver the required diketone **3** as the sole or even predominant isomer. Thus, it was necessary to revise the synthetic strategy in order to allow rings I and K to be differentiated and functionalised independently thereafter. The following discussion provides an account of construction of the I–L sub-unit by such an approach.

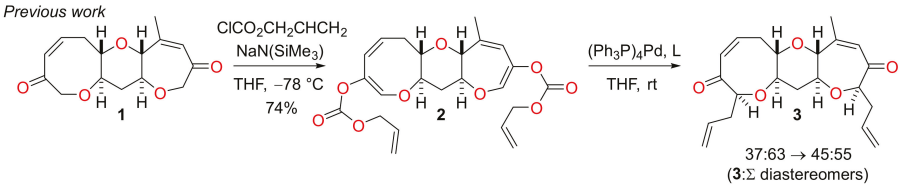

Scheme 1. Functionalisation of the I–K fragment by bidirectional double Tsuji-Trost allylation.

2. Results and Discussion

It was not possible to perform simultaneous and diastereoselective bidirectional functionalisation of the bis-enone **1** by double Tsuji-Trost allylation [24,25] and so it was necessary to elaborate rings I and K independently in order to extend the fused polyether framework (Scheme 2). The tricyclic bis-enone **1** is quasi-symmetric and so independent functionalisation of rings I and K by discrimination between reactive functional groups appears to be a challenging task at first glance. However, spectroscopic analysis of the bis-enone **1** reveals subtle structural differences between the enone functionality in rings I and K. In the IR spectrum of **1**, the carbonyl group in ring I has a stretching frequency of 1669 cm^{-1} whereas the carbonyl group in ring K has a stretching frequency of 1653 cm^{-1}—the identities of the carbonyl peaks in the IR spectrum of **1** were established unambiguously by comparison to data for the hydroxy ketones **4** and **5**, produced by partial reduction of the diketone **1** (Figure 3). The IR data suggest that the degree of enone conjugation in the eight-membered I-ring is significantly lower than that in the seven-membered K-ring. This finding was further supported by ^{13}C NMR spectroscopy where the β-carbon of the enone in ring I has a chemical shift (137 ppm) that is more typical of an unconjugated alkene at this position in an eight-membered cyclic ether, as can be seen by comparing the chemical shifts for the alkene carbons in the simple fused bicyclic ether **6** [26], whereas the corresponding carbon in ring K has a chemical shift (154 ppm) for the enone β-carbon that is consistent with a fully conjugated enone. The significant differences in the degree of conjugation in the enone groups suggested that it might be possible to functionalise them selectively by exploiting differences in their chemical reactivity. Indeed, there are pertinent examples of highly selective acid-mediated acetal formation in polycyclic substrates that contain both an enone and unconjugated ketone and so this approach was used to protect the I-ring carbonyl group selectively [27].

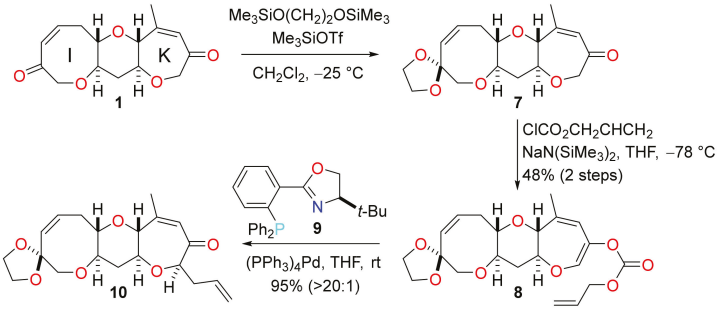

Scheme 2. Selective protection of the I-ring carbonyl group and subsequent Tsuji-Trost allylation of ring K.

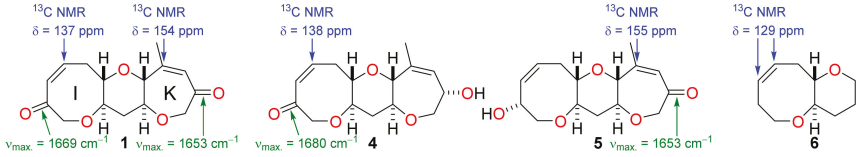

Figure 3. IR and ^{13}C data for the bis-enone **1** and comparison to data for the related compounds **4**–**6**.

Completely selective protection of the I-ring carbonyl group as a dioxolane was accomplished by reaction of the bis-enone **1** with bis(trimethylsilyl)ethylene glycol in the presence of trimethylsilyl trifluoromethanesulfonate (Scheme 2) [28]. The enone **7** was then converted into the allyl enol carbonate **8** by deprotonation with sodium bis(trimethylsilyl)amide and enolate trapping with allyl chloroformate. Tsuji-Trost allylation was then performed thereafter by treatment of the allyl enol carbonate **8** with the complex generated from tetrakis(triphenylphosphine) palladium(0) and the (*R*)-*t*-butyl-PHOX ligand (**9**) in situ [24,25,29]. The reaction was highly stereoselective (>95:5 *dr*; minor isomer not detectable by ^{1}H NMR analysis) and delivered the enone **10** in 95% yield (Scheme 2). The stereochemical outcome of this and subsequent diastereoselective reactions was confirmed by ^{1}H NMR NOE analysis (for details, see Supplementary Materials).

Ring K was elaborated further by conjugate reduction of the enone (Scheme 3). Reduction of the enone **10** with Stryker's reagent [30] resulted in a mixture of the diastereomeric ketones **11a** and **11b** (3:7 ratio) in which the required diastereomer **11a** was the minor component. This reaction also suffered from the problem that it did not proceed to completion, even when an excess of the reducing agent was used. A conjugate reduction protocol developed by Yamamoto et al. was deployed with the expectation that it would solve these reactivity and selectivity problems [31]. Coordination of the ketone to aluminium tris(2,6-diphenylphenoxide) followed by treatment with the reductant generated by the reaction of diisobutylaluminium hydride with *n*-butyllithium afforded the ketone **11b** in 39% yield and the diketone (13% yield) resulting from cleavage of the acetal protecting group of **11b**; none of the required diastereomer **11a** was obtained from the reaction. Stereocontrolled conjugate reduction of the enone **10** to give the required ketone was finally performed in good yield by reaction with the 'hot' Stryker's reagent generated from 1,2-bis(diphenylphosphino)benzene, copper(II) acetate hydrate and 1,1,3,3-tetramethyldisiloxane as described by Lipshutz and co-workers [32]. Reduction of the enone **10** with this reagent at 0 °C in toluene afforded a diastereomeric mixture of the ketones **11a** and **11b** (combined yield of 66%; 9:1 ratio) in which the required isomer was the major product. The diastereomeric ketones **11a** and **11b** could not be separated by standard silica gel chromatography.

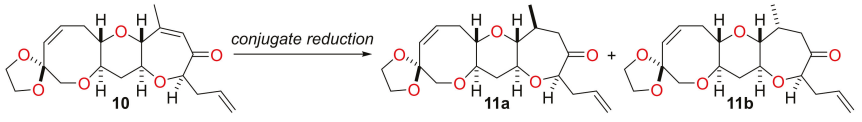

Scheme 3. Conjugate reduction of the enone **10**.

Stereoselective conjugate reduction of the enone **10** enabled the requisite K-ring hydroxyl group to be installed by enolate oxidation (Scheme 4). Regioselective deprotonation of a mixture of ketones **11a** and **11b** (4:1 ratio) with potassium bis(trimethylsilyl)amide and reaction of the resulting enolate with the *N*-sulfonyl oxaziridine **12** [33,34] produced the α-hydroxy ketone **13** in 43% yield (54% when adjusted to account for the isomer ratio of starting material **11**) and with a very high level of diastereocontrol. The same transformation was performed by generation of the triethylsilyl enol ether and subsequent Rubottom oxidation with 3-chloroperoxybenzoic acid [35], but poor yields were

obtained and so this sequence was not a viable alternative to direct enolate oxidation. The α-hydroxy ketone **13** was then subjected to stereoselective reduction with diisobutylaluminium hydride to give the diol **14** [36]. The stereochemical outcome of the reaction can be explained by a reaction mechanism in which complexation of the aluminium reagent to the hydroxyl and carbonyl groups produces a cyclic chelate and addition of diisobutylaluminium hydride occurs from the top face of the molecule (as drawn). At this stage, it was necessary to differentiate the hydroxyl groups of the *syn* diol **14** to enable construction of ring L. Selective protection of the hydroxyl group adjacent to the K-ring methyl substituent was accomplished by reaction of the diol **14** with dibutyltin oxide to give a cyclic dialkylstannylene acetal followed by regioselective fluoride-mediated alkylation with 2-bromomethylnaphthalene [37,38]. The Nap-protected alcohol **15** was obtained in reasonable yield and a small amount of unreacted diol **14** was recovered from the reaction.

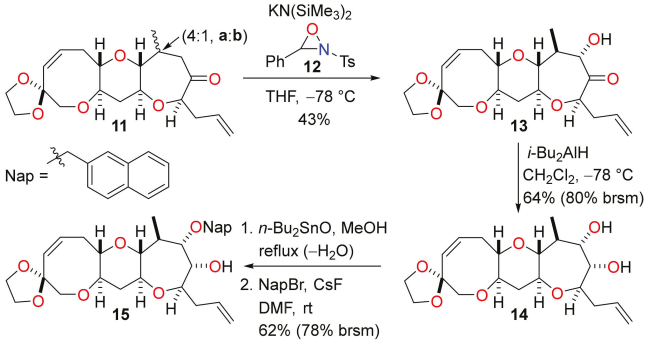

Scheme 4. Hydroxylation and further elaboration of ring K.

An alternative approach to functionalisation of ring K that did not involve sequential conjugate reduction and enolate oxidation was explored (Scheme 5). The tricyclic enone **10** was first subjected to Luche reduction which proceeded to give the allylic alcohol **16** in excellent yield and with a high level of diastereocontrol. Directed epoxidation of the allylic alcohol with *t*-butyl hydroperoxide mediated by vanadyl acetylacetonate produced the epoxide **17** in a highly stereoselective manner. Protection of the hydroxyl group as a triisopropylsilyl ether afforded the epoxide **18** in a yield of 66% from the enone **10**. It was now possible to rearrange the epoxide to give an allylic alcohol by reaction of the epoxide **18** with lithium 2,2,6,6-tetramethylpiperidide in the presence of the Lewis acid diethylaluminium chloride [39]. The allylic alcohol **19**, in which the acetal on ring I had been cleaved under the reaction conditions to reveal the enone, was obtained. Rearrangement of the epoxide **18** by treatment with *p*-toluenesulfonic acid was also successful; in this case ethylene glycol was added to the reaction mixture to ensure that the acetal protecting group was retained in product **20**. In both cases, the yield of the rearranged product was modest. Unfortunately, subsequent chemoselective and stereoselective hydrogenation of the exocyclic alkene to produce the K-ring methyl substituent proved to be difficult to accomplish. It was expected that selective directed hydrogenation of the allylic alcohol **20** would be possible by use of Crabtree's catalyst [40]. However, the hydrogenation reaction did not take place when a catalyst loading of 1 mol % was used and decomposition of the substrate occurred when higher catalysts loadings (≥10 mol %) were employed. When Wilkinson's catalyst was used to hydrogenate the alkoxide generated by deprotonation of the allylic alcohol **20** with sodium hydride in the presence of 15-crown-5 [41,42], the terminal alkene in the side chain was reduced instead of the exocyclic 1,1-disubstituted alkene in ring K.

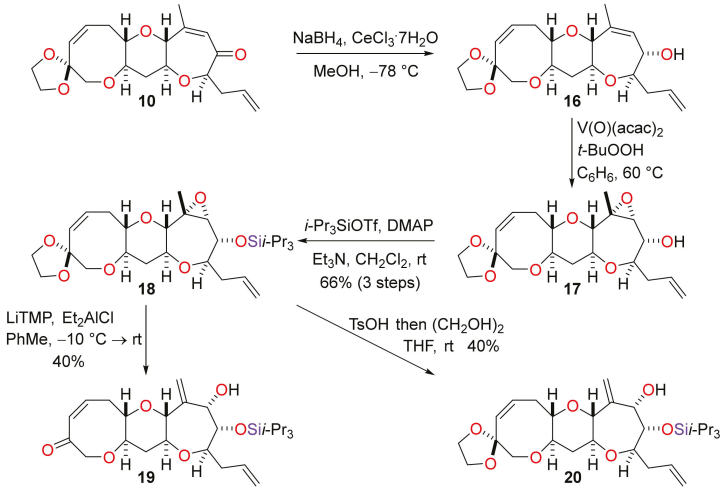

Scheme 5. An alternative approach to the elaboration of ring K.

Construction of ring L to complete the tetracyclic ciguatoxin I–L core framework was accomplished as shown in Scheme 6. The allyl side chain in the alcohol **15** was subjected to isomerisation by treatment with the ruthenium complex **21** in methanol at reflux to give the alcohol **22** as a mixture of alkene isomers (*E*/*Z*) along with some side-products [43]. At this juncture, construction of ring L as a pentenolide by conversion of the alcohol **22** into a simple acrylate ester followed by direct RCM was considered. However, there were concerns regarding the rate of initiation of the metathesis reaction because the substrate would contain an acrylate and an internal alkene branched at the α position; consequently, a relay RCM reaction was employed as a precaution [44]. Subjection of the alcohol **22** to Steglich esterification with the known carboxylic acid **23** [45] delivered the relay metathesis precursor **24** and subsequent treatment with the ruthenium complex **21** resulted in relay RCM to give the lactone **25** corresponding to the tetracyclic framework found in the I–L ring system of the Pacific ciguatoxins. The modest yield for the three-step sequence implies an average of 50% per step; it can be accounted for by the scale on which the reactions were performed and by-product formation during isomerisation (**15** → **22**). The unsaturation in ring L would enable subsequent introduction of the requisite methyl substituents by conjugate addition with a suitable methyl nucleophile and trapping of the resulting enolate with a methyl electrophile [46].

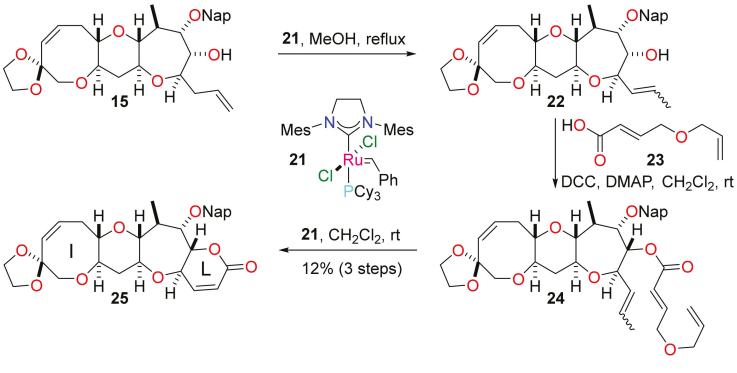

Scheme 6. Use of relay RCM to construct ring L and form the I–L ring system of the Pacific ciguatoxins.

3. Conclusions

The synthesis of the I–L ring system of the Pacific ciguatoxins has been accomplished in 10 steps starting from the tricyclic bis-enone **1**. Elaboration of ring K by stereoselective Tsuji-Trost allylation was accomplished after selective protection of the I-ring enone by acetal formation. The configuration at the methyl-bearing stereogenic centre in ring K was controlled during conjugate reduction of the enone and the hydroxyl substituent was installed in a highly stereoselective manner by enolate oxidation according to the Davis procedure. Stereoselective ketone reduction followed by selective protection of the resulting 1,2-diol then allowed the metathesis trigger to be attached to the K-ring by esterification of the hydroxyl group. Relay RCM, mediated by the Grubbs second generation ruthenium complex, resulted in formation of ring L and completed the tetracyclic framework with the functionality necessary for subsequent elaboration of ring I, installation of the methyl substituents in ring L and construction of ring M.

4. Materials and Methods

Air- and moisture-sensitive reactions were performed under an atmosphere of argon in flame-dried apparatus. Tetrahydrofuran (THF), toluene, dichloromethane and diethyl ether were purified using a Pure-SolvTM 500 Solvent Purification System. Other dry solvents and starting materials were obtained from commercial sources and used as received unless stated otherwise. Petroleum ether (pet. ether) used for column chromatography was the 40–60 °C fraction. Triethylamine and 2,2,6,6-tetramethylpiperidine were distilled and stored under argon prior to use. *n*-Butyllithium solutions were titrated against diphenylacetic acid to obtain accurate molarity. 4 Å molecular sieves were oven dried prior to use.

Reactions were monitored by thin layer chromatography (TLC) using Merck silica gel 60 covered aluminium-backed plates F254. TLC plates were visualised under UV light and stained using potassium permanganate solution or acidic ethanolic anisaldehyde solution. Flash column chromatography was performed with silica gel (Geduran Si 60 35–70 μm) as solid support.

IR spectra were recorded using a Shimadzu FT IR-8400S ATR instrument (Shimadzu UK, Milton Keynes, UK). The IR spectrum of each compound (solid or liquid) was acquired directly on a thin layer at ambient temperature.

NMR spectra were recorded on Bruker Avance III 400 MHz and 500 MHz spectrometers (Bruker UK, Coventry, UK) at ambient temperature. ^{1}H NMR chemical shifts are reported in ppm relative to $CHCl_3$ (7.26) or $CDCl_2H$ (5.32) on the δ scale followed by integration, multiplicity (s = singlet, d = doublet, t = triplet, q = quartet, m = multiplet, br. = broad, app. = apparent or a combination of these) and coupling constant(s) J (Hz). ^{13}C NMR spectra were recorded at 101 MHz and 126 MHz and chemical shifts are reported in ppm relative to $CDCl_3$ (77.16) or CD_2Cl_2 (54.00) on the δ scale.

High resolution mass spectra (HRMS) were recorded by the University of Glasgow mass spectrometry service using a JEOL MStation JMS-700 instrument [positive electron impact ionisation (EI^+)] (JEOL Ltd., Tokyo, Japan) or a Bruker micrOTOF-Q instrument [positive ion electrospray (ESI^+)] (Bruker UK, Coventry, UK).

Optical rotations were recorded with an error of ≤ ±0.1 using an automatic polarimeter Autopol V (Rudolph Research Analytical, Hackettstown, USA) and melting points were recorded with an Electrothermal IA 9100 apparatus (Cole-Parmer, Stone, UK).

(1′S,3′R,9′S,11′R,15′Z)-4′-Methyl-2′,8′,12′-trioxaspiro(1,3-dioxolane-2,14′-tricyclo-[9.6.0.0^{3,9}]heptadecane)-4′,15′-dien-6′-one (**7**)

To a solution of the bis-enone **1** (870 mg, 3.13 mmol) in dichloromethane (63 mL) at −60 °C was added, 1,2-bis(trimethylsiloxy)ethane (0.81 mL, 3.3 mmol) and trimethylsilyl trifluoromethanesulfonate (0.06 mL, 0.3 mmol). The solution was allowed to warm to −25 °C and stirred for 16 h. The reaction mixture was diluted with diethyl ether (252 mL) and the mixture was washed with sat. aq. ammonium chloride (2 × 100 mL) and brine (100 mL). The organic phase was dried ($MgSO_4$) and concentrated under reduced pressure to afford the acetal **7** (960 mg) as a brown oil. The unpurified acetal was

used directly in the next reaction. For analytical purposes, a sample was purified by flash column chromatography (5–30% ethyl acetate in pet. ether) to afford **7** as a colourless solid. M.p. 145–146 °C; R_f = 0.43 (60% ethyl acetate in pet. ether); $[\alpha]_D$ +22.6 (*c* = 0.50 in $CHCl_3$, 29 °C); ν_{max} 3028, 2953, 2932, 2884, 1655, 1443, 1348, 1115, 1086, 1074, 943, 893, 768 cm^{-1}; ^1H NMR (500 MHz, $CDCl_3$) δ 5.90 (1H, dq, *J* = 1.2, 1.2 Hz), 5.82 (1H, ddd, *J* = 11.6, 9.5, 7.5 Hz), 5.63 (1H, d, *J* = 11.6 Hz), 4.23 (1H, d, *J* = 18.3 Hz), 4.13 (1H, d, *J* = 18.3 Hz), 3.94–3.83 (4H, m), 3.67 (1H, ddq, *J* = 9.0, 1.2, 1.2 Hz), 3.61 (1H, d, *J* = 12.7 Hz), 3.50 (1H, d, *J* = 12.7 Hz), 3.47 (1H, ddd, *J* = 11.7, 9.3, 4.4 Hz), 3.33 (1H, ddd, *J* = 9.3, 5.8, 4.0 Hz), 3.30 (1H, ddd, *J* = 11.7, 9.0, 4.7 Hz), 2.89 (1H, ddd, *J* = 13.5, 9.5, 4.0 Hz), 2.56 (1H, ddd, *J* = 13.5, 7.5, 5.8 Hz), 2.36 (1H, ddd, *J* = 12.1, 4.7, 4.4 Hz), 1.97 (3H, dd, *J* = 1.2, 1.2 Hz), 1.61 (1H, ddd, *J* = 12.1, 11.7, 11.7 Hz); ^{13}C NMR (101 MHz, $CDCl_3$) δ 201.4, 155.1, 133.9, 130.3, 127.1, 108.0, 82.8, 82.5, 78.1, 77.6, 77.4, 74.2, 64.8, 64.6, 38.3, 30.1, 22.9; HRMS (ESI^+) $[C_{17}H_{22}O_6Na]^+$ found 345.1299, $[M + Na]^+$ calcld. 345.1309.

(1′S,3′R,9′S,11′R,15′Z)-4′-Methyl-2′,8′,12′-trioxaspiro(1,3-dioxolane-2,14′-tricyclo-[9.6.0.0^{3,9}]heptadecane)-4′,6′,15′-trien-6′-yl prop-2-en-1-yl carbonate (**8**)

To a solution of the acetal **7** in THF (57 mL) was added, allyl chloroformate (1.58 mL, 14.9 mmol). The resultant solution was cooled to −78 °C and sodium bis(trimethylsilyl)amide (3.0 mL of a 2.0 M solution in THF, 6.0 mmol) was added dropwise. The reaction mixture was stirred for 4 h, diluted with 5% aq. potassium dihydrogen phosphate (240 mL) and the mixture was extracted with diethyl ether (3 × 60 mL). The combined organic extracts were washed with brine (3 × 60 mL), dried ($MgSO_4$) and concentrated under reduced pressure. The residue was dissolved in toluene (100 mL) and then concentrated under reduced pressure and the procedure was repeated. Residual material was purified by flash column chromatography (5–40% diethyl ether in pet. ether) to give the allylic carbonate **8** (610 mg, 48% over 2 steps) as a colourless oil. R_f = 0.57 (60% ethyl acetate in pet. ether); $[\alpha]_D$ +96.1 (*c* = 1.00 in C_6H_6, 29 °C); ν_{max} 2951, 2891, 1759, 1663, 1451, 1364, 1246, 1225, 1198, 1126, 1090, 1055, 995, 947, 770 cm^{-1}; ^1H NMR (500 MHz, CD_2Cl_2) δ 6.62 (1H, d, *J* = 1.6 Hz), 5.96 (1H, ddt, *J* = 17.3, 10.5, 5.7 Hz), 5.86 (1H, ddd, *J* = 11.5, 9.6, 7.5 Hz), 5.67 (1H, d, *J* = 11.5 Hz), 5.54 (1H, dqd, *J* = 1.6, 1.6, 1.3 Hz), 5.37 (1H, ddt, *J* = 17.3, 1.4, 1.4 Hz), 5.29 (1H, dddd, *J* = 10.5, 1.4, 1.4, 1.4 Hz), 4.64 (2H, ddd, *J* = 5.7, 1.4, 1.4 Hz), 3.95–3.87 (4H, m), 3.74 (1H, ddq, *J* = 7.9, 1.3, 1.3 Hz), 3.65 (1H, ddd, *J* = 11.4, 7.9, 4.9 Hz), 3.63 (1H, d, *J* = 12.8 Hz), 3.54 (1H, d, *J* = 12.8 Hz), 3.52 (1H, ddd, *J* = 11.8, 9.4, 4.4 Hz), 3.32 (1H, ddd, *J* = 9.4, 5.7, 4.1 Hz), 2.92 (1H, ddd, *J* = 13.4, 9.6, 4.1 Hz), 2.56 (1H, ddd, *J* = 13.4, 7.5, 5.7 Hz), 2.49 (1H, ddd, *J* = 12.1, 4.9, 4.4 Hz), 1.89 (3H, dd, *J* = 1.6, 1.3 Hz), 1.67 (1H, ddd, *J* = 12.1, 11.8, 11.4 Hz); ^{13}C NMR (126 MHz, CD_2Cl_2) δ 155.0, 141.2, 138.5, 135.0, 134.2, 132.0, 130.7, 119.3, 118.8, 108.4, 81.8, 80.1, 78.0, 77.9, 74.6, 69.5, 65.1, 65.0, 38.7, 30.4, 21.9; HRMS (ESI^+) $[C_{21}H_{26}O_8Na]^+$ found 429.1507, $[M + Na]^+$ calcld. 529.1520.

(1′S,3′R,7′R,9′S,11′R,15′Z)-4′-Methyl-7′-(prop-2-en-1-yl)-2′,8′,12′-trioxaspiro(1,3-dioxolane-2,14′-tricyclo[9.6.0.0^{3,9}]heptadecane)-4′,15′-dien-6′-one (**10**)

A mixture of tetrakis(triphenylphosphine)palladium(0) (67 mg, 0.058 mmol, 5 mol%) and (4*R*)-*t*-butyl-2-[2-(diphenylphosphino)phenyl]-4,5-dihydroxazole (**9**) (56 mg, 0.14 mmol, 13 mol%) was dissolved in THF (20 mL). The solution was stirred for 45 min and a solution of the allylic carbonate **8** (471 mg, 1.16 mmol) in THF (38 mL) was added. The mixture was stirred at rt for a further 3.5 h and then adsorbed onto Celite. The crude material was dry loaded on to a column of silica gel and purified by flash column chromatography (5–20% ethyl acetate in pet. ether) to afford the enone **10** (398 mg, 95%, >20:1 *dr*) as a pale yellow oil. R_f = 0.57 (60% ethyl acetate in pet. ether); $[\alpha]_D$ +15.0 (*c* = 0.50 in $CHCl_3$, 30 °C); ν_{max} 2949, 2888, 2855, 1657, 1443, 1279, 1111, 1088, 999, 949, 918 cm^{-1}; ^1H NMR (500 MHz, $CDCl_3$) δ 5.89 (1H, dq, *J* = 1.1, 1.1 Hz), 5.87 (1H, ddd, *J* = 11.5, 9.6, 7.5 Hz), 5.78 (1H, dddd, *J* = 17.0, 10.2, 6.8, 6.8 Hz), 5.70 (1H, d, *J* = 11.5 Hz), 5.12–5.00 (2H, m), 4.17 (1H, dd, *J* = 7.7, 4.4 Hz), 3.98–3.89 (4H, m), 3.68 (1H, ddq, *J* = 8.9, 1.1, 1.1 Hz), 3.67 (1H, d, *J* = 12.7 Hz), 3.55 (1H, d, *J* = 12.7 Hz), 3.50 (1H, ddd, *J* = 11.7, 9.3, 4.4 Hz), 3.40 (1H, ddd, *J* = 9.3, 5.5, 4.1 Hz), 3.33 (1H, ddd,

J = 11.3, 8.9, 4.7 Hz), 2.97 (1H, ddd, *J* = 13.6, 9.6, 4.1 Hz), 2.59 (1H, ddd, *J* = 13.6, 7.5, 5.5 Hz), 2.49 (1H, ddd, *J* = 14.3, 6.8, 4.4 Hz), 2.41 (1H, ddd, *J* = 12.2, 4.7, 4.4 Hz), 2.36 (1H, ddd, *J* = 14.3, 7.7, 6.8 Hz), 2.01 (3H, dd, *J* = 1.1, 1.1 Hz), 1.70 (1H, ddd, *J* = 12.2, 11.7, 11.3 Hz); ^{13}C NMR (126 MHz, $CDCl_3$) δ 203.6, 153.7, 134.0, 133.5, 130.4, 126.7, 117.7, 107.9, 86.5, 82.5, 82.5, 77.6, 77.0, 74.2, 64.8, 64.6, 38.2, 38.1, 30.1, 22.7; HRMS (ESI$^+$) $[C_{20}H_{26}O_6Na]^+$ found 385.1606, $[M + Na]^+$ calcld. 385.1622.

(1′S,3′R,4′S,7′R,9′S,11′R,15′Z)-4′-Methyl-7′-(prop-2-en-1-yl)-2′,8′,12′-trioxaspiro(1,3-dioxolane-2,14′-tricyclo[9.6.0.0^{3,9}]heptadecan)-15′-en-6′-one (**11a**) and *(1′S,3′R,4′R,7′R,9′S,11′R,15′Z)-4′-Methyl-7′-(prop-2-en-1-yl)-2′,8′,12′-trioxaspiro(1,3-dioxolane-2,14′-tricyclo[9.6.0.0^{3,9}]heptadecan)-15′-en-6′-one* (**11b**)

(*a*) *Conjugate reduction of* **10** *with of 'hot' Stryker's reagent*

To 1,2-bis(diphenylphosphino)benzene (491 mg, 1.10 mmol) and copper(II) acetate hydrate (220 mg, 1.10 mmol) was added degassed toluene (19 mL). The resultant mixture was stirred vigorously and sparged continuously with argon for 15 min. The mixture was then sonicated for a further 30 min, at which point a pale blue suspension had formed. Tetramethyldisiloxane (0.80 mL, 4.4 mmol) was added to the mixture and it was stirred vigorously for a further 30 min, at which point the suspension developed a green colour. After refrigeration for 16 h, a red stock solution (0.055 M) had formed.

To the enone **10** (18 mg, 50 μmol) was added 'hot' Stryker's reagent (2.0 mL of a 0.055 M solution in toluene, 0.11 mmol). The solution was stirred at 0 °C for 48 h and then concentrated under reduced pressure. The residue was dissolved in THF (5 mL) and sat. aq. potassium fluoride (2 mL) was added. The biphasic mixture was stirred vigorously for 16 h and then diluted with water (10 mL). The mixture was extracted with diethyl ether (3 × 5 mL) and the combined organic extracts were dried ($MgSO_4$) and concentrated under reduced pressure. The residue was purified by flash column chromatography (10–20% ethyl acetate in pet. ether) to afford a diastereomeric mixture of the ketones **11a** and **11b** (12 mg, 66%, 9:1 **a**:**b**) as a colourless film.

(*b*) *Conjugate reduction of* **10** *with lithium n-butyl(diisobutyl)aluminium hydride*

To a solution of 2,6-diphenylphenol (380 mg, 1.50 mmol) in toluene (2 mL) at 0 °C was added dropwise trimethylaluminium (0.25 mL of a 2.0 M solution in toluene, 0.50 mmol) and the mixture was stirred for 10 min. After gas evolution had subsided, a solution of the enone **10** (145 mg, 0.400 mmol) in toluene (1 mL) was added and the resultant solution cooled to −78 °C and stirred for 10 min.

To a solution of diisobutylaluminium hydride (0.60 mL of a 1.0 M solution in heptane, 0.60 mmol) in THF (2 mL) at 0 °C was added dropwise *n*-butyllithium (0.26 mL of a 2.33 M solution in hexane, 0.60 mmol) and solution was stirred for 10 min. The solution was added to the aforementioned toluene solution of the enone **10** and aluminium tris(2,6-diphenylphenoxide) at −78 °C and the mixture was stirred for 2 h at this temperature. The mixture was then diluted with diethyl ether (50 mL) and sat. aq. Rochelle salt (50 mL) was added and the mixture was stirred vigorously for 16 h. The phases were separated and the organic phase was washed with water (25 mL) and brine (25 mL), then dried ($MgSO_4$) and concentrated under reduced pressure. The residue was purified by flash column chromatography (2.5–20% ethyl acetate in pentane) to afford the ketone **11b** (57 mg, 39%) as a colourless solid and the diketone (17 mg, 12%), resulting from deacetalation of the ketone **11b**, as a colourless film. **11a** R_f = 0.20 (20% ethyl acetate in pet. ether); $[\alpha]_D$ +117.5 (*c* = 1.00 in $CHCl_3$, 27 °C); ν_{max} 2080, 3028, 2959, 2934, 2916, 2876, 1713, 1643, 1260, 1088, 1059, 949, 912, 891, 802, 769 cm^{-1}; ^{1}H NMR (500 MHz, $CDCl_3$) δ 5.88 (1H, ddd, *J* = 11.6, 9.5, 7.5 Hz), 5.79 (1H, dddd, *J* = 17.1, 10.3, 6.9, 6.9 Hz), 5.67 (1H, d, *J* = 11.6 Hz), 5.11–5.04 (2H, m), 3.98–3.89 (4H, m), 3.80 (1H, dd, *J* = 7.9, 5.0 Hz), 3.66 (1H, d, *J* = 12.7 Hz), 3.54 (1H, d, *J* = 12.7 Hz), 3.46 (1H, ddd, *J* = 11.6, 9.3, 4.4 Hz), 3.28 (1H, ddd, *J* = 9.3, 5.8, 4.1 Hz), 2.96 (1H, ddd, *J* = 11.1, 9.3, 4.6 Hz), 2.89 (1H, ddd, *J* = 13.4, 9.5, 4.1 Hz), 2.88–2.78 (2H, m), 2.57 (1H, ddd, *J* = 13.4, 7.5, 5.8 Hz), 2.41–2.25 (3H, m), 2.12 (1H, dd, *J* = 11.5, 1.9 Hz), 1.69–1.57 (1H, m), 1.63 (1H, ddd, *J* = 12.4, 11.6, 11.1 Hz), 1.13 (3H, d, *J* = 6.6 Hz); ^{13}C NMR (126 MHz, $CDCl_3$) δ 215.2, 133.6, 133.1, 130.7, 118.0, 108.0, 86.5, 85.7, 81.6, 79.8, 77.9, 74.2, 64.8, 64.5, 45.1, 38.8, 37.2, 35.7, 30.1, 20.3; HRMS (ESI$^+$) $[C_{20}H_{28}O_7Na]^+$

found 387.1766, $[M + Na]^+$ calcld. 387.1778. **11b** M.p. 108–110 °C; R_f = 0.25 (20% ethyl acetate in pet. ether); $[\alpha]_D$ +87.1 (*c* = 2.00 in $CHCl_3$, 29 °C); ν_{max} 2957, 2936, 2884, 2855, 1711, 1641, 1288, 1090, 1061, 1042, 995, 949, 920, 770 cm^{-1}; ^1H NMR (500 MHz, $CDCl_3$) δ 5.87 (1H, ddd, *J* = 11.5, 9.6, 7.4 Hz), 5.80 (1H, dddd, *J* = 17.1, 10.2, 6.9, 6.9 Hz), 5.70 (1H, d, *J* = 11.5 Hz), 5.11–5.02 (2H, m), 3.98–3.90 (4H, m), 3.71 (1H, dd, *J* = 8.3, 4.2 Hz), 3.67 (1H, d, *J* = 12.7 Hz), 3.54 (1H, d, *J* = 12.7 Hz), 3.41–3.34 (3H, m), 3.20 (1H, ddd, *J* = 11.1, 9.6, 5.0 Hz), 3.03–2.94 (1H, m), 3.00 (1H, dd, *J* = 11.7, 2.2 Hz), 2.50 (1H, ddd, *J* = 13.5, 7.4, 4.4 Hz), 2.42 (1H, ddddd, *J* = 13.4, 6.9, 4.2, 1.3, 1.3 Hz), 2.37 (1H, ddd, *J* = 12.1, 5.0, 4.2 Hz), 2.34–2.25 (3H, m), 1.65 (1H, ddd, *J* = 12.1, 11.3, 11.1 Hz), 0.86 (3H, d, *J* = 7.0 Hz); ^{13}C NMR (126 MHz, $CDCl_3$) δ 215.5, 133.9, 133.6, 130.9, 117.8, 107.8, 87.1, 83.1, 81.7, 77.7, 74.9, 74.4, 64.8, 64.6, 44.3, 38.5, 37.5, 31.9, 30.1, 12.3; HRMS (ESI^+) $[C_{20}H_{28}O_6Na]^+$ found 387.1765, $[M + Na]^+$ calcld. 387.1778.

(1′S,3′R,4′S,5′S,7′R,9′S,11′R,15′Z)-5′-Hydroxy-4′-methyl-7′-(prop-2-en-1-yl)-2′,8′,12′-trioxaspiro(1,3-dioxolane-2,14′-tricyclo[9.6.0.0^{3,9}]heptadecan)-15′-en-6′-one (**13**)

To a solution of the ketones **11a** and **11b** (18 mg of a 4:1 mixture, 50 μmol) in THF (2.9 mL) at −78 °C, a solution of potassium bis(trimethylsilyl)amide (0.10 mL of a 0.50 M solution in toluene, 50 μmol) was added and the mixture was stirred for 1 h. A solution of the oxaziridine **12** (14 mg, 50 μmol) in THF (1 mL) was then added to the mixture dropwise and the resulting mixture was stirred for 1 h. The reaction mixture was diluted with sat. aq. sodium thiosulfate (20 mL) and the extracted with diethyl ether (3 × 10 mL). The combined organic extracts were washed with sat. aq. ammonium chloride (10 mL) and brine (2 × 10 mL), dried ($MgSO_4$) and concentrated under reduced pressure. The residue was purified by flash column chromatography (10–30% diethyl ether in pet. ether) to give the α-hydroxyketone **13** (8 mg, 43%) and recovered starting material **11a** (2 mg, 11%) as colourless oils. R_f = 0.73 (60% ethyl acetate in pet. ether); $[\alpha]_D$ +75.8 (*c* = 0.60 in $CHCl_3$, 26 °C); ν_{max} 3474, 2926, 2874, 2855, 1713, 1643, 1283, 1096, 1047, 949, 922, 770 cm^{-1}; ^1H NMR (400 MHz, $CDCl_3$) δ 5.88 (1H, ddd, *J* = 11.5, 9.5, 7.5 Hz), 5.78 (1H, ddd, *J* = 16.9, 9.8, 7.0 Hz), 5.67 (1H, d, *J* = 11.5 Hz), 5.13–5.06 (2H, m), 4.30 (1H, dd, *J* = 11.2, 6.4 Hz), 4.08 (1H, dd, *J* = 7.7, 5.0 Hz), 3.97–3.91 (4H, m), 3.66 (1H, d, *J* = 12.7 Hz), 3.54 (1H, d, *J* = 12.7 Hz), 3.46 (1H, ddd, *J* = 11.7, 9.3, 4.5 Hz), 3.33 (1H, d, *J* = 6.4 Hz), 3.28 (1H, ddd, *J* = 9.3, 5.8, 4.2 Hz), 3.01–2.94 (2H, m), 2.90 (1H, ddd, *J* = 13.5, 9.5, 4.2 Hz), 2.58 (1H, ddd, *J* = 13.5, 7.5, 5.8 Hz), 2.48–2.32 (3H, m), 1.63 (1H, app. q, *J* = 11.7 Hz), 1.54–1.44 (1H, m), 1.28 (3H, d, *J* = 6.3 Hz); ^{13}C NMR (101 MHz, $CDCl_3$) δ 215.5, 133.6, 132.4, 130.6, 118.7, 108.1, 85.5, 83.6, 81.7, 79.8, 77.7, 75.1, 74.2, 64.8, 64.5, 43.2, 38.6, 37.9, 30.1, 15.3; HRMS (ESI^+) $[C_{20}H_{28}O_7Na]^+$ found 403.1715, $[M + Na]^+$ calcld. 403.1727.

(1′S,3′R,4′S,5′S,6′S,7′R,9′S,11′R,15′Z)-4′-Methyl-7′-(prop-2-en-1-yl)-2′,8′,12′-trioxaspiro(1,3-dioxolane-2,14′-tricyclo[9.6.0.0^{3,9}]heptadecan)-15′-ene-5′,6′-diol (**14**)

To a solution of α-hydroxyketone **13** (31 mg, 81 μmol) in dichloromethane (2.9 mL) at −78°C, diisobutylaluminium hydride (0.32 mL of a 1.0 M solution in dichloromethane, 0.32 mmol) was added and the resultant solution stirred for 2 h. Further diisobutylaluminium hydride (0.32 mL of a 1.0 M solution in dichloromethane, 0.32 mmol) was added and the mixture was stirred for a further 2 h. The reaction mixture was diluted with sat. aq. Rochelle salt (20 mL) and ethyl acetate (20 mL) and stirred vigorously for 1 h. The phases were separated and the organic phase was washed with brine (2 × 10 mL), dried ($MgSO_4$) and concentrated under reduced pressure. The residue was purified by flash column chromatography (20–100% diethyl ether in pet. ether) to afford the diol **14** (20 mg, 64%) and starting material **13** (6 mg, 19%) as colourless films. R_f = 0.30 (60% ethyl acetate in pet. ether); $[\alpha]_D$ +18.4 (*c* = 0.50 in $CHCl_3$, 27 °C); ν_{max} 3447, 2926, 2874, 1647, 1456, 1285, 1090, 1042, 1013, 916, 770 cm^{-1}; ^1H NMR (400 MHz, $CDCl_3$) δ 5.90 (1H, ddd, *J* = 11.4, 9.6, 7.6 Hz), 5.85 (1H, dddd, *J* = 17.1, 10.2, 6.9, 6.9 Hz), 5.67 (1H, d, *J* = 11.4 Hz), 5.17–5.04 (2H, m), 3.94 (4H, m), 3.86 (1H br s), 3.71 (1H, d, *J* = 9.4 Hz), 3.65 (1H, d, *J* = 12.7 Hz), 3.56 (1H, ddd, *J* = 7.6, 5.5, 5.5 Hz), 3.55 (1H, d, *J* = 12.7), 3.48 (1H, ddd, *J* = 11.6, 9.3, 4.4 Hz), 3.37 (1H, ddd, *J* = 11.4, 9.3, 4.6 Hz), 3.22 (1H, ddd, *J* = 9.3, 5.9, 4.1 Hz), 2.88 (1H, ddd, *J* = 13.6, 9.6, 4.1 Hz), 2.72 (1H, dd, *J* = 9.3, 9.0 Hz), 2.59 (1H, ddd, *J* = 13.6, 7.6,

5.9 Hz), 2.39–2.24 (3H, m), 2.21 (1H, br s), 2.12 (1H, ddq, 9.4, 9.0, 6.7 Hz), 1.94 (1H, br s), 1.48 (1H, ddd, *J* = 12.1, 11.6, 11.4 Hz), 1.15 (3H, d, *J* = 6.7 Hz); ^{13}C NMR (101 MHz, $CDCl_3$) δ 134.8, 133.4, 130.8, 117.5, 108.2, 84.8, 82.7, 81.7, 78.3, 78.2, 77.7, 74.1, 73.4, 64.8, 64.5, 39.4, 39.0, 38.0, 30.3, 15.4; HRMS (ESI$^+$) $[C_{20}H_{30}O_7Na]^+$ found 405.1871, $[M + Na]^+$ calcld. 405.1884.

(1′S,3′R,4′S,5′S,6′R,7′R,9′S,11′R,15′Z)-4′-Methyl-5′-[(naphthalen-2-yl)methoxy]-7′-(prop-2-en-1-yl)-2′,8′,12′-trioxaspiro(1,3-dioxolane-2,14′-tricyclo[9.6.0.0^{3,9}]heptadecane)-15′-en-6′-ol (**15**)

To a solution of diol **14** (20 mg, 52 μmol) in methanol (5.2 mL), dibutyltin oxide (14 mg, 58 μmol) was added. The resultant suspension was stirred at reflux for 2 h to form a colourless solution. The mixture was concentrated under reduced pressure and dried by azeotropic distillation with toluene. The mixture was redissolved in DMF (5.2 mL) and 2-(bromomethyl)naphthalene (14 mg, 62 μmol) and caesium fluoride (9 mg, 0.06 mmol) were added. The reaction mixture was stirred for 16 h and then quenched with water carefully. The mixture was extracted with diethyl ether (3 × 10 mL) and the combined organic extracts were washed with brine (3 × 10 mL), dried ($MgSO_4$) and concentrated under reduced pressure. The residue was purified by flash column chromatography (20–100% diethyl ether in pet. ether) to afford the naphthyl ether **15** (17 mg, 62%) and recovered diol **14** (4 mg, 20%) as colourless films. R_f = 0.39 (80% diethyl ether in pet. ether); $[\alpha]_D$ +14.8 (*c* = 1.00 in $CHCl_3$, 27 °C); ν_{max} 3466, 2928, 2874, 2853, 1643, 1456, 1090, 949, 916, 1051, 818, 752 cm^{-1}; ^{1}H NMR (400 MHz, $CDCl_3$) δ 7.87–7.80 (3H, m), 7.76 (1H, s), 7.52–7.44 (3H, m), 5.91 (1H, ddd, *J* = 11.5, 9.6, 7.5 Hz), 5.83 (1H, dddd, *J* = 17.2, 10.3, 6.6, 6.6 Hz), 5.69 (1H, d, *J* = 11.5 Hz), 5.13–5.02 (2H, m), 4.74 (1H, d, *J* = 11.3 Hz), 4.65 (1H, d, *J* = 11.3 Hz), 3.98–3.92 (4H, m), 3.90 (1H, dd, *J* = 5.0, 2.2 Hz), 3.66 (1H, d, *J* = 12.7 Hz), 3.59 (1H, ddd, *J* = 7.9, 5.0, 5.0 Hz), 3.55 (1H, d, *J* = 12.7), 3.53 (1H, dd, *J* = 8.8, 2.2 Hz), 3.50 (1H, ddd, *J* = 11.6, 9.5, 4.3 Hz), 3.49 (1H, ddd, *J* = 11.6, 9.4, 4.5 Hz), 3.24 (1H, ddd, *J* = 9.4, 5.7, 4.1 Hz), 2.92 (1H, ddd, *J* = 13.7, 9.6, 4.1 Hz), 2.78 (1H, dd, *J* = 9.5, 7.7 Hz), 2.59 (1H, ddd, *J* = 13.7, 7.5, 5.7 Hz), 2.39–2.19 (4H, m), 1.46 (1H, ddd, *J* = 11.6, 11.6, 11.6 Hz), 1.18 (3H, d, *J* = 6.9 Hz); ^{13}C NMR (101 MHz, $CDCl_3$) δ 135.4, 134.9, 133.5, 133.3, 133.2, 130.9, 128.4, 128.0, 127.9, 127.1, 126.4, 126.3, 126.2, 117.2, 108.1, 85.4, 82.0, 81.8, 81.8, 78.2, 77.3, 74.3, 74.1, 72.6, 64.8, 64.5, 39.0, 39.0, 36.8, 30.3, 16.4; HRMS (ESI$^+$) $[C_{31}H_{38}O_7Na]^+$ found 545.2497, $[M + Na]^+$ calcld. 545.2510.

(1′S,3′R,6′S,7′R,9′S,11′R,15′Z)-4′-Methyl-7′-(prop-2-en-1-yl)-2′,8′,12′-trioxaspiro(1,3-dioxolane-2,14′-tricyclo[9.6.0.0^{3,9}]heptadecane)-4′,15′-dien-6′-ol (**16**)

To a solution of the enone **10** (292 mg, 0.806 mmol) in methanol (16 mL), cerium(III) chloride heptahydrate (361 mg, 0.969 mmol) was added. The solution was cooled to −78 °C and sodium borohydride (37 mg, 0.97 mmol) was added and the mixture was stirred for 2 h. The mixture was diluted with ethyl acetate (80 mL) and washed with sat. aq. ammonium chloride (3 × 40 mL). The organic phase was dried ($MgSO_4$) and concentrated under reduced pressure to afford the crude allylic alcohol **16** (294 mg) as a colourless gum. The residue was used directly in the next reaction without purification. For analytical purposes, a sample of the product was purified by flash column chromatography (25–75% diethyl ether in pentane) to afford the allylic alcohol **16** as a colourless gum. R_f = 0.68 (60% ethyl acetate in pet. ether); $[\alpha]_D$ +13.5 (*c* = 1.00 in $CHCl_3$, 21 °C); ν_{max} 2994, 2942, 2880, 1701, 1641, 1377, 1101, 1087, 984, 959, 854 cm^{-1}; ^{1}H NMR (400 MHz, $CDCl_3$) δ 5.91 (1H, dddd, *J* = 17.1, 10.3, 6.9, 6.9 Hz), 5.88 (1H, ddd, *J* = 11.4, 9.6, 7.6 Hz), 5.69 (1H, d, *J* = 11.4 Hz), 5.47 (1H, ddq, *J* = 2.2, 1.6, 1.6 Hz), 5.17–5.00 (2H, m), 4.05 (1H, dd, *J* = 8.8, 2.2 Hz), 3.99–3.89 (4H, m), 3.66 (1H, ddq, *J* = 9.0, 1.6, 1.6 Hz), 3.66 (1H, d, *J* = 12.7 Hz), 3.55 (1H, d, *J* = 12.7 Hz), 3.45 (1H, ddd, *J* = 11.7, 9.2, 4.4 Hz), 3.35–3.23 (1H, m), 3.29 (1H, ddd, *J* = 11.2, 9.0, 4.7 Hz), 3.26 (1H, ddd, *J* = 9.2, 5.5, 4.1 Hz), 2.94 (1H, ddd, *J* = 13.6, 9.6, 4.1 Hz), 2.55 (1H, ddd, *J* = 13.6, 7.6, 5.5 Hz), 2.49 (1H, ddddd, *J* = 14.6, 6.9, 3.5, 1.3, 1.3 Hz), 2.30 (1H, ddd, *J* = 12.1, 4.7, 4.4 Hz), 2.20 (1H, ddddd, *J* = 14.6, 8.2, 6.9, 1.3, 1.3 Hz), 1.78 (3H, dd, *J* = 1.6, 1.6 Hz), 1.58 (1H, ddd, *J* = 12.1, 11.7, 11.2 Hz); ^{13}C NMR (101 MHz, $CDCl_3$) δ 137.7, 135.3, 133.6, 130.8, 129.0, 117.0, 108.0, 83.9, 82.2, 81.7, 78.2, 77.8, 74.2, 73.4, 64.7, 64.6, 38.9, 37.8, 30.1, 21.9; HRMS (ESI$^+$) $[C_{20}H_{28}O_6Na]^+$ found 387.1771, $[M + Na]^+$ calcld. 387.1778

(1′S,3′S,4′R,6′R,7′R,8′R,10′S,12′R,16′Z)-4′-Methyl-8′-(prop-2-en-1-yl)-2′,5′,9′,13′-tetraoxaspiro(1,3-dioxolane-2,15′-tetracyclo[10.6.0.0^{3,10}.0^{4,6}]octadecane)-16′-en-7′-ol (**17**)

To a stirred solution of allylic alcohol **16** (294 mg) in benzene (41 mL), vanadyl acetylacetonate (42 mg, 0.16 mmol, >20 mol%) was added. A teal solution formed after 10 min and then *t*-butyl hydroperoxide (0.32 mL of a 5.0 M in decane, 1.6 mmol) was added to form a red solution. The solution was stirred at 60 °C for 2 h during which time the solution turned yellow. The reaction mixture was diluted with diethyl ether (40 mL) and washed with sat. aq. sodium sulfite (2 × 40 mL), sat. aq. ammonium chloride / 10% aq. ammonium hydroxide (4:1, 2 × 40 mL) and brine (2 × 40 mL). The organic phase was dried (Na_2SO_4) and concentrated under reduced pressure to afford the epoxide **17** (290 mg) as a yellow oil. The residue was used directly in the next reaction without purification. For analytical purposes, a sample of the product was purified by flash column chromatography (25–75% diethyl ether in pentane) to afford the epoxide **17** as a colourless oil. R_f = 0.39 (60% ethyl acetate in pet. ether); $[\alpha]_D$ +11.8 (*c* = 1.00 in $CHCl_3$, 22 °C); ν_{max} 3457, 2924, 2872, 2855, 1641, 1443, 1281, 1111, 1086, 1055, 1018, 882, 770 cm^{-1}; ^{1}H NMR (400 MHz, CD_2Cl_2) δ 5.93–5.81 (2H, m), 5.66 (1H, d, *J* = 11.5 Hz), 5.12–5.02 (2H, m), 3.95–3.86 (4H, m), 3.75 (1H, ddd, *J* = 8.9, 8.2, 1.0 Hz), 3.59 (1H, d, *J* = 12.7 Hz), 3.52 (1H, d, *J* = 12.7 Hz), 3.46 (1H, ddd, *J* = 11.6, 9.1, 4.5 Hz), 3.29 (1H, d, *J* = 9.1 Hz), 3.28–3.19 (2H, m), 3.15 (1H, ddd, *J* = 11.5, 9.1, 4.7 Hz), 3.08 (1H, d, *J* = 1.0 Hz), 2.86 (1H, ddd, *J* = 13.7, 9.6, 4.0 Hz), 2.60 (1H, ddd, *J* = 13.7, 6.9, 6.9 Hz), 2.53 (1H, ddd, *J* = 14.5, 6.9, 6.9 Hz), 2.26 (1H, ddd, *J* = 12.0, 4.7, 4.5 Hz), 2.12 (1H, ddd, *J* = 14.5, 7.7, 7.7 Hz), 2.02 (1H, d, *J* = 8.2 Hz), 1.42 (1H, ddd, *J* = 12.0, 11.6, 11.5 Hz), 1.40 (3H, s); ^{13}C NMR (101 MHz, CD_2Cl_2) δ 135.8, 134.1, 130.7, 117.1, 108.5, 82.7, 82.2, 80.5, 78.0, 75.7, 74.4, 72.9, 67.2, 65.1, 64.9, 61.5, 38.9, 37.8, 30.5, 21.3; HRMS (EI$^+$) $[C_{20}H_{28}O_7]^+$ found 380.1831, $[M]^+$ calcld. 380.1835.

[(1′S,3′S,4′R,6′R,7′R,8′R,10′S,12′R,16′Z)-4′-Methyl-8′-(prop-2-en-1-yl)-2′,5′,9′,13′-tetraoxaspiro(1,3-dioxolane-2,15′-tetracyclo[10.6.0.0^{3,10}.0^{4,6}]octadecane)-16′-en-7′-yloxy]tris(propan-2-yl)silane (**18**)

The reaction was performed two batches. To a solution of the epoxy alcohol **17** (145 mg) in dichloromethane (20 mL), 4-dimethylaminopyridine (244 mg, 2.00 mmol), triethylamine (1.12 mL, 8.0 mmol) and triisopropylsilyl trifluoromethanesufonate (1.61 mL, 6.0 mmol) were added. The mixture was stirred for 16 h and diluted with diethyl ether (80 mL). The mixture was washed with sat. aq. ammonium chloride (3 × 50 mL), dried (Na_2SO_4) and concentrated under reduced pressure. The residue was purified by flash column chromatography (5–15% diethyl ether in pet. ether). The batches were combined to give the silyl ether **18** (284 mg, 66% over 3 steps) as a colourless oil. R_f = 0.51 (20% ethyl acetate in pet. ether); $[\alpha]_D$ +39.2 (*c* = 0.50 in $CHCl_3$, 27 °C); ν_{max} 2943, 2893, 2866, 1641, 1464, 1109, 1089, 883, 912, 718 cm^{-1}; ^{1}H NMR (400 MHz, CD_2Cl_2) δ 5.89 (1H, ddd, *J* = 11.5, 9.6, 7.5 Hz), 5.86 (1H, dddd, *J* = 17.1, 10.3, 6.8, 6.8 Hz), 5.66 (1H, d, *J* = 11.5 Hz), 5.09–4.98 (2H, m), 3.97 (1H, dd, *J* = 9.2, 1.0 Hz), 3.94–3.86 (4H, m), 3.59 (1H, d, *J* = 12.7 Hz), 3.52 (1H, d, *J* = 12.7 Hz), 3.45 (1H, ddd, *J* = 11.6, 9.2, 4.4 Hz), 3.29–3.25 (1H, m), 3.27 (1H, d, *J* = 9.2 Hz), 3.21 (1H, ddd, *J* = 9.2, 6.0, 4.0 Hz), 3.14 (1H, ddd, *J* = 11.5, 9.2, 4.7 Hz), 3.01 (1H, d, *J* = 1.0 Hz), 2.87 (1H, ddd, *J* = 13.5, 9.6, 4.0 Hz), 2.65–2.53 (2H, m), 2.25 (1H, ddd, *J* = 11.9, 4.7, 4.4 Hz), 2.02 (1H, ddddd, *J* = 14.4, 10.1, 6.8, 1.3, 1.3 Hz), 1.40 (1H, ddd, *J* = 11.9, 11.6, 11.5 Hz), 1.38 (3H, s), 1.16–1.02 (21H, m); ^{13}C NMR (101 MHz, CD_2Cl_2) δ 136.4, 134.1, 130.7, 116.7, 108.5, 82.8, 82.3, 81.2, 78.1, 75.6, 74.4, 74.4, 67.4, 65.1, 64.9, 61.2, 38.9, 37.8, 30.6, 21.5, 18.6, 18.5, 13.6; HRMS (ESI$^+$) $[C_{29}H_{48}O_7SiNa]^+$ found 559.3047, $[M + Na]^+$ calcld. 559.3062.

(1S,3R,5S,6S,7R,9S,11R,15Z)-5-Hydroxy-4-methylidene-7-(prop-2-en-1-yl)-6-{[tris(propan-2-yl)silyl]oxy}-2,8,12-trioxatricyclo[9.6.0.0^{3,9}]heptadec-15-en-14-one (**19**)

To a solution of 2,2,6,6-tetramethylpiperidine (0.05 mL, 0.3 mmol) in toluene (0.45 mL) at −10 °C, a solution of *n*-BuLi (0.5 mL of a 0.6 M solution in toluene and hexane, 3:2, 0.3 mmol) was added dropwise. The mixture was stirred for 30 min to produce an orange solution. Diethylaluminium chloride (0.30 mL of a 1.0 M solution in hexane, 0.30 mmol) was added dropwise and the mixture was stirred for a further 30 min resulting in the formation of a colourless solution. To the resultant

solution of the complex was added a solution of the epoxide **18** (27 mg, 50 μmol) in toluene (0.70 mL). The reaction mixture was allowed to reach rt over 16 h and then diluted with diethyl ether (8 mL). Sat. aq. Rochelle salt (10 mL) was added and the mixture was stirred vigorously for 2 h. The phases were separated and the organic phase was washed with sat. aq. ammonium chloride (10 mL) and brine (10 mL), then dried ($MgSO_4$) and concentrated under reduced pressure. The residue was purified by flash column chromatography (10–40% diethyl ether in pentane) to afford the allylic alcohol **19** (10 mg, 40%) as a yellow oil. R_f = 0.60 (60% ethyl acetate in pet. ether); $[\alpha]_D$ +5.8 (*c* = 0.50 in $CHCl_3$, 27 °C); ν_{max} 3476, 2891, 2866, 1676, 1643, 1464, 1098, 1016, 997, 918, 883 cm^{-1}; ^1H NMR (400 MHz, $CDCl_3$) δ 6.47 (1H, ddd, *J* = 12.4, 8.8, 7.6 Hz), 5.87 (1H, dddd, *J* = 17.1, 10.2, 6.9, 6.6 Hz), 5.86 (1H, dddd, *J* = 12.4, 1.6, 1.6, 1.1 Hz), 5.45 (1H, ddd, *J* = 1.3, 1.3, 1.3 Hz), 5.39 (1H, ddd, *J* = 1.3, 1.3, 1.3 Hz), 5.13–5.04 (2H, m), 4.51 (1H, dd, *J* = 17.8, 1.1 Hz), 4.47 (1H, ddd, *J* = 2.5, 1.3, 1.3 Hz), 4.20 (1H, d, *J* = 17.8 Hz), 3.80 (1H, dd, *J* = 6.7, 2.5 Hz), 3.68 (1H, ddd, *J* = 11.2, 9.6, 4.3 Hz), 3.64 (1H, ddd, *J* = 9.6, 1.3, 1.3 Hz), 3.55 (1H, ddd, *J* = 9.7, 6.7, 3.0 Hz), 3.41 (1H, ddd, *J* = 11.4, 9.1, 4.2 Hz), 3.32 (1H, ddd, *J* = 9.1, 9.1, 1.6 Hz), 2.70 (1H, dddd, *J* = 14.9, 7.6, 1.6, 1.6 Hz), 2.64 (1H, dddd, *J* = 14.9, 9.1, 8.8, 1.6 Hz), 2.46 (1H, ddddd, *J* = 14.4, 6.9, 3.0, 1.3, 1.3 Hz), 2.34 (1H, ddd, *J* = 11.6, 4.3, 4.2 Hz), 2.16 (1H, ddddd, *J* = 14.4, 9.7, 6.6, 1.3, 1.3 Hz), 1.65 (1H, ddd, *J* = 11.6, 11.4, 11.2 Hz), 1.15–1.03 (21H, m); ^{13}C NMR (101 MHz, $CDCl_3$) δ 203.7, 145.1, 138.1, 135.3, 129.0, 117.7, 117.0, 85.3, 83.1, 82.0, 78.7, 78.6, 77.4, 77.0, 76.3, 38.3, 38.2, 35.1, 18.3, 13.0; HRMS (ESI^+) $[C_{27}H_{44}O_6SiNa]^+$ found 515.2775, $[M + Na]^+$ calcld. 515.2799.

(1′S,3′R,5′S,6′S,7′R,9′S,11′R,15′Z)-4′-Methylidene-7′-(prop-2-en-1-yl)-6′-{[tris(propan-2-yl)silyl]oxy}-2′,8′,12′-trioxaspiro(1,3-dioxolane-2,14′-tricyclo[9.6.0.0^{3,9}]heptadecane)-15′-en-5′-ol (**20**)

To a solution of epoxide **18** (43 mg, 80 μmol) in THF (4 mL), *p*-toluenesulfonic acid (69 mg, 0.40 mmol) and 4 Å molecular sieves (3 g) were added. The resultant mixture was stirred for 16 h and dried (4 Å molecular sieves) ethylene glycol (1 mL) was added. The reaction mixture was stirred for a further 24 h and diluted with sat. aq. sodium bicarbonate (25 mL). The organic phase was extracted with diethyl ether (3 × 10 mL) and the combined organic extracts were washed with brine (3 × 10 mL), dried ($MgSO_4$) and concentrated under reduced pressure. The residue was purified by flash column chromatography (10–30% diethyl ether in pet. ether) to afford allylic alcohol **20** (17 mg, 40%) and starting epoxide **18** (11 mg, 26%) as colourless films. R_f = 0.63 (60% ethyl acetate in pet. ether); $[\alpha]_D$ +32.4 (*c* = 1.00 in $CHCl_3$, 27 °C); ν_{max} 3476, 2941, 2866, 1643, 1464, 1090, 1018, 901, 883 cm^{-1}; ^1H NMR (400 MHz, $CDCl_3$) δ 5.92 (1H, ddd, *J* = 11.4, 9.5, 7.5 Hz), 5.87 (1H, dddd, *J* = 17.1, 10.3, 7.1, 6.5 Hz), 5.68 (1H, d, *J* = 11.4 Hz), 5.45 (1H, ddd, *J* = 1.4, 1.4, 1.4 Hz), 5.35 (1H, ddd, *J* = 1.4, 1.4, 1.4 Hz), 5.12–5.02 (2H, m), 4.44 (1H, dddd, *J* = 4.1, 2.7, 1.4, 1.4 Hz), 3.98–3.91 (4H, m), 3.79 (1H, dd, *J* = 6.9, 2.7 Hz), 3.66 (1H, d, *J* = 12.8 Hz), 3.61 (1H, ddd, *J* = 9.6, 1.4, 1.4 Hz), 3.56 (1H, d, *J* = 12.8 Hz), 3.54–3.46 (3H, m), 3.38 (1H, ddd, *J* = 9.3, 5.5, 4.1 Hz), 2.96 (1H, ddd, *J* = 13.4, 9.5, 4.1 Hz), 2.62 (1H, ddd, *J* = 13.4, 7.5, 5.5 Hz), 2.45 (1H, ddddd, *J* = 14.5, 7.1, 2.8, 1.3, 1.3 Hz), 2.31 (1H, d, *J* = 4.1 Hz), 2.30 (1H, ddd, *J* = 11.7, 4.4, 4.4 Hz), 2.15 (1H, ddddd, *J* = 14.5, 9.6, 6.5, 1.4, 1.4 Hz), 1.53 (1H, app. dt, *J* = 11.7, 11.4 Hz), 1.13–1.04 (21H, m); ^{13}C NMR (101 MHz, $CDCl_3$) δ 145.6, 135.4, 133.5, 130.9, 117.0, 116.9, 108.0, 83.2, 82.0, 82.0, 78.6, 78.2, 77.8, 76.1, 74.1, 64.8, 64.6, 38.7, 38.3, 30.3, 18.3, 13.1; HRMS (ESI^+) $[C_{29}H_{48}O_7SiNa]^+$ found 559.3041, $[M + Na]^+$ calcld. 559.3062.

(1′R,3′S,5′Z,10′R,12′S,14′R,19′S,20′S,21′S)-21′-Methyl-20′-[(naphthalen-2-yl)methoxy]-2′,9′,13′,18′-tetraoxaspiro[1,3-dioxolane-2,7′-tetracyclo(10.9.0.0^{3,10}.0^{14,19}]henicosane)-5′,15′-dien-17′-one (**25**)

To a solution of alcohol **15** (8 mg, 0.02 mmol) in methanol (0.64 mL), the ruthenium complex **21** (3 mg, 0.03 mmol, 20 mol%) was added. The solution was stirred at reflux for 1 h and concentrated under reduced pressure. The residue was purified by flash column chromatography to afford an *E* / *Z* mixture of alcohol **22** (4 mg) as a colourless film. The residue was used directly in the next reaction without purification.

To a solution of (2*E*)-4-(prop-2-en-1-yloxy)but-2-enoic acid **23** (2 mg, 0.02 mmol) in dichloromethane (0.8 mL), *N*,*N*′-dicyclohexylcarbodiimide (3 mg, 0.02 mmol) and 4-dimethylaminopyridine (0.2 mg,

0.02 mmol) were added. The resultant suspension was added to **22** (4 mg) and the mixture stirred for 16 h. The mixture was diluted with diethyl ether (4.2 mL) and filtered. The filtrate was concentrated under reduced pressure and the residue was purified by flash column chromatography (5–60% diethyl ether in pet. ether) to give an isomeric mixture of esters **24** (2 mg) as a colourless film. The residue was used directly in the next reaction without purification.

To a solution of ester **24** (2 mg) in dichloromethane (16 mL), the ruthenium complex **21** (1 mg, 1 μmol) was added. The solution was stirred for 6 h at reflux and concentrated under reduced pressure. The residue was purified by flash column chromatography (0–25% diethyl ether in dichloromethane) to deliver the tetracyclic lactone **25** (1 mg, 12% over 3 steps) as a colourless film. R_f = 0.23 (80% diethyl ether in pet. ether); $[\alpha]_D$ +48 (*c* = 0.08 in $CHCl_3$, 36 °C); ν_{max} 2922, 2851, 1734, 1636, 1559, 1119, 1042, 818 cm^{-1}; ^1H NMR (500 MHz, $CDCl_3$) δ 7.88–7.81 (3H, m), 7.80 (1H, s), 7.54–7.42 (3H, m), 6.82 (1H, dd, *J* = 9.9, 1.6 Hz), 5.93 (1H, dd, *J* = 9.9, 2.5 Hz), 5.91 (1H, ddd, *J* = 11.4, 9.7, 7.4 Hz), 5.73 (1H, d, *J* = 11.4 Hz), 4.87 (1H, d, *J* = 11.5 Hz), 4.86 (1H, ddd, *J* = 10.5, 2.5, 1.6 Hz), 4.81 (1H, d, *J* = 11.5 Hz), 4.26 (1H, dd, *J* = 10.5, 0.7 Hz), 3.96 (4H, m), 3.90 (1H, ddd, *J* = 11.0, 9.3, 5.5 Hz), 3.83 (1H, dd, *J* = 2.6, 0.7 Hz), 3.67 (1H, d, *J* = 12.7 Hz), 3.54 (1H, d, *J* = 12.7 Hz), 3.43 (1H, ddd, *J* = 12.4, 9.1, 4.3 Hz), 3.23 (1H, ddd, *J* = 9.1, 7.2, 5.5 Hz), 2.97 (1H, ddd, *J* = 13.5, 9.7, 7.2 Hz), 2.93 (1H, dd, *J* = 9.3, 5.7 Hz), 2.54 (1H, ddd, *J* = 13.5, 7.4, 5.5 Hz), 2.33 (1H, ddd, *J* = 11.8, 5.5, 4.3 Hz), 2.27 (1H, qdd, *J* = 7.4, 5.7, 2.6 Hz), 1.47 (1H, ddd, *J* = 12.4, 11.8, 11.0 Hz), 1.18 (3H, d, *J* = 7.4 Hz); ^{13}C NMR (126 MHz, $CDCl_3$) δ 163.4, 149.9, 135.6, 133.8, 133.3, 133.1, 130.8, 128.3, 128.1, 127.9, 126.8, 126.3, 126.1, 126.1, 119.4, 107.9, 86.9, 82.9, 81.8, 81.0, 77.7, 75.4, 74.4, 73.0, 69.8, 64.8, 64.7, 39.9, 39.0, 32.1, 19.9; HRMS (ESI$^+$) $[C_{31}H_{34}O_8Na]^+$ found 557.2124, $[M + Na]^+$ calcld. 557.2146.

Supplementary Materials: The following are available online at http://www.mdpi.com/2072-6651/12/12/740/s1, ^1H and ^{13}C NMR spectra for key compounds, plus additional ^1H NMR NOE data for selected intermediate compounds.

Author Contributions: J.S.C. conceived the synthetic route, supervised the project and wrote the paper; J.S.C and M.P. designed the experiments; M.P. performed all synthetic work in the laboratory. All authors have read and agreed to the published version of the manuscript.

Funding: This research was funded by EPSRC, grant numbers EP/K503058 and EP/L50497X.

Acknowledgments: The authors gratefully acknowledge studentship funding from EPSRC to support M.P. The authors also thank Alistair Boyer (University of Glasgow) for providing the carboxylic acid **23**.

Conflicts of Interest: The authors declare no conflict of interest. The funder had no role in the design of the study; in the collection, analyses, or interpretation of data; in the writing of the manuscript, or in the decision to publish the results.

References and Note

1. Murata, M.; Legrand, A.M.; Ishibashi, Y.; Yasumoto, T. Structures of Ciguatoxin and Its Congener. *J. Am. Chem. Soc.* **1989**, *111*, 8929–8931. [CrossRef]
2. Murata, M.; Legrand, A.M.; Ishibashi, Y.; Fukui, M.; Yasumoto, T. Structures and Configurations of Ciguatoxin from the Moray Eel *Gymnothorax javanicus* and Its Likely Precursor from the Dinoflagellate *Gambierdiscus toxicus*. *J. Am. Chem. Soc.* **1990**, *112*, 4380–4386. [CrossRef]
3. Yasumoto, T.; Igarashi, T.; Legrand, A.-M.; Cruchet, P.; Chinain, M.; Fujita, T.; Naoki, H. Structural Elucidation of Ciguatoxin Congeners by Fast-Atom Bombardment Tandem Mass Spectroscopy. *J. Am. Chem. Soc.* **2000**, *122*, 4988–4989. [CrossRef]
4. Nicholson, G.M.; Lewis, R.J. Ciguatoxins: Cyclic Polyether Modulators of Voltage-Gated Ion Channel Function. *Mar. Drugs* **2006**, *4*, 82–118. [CrossRef]
5. Soliño, L.; Costa, P.R. Differential Toxin Profiles of Ciguatoxins in Marine Organisms: Chemistry, Fate and Global Distribution. *Toxicon* **2018**, *150*, 124–143. [CrossRef]
6. Pasinszki, T.; Lako, J.; Dennis, T.E. Advances in Detecting Ciguatoxins in Fish. *Toxins* **2020**, *12*, 494. [CrossRef]
7. Lewis, R.J.; Vernoux, J.-P.; Brereton, I.M. Structure of Caribbean Ciguatoxin Isolated from *Caranx latus*. *J. Am. Chem. Soc.* **1998**, *120*, 5914–5920. [CrossRef]

8. Kryuchkov, F.; Robertson, A.; Miles, C.O.; Mudge, E.M.; Uhlig, S. LC-HRMS and Chemical Derivatization Strategies for the Structure Elucidation of Caribbean Ciguatoxins: Identification of C-CTX-3 and -4. *Mar. Drugs* **2020**, *18*, 182. [CrossRef]
9. Hamilton, B.; Hurbungs, M.; Jones, A.; Lewis, R.J. Multiple Ciguatoxins Present in Indian Ocean Reef Fish. *Toxicon* **2002**, 1347–1353. [CrossRef]
10. Diogène, J.; Reverté, L.; Rambla-Alegre, M.; del Río, V.; de la Iglesia, P.; Campàs, M.; Palacios, O.; Flores, C.; Caixach, J.; Ralijaona, C.; et al. Identification of Ciguatoxins in a Shark Involved in a Fatal Food Poisoning in the Indian Ocean. *Sci. Rep.* **2017**, *7*, 8240. [CrossRef]
11. Friedman, M.A.; Fernandez, M.; Backer, L.C.; Dickey, R.W.; Bernstein, J.; Schrank, K.; Kibler, S.; Stephan, W.; Gribble, M.O.; Bienfang, P.; et al. An Updated Review of Ciguatera Fish Poisoning: Clinical, Epidemiological, Environmental, and Public Health Management. *Mar. Drugs* **2017**, *15*, 72. [CrossRef] [PubMed]
12. Frelin, C.; Durand-Clément, M.; Bidard, J.-N.; Lazdunski, M. The Molecular Basis of Ciguatoxin Action. In *Marine Toxins*; Hall, S., Strichartz, G., Eds.; ACS Symposium Series; American Chemical Society: Washington, DC, USA, 1990; Volume 418, pp. 192–199.
13. Bidard, J.-N.; Vijverberg, H.M.P.; Frelin, C.; Chungue, E.; Legrand, A.-M.; Bagnis, R.; Lazdunski, M. Ciguatoxin Is a Novel Type of Na^+ Channel Toxin. *J. Biol. Chem.* **1984**, *259*, 8353–8357. [PubMed]
14. Hidalgo, J.; Liberona, J.J.; Molgó, J.; Jaimovich, E. Pacific Ciguatoxin-1b effect over Na^+ and K^+ Currents, Inositol 1,4,5-Triphosphate Content and Intracellular Ca^{2+} Signals in Cultured Rat Myotubes. *Br. J. Pharmacol.* **2002**, *137*, 1055–1062. [CrossRef] [PubMed]
15. Hirama, M.; Oishi, T.; Uehara, H.; Inoue, M.; Maruyama, M.; Oguri, H.; Satake, M. Total Synthesis of Ciguatoxin CTX3C. *Science* **2001**, *294*, 1904–1907. [CrossRef] [PubMed]
16. Inoue, M.; Miyazaki, K.; Uehara, H.; Maruyama, M.; Hirama, M. First- and Second-Generation Total Synthesis of Ciguatoxin CTX3C. *Proc. Natl. Acad. Sci. USA* **2004**, *101*, 12013–12018. [CrossRef] [PubMed]
17. Inoue, M.; Miyazaki, K.; Ishihara, Y.; Tatami, A.; Ohnuma, Y.; Kawada, Y.; Komano, K.; Yamashita, S.; Lee, N.; Hirama, M. Total Synthesis of Ciguatoxin and 51-HydroxyCTX3C. *J. Am. Chem. Soc.* **2006**, *128*, 9352–9354. [CrossRef] [PubMed]
18. Hamajima, A.; Isobe, M. Total Synthesis of Ciguatoxin. *Angew. Chem. Int. Ed.* **2009**, *49*, 2941–2945. [CrossRef]
19. Clark, J.S. Construction of Fused Polycyclic Ethers by Strategies Involving Ring-Closing Metathesis. *Chem. Commun.* **2006**, 3571–3581. [CrossRef]
20. Clark, J.S.; Grainger, D.M.; Ehkirch, A.A.-C.; Blake, A.J.; Wilson, C. Synthesis of the Fused Polycyclic Ether Core of Hemibrevetoxin B by Two-Directional Ring-Closing Metathesis. *Org. Lett.* **2007**, *9*, 1033–1036. [CrossRef]
21. Clark, J.S.; Kimber, M.C.; Robertson, J.; McErlean, C.S.P.; Wilson, C. Rapid Two-Directional Synthesis of the F–J Fragment of the Gambieric Acids by Iterative Doube Ring-Closing Metathesis. *Angew. Chem. Int. Ed.* **2005**, *44*, 6157–6162. [CrossRef]
22. Clark, J.S.; Romiti, F.; Sieng, B.; Paterson, L.C.; Stewart, A.; Chaudhury, S.; Thomas, L.H. Synthesis of the A–D Ring System of the Gambieric Acids. *Org. Lett.* **2015**, *17*, 4694–4697. [CrossRef] [PubMed]
23. Clark, J.S.; Conroy, J.; Blake, A.J. Rapid Synthesis of the A–E Fragment of CTX3C. *Org. Lett.* **2007**, *9*, 2091–2094. [CrossRef]
24. Skardon-Duncan, J.; Sparenberg, M.; Bayle, A.; Alexander, S.; Clark, J.S. Steroselective Synthesis of Medium-Sized Cyclic Ethers by Sequential Ring-Closing Metathesis and Tsuji-Trost Allylation. *Org. Lett.* **2018**, *20*, 2782–2786. [CrossRef] [PubMed]
25. Popadynec, M.; Gibbard, H.; Clark, J.S. Bidirectional Synthesis of the IJK Fragment of Ciguatoxin CTX3C by Sequential Double Ring-Closing Metathesis and Tsuji-Trost Allylation. *Org. Lett.* **2020**, *22*, 3734–3738. [CrossRef] [PubMed]
26. Clark, J.S.; Kettle, J.G. Enantioselective Synthesis of Medium-Ring Sub-Units of Brevetoxin A by Ring-Closing Metathesis. *Tetrahedron Lett.* **1997**, *17*, 127–130. [CrossRef]
27. Ciceri, P.; Demnitz, F.W.J. An Efficient, Rapid and Highly Selective Preparation of the Wieland-Miescher Ketone-9-Ethylene Ketal. *Tetrahedron Lett.* **1997**, *38*, 389–390. [CrossRef]
28. Tsunoda, T.; Suzuki, M.; Noyori, R. A Facile Procedure for Acetalization Under Aprotic Conditions. *Tetrahedron Lett.* **1980**, *21*, 1357–1358. [CrossRef]
29. Behenna, D.C.; Stoltz, B.M. The Enantioselective Tsuji Allylation. *J. Am. Chem. Soc.* **2004**, *126*, 15044–15045. [CrossRef]

30. Mahoney, W.S.; Brestensky, D.M.; Stryker, J.M. Selective Hydride-Mediated Conjugate Reduction of α,β-Unsaturated Carbonyl Compounds Using $[(Ph_3P)CuH]_6$. *J. Am. Chem. Soc.* **1988**, *110*, 291–293. [CrossRef]
31. Saito, S.; Yamamoto, H. Efficient Conjugate Reduction of α,β-Unsaturated Carbonyl Compounds by Complexation with Aluminum Tris(2,6-diphenylphenoxide). *J. Org. Chem.* **1996**, *61*, 2928–2929. [CrossRef]
32. Baker, B.A.; Bošković, Ž.V.; Lipshutz, B.H. (BDP)CuH: A "Hot" Stryker's Reagent for Use in Achiral Conjugate Reductions. *Org. Lett.* **2008**, *10*, 289–292. [CrossRef] [PubMed]
33. Davis, F.A.; Vishwakarma, L.C.; Billmers, J.M.; Finn, J. Synthesis of α-Hydroxy Carbonyl Compounds (Acyloins): Direct Oxidation of Enolates Using 2-Sulfonyloxaziridines. *J. Org. Chem.* **1984**, *49*, 3241–3243. [CrossRef]
34. Davis, F.A.; Sheppard, A.C. Applications of Oxaziridines in Organic Synthesis. *Tetrahedron* **1989**, *45*, 5703–5742. [CrossRef]
35. Rubottom, G.M.; Vazquez, M.A.; Pelegrina, D.R. Peracid Oxidation of Trimethylsilyl Enol Ethers: A Facile α-Hydroxylation Procedure. *Tetrahedron Lett.* **1974**, *15*, 4319–4322. [CrossRef]
36. Zhang, Y.; Rohanna, J.; Zhou, J.; Iyer, K.; Rainier, J.D. Total Synthesis of Brevenal. *J. Am. Chem. Soc.* **2011**, *133*, 3208–3216. [CrossRef]
37. Nashed, M.A.; Anderson, L. Organotin Derivatives and the Selective Acylation and Alkylation of the Equatorial Hydroxy Group in a Vicinal, Equatorial-Axial Pair. *Tetrahedron Lett.* **1976**, *17*, 3503–3506. [CrossRef]
38. Zou, X.; Qin, C.; Pereira, C.L.; Tian, G.; Hu, J.; Seeberger, P.H.; Yin, J. Synergistic Glycosylation as Key to the Chemical Synthesis of an Outer Core Octasaccharide of *Helicobacter pylori*. *Chem. Eur. J.* **2018**, *24*, 2868–2872. [CrossRef]
39. Yasuda, A.; Tanaka, S.; Oshima, K.; Yamamoto, H.; Nozaki, H. Organoaluminum Reagents of Type $R^1R^2NAlEt_2$ Which Allow Regiospecific Isomerization of Epoxides to Allylic Alcohols. *J. Am. Chem. Soc.* **1974**, *96*, 6513–6514. [CrossRef]
40. Crabtree, R.H.; Davis, M.W. Directing Effects in Homogeneous Hydrogenation with $[Ir(cod)(PCy_3)(py)]PF_6$. *J. Org. Chem.* **1986**, *51*, 2655–2661. [CrossRef]
41. Thompson, H.W.; McPherson, E. Control of Hydrogenation Stereochemistry by Intramolecular Anionic Coordination to Homogeneous Catalysts. *J. Am. Chem. Soc.* **1974**, *96*, 6232–6233. [CrossRef]
42. Machado, A.S.; Olesker, A.; Castillon, S.; Lukacs, G. Hydroxy Group Directed Hydrogenation with Rhodium and Iridium Catalysts. Synthesis of a Protected Chiral Carbocyclic Analogue of Daunosamine. *J. Chem. Soc. Chem. Commun.* **1985**, *6*, 330–332. [CrossRef]
43. Hanessian, S.; Giroux, S.; Larsson, A. Efficient Allyl to Propenyl Isomerization in Functionally Diverse Compounds with a Thermally Modified Grubbs Second-Generation Catalyst. *Org. Lett.* **2006**, *8*, 5481–5484. [CrossRef] [PubMed]
44. Hoye, T.R.; Jeffrey, C.S.; Tennakoon, M.A.; Wang, J.; Zhao, H. Relay Ring-Closing Metathesis (RRCM): A Strategy for Directing Metal Movement Throughout Olefin Metathesis Sequences. *J. Am. Chem. Soc.* **2004**, *126*, 10210–12211. [CrossRef] [PubMed]
45. Harding, K.E.; Clement, B.A.; Moreno, L.; Peter-Katalinic, J. Synthesis of Some Polyfunctionalized Bicyclo[3.3.1]nonane-2,9-diones and Bicyclo[4.3.1]decane-2,10-diones. *J. Org. Chem.* **1981**, *46*, 940–948. [CrossRef]
46. For installation of the C-47 and C-48 methyl substituents and the M-ring spiroacetal in a related but simpler α,β-unsaturated lactone, see: Domon, D.; Fujiwara, K.; Ohtaniuchi, Y.; Takezawa, A.; Takeda, S.; Kawasaki, H.; Murai, A.; Kawai, H.; Suzuki, T. Synthesis of the C42–C52 Part of Ciguatoxin CTX3C. *Tetrahedron Lett.* **2005**, *46*, 8279–8283.

toxins

MDPI

Article

Evidence for the Range Expansion of Ciguatera in French Polynesia: A Revisit of the 2009 Mass-Poisoning Outbreak in Rapa Island (Australes Archipelago)

Mireille Chinain [1,*], Clémence Mahana iti Gatti [1], André Ung [1], Philippe Cruchet [1], Taina Revel [1], Jérôme Viallon [1], Manoëlla Sibat [2], Patrick Varney [3], Victoire Laurent [3], Philipp Hess [2] and Hélène Taiana Darius [1]

1 Institut Louis Malardé, Laboratory of Marine Biotoxins—UMR EIO (IFREMER-ILM-IRD-UPF), P.O. Box 30, 98713 Papeete, Tahiti, French Polynesia; cgatti@ilm.pf (C.M.i.G.); aung@ilm.pf (A.U.); pcruchet@ilm.pf (P.C.); trevel@ilm.pf (T.R.); jviallon@ilm.pf (J.V.); tdarius@ilm.pf (H.T.D.)

2 Institut Français de Recherche Pour l'Exploitation de la Mer, Phycotoxins Laboratory, 44311 Nantes, France; manoella.sibat@ifremer.fr (M.S.); philipp.hess@ifremer.fr (P.H.)

3 Météo France, Direction Inter-Régionale en Polynésie Française, P.O. Box 6005, 98702 Faa'a, Tahiti, French Polynesia; patrick.varney@pfmail.dirpf.meteo.fr (P.V.); victoire.laurent@meteo.fr (V.L.)

* Correspondence: mchinain@ilm.pf

Received: 29 October 2020; Accepted: 28 November 2020; Published: 1 December 2020

Abstract: Ciguatera poisoning (CP) results from the consumption of seafood contaminated with ciguatoxins (CTXs). This disease is highly prevalent in French Polynesia with several well-identified hotspots. Rapa Island, the southernmost inhabited island in the country, was reportedly free of CP until 2007. This study describes the integrated approach used to investigate the etiology of a fatal mass-poisoning outbreak that occurred in Rapa in 2009. Symptoms reported in patients were evocative of ciguatera. Several *Gambierdiscus* field samples collected from benthic assemblages tested positive by the receptor binding assay (RBA). Additionally, the toxicity screening of ≈250 fish by RBA indicated ≈78% of fish could contain CTXs. The presence of CTXs in fish was confirmed by liquid chromatography tandem mass spectrometry (LC-MS/MS). The potential link between climate change and this range expansion of ciguatera to a subtropical locale of French Polynesia was also examined based on the analysis of temperature time-series data. Results are indicative of a global warming trend in Rapa area. A five-fold reduction in incidence rates was observed between 2009 and 2012, which was due in part to self-regulating behavior among individuals (avoidance of particular fish species and areas). Such observations underscore the prominent role played by community outreach in ciguatera risk management.

Keywords: ciguatera poisoning; French Polynesia; *Gambierdiscus*; ciguatoxins; epidemiology; toxicological analyses; risk management; climate change

Key Contribution: This study describes the epidemiological and ecotoxicological features of an unprecedented ciguatera poisoning (CP) event in Rapa Island (Australes archipelago, French Polynesia). Confirmation of the bioaccumulation of several Pacific ciguatoxins (P-CTXs) in Rapa fish is provided for the first time. Results of temperature time-series data analyses are indicative of a global warming trend in Rapa area. The prominent role of education and community outreach in ciguatera policy and management is highlighted.

1. Introduction

Increasing numbers of poisonings linked to the consumption of seafood contaminated with marine toxins are being reported worldwide [1–4]. Among the dozen of poisoning syndromes described so far [5], ciguatera poisoning (CP) represents the most common non-bacterial seafood poisoning globally. Ciguatera results from the consumption of fish contaminated with lipid soluble toxins known as ciguatoxins (CTXs), which originate from assemblages of epiphytic dinoflagellates of the genera *Gambierdiscus* and *Fukuyoa* [6–8] (for reviews, and references therein). Yet, other marine organisms such as bivalves, echinoderms, gastropods, and arthropods may also be involved [9–14]. *Gambierdiscus* and *Fukuyoa* spp. algal ciguatoxins are readily transferred through the food web from algae to herbivorous and then carnivorous fish, and ultimately to humans [15,16].

Ciguatera is characterized by a complex array of gastrointestinal, neurological, and cardiovascular symptoms of variable intensity, which are often complicated by chronic manifestations that can last for months to years [17–20]. The most commonly reported symptoms include diarrhea, vomiting, paresthesia of extremities, circumoral paresthesia, cold allodynia, generalized pruritus, myalgia, arthralgia, bradycardia, hypotension, extreme fatigue, etc. [19]. Although ciguatera-related fatalities are rare (<0.1% of reported cases), the high morbidity of this debilitating and sometimes long-lasting illness makes it both a prominent public health issue [4,15,19] and a major impediment for subsistence and recreational fisheries worldwide [21–24].

Until the 2000s, the distribution of ciguatera-causing organisms and ciguatoxic fish were thought to be limited to regions between latitudes 35° N and 35° S, with the highest poisoning incidence rates consistently reported from two tropical, historical CP-endemic areas, the Pacific and Caribbean regions [4] (for review and references therein) and [25,26], which is a situation due in part to the strong reliance of local communities on marine resources. The first reports of consumer illness and/or detection of ciguatoxic fish caught in previously non-endemic areas can be found in the literature as early as 2004 from localized areas such as the Macaronesia (Canary Islands, Madeira) [27–36], the eastern Mediterranean [37], the Gulf of Mexico [38], or the coast of Cameroon in West Africa [21]. In most of these instances, confirmation of the presence of CTXs in implicated toxic meals was consistent with the detection of *Gambierdiscus* species within the respective regions [38–48].

The current expansion of CP to novel areas such as Macaronesia and east and southeast Asia since the 2000s is now well established [4]. Multiple factors are believed to contribute to this expansion of the geographical range of CP, such as anthropogenic disturbances [49–51], naturally occurring environmental changes, including long-term climatic oscillations and global warming [52,53], which likely provide favorable conditions for the migration and settlement of CP causative organisms in temperate-like (and warmer) areas of the globe [4,54] (for reviews and references therein). Modeling CP occurrences based on long-term time-series data and/or temperature projections has also been addressed in several papers [55,56]; however, few studies have actually provided a clear assessment of the link between global warming and increased number of CP cases [25,57–59].

French Polynesia is a long-standing ciguatera hotspot as evidenced by the epidemiological data available for this country since 1960 [17,60–62]. Since 2007, a country-wide epidemiological surveillance program of CP cases is conducted jointly by the Institut Louis Malardé and the Public Health Directorate of French Polynesia (www.ciguatera.pf [63]). None of the five archipelagoes of French Polynesia is completely immune from ciguatera [23]. Although the general trend observed in ciguatera annual incidence rate (IR) points toward a stable IR in French Polynesia as a whole, IR rates can differ considerably from one island to another, ranging from 2 to over 1800 cases per 10,000 inhabitants [4]. As previously reported in other endemic localities of the South Pacific [62], these figures are likely under-estimated and could quite possibly be at least doubled [64]. Of note, a distance gradient is generally observed in the IRs, with the island groups furthest from Tahiti (Society archipelago) showing the highest IRs, due mainly to dietary differences observed between island groups [17]. In this respect, Rapa (Iti) Island located in the southernmost part of the Australes archipelago (Figure 1a) stood as an exception: until 2007, this island was reputed free of ciguatera [60], whereas its sister island Raivavae

consistently showed some of the highest IRs in the Australes between 2007 and 2008 [50]. This small island (40 km^2) is commonly referred to as the "little sister" of Rapa Nui (Easter Island), and it is regarded as one of the most isolated islands in the South Pacific, along with Pitcairn and Easter Island: indeed, there is no airport on Rapa Island (Figure 1b) and it takes around 50 h to reach the island by cargo ship from Tahiti. Boats traveling there are few and far between (every two to three months), and patrol boats of the French Navy also carry out episodic liaison missions from Tahiti. Due to its extreme southern location at a temperate-like latitude, Rapa's climate is characterized by seasonal variations more pronounced than in the rest of French Polynesia, with an annual average temperature of 20 °C and an important precipitation regime [65].

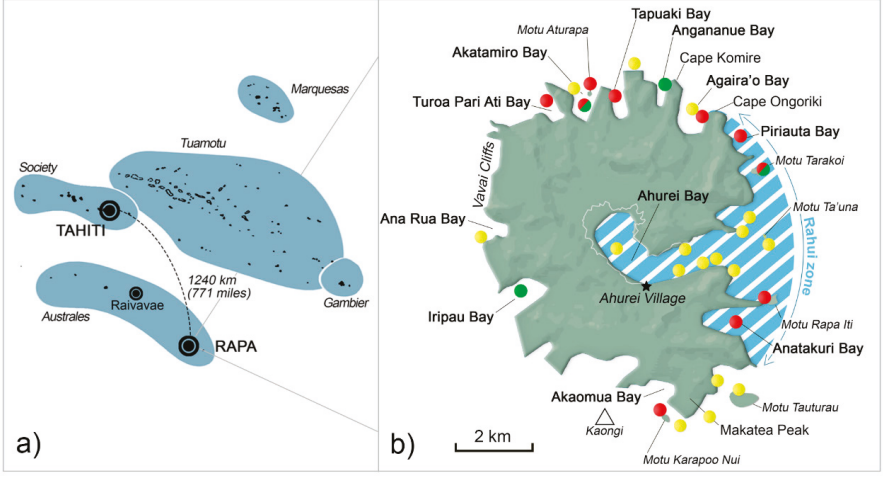

Figure 1. Maps of (**a**) French Polynesia and (**b**) Rapa Island (Australes archipelago). Yellow dots represent the 29 sampling sites prospected during the 2010 field study. The sampling sites highlighted in green and/or red indicate the locations where assemblages of *Gambierdiscus* spp. and/or *Ostreopsis* spp., respectively, were found on various macroalgal host species.

In October 2009, an unprecedented mass-poisoning outbreak occurred in this island following community fishing in the *rāhui* (conservation) area. Within months, this outbreak is believed to have affected nearly half of the resident population and even resulted in two fatalities. Faced with the magnitude and severity of this outbreak, the local public health authorities mandated scientists from the Institut Louis Malardé to conduct environmental and toxicological investigations in Rapa Island in order to investigate the etiology of this mass poisoning. In parallel to the field survey, a community outreach program was also conducted among the local population, as early as January 2010, and was continued throughout 2010 and in the ensuing years. In particular, individuals were advised not to consume specific parts of the fish (head, viscera) and to avoid particular fish species and fishing areas. The importance of a systematic report of CP incidents was also emphasized.

The present paper describes the epidemiological and field investigations conducted in 2010 in Rapa, as well as the benefits that aroused from community outreach interventions among the local population. In addition to analyses by the receptor-binding assay conducted in 2010, fish samples from the event were re-analyzed with recently optimized methods (Neuro2a assay and tandem mass spectrometry). Finally, retrospective temperature data series collated from different sources were also examined to assess the current climate trend in Rapa area. Taken together, our results confirm the current expansion of ciguatera to this temperate-like locale of French Polynesia, as well as the relevance and usefulness of an integrated approach in CP risk management in newly affected hotspots.

2. Results

2.1. Epidemiology of the 2009 Outbreak in Rapa Island

While no case was reported in 2007, six isolated CP incidents occurred starting from 2008, involving a carnivorous fish, *Seriola lalandi* (king fish, or *ma'aki* in native language), and an herbivorous fish, *Kyphosus cinerascens* (highfin chub or *karamami* in native language), for three (50%) and two (33%) of these cases, respectively (Table 1).

At the peak of the 2009 outbreak, a total of 87 resident people was seen in consultation at the infirmary, giving an IR of 1805 cases per 10,000 people for 2009. Of note, the majority of poisoning cases (78%) occurred in October (28%) and November 2009 (50%). The unusual severity of this outbreak even resulted in two fatalities. However, between 2009 and 2012, an 80% reduction in the number of poisoning cases was reported. Recent data point to an IR (128 cases/10,000 people on average in the past two years) comparable to the one reported in 2008 (IR = 145 cases/10,000 people) (Table 1). According to observations made by the nurse on site, first symptoms appeared between 1 and 72 h following the ingestion of the toxic meal (Table 2), except for one female patient, aged 52, who developed symptoms within minutes after consumption of the viscera of a seagrass parrotfish (*Leptoscarus vaigiensis*). Yet, apart from this rapid onset of poisoning symptoms, this patient displayed clinical signs typical of a moderate CP. Individuals presented with digestive and neurological symptoms highly evocative of ciguatera: in 2009–2010, during the peak of the epidemic, digestive disorders (diarrhea) were recorded in 68% of affected patients, while cold allodynia (84%), paresthesia (88%), dysesthesia (79%) and itching (71%) were among the predominant neurological symptoms (Table 2).

The prevalence of symptoms reported in patients according to the trophic status of the implicated fish was also examined, showing a strong dietary preference for herbivores (n = 84) vs. carnivores (n = 24) among Rapa residents. Data in Figure 2 indicate that digestive and cardiovascular disorders were more prevalent in carnivore-based poisoning, with the caveat that this comparison is based on groups with different and limited sample size. Interestingly, behavioral disorders were reported only in toxic incidents following the consumption of herbivores (Figure 2).

Of the 87 patients seen at the Rapa infirmary in 2009, 54% declared having previously experienced at least one or multiple (two to three) CP-like poisoning events. Moreover, for 52% and 47% of them, fish meal included viscera and head, respectively, vs. 33% who limited their fish consumption to the flesh only. By 2010, the proportion of CP cases involving the consumption of viscera and head had decreased to 22% and 37%, respectively, whereas the percentage of patients who consumed only flesh had increased by almost two-fold (60%). Of note, two fatalities were recorded in 2009, while one patient required hospitalization in 2010. Moreover, based on declaration forms, the percentage of unreported cases (i.e., guests who had shared a toxic meal with reporting patients and went on developing symptoms, but for whom no declaration form was completed) was estimated at 40% and 10% in 2009 and 2010, respectively. Of note, this rate remained around 18% on average until 2014.

Data collected at the infirmary revealed the fish involved in poisoning events were caught from two main areas, i.e., in the *rāhui* zone located in the vicinity of Ahurei village and Akatamiro Bay, a daily fishing site for local residents located north of the island, which accounted for 49 and 33% of reported events respectively, in 2009 (Figure 1 and Table 1). In addition to *S. lalandi* and *K. cinerascens*, another herbivorous species was frequently mentioned in declaration forms, namely *Leptoscarus vaigiensis* (seagrass parrotfish, or komokomo in native language) (Figure 3). All together, these three species accounted for 80 and 72% of the reported events in 2009 and 2010, respectively. Interestingly, a noticeable shift in both the fish species and fishing areas involved in CP events was observed following the 2010 field campaign and public outreach interventions in the island: indeed, this group of fish represented no more than 12, 38, and 27% of the fish involved in poisoning events in 2012, 2013, and 2014, respectively (Table 1).

Table 1. Number of ciguatera poisoning (CP) events, CP cases, and corresponding incidence rates (IR) reported from the medical facility of Rapa Island between 2007 and 2019. The prevalence (in %) of fish species and fishing sites involved in CP events is also given.

Year	2007	2008	2009	2010	2011	2012	2013	2014	2015	2016	2017 [1]	2018	2019
Number of CP events		6	71	21	11	17	32	11	9	6	-	4	6
Number of reported CP cases	-	7	87	27	13	17	33	11	15	7	-	6	7
Number of unreported cases [2]	-	5	59	3	6	2	1	-	7	5	-	1	6
Number of fatal cases	-	-	2 [3]	-	-	-	-	-	-	-	-	-	-
Incidence rates (IR) [4] (reported cases/10,000 inhab.)	-	145	1805	560	269	330	660	214	291	136	-	118	138
Fish species involved (% of event)													
Seriola lalandi	-	50	6	24	18	-	7	-	44	17	-	25	33
Kyphosus cinerascens	-	33	29	29	27	6	3	-	-	33	-	-	17
Leptoscarus vaigiensis	-	-	45	19	9	6	28	27	-	-	-	-	17
Others:	-	17	20	28	46	88	62	73	56	50	-	75	33
Scombridae		*17* [5]	*3*										
Carangidae				*9*	*9*	*17*	*3*	*9*		*17*		*25*	
Acanthuridae						*17*			*11*				
Scaridae			*1*	*9*		*12*	*19*	*27*	*34*	*17*			*17*
Serranidae			*3*		*9*	*12*	*34*	*18*	*11*			*50*	*16*
miscellaneous			*13*	*10*	*28*	*30*	*6*	*19*		*16*			
Fishing sites involved (% of event)													
Rāhui zone	-	67	49	33	45	35	12	18	11	67	-	25	17
Akatamiro Bay	-	-	33	-	-	6	16	9	-	-	-	-	17
Others:	-	-	14	53	27	35	44	18	*67*	-	-	50	33
Turoa Pari Ati Bay			*2*	*10*									
Tapuaki Bay			*4*	*5*									
Agaira'o Bay							*10*						
Kaongi				*5*									
Motu Tauturau							*10*		*11*				
Akaomua Bay				*5*			*3*						
Iripau Bay				*14*			*6*	*9*	*11*				
Ana Rua Bay				*5*	*9*			*9*				*25*	
Vavai Cliffs			*1*		*9*	*23*	*3*					*25*	
offshore			*7*	*9*	*9*	*12*	*12*		*45*				*33*
Unknown	-	33	4	14	28	24	28	55	22	33		25	33

[1] No data available for 2017. [2] Number of guests who shared a toxic meal with reporting patients and developed poisoning symptoms, but for whom no declaration form was completed. [3] Fatal cases involved an elderly woman with known comorbidity factors and a middle-aged man, who both presented pronounced cardiovascular symptoms. [4] IRs were calculated according to the population data from the 2007, 2012, and 2017 census. [5] Numbers in italics give the respective prevalence of fish families and fishing sites involved in CP events totalized under the "Others" headings.

Table 2. Clinical signs experienced by patients during the 2009–2010 mass ciguatera outbreak in Rapa Island. The number of patients concerned by each clinical sign and corresponding percentage (%) is given. Symptoms most frequently recorded are highlighted in bold characters.

Year	2009	2010
Total number of CP cases reported	87	27
Digestive disorders		
Nausea/vomiting	28 (32%)	11 (39%)
Diarrhea	**59 (68%)**	19 (68%)
Cardiovascular disorders [1]		
Bradycardia	10 (14%) [1]	6 (22%)
Hypotension	9 (12%) [1]	3 (11%)
Neurological and systemic disorders		
Cold allodynia	**80 (92%)**	15 (54%)
Paresthesia	**83 (95%)**	17 (61%)
Dysesthesia	**75 (86%)**	15 (54%)
Itching	**69 (79%)**	12 (43%)
Dizziness/headaches	50 (57%)	10 (36%)
Muscular disorders	**67 (77%)**	19 (68%)
Joint pains	**56 (64%)**	11 (39%)
Chills/hypothermia	**54 (62%)**	8 (29%)
Burning sensation (throat, mouth)/"metallic" taste	43 (49%)	4 (14%)
Urogenital burning/pain/discomfort	15 (17%)	4 (14%)
Behavioral disorders (agitation, disorientation)	9 (10%)	2 (7%)

[1] For 2009, the prevalence of cardiovascular symptoms was estimated from n = 72 declaration forms (data not available for 15 patients). Data source: Bureau de Veille Sanitaire, Public Health Directorate of French Polynesia, and Institut Louis Malardé.

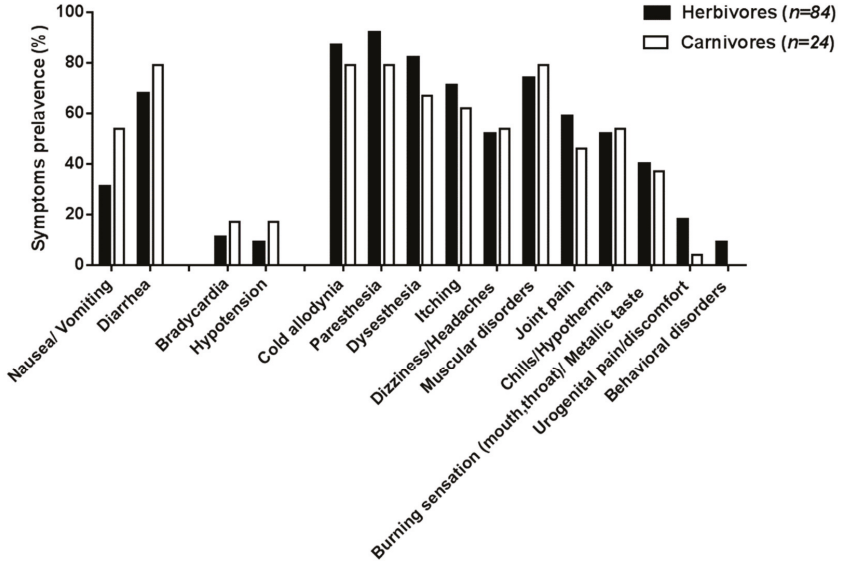

Figure 2. Prevalence (in percentage) of the major clinical symptoms reported in patients following the ingestion of herbivorous vs. carnivorous toxic fish during the 2009–2010 poisoning outbreak in Rapa Island. The prevalence of cardiovascular symptoms was calculated from n = 74 and n = 19 declaration forms for herbivores and carnivores, respectively.

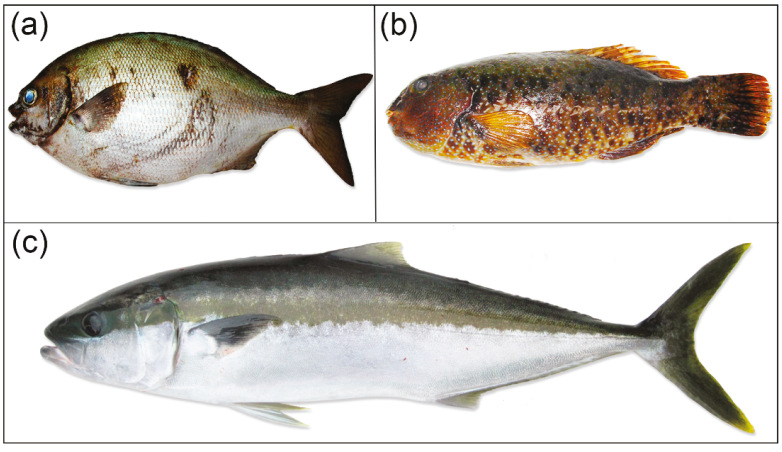

Figure 3. Photographs of three of the fish species regarded as major contributors to the mass-poisoning outbreak reported in Rapa Island: (**a**) *Kyphosus cinerascens* (highfin chub—karamami, herbivore); (**b**) *Leptoscarus vaigiensis* (seagrass parrotfish—komokomo, herbivore); (**c**) *Seriola lalandi* (king fish—ma'aki, carnivore). (photo credit: © Institut Louis Malardé).

Likewise, altogether, the *rāhui* zone and Akatamiro Bay, which were implicated in 82% of poisoning events in 2009, were mentioned in 41 and 28% of declaration forms in 2012 and 2013, respectively. Conversely, 35 and 44% of the implicated fishing sites in 2012 and 2013, respectively, corresponded to new fishing areas located in the north (e.g., Turoa Pari Ati Bay), south (e.g., Motu Tauturau, Akaomua Bay, Kaongi offshore shoals), or west (e.g., Iripau Bay, Ana Rua Bay, Vavai Cliffs) of Rapa Island (Figure 1 and Table 1). In 2017, no declaration form was received at all, while in 2018, 50% of the implicated fishing sites corresponded to locations other than the *rāhui* zone and Akatamiro Bay (Table 1).

2.2. Abundance, Distribution, and Toxicity of Gambierdiscus Populations

Overall, 50 macroalgal samples were collected in 29 distinct locations and analyzed for the presence of ciguatera-causing organisms. *Gambierdiscus* populations were present in four of the sampling sites (Figure 1 and Table 3), i.e., Motu Tarakoi, Akatamiro Bay, Cape Komire, and Iripau Bay.

Table 3. *Gambierdiscus* spp. and *Ostreopsis* spp. cell abundance in benthic assemblages found on various macroalgal host species. The ciguatoxins (CTX)-like activity data for *Gambierdiscus* wild samples as assessed by the radioactive receptor binding assay (rRBA) are also presented.

Genus	*Gambierdiscus* spp.			*Ostreopsis* spp.	
Sampling Sites	**Macroalgal Host Species**	**Abundance (Cells)**	**CTX-Like Activity [2]**	**Macroalgal Host Species**	**Abundance (Cells)**
Turoa Pari Ati Bay				*Lobophora variegata*	6.1×10^6
Akatamiro Bay	*Lobophora variegata*	2250	13.5	*Lobophora variegata*	5.4×10^6
Motu Aturapa				*Dictyota bartayresiana*	13×10^6
Cape Komire	*Dictyota dichotoma*	10,300	0.5		
Cape Ongoriki				*Sargassum* sp.	15.7×10^6
Piriauta Bay [1]				*Sargassum* sp.	19×10^6
Motu Tarakoi [1]	*Lobophora variegata*	5000	1.6 *	*Sargassum* sp.	3.4×10^6
Motu Rapa Iti [1]				*Lobophora variegata*	15.8×10^6
Anatakuri Bay [1]				*Lobophora variegata*	2.2×10^6
Motu Karapoo Nui				*Lobophora variegata*	1.7×10^6
Iripau Bay	*Lobophora variegata*	10,350	3.5		

[1] *Rāhui* zone. [2] Composite CTX-like activity expressed in pg CTX3C eq $cell^{-1}$ (n = 1). * Wild sample collected in January 2010 during the peak of the outbreak.

Cell yields in *Gambierdiscus* wild samples ranged from 2250 cells (Akatamiro Bay) to 10,350 cells (Iripau Bay). *Gambierdiscus* species are not easily distinguishable by light microscopy and, unfortunately, quantitative PCR assays useful to discriminate between species of this dinoflagellate were not yet available at the time of this study. Thus, it was not possible to document the diversity and relative abundance of the different *Gambierdiscus* species present in these wild samples. *Gambierdiscus* preferred macroalgal host was *Lobophora variegata* (*kautake* in native language) (Table 3). The other dominant Fucophycea observed in Rapa waters was *Sargassum* sp. (Figure 4a,b). Interestingly, these two macroalgae were also colonized by dense populations of *Ostreopsis* spp., most notably in three sites within the *rāhui* zone where an abundance of up to 19×10^6 (Piriauta Bay), 15.8×10^6 (Motu Rapa Iti, Figure 4c), and 15.7×10^6 cells (Cape Ongoriki) were recorded. It should be noted that an additional *Ostreopsis* spp. bloom (13×10^6 cells) was also sampled from the species *Dictyota bartayresiana* (Fucophycea) collected near Motu Aturapa (Table 3).

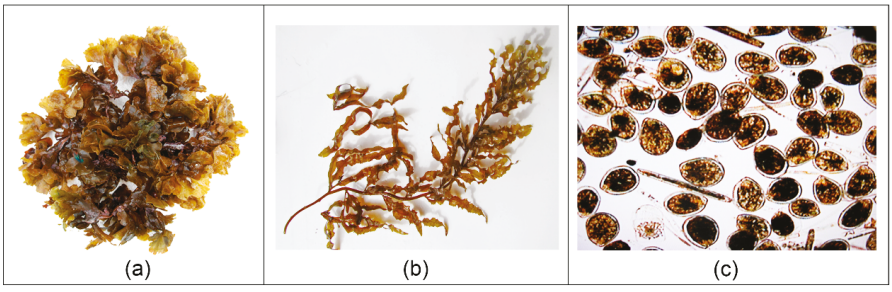

Figure 4. Photographs of the two dominant macroalgal hosts present in Rapa waters and wild sample of benthic microalgal species found on these substrates: (**a**) *Lobophora variegata* (Fucophyceae); (**b**) *Sargassum* sp. (Fucophyceae); (**c**) benthic assemblage composed almost exclusively of *Ostreopsis* spp cells collected from Motu Rapa Iti (photo credit: © Institut Louis Malardé).

Toxicity analyses conducted by the radioactive receptor binding assay (rRBA) confirmed a composite CTX-like activity in extracts of *Gambierdiscus* wild samples, ranging from 0.5 to 13.5 pg CTX3C eq $cell^{-1}$ (Table 3). Of note, the sample collected from Motu Tarakoi at the peak of the poisoning outbreak (i.e., in January 2010) displayed a CTX-like activity of 1.6 pg CTX3C eq $cell^{-1}$.

2.3. rRBA, CBA-N2a and LC-MS/MS Toxicity Data in Fish

A total of 251 fish specimens representing different feeding types (i.e., herbivores, carnivores, and to a lesser extent omnivores) were spear-fished and tested individually using the rRBA in the frame of a large-scale toxicity survey conducted in the same study sites as those screened for the presence of *Gambierdiscus* assemblages. Species commonly consumed in Rapa were primarily targeted, including surgeonfish, parrotfish, chubs, goatfish, groupers, and jacks (Table S1). The rRBA data allowed confirmation of a CTX-like activity in 78% of fish (Table S1), with a similar contamination rate in herbivores (85%, n = 159) vs. carnivores (78%, n = 89) (Table S1), and no significant differences between the rRBA values monitored in herbivores vs. carnivores (p value = 0.8109). Concerning specifically *L. vaigiensis* and *K. cinerascens*, the two herbivore fish species primarily involved in the 2009 outbreak (Table 1), rRBA data showed 92 and 79% of samples, respectively, tested rRBA positive, with maximum CTX-like activity of 12.4 and 4.1 µg CTX3C eq kg^{-1}, respectively (Table S1). It should be noted that a majority of the tested fish harbored exceptionally high levels of CTX-like compounds, which are well above the concentration that causes ciguatera in humans in the Pacific, i.e., 0.1 ppb or 0.1 µg CTX1B eq kg^{-1} [15]. For example, the highest CTX-like activity found in the herbivore *L. vaigiensis* #237 and the carnivore *G. plessisi* #156 were 12.4 µg CTX3C eq kg^{-1} (or 5.2 µg CTX1B eq kg^{-1}) and 14.5 µg CTX3C eq kg^{-1} (or 6.1 µg CTX1B eq kg^{-1}), respectively (Table S1). No correlation was found between the size/weight of fish and rRBA values (linear correlation test, p values > 0.05). Interestingly,

several of the study sites within the *rāhui* zone and the northern bays clearly appeared as high-risk locations for ciguatera, with >80% of positive samples. In contrast, the frequency of rRBA CTX positive fish was remarkably low in areas sampled in the south of the island, i.e., Akaomua Bay (7%, n = 15), Makatea Peak (0%, n = 4), and to a lesser extent, Ana Rua Bay (46%, n = 13) (Table S1).

Twelve fish selected among the rRBA negative (x5) and positive (x7) samples were subsequently analyzed using recently optimized protocols of the CBA-N2a [66] and liquid chromatography tandem mass spectrometry (LC-MS/MS) for confirmation of the presence of CTX congeners [67] (Table 4).

Table 4. CTX-like activity estimates (expressed in μg CTX3C eq kg^{-1}) as assessed by rRBA, CBA-N2a, and LC-MS/MS in a selection of 12 fish specimens sampled from Rapa Island. Results were obtained from one (rRBA and LC-MS/MS) and three independent experiments (CBA-N2a). For additional details, see Section 5.5.

Sampling Site	ID #	Scientific Name	Diet	rRBA	CBA-N2a *	LC-MS/MS
Iripau Bay	74	*Ctenochaetus striatus*	H	7.3	0.33 ± 0.05	<LOQ
Akaomua Bay	159	*Kyphosus cinerascens*	H	<LOD	<LOD	<LOQ
Motu Ta'una	143	*Kyphosus cinerascens*	H	1.4	0.52 ± 0.09	<LOQ
Akaomua Bay	161	*Chlorurus microrhinos*	H	<LOD	0.05 ± 0.01	<LOD
Motu Rapa Iti	209	*Chlorurus microrhinos*	H	7.8	0.31 ± 0.03	<LOQ
Akaomua Bay	163	*Leptoscarus vaigiensis*	H	<LOD	<LOD	<LOD
Motu Rapa Iti	214	*Leptoscarus vaigiensis*	H	5.0	4.75 ± 0.25	0.75
Akaomua Bay	167	*Epinephelus fasciatus*	C	<LOD	<LOD	<LOD
Tapuaki Bay	48	*Epinephelus fasciatus*	C	0.8	0.23 ± 0.02	<LOD
Ahurei Bay	229	*Epinephelus merra*	C	1.4	0.11 ± 0.02	<LOQ
Anatakuri Bay	198	*Monotaxis grandoculis*	C	<LOD	0.10 ± 0.01	<LOD
Motu Rapa Iti	211	*Pseudocaranx dentex*	C	1.0	1.18 ± 0.08	<LOQ

H: Herbivore. C: Carnivore. LOD: Limit of detection. LOQ: Limit of quantification. * CBA-N2a data correspond to the sum of the CTX-like activity measured in both LF90/10 and LF100 dry extracts.

For rRBA negative samples, CBA-N2a was able to detect a low CTX-like cytotoxic activity in *C. microrhinos* #161 and *M. grandoculis* #198 (Table 4), whereas a fairly good concordance was found between rRBA and LC-MS/MS results, i.e., all negative samples by rRBA were also identified as negative by LC-MS/MS, except for *Kyphosus cinerascens* #159 in which CTXs <LOQ (limit of quantification) were detected (Table 4).

For rRBA positive samples, data showed the rRBA consistently gave higher estimates than CBA-N2a for five of these samples, except for *L. vaigiensis* #214 and *P. dentex* #211 for which similar CTX-like activity estimates were obtained (Table 4). When N2a cells were exposed to increasing concentrations of LF90/10 dry extracts of *L. vaigiensis* #214 (Figure 5a) and *P. dentex* #211 (Figure 5b), no cytotoxic effects were observed in the absence of ouabain (O) and veratridine (V) (i.e., OV- conditions). Conversely, a sigmoidal dose–response curve with a negative slope was obtained in OV+ conditions for both fish (Figure 5a,b). A similar pattern was observed with the LF100 dry extracts of both fish (Figure S1a,b). This response is typical of the activity of voltage gated sodium channel (VGSC) activators such as CTX3C and CTX1B (Figure S1c,d). Of note, the LF90/10 fraction concentrated 82.5 and 94.6% of the total composite CTX-like activity of *L. vaigiensis* #214 and *P. dentex* #211, respectively.

Analyses by LC-MS/MS also confirmed the presence of CTX compounds in all positive samples, but at levels below the LOQ, except in *L. vaigiensis* #214, for which both the toxin profile and CTX estimate (0.75 μg CTX3C eq kg^{-1}) were provided (Figure 6 and Table S2). Overall, six different CTX congeners could be detected in this highly toxic herbivore, i.e., in decreasing order, 49-*epi*CTX3C or CTX3B (0.24 μg CTX3C eq kg^{-1}), CTX3C (0.2 μg kg^{-1}), 2-hydroxyCTX3C (0.17 μg CTX3C eq kg^{-1}), and a mix of 52-*epi*-54-deoxyCTX1B (or CTX2), and possibly 54-deoxyCTX1B (or CTX3) and a CTX3C isomer (4) not yet characterized at levels below the LOQ (i.e., 0.15 μg CTX3C eq kg^{-1} of fish tissue, (see Section 5.5.3) (Figure 6c). Moreover, there are some indications that the CTX-like compounds present <LOQ in other positive samples, including *P. dentex* #211, actually correspond to two additional unidentified CTX3C isomers (1) and (3) (Figure 6d). It should be noted that the three CTX3C isomers

(1), (3), and (4) detected in Rapa fish are also currently found in the culture extracts of a highly toxic strain of *G. polynesiensis* (Figure 6b).

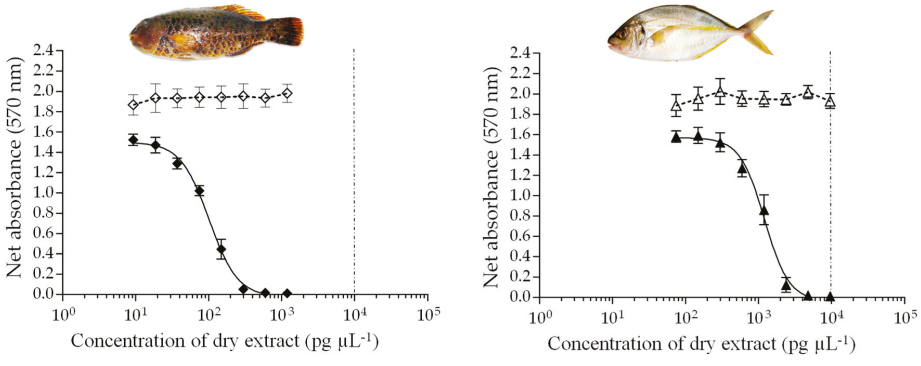

Figure 5. Composite cytotoxicity dose-response curves of N2a cells in OV- (open symbols) and OV+ (solid symbols) conditions when exposed to increasing concentrations of LF90/10 extracts of (**a**) *Leptoscarus vaigiensis* #214 and (**b**) *Pseudocaranx dentex* #211 collected from Rapa Island. Data represent the mean ± SD of three independent experiments, each concentration run in triplicate (n = 9). The dotted vertical line corresponds to the maximum concentration of LF90/10 dry extracts for matrix interference (MCE = 10,000 pg µL^{-1}).

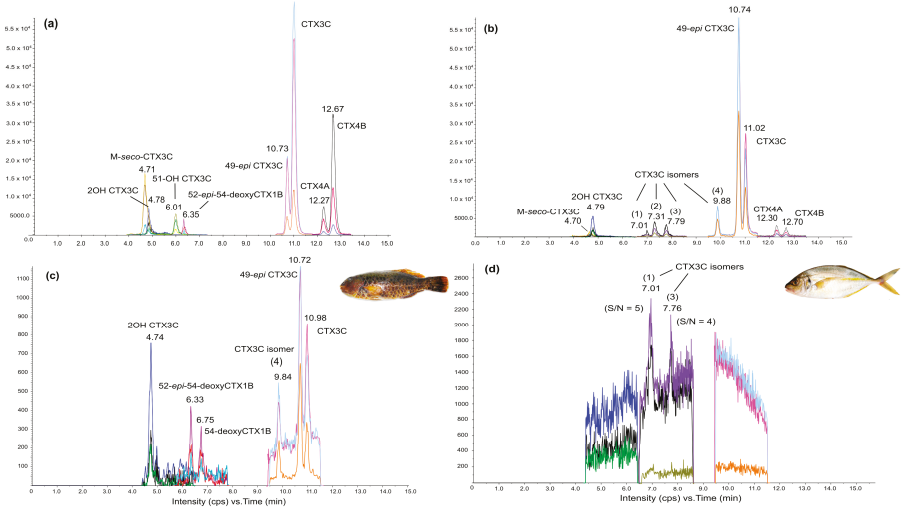

Figure 6. LC-MS/MS chromatograms of (**a**) mix of Pacific ciguatoxins (P-CTXs) standards (Institut Louis Malardé, Papeete, Tahiti, French Polynesia), (**b**) *Gambierdiscus polynesiensis* culture extract (NHA4, Marquesas Island), (**c**) *Leptoscarus vaigiensis* #214 fish extract, and (**d**) *Pseudocaranx dentex* #211 fish extract. The signal-to-noise (S/N) represented on chromatogram (**d**) was calculated with three standard deviations for the m/z transition 1023.6 > 1005.6.

2.4. Temperature Trends in Rapa Island

The trends observed in the average annual minimum (Tmin), maximum (Tmax), and mean (Tmean) values of atmospheric temperature values recorded at the Rapa synoptic weather station between 1960 and 2016, were analyzed by means of the Mann–Kendall test. Results showed a significant increase of +0.86 °C in the average annual temperature values over the 57-years time period (Table 5 and Figure 7).

Table 5. Results of the non-parametric Mann–Kendall test when applied to the average annual minimum (Tmin), maximum (Tmax), mean (Tm) values of atmospheric temperature, and sea surface temperature (SST) datasets available for Rapa between 1960 and 2016. This test was used to detect monotonic trends in the data series. The H0 hypothesis states that temperature data come from a population with independent measures and are identically distributed, whereas the HA hypothesis states temperature data follow a monotonic trend.

Temperature Data Series	Kendall's Tau	2-Sided *p* Value	Alpha	Conclusion
Tmax	0.202 (2.14)	3.2×10^{-2}	0.05	HA
Tmin	0.473 (5.07)	3.58×10^{-7}	0.05	HA
Tmean	0.347 (3.71)	2.1×10^{-4}	0.05	HA
SST (ERSSTv5)	0.067 (0.71)	0.48	0.05	H0

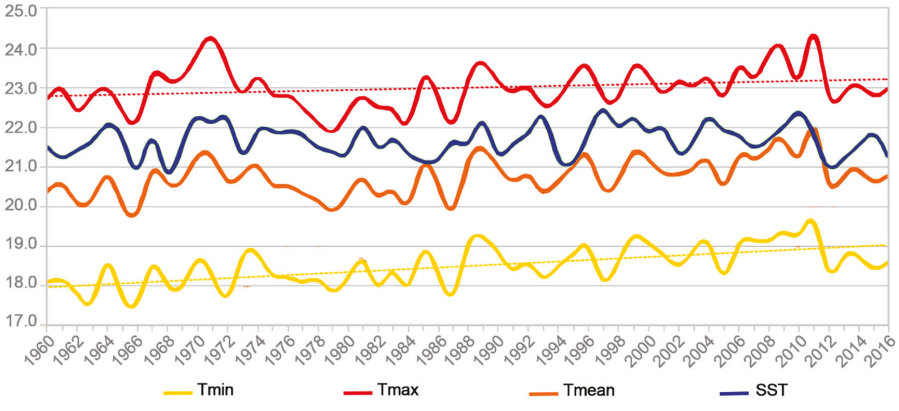

Figure 7. Average annual sea surface (SST) and atmospheric i.e., minimum (Tmin), maximum (Tmax), and mean (Tmean) temperatures recorded in Rapa area between 1960 and 2016. Yellow and red dotted lines represent the trend curves observed for Tmin (f(x) = 0.0188x + 17.9646) and Tmax (f(x) = 0.0085x + 22.7549), respectively.

Of note, this increase was due more to a warming of annual minimum temperatures (+1.07 °C) than to the one of maximum temperatures (+0.48 °C) (Figure 7). Contrastingly, the positive trend (+0.48 °C) noted in the sea surface temperatures (SST) obtained from the Extended Reconstructed Sea Surface Temperature (ERSST)v5 database was not considered significant. Likewise, no significant increase was observed in the SST data provided by the Group for High Resolution Sea Surface Temperature (GHRSST) Level 4 MW_OI (data not shown).

Next, given the limited spatial resolution of ERSSTv5 (too sparse data for the Rapa area), we chose another approach by examining the potential correlations between the mean annual GHRSST, ERSSTv5, and atmospheric temperatures in Rapa. Results of the Pearson correlation test show a strong positive correlation between the GHRSST high resolution SST data and Tmin, Tmax, and Tmean for the 1998–2016 time period, both on a monthly and annual time scale (correlation coefficients $r > 0.8$, on average) (Table 6). In contrast, no significant correlation was found between the GHRSST and

ERSSTv5 data, whatever the study period, i.e., 1998-2016 (r = 0.25) or 1960–2016 (data not shown) (Table 6).

Table 6. Pearson correlation coefficient values (r, CI = 0.95) between Group for High Resolution Sea Surface Temperature (GHRSST) Level 4 MW_OI and Extended Reconstructed Sea Surface Temperature (ERSST)v5 sea surface temperature data series, and the Tmax, Tmin, and Tmean of atmospheric temperatures data series obtained from the Rapa synoptic weather station between 1998 and 2016.

Time Period (Scale)	GHRSST/ERSST	GHRSST/Tmax	GHRSST/Tmin	GHRSST/Tmean
1998–2016 (month)	0.91	0.95	0.92	0.94
1998–2016 (year)	0.25	0.86	0.78	0.87

3. Discussion

The present study describes the integrated approach used to investigate the etiology of an unprecedented mass-poisoning event that occurred in Rapa Island (Australes, French Polynesia) between 2009 and 2010. This approach, which combined epidemiological, environmental, and toxicological investigations, confirms this toxic outbreak as a ciguatera event and is consistent with a range expansion in the spatial distribution of both *Gambierdiscus* spp. and ciguatoxic fish to temperate-like locales of French Polynesia.

The first evidence provided is the symptomatology of the illness described in patients' declaration forms during the peak of the outbreak. Clinically, CP is characterized by a complex combination of non-specific manifestations, with up to 175 different symptoms recorded in both the acute and chronic phases of the illness, including gastrointestinal, cardiovascular, and neurological disturbances appearing in a non-pyretic and non-allergic context [68]. In the absence of a refined, universal case definition of this illness, defining ciguatera in terms of a small, reliable group of symptoms remains difficult. However, some clues should be regarded as strong indicators of CP, especially if two or more consumers of fish at the same meal experience symptoms. Highly evocative of CP are neurological pruritus and complainants of cold allodynia, an intense and painful tingling, burning, or electric sensation in response to cold stimuli [69], which is considered characteristic of CP [17,19,70–72]. In the present study, almost all patients during 2009 experienced cold allodynia. The predominance of neurological symptoms over other symptoms among Rapa patients (>80% on average) is also another characteristic feature of CP illness in French Polynesia [17] and more broadly in the Pacific [19] (for a review and references therein).

Classically, ciguatera-related fatalities are rare (<0.1% of reported cases) [15,73]. In this regard, the mass-poisoning event in Rapa that resulted in two fatalities in 2009 stands out by its unusual magnitude and severity. Chan 2016 [74] has identified several contributory factors to ciguatera-related deaths, including the consumption of large portions of fish parts rich in CTXs such as viscera and head. Here, approximately half of the victims declared they had consumed the viscera and head of the fish. Yet, the limited medical resources available at the Rapa infirmary, both in terms of drug supply and supportive care capacity, may have also contributed to this high fatality rate. Finally, the potential co-exposure of Rapa Island residents to other toxin suites cannot be completely ruled out and may explain the unusual severity of the toxic incident reported in Rapa. Indeed, massive blooms of *Ostreopsis* spp were consistently observed in numerous fishing locations within the *rāhui* zone (e.g., Motu Rapa Iti, Piriauta Bay), which was incriminated in ≈50% of the reported events in 2009. *Ostreopsis* proliferation has become highly problematic in several temperate and subtropical areas due to the formation of intense blooms associated with the production of palytoxin (PLTX) and related analogs (ovatoxins, ostreocins, etc.) that have deleterious impacts on human health [54] (for review and references therein). Three distinct species, *O. lenticularis*, *O.* cf. *ovata*, and *O. siamensis*, were tentatively identified in wild samples of Rapa on the basis of their morphological characteristics [75]. These findings are consistent with previous and recent observations that these potentially toxic species frequently co-occur with *Gambierdiscus* spp. in benthic assemblages of ciguateric biotopes in French Polynesia [76–79].

Interestingly, further CBA-N2a screening of the major *Ostreopsis* spp. bloom sampled from Piriauta Bay suggested the presence of trace amounts of PLTX in this wild sample [75]. In tropical areas, PLTX-like compounds may accumulate and contaminate fish and marine invertebrates, and their ingestion by humans can have dramatic health impacts, in addition to the well-known risk of CP [80–82]. In Japan, Taniyama et al. (2003) [83] provided evidence that *Ostreopsis* spp. was the likely origin of PLTX bioaccumulated in the parrotfish *Scarus ovifrans* through food chain. Thus, the unusual severity of the CP toxic episode in Rapa raises the question of the potential contribution of *Ostreopsis* spp. and PLTX in the observed fatalities. Of note, LC-MS/MS analyses performed on the twelve fish specimens selected in this study failed to confirm the presence of PLTX and its derivatives in samples (data not shown).

The environmental investigations conducted in various locations around the island also confirmed the presence of *Gambierdiscus* spp. in several benthic assemblages, although these latter were often dominated by *Ostreopsis* spp. (*Ostreopsis* spp. cells were 1000-fold more abundant on average than *Gambierdiscus* spp.). Antagonist relationships between *Gambierdiscus* spp. and co-occurring *Ostreopsis* spp. have been documented in a number of field surveys [6] (for review and references therein). In vitro studies also showed that extracts of *Ostreopsis* sp. were able to suppress *Gambierdiscus* growth and adherence capacity [84,85] and that these allelopathic effects may be under the control of various environmental factors such as temperature or salinity [85]. It is hypothesized that during the time lapse between the peak of the outbreak in 2009 and samplings conducted in the frame of the present study, *Ostreopsis* spp. filled the ecological niche following *Gambierdiscus* outbreaks, as previously observed in other ciguateric locations of French Polynesia [77].

This low abundance of *Gambierdiscus* populations contrasted with the remarkably high CTX-like activities detected by rRBA in some of these samples, which were in the range of the toxic potency displayed by Pacific strains of *G. polynesiensis* as determined by either CBA-N2a or LC-MS/MS [75,86,87]. Previous field studies have outlined the frequent lack of correlation between sample toxicity and biomass [88,89] suggesting bloom toxicity and hence, the severity of CP incidents, which is primarily driven by the presence of selected, highly toxic species/strains, even if they may not be the numerically dominant ones [7,13,87]. In any case, the current knowledge gap concerning the taxonomic diversity of *Gambierdiscus* species present in Rapa waters warrants further investigations.

A total of 251 fish representative of different trophic levels were screened for their toxicity using a functional test (rRBA). This large-scale survey brought to light the high CTX-like activity measured in numerous herbivorous and carnivorous fish specimens in the Rapa food web: indeed, the highest rRBA values were measured in a herbivore (*L. vaigiensis*) and a carnivore (*G. plessisi*), and exceeded by 500 and 600 times, respectively, the advisory level of 0.01 μg CTX1B eq kg^{-1} recommended by the US Food and Drug Administration (FDA) [90], which is considered by the European Food Safety Authority (EFSA) as the concentration expected not to exert effects in sensitive individuals [91]. Long-term surveys showed there is usually a lag time of several months between the appearance of *Gambierdiscus*, the subsequent transfer of ciguatoxins into the food web, and the first reported CP cases in consumers [58,92]. The transfer of algal CTXs in the food web requires passage through herbivorous fish; therefore, in ciguatera-prone reef ecosystems, shifts in the types of reef fishes involved in CP are generally observed beginning with herbivores and then followed by carnivores years later [10,93,94]. Herein, the detection of significant amounts of ciguatoxins in a variety of fish species, including those from higher trophic levels (groupers, snappers, and jacks) suggests that ciguatera was well established in the island long before this major 2009 outbreak. The proof is, in 2009 declaration forms, an unexpected high number of patients (54%) that declared they had previously experienced one or multiple poisoning episodes, suggesting a significant number of CP cases may have been overlooked or under-reported in Rapa in months or years prior to the 2009 toxic episode. The under-reporting of ciguatera cases is one of the major causes of the underestimation in CP prevalence worldwide [4] (for a review and references therein). In the South Pacific, reported CP cases likely represent only 20% of the actual cases [62]. Based on the number of guests who shared a toxic meal with declarants and

subsequently presented with symptoms, but did not report at the Rapa infirmary, it is believed that the 2009 statistics could be at least doubled.

Toxicity data from this large-scale fish survey also supported the epidemiological findings that *L. vaigiensis* and *K. cinerascens* were indeed major contributors to the mass-poisoning outbreak in Rapa in 2009, as 92% and 71% of these fish were found to be rRBA positive. Interestingly, according to the local fishermen, komokomo (*L. vaigiensis*) and karamami (*K. cinerascens*) are known to feed preferentially on *Lobophora variegata* and *Sargassum* sp., the two dominant brown macroalgal species in Rapa waters, which also appeared as *Gambierdiscus* spp. and/or *Ostreopsis* spp. preferred algal host substrates. Unlike what is observed in other CP endemic areas such as the Indian Ocean, the Caribbean, the eastern Atlantic Ocean, and the western Pacific [95–99], where CP events rarely involve herbivorous species, Scaridae, Acanthuridae, and Kyphosidae are frequently reported in CP cases occurring in French Polynesia and the Cook Islands [10,50,75,100]. By way of example, between 2008 and 2018, herbivorous species consistently ranked among the top five species most frequently involved in CP cases recorded annually in French Polynesia (www.ciguatera.pf [63]). Finally, analysis of the clinical data showed no striking differences in the prevalence of symptoms with regard to the trophic status of implicated fish, although the limited sample size of declaration forms prevents any definite conclusion. It is believed that the severity of CP incidents in a given area may be driven by both the genetic diversity in wild populations of the causative microalgae *Gambierdiscus* and the species-specific CTX profiles in fish, which have been shown to vary regionally [101,102]. Yet, a previous study conducted between 2002 and 2008 in French Polynesia on 3222 CP cases showed no link between the fish feeding type and the severity of CP cases (sum of symptoms) [61].

Twelve fish selected among the rRBA negative and positive fish samples were subsequently analyzed by CBA-N2a and LC-MS/MS for confirmation of the presence of CTXs. Although the limited sample size for CBA-N2a and LC-MS/MS data limits constructive comparison with rRBA results, several interesting findings were highlighted. First, for all five negative samples identified by rRBA, toxicity data were well correlated, with none of these samples containing more than trace amounts of CTX when measured by CBA-N2a ($\leq$0.1 μg CTX3C eq kg^{-1}). All positive samples by rRBA were also found positive by CBA-N2a, although rRBA consistently gave higher estimates than CBA-N2a for five of these samples, which is a result confirming previous observations in fish from the Caribbean [24,103–105]. This well-known tendency for overestimation by the rRBA as compared to the CBA-N2a, which has been consistently observed for samples submitted to identical extraction procedures [103,105], somewhat questions the strikingly high prevalence of toxic fish monitored in Rapa. However, from a risk management perspective, the use of rRBA as a screening tool in the present study proved highly relevant, as it likely contributed to raise immediate awareness among Rapa residents and thus limit the spread of CP. Another observed difference concerns the single fish (i.e., *L. vaigiensis* #211) in which CTXs could be detected in quantifiable amounts by LC-MS/MS, whereas rRBA and CBA-N2a were able to quantify CTX-like toxicity in all seven positive samples. This quantitation divergence between functional and chemical methods has been previously documented in large-scale field surveys conducted in the Kiribati and the Canary Islands [11,36]. It is well established that LC-MS/MS is a methodology with higher detection limits, which, additionally, can quantify only known targeted CTX analogs and may overlook congeners not yet described, while rRBA and CBA-N2a rather reflect a global response indicative of the binding affinity or cytotoxic effects of the suite of CTX compounds present in fish samples [11,36]. Additional factors may also explain these observed differences, such as the use of various extraction techniques for samples analyzed in the present study (see Section 5.4), which may have affected both the extraction efficiency and recovery of CTX compounds. Indeed, Harwood et al. (2017) [106] found that the use of methanol as the extraction solvent gives good extraction efficiency of CTXs but results in high levels of co-extractives, causing severe ion suppression with LC-MS.

The toxin profile in Rapa fish consisted of 49-*epi*CTX3C (or CTX3B), CTX3C, 2-hydroxyCTX3C, one uncharacterized CTX3C isomer, as well as two CTX analogs belonging to the CTX1B type, i.e.,

52-*epi*-54-deoxyCTX1B (or CTX2) and 54-deoxyCTX1B (or CTX3), as formally identified by LC-MS/MS in the highly toxic herbivore *L. vaigiensis* #214. Two potential unidentified CTX3C isomers were also detected at levels below the LOQ in most of the positive samples identified by LC-MS/MS, including in the carnivorous fish species *P. dentex* #211. Previous field surveys have confirmed CTX3B, CTX3C, and unidentified CTX3C isomers are commonly present in food webs and marine environments of ciguateric biotopes in French Polynesia [13,14,107]. By way of example, in Anaho Bay, a long-standing CP hotspot in Nuku Hiva Island (Marquesas archipelago), a complex toxin suite comprised of CTX3B and CTX3C, 51-hydroxyCTX3C, and two congeners of the CTX1B group, i.e., CTX4A (or 52-*epi*-CTX4B) and CTX4B has been characterized in various marine invertebrates responsible for acute poisoning cases [13,14]. In the present study, the bioaccumulation of two additional CTX1B-type congeners (i.e., 52-*epi*-54-deoxyCTX1B and 54-deoxyCTX1B) was evidenced for the first time in Rapa food web, which is a finding consistent with observations in food web components of Pacific coral reef ecosystems [11]. Interestingly, several of these CTX congeners have also been formally identified in cultures of highly toxic strains of *Gambierdiscus* such as *G. polynesiensis* [87], which is a species regarded as the primary source of CTXs in French Polynesia, and the South Pacific area in general [8] (for review and references therein). These observations suggest that *Gambierdiscus* is the actual source of CTXs detected in Rapa fish, at least in herbivores. Since the genetic composition of *Gambierdiscus* populations in toxic areas may contribute in shaping the toxin profile in fish [102,108], further investigations are most needed to clarify the taxonomic diversity of *Gambierdiscus* populations in Rapa and gain insights into the toxin suites involved in local CP cases.

With regard to the climate trend status in the Rapa area, our results showed the average annual Tmin, Tmax, and Tmean values of atmospheric temperatures recorded at Rapa from 1960 to present days are trending upward, which is a strong indication of climate change in the area. However, analysis of the SST data available from both ERSST and GHRSST using the Mann–Kendall method failed to confirm this finding. This can be explained by the low spatial resolution of ERSST data that may have contributed to smooth the climate change signal and the low temporal resolution of GHRSST data. Nevertheless, the strong positive correlation between the average annual values of atmospheric temperature and GHRSST SST data for the 1998–2016 time period suggests these two datasets likely followed similar trends, thus allowing to conclude that the Rapa area is currently affected by global warming. Numerous field observations linking climate change to CP outbreaks in the tropical Pacific can be found in the literature: cyclical weather patterns such as El Niño, associated with unusual warming of Pacific Ocean waters, have resulted in spikes of ciguatera cases in the Republic of Kiribati, Western Samoa, the State of Tuvalu, and the Cook Islands [57], which is consistent with observations by Tester et al. (2010) [25] and Gingold et al. (2014) [59], who found an association between CP incidence and warmer sea surface temperatures in the Caribbean basin. While studying the fluctuations of *Gambierdiscus* populations in a ciguateric site in Tahiti Island (French Polynesia), Chinain et al. (1999) [88] found an increase in both the density and frequency of *Gambierdiscus* blooms following unusually elevated water temperatures, which is concomitant with a severe coral bleaching episode affecting large areas of the study site. As a result, the peak number of CP cases was recorded three months after these peak densities of *Gambierdiscus* [58]. Recently, Zheng et al. (2020) [56] examined the potential link between several indicators relating to SST data and ciguatera occurrences in French Polynesia and the Cook Islands, and they found that SST anomaly is proven to be a strong positive predictor of an increased ciguatera incidence for both countries. A general consensus is that global warming may lead to a substantial shift in both the distribution and abundance of ciguatera dinoflagellates [55,109], provided that species-specific habitat requirements are met [54] (for review and references therein). In addition to temperature as a potential forcing factor of CP, previous studies have also outlined reef disturbances or degradations linked to extreme climatic events (e.g., cyclone activity, heavy rains) or infestations of crown-of-thorns starfish often precede ciguatoxic events [15,23,51]. All these observations substantiate the idea that global warming as a result of climate change is among the likely causes of the observed expansion of ciguatera to Rapa Island.

However, climate may not be the only driver for ciguatera occurrence in Rapa. Local human activities resulting in significant environmental changes may also be tangible contributors to the problem, as is the case in Akatamiro Bay and Iripau Bay. Indeed, these two areas regarded as at high risk of CP (i.e., confirmed presence of *Gambierdiscus* spp. and/or *Ostreopsis* spp. in benthic assemblages, and high prevalence of toxic fish) are also the sites of major anthropogenic pressure: Akatamiro Bay is characterized by highly altered habitats, which is a likely consequence of soil erosion and subsequent runoffs (nutrient-rich inputs) from land masses due to unrestrained goat ranching, and Iripau Bay is used on a daily basis for the community-based cultivation of taro (*Colocasia esculenta*). There are some indications that nutrient levels in ciguateric biotopes correlate well with *Gambierdiscus* abundance [110,111], but this is not a consistent finding [112–114]. Nutrient inputs can also cause a major shift in the distribution and abundance of ciguatera-related dinoflagellates: in several locations of the Northern Great Barrier Reef (Australia) affected by ongoing coastal eutrophication, benthic assemblages in inshore reefs once dominated by *Gambierdiscus* were composed primarily of *Prorocentrum* and *Ostreopsis*, whilst *Gambierdiscus* was still dominant in offshore locations [26].

In parallel to the 2010 field survey, a community outreach program was conducted in Rapa to warn individuals against specific risk-taking behaviors and stress the importance of systematic report of CP incidents. Information about the fish species and fishing areas most at risk of ciguatera were also provided. These outreach interventions appeared to create self-regulating behavior among individuals in the years following the 2010 field campaign, as shown by (i) the noticeable shift in both fish species and fishing areas involved in CP cases; (ii) the significant drop in the prevalence of patients who declared they consumed fish viscera and/or head, and (iii) the lower under-reporting rate of CP incidents perceptible until 2014, which could also be attributed, in part, to a significant change in the population's eating habits evidenced in the 2012–2014 declaration forms (data not shown), i.e., individuals clearly avoided sharing meals of potentially toxic fish with other (multiple) guests to limit poisoning risk. All these adjustments to CP among the local community may have contributed to the five-fold reduction in CP incidence rate between 2009 and 2012. Moreover, IRs recorded in recent years have also returned to a level comparable to 2008. It should be noted that similar results following outreach programs were achieved in Raivavae, which is another CP-prone island in the Australes archipelago [50]. In this island, educating the resident public (e.g., local leaders, fishermen, the general public, school children, etc.) about the origin of the disease and preventive measures proved useful to the community by reducing poisoning cases by two-fold. This was achieved through public meetings, dissemination of guidebooks, flyers, informational posters available in French and native language, and distributed to health centers, schools, and the town hall, as well as educational modules targeted at primary schools. All these observations support the idea that consumers' education is critically important in the management of seafood poisonings [2].

4. Conclusions

The field study conducted in Rapa Island following an unprecedented toxic episode among its resident population allowed confirming that CP is no longer confined to the tropical part of French Polynesia, which is a long-standing endemic area, but should now also be considered to be well established in subtropical zones. The integrated (multi-disciplinary) approach, which combined epidemiological, environmental, and toxicological investigations, proved effective in confirming the presence of toxin-producing *Gambierdiscus* assemblages in Rapa waters. Moreover, CTX bioaccumulation in a locally caught herbivorous fish species identified as a primary contributor to the 2009 poisoning outbreak was confirmed by using three different analytical techniques. Speculation that additional toxins such as those linked to the proliferation of *Ostreopsis* spp. in the Rapa environment might have contributed to the unusual severity and magnitude of this toxic incident warrants more thorough investigations. Finally, this study also underscores the relevance and benefits of education and public outreach interventions, in parallel to field investigations, for an effective management of

ciguatera risk. Expanding this sentinel approach to other ciguatera-prone areas will undoubtedly help break the persistence of this disease among French Polynesian communities.

5. Materials and Methods

5.1. Study Site

Located in the South Pacific Ocean, French Polynesia is composed of five island groups, namely Society, Marquesas, Tuamotu, Gambier, and Australes archipelagoes, spread over a surface as large as Europe (Figure 1a). Rapa Island is located in the Australes archipelago, equidistant between New Zealand and Easter Island (27.595369 S–144.362151 W) and approximately 1240 km (771 miles) south of the main island of Tahiti (Figure 1a). Monthly average maximum and minimum temperatures in Rapa range from 20.4 to 26.4 °C, and from 15.8 to 22.4 °C, respectively, with a precipitation regime of 251.7 cm of water per year on average (median value for 1981–2010) [65].

Based on the 2007 census, Rapa counted 482 inhabitants (www.ISPF.pf [115]) regrouped primarily in the main village of Ahurei (Figure 1b). The population in Rapa relies primarily on agriculture and subsistence fishing, and it is a very close-knit community. Rapa is subject to the custom of *rāhui*, which is a form of fishing taboo for conservation purposes [96,97] that restricts access to specific fishing grounds tenured by the "Conseil des Sages" of Rapa. This customary practice imposes the spatial closure of the main fishing grounds in the island during most of the year, and fish catch is allowed only at specified celebration periods.

Samples analyzed in this study were collected in the frame of a field campaign conducted in December 2010, i.e., approximately one year after the report of the mass-poisoning outbreak. A total of 29 sampling locations distributed around the island were screened for the presence of toxic *Gambierdiscus* assemblages and fish (Figure 1b).

5.2. Biological Samples

5.2.1. Macroalgal Samples

All *Gambierdiscus* wild samples examined in the present study were collected from macroalgal substrates according to the method described in Chinain et al. (2010) [50] since the artificial substrate method (i.e., windows screens) developed by Tester et al. (2014) [116] was not yet available at the time of these field investigations. Briefly, 200 to 400 g of the most abundant and widely distributed macroalgal substrates (e.g., *Lobophora variegata* and *Sargassum* sp.) were collected at water depths between 1 and 5 m and examined for the presence of *Gambierdiscus* cells and other benthic dinoflagellate species often found in association with ciguatera-causing organisms in benthic assemblages of ciguateric biotopes, e.g., *Ostreopsis* spp. and *Prorocentrum* spp [117]. Macroalgal samples were sealed within plastic bags underwater and shaken and kneaded vigorously to dislodge dinoflagellate cells. For each macroalgal sample, the detrital suspension was successively filtered through 125, 40, and 20 µm mesh sieves. Thus, sub-samples (1 mL) of the 40 and 20 µm fractions obtained were preserved in 50 mL of 5% formalin–seawater for cell enumeration. The total cell yields were assessed under light microscopy from n = 2 to 5 counts of 100 µL aliquots. The remaining 40 and 20 µm fractions were centrifuged at 2000× *g* for 20 min, and the resulting cell pellets stored at −20 °C until further extraction.

5.2.2. Fish Samples

The fish species primarily targeted in this study were those deemed edible by the local population and those most frequently involved in poisoning cases based on the ciguatera declaration forms available at the infirmary of Rapa (the only medical structure on the island) and on a questionnaire survey conducted prior to field samplings, respectively. As fish toxicity is likely to vary depending on age, several individuals per species were spear-fished to screen the largest range of size/weight possible: for instance, for *Kyphosus cinerascens*, *Leptoscarus vaigiensis*, and *Chlorurus microrhinos* catches,

sample weights ranged from 235 to 3450 g, from 290 to 1070 g, and from 465 to 2300 g, respectively (Table S1). Each fish was measured and weighed, and its flesh conditioned in the form of fillets stored at −20 °C. Back at the laboratory, pooled fillets obtained from each fish specimen were thawed and homogenized by grinding in a blender (Groupe SEB, Lourdes, France) waste disposal unit and stored at −20 °C until extraction. In addition, for each fish specimen, 50 g of ground flesh tissue were transferred into a ziplock plastic bag, and freeze-dried for 20 h, at −20 °C, 1 mbar, then for 4 h, at −60 °C, 0.01 mbar (Martin Christ, Beta 1-8 LDplus) prior to LC-MS/MS analyses.

5.3. Epidemiological Data

The epidemiological data presented herein were compiled from patients' declaration forms filled out by the medical staff of Rapa infirmary between 2008 and 2019. These data were collected in the frame of the country-wide epidemiological survey on CP cases currently in place in French Polynesia [4] (www.ciguatera.pf [63]). Information is gathered on age, gender, clinical symptoms reported following fish intake, number of previous poisonings, number of affected guests, as well as details of the toxic meal, e.g., fishing area, marine species involved, parts of the fish eaten, etc. (see Supplementary Material Figure S2).

5.4. Toxin Extraction

5.4.1. Micro-Algal Samples

Gambierdiscus sample extracts were prepared following the protocols described in Chinain et al. (2010) [50]. Briefly, each cell pellet was extracted twice in pure methanol (MeOH) and twice in MeOH/H_2O (50/50) under sonication for 30 min. After centrifugation, the resulting supernatants were pooled and dried under vacuum. The crude extract thus obtained was further partitioned between dichloromethane (CH_2Cl_2) and MeOH/H_2O (60/40). The resulting CH_2Cl_2 phase, in which CTXs-like compounds are preferentially recovered, was dried under vacuum. Then, dry extracts of *Gambierdiscus* wild samples corresponding to 2250 to 10,350 cells eq (Table 3) were resuspended in 1 mL of rRBA incubation buffer [118] and stored at +4 °C until tested for their composite binding affinity via the rRBA.

5.4.2. Fish Samples

For rRBA analyses: The extraction protocol used in 2010 followed the one described in Darius et al. (2007) [100], with slight modifications. For each fish sample, a portion of 10 g of flesh was extracted in 14 mL MeOH under sonication for 2 h and left to stand at −20 °C overnight. Then, the resulting crude extract was centrifuged and purified by solid phase extraction (SPE) technique. The supernatant from each tube was adjusted to MeOH/H_2O (70/30) and passed through Sep-Pak C18 cartridges (360 mg; Waters®, Saint-Quentin, France) pre-conditioned with MeOH/H_2O (70/30) before loading extracts. Then, after an initial washing step with MeOH/H_2O (70/30), each column was eluted successively with MeOH/H_2O (90/10) and pure MeOH. The resulting liposoluble fraction likely to contain the majority of CTXs (LF90/10) was further dried under vacuum, resuspended in rRBA incubation buffer at a concentration of 10 g flesh equivalent (eq) mL^{-1}, and stored at +4 °C until tested for its composite binding affinity. Due to the high lipid nature of the flesh of herbivorous fish from Rapa, the precipitation (delipidation) step at −20 °C was repeated followed by a washing step using MeOH/H_2O (80/20) prior to the elution step with MeOH/H_2O (90/10).

For CBA-N2a analyses: Samples intended for CBA-N2a analyses were extracted using an optimized protocol described in Darius et al. (2018) [13]. Briefly, each sample (10 g) was extracted twice in methanol and twice in MeOH/H_2O (50/50), under sonication for 4 h, followed by a liquid/liquid partition between CH_2Cl_2 and MeOH/H_2O (60/40). The CH_2Cl_2 phase was dried under vacuum and defatted by a second solvent partition using cyclohexane and MeOH/H_2O (80/20). Then, the aqueous methanol fraction was evaporated and purified on Sep-Pak C18 cartridges as previously described [13]. Then, the resulting liposoluble fractions likely to contain CTXs (i.e., LF90/10 and LF100) were dried in a

SpeedVac concentrator (ThermoFisherScientific, Waltham, MA, USA) and weighed on a microbalance (model MC 410 S, Sartorius, Göttingen, Germany) at a reading accuracy of 0.1 mg. Finally, each dry extract was resuspended in MeOH at a concentration of 10 mg mL^{-1} and stored at −20 °C until tested for composite cytotoxicity.

For LC-MS/MS analyses: Fish extracts were prepared according to the protocols described in Sibat et al. (2018) [67], with slight modifications. Briefly, for each fish sample, freeze-dried samples corresponding to 50 g (wet weight) of flesh tissue were extracted twice with MeOH/H_2O (90/10) (150 mL). After centrifugation at 3500× *g* for 10 min, the supernatants were pooled and evaporated at 60 °C with a rotary evaporator under reduced pressure. The residue was resuspended in MeOH/H_2O (90/10) (30 mL) and defatted twice with *n*-hexane (60 mL). The aqueous MeOH layer was concentrated to dryness under nitrogen (N2) flux at 40 °C. The resulting crude extract was dissolved in 5 mL of ethyl acetate (EtOAc)/MeOH (85/15 v/v) prior to purification using two successive SPE clean-up steps. After conditioning with 3 mL of EtOAc/MeOH (85/15 v/v), sample extracts (2 mL, equivalent to 20 g of fish flesh wet weight) were loaded onto Bond Elut Florisil® cartridges (500mg, Agilent technologies, Santa Clara, CA, USA). Cartridges were eluted with 2 × 2 mL of the same solvent. The three fractions were combined (6 mL) and evaporated under N2 flux at 40 °C. The resulting residue (E1) was dissolved in MeOH/H_2O (70/30) (2 mL). For the second SPE purification step, Bond Elut LRC C18 cartridges (500 mg, Agilent technologies, Santa Clara, CA, USA) were used. The cartridges were first conditioned with MeOH/H_2O (70/30) (3 mL), prior to the loading of the purified extract. Then, the C18 cartridges were washed with MeOH/H_2O (75/25) (3 mL) and the P-CTXs were eluted with MeOH/H_2O (90/10) (2 × 3 mL). The two eluting fractions were combined and evaporated under N2 flux at 40 °C. The resulting purified extract (E2) was resuspended in 500 µL of pure MeOH prior to LC-MS/MS analysis.

5.5. Toxicological Analyses

5.5.1. Radioactive Receptor Binding Assay (rRBA)

Gambierdiscus and fish samples were initially tested for their CTX binding affinity via the radioactive receptor binding assay (rRBA) performed in a tube format following the method previously described by Darius et al. (2007) [100]. For wild *Gambierdiscus* samples, a full curve was run based on eight concentrations ranging from 2 to 900 and 12 to 4140 cell mL^{-1} for the lowest to highest cell amounts available and tested in one rRBA experiment. For fish samples, four to eight concentrations were tested in duplicate in one rRBA experiment. Radioactivity (counts per minute, cpm) was determined using a Microbeta Trilux 1450 liquid scintillation counter (Perkin Elmer, Courtaboeuf, France). The cpm data were fitted to a sigmoidal dose–response curve based on the four parameters model (4PL) using GraphPad Prism v8.4.3 software (GraphPad, San Diego, CA, USA) allowing the calculation of IC_{50} values (concentrations causing 50% inhibition of [^{3}H]PbTx-3 binding on rat brain synaptosomes) expressed in cells mL^{-1} or flesh equivalent mg mL^{-1} for *Gambierdiscus* and fish samples, respectively. Calibration of the assay was achieved using CTX3C and CTX1B toxin standard solutions sourced from the Institut Louis Malardé (Papeete, French Polynesia). The CTX-like toxicity in *Gambierdiscus* and fish samples was estimated based on the comparison of their IC_{50} values with the one of CTX3C standard (IC_{50} of CTX3C/IC_{50} of sample). The CTX-like toxicity was expressed in pg CTX3C eq $cell^{-1}$ and µg CTX3C eq kg^{-1} of fish flesh for *Gambierdiscus* and fish samples, respectively. The mean IC_{50} values obtained for CTX3C and CTX1B were 0.62 ± 0.16 and 0.26 ± 0.14 ng mL^{-1}, respectively [100]; hence, to obtain rRBA values expressed in µg CTX1B eq kg^{-1}, a conversion factor of x0.42 should be applied. The limit of detection (LOD) and limit of quantification (LOQ) of the assay were established at 0.015 and 0.31 pg CTX3C eq $cell^{-1}$ for *Gambierdiscus* and 0.16 and 0.31 µg CTX3C eq kg^{-1} for fish samples. All fish samples <LOD were identified as negative samples.

5.5.2. Neuroblastoma Cell-Based Assay (CBA-N2a)

Several negative and positive herbivorous and carnivorous fish specimens identified by rRBA were selected among the species primarily involved in CP incidents and/or preferentially consumed by the local population and subsequently analyzed by the neuroblastoma cell-based cytotoxicity assay (CBA-N2a) using the recently optimized protocol detailed in Viallon et al. (2020) [66]. The maximum concentrations of dry extract (MCE) that did not induce unspecific cytotoxic effects in neuroblastoma (N2a) cells were established at 10,000 and 50,000 pg μL^{-1} for F90/10 and LF100 fish extracts, respectively. First, a qualitative screening of both fractions was performed using the MCE in OV- and OV+ conditions, i.e., non-destructive Ouabain (O) and Veratridine (V) treatments between 80/8 and 90/9 µM (final concentrations) [66]. For positive fractions, the first dilution was adjusted, and a serial dilution 1:2 (eight concentrations) was undertaken to obtain a full dose–response curve run in parallel with CTX3C as the toxin standard. Another standard, namely CTX1B, was also run in parallel with the two positive samples showing the highest CTX-like activity (Figure S1c,d). Each positive fraction was tested in three independent experiments, and each concentration was run in triplicate (n = 9). Net absorbance data were fitted to a sigmoidal dose–response curve based on the 4PL model allowing the calculation of half-maximal effective concentration (EC_{50}) values using GraphPad Prism v8.4.3 software. Following the determination of the EC_{50} values of CTX3C standard (EC_{50} of CTX3C, fg μL^{-1}) and of the tested fraction (EC_{50} of dry extract, pg μL^{-1}), the CTX-like toxicity in the fish sample (T) was estimated according to Viallon et al. 2020 [66], using the following equation:

$$(T) = [(EC_{50} \text{ of CTX3C})/(EC_{50} \text{ of dry extract})]*(DEW/FW),$$

in which T (µg CTX3C eq kg^{-1} of fish flesh) is the CTX-like toxicity, and DEW and FW represent the dry extract weight (mg) and the sample fresh weight (g), respectively. Of note, the (T) values for each fish sample indicated in Table 4 corresponded to the CTX-like activity measured in both LF90/10 and LF100 dry extracts. The LOD and LOQ of the assay for the LF90/10 fraction, which concentrates the majority of the cytotoxic activity, were determined at 0.03 ± 0.01 and 0.06 ± 0.02 µg CTX3C eq kg^{-1}, respectively [66].

5.5.3. Liquid Chromatography Tandem Mass Spectrometry (LC-MS/MS)

LC-MS/MS analyses were also performed on the previously selected fish samples in order to provide unequivocal confirmation of the presence of P-CTXs congeners in toxic fish and gain information on their specific toxin profiles. These analyses were conducted using a UHPLC system (UFLC Nexera, SHIMADZU, Kyoto, Japan) coupled to a hybrid triple quadrupole-linear ion-trap API4000 QTRAP mass spectrometer (SCIEX, Redwood City, CA, USA) equipped with a TurboV® electrospray ionization source (ESI). A 1.8 µm C18 Zorbax Eclipse plus column (50*2.1 mm, AGILENT TECHNOLOGIES, Santa Clara, CA, USA) was employed at 40 °C and eluted at 400 µL/min with a linear gradient. Eluent A is water and eluent B is methanol, both eluents containing 2 mM ammonium formiate and 50 mM formic acid. The elution gradient ran from 78 to 88% over 10 min and was held for 4 min before re-equilibration during 5 min.

Mass spectrometry detection was operated in positive Multiple Reaction Monitoring (MRM) mode. The MRM acquisition method was created using the scheduled MRM algorithm. This algorithm optimizes the dwell times and cycle time to provide a better peak detection and improve reproducibility. A detection window of 120 s and a target scan time of 2 s were chosen for the MRM method. The selected *m/z* transitions are repertories in Table S2. The MRM experiments were established by using the following source settings: curtain gas set at 25, ion spray at 5500 V, a turbogas temperature of 300 °C, gas 1 set at 40 and gas 2 set at 60 psi, with an entrance potential of 10 V. The instrument control, data processing, and analysis were conducted using Analyst software 1.6.3 (SCIEX, Redwood City, CA, USA).

A calibration solution of CTX3C (Institut Louis Malardé, Papeete, Tahiti, French Polynesia) was prepared in MeOH with concentration ranging from 10 to 500 ng mL^{-1}. The LOD and LOQ were respectively determined at 0.05 and 0.15 µg CTX3C eq $kg^{-1}$of fish tissue, respectively. To complete chromatogram profile, a mix of Pacific CTX standards (Institut Louis Malardé, Papeete, Tahiti, French Polynesia) was injected in the sequence.

In order to quantify the P-CTX congeners and due to the lack of standards, concentrations were estimated from the P-CTX3C calibration curve assuming equivalent molar response. Thus, the respective CTX concentrations were expressed in µg CTX3C eq kg^{-1} of fish tissue.

5.6. Time-Series Temperature Data

Classically, 50-year temperature datasets are required to assess global warming trends, as at this timescale, low-frequency oscillations in sea surface temperature (SST) such as the Inter decadal Pacific Oscillation (IPO) interfere little with the climate change signal [119]. In the present study, both atmospheric temperature (AMT) and SST data were used to analyze the current climate change state in the Rapa area. The AMT data series for the 1960–2016 time period were obtained from the Météo France synoptic weather station located in Ahurei village in Rapa, and they were used to calculate the daily minimum (Tmin), maximum (Tmax), and mean (Tmean) values of atmospheric temperatures, as well as the average annual Tmin, Tmax, and Tmean values. The mean annual SST values were estimated from global monthly SST data available from the Extended Reconstructed Sea Surface Temperature version 5 (ERSSTv5) database that covers a time period from 1854 to present days. ERSSTv5 combines both data from in situ observations by ships and buoys and a decade of near-surface data from Argo floats [120]. For the present study, we focused on the 1960–2016 time-period using a 2° × 2° grid resolution. As a result of the poor spatial resolution of the ERSSTv5 dataset particularly in the Southern Hemisphere, we also utilized daily SST data obtained from the Group for High Resolution Sea Surface Temperature (GHRSST Level 4 MW_OI) available only from 1998/01/01 to 2017/12/31, but with a spatial resolution of 0.25° × 0.25°, which is best adapted to the scale of Rapa Island. Then, the average monthly and annual temperature data thus obtained were used to assess the potential correlations between GHRSST, ERSSTv5, and Météo France station data series, and qualify the global warming trend in the Rapa area.

5.7. Statistical Analyses

To determine whether rRBA values differed significantly between the herbivorous and carnivorous fish, standard deviations (SD) and 95% confidence interval (CI; p value < 0.05) were first calculated, and a Mann–Whitney test (non-parametric test) was performed using GraphPad Prism v8.4.3. To analyze whether there was a significant correlation between the size/weight of fish and rRBA values, a linear correlation test was performed using RStudio v1.0.153 (RStudio, Inc., Boston, MA, USA).

Climatic trend in Rapa was assessed using the Mann–Kendall test at a 95% confidence interval. Analysis was completed by estimating the linear trend with the least squares method. Given the limited sample size of the GHRSST data set (i.e., time coverage < 50 years), only the correlations between GHRSST, ERSSTv5 and Météo France data series were tested using the Pearson correlation test (CI = 0.95).

Supplementary Materials: The following are available online at http://www.mdpi.com/2072-6651/12/12/759/s1, Table S1: Toxicity data of Rapa fish, according to species and sampling sites, as assessed by rRBA, Table S2: Selected *m/z* transitions and LC-MS/MS instrument parameters used for the scheduled MRM method, Figure S1: Composite toxicity dose-response curves of N2a cells in OV- (open symbols) and OV+ (solid symbols) conditions when exposed to increasing concentrations of LF100 fish extracts and pure Pacific CTXs, Figure S2: Standardized declaration form for Ciguatera and seafood poisoning cases.

Author Contributions: Conceptualization, M.C. and H.T.D.; Methodology, M.C., C.M.i.G., J.V., M.S., V.L. and H.T.D.; Field-data collection: M.C., C.M.i.G., A.U., P.V., and V.L.; Formal analysis, A.U., P.C., T.R., J.V., M.S., and H.T.D.; Data curation, M.C., C.M.i.G., J.V., M.S., V.L. and H.T.D.; Supervision, M.C. and H.T.D.; Funding acquisition, M.C.; Project administration, M.C.; Writing—original draft, M.C., C.M.i.G., M.S., V.L. and H.T.D.;

Writing—review & editing, M.C., C.M.i.G., A.U., P.C., T.R., J.V., M.S., P.V., V.L., P.H. and H.T.D. All authors have read and agreed to the published version of the manuscript.

Funding: This research was funded by the countries of France and French Polynesia in the frame of the research program "Contrat de Projet RAPA", Convention No. 12 838/MSS/DS/DAF of 22 November 2011.

Acknowledgments: The authors wish to thank Mote Tchou Fouc for his help during field sampling, Amandine Caillaud for her contribution in the design of this study, and Sébastien Longo for performing the statistical analyses on RBA data. They are most indebted to Eric Berthon, Administrateur d'Etat des Australes from 2009 to 2011, the crews of the French Navy patrol boat La Tapageuse and the cargo ship Tahiti Nui 1, as well as the population of Rapa Island for their invaluable help during the 2010 field campaign. The authors are also grateful to the two anonymous reviewers whose comments greatly helped improve the manuscript.

Conflicts of Interest: The authors declare no conflict of interest. The funders had no role in the design of the study; in the collection, analyses, or interpretation of data; in the writing of the manuscript; or in the decision to publish the results.

References

1. Van Dolah, F.M. Marine algal toxins: Origins, health effects, and their increased occurrence. *Environ. Health Perspect.* **2000**, *108* (Suppl. 1), 133–141. [CrossRef] [PubMed]
2. Toda, M.; Uneyama, C.; Toyofuku, H.; Morikawa, K. Trends of food poisonings caused by natural toxins in Japan. *J. Food Hyg. Soc. Jpn.* **2012**, *53*, 105–120. [CrossRef] [PubMed]
3. Ansdell, V. Seafood Poisoning. In *Travel Medicine*, 4th ed.; Keystone, J.S., Kozarsky, P.E., Connor, B.A., Nothdurft, H.D., Mendelson, M., Leder, K., Eds.; Elsevier: London, UK, 2019; pp. 449–456. [CrossRef]
4. Chinain, M.; Gatti, C.M.I.; Darius, H.T.; Quod, J.P.; Tester, P.A. Ciguatera poisonings: A global review of occurrences and trends. *Harmful Algae* **2020**, 101873. [CrossRef]
5. Daneshian, M.; Botana, L.M.; Dechraoui Bottein, M.-Y.; Buckland, G.; Campàs, M.; Dennison, N.; Dickey, R.W.; Diogène, J.; Fessard, V.; Hartung, T.; et al. A roadmap for hazard monitoring and risk assessment of marine biotoxins on the basis of chemical and biological test systems. *Altern. Anim. Exp. ALTEX* **2013**, *30*, 487–545. [CrossRef]
6. Parsons, M.L.; Aligizaki, K.; Dechraoui Bottein, M.-Y.; Fraga, S.; Morton, S.L.; Penna, A.; Rhodes, L. *Gambierdiscus* and *Ostreopsis*: Reassessment of the state of knowledge of their taxonomy, geography, ecophysiology, and toxicology. *Harmful Algae* **2012**, *14*, 107–129. [CrossRef]
7. Litaker, R.W.; Holland, W.C.; Hardison, D.R.; Pisapia, F.; Hess, P.; Kibler, S.R.; Tester, P.A. Ciguatoxicity of *Gambierdiscus* and *Fukuyoa* species from the Caribbean and Gulf of Mexico. *PLoS ONE* **2017**, *12*, e0185776. [CrossRef]
8. Chinain, M.; Gatti, C.M.; Roué, M.; Darius, H.T. Ciguatera-causing dinoflagellates in the genera *Gambierdiscus* and *Fukuyoa*: Distribution, ecophysiology and toxicology. In *Dinoflagellates: Morphology, Life History and Ecological Significance*; Subba Rao, D.V., Ed.; The Nova Science Publishers, Inc.: New York, NY, USA, 2020; pp. 405–457.
9. Earle, K.V. Pathological effects of two West Indian echinoderms. *Trans. R. Soc. Trop. Med. Hyg.* **1940**, *33*, 447–452. [CrossRef]
10. Rongo, T.; van Woesik, R. Ciguatera poisoning in Rarotonga, Southern Cook Islands. *Harmful Algae* **2011**, *10*, 345–355. [CrossRef]
11. Mak, Y.L.; Wai, T.-C.; Murphy, M.B.; Chan, W.H.; Wu, J.J.; Lam, J.C.W.; Chan, L.L.; Lam, P.K.S. Pacific ciguatoxins in food web components of coral reef systems in the Republic of Kiribati. *Environ. Sci. Technol.* **2013**, *47*, 14070–14079. [CrossRef]
12. Roué, M.; Darius, H.T.; Picot, S.; Ung, A.; Viallon, J.; Gaertner-Mazouni, N.; Sibat, M.; Amzil, Z.; Chinain, M. Evidence of the bioaccumulation of ciguatoxins in giant clams (*Tridacna maxima*) exposed to *Gambierdiscus* spp. cells. *Harmful Algae* **2016**, *57*, 78–87. [CrossRef]
13. Darius, H.T.; Roué, M.; Sibat, M.; Viallon, J.; Gatti, C.M.; Vandersea, M.W.; Tester, P.A.; Litaker, R.W.; Amzil, Z.; Hess, P.; et al. *Tectus niloticus* (Tegulidae, Gastropod) as a novel vector of Ciguatera Poisoning: Detection of Pacific ciguatoxins in toxic samples from Nuku Hiva Island (French Polynesia). *Toxins* **2018**, *10*, 2. [CrossRef] [PubMed]

14. Darius, H.T.; Roué, M.; Sibat, M.; Viallon, J.; Gatti, C.M.i.; Vandersea, M.W.; Tester, P.A.; Litaker, R.W.; Amzil, Z.; Hess, P.; et al. Toxicological investigations on the sea urchin *Tripneustes gratilla* (Toxopneustidae, Echinoid) from Anaho Bay (Nuku Hiva, French Polynesia): Evidence for the presence of Pacific ciguatoxins. *Mar. Drugs* **2018**, *16*, 122. [CrossRef] [PubMed]
15. Lehane, L.; Lewis, R.J. Ciguatera: Recent advances but the risk remains. *Int. J. Food Microbiol.* **2000**, *61*, 91–125. [CrossRef]
16. Ikehara, T.; Kuniyoshi, K.; Oshiro, N.; Yasumoto, T. Biooxidation of ciguatoxins leads to species-specific toxin profiles. *Toxins* **2017**, *9*, 205. [CrossRef]
17. Chateau-Degat, M.L.; Dewailly, E.; Cerf, N.; Nguyen, N.L.; Huin-Blondey, M.O.; Hubert, B.; Laudon, F.; Chansin, R. Temporal trends and epidemiological aspects of ciguatera in French Polynesia: A 10-year analysis. *Trop. Med. Int. Health* **2007**, *12*, 485–492. [CrossRef]
18. Stempf, E. *Incidence des Formes Chroniques de la Ciguatera au Sein de la Population Réunionnaise de 2000 à 2014*; Université de Bordeaux Segalen: Bordeaux, France, 2015; p. 58.
19. Friedman, M.A.; Fernandez, M.; Backer, L.C.; Dickey, R.W.; Bernstein, J.; Schrank, K.; Kibler, S.; Stephan, W.; Gribble, M.O.; Bienfang, P.; et al. An updated review of Ciguatera Fish Poisoning: Clinical, epidemiological, environmental, and public health management. *Mar. Drugs* **2017**, *15*, 72. [CrossRef]
20. Gatti, C.M.; Lonati, D.; Darius, H.T.; Zancan, A.; Roué, M.; Schicchi, A.; Locatelli, C.A.; Chinain, M. *Tectus niloticus* (Tegulidae, Gastropod) as a novel vector of Ciguatera Poisoning: Clinical characterization and follow-up of a mass poisoning event in Nuku Hiva Island (French Polynesia). *Toxins* **2018**, *10*, 102. [CrossRef]
21. Bienfang, P.; Oben, B.; DeFelice, S.; Moeller, P.; Huncik, K.; Oben, P.; Toonen, R.; Daly-Engel, T.; Bowen, B. Ciguatera: The detection of neurotoxins in carnivorous reef fish from the coast of Cameroon, West Africa. *Afr. J. Mar. Sci.* **2008**, *30*, 533–540. [CrossRef]
22. Rongo, T.; van Woesik, R. Socioeconomic consequences of ciguatera poisoning in Rarotonga, Southern Cook Islands. *Harmful Algae* **2012**, *20*, 92–100. [CrossRef]
23. Morin, E.; Gatti, C.; Bambridge, T.; Chinain, M. Ciguatera fish poisoning: Incidence, health costs and risk perception on Moorea Island (Society Archipelago, French Polynesia). *Harmful Algae* **2016**, *60*, 1–10. [CrossRef]
24. Hardison, D.R.; Holland, W.C.; Darius, H.T.; Chinain, M.; Tester, P.A.; Shea, D.; Bogdanoff, A.K.; Morris, J.A., Jr.; Flores Quintana, H.A.; Loeffler, C.R.; et al. Investigation of ciguatoxins in invasive lionfish from the greater Caribbean region: Implications for fishery development. *PLoS ONE* **2018**, *13*, e0198358. [CrossRef] [PubMed]
25. Tester, P.A.; Feldman, R.L.; Nau, A.W.; Kibler, S.R.; Litaker, W.R. Ciguatera fish poisoning and sea surface temperatures in the Caribbean Sea and the West Indies. *Toxicon* **2010**, *56*, 698–710. [CrossRef]
26. Skinner, M.P.; Lewis, R.J.; Morton, S. Ecology of the ciguatera causing dinoflagellates from the Northern Great Barrier Reef: Changes in community distribution and coastal eutrophication. *Mar. Pollut. Bull.* **2013**, *77*, 210–219. [CrossRef] [PubMed]
27. Perez-Arellano, J.L.; Luzardo, O.P.; Perez Brito, A.; Hernandez Cabrera, M.; Zumbado, M.; Carranza, C.; Angel-Moreno, A.; Dickey, R.W.; Boada, L.D. Ciguatera fish poisoning, Canary Islands. *Emerg. Infect. Dis.* **2005**, *11*, 1981–1982. [CrossRef]
28. Boada, L.D.; Zumbado, M.; Luzardo, O.P.; Almeida-González, M.; Plakas, S.M.; Granade, H.R.; Abraham, A.; Jester, E.L.E.; Dickey, R.W. Ciguatera fish poisoning on the West Africa Coast: An emerging risk in the Canary Islands (Spain). *Toxicon* **2010**, *56*, 1516–1519. [CrossRef]
29. Otero, P.; Pérez, S.; Alfonso, A.; Vale, C.; Rodriguez, P.; Gouveia, N.N.; Gouveia, N.; Delgado, J.; Vale, P.; Hirama, M.; et al. First toxin profile of ciguateric fish in Madeira Arquipelago (Europe). *Anal. Chem.* **2010**, *82*, 6032–6039. [CrossRef] [PubMed]
30. Nuñez, D.; Matute, P.; Garcia, A.; Garcia, P.; Abadía, N. Outbreak of ciguatera food poisoning by consumption of amberjack (*Seriola* spp.) in the Canary Islands, may 2012. *Euro Surveill.* **2012**, *17*, 20188.
31. Caillaud, A.; Eixarch, H.; de la Iglesia, P.; Rodriguez, M.; Dominguez, L.; Andree, K.B.; Diogène, J. Towards the standardisation of the neuroblastoma (neuro-2a) cell-based assay for ciguatoxin-like toxicity detection in fish: Application to fish caught in the Canary Islands. *Food Addit. Contam. Part A* **2012**, *29*, 1000–1010. [CrossRef]
32. Bravo, J.; Suarez, F.C.; Ramirez, A.S.; Acosta, F. Ciguatera, an emerging human poisoning in Europe. *J. Aquac. Mar. Biol.* **2015**, *3*, 00053. [CrossRef]

33. Estevez, P.; Castro, D.; Manuel Leao, J.; Yasumoto, T.; Dickey, R.; Gago-Martinez, A. Implementation of liquid chromatography tandem mass spectrometry for the analysis of ciguatera fish poisoning in contaminated fish samples from Atlantic coasts. *Food Chem.* **2019**, *280*, 8–14. [CrossRef]
34. Estevez, P.; Castro, D.; Pequeño-Valtierra, A.; Leao, J.M.; Vilariño, O.; Diogène, J.; Gago-Martínez, A. An attempt to characterize the ciguatoxin profile in *Seriola fasciata* causing ciguatera fish poisoning in Macaronesia. *Toxins* **2019**, *11*, 221. [CrossRef] [PubMed]
35. Sanchez-Henao, J.A.; García-Álvarez, N.; Fernández, A.; Saavedra, P.; Silva Sergent, F.; Padilla, D.; Acosta-Hernández, B.; Martel Suárez, M.; Diogène, J.; Real, F. Predictive score and probability of CTX-like toxicity in fish samples from the official control of ciguatera in the Canary Islands. *Sci. Total Environ.* **2019**, *673*, 576–584. [CrossRef] [PubMed]
36. Sanchez-Henao, A.; García-Álvarez, N.; Silva Sergent, F.; Estévez, P.; Gago-Martínez, A.; Martín, F.; Ramos-Sosa, M.; Fernández, A.; Diogène, J.; Real, F. Presence of CTXs in moray eels and dusky groupers in the marine environment of the Canary Islands. *Aquat. Toxicol.* **2020**, 105427. [CrossRef] [PubMed]
37. Bentur, Y.; Spanier, E. Ciguatoxin-like substances in edible fish on the Eastern Mediterranean. *Clin. Toxicol.* **2007**, *45*, 695–700. [CrossRef] [PubMed]
38. Villareal, T.A.; Hanson, S.; Qualia, S.; Jester, E.L.E.; Granade, H.R.; Dickey, R.W. Petroleum production platforms as sites for the expansion of ciguatera in the northwestern Gulf of Mexico. *Harmful Algae* **2007**, *6*, 253–259. [CrossRef]
39. Aligizaki, K.; Nikolaidis, G. Morphological identification of two tropical dinoflagellates of the genera *Gambierdiscus* and *Sinophysis* in the Mediterranean Sea. *J. Biol. Res. Thessalon.* **2008**, *9*, 75–82.
40. Fraga, S.; Rodriguez, F.; Caillaud, A.; Diogɛne, J.; Raho, N.; Zapata, M. *Gambierdiscus excentricus* sp. nov. (Dinophyceae), a benthic toxic dinoflagellate from the Canary Islands (NE Atlantic Ocean). *Harmful Algae* **2011**, *11*, 10–22. [CrossRef]
41. Tester, P.A.; Vandersea, M.W.; Buckel, C.A.; Kibler, S.R.; Holland, W.C.; Davenport, E.D.; Clark, R.D.; Edwards, K.F.; Taylor, J.C.; Vander Pluym, J.L.; et al. *Gambierdiscus* (Dinophyceae) species diversity in the Flower Garden Banks National Marine Sanctuary, Northern Gulf of Mexico, USA. *Harmful Algae* **2013**, *29*, 1–9. [CrossRef]
42. Fraga, S.; Rodriguez, F. Genus *Gambierdiscus* in the Canary Islands (NE Atlantic Ocean) with description of *Gambierdiscus silvae* sp. nov., a new potentially toxic epiphytic benthic dinolflagellate. *Protist* **2014**, *165*, 839–853. [CrossRef]
43. Rodríguez, F.; Fraga, S.; Ramilo, I.; Rial, P.; Figueroa, R.I.; Riobó, P.; Bravo, I. Canary Islands (NE Atlantic) as a biodiversity 'hotspot' of *Gambierdiscus*: Implications for future trends of ciguatera in the area. *Harmful Algae* **2017**, *67*, 131–143. [CrossRef]
44. Pisapia, F.; Holland, W.C.; Hardison, D.R.; Litaker, R.W.; Fraga, S.; Nishimura, T.; Adachi, M.; Nguyen-Ngoc, L.; Séchet, V.; Amzil, Z.; et al. Toxicity screening of 13 *Gambierdiscus* strains using neuro-2a and erythrocyte lysis bioassays. *Harmful Algae* **2017**, *63*, 173–183. [CrossRef] [PubMed]
45. Reverté, L.; Toldrà, A.; Andree, K.B.; Fraga, S.; Falco, G.; Campàs, M.; Diogène, J. Assessment of cytotoxicity in ten strains of *Gambierdiscus australes* from Macaronesian Islands by neuro-2a cell-based assays. *J. Appl. Phycol.* **2018**, *30*, 2447–2461. [CrossRef]
46. Rossignoli, A.E.; Tudó, A.; Bravo, I.; Díaz, P.A.; Diogène, J.; Riobó, P. Toxicity characterisation of *Gambierdiscus* species from the Canary Islands. *Toxins* **2020**, *12*, 134. [CrossRef] [PubMed]
47. Tudó, À.; Toldrà, A.; Rey, M.; Todolí, I.; Andree, K.B.; Fernández-Tejedor, M.; Campàs, M.; Sureda, F.X.; Diogène, J. *Gambierdiscus* and *Fukuyoa* as potential indicators of ciguatera risk in the Balearic Islands. *Harmful Algae* **2020**, *99*, 101913. [CrossRef] [PubMed]
48. Tudó, À.; Gaiani, G.; Rey Varela, M.; Tsumuraya, T.; Andree, K.B.; Fernández-Tejedor, M.; Campàs, M.; Diogène, J. Further advance of *Gambierdiscus* species in the Canary Islands, with the first report of *Gambierdiscus belizeanus*. *Toxins* **2020**, *12*, 692. [CrossRef] [PubMed]
49. Ruff, T.A. Ciguatera in the Pacific: A link with military activities. *Lancet* **1989**, *333*, 201–205. [CrossRef]
50. Chinain, M.; Darius, H.T.; Ung, A.; Tchou Fouc, M.; Revel, T.; Cruchet, P.; Pauillac, S.; Laurent, D. Ciguatera risk management in French Polynesia: The case study of Raivavae Island (Australes Archipelago). *Toxicon* **2010**, *56*, 674–690. [CrossRef] [PubMed]
51. Rongo, T.; van Woesik, R. The effects of natural disturbances, reef state, and herbivorous fish densities on ciguatera poisoning in Rarotonga, southern Cook Islands. *Toxicon* **2013**, *64*, 87–95. [CrossRef]

52. Rongo, T.; Bush, M.; Van Woesik, R. Did ciguatera prompt the late Holocene Polynesian voyages of discovery? *J. Biogeogr.* **2009**, *36*, 1423–1432. [CrossRef]
53. Llewellyn, L.E. Revisiting the association between sea surface temperature and the epidemiology of fish poisoning in the South Pacific: Reassessing the link between ciguatera and climate change. *Toxicon* **2010**, *56*, 691–697. [CrossRef]
54. Tester, P.A.; Berdalet, E.; Litaker, R.W. Climate change and benthic harmful microalgae. *Harmful Algae* **2020**, *91*, 101655. [CrossRef] [PubMed]
55. Kibler, S.R.; Tester, P.A.; Kunlec, K.E.; Moored, S.K.; Litaker, W.R. Effects of ocean warming on growth and distribution of dinoflagellates associated with ciguatera fish poisoning in the Caribbean. *Ecol. Model.* **2015**, *316*, 194–210. [CrossRef]
56. Zheng, L.; Gatti, C.M.i.; Garrido Gamarro, E.; Suzuki, A.; Teah, H.Y. Modeling the time-lag effect of sea surface temperatures on ciguatera poisoning in the South Pacific: Implications for surveillance and response. *Toxicon* **2020**, *182*, 21–29. [CrossRef] [PubMed]
57. Hales, S.; Weinstein, P.; Woodward, A. Ciguatera (Fish Poisoning), El Nino, and Pacific sea surface temperatures. *Ecosyst. Health* **1999**, *5*, 20–25. [CrossRef]
58. Chateau-Degat, M.-L.; Chinain, M.; Cerf, N.; Gingras, S.; Hubert, B.; Dewailly, E. Seawater temperature, *Gambierdiscus* spp. variability and incidence of ciguatera poisoning in French Polynesia. *Harmful Algae* **2005**, *4*, 1053–1062. [CrossRef]
59. Gingold, D.B.; Strickland, M.J.; Hess, J.J. Ciguatera fish poisoning and climate change: Analysis of National Poison Center Data in the United States, 2001–2011. *Environ. Health Perspect.* **2014**, *122*, 580–586. [CrossRef]
60. Bagnis, R.; Bennet, J.; Barsinas, M.; Chebret, M.; Jacquet, G.; Lechat, I.; Mitermite, Y.; Perolat, P.H.; Rongeras, S. Epidemiology of ciguatera in French Polynesia from 1960 to 1984. In Proceedings of the Fifth International Coral Reef Congress, Tahiti, French Polynesia, 27 May–1 June 1985; Gabrie, C., Salvat, B., Eds.; Antenne Museum-EPHE: Moorea, French Polynesia, 1985; pp. 475–482.
61. Chateau-Degat, M.-L.; Chinain, M.; Darius, H.T.; Dewailly, E.; Mallet, H.-P. Epidemiological survey of ciguatera in French Polynesia. *Bull. Epidemiol. Hebd.* **2009**, *48/50*, 522–525.
62. Skinner, M.P.; Brewer, T.D.; Johnstone, R.; Fleming, L.E.; Lewis, R.J. Ciguatera fish poisoning in the Pacific Islands (1998 to 2008). *PLoS Negl. Trop. Dis.* **2011**, *5*, e1416. [CrossRef]
63. Available online: https://www.ciguatera.pf (accessed on 27 October 2020).
64. Chinain, M.; Darius, H.T.; Gatti, C.M.; Roué, M. Update on ciguatera research in French Polynesia. *SPC Fish. Newsl.* **2016**, *150*, 42–51.
65. Laurent, V.; Maamaatuaiahutapu, K. *Atlas Climatologique de la Polynésie Française*, 2nd ed.; Météo France: Tahiti, French Polynesia, 2019; 228p.
66. Viallon, J.; Chinain, M.; Darius, H.T. Revisiting the neuroblastoma cell-based assay (CBA-N2a) for the improved detection of marine toxins active on voltage gated sodium channels (VGSCs). *Toxins* **2020**, *12*, 281. [CrossRef]
67. Sibat, M.; Herrenknecht, C.; Darius, H.T.; Roué, M.; Chinain, M.; Hess, P. Detection of Pacific ciguatoxins using liquid chromatography coupled to either low or high resolution mass spectrometry (LC-MS/MS). *J. Chromatogr. A* **2018**, *1571*, 16–28. [CrossRef] [PubMed]
68. Wang, D.Z. Neurotoxins from marine dinoflagellates: A brief review. *Mar. Drugs* **2008**, *6*, 349–371. [CrossRef] [PubMed]
69. Vetter, I.; Touska, F.; Hess, A.; Hinsbey, R.; Sattler, S.; Lampert, A.; Sergejeva, M.; Sharov, A.; Collins, L.S.; Eberhardt, M.; et al. Ciguatoxins activate specific cold pain pathways to elicit burning pain from cooling. *EMBO J.* **2012**, *31*, 3795–3808. [CrossRef] [PubMed]
70. Cameron, J.; Capra, M.F. The basis of the paradoxical disturbance of temperature perception in ciguatera poisoning. *J. Toxicol. Clin. Toxicol.* **1993**, *31*, 571–579. [CrossRef]
71. Pearn, J. Neurology of ciguatera. *J. Neurol. Neurosurg. Psychiatry* **2001**, *70*, 4–8. [CrossRef]
72. Edwards, A.; Zammit, A.; Farrell, H. Four recent ciguatera fish poisoning incidents in New South Wales, Australia linked to imported fish. *Commun. Dis. Intell.* **2019**, *43*, 1–9. [CrossRef]
73. Hamilton, B.; Whittle, N.; Shaw, G.; Eaglesham, G.; Moore, M.R.; Lewis, R.J. Human fatality associated with Pacific ciguatoxin contaminated fish. *Toxicon* **2010**, *56*, 668–673. [CrossRef]
74. Chan, T.Y.K. Characteristic features and contributory factors in fatal ciguatera fish poisoning—Implications for prevention and public education. *Am. J. Trop. Med. Hyg.* **2016**, *94*, 704–709. [CrossRef]

75. Pawlowiez, R.; Darius, H.T.; Cruchet, P.; Rossi, F.; Caillaud, A.; Laurent, D.; Chinain, M. Evaluation of seafood toxicity in the Australes archipelago (French Polynesia) using the neuroblastoma cell-based assay. *Food Addit. Contam. Part A* **2013**, *30*, 567–586. [CrossRef]
76. Fukuyo, Y. Taxonomical study on benthic dinoflagellates collected in coral reefs. *Bull. Jpn. Soc. Sci. Fish.* **1981**, *47*, 967–978. [CrossRef]
77. Bagnis, R.; Bennett, J.; Prieur, C.; Legrand, A.M. The dynamics of three toxic benthic dinoflagellates and the toxicity of ciguateric surgeonfish in French Polynesia. In *Toxic Dinoflagellates*; Anderson, D.M., White, A.N., Baden, D.G., Eds.; Elsevier: New York, NY, USA, 1985; pp. 177–182.
78. Chomérat, N.; Bilien, G.; Derrien, A.; Henry, K.; Ung, A.; Viallon, J.; Darius, H.T.; Gatti, C.; Roué, M.; Hervé, F.; et al. *Ostreopsis lenticularis* Y. Fukuyo (Dinophyceae, Gonyaulacales) from French Polynesia (South Pacific Ocean): A revisit of its morphology, molecular phylogeny and toxicity. *Harmful Algae* **2019**, *84*, 95–111. [CrossRef] [PubMed]
79. Chomérat, N.; Bilien, G.; Couté, A.; Quod, J.-P. Reinvestigation of *Ostreopsis mascarenensis* Quod (Dinophyceae, Gonyaulacales) from Réunion Island (SW Indian Ocean): Molecular phylogeny and emended description. *Phycologia* **2020**, *59*, 1–14. [CrossRef]
80. Alcala, A.C.; Alcala, L.C.; Garth, J.S.; Yasumura, D.; Yasumoto, T. Human fatality due to ingestion of the crab *Demania reynaudii* that contained a palytoxin-like toxin. *Toxicon* **1988**, *26*, 105–107. [CrossRef]
81. Randall, J.E. Review of clupeotoxism, an often fatal illness from the consumption of clupeoid fishes. *Pac. Sci.* **2005**, *59*, 73–77. [CrossRef]
82. Deeds, J.R.; Schwartz, M.D. Human risk associated with palytoxin exposure. *Toxicon* **2010**, *56*, 150–162. [CrossRef]
83. Taniyama, S.; Arakawa, O.; Terada, M.; Nishio, S.; Takatani, T.; Mahmud, Y.; Noguchi, T. *Ostreopsis* sp., a possible origin of palytoxin (PTX) in parrotfish *Scarus ovifrons*. *Toxicon* **2003**, *42*, 29–33. [CrossRef]
84. García-Portela, M.; Riobó, P.; Franco, J.M.; Bañuelos, R.M.; Rodríguez, F. Genetic and toxinological characterization of North Atlantic strains of the dinoflagellate *Ostreopsis* and allelopathic interactions with toxic and non-toxic species from the genera *Prorocentrum*, *Coolia* and *Gambierdiscus*. *Harmful Algae* **2016**, *60*, 57–69. [CrossRef]
85. Sparrow, L.; Momigliano, P.; Russ, G.R.; Heimann, K. Effects of temperature, salinity and composition of the dinoflagellate assemblage on the growth of *Gambierdiscus carpenteri* isolated from the Great Barrier Reef. *Harmful Algae* **2017**, *65*, 52–60. [CrossRef]
86. Rhodes, L.; Harwood, T.; Smith, K.; Argyle, P.; Munday, R. Production of ciguatoxin and maitotoxin by strains of *Gambierdiscus australes*, *G. pacificus* and *G. polynesiensis* (Dinophyceae) isolated from Rarotonga, Cook Islands. *Harmful Algae* **2014**, *39*, 185–190. [CrossRef]
87. Longo, S.; Sibat, M.; Viallon, J.; Darius, H.T.; Hess, P.; Chinain, M. Intraspecific variability in the toxin production and toxin profiles of in vitro cultures of *Gambierdiscus polynesiensis* (Dinophyceae) from French Polynesia. *Toxins* **2019**, *11*, 735. [CrossRef]
88. Chinain, M.; Germain, M.; Deparis, X.; Pauillac, S.; Legrand, A.M. Seasonal abundance and toxicity of the dinoflagellate *Gambierdiscus* spp. (Dinophyceae), the causative agent of ciguatera in Tahiti, French Polynesia. *Mar. Biol.* **1999**, *135*, 259–267. [CrossRef]
89. Litaker, R.W.; Vandersea, M.W.; Faust, M.A.; Kibler, S.R.; Nau, A.W.; Holland, W.C.; Chinain, M.; Holmes, M.J.; Tester, P.A. Global distribution of ciguatera causing dinoflagellates in the genus *Gambierdiscus*. *Toxicon* **2010**, *56*, 711–730. [CrossRef] [PubMed]
90. Food and Drug Administration (FDA). Appendix 5—FDA and EPA Safety Levels in Regulations and Guidance. In *Fish and Fishery Products Hazards and Control Guidance*, 4th ed.; University of Florida: Gainesville, FL, USA, 2020; p. A5-1.
91. European Food Safety Authority (EFSA). Scientific opinion on marine biotoxins in shellfish—Emerging toxins: Ciguatoxin group. *EFSA J.* **2010**, *8*, 1627. [CrossRef]
92. Clausing, R.J.; Chinain, M.; Dechraoui Bottein, M.Y. Practical sampling guidance for determination of ciguatoxin in fish. In *Guide for Designing and Implementing a Plan to Monitor Toxin-Producing Microalgae*, 2nd ed.; Reguera, B., Alonso, R., Moreira, Á., Méndez, S., Dechraoui Bottein, M.-Y., Eds.; IOC Manuals & Guides: Paris, France; Vienna, Austria, 2016; Volume 59, pp. 51–61.

93. Bagnis, R.; Bennet, J.; Barsinas, M.; Drollet, J.H.; Jacquet, G.; Legrand, A.M.; Cruchet, P.H.; Pascal, H. Correlation between ciguateric fish and damage to the reefs in the Gambier Islands (French Poynesia). In Proceedings of the Sixth International Coral Reef Symposium, Townsville, Australia, 8–12 August 1988; Choat, J.H., Barnes, D., Borowitzka, M.A., Coll, J.C., Davies, P.J., Flood, P., Hatcher, B.G., Hopley, D., Hutchings, P.A., Kinsey, G.R., et al., Eds.; 6th International Coral Reef Symposium Executive Committee: Townsville, Australia, 1988; pp. 195–200.
94. Lewis, R.J.; Holmes, M.J. Origin and transfer of toxins involved in ciguatera. *Comp. Biochem. Physiol. C* **1993**, *106*, 615–628. [CrossRef]
95. Pottier, I.; Vernoux, J.P.; Lewis, R.J. Ciguatera Fish Poisoning in the Caribbean Islands and Western Atlantic. In *Reviews of Environmental Contamination and Toxicology: Continuation of Residue Reviews*; Ware, G.W., Ed.; Springer: New York, NY, USA, 2001; pp. 99–141.
96. Oshiro, N.; Yogi, K.; Asato, S.; Sasaki, T.; Tamanaha, K.; Hirama, M.; Yasumoto, T.; Inafuku, Y. Ciguatera incidence and fish toxicity in Okinawa, Japan. *Toxicon* **2010**, *56*, 656–661. [CrossRef]
97. Chan, T.Y.K. Emergence and epidemiology of ciguatera in the coastal cities of Southern China. *Mar. Drugs* **2015**, *13*, 1175–1184. [CrossRef]
98. Hossen, V.; Soliño, L.; Leroy, P.; David, E.; Velge, P.; Dragacci, S.; Krys, S.; Flores Quintana, H.; Diogène, J. Contribution to the risk characterization of ciguatoxins: LOAEL estimated from eight ciguatera fish poisoning events in Guadeloupe (French West Indies). *Environ. Res.* **2015**, *143*, 100–108. [CrossRef]
99. Ha, D.V.; Uesugi, A.; Uchida, H.; Ky, P.X.; Minh, D.Q.; Watanabe, R.; Matsushima, R.; Oikawa, H.; Nagai, S.; Iwataki, M.; et al. Identification of causative ciguatoxins in red snappers *Lutjanus bohar* implicated in ciguatera fish poisonings in Vietnam. *Toxins* **2018**, *10*, 420. [CrossRef]
100. Darius, H.T.; Ponton, D.; Revel, T.; Cruchet, P.; Ung, A.; Tchou Fouc, M.; Chinain, M. Ciguatera risk assessment in two toxic sites of French Polynesia using the receptor-binding assay. *Toxicon* **2007**, *50*, 612–626. [CrossRef]
101. Yogi, K.; Oshiro, N.; Inafuku, Y.; Hirama, M.; Yasumoto, T. Detailed LC-MS/MS analysis of ciguatoxins revealing distinct regional and species characteristics in fish and causative alga from the Pacific. *Anal. Chem.* **2011**, *83*, 8886–8891. [CrossRef]
102. Yogi, K.; Sakugawa, S.; Oshiro, N.; Ikehara, T.; Sugiyama, K.; Yasumoto, T. Determination of toxins involved in Ciguatera Fish Poisoning in the Pacific by LC/MS. *J. AOAC Int.* **2014**, *97*, 398–402. [CrossRef] [PubMed]
103. Bottein Dechraoui, M.Y.; Tiedeken, J.A.; Persad, R.; Wang, Z.; Granade, H.R.; Dickey, R.W.; Ramsdell, J.S. Use of two detection methods to discriminate ciguatoxins from brevetoxins: Application to great barracuda from Florida Keys. *Toxicon* **2005**, *46*, 261–270. [CrossRef]
104. Hardison, D.R.; Holland, W.C.; McCall, J.R.; Bourdelais, A.J.; Baden, D.G.; Darius, H.T.; Chinain, M.; Tester, P.A.; Shea, D.; Flores Quintana, H.A.; et al. Fluorescent Receptor Binding Assay for detecting ciguatoxins in fish. *PLoS ONE* **2016**, *11*, e0153348. [CrossRef] [PubMed]
105. Díaz-Asencio, L.; Clausing, R.J.; Vandersea, M.; Chamero-Lago, D.; Gómez-Batista, M.; Hernández-Albernas, J.I.; Chomérat, N.; Rojas-Abrahantes, G.; Litaker, R.W.; Tester, P.; et al. Ciguatoxin occurrence in food-web components of a Cuban coral reef ecosystem: Risk-assessment implications. *Toxins* **2019**, *11*, 722. [CrossRef] [PubMed]
106. Harwood, D.T.; Murray, S.; Boundy, M.J. Chapter Three—Sample preparation prior to marine toxin analysis. In *Comprehensive Analytical Chemistry*; Diogène, J., Campàs, M., Eds.; Elsevier: Amsterdam, The Netherlands, 2017; Volume 78, pp. 89–136. [CrossRef]
107. Roué, M.; Smith, K.F.; Sibat, M.; Viallon, J.; Henry, K.; Ung, A.; Biessy, L.; Hess, P.; Darius, H.T.; Chinain, M. Assessment of ciguatera and other phycotoxin-related risks in Anaho Bay (Nuku Hiva Island, French Polynesia): Molecular, toxicological, and chemical analyses of passive samplers. *Toxins* **2020**, *12*, 321. [CrossRef]
108. Soliño, L.; Costa, P.R. Differential toxin profiles of ciguatoxins in marine organisms: Chemistry, fate and global distribution. *Toxicon* **2018**, *150*, 124–143. [CrossRef]
109. Parsons, M.L.; Settlemier, C.J.; Bienfang, P.K. A simple model capable of simulating the population dynamics of *Gambierdiscus*, the benthic dinoflagellate responsible for ciguatera fish poisoning. *Harmful Algae* **2010**, *10*, 71–80. [CrossRef]
110. Carlson, R.D.; Tindall, D.R. Distribution and periodicity of toxic dinoflagellates in the Virgin Islands. In *Toxic Dinoflagellates*; Anderson, D.M., White, A.W., Baden, D.G., Eds.; Elsevier: Amsterdam, The Netherlands, 1985; pp. 171–176.

111. Loeffler, C.R.; Richlen, M.L.; Brandt, M.E.; Smith, T.B. Effects of grazing, nutrients, and depth on the ciguatera-causing dinoflagellate *Gambierdiscus* in the US Virgin Islands. *Mar. Ecol. Prog. Ser.* **2015**, *531*, 91–104. [CrossRef]
112. Yasumoto, T.; Inoue, A.; Ochi, T.; Fujimoto, K.; Oshima, Y.; Fukuyo, Y.; Adachi, R.; Bagnis, R. Environmental studies on a toxic dinoflagellate responsible for ciguatera. *Bull. Jpn. Soc. Sci. Fish.* **1980**, *46*, 1397–1404. [CrossRef]
113. Ichinotsubo, D.; Asahina, A.Y.; Titus, E.; Chun, S.; Hong, T.W.P.; Shirai, J.L.; Hokama, Y. Survey for ciguatera fish poisoning in west Hawaii. *Mem. Qld. Mus.* **1994**, *34*, 513–522.
114. Parsons, M.L.; Preskitt, L.B. A survey of epiphytic dinoflagellates from the coastal waters of the island of Hawai'i. *Harmful Algae* **2007**, *6*, 658–669. [CrossRef]
115. Institut de la Statistique de la Polynésie Française. Available online: https://www.ispf.pf/ (accessed on 27 October 2020).
116. Tester, P.A.; Kibler, S.R.; Holland, W.C.; Usup, G.; Vandersea, M.W.; Leaw, C.P.; Teen, L.P.; Larsen, J.; Mohammad-Noor, N.; Faust, M.A.; et al. Sampling harmful benthic dinoflagellates: Comparison of artificial and natural substrate methods. *Harmful Algae* **2014**, *39*, 8–25. [CrossRef]
117. Smith, K.F.; Biessy, L.; Argyle, P.A.; Trnski, T.; Halafihi, T.; Rhodes, L.L. Molecular identification of *Gambierdiscus* and *Fukuyoa* (Dinophyceae) from environmental samples. *Mar. Drugs* **2017**, *15*, 243. [CrossRef] [PubMed]
118. Chinain, M.; Darius, H.T.; Ung, A.; Cruchet, P.; Wang, Z.; Ponton, D.; Laurent, D.; Pauillac, S. Growth and toxin production in the ciguatera-causing dinoflagellate *Gambierdiscus polynesiensis* (Dinophyceae) in culture. *Toxicon* **2010**, *56*, 739–750. [CrossRef]
119. Power, S.; Casey, T.; Folland, C.K.; Colman, A.; Mehta, V. Interdecadal modulation of the impact of ENSO on Australia. *Clim. Dyn.* **1999**, *15*, 319–323. [CrossRef]
120. Huang, B.; Thorne, P.W.; Banzon, V.F.; Boyer, T.; Chepurin, G.; Lawrimore, J.H.; Menne, M.J.; Smith, T.M.; Vose, R.S.; Zhang, H. Extended reconstructed sea surface temperature, Version 5 (ERSSTv5): Upgrades, validations, and intercomparisons. *J. Clim.* **2017**, *30*, 8179–8205. [CrossRef]

toxins

MDPI

Article

Effects of pH and Nutrients (Nitrogen) on Growth and Toxin Profile of the Ciguatera-Causing Dinoflagellate *Gambierdiscus polynesiensis* (Dinophyceae)

Sébastien Longo [1,*], Manoëlla Sibat [2], Hélène Taiana Darius [1], Philipp Hess [2] and Mireille Chinain [1]

[1] Laboratory of Marine Biotoxins, Institut Louis Malardé-UMR241 EIO (IFREMER, ILM, IRD, UPF), 98713 Papeete, Tahiti, French Polynesia; tdarius@ilm.pf (H.T.D.); mchinain@ilm.pf (M.C.)

[2] Phycotoxins Laboratory, IFREMER, Rue de l'Ile d'Yeu, 44311 Nantes, France; Manoella.Sibat@ifremer.fr (M.S.); Philipp.Hess@ifremer.fr (P.H.)

* Correspondence: slongo@ilm.pf

Received: 7 October 2020; Accepted: 25 November 2020; Published: 4 December 2020

Abstract: Ciguatera poisoning is a foodborne disease caused by the consumption of seafood contaminated with ciguatoxins (CTXs) produced by dinoflagellates in the genera *Gambierdiscus* and *Fukuyoa*. Ciguatera outbreaks are expected to increase worldwide with global change, in particular as a function of its main drivers, including changes in sea surface temperature, acidification, and coastal eutrophication. In French Polynesia, *G. polynesiensis* is regarded as the dominant source of CTXs entering the food web. The effects of pH (8.4, 8.2, and 7.9), Nitrogen:Phosphorus ratios (24N:1P vs. 48N:1P), and nitrogen source (nitrates vs. urea) on growth rate, biomass, CTX levels, and profiles were examined in four clones of *G. polynesiensis* at different culture age (D10, D21, and D30). Results highlight a decrease in growth rate and cellular biomass at low pH when urea is used as a N source. No significant effect of pH, N:P ratio, and N source on the overall CTX content was observed. Up to ten distinct analogs of Pacific ciguatoxins (P-CTXs) could be detected by liquid chromatography-tandem mass spectrometry (LC-MS/MS) in clone NHA4 grown in urea, at D21. Amounts of more oxidized P-CTX analogs also increased under the lowest pH condition. These data provide interesting leads for the custom production of CTX standards.

Keywords: *Gambierdiscus polynesiensis*; French Polynesia; ciguatera; ciguatoxins; LC-MS/MS; toxin profile; nitrate; urea; culture medium acidification

Key Contribution: This study documents for the first time the response of *Gambierdiscus polynesiensis* strains to some key drivers of global change, i.e., pH and nutrients availability. Both the acidification and the use of different sources and/or concentrations of nitrogen in culture medium had significant effects on *G. polynesiensis* growth and ciguatoxin production. The acidification of the culture medium also stimulates the production of more oxidized forms of P-CTXs in *G. polynesiensis*. This study may benefit Research and Development (R&D) programs aiming at the custom production of CTX standards.

1. Introduction

Ciguatera poisoning (CP) is the most prevalent, phycotoxin-related seafood intoxication affecting mainly populations living in tropical and subtropical areas of the world. CP cases occur after the consumption of seafood contaminated with toxins known as ciguatoxins (CTXs) that are produced by dinoflagellates in the genera *Gambierdiscus* and *Fukuyoa*. Ciguatera toxins enter marine food webs through grazing by herbivores and detritivores and are further accumulated through predation and

bio-transformed in carnivores [1,2]. Overall, eighteen species of *Gambierdiscus* are now recognized worldwide [3–14]. The phylogeny of these species based on large subunit ribosomal ribonucleic acid (LSU rDNA) D8–D10 region sequences is provided by Kretzschmar et al. [11]. Ciguatoxin production has been shown by the neuroblastoma cell-based assay (CBA-N2a) to vary considerably according to species [15,16] but, interestingly, has only been confirmed by liquid chromatography-tandem mass spectrometry (LC-MS/MS) in *G. polynesiensis* since the genus *Gambierdiscus* has been enlarged from *G. toxicus* to other species [3,17].

Numerous field observations linking the effects of climate change to CP events can be found in the literature [18–24]. In particular, cyclical weather patterns such as El Niño, associated with unusual warming of ocean waters in the Pacific, have resulted in spikes of ciguatera [25], consistent with observations by Gingold et al. [26], who found an association between CP incidence and warmer sea surface temperatures in the Caribbean basin. Many laboratory studies have also investigated *Gambierdiscus* and *Fukuyoa* spp. growth responses and/or toxin production under varying environmental conditions, including temperature, salinity, and irradiance (for reviews, see References [27] and [28], and references therein). Results confirm that differences among strains exist not only across but also within species [15,29–33]. All these observations substantiate the idea that ocean warming as a result of climate change may increase the global distribution of CTX-producing dinoflagellates and, hence, CP incidence worldwide. However, the influence of other environmental drivers commonly associated with global change, such as ocean acidification and increasing eutrophication of coastal marine ecosystems, also deserve to be investigated.

Oceans serve as one of the largest carbon reserves on earth, absorbing nearly one third of all carbon dioxide emissions [34]. Increasing amounts of CO_2 diffusing from the atmosphere into the oceans results, among others, in ocean acidification [35], currently estimated as a decrease in seawater pH by 0.11 units since the 1870s [36], with the current pH being 8.06 on average [37]. Following the fifth Intergovernmental Panel on Climate Change report, forecasts predict an additional decrease in ocean pH from 0.07 (Representative Concentration Pathway 2.6; RCP 2.6) to 0.33 units (RCP 8.5) by 2100 [37,38]. Furthermore, over the past decades, there have also been significant increases in marine eutrophication globally [39]. Still, eutrophication should be considered a localized phenomenon and, in some regions, improvements have shown to lead to reduction of harmful algal blooms (HABs), e.g., in the Japanese Inland Sea [40]. Nitrogen (N) and phosphorus (P), two major drivers of marine eutrophication, are commonly regarded as key limiting nutrients in most aquatic ecosystems [41]. Eutrophication episodes can lead to hypoxia and anoxia, reduced water quality, alteration of food web structure, habitat degradation, loss of biodiversity, and even harmful algal bloom (HAB) events [39,42–44], which in turn may result in health risks and economic losses, including losses of fish and wildlife production and losses of recreational amenities [45,46]. By way of example, French Polynesian lagoons are well-known oligotrophic ecosystems characterized by low concentrations of dissolved mineral nitrogen [47–49]. However, more recently, intensified agriculture and aquaculture (e.g., pearl-farming) practices, as well as increasing development of coastal activities, have caused major changes in local environments via the release of nutrient-rich inputs [44,50,51].

The influence nutrients and pH have on the ecophysiology and toxicity of ciguatera-causing dinoflagellates is still poorly documented. To our knowledge, no published study has currently investigated the effects of pH on the growth and toxin production of *Gambierdiscus* and *Fukuyoa* spp. However, several studies have shown the effect of pH on various HAB species (Reference [47] and references therein), such as *Alexandrium* and *Pseudo-Nitzschia* spp. [48–57]. Likewise, few field studies have examined the correlation between *Gambierdiscus* cell densities and nutrient levels in various ciguatera-prone areas of the Pacific (French Polynesia, Hawaii) [57–59], Caribbean (British and U.S. Virgin Islands) [60–62], and Indian Ocean (Mauritius) [63]. While some of these studies were limited by non-detectable nutrient concentrations [63], others gave contradictory results [57–62]. There is also limited data on the role of nutrients in stimulating *Gambierdiscus* and *Fukuyoa* spp. toxin production [32,64–67]. These studies, which examined the effects of both nutrient levels and

various nitrogen sources (i.e., nitrate, ammonium, urea), showed that species matters, as results suggest that the various species of *Gambierdiscus* may have different nutrient physiologies and uptake kinetics.

In French Polynesia, *G. polynesiensis* is regarded as the dominant source of CTXs entering the food web [68]. A recent study conducted on four *G. polynesiensis* isolates originating from distinct geographic locations in French Polynesia, showed that these strains produce at least nine distinct P-CTX analogs in culture, namely P-CTX4B, P-CTX4A (52-epi-P-CTX4B), P-CTX3C, P-CTX3B (49-epi-P-CTX3C), 2-hydroxy-P-CTX3C, M-seco-P-CTX3C, and three P-CTX3B/C isomers not fully characterized yet, and confirmed that clonal variation in toxin production exists in this species [33].

As a follow-up study, the present work aimed at assessing the in vitro growth and toxin production in *G. polynesiensis* at different growth phases, when cultured under various combinations of pH (8.4, 8.2, and 7.9) and Nitrogen:Phosphorus (N:P) ratios (24N:1P vs. 48N:1P), while using two distinct N sources, i.e., nitrate vs. urea. Variations in both overall cellular CTX concentrations and toxin profiles were characterized by LC-MS/MS. How these data can help promote the custom production of algal CTX standards currently needed for the implementation of CP risk and management programs is further discussed.

2. Results

2.1. Effects of Culture Age, pH, Nitrogen Source, and N:P Ratio on G. polynesiensis Growth Rate and Biomass

The mean growth rates exhibited by each *G. polynesiensis* strain 10 days (D10) and 21 days (D21) post-inoculation, under three different pH and two N:P ratios using either nitrate or urea as N source, are presented in Table 1.

In nitrate growth experiments, all strains displayed a typical growth pattern at pH = 8.4 and 8.2, characterized by a maximum growth rate of 0.2 division day^{-1} (div day^{-1}) on average at the exponential growth phase (from D0 to D10) and a mean growth rate of 0.1 div day^{-1} at the stationary phase (from D10 to D21), whatever the N:P ratio tested. At pH = 7.9, although a similar growth rate around 0.2 div day^{-1} was reached at the exponential growth phase, cultures rapidly declined after 10 days contrarily to cultures maintained at pH 8.4 or 8.2. Overall, for *G. polynesiensis* considered as a whole, statistical analyses revealed no significant effect of pH or N:P ratio on the growth rate in nitrate-based culture media (data not shown).

In urea growth experiments, a different growth pattern was demonstrated in all four strains as compared to nitrate conditions (Table 1). From D0 to D10, growth rates never exceeded 0.14 div day^{-1} (clone RIK7, 48N:1P) at pH = 8.4, for the two N:P ratios tested. At pH = 8.2, strains showed a different growth response characterized by a latency phase from D0 to D10, an exponential phase from D10 to D21 with a maximum growth rate of 0.2 div day^{-1} (RIK7, 48N:1P), followed by a stationary phase from D21 to D30 for all strains (data not shown). At pH = 7.9, a similar growth trend was observed, although growth rates were generally lower than at pH = 8.2 (Table 1).

The cell biomass reached after 30 days of culture are presented in Table 2. It can be noted that data significantly differed between nitrate and urea supply, most notably at 24N:1P ratio (Table 2), with final cell yields in nitrate being 3-fold higher on average than those obtained in urea. At a given pH, no N:P ratio effect on cell biomass was noticed when strains were grown in nitrate, whereas cell yields obtained for all strains at 48N:1P were almost 2-fold higher on average than at 24N:1P in urea. For a given N source, cell yields were also lower at pH = 7.9 than at pH = 8.4 at the two N:P ratios tested. Of note, in nitrate conditions, the lowest cell yields were generally observed in the RAI-1 strain.

Table 1. Mean growth rates ± standard deviation (SD) (in div day^{-1}, n = 2) of *G. polynesiensis* clones (NHA4, RAI-1, RIK7, and RG92) as assessed at day 10 (D10) and day 21 (D21), under three different pH conditions (8.4, 8.2, and 7.9), using either nitrate or urea as nitrogen (N) source when tested at two distinct N:P ratios (24N:1P and 48N:1P).

Culture Age	N Source	N:P Ratio	PH	NHA4	RAI-1	RIK7	RG92
D0→D10	Nitrate	24N:1P	8.4	0.20 ± 0.01	0.18 ± 0.00	0.20 ± 0.03	0.15 ± 0.00
			8.2	0.17 ± 0.01	0.20 ± 0.02	0.17 ± 0.00	0.21 ± 0.01
			7.9	0.22 ± 0.01	0.23 ± 0.00	0.22 ± 0.00	0.18 ± 0.00
		48N:1P	8.4	0.23 ± 0.00	0.15 ± 0.00	0.22 ± 0.02	0.19 ± 0.00
			8.2	0.22 ± 0.01	0.20 ± 0.03	0.21 ± 0.03	0.13 ± 0.00
			7.9	0.26 ± 0.01	0.12 ± 0.01	0.16 ± 0.00	0.21 ± 0.01
	Urea	24N:1P	8.4	0.04 ± 0.01	0.03 ± 0.02	0.08 ± 0.01	0.03 ± 0.02
			8.2	−0.08 ± 0.01	−0.06 ± 0.03	−0.07 ± 0.00	−0.11 ± 0.07
			7.9	−0.05 ± 0.01	−0.05 ± 0.01	−0.04 ± 0.03	−0.05 ± 0.01
		48N:1P	8.4	0.12 ± 0.02	0.11 ± 0.01	0.14 ± 0.01	0.04 ± 0.01
			8.2	0.02 ± 0.03	−0.06 ± 0.01	0.00 ± 0.02	0.00 ± 0.02
			7.9	0.01 ± 0.01	−0.01 ± 0.01	0.00 ± 0.01	−0.02 ± 0.00
D10→D21	Nitrate	24N:1P	8.4	0.09 ± 0.02	0.09 ± 0.00	0.08 ± 0.01	0.13 ± 0.00
			8.2	0.15 ± 0.00	0.07 ± 0.03	0.13 ± 0.01	0.09 ± 0.01
			7.9	−0.02 ± 0.02	−0.06 ± 0.04	0.00 ± 0.01	−0.07 ± 0.03
		48N:1P	8.4	0.08 ± 0.01	0.13 ± 0.01	0.08 ± 0.03	0.11 ± 0.00
			8.2	0.07 ± 0.04	0.04 ± 0.04	0.08 ± 0.02	0.15 ± 0.00
			7.9	0.04 ± 0.08	−0.05 ± 0.02	0.00 ± 0.00	−0.07 ± 0.01
	Urea	24N:1P	8.4	0.05 ± 0.01	0.05 ± 0.02	0.07 ± 0.05	0.05 ± 0.01
			8.2	0.15 ± 0.02	0.11 ± 0.01	0.16 ± 0.01	0.17 ± 0.05
			7.9	0.04 ± 0.02	0.07 ± 0.02	0.06 ± 0.07	0.02 ± 0.01
		48N:1P	8.4	0.07 ± 0.01	0.10 ± 0.01	0.09 ± 0.02	0.10 ± 0.03
			8.2	0.17 ± 0.03	0.16 ± 0.04	0.20 ± 0.03	0.17 ± 0.01
			7.9	0.09 ± 0.01	0.11 ± 0.00	0.13 ± 0.01	0.10 ± 0.01

Table 2. Mean ± SD (n = 2) of final cell biomass yielded at D30 for each *G. polynesiensis* clones (NHA4, RAI-1, RIK7. and RG92), under three different pH conditions (8.4, 8.2, and 7.9), and two distinct N:P ratios (24N:1P and 48N:1P) when nitrate or urea were used as N source.

N Source	N:P Ratio	PH	NHA4	RAI-1	RIK7	RG92
Nitrate	24N:1P	8.4	359,210 ± 62,793	235,365 ± 42,083	327,392 ± 27,340	355,867 ± 10,714
		8.2	369,212 ± 16,423	187,680 ± 13,356	351,475 ± 36,808	224,060 ± 33,932
		7.9	130,333 ± 11,857	151,357 ± 17,596	166,912 ± 64,067	171,303 ± 38,440
	48N:1P	8.4	295,035 ± 49,244	222,077 ± 39,746	264,010 ± 49,939	412,392 ± 19,155
		8.2	386,863 ± 69,359	165,353 ± 24,543	299,937 ± 7,630	203,235 ± 17,276
		7.9	189,182 ± 12,229	122,088 ± 23,412	238,283 ± 14,594	169,433 ± 16,245
Urea	24N:1P	8.4	95,207 ± 1,202	102,435 ± 27,400	198,646 ± 48,861	108,437 ± 44,900
		8.2	87,269 ± 21,779	101,969 ± 11,809	100,867 ± 21,885	94,374 ± 2,404
		7.9	59,397 ± 1,465	75,607 ± 17,721	67,019 ± 9,035	55,444 ± 11,268
	48N:1P	8.4	283,196 ± 81,070	259,798 ± 14,566	256,197 ± 8,309	120,589 ± 38,608
		8.2	245,882 ± 23,122	212,219 ± 27,011	249,582 ± 37,724	243,359 ± 13,188
		7.9	125,726 ± 15,384	175,371 ± 18,907	164,946 ± 6,384	110,912 ± 15,593

2.2. Diversity of P-CTX Analogs in G. polynesiensis

The LC-MS/MS analyses performed on crude methanol extracts of all four clones revealed that depending on the strain and culture conditions applied, the number of detectable P-CTX analogs in cultures of *G. polynesiensis* could range from four up to ten analogs consisting of: (i) two major compounds, P-CTX3B and P-CTX3C, and (ii) eight minor CTXs analogs: two non-polar analogs from the P-CTX1B group, i.e., P-CTX4A and P-CTX4B, two oxidized forms of P-CTX3C, i.e., 2-OH-P-CTX3C and M-seco-P-CTX3C, and four hitherto undescribed isomers belonging to the P-CTX3B/C group, referred to as P-CTX3B/C group isomers 1, 2, 3, and 4 (Figure 1).

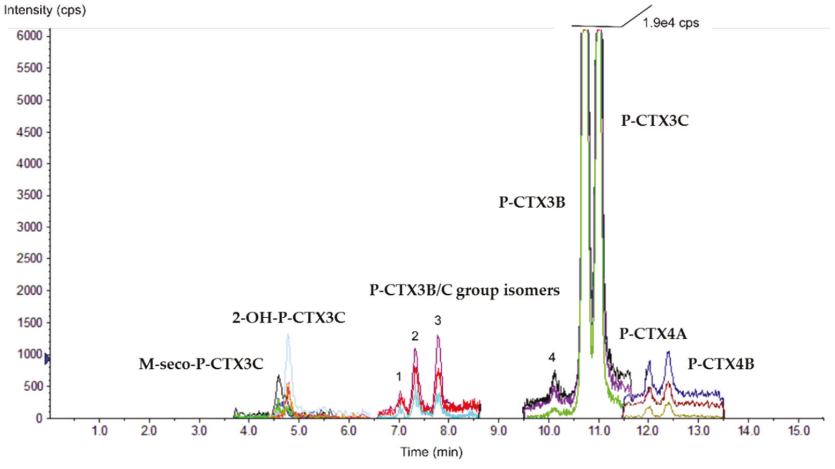

Figure 1. Chromatogram of scheduled Multiple Reaction Monitoring (MRM) LC-MS/MS showing the different P-CTX analogs detected in crude methanol extracts of *G. polynesiensis* strain NHA4 cultivated during 21 days in urea 48N:1P at pH = 7.9. The different colors correspond to the different MRM transitions (*m*/*z*) selected for the analysis method, scanning three transitions for each P-CTX analogs (see Supplementary Table S1 for further information about *m*/*z* transitions selected).

Of note, only P-CTX3B/C group isomers 2 and 3 were produced at quantifiable amounts, whereas P-CTX3B/C isomers 1 and 4 were consistently present at levels below the limit of quantification (LOQ = 10 ng mL^{-1}) and, therefore, are not represented in the following figures and tables.

Quantitation of the different P-CTXs analogs was carried out using P-CTX3C, the only commercially available reference material. Assuming equal molar response and applying the same LOD and LOQ, the estimated concentrations were calculated against the P-CTX3C calibration curve and expressed in equivalent P-CTX3C. The sum of the estimated concentrations of all analogs allowed estimation of the overall cellular toxin content (expressed in pg P-CTX3C eq $cell^{-1}$).

2.3. Effects of Strain, Culture Age, Nitrogen, and pH on the Overall P-CTX Cell Content in G. polynesiensis

The overall P-CTX cell content in the four strains ranged from 0.1 to 4.0 pg P-CTX3C eq $cell^{-1}$, depending on culture age, strain, and culture conditions (Figure 2). Of note, the P-CTX content in NHA4 (i.e., 2.12 ± 0.99 pg P-CTX3C eq $cell^{-1}$, on average) was significantly higher than the one measured in the three other clones (*p*-values ranged from <0.0001 to 0.004). Conversely, RG92 showed the lowest P-CTX content with an average of 0.44 ± 0.24 pg P-CTX3C eq $cell^{-1}$ (Figure 2). Also, P-CTX contents measured at D10 were significantly lower than at D21 and D30 (p-value < 0.05). In contrast, the pH, N source, or N:P ratio had no significant effects on the overall cellular CTX content of *G. polynesiensis* strains.

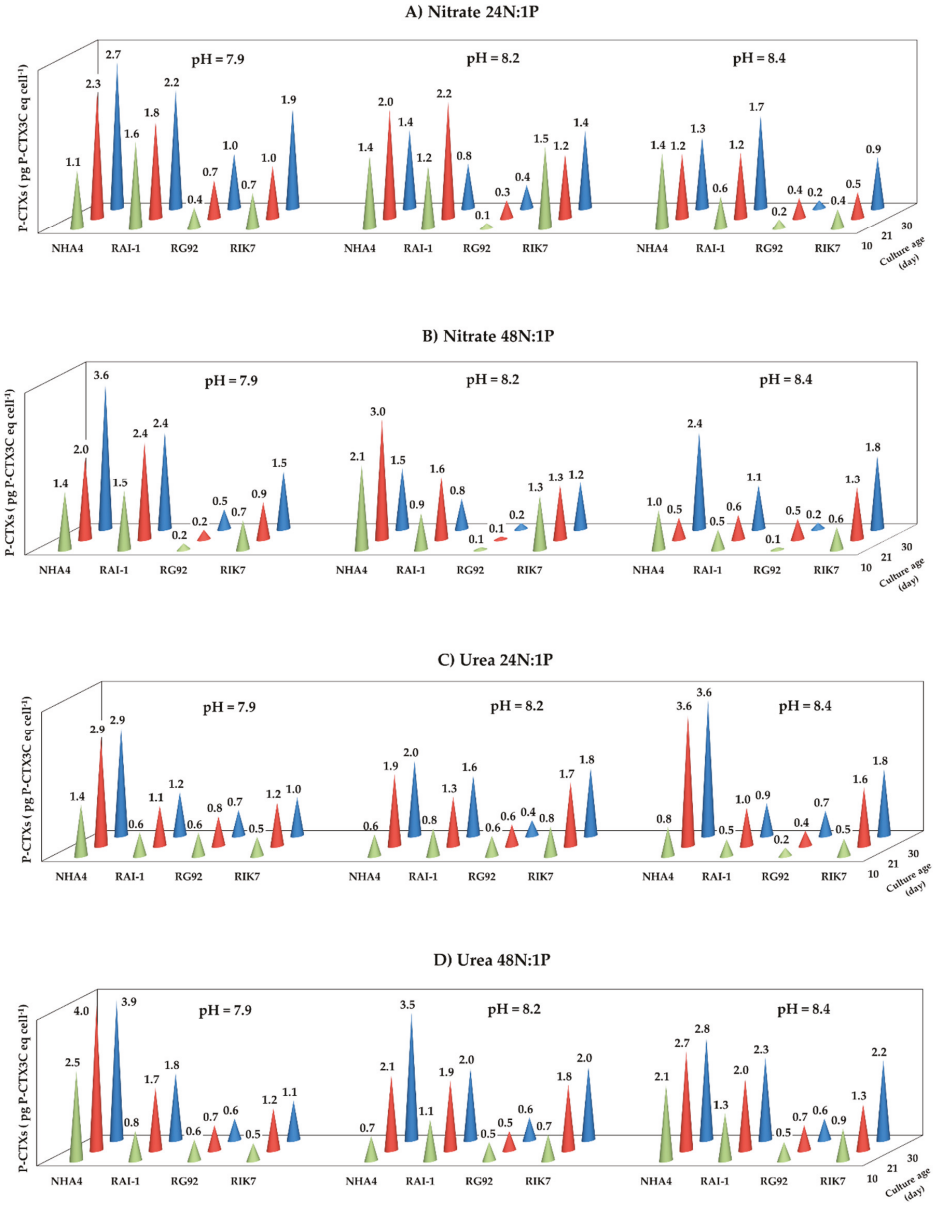

Figure 2. Mean overall P-CTX content (expressed in pg P-CTX3C eq cell^{-1}) measured by LC-MS/MS at three distinct culture ages (D10, D21, and D30) in four *G. polynesiensis* strains (NHA4, RAI-1, RG92, and RIK7) when grown at three different pH (7.9, 8.2, and 8.9), in nitrate: 24N:1P (**A**) and 48N:1P (**B**) vs. urea: 24N:1P (**C**) and 48N:1P (**D**). Data represent the mean P-CTX content in each strain tested in two technical replicates.

2.4. Effects of Strain, Culture Age, Nitrogen, and pH on G. polynesiensis Toxin Profiles

2.4.1. Clonal Variations in P-CTX Profiles

While RAI-1 (Australes strain) and RIK7 (Gambier strain) had similar toxin profiles composed of six analogs in all experiments (Figure 3), two additional analogs, i.e., 2-OH-P-CTX3C and M-seco-P-CTX3C, were quantified in NHA4 (Marquesas strain) cultures, whereas P-CTX4A analog was not quantified in RG92 (Tuamotu strain). Figure 3 shows that the amounts of P-CTX3B and P-CTX3C were significantly higher in NHA4 than in the three other clones (p-value < 0.0001), and significantly lower in RG92 than in other clones (p-value < 0.0001), based on pairwise comparisons.

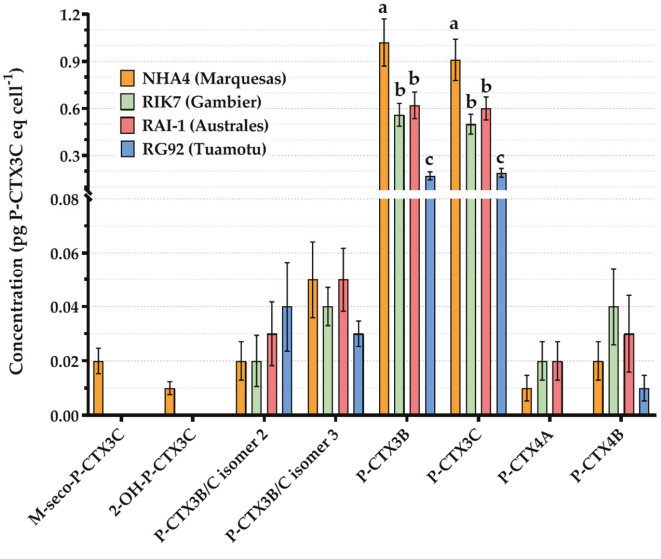

Figure 3. Mean cellular concentrations expressed in pg P-CTX3C equivalent cell^{-1} (eq cell^{-1}) of each P-CTX analog measured by LC-MS/MS in four *G. polynesiensis* strains (NHA4, RIK7, RAI-1, and RG92). Data represent the mean ± 95% confidence interval (CI) of n = 72 samples (two technical replicates per strain when grown under three pH conditions and two different N sources tested at two N:P ratios, at three culture ages). The letters a, b and c shown on P-CTX3B and -3C bars indicate statistical differences observed between clones based on pairwise comparisons.

2.4.2. Effects of Culture Age on *G. polynesiensis* P-CTX Concentrations

The concentrations of the different P-CTX analogs detected in each of the four clones at different culture ages, i.e., D10, D21, and D30, are presented in Figure 4. Overall, only five analogs could be quantified at D10 vs. up to eight analogs at D30 depending on the strain considered (Figure 4). Moreover, a progressive increase in P-CTX3B and -3C concentrations, the two major toxins produced by *G. polynesiensis* strains, was noticed in RIK7 from D10 to D30 (Figure 4B), whereas for the three other clones, no significant differences were observed between D21 and D30 for these two compounds (Figure 4A,C,D). Interestingly, while P-CTX3B/C isomer 2 significantly decreased between D10 and D30 in strain RG92 (Figure 4D), P-CTX4A and -4B concentrations increased in the three other strains (Figure 4A–C).

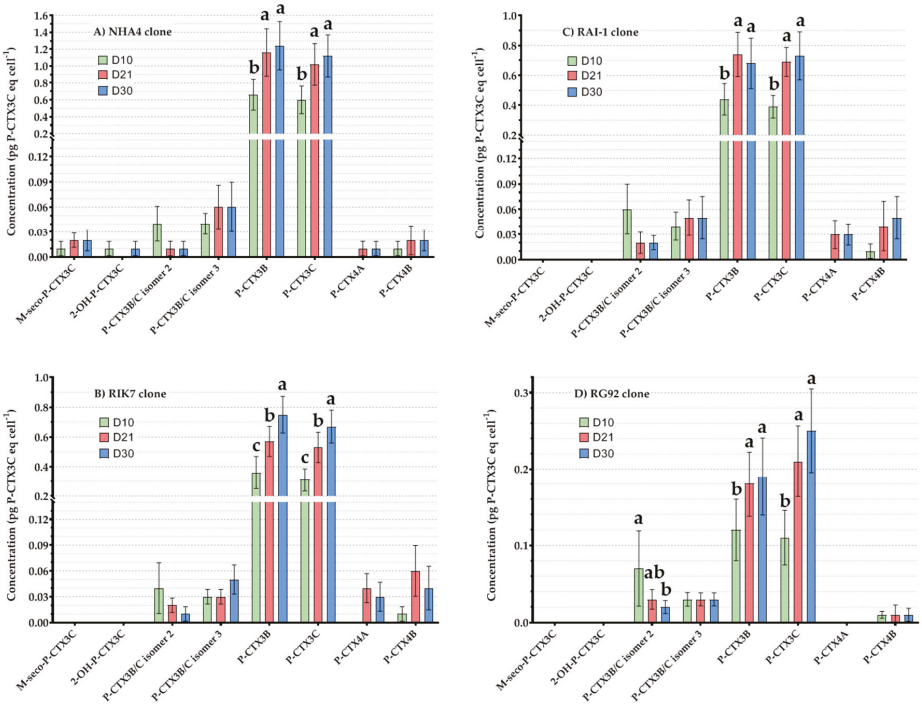

Figure 4. Mean cellular concentrations (expressed in pg P-CTX3C eq cell^{-1}) of P-CTX analogs measured by LC-MS/MS in four *G. polynesiensis* clones at three different culture ages (D10, D21, and D30): (**A**) NHA4, (**B**) RIK7, (**C**) RAI-1, and (**D**) RG92. Data represent the mean ± 95% CI of n = 24 samples (two technical replicates per strain when grown under three pH conditions and two different N sources tested at two N:P ratios). Letters indicate statistical differences observed between samples based on pairwise comparisons.

2.4.3. Effects of N Source and N:P Ratio on *G. polynesiensis* P-CTXs Concentrations

The variations in P-CTX analogs diversity observed between four strains of *G. polynesiensis* when grown under different N sources and N:P ratios are presented in Figure 5 In nitrate-based experiments, only three quantifiable analogs were detected in cultures, i.e., P-CTX3B/C isomer 3, P-CTX3B and -3C with no significant effects of N:P ratio on their respective levels, except for clone RG92 (Figure 5D). In urea-based experiments, the number of quantifiable analogs substantially increased to five analogs in RG92 (Figure 5D), six in RAI-1 and RIK7 (Figure 5B,C), and eight in NHA4 (Figure 5A).

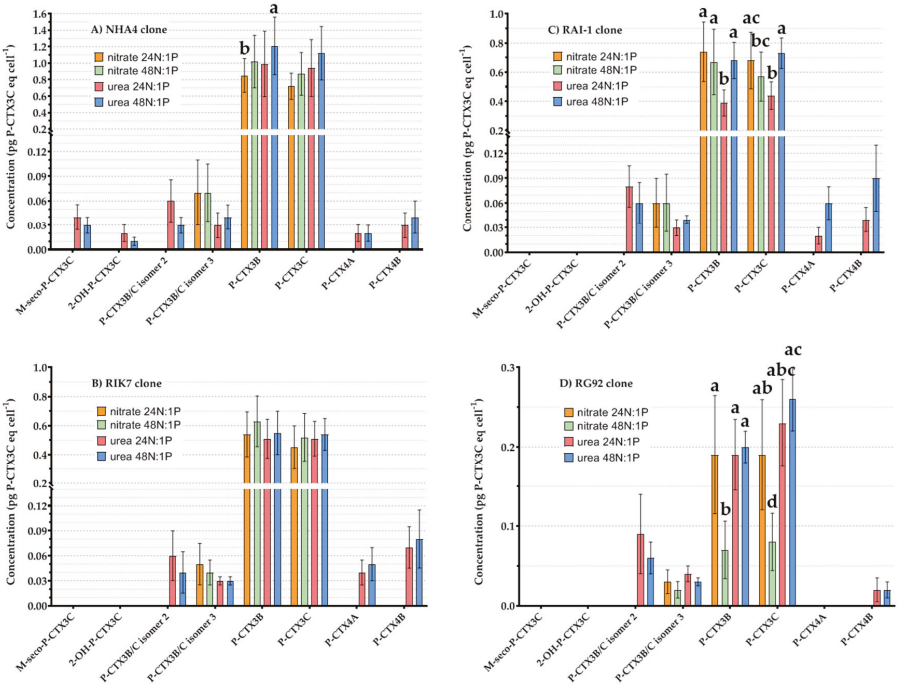

Figure 5. Mean cellular concentrations (expressed in pg P-CTX3C eq cell^{-1}) of P-CTX analogs measured by LC-MS/MS in NHA4 (**A**), RIK7 (**B**), RAI-1 (**C**), and RG92 (**D**) clones grown in nitrate 24N:1P and 48N:1P vs. urea 24N:1P and 48N:1P. Data represent the mean ± 95% CI of n = 18 samples (two technical replicates analyzed at three culture ages and three pH conditions). Letters indicate statistical differences observed between samples based on pairwise comparisons.

2.4.4. Effects of pH on *G. polynesiensis* P-CTX Concentrations

The variations in P-CTX analogs diversity observed in strains of *G. polynesiensis* when grown under different pH conditions are illustrated in Figure 6. It can be seen that in RAI-1, amounts of P-CTX3B increased significantly from pH = 8.4 to pH = 7.9 (Figure 6C). In NHA4 and RG92, amounts of P-CTX3B and -3C did not vary significantly at pH = 8.2 and pH = 8.4 but were significantly higher at pH = 7.9 (Figure 6A,D). In RIK7, amounts of P-CTX3B and -3C were significantly higher at pH = 8.2 (Figure 6B). In addition, the levels of a minor, more polar analog, namely P-CTX3B/C isomer 3, tended to increase at pH = 7.9 in all the clones as compared to 8.4 (Figure 6A–D). The same observations apply to two other analogs, i.e., 2-OH-P-CTX3C and M-seco-P-CTX3C, which were detected at quantifiable amounts only in NHA4 (Figure 6A). In contrast, P-CTX3B/C isomer 2 and P-CTX4A/4B amounts remained stable across all pH values (Figure 6), except for P-CTX3B/C isomer 2 in RG92, which was significantly higher in pH = 8.2 (Figure 6D).

Table 3 summarizes the different parameters showing significant positive or negative effects on cell yields, overall toxin content, and/or individual analog concentrations in *G. polynesiensis* strains, based on multiple statistical comparisons. Results indicate that the clonal strain influenced both the diversity (number of analogs) and concentrations of each P-CTX analog produced. The final cell yield, the overall cell toxin content, and the levels of P-CTX analogs with low polarity significantly increased in aged cultures, whereas growth stage had no significant effect on the amounts of more polar analogs, except for P-CTX3B/C isomer 2. Contrastingly, decreasing the pH in the culture medium led to reduced cell yields and stimulated the production of more polar forms of P-CTX analogs, while no

significant effect was noticed on less polar analogs, except for P-CTX3B. Overall, a 2-fold increase in nitrogen concentrations (from 24N:1P to 48N:1P) resulted in enhanced cell biomass but had little effect (if any) on the overall cell toxin content and the amounts of the various P-CTX analogs composing *G. polynesiensis* toxin profile. Finally, modifying the nitrogen source from nitrate to urea significantly reduced the final cell yields but was highly beneficial to the production of several P-CTX analogs.

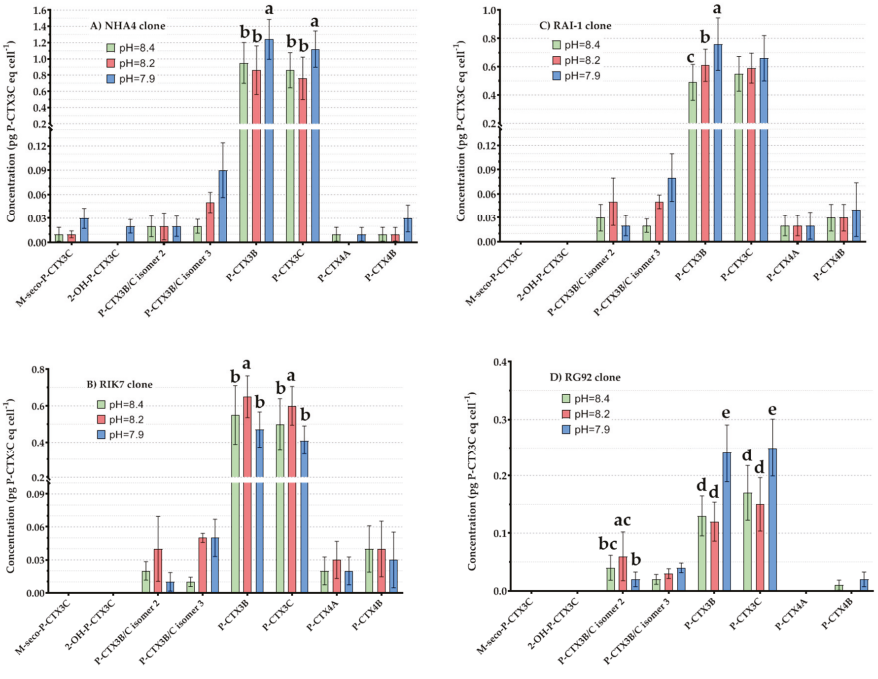

Figure 6. Mean cellular concentrations (expressed in pg P-CTX3C eq cell^{-1}) of P-CTX analogs measured by LC-MS/MS in NHA4 (**A**), RIK7 (**B**), RAI-1 (**C**), and RG92 (**D**) clones under three different pH conditions. Data represent the mean ± 95% CI of n = 24 samples (two technical replicates analyzed at three culture ages and two different N sources tested at two N:P ratios). Letters indicate statistical differences observed between samples based on pairwise comparisons.

Table 3. Effects of strain, culture age, N:P ratio, N source, and pH on the cell biomass, overall toxin content, and P-CTXs profile in *G. polynesiensis*. The statistical significance of each of these parameters is indicated. The different P-CTX analogs are listed by increasing polarity. The "→ "symbol indicates which condition comparison has been conducted.

Parameter	Strain	Culture Age D10→D21/D30	N:P Ratio 24N:1P→48N:1P	N Source Nitrate→Urea	pH 8.4→8.2/7.9
Cell yields at D30	ns	↗ ***	↗ *	↘ ***	↘ **
Overall toxin content	***	↗ *	ns	ns	ns
P-CTX4A	***	↗ ***	↗ *	↗ ***	ns
P-CTX4B	***	↗ ***	↗ **	↗ ***	ns
P-CTX3B	***	↗ ***	ns	ns	↗ *
P-CTX3C	***	↗ ***	ns	↗ *	ns
P-CTX3B/C isomer 2	*	↘ ***	↘ *	↗ ***	↗ ***
P-CTX3B/C isomer 3	***	ns	ns	↘ ***	↗ ***
2-OH-P-CTX3C	***	ns	ns	↗ ***	↗ **
M-seco-P-CTX3C	***	ns	ns	↗ ***	↗ **

* p-value < 0.05, ** p-value < 0.01, *** p-value < 0.001, ns = non significant, ↗ increase, ↘ decrease.

3. Discussion

Ciguatera occurrences at a global scale depend on a combination of trend drivers. Among them, global ocean warming attributable to global change is often cited as a main driver of the current expansion of CP to novel areas and reportedly increased CP incidence (see References [23,24] for reviews and references therein). In contrast, the potential impacts of ocean acidification and eutrophication on CP trends is a topic that remains largely under-studied. The present work aimed at assessing the growth and toxin production in four toxic clones of *G. polynesiensis* isolated from French Polynesia when grown under different combinations of pH, nitrogen ratios, and sources, three environmental parameters regarded as representative of ocean acidification and eutrophication. Several experimental constraints were encountered in the course of this study, such as the limited number of technical replicates set up in growth experiments, or the lack of replicate measures and certified reference standards in LC-MS/MS analyses. Also, the direct addition of HCl drops in *G. polynesiensis* culture medium for pH stabilization appears as a less ecologically relevant method than bubbling with CO_2-enriched air. Hence, the data presented here should be regarded as preliminary results pending further confirmatory studies.

Despite these limits, this study yielded interesting novel results. In particular, it was shown for the first time that when grown at pH = 7.9, a value close to the predicted ocean pH for the end of this century, cells of *G. polynesiensis* were able to survive, even if they required higher pH to achieve optimal growth. Cellular processes (such as phytoplankton productivity and toxin production) have been shown to be sensitive to shifts in CO_2 concentrations, including in diatoms and dinoflagellates [69–72], but there is still a striking lack of published data on the response of *Gambierdiscus* spp. to varying pH. To our knowledge, only one other study has examined the effects of pH on the growth and toxicity of two strains isolated from Marakei Island (Republic of Kiribati) and identified as *G. balechii* [73] and *Gambierdiscus* sp. type 5 [74] (*Chan, pers. comm.*). In that study, low pH values stimulated the growth while negatively impacting the toxin production in *Gambierdiscus* sp. type 5, which is in marked contrast with our results on *G. polynesiensis*. These contrasting findings suggest that *Gambierdiscus* growth as a response to acidification might differ across species, and that ocean acidification may result in a shift in both the composition and abundance of *Gambierdiscus* spp. in the environment. Regarding the effect of pH on *G. polynesiensis* toxin production, this study showed that acidification of the culture medium stimulated the production of more polar (oxidized) forms of P-CTXs in this species, i.e., P-CTX3B/C isomer 3 in all four clones, and 2-OH-P-CTX3C and M-seco-P-CTX3C in NHA4. It is well established that the biooxidation undergone by CTXs in the food chain leads to more toxic analogs [2]. Our findings thus suggest that ocean acidification may result in less abundant but also more toxic populations of *G. polynesiensis*, a major contributor to toxin flux in ciguateric biotopes in the Pacific [30,33,68,75,76], which, in turn, may lead to increased CP risk. Indeed, it is recognized that the toxicity in a given area depends primarily on the presence of selected highly toxic species of *Gambierdiscus* that may not be the numerically dominant species, but which contribute disproportionately to the overall toxicity of the region [33,77]. In any case, since ciguatera occurrence is generally associated with complex assemblages of multiple *Gambierdiscus* species [15,68,78], these preliminary observations warrant further studies on the physiological and toxicological responses of the other *Gambierdiscus* species frequently encountered in benthic assemblages of ciguateric biotopes, in order to inform reliable risk models on CP trends in the context of global change.

The role played by nutrients in ciguatera events remains unclear. Again, very few field studies with reported statistical results have measured nutrient concentrations concurrently to ciguatera dinoflagellate densities. Of these, both Carlson and Tindall [62] and Loeffler et al. [60] reported a positive correlation between nutrient concentrations and *Gambierdiscus* abundance in the U.S. Virgin Islands. Conversely, Yasumoto et al. [57] and Ichinotsubo et al. [59] found no direct correlation between nutrients and cell densities in French Polynesia and Hawaii respectively, consistent with the observations by Parsons and Preskitt [58] in several Hawaiian locations, although according to these authors, the highest cell densities occurred at the site with the highest nutrient concentrations. All this data suggest that nutrient loadings in coastal environments may not necessarily lead to *Gambierdiscus*

blooms and, in fact, the linkage between increased HAB occurrences and eutrophication remains largely inconclusive for a number of microalgal taxa (References [63,78,79] and references therein). However, according to Skinner et al. [80], nutrient inputs can cause a major shift in the distribution and abundance of ciguatera-related dinoflagellates, as evidenced in the Northern Great Barrier Reef (Australia): in several locations affected by on-going coastal eutrophication, benthic assemblages in inshore reefs once dominated by *Gambierdiscus* were composed primarily of *Prorocentrum* and *Ostreopsis*, whilst *Gambierdiscus* was still dominant in offshore locations.

In the present study, the influence of nitrogen (nutrient levels and nitrogen sources) on the growth and toxicity of *G. polynesiensis* was examined in in vitro conditions. Nitrogen was selected because French Polynesian lagoons are usually characterized by low concentrations of dissolved mineral nitrogen [47–49]. Our results indicate that growth rates did not significantly vary with N:P ratio, consistent with the findings of Sperr and Doucette [67], who tested a wide range of N:P ratios from 5:1 to 50:1 on several Caribbean strains. Another main finding was that all four *G. polynesiensis* strains achieved higher growth rates with nitrate rather than with urea. Likewise, the cell biomass yielded at D30 were 3-fold higher on average in nitrate than in urea at 24N:1P for all four strains. These results substantiate previous observations by Lartigue et al. [32], who tested the effects of different nitrogen sources on the growth and toxicity of two *Gambierdiscus* strains subsequently classified as *G. caribaeus* and *Gambierdiscus* ribotype 2 [8,77]. They noted that both strains grew well when the nitrogen source was nitrate while neither species grew on urea. These findings are in marked contrast with those of Durand-Clement [65,66], who reported increased growth in *Gambierdiscus* when urea concentration was increased from 0 to 1 mM. Parsons et al. [27] hypothesized that one possible explanation for this apparent contradiction is that Durand-Clément [66] tested a different species of *Gambierdiscus*, thereby implying that the various *Gambierdiscus* species likely have different nutrient physiologies.

The influence of nutrients in stimulating *Gambierdiscus* toxin production is also poorly documented and remains ambiguous. The field study conducted by Okolodkov et al. [61] in the Yucatan peninsula (Gulf of Mexico) outlined the importance of potential linked effects of various environmental parameters as the authors hypothesized that the greatest potential for ciguatoxin flux into the food web may occur in protected, low turbulence environments, where salinities are high, nutrients abundant, and water temperatures are between 24 and 31 °C.

In cultured-based studies, Lechat et al. [64] showed that variations in media (use of media with a high metallic salt content) resulted in increased ciguatoxin production, whereas Lartigue et al. [32] claimed that CTX production in Caribbean *G. toxicus* clones was not affected by organic (nitrate or ammonium) or inorganic (urea, free amino acids or putrescine) nitrogen sources. In the present study, we were able to confirm that the use of either nitrate or urea in the growth medium had no significant effect on the overall toxin yield in *G. polynesiensis* cultures, but did result in a substantial increase of quantifiable analogs, from three to a maximum of eight P-CTX analogs depending on the strain considered. The reason for this drastic change in *G. polynesiensis* toxin profile following the shift to urea in the culture medium is unclear. Epiphytic/benthic dinoflagellates have classical nitrogen requirements: they are known to readily utilize nitrate and ammonium with some taxa showing an apparent preference for the latter [81,82]. Both Bomber [83] and Lartigue et al. [32] found an increase in cellular ciguatoxicity of *Gambierdiscus* with increasing NH_4^+, which might indicate a functional role of this compound in the biosynthesis of CTXs. However, the potential role played by intracellular phosphorus utilization in toxin synthesis should not be overlooked [84,85]. Concerning the influence of N:P ratio on toxin production, Durand-Clement [65] indicated that overall toxin production remained constant with nutrient levels, whereas Sperr and Doucette [67] concluded that CTX production can be determined by high N:P ratio (i.e., N:P ≥ 30:1) in Caribbean strains of *G. toxicus*.

It should be noted that many of these earlier studies have not evaluated toxicity with CTX-specific protocols and that none of these studies have evaluated individual toxins in the response of *Gambierdiscus* clones to different nutrient regimes. Indeed, quantitation methods used in studies by Durand-Clement [65] and Sperr and Doucette [67] were based on an overall toxins concentration

estimate (i.e., crude extract evaluated by mouse bioassay) which is not directly comparable with our use of LC-MS/MS method in the present study, which is more specific for P-CTX detection and in which each known P-CTX analog concentration is investigated. Another issue which makes comparisons with previous studies difficult is that much of the early work with *Gambierdiscus* referred solely to *G. toxicus*, while it is now well established that multiple species exist within this genus.

Dinoflagellates in the genus *Gambierdiscus* are the source of a number of non-structurally related groups of secondary metabolites of interest (see Reference [20] for a review and references therein). Of these, CTXs are by far the most studied group due to their direct involvement in ciguatera poisoning. At present, only P-CTX3C is commercially available for detection and quantitation purposes. The current scarcity of CTX analytical standards constitutes a serious hindrance to the quantitation of these compounds in seafood and the implementation of food safety surveillance programs. Hence, significant efforts have been devoted in the past decade to determine which species of *Gambierdiscus* are more toxic than the others, and assess the variations in toxin production in response to different stressors (see References [27,28] for reviews and references therein). Not all species of *Gambierdiscus* are known to produce CTXs. Among the eighteen species described to date, *G. polynesiensis*—a species allegedly endemic to the Pacific Ocean—is recognized as the highest CTX producer with published toxicity data ranging from 1.2 up to 20.9 pg P-CTX3C eq cell^{-1} [17,19,30,33,86]. In the present study, we showed that *G. polynesiensis* cellular toxicity could vary by up to 46 orders of magnitude in French Polynesian clones from geographically distinct origins. Although part of these variations was attributable to different culture conditions and growth stage, these observations highlight the fact that an adequate selection of the appropriate candidate-strains is preponderant in R&D programs aiming at the custom production of high-value CTX standards. Of note, this strain-dependent production of CTXs demonstrated in *G. polynesiensis* is also well established in other species such as *G. australes*, *G. balechii*, *G. pacificus*, *G. toxicus*, *F. paulensis*, and *F. ruetzleri* [3,9,15,74,75,87,88]. In addition, numerous studies have demonstrated that cellular toxin levels often increase with the age of the culture [17,29,32,33,67], implying that the culture conditions for optimal growth of *Gambierdiscus* are likely to differ from the ones ensuring optimal toxin production. The LC-MS/MS data presented here (and those of Longo et al. [33]) also revealed that an increase in the number of CTXs analogs produced in cultures generally takes place from the exponential to the stationary phase. Finally, another important issue that needs to be considered in toxin production programs is the gradual drop in toxin yields likely to affect high toxin-producing clones over time, as already reported in *G. polynesiensis* clones isolated from the Cook Islands and French Polynesia, respectively [33,89]. These observations suggest that high toxin production may not be a stable characteristic in long-term cultures of *G. polynesiensis*, contradicting earlier observations by Chinain et al. [17].

4. Conclusions

This study has provided clear evidence that manipulation of environmental variables can result in enhanced growth and toxicity (types of P-CTX analogs in addition to amounts) in *G. polynesiensis*. However, the importance of other factors such as culture age, clonal differences, and harvest time should not be overlooked if the pursued objective is to maximize toxin yield and diversity. More widely, increasing attention is paid to the secondary metabolites produced by microalgae, particularly dinoflagellates, due to their potential uses in the biological, biomedical, and toxicological fields [90]. *Gambierdiscus* is no exception to the rule. Further studies are needed on the other species of *Gambierdiscus* also regarded as major contributors to toxin flux in CP-prone areas, e.g., *G. excentricus*, *G. australes*, and possibly *G. silvae* [14,16,91], thereby providing important information that can greatly benefit current efforts to establish a sustainable source of CTX standards. Indeed, numerous studies have shown the ability of *Gambierdiscus* to produce a wide variety of P-CTX analogs as well as their bioaccumulation at each trophic level, from herbivorous to carnivorous fish or marine invertebrates [28,92]. However, despite the identification of several C-CTX and I-CTX analogs in carnivorous fish and sharks [93–100], no study has yet been able to demonstrate the toxin production of C-CTXs or I-CTXs in *Gambierdiscus*.

This fact is of major importance as toxin-producing in vitro cultures can provide a continuous source of CTX standards. Easier access to a variety of CTX standards will undoubtedly help improve the testing capabilities in ciguatera management and hence, accelerate the implementation of food safety surveillance programs globally. In this process, studies on the complementarity between several detection methods classically used in CP risk monitoring program (e.g., LC-MS/MS, CBA-N2a, and Receptor Binding Assay) need to be pursued [92,101–103] to better understand quantitation differences across methods and laboratories, and hence foster trans-regional comparative studies on ciguatera. Concurrently, the recent development of metabolomics appears as a unique opportunity to conduct in-depth investigations on the chemodiversity of these dinoflagellates, in order to, e.g., describe new compounds (including toxins), assess the variations of their productions in response to different stressors, or identify chemical markers at different taxonomic levels [103].

5. Materials and Methods

5.1. Source of G. polynesiensis Isolates

The four clones of *G. polynesiensis* used in this study (RIK7, NHA4, RAI-1, and RG92), originate from different islands of French Polynesia, i.e., Mangareva Island (Gambier archipelago), Nuku Hiva Island (Marquesas archipelago), Raivavae Island (Australes archipelago), and Rangiroa atoll (Tuamotu archipelago) (Table 4). These clones were isolated from macro-algal and/or artificial substrate (window screens) samples collected following the methods described by Chinain et al. [17] and Tester et al. [104], respectively. All four strains are part of the Laboratory of Marine Biotoxins culture collection at the *Institut Louis Malardé* (Tahiti, French Polynesia), where cultures are deposited.

Table 4. Geographic origin and year of isolation of the four *G. polynesiensis* clones selected for this study.

ID Code	RIK7	NHA4	RAI-1	RG92
Year of isolation	2013	2015	2008	1992
Archipelago	Gambier	Marquesas	Australes	Tuamotu
Island	Mangareva	Nuku Hiva	Raivavae	Rangiroa

5.2. In Vitro Cultures

All four *G. polynesiensis* clones selected for this study had been maintained in natural seawater (pH = 8.4 on average) supplemented with f_{10k} medium [105], at 26 ± 1 °C under 60 ± 10 µmol photons m^{-2} s^{-1} irradiance (12 h light:12 h dark photoperiod) for years prior to experimentation. When culture conditions were changed, clones were acclimated for 40 days to the ambient regime prior to growth experiments.

Six consecutive experiments were conducted, three using nitrate as N source at three distinct pH, and the other three, using urea (Sigma-Aldrich, St. Louis, MO, USA). For each experiment at a given pH, the four strains were tested under two N:P ratios and at three culture ages in two technical replicates.

Regarding the two N:P ratios tested, i.e., N:P of 24 and 48, the composition of the f_{10k} medium was modified accordingly. Practically, N and P concentrations were 0.05 µM and 2.1×10^{-3} µM in 24N:1P experiments respectively, which are consistent with concentrations observed in oligotrophic ocean water [106]. In 48N:1P experiments, concentrations used for N and P elements were 0.1 µM and 2.1×10^{-3} µM, respectively. Even though the N:P ratio 24 is significantly higher than the Redfield ratio (16), it was used as the standard condition since it has been used for many years in the maintenance of cultures at Institut Louis Malardé. It was also verified to be locally found in the Polynesian coastal environment [107,108] and to be comprised between the median N:P ratio measured in warm oligotrophic mid-latitude oceans, i.e., 28N:1P [109], and in global ocean water, i.e., 22N:1P [106].

In pH experiments, the pH in culture flasks was monitored twice a day and stabilized at three different values, i.e., 8.4, 8.2, and 7.9, by direct addition of a few drops of 1 M HCl into the culture medium. Overnight, a +0.3 pH unit variation was observed on average and daily corrected.

Overall, different combinations of culture conditions under varying pH, N:P ratio, and nitrogen sources (N = 144 combinations) were thus tested on *G. polynesiensis* strains. To this end, batch cultures of each of the four clones were established in technical duplicates by inoculating 40,000 cells into 200 mL of seawater supplemented with 200 µL of f_{10k} in 250 mL Erlenmeyer flasks. Seawater was previously aged for 1 month, filtered through a 0.2 µm GF/F Whatman filters (Dutscher, Brumath, France), and sterilized by autoclaving for 20 mn at 120 °C. All cultures were grown in an incubator (ThermoStable IR250, Wigel, Eichel, Germany). Flasks were incubated at randomly determined sites in the incubator and flask position was changed on a daily basis.

5.3. Growth Rate

Growth rate was assessed using in vivo fluorescence following the method described in Longo et al. [33]. Briefly, cell growth was assessed by measuring chlorophyll fluorescence at 485 nm, at two-day intervals, using a spectrophotometer (Victor X2, PerkinElmer, Waltham, MA, USA). To limit error during fluorescence measurements, cultures were fully mixed prior to fluorescence reading, then a 100 µL aliquot of each culture was deposited in 96-well plates, where cells were lysed by the addition of 100 µL dimethyl sulfoxide (DMSO; n = 3 wells per batch culture). Five fluorescence readings were performed on each well.

Growth rates (µ) were determined using the following Equation (1):

$$\mu = [\ln^*(rfu_{t1}/rfu_{t0})]/[\ln(2) * (t_1 - t_0)] \quad (1)$$

in which µ (division day^{-1}) is the growth rate, and rfu_{t1} and rfu_{t0} represent the fluorescence measured at times t_1 (days) and t_0 respectively, corresponding to the exponential growth phase portion of the growth curve.

5.4. Cells Harvest and Toxin Extraction

Cells were harvested at D30 post-inoculation. Prior to cell harvest, the total cell yield was determined by automated counting using a Multisizer III^{TM} particle counter (Beckman Coulter, Inc., Brea, CA, USA). Cultures were harvested by filtration onto a 40 µm sieve in their late exponential, early stationary, and senescence growth phase (i.e., at D10, D21, and D30 post-inoculation, respectively). Each filter was then transferred into a 50 mL Greiner tube using seawater, and centrifuged at 2800× *g* for 2 min. After discarding the supernatants, filters were freeze-dried for 20 h at −20 °C, 1 mbar, then 4 h at −60 °C, 0.01 mbar (Martin Christ, Beta 1–8 LDplus, Osterode am Harz, Germany). Each sample was then stored at −20 °C until further extraction for toxicity screening.

G. polynesiensis cells were extracted by adding 20 mL of methanol (MeOH) directly into the tubes containing each freeze-dried cell sample. Tubes were then vortexed for a few seconds and then placed in an ultrasound tank for one hour. Following a centrifugation step at 2800× *g* for 10 min, the resulting supernatant was recovered in a 250 mL flask. This extraction step was repeated once in MeOH and then once in aqueous methanol (MeOH: H_2O 1:1). The three supernatants were further pooled and dried under vacuum using a rotary evaporator (Rotavapor RII, Büchi, Flawil, Switzerland), and the resulting crude cellular extract suspended in 4 mL of pure methanol.

Half of this solution (2 mL MeOH) was filtered through a Sartorius filter (3 cm diameter, 0.45 µm porosity), then evaporated under nitrogen to dryness to obtain a crude extract destined for the LC-MS/MS analysis. In total, 288 samples have been generated and analyzed.

5.5. Liquid Chromatography Coupled with Tandem Mass Spectrometry (LC-MS/MS) Analysis

The toxin screening of *G. polynesiensis* cell extracts was performed using a Ultra High Performance Liquid Chromatography (UHPLC) system (UFLC Nexera, SHIMADZU, Kyoto, Japan) coupled to a hybrid triple quadrupole-linear ion-trap API4000 QTRAP mass spectrometer (SCIEX, Redwood City, CA, USA) equipped with a TurboV® electrospray ionization source (ESI). The instrument control,

data processing, and analysis were conducted using Analyst software 1.6.2 (Sciex, CA, USA). A linear gradient using water as eluent A and MeOH as eluent B, both eluents containing 2 mM ammonium formate and 50 mM formic acid, was run on a Zorbax Eclipse Plus C18 column, 50*2.1 mm, 1.8 µm, 95 Å (Agilent Technologies, Santa Clara, CA, USA). The flow rate was 0.4 mL min^{-1}, the injection volume was 5 µL, and the column temperature 40 °C.

The elution gradient was as follows: 78% B to 88% B from 0 to 10 min, hold at 88% B for 4 min, decrease from 88% to 78% in 1 min, and hold for 5 min at 78% B. Mass spectrometric detection was performed in positive ionization mode using Multiple Reaction Monitoring (MRM) scanning.

The optimized ESI+ parameters were set as follows: curtain gas at 25 pounds per square inch (psi), ion spray at 5500 V, turbo gas temperature at 300 °C, gas 1 and 2 were set at 40 and 60 psi respectively, and an entrance potential at 10 V.

MRM acquisition method was created using the scheduled MRM algorithm. This algorithm optimizes dwell times and cycle time to provide better peak detection and improve reproducibility. A detection window of 90 s and a target scan time of 2 s were chosen for the MRM method. In order to quantify P-CTX analog, a calibration solution of P-CTX3C (Wako, Japan) was prepared in MeOH, with concentration ranging from 12 to 200 ng mL^{-1}. LOQ is determined to 10 ng mL^{-1} and LOD to 5 ng mL^{-1}. Due to the lack of analytical standards, contents of each P-CTX analog were quantified from the P-CTX3C calibration curve prepared, assuming equivalent molar response. The sum of the estimated concentrations of all analogs allowed characterization of the respective toxin profiles and calculation of the overall cellular toxin content (expressed in pg P-CTX3C eq $cell^{-1}$).

5.6. Statistical Analyses

To determine whether growth rates and toxin profiles differences observed between the different culture conditions tested (i.e., different combinations of pH and N:P ratio values as well as the use of different nitrogen sources in the growth medium) were statistically significant, standard deviations (SD) and 95% confidence interval (CI; p-value < 0.05) were calculated. Then, an analysis of variance (ANOVA) (normality, homoscedasticity) was performed using RStudio v1.0.153 (Boston, MA, USA) or GraphPad Prism v8.1.2. (GraphPad, San Diego, CA, USA). In order to ensure more robust analyses about the general effects on toxin production, data were merged to increase sample size and allow parametric analysis, even if normality sometimes was not verified. By way of example, to study the effect of geographic origin on P-CTX amounts, results obtained for the 288 samples were grouped into 4 datasets (with n = 72 per dataset) corresponding to the four *G. polynesiensis* clones, regardless of the pH, cell age, and N levels and source. A similar rationale was applied to assess the effects of pH (n = 24), culture age (n = 24), N:P ratio and N source (n = 18) on P-CTX levels of each clone.

Supplementary Materials: The following are available online at http://www.mdpi.com/2072-6651/12/12/767/s1, Table S1. List of all *m/z* transitions required in scheduled MRM LC-MS/MS analysis to detect and quantify P-CTX compounds.

Author Contributions: Conceptualization, methodology and validation, S.L., P.H., and M.C.; formal analyses, S.L., and M.S.; data curation, S.L.; writing-original draft preparation, S.L., and M.C.; writing-review and editing, S.L., M.S., H.T.D., P.H., and M.C.; supervision, M.C, P.H., M.S. and H.T.D.; project administration, M.C.; funding acquisition, M.C. All authors have read and agreed to the published version of the manuscript.

Funding: This work was conducted in the framework of the GLOBALCIG PhD program which was supported in part by funds from the Délégation à la Recherche de la Polynésie française (Conv. N° 02813/MTF/REC of April 28th 2017) and the University of French Polynesia.

Acknowledgments: The authors wish to thank Philippe Cruchet, Kévin Henry, and André Ung from LBM for their technical assistance, as well as the three anonymous reviewers who helped improving the manuscript.

Conflicts of Interest: The authors declare no conflict of interest. The funders had no role in the design of the study; in the collection, analyses, or interpretation of data; in the writing of the manuscript; or in the decision to publish the results.

References

1. Anderson, D.M.; Lobel, P.S. The continuing enigma of ciguatera. *Biol. Bull.* **1987**, *172*, 89–107. [CrossRef]
2. Ikehara, T.; Kuniyoshi, K.; Oshiro, N.; Yasumoto, T. Biooxidation of ciguatoxins leads to species-specific toxin profiles. *Toxins* **2017**, *9*, 205. [CrossRef] [PubMed]
3. Chinain, M.; Faust, M.; Pauillac, S. Morphology and molecular analyses of three toxic species of *Gambierdiscus* (Dinophyceae): *G. pacificus*, sp. nov., *G. australes*, sp. nov., and *G. polynesiensis*, sp. nov. *J. Phycol.* **1999**, *35*, 1282–1296. [CrossRef]
4. Fraga, S.; Rodríguez, F. Genus *Gambierdiscus* in the Canary Islands (NE Atlantic Ocean) with description of *Gambierdiscus silvae* sp. nov., a new potentially toxic epiphytic benthic dinoflagellate. *Protist* **2014**, *165*, 839–853. [CrossRef] [PubMed]
5. Fraga, S.; Rodríguez, F.; Riobó, P.; Bravo, I. *Gambierdiscus balechii* sp. nov (Dinophyceae), a new benthic toxic dinoflagellate from the Celebes Sea (SW Pacific Ocean). *Harmful Algae* **2016**, *58*, 93–105. [CrossRef]
6. Smith, K.F.; Rhodes, L.; Verma, A.; Curley, B.G.; Harwood, D.T.; Kohli, G.S.; Solomona, D.; Rongo, T.; Munday, R.; Murray, S.A. A new *Gambierdiscus* species (Dinophyceae) from Rarotonga, Cook Islands: *Gambierdiscus cheloniae* sp. nov. *Harmful Algae* **2016**, *60*, 45–56. [CrossRef]
7. Jang, S.H.; Jeong, H.J.; Yoo, Y.D. *Gambierdiscus jejuensis* sp. nov., an epiphytic dinoflagellate from the waters of Jeju Island, Korea, effect of temperature on the growth, and its global distribution. *Harmful Algae* **2018**, *80*, 149–157. [CrossRef]
8. Litaker, R.W.; Vandersea, M.W.; Faust, M.A.; Kibler, S.R.; Chinain, M.; Holmes, M.J.; Holland, W.C.; Tester, P.A. Taxonomy of *Gambierdiscus* including four new species, *Gambierdiscus caribaeus*, *Gambierdiscus carolinianus*, *Gambierdiscus carpenteri* and *Gambierdiscus ruetzleri* (Gonyaulacales, Dinophyceae). *Phycologia* **2009**, *48*, 344–390. [CrossRef]
9. Nishimura, T.; Sato, S.; Tawong, W.; Sakanari, H.; Yamaguchi, H.; Adachi, M. Morphology of *Gambierdiscus scabrosus* sp. nov. (Gonyaulacales): A new epiphytic toxic dinoflagellate from coastal areas of Japan. *J. Phycol.* **2014**, *50*, 506–514. [CrossRef]
10. Rhodes, L.L.; Smith, K.F.; Verma, A.; Curley, B.G.; Harwood, D.T.; Murray, S.; Kohli, G.S.; Solomona, D.; Rongo, T.; Munday, R.; et al. A new species of *Gambierdiscus* (Dinophyceae) from the south-west Pacific: *Gambierdiscus honu* sp. nov. *Harmful Algae* **2017**, *65*, 61–70. [CrossRef]
11. Kretzschmar, A.L.; Larsson, M.E.; Hoppenrath, M.; Doblin, M.A.; Murray, S.A. Characterisation of two toxic *Gambierdiscus* spp. (Gonyaulacales, Dinophyceae) from the Great Barrier Reef (Australia): *G. lewisii* sp. nov. and *G. holmesii* sp. nov. *Protist* **2019**, *170*, 125699. [CrossRef] [PubMed]
12. Adachi, R.; Fukuyo, Y. The thecal structure of a marine toxic dinoflagellate *Gambierdiscus toxicus* gen. et sp. nov. collected in a ciguatera-endemic area. *Bull. Jpn. Soc. Sci. Fish.* **1979**, *45*, 67–71. [CrossRef]
13. Faust, M.A. Observation of sand-dwelling toxic dinoflagellates (Dinophyceae) from widely differing sites, including two new species. *J. Phycol.* **1995**, *31*, 996–1003. [CrossRef]
14. Fraga, S.; Rodríguez, F.; Caillaud, A.; Diogène, J.; Raho, N.; Zapata, M. *Gambierdiscus excentricus* sp. nov. (Dinophyceae), a benthic toxic dinoflagellate from the Canary Islands (NE Atlantic Ocean). *Harmful Algae* **2011**, *11*, 10–22. [CrossRef]
15. Litaker, R.W.; Holland, W.C.; Hardison, D.R.; Pisapia, F.; Hess, P.; Kibler, S.R.; Tester, P.A. Ciguatoxicity of *Gambierdiscus* and *Fukuyoa* species from the Caribbean and Gulf of Mexico. *PLoS ONE* **2017**, *12*, e0185776. [CrossRef]
16. Pisapia, F.; Holland, W.C.; Hardison, D.R.; Litaker, R.W.; Fraga, S.; Nishimura, T.; Adachi, M.; Nguyen-Ngoc, L.; Séchet, V.; Amzil, Z.; et al. Toxicity screening of 13 *Gambierdiscus* strains using neuro-2a and erythrocyte lysis bioassays. *Harmful Algae* **2017**, *63*, 173–183. [CrossRef]
17. Chinain, M.; Darius, H.T.; Ung, A.; Cruchet, P.; Wang, Z.; Ponton, D.; Laurent, D.; Pauillac, S. Growth and toxin production in the ciguatera-causing dinoflagellate *Gambierdiscus polynesiensis* (Dinophyceae) in culture. *Toxicon* **2010**, *56*, 739–750. [CrossRef]
18. Barton, E.D.; Tanner, P.; Turchen, S.G.; Tunget, C.L.; Manoguerra, A.; Clark, R.F. Ciguatera fish poisoning a Southern California epidemic. *West. J. Med.* **1995**, *163*, 31–35.
19. Chinain, M.; Germain, M.; Deparis, X.; Pauillac, S.; Legrand, A.-M. Seasonal abundance and toxicity of the dinoflagellate *Gambierdiscus* spp. (Dinophyceae), the causative agent of ciguatera in Tahiti, French Polynesia. *Mar. Biol.* **1999**, *135*, 259–267. [CrossRef]

20. Tosteson, T.R. Caribbean ciguatera: A changing paradigm. *Rev. Biol. Trop.* **2004**, *52*, 109–113.
21. Llewellyn, L.E. Revisiting the association between sea surface temperature and the epidemiology of fish poisoning in the South Pacific: Reassessing the link between ciguatera and climate change. *Toxicon* **2010**, *56*, 691–697. [CrossRef] [PubMed]
22. Tester, P.A.; Feldman, R.L.; Nau, A.W.; Kibler, S.R.; Litaker, W.R.; Litaker, R.W. Ciguatera fish poisoning and sea surface temperatures in the Caribbean Sea and the West Indies. *Toxicon* **2010**, *56*, 698–710. [CrossRef] [PubMed]
23. Tester, P.A.; Berdalet, E.; Litaker, R.W. Climate change and harmful benthic microalgae. *Harmful Algae* **2020**, *91*, 101655. [CrossRef] [PubMed]
24. Chinain, M.; Gatti, C.M.; Darius, H.T.; Quod, J.P.; Tester, P.A. Ciguatera Poisonings: A global review of occurences and trends. *Harmful Algae* **2020**. [CrossRef]
25. Hales, S.; Weinstein, P.; Woodward, A. Ciguatera (Fish Poisoning), El Niño, and Pacific Sea Surface Temperature. *Ecosyst. Health* **1999**, *5*, 20–25. [CrossRef]
26. Gingold, D.B.; Strickland, M.J.; Hess, J.J. Ciguatera fish poisoning and climate change: Analysis of national poison center data in the United States, 2001–2011. *Environ. Health Perspect.* **2014**, *122*, 580–586. [CrossRef]
27. Parsons, M.L.; Aligizaki, K.; Dechraoui Bottein, M.; Fraga, S.; Morton, S.L.; Penna, A.; Rhodes, L. *Gambierdiscus* and *Ostreopsis*: Reassessment of the state of knowledge of their taxonomy, geography, ecophysiology, and toxicology. *Harmful Algae* **2012**, *14*, 107–129. [CrossRef]
28. Chinain, M.; Gatti, C.M.; Roué, M.; Darius, H.T. Ciguatera-causing dinoflagellates in the genera *Gambierdiscus* and *Fukuyoa*: Distribution, ecophysiology and toxicology. In *Dinoflagellates: Morphology, Life History and Ecological Significance*; Subba Rao, D.V., Ed.; Nova Science: New York, NY, USA, 2020; pp. 405–457.
29. Vacarizas, J.; Benico, G.; Austero, N.; Azanza, R. Taxonomy and toxin production of *Gambierdiscus carpenteri* (Dinophyceae) in a tropical marine ecosystem: The first record from the Philippines. *Mar. Pollut. Bull.* **2018**, *137*, 430–443. [CrossRef]
30. Rhodes, L.; Harwood, T.; Smith, K.; Argyle, P.; Munday, R. Production of ciguatoxin and maitotoxin by strains of *Gambierdiscus australes*, *G. pacificus* and *G. polynesiensis* (Dinophyceae) isolated from Rarotonga, Cook Islands. *Harmful Algae* **2014**, *39*, 185–190. [CrossRef]
31. Kibler, S.R.; Litaker, R.W.; Holland, W.C.; Vandersea, M.W.; Tester, P.A. Growth of eight *Gambierdiscus* (Dinophyceae) species: Effects of temperature, salinity and irradiance. *Harmful Algae* **2012**, *19*, 1–14. [CrossRef]
32. Lartigue, J.; Jester, E.L.E.; Dickey, R.W.; Villareal, T.A. Nitrogen source effects on the growth and toxicity of two strains of the ciguatera-causing dinoflagellate *Gambierdiscus toxicus*. *Harmful Algae* **2009**, *8*, 781–791. [CrossRef]
33. Longo, S.; Sibat, M.; Viallon, J.; Darius, H.T.; Hess, P.; Chinain, M. Intraspecific variability in the toxin production and toxin profiles of in vitro cultures of *Gambierdiscus polynesiensis* (Dinophyceae) from French Polynesia. *Toxins* **2019**, *11*, 735. [CrossRef] [PubMed]
34. Zeebe, R.E. History of Seawater Carbonate Chemistry, Atmospheric CO_2, and Ocean Acidification. *Annu. Rev. Earth Planet. Sci.* **2012**, *40*, 141–165. [CrossRef]
35. Doney, S.; Fabry, V.; Feely, R.; Kleypas, J. Ocean acidification: The other CO_2 problem. *Ann. Rev. Mar. Sci.* **2009**, *1*, 169–192. [CrossRef] [PubMed]
36. Gattuso, J.-P.; Magnan, A.; Billé, R.; Cheung, W.W.L.; Howes, E.L.; Joos, F.; Allemand, D.; Bopp, L.; Cooley, S.R.; Eakin, C.M.; et al. Contrasting futures for ocean and society from different anthropogenic CO_2 emissions scenarios. *Science* **2015**, *349*, aac4722. [CrossRef] [PubMed]
37. Bopp, L.; Resplandy, L.; Orr, J.C.; Doney, S.C.; Dunne, J.P.; Gehlen, M.; Halloran, P.; Heinze, C.; Ilyina, T.; Séférian, R.; et al. Multiple stressors of ocean ecosystems in the 21st century: Projections with CMIP5 models. *Biogeosciences* **2013**, *10*, 6225–6245. [CrossRef]
38. Solomon, S. IPCC (2007): Climate Change The Physical Science Basis. In Proceedings of the 2007 American Geophysical Union Fall Meeting, San Francisco, CA, USA, 10–14 December 2007.
39. Howarth, R.W. Coastal nitrogen pollution: A review of sources and trends globally and regionally. *Harmful Algae* **2008**, *8*, 14–20. [CrossRef]
40. Lassus, P.; Chomérat, N.; Hess, P.; Nézan, E. *Micro-Algues Toxiques et Nuisibles de L'océan Mondial*; COI Manuels et Guides, 68; International Society for the Study of Harmful Algae, Ed.; ISSHA: Copenhagen, Denmark, 2016.

41. Elser, J.J.; Bracken, M.E.S.; Cleland, E.E.; Gruner, D.S.; Harpole, W.S.; Hillebrand, H.; Ngai, J.T.; Seabloom, E.W.; Shurin, J.B.; Smith, J.E. Global analysis of nitrogen and phosphorus limitation of primary producers in freshwater, marine and terrestrial ecosystems. *Ecol. Lett.* **2007**, *10*, 1135–1142. [CrossRef]
42. Rosenberg, R.; Loo, L.-O. Marine eutrophication induced oxygen deficiency: Effects on soft bottom fauna, Western Sweden. *Ophelia* **1988**, *29*, 213–225. [CrossRef]
43. Rabalais, N.N.; Turner, R.E.; Díaz, R.J.; Justić, D. Global change and eutrophication of coastal waters. *ICES J. Mar. Sci.* **2009**, *66*, 1528–1537. [CrossRef]
44. Rodier, M.; Longo, S.; Henry, K.; Ung, A.; Lo-Yat, A.; Darius, H.T.; Viallon, J.; Beker, B.; Delesalle, B.; Chinain, M. Diversity and toxic potential of algal bloom-forming species from Takaroa lagoon (Tuamotu, French Polynesia): A field and mesocosm study. *Aquat. Microb. Ecol.* **2019**, *83*, 15–34. [CrossRef]
45. Carpenter, S.R.; Caraco, N.F.; Correll, D.L.; Howarth, R.W.; Sharpley, A.N.; Smith, V.H. Nonpoint pollution of surface waters with Phosphorus and Nitrogen. *Ecol. Appl.* **1998**, *8*, 559–568. [CrossRef]
46. Wilson, M.A.; Carpenter, S.R. Economic Valuation of Freshwater Ecosystem Services in the United States: 1971–1997. *Ecol. Appl.* **1999**, *9*, 772–783.
47. Dufour, P.; Berland, B. Nutrient control of phytoplanktonic biomass in atoll lagoons and Pacific ocean waters: Studies with factorial enrichment bioassays. *J. Exp. Mar. Biol. Ecol.* **1999**, *234*, 147–166. [CrossRef]
48. Dufour, P.; Charpy, L.; Bonnet, S.; Garcia, N. Phytoplankton nutrient control in the oligotrophic South Pacific sub tropical gyre (Tuamotu archipelago). *Mar. Ecol. Prog. Ser.* **1999**, *179*, 285–290. [CrossRef]
49. Charpy, L.; Rodier, M.; Fournier, J.; Langlade, M.J.; Gaertner-Mazouni, N. Physical and chemical control of the phytoplankton of Ahe lagoon, French Polynesia. *Mar. Pollut. Bull.* **2012**, *65*, 471–477. [CrossRef]
50. Stollsteiner, P. *BRGM, Programme ARAI 3. Erosion, transport solide et dynamique torrentielle des rivières de Polynésie française*; Rapport final BRGM/RP-60251-FR; BRGM: Tahiti, French Polynesia, 2011; 140p.
51. Gaertner-Mazouni, N.; Lacoste, E.; Bodoy, A.; Peacock, L.; Rodier, M.; Langlade, M.J.; Orempuller, J.; Charpy, L. Nutrient fluxes between water column and sediments: Potential influence of the pearl oyster culture. *Mar. Pollut. Bull.* **2012**, *65*, 500–505. [CrossRef]
52. Raven, J.A.; Gobler, C.J.; Hansen, P.J. Dynamic CO_2 and pH levels in coastal, estuarine, and inland waters: Theoretical and observed effects on harmful algal blooms. *Harmful Algae* **2020**, *91*, 101594. [CrossRef]
53. Flores-Moya, A.; Rouco, M.; García-Sánchez, M.J.; García-Balboa, C.; González, R.; Costas, E.; López-Rodas, V. Effects of adaptation, chance, and history on the evolution of the toxic dinoflagellate *Alexandrium minutum* under selection of increased temperature and acidification. *Ecol. Evol.* **2012**, *2*, 1251–1259. [CrossRef]
54. Hattenrath-Lehmann, T.K.; Smith, J.L.; Wallace, R.B.; Merlo, L.R.; Koch, F.; Mittelsdorf, H.; Goleski, J.A.; Anderson, D.M.; Gobler, C.J. The effects of elevated CO_2 on the growth and toxicity of field populations and cultures of the saxitoxin-producing dinoflagellate *Alexandrium fundyense*. *Limnol. Oceanogr.* **2015**, *60*, 198–214. [CrossRef]
55. Tatters, A.O.; Fu, F.X.; Hutchins, D.A. High CO_2 and silicate limitation synergistically increase the toxicity of *Pseudo-nitzschia fraudulenta*. *PLoS ONE* **2012**, *7*, e32116. [CrossRef] [PubMed]
56. Sun, J.; Hutchins, D.A.; Feng, Y.; Seubert, E.L.; Caron, D.A.; Fu, F.X. Effects of changing pCO_2 and phosphate availability on domoic acid production and physiology of the marine harmful bloom diatom *Pseudo-nitzschia multiseries*. *Limnol. Oceanogr.* **2011**, *56*, 829–840. [CrossRef]
57. Yasumoto, T.; Inoue, A.; Ochi, T.; Fujimoto, K.; Oshima, Y.; Fukuyo, Y.; Adachi, R.; Bagnis, R. Environmental studies on a toxic dinoflagellate responsible for ciguatera. *Bull. Jpn. Soc. Sci. Fish.* **1980**, *46*, 1397–1404. [CrossRef]
58. Parsons, M.L.; Preskitt, L.B. A survey of epiphytic dinoflagellates from the coastal waters of the island of Hawaii. *Harmful Algae* **2007**, *6*, 658–669. [CrossRef]
59. Ichinotsubo, D.; Asahina, A.Y.; Titus, E.; Chun, S.; Hong, T.W.P.; Shirai, J.L.; Hokama, Y. Survey for ciguatera fish poisoning in West Hawaii. *Mem. Queensl. Mus.* **1994**, *34*, 513–522.
60. Loeffler, C.R.; Richlen, M.L.; Brandt, M.E.; Smith, T.B. Effects of grazing, nutrients, and depth on the ciguatera-causing dinoflagellate *Gambierdiscus* in the US Virgin Islands. *Mar. Ecol. Prog. Ser.* **2015**, *531*, 91–104. [CrossRef]
61. Okolodkov, Y.; Merino-Virgilio, F.; Aké-Castillo, J.; Aguilar-Trujillo, A.; Espinosa-Matías, S.; Herrera-Silveira, J. Seasonal changes in epiphytic dinoflagellate assemblages near the northern coast of the Yucatan peninsula, Gulf of Mexico. *Acta Bot. Mex.* **2014**, *107*, 121–151. [CrossRef]

62. Carlson, R.D.; Tindall, D.R. Distribution and periodicity of toxic dinoflagellates in the Virgin Islands. In *Toxic Dinoflagellates*; Anderson, D.M., White, A.W., Baden, D.G., Eds.; Elsevier: Amsterdam, The Netherlands, 1985; pp. 171–176.
63. Hurbungs, M.D.; Jayabalan, N.; Chineah, V. Seasonal distribution of potentially toxic benthic dinoflagellates in the lagoon of Trou aux Biches, Mauritius. In Proceedings of the 5th Annual Meeting of Agricultural Scientists, Reduit, Mauritius, 3–4 May 2001; Lalouette, J.A., Bachraz, D.Y., Eds.; The Food and Agricultural Research Council: Reduit, Mauritius, 2002; pp. 211–217.
64. Lechat, I.; Partenski, F.; Chungue, E. *Gambierdiscus toxicus*: Culture and toxin production. In Proceedings of the 5th International Coral Reef Congress, Tahiti, French Polynesia, 27 May–1 June 1985; Volume 4, pp. 443–448.
65. Durand-Clement, M. A study of toxin production by *Gambierdiscus toxicus* in culture. *Toxicon* **1986**, *24*, 1153–1157. [CrossRef]
66. Durand-Clement, M. Study of production and toxicity of cultured *Gambierdiscus toxicus*. *Biol. Bull.* **1987**, *172*, 108–121. [CrossRef]
67. Sperr, A.E.; Doucette, G. Variation in growth rate and ciguatera toxin production among geographically distinct isolates of *Gambierdiscus toxicus*. In *Harmful and Toxic Algal Blooms*; Intergovernmental Oceanographic Commission of UNESCO: Paris, France, 1996; pp. 309–312.
68. Darius, H.T.; Roué, M.; Sibat, M.; Viallon, J.; Gatti, C.M.I.; Vandersea, M.W.; Tester, P.A.; Litaker, R.W.; Amzil, Z.; Hess, P.; et al. *Tectus niloticus* (Tegulidae, Gastropod) as a novel vector of ciguatera poisoning: Detection of pacific ciguatoxins in toxic samples from Nuku Hiva Island (French Polynesia). *Toxins* **2018**, *10*, 2. [CrossRef]
69. Hansen, P.; Lundholm, N.; Rost, B. Growth limitation in marine red-tide dinoflagellates: Effects of pH versus inorganic carbon availability. *Mar. Ecol. Prog. Ser.* **2007**, *334*, 63–71. [CrossRef]
70. Hinga, K.A. Co-occurrence of dinoflagellate blooms and high pH in marine enclosures. *Mar. Ecol. Prog. Ser.* **1992**, *86*, 181–187. [CrossRef]
71. Lundholm, N.; Hansen, P.J.; Kotaki, Y. Effect of pH on growth and domoic acid production by potentially toxic diatoms of the genera *Pseudo-nitzschia* and *Nitzschia*. *Mar. Ecol. Prog. Ser.* **2004**, *273*, 1–15. [CrossRef]
72. Schippers, P.; Lürling, M.; Scheffer, M. Increase of atmospheric CO_2 promotes phytoplankton productivity. *Ecol. Lett.* **2004**, *7*, 446–451. [CrossRef]
73. Dai, X.; Mak, Y.L.; Lu, C.K.; Mei, H.H.; Wu, J.J.; Lee, W.H.; Chan, L.L.; Lim, P.T.; Mustapa, N.I.; Lim, H.C.; et al. Taxonomic assignment of the benthic toxigenic dinoflagellate *Gambierdiscus* sp. type 6 as *Gambierdiscus balechii* (Dinophyceae), including its distribution and ciguatoxicity. *Harmful Algae* **2017**, *67*, 107–118. [CrossRef]
74. Xu, Y.; Richlen, M.L.; Morton, S.L.; Mak, Y.L.; Chan, L.L.; Tekiau, A.; Anderson, D.M.; Ling, Y.; Lai, L. Distribution, abundance and diversity of *Gambierdiscus* spp. from a ciguatera-endemic area in Marakei, Republic of Kiribati. *Harmful Algae* **2014**, *34*, 56–68. [CrossRef]
75. Chinain, M.; Darius, H.T.; Ung, A.; Tchou Fouc, M.; Revel, T.; Cruchet, P.; Pauillac, S.; Laurent, D. Ciguatera risk management in French Polynesia: The case study of Raivavae Island (Australes Archipelago). *Toxicon* **2010**, *56*, 674–690. [CrossRef]
76. Smith, K.F.; Biessy, L.; Argyle, P.A.; Trnski, T.; Halafihi, T.; Rhodes, L.L. Molecular identification of *Gambierdiscus* and *Fukuyoa* (Dinophyceae) from environmental samples. *Mar. Drugs* **2017**, *15*, 243. [CrossRef]
77. Litaker, R.W.; Vandersea, M.W.; Faust, M.A.; Kibler, S.R.; Nau, A.W.; Holland, W.C.; Chinain, M.; Holmes, M.J.; Tester, P.A. Global distribution of ciguatera causing dinoflagellates in the genus *Gambierdiscus*. *Toxicon* **2010**, *56*, 711–730. [CrossRef]
78. Lyu, Y.; Richlen, M.L.; Sehein, T.R.; Chinain, M.; Adachi, M.; Nishimura, T.; Xu, Y.; Parsons, M.L.; Smith, T.B.; Zheng, T.; et al. LSU rDNA based RFLP assays for the routine identification of *Gambierdiscus* species. *Harmful Algae* **2017**, *66*, 20–28. [CrossRef]
79. Davidson, K.; Gowen, R.J.; Harrison, P.J.; Fleming, L.E.; Hoagland, P.; Moschonas, G. Anthropogenic nutrients and harmful algae in coastal waters. *J. Environ. Manag.* **2014**, *146*, 206–216. [CrossRef] [PubMed]
80. Skinner, M.P.; Lewis, R.J.; Morton, S. Ecology of the ciguatera causing dinoflagellates from the Northern Great Barrier Reef: Changes in community distribution and coastal eutrophication. *Mar. Pollut. Bull.* **2013**, *77*, 210–219. [CrossRef] [PubMed]
81. Bomber, J.W.; Aikman, K. The ciguatera dinoflagellates. *Biol. Ocean* **1989**, *6*, 291–311.

82. Aikman, K.; Tindall, D.; Morton, S. Physiology and potency of the dinoflagellate *Prorocentrum hoffmannianum* (Faust) during one complete growth cycle. In *5th International Conference on Toxic Marine Phytoplankton, Toxic Phytoplankton Blooms in the Sea*; Smayda, T.J., Shimizu, Y., Eds.; Elsevier Science Publishers: New York, NY, USA, 1993; pp. 463–468.
83. Bomber, J.W. Toxinogenesis in dinoflagellate: Genetic and physiological factors. In *Ciguatera Seafood Toxin*; Miller, D.M., Ed.; CRC Press: Boca Raton, FL, USA, 1991; pp. 135–170.
84. Tindall, D.; Morton, S. Community dynamics and physiology of epiphytic/benthic dinoflagellates associated with ciguatera. In *Physiological Ecology of Harmful Algal Blooms*; Anderson, D.M., Cembella, A.D., Hallegraeff, G.M., Eds.; NATO ASI Series; Springer: Berlin, Germany, 1998; Volume 41, pp. 291–313.
85. Hardison, D.R.; Holland, W.C.; McCall, J.R.; Bourdelais, A.J.; Baden, D.G.; Darius, H.T.; Chinain, M.; Tester, P.A.; Shea, D.; Quintana, H.A.F.; et al. Fluorescent receptor binding assay for detecting ciguatoxins in fish. *PLoS ONE* **2016**, *11*, e0153348. [CrossRef]
86. Pawlowiez, R.; Darius, H.T.; Cruchet, P.; Rossi, F.; Caillaud, A.; Laurent, D.; Chinain, M. Evaluation of seafood toxicity in the Australes Archipelago (French Polynesia) using the neuroblastoma cell-based assay. *Food Addit. Contam. A* **2013**, *30*, 567–586. [CrossRef]
87. Gómez, F.; Qiu, D.; Lopes, R.M.; Lin, S. *Fukuyoa paulensis* gen. et sp. nov., a new genus for the globular species of the dinoflagellate *Gambierdiscus* (Dinophyceae). *PLoS ONE* **2015**, *10*, e0119676. [CrossRef]
88. Laza-Martínez, A.; David, H.; Riobó, P.; Miguel, I.; Orive, E. Characterization of a strain of *Fukuyoa paulensis* (Dinophyceae) from the Western Mediterranean Sea. *J. Eukaryot. Microbiol.* **2015**, *63*, 481–497. [CrossRef]
89. Munday, R.; Murray, S.; Rhodes, L.L.; Larsson, M.E.; Harwood, D.T. Ciguatoxins and maitotoxins in extracts of sixteen *Gambierdiscus* isolates and one *Fukuyoa* isolate from the South Pacific and their toxicity to mice by intraperitoneal and oral administration. *Mar. Drugs* **2017**, *15*, 208. [CrossRef]
90. Assunção, J.; Guedes, A.C.; Malcata, F.X. Biotechnological and pharmacological applications of biotoxins and other bioactive molecules from dinoflagellates. *Mar. Drugs* **2017**, *15*, 393. [CrossRef]
91. Robertson, A.; Richlen, M.L.; Erdner, D.; Smith, T.B.; Anderson, D.M.; Liefer, J.; Xu, Y.; McCarron, P.; Miles, C.; Parsons, M.L. Toxicity, chemistry, and implications of *Gambierdiscus silvae*: A ciguatoxin superbug in the Greater Caribbean Region. In Proceedings of the 18th International Conference on Harmful Algae, Nantes, France, 21–26 October 2018.
92. Pasinszki, T.; Lako, J.; Dennis, T.E. Advances in Detecting Ciguatoxins in Fish. *Toxins* **2020**, *12*, 494. [CrossRef]
93. Vernoux, J.P.; Lewis, R.J. Isolation and characterisation of Caribbean ciguatoxins from the horse-eye jack (*Caranx latus*). *Toxicon* **1997**, *35*, 889–900. [CrossRef]
94. Hamilton, B.; Hurbungs, M.; Vernoux, J.P.; Jones, A.; Lewis, R.J. Isolation and characterisation of Indian Ocean ciguatoxin. *Toxicon* **2002**, *40*, 685–693. [CrossRef]
95. Hamilton, B.; Hurbungs, M.; Jones, A.; Lewis, R.J. Multiple ciguatoxins present in Indian Ocean reef fish. *Toxicon* **2002**, *40*, 1347–1353. [CrossRef]
96. Pottier, I.; Vernoux, J.; Jones, A.; Lewis, R.J. Characterisation of multiple Caribbean ciguatoxins and congeners in individual specimens of horse-eye jack (*Caranx latus*) by high-performance liquid chromatography/mass spectrometry. *Toxicon* **2002**, *40*, 929–939. [CrossRef]
97. Diogène, J.; Reverté, L.; Rambla-Alegre, M.; del Rio, V.; de la Iglesia, P.; Campas, M.; Palacios, O.; Flores, C.; Caixach, J.; Ralijaona, C.; et al. Identification of ciguatoxins in a shark involved in a fatal food poisoning in the Indian Ocean. *Sci. Rep.* **2017**, *7*, 8240. [CrossRef]
98. Kryuchkov, F.; Robertson, A.; Miles, C.O.; Mudge, E.M.; Uhlig, S. LC–HRMS and chemical derivatization strategies for the structure elucidation of Caribbean ciguatoxins: Identification of C-CTX-3 and -4. *Mar. Drugs* **2020**, *18*, 182. [CrossRef]
99. Lewis, R.J.; Vernoux, J.-P.; Brereton, I.M. Structure of Caribbean ciguatoxin isolated from *Caranx latus*. *J. Am. Chem. Soc.* **1998**, *120*, 5914–5920. [CrossRef]
100. Abraham, A.; Jester, E.L.E.; Granade, H.R.; Plakas, S.M.; Dickey, R.W. Caribbean ciguatoxin profile in raw and cooked fish implicated in ciguatera. *Food Chem.* **2012**, *131*, 192–198. [CrossRef]
101. Wu, J.J.; Mak, Y.L.; Murphy, M.B.; Lam, J.C.W.; Chan, W.C.H.; Wang, M.; Chan, L.L.; Lam, P.K.S. Validation of an accelerated solvent extraction liquid chromatography tandem mass spectrometry method for Pacific ciguatoxin-1 in fish flesh and comparison with the mouse neuroblastoma assay. *Anal. Bioanal. Chem.* **2011**, *400*, 3165–3175. [CrossRef]

102. Reverté, L.; Soliño, L.; Carnicer, O.; Diogène, J.; Campàs, M. Alternative methods for the detection of emerging marine toxins: Biosensors, biochemical assays and cell-based assays. *Mar. Drugs* **2014**, *12*, 5719–5763. [CrossRef]
103. Hess, P.; Mondeguer, F.; Glauner, T.; Wust, B.; Sibat, M.; Zendong, S.Z.; Herrenknecht, C.; Séchet, V. Metabolomic analysis of marine microalgae using high resolution mass spectrometry for taxonomic comparisons and screening of marine biotoxins. In Proceedings of the 61st American Society for Mass Spectrometry (ASMS), Minneapolis, MN, USA, 9–13 June 2013.
104. Tester, P.A.; Kibler, S.R.; Holland, W.C.; Usup, G.; Vandersea, M.W.; Leaw, C.P.; Teen, L.P.; Larsen, J.; Mohammad-Noor, N.; Faust, M.A.; et al. Sampling harmful benthic dinoflagellates: Comparison of artificial and natural substrate methods. *Harmful Algae* **2014**, *39*, 8–25. [CrossRef]
105. Holmes, M.J.; Lewis, R.J.; Poli, M.A.; Gillespie, N.C. Strain dependent production of ciguatoxin precursors (gambiertoxins) by *Gambierdiscus toxicus* (Dinophyceae) in culture. *Toxicon* **1991**, *29*, 761–775. [CrossRef]
106. Martiny, A.C.; Pham, C.T.A.; Primeau, F.W.; Vrugt, J.A.; Moore, J.K.; Levin, S.A.; Lomas, M.W. Strong latitudinal patterns in the elemental ratios of marine plankton and organic matter. *Nat. Geosci.* **2013**, *6*, 279–283. [CrossRef]
107. Dufour, P.; Andréfouët, S.; Charpy, L.; Garcia, N. Atoll morphometry controls lagoon nutrient regime. *Limnol. Oceanogr.* **2001**, *46*, 456–461. [CrossRef]
108. Harris, P.; Fichez, R. *Observations et mécanismes de la crise dystrophique de 1994 dans le lagon de l'atoll d'Hikueru (archipel des Tuamotu, Polynésie française)*; ORSTOM-Tahiti, Ed.; ORSTOM: Tahiti, French Polynesia, 1995; Volume 45, 25 p.
109. Sharoni, S.; Halevy, I. Nutrient ratios in marine particulate organic matter are predicted by the population structure of well-adapted phytoplankton. *Sci. Adv.* **2020**, *6*, eaaw9371. [CrossRef] [PubMed]

toxins

MDPI

Article

Characteristic Distribution of Ciguatoxins in the Edible Parts of a Grouper, *Variola louti*

Naomasa Oshiro [1,*], Hiroya Nagasawa [1,2], Kyoko Kuniyoshi [1], Naoki Kobayashi [2], Yoshiko Sugita-Konishi [2,†], Hiroshi Asakura [1] and Takeshi Yasumoto [3]

[1] National Institute of Health Sciences, 3-25-26 Tonomachi, Kawasaki, Kanagawa 210-9501, Japan; h1r08a.n@gmail.com (H.N.); k-kuniyoshi@nihs.go.jp (K.K.); hasakura@nihs.go.jp (H.A.)
[2] Department of Food and Life Science, School of Life and Environmental Science, Azabu University, 1-17-71 Fuchinobe, Chuo-ku, Sagamihara, Kanagawa 252-5201, Japan; n-kobayashi@azabu-u.ac.jp (N.K.); yoshikoni2020@gmail.com (Y.S.-K.)
[3] Tama Laboratory, Japan Food Research Laboratories, 6-11-10 Nagayama, Tama, Tokyo 206-0025, Japan; yasumotot@jfrl.or.jp
* Correspondence: n-oshiro@nihs.go.jp; Tel.: +81-44-270-6568
† Present address: Department of Nutritional Science, Faculty of Applied Bio-Science, Tokyo University of Agriculture, 1-1-1 Sakuragaoka, Setagaya 156-8502, Japan.

Abstract: Ciguatera fish poisoning (CFP) is one of the most frequently encountered seafood poisoning syndromes; it is caused by the consumption of marine finfish contaminated with ciguatoxins (CTXs). The majority of CFP cases result from eating fish flesh, but a traditional belief exists among people that the head and viscera are more toxic and should be avoided. Unlike the viscera, scientific data to support the legendary high toxicity of the head is scarce. We prepared tissue samples from the fillet, head, and eyes taken from five yellow-edged lyretail (*Variola louti*) individuals sourced from Okinawa, Japan, and analyzed the CTXs by LC-MS/MS. Three CTXs, namely, CTX1B, 52-*epi*-54-deoxyCTX1B, and 54-deoxyCTX1B, were confirmed in similar proportions. The toxins were distributed nearly evenly in the flesh, prepared separately from the fillet and head. Within the same individual specimen, the flesh in the fillet and the flesh from the head, tested separately, had the same level and composition of toxins. We, therefore, conclude that flesh samples for LC-MS/MS analysis can be taken from any part of the body. However, the tissue surrounding the eyeball displayed CTX levels two to four times higher than those of the flesh. The present study is the first to provide scientific data demonstrating the high toxicity of the eyes.

Keywords: ciguatera; ciguatoxin; LC-MS/MS; CTX1B; 52-*epi*-54-deoxyCTX1B; 54-deoxyCTX1B

Key Contribution: CTXs were evenly distributed in the flesh, indicating that tissue samples for monitoring can be taken from any part of the body except the eyes, which contained CTX levels two to three times higher than the flesh. In all samples, the relative ratio of the CTX analogs did not vary within the specimens.

Citation: Oshiro, N.; Nagasawa, H.; Kuniyoshi, K.; Kobayashi, N.; Sugita-Konishi, Y.; Asakura, H.; Yasumoto, T. Characteristic Distribution of Ciguatoxins in the Edible Parts of a Grouper, *Variola louti*. *Toxins* **2021**, *13*, 218. https://doi.org/10.3390/toxins13030218

Received: 30 December 2020
Accepted: 15 March 2021
Published: 17 March 2021

1. Introduction

Ciguatera fish poisoning (CFP) is one of the most frequently encountered seafood poisoning syndromes; it is caused by the consumption of the marine finfish contaminated with ciguatoxins (CTXs) [1–4]. CTXs bind to receptor-site 5 of the alpha subunit of the voltage-gated sodium channel and cause hyperexcitability of the nerve membrane [5]. CFP is associated with gastrointestinal, cardiovascular, and neurological disorders, and more than 170 symptoms and signs have been reported [1]. The patients recover within a few days in mild cases, but the symptoms last for months or years in severe cases [5]. CFP mostly occurs in tropical and subtropical regions of the Pacific, the Indian Ocean, and the Caribbean Sea and is commonly reported in the South Pacific islands, including French

Polynesia, Fiji, Cook Island, and Kiribati, among others [4,6]. In recent years, there have been a series of reports of CFP in areas where it does not typically occur. For example, cases were recorded in the Canary (Spain) and Madeira (Portugal) Islands, which belong to Macaronesia in northwestern Africa in the eastern Atlantic Ocean, in 2004, and occurrences have continued since then [7,8]. Therefore, there are concerns about the expansion of CFP endemic areas. In Japan, Okinawa and the Amami Islands are located in the subtropical region; several cases of CFP are reported annually, though at much lower numbers than in the South Pacific Islands [9–11]. From 1989 to 2011, 78 CFP events were officially reported to the Government of Japan, 90% (70 events) of which were in Okinawa. The most implicated fish was the yellow-edged lyretail *Variola louti* (16 events, 21%), followed by one-spot snapper *Lutjanus monostigma* (12 events, 15%), and red snapper *Lutjanus bohar* (11 events, 14%) [12].

CTXs are produced by some species from the dinoflagellate genera *Gambierdiscus* and *Fukuyoa* and transmitted to herbivorous animals and carnivorous fish via the food chain [13,14]. CTXs are naturally occurring macromolecules consisting of ladder-shaped polyether, with more than 20 analogs reported from the Pacific Ocean and classified into CTX1B-type and CTX3C-type toxins based on their skeletal structure [15]. In our previous studies, we reported the regional and species-specific features of the CTX profiles of fish in the Pacific using liquid chromatography–tandem mass spectrometry (LC-MS/MS) analysis [16–19]. In the specimens captured in Hawaii, French Polynesia, Minamitorishima (Marcus Island), and mainland Japan, both CTX1B-type and CTX3C-type toxins were detected [16]. In contrast, only CTX1B-type toxins were detected in the Okinawa and Amami regions' specimens. In *V. louti* captured from Okinawan waters, only three CTX1B analogs (CTX1B, 52-*epi*-54deoxyCTX1B and 54-deoxyCTX1B; Figure 1), were present and the relative levels of these three analogs were comparable.

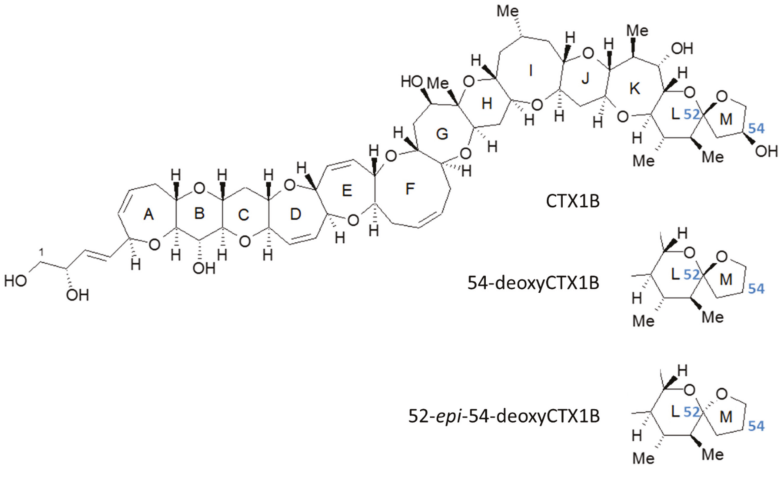

Figure 1. Structures representative of ciguatoxin-1B (CTX1B), 52-*epi*-54-deoxyCTX1B, and 54-deoxyCTX1B, implicated in CFP in Okinawa, Japan.

The majority of CFP cases arise from consumption of the fish fillet, but among the inhabitants of tropical islands, it is believed that the head and viscera are more toxic than the fillet [4,9]. Additionally, there have been reports that the symptoms are more severe among patients who consumed the head and/or the viscera than in those who consumed only the flesh [4,20–24]. Usually, the whole or half-cut head, without removing the eyes, is broiled, steamed, stewed, deep-fried, or souped. The legends of Okinawa, Japan, point out the high risks of eating the heads, and the actual number of incidents was reported in an early epidemiological study in Okinawa [25,26]. Thus, avoiding the consumption of the

viscera and the head is recommended [4,27]. The presence of high levels of CTXs in the liver of ciguateric fish is well documented [26,28–30], providing the basis for the use of the livers as the source of toxin isolation [31,32]. Conversely, toxicity data on the CTX levels in head samples are scarce [29].

In this study, we analyze CTXs by LC-MS/MS to disclose their levels and profiles in the flesh samples dissected from the fillet and head (cheek, collar, and cavalry) and the eye samples, the edible parts of fish mentioned in the legends. We used five individuals of the carnivorous fish *V. louti*, the yellow-edged lyretail (Figure 2A), one of the representative species of CFP in Okinawa, Japan. The presence of CTX1B, 52-*epi*-54deoxyCTX1B, and 54-deoxyCTX1B in these specimens was confirmed by preliminary analysis.

Table 1. Sample preparation from the eyeball and the surrounding tissue taken from the fish specimens.

Specimen	ID [1]	SL [2] (mm)	Weight (g)	Eye Sample Preparation [3]
A	160024	490	2934	whole parts were mixed (#10)
B	160085	410	1734	surrounding tissue (#11), inner contents, including a lens (#12) and the outer membrane of the eyeball (#13)
C	163077	456	2719	surrounding tissue (#11), inner contents, including a lens (#12) and the outer membrane of the eyeball (#13)
D	160135	490	2594	surrounding tissue (#11), inner contents of the eyeball (#12) and lens (#14)
E	160136	450	2430	surrounding tissue (#11), inner contents of the eyeball (#12) and lens (#14)

[1] Specimen ID at the National Institute of Health Sciences. [2] SL: standard length; [3] preparation of the sample from the eyeball and surrounding tissue for LC-MS/MS analysis. Numbers in brackets are the sample codes.

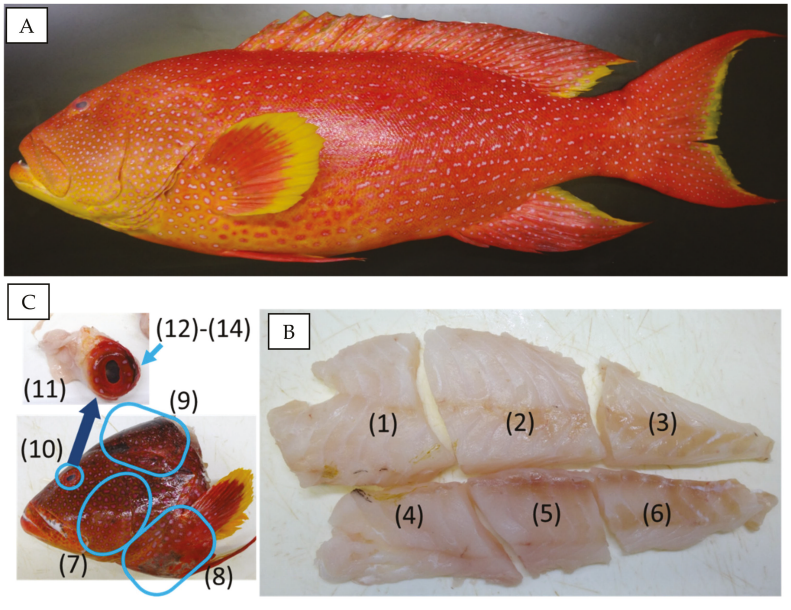

Figure 2. A specimen (D, ID 160135) of *V. louti* used for this study (**A**) and the locations of samples used for LC-MS/MS analyses. (**B**) The half-body fillet was divided into six parts (#1–#6, bottom right). (**C**) From the head, the flesh samples taken from the cheek (#7), the collar (#8), and the cavalry (#9); the eyeball (#10) and the tissue surrounding eyeball (#11). The eyeball was further separated into samples #12–#14, as shown in Table 1.

2. Results

Six and three flesh samples were prepared from the fillet (#1–#6) and head (#7–#9), respectively, as shown in Figure 2B,C. Eye samples (#10), composed of the eyeball and the surrounding tissue (#11), were taken, and the eyeballs were further separated from Specimens B–E (#12–#14), as shown in Table 1.

Three CTX1B-type analogs, including CTX1B, 52-*epi*-54-deoxyCTX1B, and 54-deoxyCTX1B, were detected in all specimens. However, neither the fourth CTX1B-type nor the CTX3C-type analog was detected in any samples (Figure 3; Figure 4). Detection of only three CTX1B analogs is characteristic in the carnivorous fish from Okinawa [16,17]. Representative chromatograms are shown in Figure 3. The ratios of the three CTX1B analogs were similar within all specimens (Figure 4).

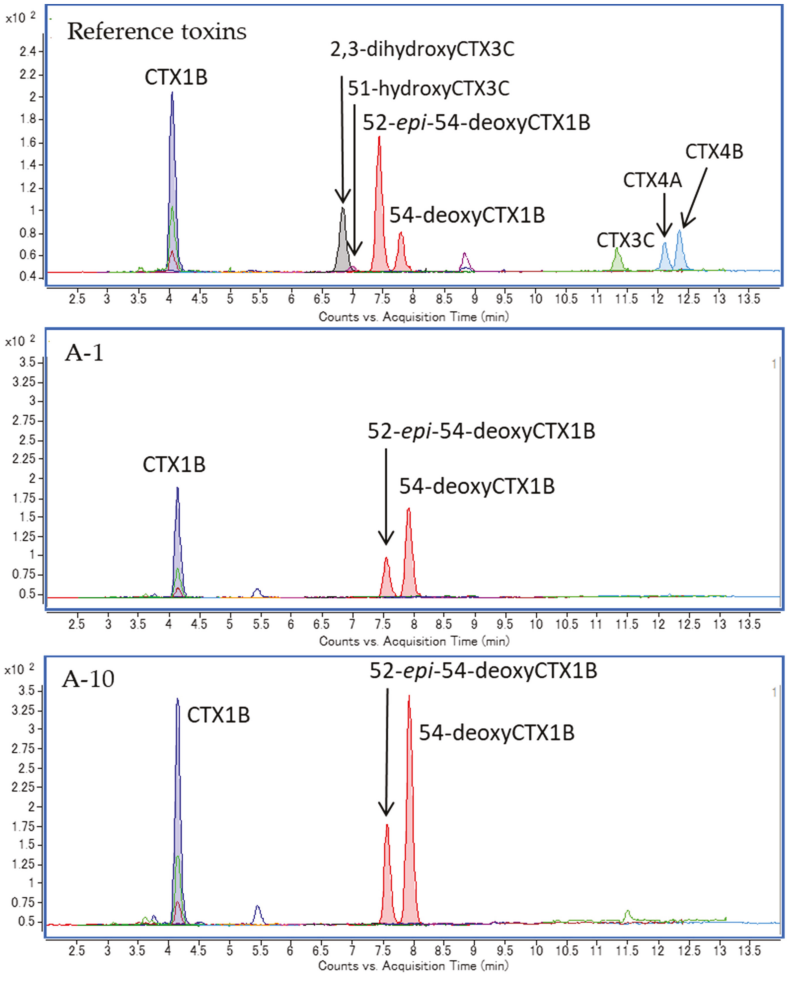

Figure 3. LC-MS/MS chromatograms of reference toxin mixture (top), flesh (A-1, middle), and eye (A-10, bottom) samples of Specimen A.

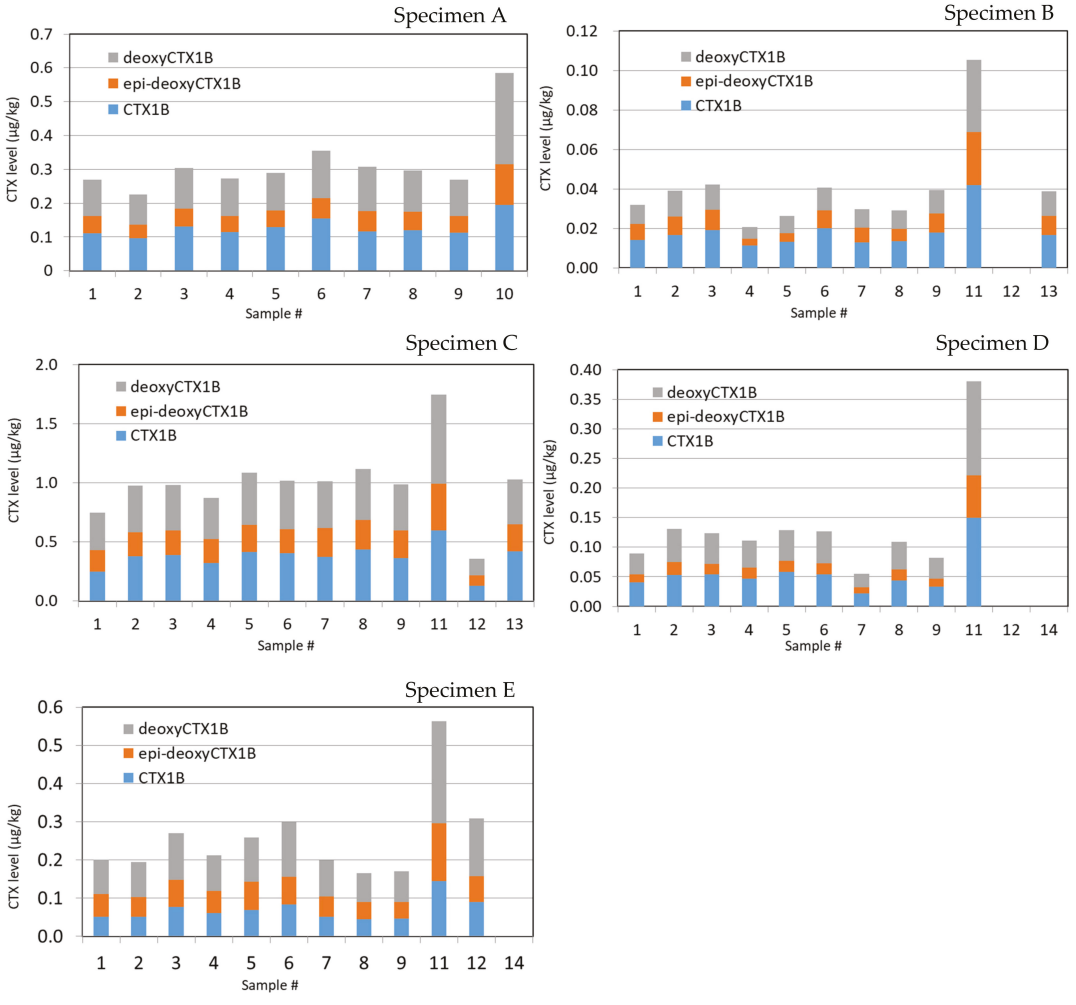

Figure 4. The levels of CTX1B analogs detected in samples prepared from Specimens A–E.

2.1. Specimen A

The total CTX levels (average ± SD (standard deviation)) in the flesh samples from the filet (#1–#6) and the head (#7–#9) were similar, measuring 0.287 ± 0.043 and 0.292 ± 0.012 μg/kg, respectively (Table 2 and Figure 4). The eye sample (#10), comprised of the eyeball and the surrounding tissue, was mixed, and LC-MS/MS analysis was applied. The level of CTXs was 0.585 μg/kg, twice as high as that of the flesh samples (Table 3). The ratios of three CTX analogs within the specimens were similar (Figure 4).

Table 2. CTX levels in flesh prepared from the fillet (#1–#6) and head (#7–#9).

Specimen	CTXs Levels (μg/kg) in the Fillet [1]								CTXs Levels (μg/kg) in the Head [1]				
	#1	#2	#3	#4	#5	#6	Average	SD [2]	#7	#8	#9	Average	SD
A	0.270	0.226	0.305	0.274	0.290	0.355	0.287	0.043	0.308	0.297	0.270	0.292	0.019
B	0.032	0.039	0.042	0.021	0.026	0.041	0.033	0.009	0.030	0.029	0.039	0.033	0.006
C	0.749	0.978	0.984	0.873	1.088	1.018	0.948	0.120	1.011	1.117	0.989	1.039	0.068
D	0.089	0.131	0.124	0.111	0.129	0.126	0.118	0.016	0.055	0.110	0.082	0.082	0.027
E	0.201	0.195	0.270	0.212	0.259	0.300	0.239	0.043	0.200	0.166	0.171	0.179	0.018

[1] The sum of the levels of CTX1B, 52-*epi*-54deoxyCTX1B, and 54-deoxyCTX1B. [2] SD: standard deviation.

Table 3. CTXs levels in flesh (fillet and head) and eye samples.

Specimen	CTXs Levels (μg/kg) [1]						
	Fillet [2]	Head [3]	#10	#11	#12	#13	#14
A	0.287	0.292	0.585	- [4]	-	-	-
B	0.033	0.033	-	0.106	<LOD [5]	0.039	-
C	0.948	1.039	-	1.747	0.360	1.031	-
D	0.118	0.082	-	0.380	<LOD	-	<LOD
E	0.239	0.179	-	0.563	0.308	-	<LOD

[1] The sum of the levels of CTX1B, 52-*epi*-54deoxyCTX1B, and 54-deoxyCTX1B. [2] Average of samples #1-#6. [3] Average of samples #7–#9. [4] -: not analyzed. [5] <LOD: less than the limit of detection (0.001 μg/kg).

2.2. Specimen B

The CTX levels in the flesh samples were 0.033 ± 0.009 μg/kg in the filet (#1–#6) and 0.033 ± 0.006 μg/kg in the head (Table 2). To clarify the source of the high CTX levels in the eye sample, as observed in Specimen A, the eye sample was further separated into three portions in Specimen B: the surrounding tissue (#11), the inner contents of the eyeball, including the lens (#12), and the outer membrane of the eyeball (#13). The highest levels of CTX1B analogs were detected in #11, with 0.106 μg/kg, which was three times higher than of the flesh samples (#1–#9). The level in #13 was 0.039 μg/kg, and in #12, it was less than the limit of detection (LOD, <0.001 μg/kg) (Table 3).

2.3. Specimens C

The samples were prepared in the same way as those of Specimen B. The levels in the filet, the head, and samples #11–#13 were 0.948 ± 0.120, 1.039 ± 0.068, 1.747, 0.360, and 1.031 μg/kg, respectively (Table 2; Table 3). While the detected levels in Specimen C (0.360–1.747 μg/kg) were much higher than in Specimen B (0.021–0.106 μg/kg), the relative levels in respective sample portions were similar (Table 3).

2.4. Specimens D

CTXs were detected at the levels of 0.118 ± 0.016 and 0.082 ± 0.027 μg/kg in the filet and the head, respectively (Table 2). We prepared separate tissue samples, consisting of the surrounding tissue (#11), inner contents (#12), and lens (#14) from the eye, to locate where the highest levels of CTXs had originated. Among them, CTXs were detected only in #11 (0.380 μg/kg), which exhibited levels 3.2 and 4.6 times higher than in the filet and the head, respectively (Table 3).

2.5. Specimen E

Although the levels of CTX1B and 54-deoxyCTX1B in all flesh samples (#1–#9) were similar, the levels of 52-*epi*-54-deoxyCTX1B were much higher in the fillet samples #1–#6 than in #7–#9 taken from the head of Specimen E (Figure 4A, Figure S1). In addition to the

different ratios of the three CTX1B analogs in the flesh and head, splitting the peak top of 52-*epi*-54-deoxyCTX1B of samples of the filet made us suspect the presence of interfering substances in these samples. These samples were reanalyzed using a different gradient system (Gradient II), and the peaks of 52-*epi*-54-deoxyCTX1B were separated from those of the interferent, as shown in Figure 4B and Figure S2. The levels in the filet and the head were at 0.239 ± 0.043 and 0.179 ± 0.018 μg/kg, respectively (Table 2).

The eye samples were prepared equally to those of Specimen D (Table 1), and CTXs were detected in #11 and #12 at 0.563 and 0.308 μg/kg, respectively (Table 3). The level in #11 was two to three times higher than of the filet and the head (Table 3). No CTXs were detected in #14. While no CTXs were detected in #12 of Specimen D, the same analogs were detected at relatively high levels in the corresponding sample of Specimen E (Table 3). The different results between Specimens D and E might be ascribable to the cross-contamination of surrounding tissues.

3. Discussion

According to the inhabitants of the tropical islands where CFP is prevalent, the head and viscera are more likely to cause CFP than the fillet. In addition, many papers reported that the patients who consumed these portions displayed the most severe symptoms among individuals who had shared the same fish [4,21–23]. In order to obtain evidence upholding this legend, we prepared samples from the fillet and the head, the edible parts of the fish, and separately analyzed CTXs by LC-MS/MS. The gills, scales, and viscera were not tested in this study because they are not considered edible tissues. We separated the fillet further into small six sections, depending on the distances from the head and tail. The fillet from the belly side is believed to be fatty compared to the dorsal side. For the head, we took the flesh from the cheek, collar, and calvary. CTX levels across the specimens and the levels and profiles in the flesh samples were similar across the specimens. The toxin contents and toxin profiles in these small sections are important—first, to prevent food poisoning, and secondly, for the accurate evaluation of the fish under testing. In the case of beef, the variations of quality among the body parts are well understood. No comparable data exist as to the variation in fish or the profiles of toxins. Much attention has been paid to the accuracy of the analytical method to quantify CTXs. If CTXs are unevenly distributed in the fish body, the validity of the analytical data will be governed by which part the sample has been taken from. The present study demonstrates that flesh samples for toxin analysis can be arbitrarily taken from all parts of the body of *V. louti* except the eye areas. This finding is important for designing the protocol for testing fish for various purposes, including food safety, business, legal actions, and more.

In Specimen E, interference peaks were detected in the fillet samples but not in the flesh from the head or the tissues of the eye (Figure 5). The presence of the interferences only in the filet is interesting, and further investigation to uncover the structural information of these substances will be carried out.

In the samples prepared from the eyes, namely, the tissue surrounding the eyeball, CTXs were detected at two to four times higher levels than in the flesh samples. This tissue is known to contain high contents of polyunsaturated fatty acids, docosahexaenoic acid (DHA) and icosapentaenoic acid (eicosapentaenoic acid (EPA)) [33–35]. The high levels of CTXs in the eyes will be an interesting phenomenon for future studies. Although high in concentration, the eyes alone cannot account for the legends of higher toxicity of the head. According to Li et al. [29], CTXs were consistently detected in various tissues of grouper *Epinephelus coioides* over 30 days of exposure. CTX levels ranked from high to low in the following order: liver, intestine, gill, skin, brain, and muscle. The brain and other cerebrum tissues in the head were suspected to be rich in CTXs because of the abundance of the voltage-dependent sodium channels [5,36]. However, the difficulty of separation and the small quantity available for analysis prevented us from analyzing CTXs from those tissues in this study. Attempts will be made in the future to test the cerebrum tissues in the

head and the backbone. Finally, the reliability and high efficacy of LC-MS/MS analysis in studying food safety and the body distribution of CTXs have been demonstrated.

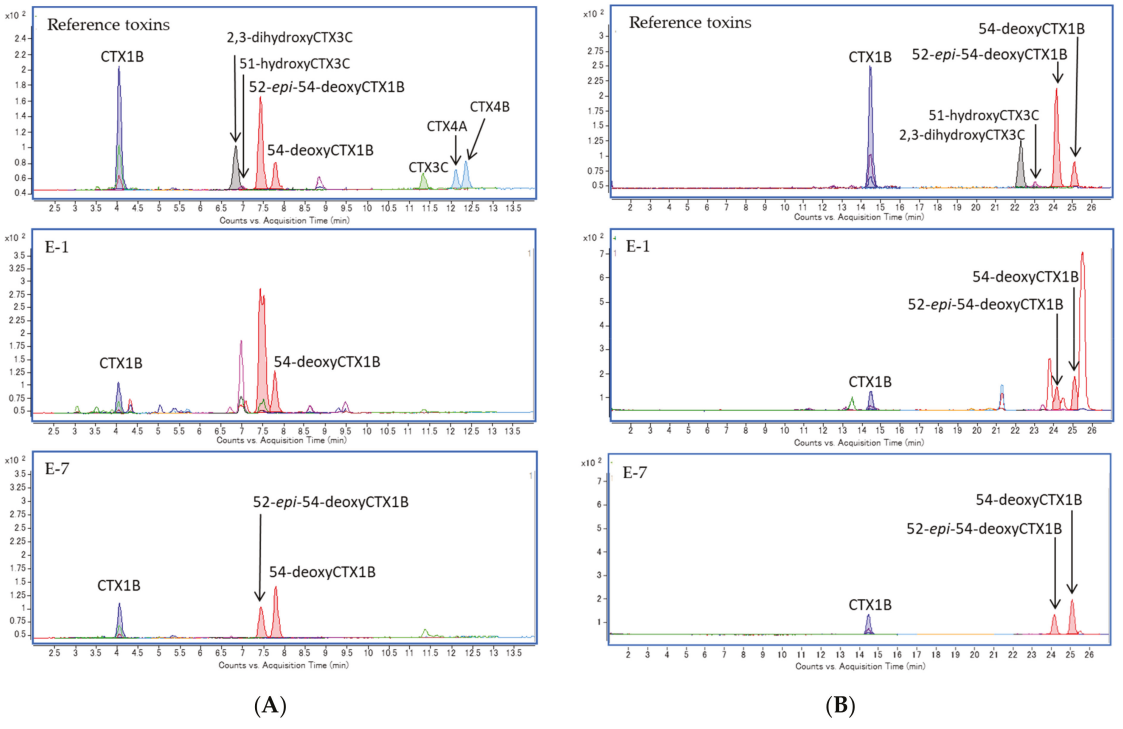

Figure 5. LC-MS/MS chromatograms of reference toxin mixture (top) and flesh samples of the fillet (E-1, middle) and cheek (E-7, bottom) of Specimen E. The gradient systems used were conditions Gradient I (**A**) and II (**B**).

4. Conclusions

The levels and profiles of the CTXs (CTX1B, 52-*epi*-54-deoxyCTX1B, and 54-deoxyCTX1B) in tissues were shown to be comparable among samples prepared from the same individual. This even distribution was revealed by LC-MS/MS analyses using the fillet and head and eye samples of five specimens of a representative ciguateric fish, *Variola louti.* Any part of the flesh, except for the eyes, can be used for analyses to judge the safety of the fish or to produce ecological data. The tissues of the eyes were found, for the first time, to contain CTX levels two or four times higher than that of the flesh.

5. Materials and Methods

5.1. Reference Toxins and Reagents

The reference toxin mixture was comprised of eight CTX analogs, including CTX1B, 52-*epi*-54-deoxyCTX1B, 54-deoxyCTX1B, CTX4A, CTX4B, 2,3-dihydroxyCTX3C, 51-hydroxyCTX3C, and CTX3C, all of which were pure or near-pure toxins prepared from natural sources and identified by spectroscopic analysis [15,37–41]. The levels of the detected toxins were quantified using the reference toxins Ciguatoxin-1B (43.3 ± 1.3 ng) and 52-*epi*-54-deoxyCTX1B (58.4 ± 2.5 ng). Since the reference material for 54-deoxyCTX1B was unavailable, its levels were quantified using 52-*epi*-54-deoxyCTX1B.

Acetone, hexane, and ethyl acetate of Primepure grade, diethyl ether of Guaranteed reagent grade, and methanol and acetonitrile of liquid chromatography–mass spectrometry

(LC-MS) grade were purchased from Kanto Chemical Co., Inc. (Tokyo, Japan). Ammonium formate solution (1 mol/L) and formic acid were of high-performance liquid chromatography (HPLC) grade (Wako Chemical Industry, Ltd., Osaka, Japan). Ultra-pure water was supplied by the Milli-Q® Integral Water Purification System for Chemical Analysis (Millipore, Bedford, MA, USA).

5.2. Fish Specimens

The five individuals of *V. louti* used were found to be contaminated with CTX1B, 52-*epi*-54-deoxyCTX1B, and 54-deoxyCTX1B and selected from our ciguateric fish collection, purchased in Okinawa, Japan (Specimens A–E, Table 1, Figure 2A). The head and a fillet were taken from the body. The fillet was cut into 6 parts (#1–#6), as shown in Figure 2B. The following four samples were prepared from the heads: the flesh from the cheek (#7), the collar (#8), and cavalry (#9), and the eyeball combined with surrounding tissue (#10), as shown in Figure 2C. Each eye sample was separated, as shown in Table 1. In Specimen A, the whole part was mixed (#10). Since the CTX level of the eye sample (#10) was the highest within the samples (#1–#10) of Specimen A, and in order to explore the highly contaminated portion in the eye, eye samples (#10) in Specimens B and C were separated into the surrounding tissue (#11), inner contents including the lens (#12), and outer membrane (#13). In Specimens D and F, to confirm the existence of high-level CTXs in the surrounding tissue and to verify whether the CTXs are present in the eyeball's inner contents or lens, samples #11, #12, and #14 were prepared and analyzed.

5.3. Extraction and Sample Preparation for LC-MS/MS

Extraction and preparation of the fish flesh followed the method in previous studies (Figure S3) [18,19]. Flesh (5 g) was extracted with acetone (15 mL) twice, and the extracts were combined and evaporated to remove the acetone. The remaining aqueous extracts were partitioned with diethyl ether (5 mL) twice, and the combined diethyl ether layer was dried completely and dissolved in 90% methanol (*v/v*, 1.5 mL). The aqueous methanol was defatted with hexane (3 mL, twice), and the remaining solution was dried completely to obtain the crude extract.

The crude extract was dissolved in ethyl acetate-methanol (9:1, *v/v*, 5 mL) and applied to a Florisil column (500 mg, GL Sciences Inc., Tokyo, Japan) that had been preconditioned with the same solvent. The eluent, containing nonabsorbed substances, was collected and dried under a nitrogen stream. The residue was dissolved with acetonitrile (5 mL) and applied to a primary and secondary amine cartridge column (PSA, 200 mg, GL Sciences Inc., Tokyo, Japan), preconditioned with methanol and acetonitrile. CTXs were eluted first with acetonitrile and then methanol (3 mL). Both acetonitrile and methanol eluates were dried under a nitrogen stream and dissolved in methanol to be analyzed by LC-MS/MS. A 1-mL portion of the solution was equivalent to 5 g of the flesh.

The preparation of the eye samples (#10–#14) followed that of the flesh samples. When the sample was smaller than 5 g, the whole sample was used, and the extraction and pretreatment procedures were carried out without any change. The sample solution used for LC-MS/MS was adjusted to 5 g tissue-equivalent/mL.

5.4. LC-MS/MS Analysis

LC-MS/MS analysis was carried out with the Agilent 1290 HPLC system coupled with an Agilent 6460 Triple Quadrupole MS instrument (Santa Clara, CA, USA) (Table S1). Briefly, 5 µL of sample solution was injected into a Zorbax Eclipse Plus C18 column (2.1 × 50 mm id, 1.8 µm, Agilent Technologies, Santa Clara, CA, USA), at 40 °C. Eluate A was water containing 5 mM ammonium formate and 0.1% formic acid. and Eluate B was methanol. The gradient system (Gradient I) was as follows: 0.0–0.25 min (60% B); 0.25–0.50 min (60–75% B); 0.50–12.0 min (75% B); 12.0–14.0 min (90% B); 14.1–20 min (100% B). When the presence of an interfering substance was suspected, the sample was reanalyzed using another gradient system. The gradient condition for Gradient II was as

follows: 0–0.25 min (50% B); 0.25–0.5 min (50–65% B); 0.5–25 min (65–80% B); 25–27 min (80% B); 27–33 min t(100% B). The flow rate was 0.4 mL/min. The target toxins were ionized with electron spray ionization (ESI) equipped with Agilent Jet Stream, and positive ions were monitored with multiple reaction monitoring (MRM) mode. Since $[M + Na]^+$ ions were stable and gave no fragment ions, $[M + Na]^+$ of each analog was set for both precursor and product ions ($[M + Na]^+ > [M + Na]^+$), with high collision energy to achieve sensitive analysis. The optimized MS parameters were dry gas N_2, 300 °C, 10 L/min; nebulizer gas N_2, 50 psi; sheath gas N_2, 380 °C, 11 L/min; capillary voltage 5000 V; fragmentor voltage 300 V; collision gas N_2, collision energy 40 eV. The limit of detection (LOD) and the limit of quantitation (LOQ) of CTX1B, 52-*epi*-54-deoxyCTX1B, and 54-deoxyCTX1B were 0.001 and 0.005 µg/kg, respectively.

Supplementary Materials: The following materials are available online at https://www.mdpi.com/2072-6651/13/3/218/s1. Figure S1: LC-MS/MS chromatograms in Gradient I of samples (#1–#9, #11, #12, and #14) prepared from Specimen E (ID 160136). Figure S2: LC-MS/MS chromatograms in Gradient II of samples (#1–#9, #11, #12, and #14) prepared from Specimen E (ID 160136). Figure S3: Sample preparation from fish flesh for LC-MS/MS. Table S1: LC-MS/MS conditions for CTX analysis.

Author Contributions: Conceptualization, N.O., Y.S.-K., H.A. and T.Y.; methodology, N.O.; validation, N.O., and K.K.; formal analysis, N.O., H.N. and K.K.; investigation, N.O. and H.N.; resources, N.O.; data curation, N.O., H.N. and K.K.; writing—original draft preparation, N.O. and H.N.; writing—review and editing, N.O., N.K., Y.S.-K., H.A. and T.Y.; visualization, H.N. and K.K.; supervision, H.A., Y.S.-K. and T.Y.; project administration, N.O.; funding acquisition, N.O. All authors have read and agreed to the published version of the manuscript.

Funding: Part of this research was funded by the Japan Food Chemical Research Foundation.

Informed Consent Statement: Not applicable.

Data Availability Statement: The data presented in this study are available on request from the corresponding author.

Conflicts of Interest: The authors declare no conflict of interest.

References

1. FAO; WHO. *Report of the Expert Meeting on Ciguatera Poisoning: Rome, 19–23 November 2018*; FAO: Rome, Italy, 2020; Volume 9, p. 156. [CrossRef]
2. Yasumoto, T.; Satake, M. Chemistry, Etiology and Determination Methods of Ciguatera Toxins. *J. Toxicol. Toxin Rev.* **1996**, *15*, 91–107. [CrossRef]
3. Yasumoto, T. Chemistry, etiology, and food chain dynamics of marine toxins. *Proc. Jpn. Acad. Ser. B* **2005**, *81*, 43–51. [CrossRef]
4. Friedman, M.A.; Fernandez, M.; Backer, L.C.; Dickey, R.W.; Bernstein, J.; Schrank, K.; Kibler, S.; Stephan, W.; Gribble, M.O.; Bienfang, P.; et al. An Updated Review of Ciguatera Fish Poisoning: Clinical, Epidemiological, Environmental, and Public Health Management. *Mar. Drugs* **2017**, *15*, 72. [CrossRef]
5. Pearn, J. Neurology of ciguatera. *J. Neurol. Neurosurg. Psychiatry* **2001**, *70*, 4–8. [CrossRef] [PubMed]
6. Chinain, M.; Gatti, C.; Darius, H.; Quod, J.-P.; Tester, P. Ciguatera poisonings: A global review of occurrences and trends. *Harmful Algae* **2020**, 101873. [CrossRef]
7. Pérez-Arellano, J.-L.; Luzardo, O.P.; Brito, A.P.; Cabrera, M.H.; Zumbado, M.; Carranza, C.; Angel-Moreno, A.; Dickey, R.W.; Boada, L.D. Ciguatera Fish Poisoning, Canary Islands. *Emerg. Infect. Dis.* **2005**, *11*, 1981–1982. [CrossRef] [PubMed]
8. Sanchez-Henao, A.; García-Álvarez, N.; Sergent, F.S.; Estévez, P.; Gago-Martínez, A.; Martín, F.; Ramos-Sosa, M.; Fernández, A.; Diogène, J.; Real, F. Presence of CTXs in moray eels and dusky groupers in the marine environment of the Canary Islands. *Aquat. Toxicol.* **2020**, *221*, 105427. [CrossRef]
9. Hashimoto, Y.; Konosu, S.; Yasumoto, T.; Kamiya, H. Ciguatera in the Ryukyu and Amami Islands. *Bull. Jpn. Soc. Sci. Fish.* **1969**, *35*, 316–326. [CrossRef]
10. Oshiro, N.; Yogi, K.; Asato, S.; Sasaki, T.; Tamanaha, K.; Hirama, M.; Yasumoto, T.; Inafuku, Y. Ciguatera incidence and fish toxicity in Okinawa, Japan. *Toxicon* **2010**, *56*, 656–661. [CrossRef]
11. Oshiro, N.; Matsuo, T.; Sakugawa, S.; Yogi, K.; Matsuda, S.; Yasumoto, T.; Inafuku, Y. Ciguatera Fish Poisoning on Kakeroma Island, Kagoshima Prefecture, Japan. *Trop. Med. Health* **2011**, *39*, 53–57. [CrossRef]
12. Toda, M.; Uneyama, C.; Toyofuku, H.; Morikawa, K. Trends of Food Poisonings Caused by Natural Toxins in Japan, 1989–2011. *Shokuhin Eiseigaku Zasshi (Food Hyg. Saf. Sci.)* **2012**, *53*, 105–120. [CrossRef]

13. Yasumoto, T.; Nakajima, I.; Bagnis, R.; Adachi, R. Finding of a dinoflagellate as a likely culprit of ciguatera. *Bull. Jpn. Soc. Sci. Fish.* **1977**, *43*, 1021–1026. [CrossRef]
14. Chinain, M.; Gatti, C.M.; Roué, M.; Darius, H.T.; Subba Rao, D. Ciguatera-causing dinoflagellates in the genera *Gambierdiscus* and *Fukuyoa*: Distribution, ecophysiology and toxicology. In *Dinoflagellates: Classification, Evolution, Physiology and Ecological Significance*; Durvasula, S.R.V., Ed.; Nova Science Publishers: New York, NY, USA, 2020; pp. 405–457. ISBN 978-1-53617-888-3.
15. Yasumoto, T.; Igarashi, T.; Legrand, A.-M.; Cruchet, P.; Chinain, M.; Fujita, T.; Naoki, H. Structural Elucidation of Ciguatoxin Congeners by Fast-Atom Bombardment Tandem Mass Spectroscopy. *J. Am. Chem. Soc.* **2000**, *122*, 4988–4989. [CrossRef]
16. Yogi, K.; Oshiro, N.; Inafuku, Y.; Hirama, M.; Yasumoto, T. Detailed LC-MS/MS Analysis of Ciguatoxins Revealing Distinct Regional and Species Characteristics in Fish and Causative Alga from the Pacific. *Anal. Chem.* **2011**, *83*, 8886–8891. [CrossRef] [PubMed]
17. Yogi, K.; Sakugawa, S.; Oshiro, N.; Ikehara, T.; Sugiyama, K.; Yasumoto, T. Determination of Toxins Involved in Ciguatera Fish Poisoning in the Pacific by LC/MS. *J. AOAC Int.* **2014**, *97*, 398–402. [CrossRef]
18. Oshiro, N.; Tomikawa, T.; Kuniyoshi, K.; Kimura, K.; Kojima, T.; Yasumoto, T.; Asakura, H. Detection of Ciguatoxins from Fish Introduced into a Wholesale Market in Japan. *Shokuhin Eiseigaku Zasshi (Food Hyg. Saf. Sci.)* **2021**, *62*, 8–13. [CrossRef]
19. Oshiro, N.; Tomikawa, T.; Kuniyoshi, K.; Ishikawa, A.; Toyofuku, H.; Kojima, T.; Asakura, H. LC–MS/MS Analysis of Ciguatoxins Revealing the Regional and Species Distinction of Fish in the Tropical Western Pacific. *J. Mar. Sci. Eng.* **2021**, *9*, 299. [CrossRef]
20. Chateau-Degat, M.-L.; Legrand, A.-M.; Darius, T.; Chansin, R.; Dewailly, E.; Laudon, F.; Chinain, M.; Huin-Blondey, M.-O.; Nguyen, N.L. Prevalence of Chronic Symptoms of Ciguatera Disease in French Polynesian Adults. *Am. J. Trop. Med. Hyg.* **2007**, *77*, 842–846. [CrossRef] [PubMed]
21. Edwards, A.; Zammit, A.; Farrell, H. Four recent ciguatera fish poisoning incidents in New South Wales, Australia linked to imported fish. *Commun. Dis. Intell.* **2019**, *43*, 43. [CrossRef]
22. Chateau-Degat, M.-L.; Dewailly, E.; Cerf, N.; Nguyen, N.L.; Huin-Blondey, M.-O.; Hubert, B.; Laudon, F.; Chansin, R. Temporal trends and epidemiological aspects of ciguatera in French Polynesia: A 10-year analysis. *Trop. Med. Int. Health* **2007**, *12*, 485–492. [CrossRef] [PubMed]
23. Muecke, C.; Hamper, L.; Skinner, A.; Osborne, C. Ciguatera fish poisoning in an international ship crew in Saint John Canada: 2015. *Can. Commun. Dis. Rep.* **2015**, *41*, 285–288. [CrossRef] [PubMed]
24. Chan, T.Y.K. Characteristic Features and Contributory Factors in Fatal Ciguatera Fish Poisoning—Implications for Prevention and Public Education. *Am. J. Trop. Med. Hyg.* **2016**, *94*, 704–709. [CrossRef] [PubMed]
25. Hashimoto, Y.; Fusetani, N. A Preliminary Report on the Toxicity of an Amberjack, *Seriola aureovittata*. *Bull. Jpn. Soc. Sci. Fish.* **1968**, *34*, 618–626. [CrossRef]
26. Yasumoto, T.; Scheuer, P.J. Marine toxins of the pacific—VIII ciguatoxin from moray eel livers. *Toxicon* **1969**, *7*, 273–276. [CrossRef]
27. Dickey, R.W.; Plakas, S.M. Ciguatera: A public health perspective. *Toxicon* **2010**, *56*, 123–136. [CrossRef] [PubMed]
28. Chan, W.H.; Mak, Y.L.; Wu, J.J.; Jin, L.; Sit, W.H.; Lam, J.C.W.; De Mitcheson, Y.S.; Chan, L.L.; Lam, P.K.S.; Murphy, M.B. Spatial distribution of ciguateric fish in the Republic of Kiribati. *Chemosphere* **2011**, *84*, 117–123. [CrossRef] [PubMed]
29. Li, J.; Mak, Y.L.; Chang, Y.-H.; Xiao, C.; Chen, Y.-M.; Shen, J.; Wang, Q.; Ruan, Y.; Lam, P.K.S. Uptake and Depuration Kinetics of Pacific Ciguatoxins in Orange-Spotted Grouper (*Epinephelus coioides*). *Environ. Sci. Technol.* **2020**, *54*, 4475–4483. [CrossRef]
30. Kohli, G.S.; Haslauer, K.; Sarowar, C.; Kretzschmar, A.L.; Boulter, M.; Harwood, D.; Laczka, O.; Murray, S.A. Qualitative and quantitative assessment of the presence of ciguatoxin, P-CTX-1B, in Spanish Mackerel (*Scomberomorus commerson*) from waters in New South Wales (Australia). *Toxicol. Rep.* **2017**, *4*, 328–334. [CrossRef]
31. Legrand, A.M.; Litaudon, M.; Genthon, J.N.; Bagnis, R.; Yasumoto, T. Isolation and some properties of ciguatoxin. *Environ. Boil. Fishes* **1989**, *1*, 183–188. [CrossRef]
32. Lewis, R.J.; Sellin, M.; Poli, M.A.; Norton, R.S.; MacLeod, J.K.; Sheil, M.M. Purification and characterization of ciguatoxins from moray eel (*Lycodontis javanicus*, Muraenidae). *Toxicon* **1991**, *29*, 1115–1127. [CrossRef]
33. Sawada, T.; Takahashi, K.; Hatano, M. Molecular Species Analysis of Fish Oil Triglyceride by Light Scattering Mass Detector Equipped Liquid Chromatograph II. Triglyceride Composition of Tuna and Bonito Orbital Fats. *Nippon Suisan Gakkaishi* **1993**, *59*, 285–290. [CrossRef]
34. Ishihara, K.; Saito, H. The Docosahexaenoic Acid Content of the Lipid of Juvenile Bluefin Tuna *Thunnus thynnus* Caught in the Sea off Japanese Coast. *Fish. Sci.* **1996**, *62*, 840–841. [CrossRef]
35. Kitamura, Y.; Nomura, A.; Wada, S. Seasonal Variation in Lipid Content and Fatty Acid Composition of Round Frigate Mackerel, *Auxis rochei* Risso, in Tosa Bay. *J. Jpn. Oil Chem. Soc.* **1996**, *45*, 1267–1270. [CrossRef]
36. Wang, J.; Ou, S.-W.; Wang, Y.-J. Distribution and function of voltage-gated sodium channels in the nervous system. *Channels* **2017**, *11*, 534–554. [CrossRef] [PubMed]
37. Murata, M.; Legrand, A.M.; Ishibashi, Y.; Yasumoto, T. Structures of ciguatoxin and its congener. *J. Am. Chem. Soc.* **1989**, *111*, 8929–8931. [CrossRef]
38. Murata, M.; Legrand, A.M.; Ishibashi, Y.; Fukui, M.; Yasumoto, T. Structures and configurations of ciguatoxin from the moray eel *Gymnothorax javanicus* and its likely precursor from the dinoflagellate *Gambierdiscus toxicus*. *J. Am. Chem. Soc.* **1990**, *112*, 4380–4386. [CrossRef]

39. Satake, M.; Murata, M.; Yasumoto, T. The structure of CTX3C, a ciguatoxin congener isolated from cultured *Gambierdiscus toxicus*. *Tetrahedron Lett.* **1993**, *34*, 1975–1978. [CrossRef]
40. Satake, M.; Ishibashi, Y.; Legrand, A.-M.; Yasumoto, T. Isolation and Structure of Ciguatoxin-4A, a New Ciguatoxin Precursor, from Cultures of Dinoflagellate *Gambierdiscus toxicus* and Parrotfish *Scarus gibbus*. *Biosci. Biotechnol. Biochem.* **1996**, *60*, 2103–2105. [CrossRef] [PubMed]
41. Satake, M.; Fukui, M.; Legrand, A.-M.; Cruchet, P.; Yasumoto, T. Isolation and structures of new ciguatoxin analogs, 2,3-dihydroxyCTX3C and 51-hydroxyCTX3C, accumulated in tropical reef fish. *Tetrahedron Lett.* **1998**, *39*, 1197–1198. [CrossRef]

toxins

MDPI

Article

Asynchrony of *Gambierdiscus* spp. Abundance and Toxicity in the U.S. Virgin Islands: Implications for Monitoring and Management of Ciguatera

Justin D. Liefer [1,2], Mindy L. Richlen [3], Tyler B. Smith [4], Jennifer L. DeBose [5], Yixiao Xu [3,6], Donald M. Anderson [3] and Alison Robertson [5,7,*]

1 Department of Biology, Mount Allison University, New Brunswick, NJ E4L 1E4, Canada; jliefer@mta.ca
2 U.S. Food and Drug Administration, Dauphin Island, Alabama, AL 36528, USA
3 Woods Hole Oceanographic Institute, Woods Hole, MA 02543, USA; mrichlen@whoi.edu (M.L.R.); xuyixiao_77@163.com (Y.X.); danderson@whoi.edu (D.M.A.)
4 Center for Marine and Environmental Studies, University of the Virgin Islands, St. Thomas, MN 00802, USA; tsmith@uvi.edu
5 School of Marine and Environmental Sciences, University of South Alabama, Mobile, Alabama, AL 36688, USA; jdebose@southalabama.edu
6 Key Laboratory of Environment Change and Resources Use in Beibu Gulf, Ministry of Education, Nanning Normal University, Nanning 530001, China
7 Dauphin Island Sea Lab., Dauphin Island, Alabama, AL 36528, USA
* Correspondence: arobertson@disl.org; Tel.: +1-251-404-8163

Abstract: Ciguatera poisoning (CP) poses a significant threat to ecosystem services and fishery resources in coastal communities. The CP-causative ciguatoxins (CTXs) are produced by benthic dinoflagellates including *Gambierdiscus* and *Fukuyoa* spp., and enter reef food webs via grazing on macroalgal substrates. In this study, we report on a 3-year monthly time series in St. Thomas, US Virgin Islands where *Gambierdiscus* spp. abundance and Caribbean-CTX toxicity in benthic samples were compared to key environmental factors, including temperature, salinity, nutrients, benthic cover, and physical data. We found that peak *Gambierdiscus* abundance occurred in summer while CTX-specific toxicity peaked in cooler months (February–May) when the mean water temperatures were approximately 26–28 °C. These trends were most evident at deeper offshore sites where macroalgal cover was highest year-round. Other environmental parameters were not correlated with the CTX variability observed over time. The asynchrony between *Gambierdiscus* spp. abundance and toxicity reflects potential differences in toxin cell quotas among *Gambierdiscus* species with concomitant variability in their abundances throughout the year. These results have significant implications for monitoring and management of benthic harmful algal blooms and highlights potential seasonal and highly-localized pulses in reef toxin loads that may be transferred to higher trophic levels.

Keywords: *Gambierdiscus*; ciguatera poisoning; *Dictyota*; ciguatoxin; Caribbean; dinoflagellate; benthic algae; algal toxin; harmful algal bloom

Key Contribution: This study demonstrates a seasonal asynchrony between *Gambierdiscus* abundance and C-CTX toxicity through monthly long-term monitoring, with the most significant trends observed at offshore field sites where depth and other factors may favor toxin production. This asynchronicity reflects potential differences in the toxin cell quota of individual *Gambierdiscus* species and their variations in relative abundance with the species assemblage through time. These data highlight the need for increased spatio-temporal monitoring focused on identifying seasonal and site-specific pulses in CTX production in order to estimate potential CP risk rather than depending on genus-level abundance data.

Citation: Liefer, J.D.; Richlen, M.L.; Smith, T.B.; DeBose, J.L.; Xu, Y.; Anderson, D.M.; Robertson, A. Asynchrony of *Gambierdiscus* spp. Abundance and Toxicity in the U.S. Virgin Islands: Implications for Monitoring and Management of Ciguatera. *Toxins* **2021**, *13*, 413. https://doi.org/10.3390/toxins13060413

Received: 3 May 2021
Accepted: 7 June 2021
Published: 10 June 2021

1. Introduction

Of all the human poisoning syndromes associated with harmful algal blooms (HABs), ciguatera poisoning (CP) has the most significant human health and economic impacts globally [1]. CP is caused by consumption of fish or shellfish, generally associated with coral reef systems, that are contaminated with a suite of lipid-soluble toxins known collectively as ciguatoxins. These toxins and their precursors are produced by certain species or strains of benthic dinoflagellates in the genera *Gambierdiscus* and *Fukuyoa* that live on algal substrates or other surfaces, such as dead corals and sand, in many coral reef communities [2–4]. Ciguatoxins (CTX) and related metabolites enter and accumulate in coral reef food webs through grazing by herbivorous fish and invertebrates, reaching their highest concentrations in carnivorous finfish [5–7], where they pose the greatest public health risk [8]. With increased globalization, CTX and *Gambierdiscus* have been reported from temperate locations including the northern Gulf of Mexico, New Zealand, Japan, and the Canary Islands; however, CP is endemic to many tropical and subtropical coral reef ecosystems globally and primarily affects coastal communities [9–12]. Global estimates of CP incidence vary widely, ranging from tens of thousands to as many as 500,000 poisonings per year [1,13]. Producing accurate estimates of the true incidence of CP is challenged by a high degree of underreporting and misdiagnoses [14], and consequently, CP remains an overlooked and under-appreciated problem. Prevention and management strategies for CP have been hindered by knowledge gaps regarding the environmental and physiological factors contributing to toxin dynamics, as well as the lack of commercially available toxin standards and affordable and practical methods for toxin detection.

CP differs from other HABs in that poisoning events are not associated with large-scale planktonic blooms of a single causative species but are often an ongoing and chronic problem in endemic regions. Over the past two decades, renewed scientific interest and research has resulted in significant advances in our understanding of the biogeography and ecophysiology of *Gambierdiscus* and *Fukuyoa,* including a fuller characterization of species diversity and global distribution [2,15], intra- and inter-specific [16–19] growth characteristics [20,21], and habitat or substrate preferences (reviewed by [2]). These studies have provided a fuller understanding of the factors governing population and toxin dynamics, including the identification of highly toxic species that may dominate CTX production and flux into food webs. Key drivers of CTX prevalence and CP risk are thought to involve a combination of several environmental and ecological factors, including: (1) environmental conditions that promote growth, leading to high *Gambierdiscus* and *Fukuyoa* cell concentrations, (2) prevalence of CTX-producing species and strains, (3) environmental conditions that promote cellular toxin production, and (4) increased substrate availability that promotes the proliferation and increased areal abundance of benthic dinoflagellates in reef ecosystems. Additionally, patterns of toxicity are affected by bioconversion of the toxin precursors produced by *Gambierdiscus* to more potent compounds during toxin uptake, metabolism, and transfer.

As research on *Gambierdiscus* has expanded and progressed, so have efforts to characterize linkages between key environmental factors (e.g., seawater temperature), *Gambierdiscus* and *Fukuyoa* population and toxin dynamics, and subsequent CP risk and incidence. Early efforts by Tosteson [22] reported a relationship between warming seawater temperatures and barracuda toxicity, in which barracuda ciguatoxicity was correlated with both increases in seawater temperatures as well as with total cases of human ciguatera intoxications. In Tahiti, Chinain et al. [23] carried out weekly sampling of *Gambierdiscus* abundance and toxicity over a seven-year period (1993–1999), which identified seasonal trends in peak cell densities that occurred during the warmest months (October, November, December). They concluded that ciguatera outbreaks more likely reflected the presence of highly toxic strains rather than high overall biomass, as no correlation was found between sample toxicity and *Gambierdiscus* spp. abundance. These data were subsequently used by Chateau-Degat et al. [24] to construct a temporal model that related seawater temperatures to *Gambierdiscus* spp. growth, and subsequent onset of ciguatera cases. A key challenge

in these and other ongoing efforts to link spatiotemporal dynamics of *Gambierdiscus* spp. abundance and CTX production with CP risk is the high spatial heterogeneity observed for both *Gambierdiscus/Fukuyoa* populations and the ciguatoxicity of potential seafood vectors. Within small spatial scales (<3 km) on a single island, fish at one reef site may be safe to eat, while neighboring reefs can harbor "hot-spots" where ciguatoxic fish are prevalent [25–28]. This variation in CTX accumulation within higher trophic levels may reflect corresponding spatial heterogeneity in *Gambierdiscus* population structure, coupled with the large differences in CTX production documented among co-occurring *Gambierdiscus* and *Fukuyoa* species [9,16,17,29,30]. For example, there can be an over 1500-fold difference in toxin content among *Gambierdiscus* species, with *G. polynesiensis* identified as a toxic species from the Pacific [7], and *G. excentricus* and *G. silvae* as the most toxic species from the Caribbean [17,19,31,32].

In this study, we assessed *Gambierdiscus* abundance and CTX content within natural epiphyte assemblages from St. Thomas, USVI (Figure 1), an area hyperendemic for CP [33], to determine the seasonality, spatial variability, and environmental correlates of CTX production. Field activities were conducted monthly over 3 years at four coral reef sites located on the south side of the island, including two nearshore (Black Point, BP; Coculus Rock, CRK) and two offshore locations (Flat Cay, FC; Seahorse Shoal, SH), ranging in depth from ~6–22 m depth (see Figure 1). Populations of *Gambierdiscus* found at these sites are known to comprise five of the seven *Gambierdiscus* species documented in the Caribbean and one ribotype: *G. belizeanus*, *G. caribaeus*, *G. carolinianus*, *G. carpenteri*, *G. silvae,* and *G.* sp, *ribotype 2* (Richlen, M.L. unpublished data, and [34]). Clear, yet decoupled, seasonal patterns of *Gambierdiscus* abundance and CTX levels were observed, as well as marked differences in CTX levels among adjacent sites. Our findings indicate that variability in CTX production within *Gambierdiscus* populations over small spatial scales may be a key driver of CP risk. This work also highlights the importance of time-integrated monitoring of in situ CTX production, which provides a more direct determination of the sites and conditions that are the ultimate source of CP risk.

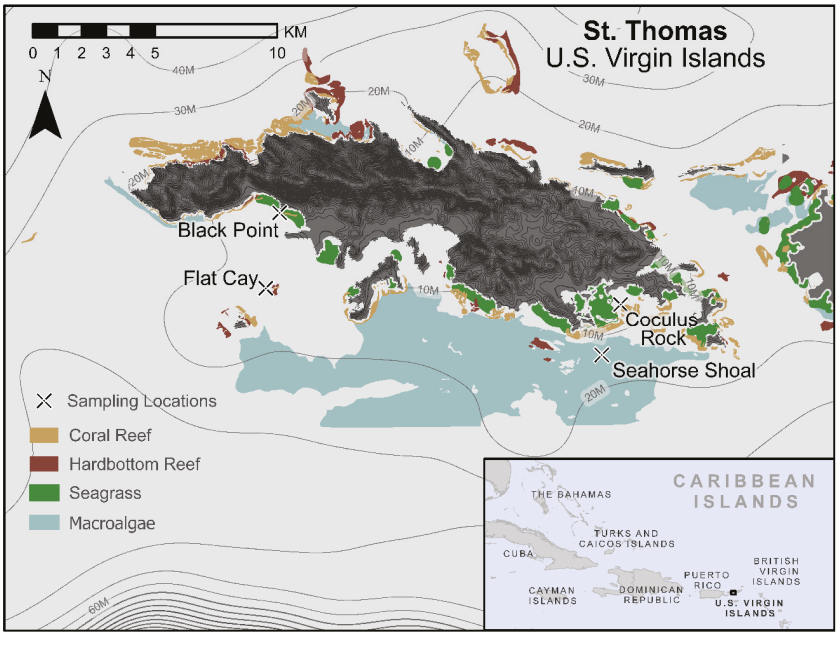

Figure 1. Map of long-term field sampling sites in St. Thomas, US Virgin Islands. Map created in ArcGIS Professional with

overlaid shapefiles of benthic cover with coral, hardbottom, and seagrass from [35] and macroalgae from the St. Thomas and St. John benthic habitat dataset [36], both from the National Oceanic and Atmospheric Administration, U.S. Dept. Commerce.

2. Results

2.1. Variation in Environmental Conditions and Benthic Composition

Mean daily temperature and salinity (not shown) were similar at all four sites and followed seasonal patterns. Benthic temperatures ranged from 25.5–29.9 °C with a mean of 27.8 ± 1.6 °C and displayed a seasonal pattern typical of the tropical northern hemisphere, with peak temperatures in summer (June–October) and minimum temperatures in winter (December–March). Salinity variations were small and ranged from 34.6–36.2 psu with a mean of 35.5 ± 0.5 psu, with maximum values in March–May and minimum values in September–November. Dissolved nutrients were low overall and varied over a small range. For instance, mean dissolved inorganic phosphorus (DIP) was 0.09 ± 0.04 μM, while mean dissolved inorganic nitrogen was 0.90 ± 0.8 μM. There were also no strong seasonal patterns in available data on climate variables (precipitation, wind speed and direction). Spatial and seasonal variation in environmental and physical parameters (i.e., wind speed and direction, precipitation, benthic temperature, and nutrients) were also examined with multivariate techniques and no clear ordination of parameters or clustering of sites was apparent (see Table S1). Analyses were limited to these parameters due to frequent gaps in other data (e.g., salinity and other CTD vertical profile measurements). Selected environmental parameters were compared using a principal components analysis (PCA) and no principal components explained more than 22.8% of overall variation (Table S1). Environmental variation among sites was examined with a cluster analysis, multidimensional scaling, and an ANOSIM test (Primer-E) for parameters that were measured directly at each site (benthic temperature and nutrients). All sites showed high multivariate similarity (ANOSIM Global R = 0.28) and no clear spatial patterns.

Benthic composition at all sites was mostly dominated by macroalgae, which ranged from 11.7–75.0% of benthic cover with a mean of 39.6 ± 12.5%, and was variable over time (Figure 2). Other major components were dead coral with turf algae, non-living substrate, and corals, with mean benthic cover ranging from 11.7–23.0%. Minor components included gorgonians, sponges, coralline algae, and cyanobacteria. As with the site environmental conditions, there were no clear spatiotemporal patterns and a high multivariate similarity (ANOSIM test, Primer-E) in overall benthic cover among sample years and study sites. Macroalgal cover was dominated by fleshy macroalgae which mainly consisted of *Dictyota* spp. (24.1 ± 10.0% of macroalgal cover; see monthly trends in Figure 2), followed by *Lobophora variegata* (7.7 ± 10.4%), and *Halimeda* spp. (0.4 ± 1.2%). Macroalgae composition was distinct among the sites (ANOSIM Global R = 0.568) (Supplementary Figure S1), primarily due to differences between the nearshore sites (CRK and BP) and the offshore Sites FC (R = 0.501–0.539) and SH (R = 0.824–0.935) (Table S1). A SIMPER analysis showed these dissimilarities were driven by the higher abundance of *L. variegata* at the offshore sites, which accounted for 41.7–60.7% of the dissimilarity between pairwise comparisons.

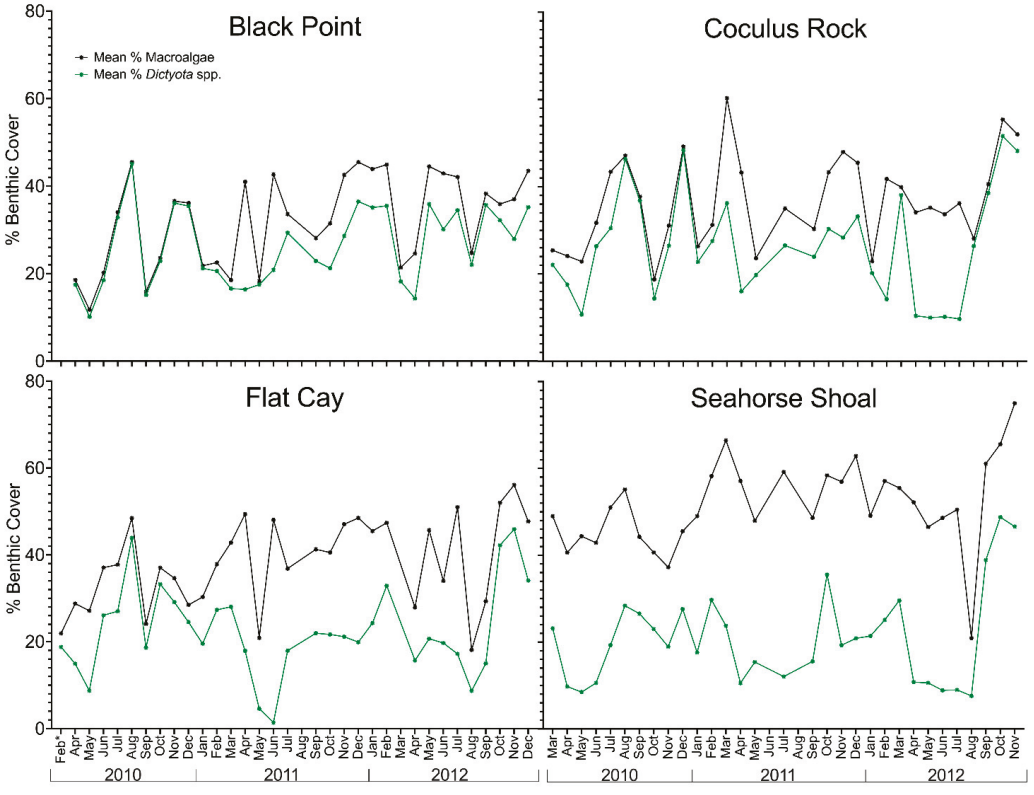

Figure 2. Time-series of benthic cover over the study period as determined by benthic habitat video surveys. Data highlights the temporal change in the percent (%) cover of combined macroalgae (black) and % *Dictyota* spp. cover (green) at each sampling site. Missing data points are time periods when benthic surveys were not conducted. Feb* denotes that FC was surveyed on 23 February 2010.

2.2. *Gambierdiscus spp.* Abundance

Gambierdiscus spp. were detected in all 135 samples collected in this study. Abundances of *Gambierdiscus* were highly variable, both in terms of overall range (2.5–63.3 cells g *Dictyota*$^{-1}$, mean 69.0 ± 63.3 cells g *Dictyota*$^{-1}$) and periodicity (Figure 3). The only apparent seasonal pattern in abundance was the occurrence of an annual maximum in September–October of each study year at each site that coincided with the thermal maximum of sea surface temperature and doldrum-like conditions. The variation in *Gambierdiscus* spp. abundance was dissimilar among sites, with the exception of the annual abundance peaks in September–October of 2010 and 2012 (see Figure 3). The highest overall abundances at CRK, FC, and SH were observed in September–October 2010, and annual mean *Gambierdiscus* spp. abundance was also significantly higher ($p < 0.001$, ANOVA with Tukey's test post hoc) in 2010 (111.5 ± 80.8 cells g *Dictyota*$^{-1}$) compared to 2011 and 2012 (49.4 ± 35.6 and 52.7 ± 51.3 cells g *Dictyota*$^{-1}$, respectively). Mean abundances were generally higher at BP (84.7 ± 69.3 cells g *Dictyota*$^{-1}$) and FC (80.4 ± 56.9 cells g *Dictyota*$^{-1}$) near the western end of St. Thomas compared to the eastern sites of CRK and SH (56.6 ± 62.0 and 54.7 ± 61.6 cells g *Dictyota*$^{-1}$, respectively), with overall abundance at BP being significantly higher than at CRK and SH ($p < 0.05$). There was no significant correlation between abundance and any of the environmental factors assessed, based on both direct parametric correlation tests and multivariate correlation analysis (BEST in Primer-E).

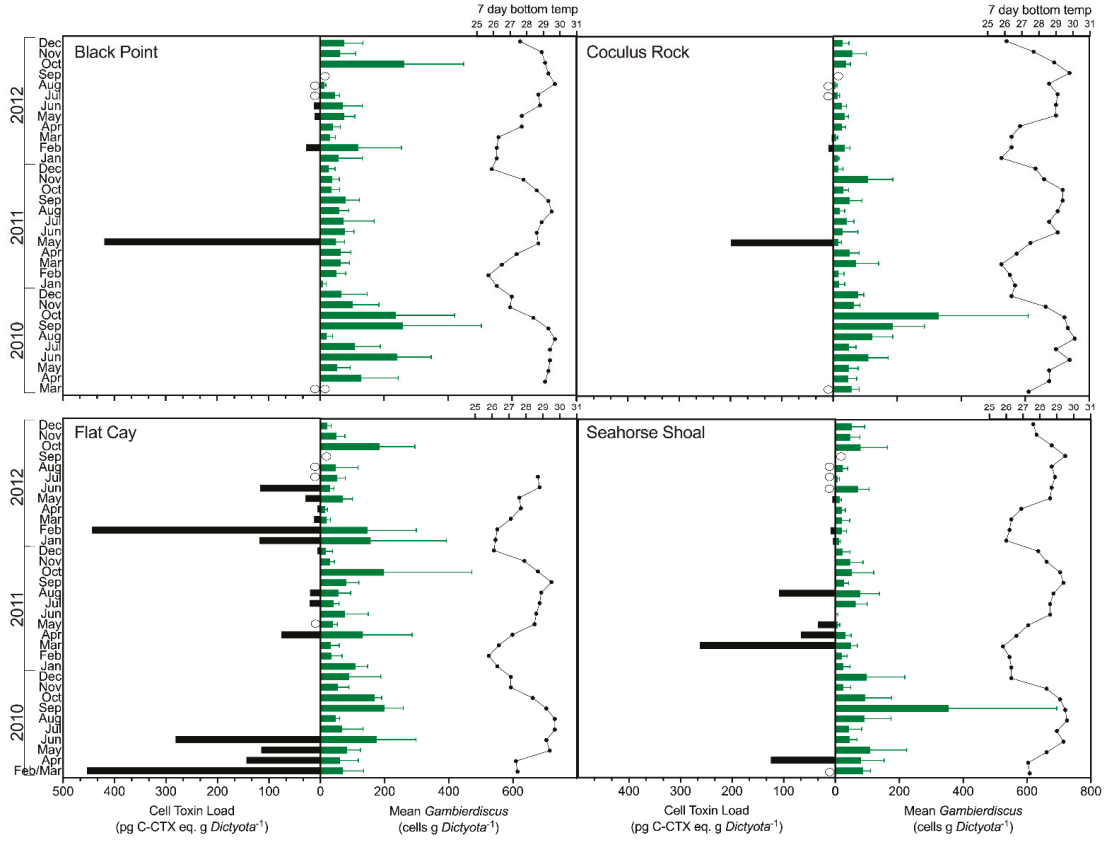

Figure 3. Asynchrony between cell toxin load (C-CTX eq cell^{-1} * cells g *Dictyota*$^{-1}$) and mean (+s.d.) *Gambierdiscus* spp. abundance (cells g *Dictyota*$^{-1}$), with 7-day averaged bottom temperatures from each site. Open circles represent "No Data" for either toxin load or *Gambierdiscus* abundance count.

2.3. Detection of Ciguatoxins in Field Samples

The specific sodium channel agonist activity detected by N2a assay was attributed to CTX congeners in all samples based on several lines of evidence: (1) the direction, shape, and slope of dose-response curves generated from field sample extracts were congruent with C-CTX-1 standards indicating similar activities and potencies by N2a assay (see Supplementary Figure S2); (2) *Gambierdiscus* spp. (a known source of CTXs) was present in all samples; (3) the extraction procedure used was not suitable for isolation of the polar alkaloid sodium channel blockers known to occur in marine systems (e.g., saxitoxin, tetrodotoxin); (4) non-specific activity potentially generated by other toxin classes (with alternate modes of action) were excluded from our analyses (as described in the Methods); and, (5) dinoflagellate sources and toxins of other site 5 sodium channel agonists, e.g., *Karenia*-produced brevetoxins, have not been reported in algae, fish, or shellfish from the study region. Considering the biotransformation of CTXs characterized in other regions, the CTX congeners detected in Caribbean *Gambierdiscus* spp. are likely to be uncharacterized precursors of C-CTX-1 or C-CTX-2, the most abundant congeners found in higher trophic level Caribbean fish [37,38]. The Caribbean CTX standard used in the N2a bioassays was C-CTX-1, the only quantified reference material that was available at the time of this study, hence all detected CTX levels are expressed as C-CTX-1 equivalents (C-CTX eq.).

The identity, structure, and toxicity of Caribbean CTX congeners present in *Gambierdiscus* spp. are poorly understood and no reference materials are presently available. This lack of knowledge complicates the use of clean-up methods, such as solid-phase extraction (SPE), for sample extracts as they may remove the target analytes. As detailed in the methods, four samples, representing a range of determined CTX activities, were purified using silica (Si) SPE column (Agilent) to assess the effect of sample clean up on measured composite toxicity. In all four samples, Si SPE purification caused a reduction in assay response in both the ouabain-veratridine-treated cells (i.e., reduction in CTXs) and PBS control cells (i.e., a reduction in cytotoxic matrix compounds). This indicates that Si SPE clean-up may have removed cytotoxic matrix compounds that affect negative control N2a cells, but also removed some of the target analyte with no improvement in quantification and hence was not used for sample quantitation. Dilution of samples (reducing both interfering matrix and analyte) that did not undergo clean-up or purification resulted in a 7–16% variation in quantitation. Considering the lack of precision in cell-based and other bioassays, as compared to instrumental methods (e.g., LC-MS/MS), this was considered an acceptable degree of variation.

CTX activity was quantifiable in 24.6% of benthic algal samples without purification while also meeting quality assessment controls of the N2a assay (summarized in Table 1). In the vast majority of remaining samples, CTX activity was below the limit of quantitation. The lowest CTX concentration quantified in our samples was 0.33 ± 0.06 ng C-CTX-1 eq. mL^{-1}, which was above the determined limit of quantitation for CTX in unpurified extracts of environmental algal samples using the N2a assay (see Section 4.4.4).

Table 1. The distribution of positive and quantifiable samples as well as the mean and range of cell toxin quota and toxin load across all sites.

Field Site	Black Point	Flat Cay	Coculus Rock	Seahorse Shoal	Overall
Total Samples Collected	30	32	31	32	125
No. Positive Samples	8	15	7	16	46
No. Quantifiable Samples	4	14	3	9	30
% Total Positive Samples	17.4	32.6	15.2	34.8	% of total
% Total Quantifiable Samples	13.3	46.7	10	30	% of total
Mean Cell Toxin Quota (pg C-CTX-1 eq. $cell^{-1}$)	0.3 ± 1.5	0.7 ± 1.4	0.4 ± 2.3	0.5 ± 1.3	0.5 ± 1.63
Cell Toxin Quota Range (pg C-CTX-1 eq. $cell^{-1}$)	0–8.3	0–6.4	0–12.6	0–5.4	0–12.6
Mean Toxin Load (pg C-CTX-1 eq. g *Dictyota*$^{-1}$)	15.1 ± 75.2	59.4 ± 121.3	6.8 ± 35.8	20.5 ± 55.5	25.5 ± 72.0
Toxin Load Range (pg C-CTX-1 eq. g *Dictyota*$^{-1}$)	0–419.4	0–453.8	0–199.5	0–262.2	0–453.8

2.4. Spatial and Temporal Variability of In Situ Ciguatoxin Levels

Among the 135 sampling events, 125 samples were available for assessing CTX production by *Gambierdiscus*. Among these, 46 (37.7%) were positive for CTX activity (Table 1), meaning that there was ≤50% survival in ouabain-veratridine-treated (i.e., sensitized to sodium channel agonist) N2a cells and ≥95% survival in untreated N2a cells at the same dosage. CTX levels were high enough to be quantified in 30 (24.6%) samples (Table 1). Samples deemed positive for CTX (specific activity for a sodium channel agonist), but not meeting quantitation criteria, were considered "trace" detections. Three samples were also considered trace measurements due to detection of CTX in the toxin samples and a

corresponding detection of *Gambierdiscus* spp. in the abundance samples at the same sampling points, but a measurement of *Gambierdiscus* cell abundance in the samples collected to assess toxicity was not available. Cell toxin quotas for *Gambierdiscus* spp. were calculated by normalizing the measured CTX concentration to the *Gambierdiscus* cell abundance measured within a given toxin sample. The toxin load for each sample was calculated as the product of the cell toxin quota and the *Gambierdiscus* spp. abundance measured on *Dictyota* hosts (i.e., cells per g *Dictyota*) during the same sample collection. This toxin load represents the amount of toxin present per mass of macroalgal substrate (units of pg C-CTX-1 eq. g *Dictyota*$^{-1}$) and is used as a proxy for the amount of toxin available for trophic transfer during each sampling event.

The toxin quota of *Gambierdiscus* ranged from 0–12.6 pg C-CTX-1 eq. cell^{-1} (Table 1; Figure 4) and toxin load ranged from 0–453.8 pg C-CTX-1 eq. g *Dictyota*$^{-1}$ (Table 1; Figure 3). Unlike *Gambierdiscus* spp. abundance, both toxin quota and toxin load appeared to have a distinct annual seasonality. The majority of positive samples (80.0%) and quantifiable toxin samples (76.6%) were collected during February–June of each sample year (Figures 3 and 4). The six quantifiable toxin samples observed outside of this February–June season were collected from Sites FC and SH in July–August 2011 and January–February 2012, months adjacent to the greatest periods of toxin occurrence (February–June 2011 and 2012). Only four trace toxin detections were observed in September–November of all sample years. There were no significant differences in mean toxin quota or toxin load between sample years (p = 0.057–0.061), although the largest proportion of quantifiable toxin samples occurred in 2012 (50.0%) followed by 2011 (33.3%) and 2010 (16.7%).

The majority of positive (67.2%) and quantifiable samples (76.7%) originated from the offshore sites FC and SH, with 46.7% of quantifiable samples originating from site FC alone and 30% from site SH (Table 1). The highest toxin quotas were detected at nearshore sites CRK (12.6 pg C-CTX-1 eq. cell^{-1}) and BP (8.4 pg C-CTX-1 eq. cell^{-1}), though these values were far higher than the other, infrequent toxin detections at these sites (Figure 4). A Welch's ANOVA (a one-way ANOVA that assumes unequal variance) showed a significant difference in toxin quota ($p < 0.005$) and toxin load ($p < 0.01$) among sites. A post hoc Games–Howell test showed that both toxin quota ($p < 0.01$) and toxin load ($p < 0.05$–0.01) were significantly higher at FC compared to CRK and BP (Figure 5). Considering both spatial and temporal variability, 50.0% of positive samples and 63.3% of quantified samples occurred at offshore sites and during the high toxicity period of February–June.

There was no strong or significant correlation between toxin quota or toxin load and any of the environmental factors assessed, based on both direct parametric correlation tests and multivariate correlation analysis (BEST in Primer-E). This is not surprising considering that CTX was not quantifiable in ~75% of samples and the lack of ordination or apparent structure in the environmental data. Although no monitored environmental variables were directly correlated with toxin parameters, the vast majority of positive (69.6%) and quantifiable (90.0%) samples were collected when temperatures were below the mean of the study period (27.8 ± 1.6 °C). Additionally, greater majorities of positive (91.3%) and quantifiable (96.7%) samples were collected when salinity was above the mean of the study period (35.5 ± 0.5 °C).

The toxin quota of the *Gambierdiscus* present, rather than *Gambierdiscus* abundance, appeared to determine toxin load throughout the study. There was no correlation between *Gambierdiscus* abundance (Spearman's R = −0.090, p = 0.51) and toxin load overall (Spearman's R = −0.054, p = 0.68) Additionally, there were only four trace detections during the months of peak abundance in each year (September–November), while some of the highest toxin quotas and loads occurred when abundances were relatively low (Figure 3).

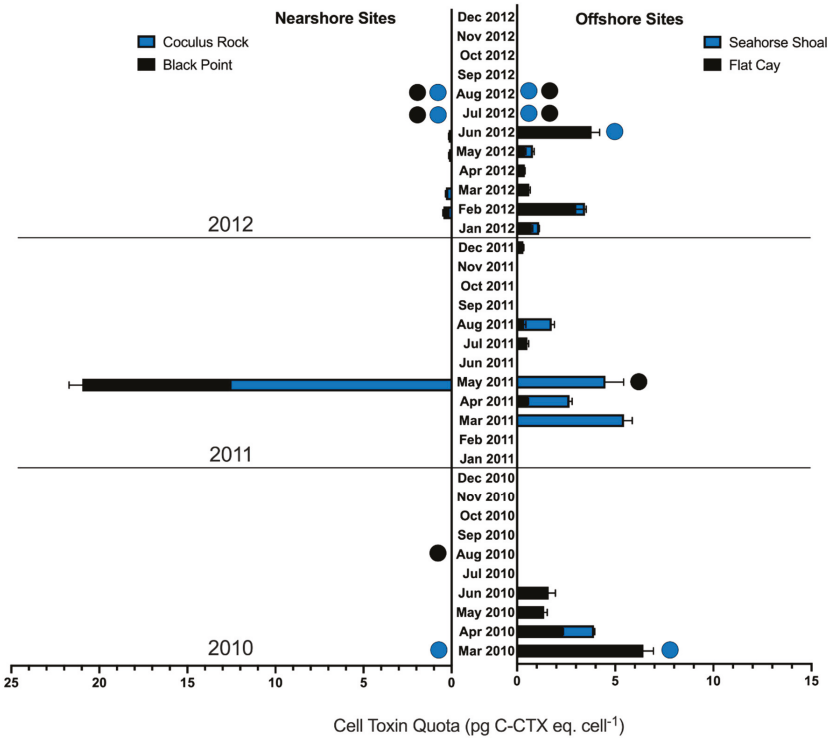

Figure 4. Time series of toxin cell quota (pg C-CTX-1 eq. cell^{-1}) determined from benthic microalgal (20–200 μM fraction) field samples collected monthly from nearshore (Black Point; Coculus Rock) and offshore sites (Flat Cay; Seahorse Shoal) of St. Thomas, Virgin Islands. Black Point and Flat Cay (black bars) are western sites, whereas Coculus Rock and Seahorse Shoal (blue bars) are eastern sites. Colored circles represent "No Data" collected from the corresponding sites, with all other zeros indicating true non-detections of toxicity.

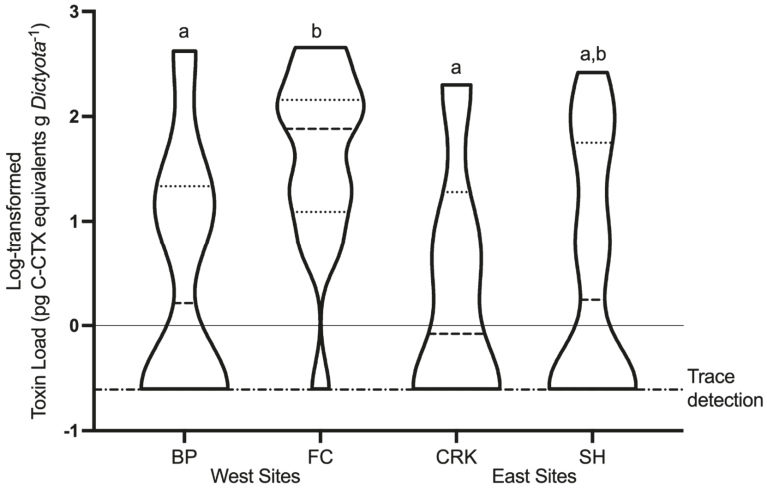

Figure 5. Truncated violin plot of log-transformed toxin load. Medians (dashed) and quartiles (dotted) shown. Trace detections were designated at toxin load 0.25 pg C-CTX-1 eq. g *Dictyota*$^{-1}$ (log-transformed to −0.6). Letters on plot indicate significant differences in toxin load between sites.

3. Discussion

Laboratory studies of isolated toxic microalgae are essential for confirming their toxicity and mechanisms of toxin production, but these measurements often differ from the levels of toxin production observed in natural systems. Thus, robust assessments of in situ toxin production by harmful microalgae are critical for understanding their true toxin dynamics and potential threat to ecosystem function or public health. This work is the most comprehensive and quantitative assessment to date of the in situ toxicity of *Gambierdiscus* in the Caribbean, the ultimate cause of more cases of human illnesses than any other harmful alga [1]. We also express this in situ toxicity in proportion to the mass of an abundant benthic substrate (the macroalga *Dictyota* spp.) consumed by potential vectors of CTX, providing a quantitative link between toxin production and trophic transfer. As these values were determined in a location where CP is endemic with monthly sampling over 3 years, our findings provide valuable constraints for efforts to model in situ CTX levels and the trophic transfer of CTX in the Greater Caribbean region.

3.1. Relative Toxicity of In Situ Gambierdiscus

The cell toxin quotas determined in this study, ranging from 0–12.62 pg C-CTX-1 eq. cell^{-1} with a mean of 0.5 ± 1.63 pg C-CTX-1 eq. cell^{-1}, are comparable to the limited number of other available in situ values (see Table 2). Values in Table 2 that were determined with the mouse bioassay, originally compiled as mouse units by Litaker et al. [15], were converted to composite CTX toxin quotas by assuming that one mouse unit is equivalent to 18 ng of CTX3C for Pacific samples and 72 ng of C-CTX-1 for Caribbean samples [39,40]. Though comparable to other in situ values, the toxin quotas we observed are also considerably higher than those of most cultured *Gambierdiscus* strains of Caribbean, eastern Atlantic, or Pacific origin measured using similar applications of the N2a assay as used in this study [17,19,41]. Most of these N2a toxin quotas were determined as CTX3C equivalents [17,19], a common Pacific congener of CTX that has been reported to be 2-fold more toxic than the Caribbean congener we used as a reference standard, C-CTX-1 [42]. This difference in standard toxicity could cause a lower CTX content to be determined in Caribbean strains measured with CTX3C as a standard rather than C-CTX-1. Even when taking this difference into account, the only Caribbean strains with toxin quota values comparable to the in situ values measured in this study are those from the species *G. silvae* (2.1–4.8 pg C-CTX-1 eq. cell^{-1} [31]) and *G. excentricus* (0.47 pg CTX3C eq. cell^{-1} and 1.43 pg CTX3C eq. cell^{-1}, respectively [17,19]).

Table 2. Published values of in situ *Gambierdiscus* toxin quota. Toxin measurements determined by mouse bioassay (MBA) were originally compiled by Litaker et al. [15] and were standardized prior to conversion to toxin quotas, assuming one mouse unit = 18 ng of CTX3C and 72 ng of C-CTX-1 for Pacific and Caribbean samples, respectively [39,40].

Location	Cell Toxin Quota (pg CTX eq. Cell^{-1})		Method	*N*	Reference
	Range	Mean			
Northwest Hawaiian Is., Hawaii	-	24	[1] MBA	1	[43]
Papara, Tahiti, French Polynesia	0.09–3.60	0.25 ± 0.18	[1] MBA	34	[23]
Rapa Island, French Polynesia	0.5–13.5	-	[2] RBA	4	[44]
Gambier Islands, French Polynesia	0.03–1.00	0.15 ± 0.26	[1] MBA	6	[45]
Hitiaa Reef, Tahiti, French Polynesia	0.05–1.35	0.16 ± 0.20	[1] MBA	10	[46]
Gambier Islands, French Polynesia	0.96–1.42	1.15 ± 0.32	[1] MBA	2	[47]

Table 2. *Cont.*

Location	Cell Toxin Quota (pg CTX eq. Cell^{-1})		Method	*N*	Reference
	Range	Mean			
Platypus Bay, Australia	-	0.23	[1] MBA	1	[48]
Nuku Hiva, French Polynesia	0.85–3.90	2.38 ± 2.15	[2] RBA		[49]
Rapa, French Polynesia	-	0.03 ± 0.004	[3] N2a	1	[50]
^ St. Thomas, US Virgin Islands	1.14–5.14	1.54 ± 0.94	[1] MBA	3	[51]
^ St. Thomas, US Virgin Islands	0.00–12.62	0.56 ± 1.75	[3] N2a	125	This Study

[1] Mouse Bioassay (MBA); [2] Radioligand Receptor Binding Assay (RBA), [3] In vitro mouse neuroblastoma MTT based assay (N2a); [4] sample number (*N*). ^ Caribbean Region.

3.2. Cellular CTX Quota and Not Gambierdiscus Abundance Determines CTX Production

One of the most notable findings of this study is the greater influence of toxin quota rather than *Gambierdiscus* abundance on CTX load overall and within any given site. The vast majority of CTX detections occurred from February to June of each study year when *Gambierdiscus* abundance was relatively low, while CTX was generally not detected during periods with the highest *Gambierdiscus* abundances. The only other study to our knowledge that has monitored site-specific *Gambierdiscus* abundance and in situ toxicity over time [23] found a similar asynchrony between abundance and toxicity, with the highest in situ toxin measurements observed at relatively low *Gambierdiscus* abundance, and *Gambierdiscus* abundance being a poor predictor of in situ toxicity. This decoupling or asynchrony of *Gambierdiscus* abundance and CTX production is consistent with wide variation in toxicity that has been observed among *Gambierdiscus* species in all regions where the genus is endemic [7,17,19,30,32]. The far greater variation in toxicity among species compared to the variation within a species [19,41,52–54] indicates that CTX source levels are mostly determined by species composition rather than *Gambierdiscus* abundance at the genus level [17]. Additionally, the species that appear to be most common and widespread in the Caribbean, such as *G. caribaeus*, *G. carolinianus*, *G. belizeanus*, and *G. carpenteri*, have low toxicities [17,19], thus periods when these species are abundant may not be expected to result in high CTX levels. In contrast, Caribbean species such as *G. silvae* have been shown through our prior efforts to have high toxin quotas [31], while others have reported similar trends for *G. excentricus* [17,19]. In both cases, the reported cell toxin quotas reported in these high toxin-producing strains of the respective species, could have the capacity to produce the in situ CTX loads observed in this study, even at low abundances. The discovery of "super-producing" strains of *G. polynesiensis* in Pacific waters has generated the hypothesis that a small relative abundance of highly toxic *Gambierdiscus* species may dominate CTX production that leads to CP outbreaks [7,40,48]. The high CTX loads observed at relatively low in situ *Gambierdiscus* abundances, the high toxicity of some *Gambierdiscus* species, and the low toxicity of the most common *Gambierdiscus* species in our study region all support the hypothesis that highly toxic, low-abundance species of *Gambierdiscus* dominate CTX production in the Caribbean.

3.3. Nearshore vs. Offshore Sites

Gambierdiscus CTX production also displayed spatial patterns that were generally consistent across three years of monitoring. *Gambierdiscus* was present in all samples collected over the study period, yet the majority of samples containing quantifiable CTX were collected at offshore sites (FC and SH) during February–June. Though distinct in their contribution to regional CTX levels, sites FC and SH were similar to nearshore sites with respect to measured physical and chemical features. Despite these apparent similarities, depth may be a factor that distinguishes the high CTX offshore sites (FC and SH), where sampling depths were greater (~18 m bottom depth) than at the nearshore sites CRK and

BP (~9 m bottom depth). This difference in depth may generate distinct light and water motion conditions for epiphytic *Gambierdiscus* populations between offshore and nearshore sites, the measurement of which were beyond the scope of this work. Measurements of light availability or optical qualities of the overlying water column were not available for the samples used in this study and physical conditions at all study sites were inferred from current and wave activity at one nearby buoy-monitoring location. However, water motion has been shown to be low, with little effect on *Gambierdiscus* populations in this study area [55], and is considerably lower than at locations where depth and water motion seem to affect *Gambierdiscus* abundance within epiphytic communities [56]. There is limited and conflicting evidence as to the physiological effect of light on toxin production within *Gambierdiscus* species or strains [44,57], but there are distinct growth-irradiance responses among co-occurring Caribbean *Gambierdiscus* species [20,21]. More favorable light conditions for constitutively more toxic species at deeper offshore sites could support the observed spatial patterns in CTX production. Future studies could test this supposition by determining if the most toxic species found at the offshore locations in this study or similar locations have lower optimal or maximum growth irradiances or are better adapted to the likely lower variability in irradiance of deeper benthic habitats.

Nearshore and offshore sites also varied in terms of the relative abundance and composition of macroalgae substrate. At the nearshore sites (BP and CRK), *Dictyota* spp. made up the majority of the macroalgal substrate for *Gambierdiscus* attachment. However, at the offshore sites (FC and SH), there was generally a higher percent-cover of fleshy macroalgae, as well as a greater proportion of species other than *Dictyota* present (e.g., *Lobophora variegata*). Although, beyond this study, to differentiate, there are multiple aspects where macroalgal abundance and composition might impact *Gambierdiscus* abundance and ciguatoxin transferability. Specifically, *Gambierdiscus*–macroalgae host interactions, which can be species-specific, might depend on shading potential, chemical cues, and host-palatability to higher trophic levels [58–60]. Since *Gambierdiscus* species determination has further developed since this study, future studies could determine if there are particular in situ host associations or macroalgal abundance that favor particularly toxic species/strains and if these associations are linked to the environmental conditions and benthic community compositions that vary between these nearshore and offshore sites.

3.4. Seasonality of CTX Production

Seasonal patterns of *Gambierdiscus* CTX quota and CTX loads were observed, with the vast majority (80.0%) of CTX detections occurring in February–June, which provides key insights into the environmental and ecological factors controlling CTX exposure risk. A similar seasonal pattern for in situ toxicity was also observed by Chinain et al. [23] in Tahiti, with the majority of high in situ CTX levels observed at temperatures below annual means and low or no in situ toxicity observed in the warmest months. If CTX loads are indeed determined by highly toxic species occurring at relatively low abundances, then the temporal patterns observed in this study indicate that these species show seasonality in their occurrence. Of the wide set of monitored environmental conditions that may affect *Gambierdiscus* populations, temperature and salinity showed the strongest seasonal patterns. However, neither of these factors were directly correlated with CTX quotas or loads. Salinity varied over a relatively small range (34.6–36.2 psu), which is unlikely to have an effect among species or a physiological impact within a species [20]. Temperature showed a considerably larger seasonal variation (25.5–29.9 °C) that spans the known range of temperature optima for *Gambierdiscus* species [20,21]. Despite the lack of a direct correlation between temperature and CTX levels, it is striking that the vast majority of positive (69.6%) and quantifiable (90.0%) samples were detected when benthic temperatures were below the mean temperature of the study area (27.8 ± 1.6 °C). This mean temperature is also well above the growth optimum for *G. silvae*, the most toxic Caribbean species examined by Xu et al. [20], which had the lowest upper temperature limit for growth (29.8 °C) among eight *Gambierdiscus* species. Additionally, the strain of *G. excentricus* that

has produced the highest CTX quotas for an Atlantic species to date [19] was isolated from waters off the Canary Islands with relatively cool temperatures for *Gambierdiscus* (18–24 °C). The strain of *G. excentricus* that has produced the highest CTX quotas for a Caribbean species [17] was isolated from Pulley Ridge, located ~150 km offshore of Florida at a depth of 60–80 m where temperatures would be considerably lower than the mean temperature observed in the present study. The adaptation of the most toxic Caribbean strains to cooler temperatures is consistent with CTX detections being restricted to below-average temperatures in this study and may provide a key environmental constraint on CTX exposure risk.

3.5. Implications for Assessing CTX Exposure Risk

Our observation that CTX source levels in St. Thomas are determined by the toxin quota of *Gambierdiscus* cells rather than their abundance at the genus level has implications for efforts to predict CP risk in regions where this illness is endemic. Many proposed management efforts or models of potential CP risk are based on monitoring or predicting overall *Gambierdiscus* abundance [24,61–63]. Our findings and the apparent importance of species composition in determining the CTX production of a *Gambierdiscus* population [7,17] indicate that monitoring *Gambierdiscus* abundance alone would not help determine when and where trophic systems are likely to encounter and biomagnify CTX. Determining the most toxic *Gambierdiscus* species in an endemic CP location and using new molecular identification tools [34,64,65] to determine their spatiotemporal distribution may be more conducive to estimating CP exposure risk.

Even if the occurrence of CTX in the first trophic level could be accurately predicted in systems that yield ciguatoxic fish, predicting the spatial and temporal links between algal CTX production, bioaccumulation of CTX in higher trophic levels, and potential human exposure remain challenging. Our findings provide the basis for linking these phenomena by demonstrating that CTX production is restricted both spatially, within a relatively small study area (offshore sites in St. Thomas), and seasonally (~February–June). Determining the locations most likely to produce CTX allows studies of trophic dynamics of CTX (e.g., [26]) or of the site fidelity of key CTX vectors like large, mobile fish species to be related to a limited spatial source of CTX. By establishing a time-frame when CTX vectors are most likely to consume highly toxic *Gambierdiscus*, the lag between CTX production and potential human exposure can be better assessed. The restriction of CTX production to below-average temperatures and the possible importance of cool-adapted highly toxic species [8] also suggests lower temperature limits and a broader potential geographic range for CP risk in shallow marine habitats than previously estimated [63]. These implications (i.e., potential range expansion of cool-adapted toxigenic *Gambierdiscus* species) have also been suggested by others in the field [8,66,67], highlighting the importance of further evaluation so that monitoring and predictive models meet the needs of future risk assessment.

4. Materials and Methods

4.1. Site Descriptions

Samples were collected at four sites around St. Thomas (Figure 1) between late February/early March 2010 and December 2012. All St. Thomas sites are located south of the island on a nearshore to offshore gradient. Coculus Rock (CRK; 18.31257 N, 64.86058 W) is located near an emergent rock reef and is composed of diverse scattered stony corals on bedrock (6–7 m depth). Black Point (BP; 18.3445 N, 64.98595 W) is a nearshore fringing coral reef (7–16 m depth). Flat Cay (FC; 18.31822 N, 64.99104 W) is a fringing coral reef on the leeward side of a small uninhabited island (11–16 m depth). Seahorse Shoal (SH; 18.29467 N, 64.8675 W) is a deep patch reef 2 km offshore of St. Thomas (19–22 m depth). The latter three sites are star coral (*Orbicella* spp.) reefs with diverse coral and sponge communities. Further site descriptions can be found in [68]. During the sampling period for this study, these sites were impacted by a moderate thermal stress and coral bleaching event in August 2010 (widespread colony paling and bleaching, but limited mortality), which was

truncated by the passage of Hurricane Earl on 3 August [69,70]. This storm passed about 105 km NE of St. Thomas, causing wind gusts of up to 120 km hr^{-1} and rainfall of 7.6 cm at the St. Thomas airport (see https://www.nhc.noaa.gov/data/tcr/AL072010_Earl.pdf, accessed on 22 April 2021).

4.2. Environmental Sampling

4.2.1. Oceanographic Measurements

Salinity measurements were obtained at each site from vertical profiles taken with a shallow-water Seabird SBE 25 recording at 8 Hz (Sea-Bird Electronics, Bellevue, WA, USA). Sensors were factory-calibrated within one year of deployment. Casts were made at anchor or on drift within 100 m (horizontal) of the research site. Casts were made within 1 m of the seafloor. Resulting data files were trimmed to the bottom meter of the downcast and averaged over this meter for use in analysis as this reflected the closest point to the reef organisms. Additional physical data was retrieved from the Caribbean Ocean Observing System St. John Oceanographic Buoy (VI 104; 18°15.09′ N, 64°46.02′ W; https://www.caricoos.org/station/st-john/us, accessed on 22 March 2021).

4.2.2. Benthic Temperatures

Benthic temperatures were taken at each site by a shaded Hobo Water Temperature Pro V2, Onset Computer Corp., Bourne, MA, USA) affixed to a steel rod within 20 cm of the reef surface following prior methods [69,71]. Probes were calibration-checked prior to deployment in an ice bath and took readings every 15 min. Data were averaged over each day to determine 1-day mean, and further averaged over 7, 14, 21, and 30 days for the respective means for use in analyses.

4.2.3. Precipitation

Precipitation and wind data for the region was recorded at the St. Thomas Cyril E. King Airport by a US National Weather Service station (TIST) and data was accessed at the National Climate Data Center https://www.ncdc.noaa.gov/cdo-web/datasets/GHCND/stations/GHCND:VQW00011640/detail, accessed on 22 March 2021). The mean daily precipitation for the 14 days prior to a sampling event was calculated from daily summaries.

4.2.4. Nutrient Analyses

Water samples for nutrient analyses were collected in whirlpak bags and stored on ice until return to the University of the Virgin Islands (UVI; within 5 h). Once at the laboratory, samples were transferred to acid-washed, sample-rinsed polypropylene bottles and frozen at −20 °C. Samples were shipped frozen to Woods Hole Oceanographic Institute (WHOI) and analyzed for inorganic nitrate plus nitrite (hereafter termed "nitrate"), ammonium, silicate, and phosphate using a Lachat Instruments QuickChem 800 four-channel continuous flow injection system. This method is USEPA approved for nutrient analysis ranging from groundwater to the open ocean.

4.2.5. Benthic Community Composition

Benthic cover at each study site was estimated using digital video along six randomly sited permanent transects as described in [71]. Each transect was 10 m in length and marked with steel rods, with transects spaced at least 3 m apart. Digital video was recorded perpendicular to the substrate and resultant images were cut into non-overlapping images, typically 15 per transect. Fifteen random points were placed on the image using Coral Point Count software [72] and characterized to the lowest identifiable taxonomic or abiotic level by a trained expert. Cover of each category (i.e., Coral, Gorgonians, Sponges, Zoanthids, Macroalgae, Coralline Algae, Dead Coral with Turf Algae, Non-Living Substrate, Other Living) was calculated for each transect by dividing the number of occurrences by the total number of points surveyed. Macroalgal cover was partitioned into % fleshy macroalgae, % *Dictyota* spp., % *Lobophora variegata*, % *Halimeda* spp., and % other.

4.3. Biological Sampling

4.3.1. Collection of *Gambierdiscus* Epiphytes

Gambierdiscus were collected as epiphytes on macroalgae to determine their abundance and toxin content and scientific collection permits for this project were approved by the Virgin Islands Department of Fish and Wildlife, Marine Resources Division.

Dictyota spp. were the most widely distributed algae at the sampling sites (and frequently was the only macroalgal taxa present), so only *Dictyota* spp. were sampled for this study. Eight replicate samples of *Dictyota* spp. (four for *Gambierdiscus* abundance and four for toxin measurements) were collected by SCUBA divers from each study site in each month of the study period, with these exceptions: February 2010—only Flat Cay was sampled, March 2010—only Coculus Rock and Seahorse Shoal were sampled, and September 2012—no sites were sampled. Multiple thalli of *Dictyota* spp. were collected by carefully cropping and transferring to a Ziploc bag, which was then sealed underwater. Samples were stored in a cooler until processing within the same day. For sample processing, macroalgae were vigorously shaken for at least one minute to loosen the dinoflagellates, which were then sieved sequentially using 200 μm and 20 μm nitex sieves. *Dictyota* spp. retained in the 200 μm filter were removed, blotted dry with a paper towel, and weighed. With samples for *Gambierdiscus* abundance, the fraction of material retained on the 20 μm sieve was rinsed into a 15 mL conical tube, brought up to 10 mL with filtered seawater, and preserved with 0.5 mL formalin. For toxin samples, material retained on the 20 μm sieve was pooled from all four samples and rinsed into a shallow tray. The tray was maintained under low light (cool white fluorescent) and larger particulate material was allowed to settle to the bottom of the tray while living, detached *Gambierdiscus* cells (or other motile epiphytes) would remain in the overlying water due to active swimming and phototaxis. This overlying water was gently siphoned off and sieved again with a 20 μm sieve. Material collected with this final sieving was rinsed into 50 mL polypropylene centrifuge tubes (total capacity 60 mL) with filtered seawater and samples centrifuged at low speed (<1000× *g*) for 5 min to pellet cells. A small volume of overlying seawater was discarded to reach a final volume of 50 mL for each sample. This sample was then inverted several times to mix and a 1 mL aliquot was collected and preserved as described above for *Gambierdiscus* abundance measurements to determine the *Gambierdiscus* cell density within the toxin sample. After low-speed centrifugation of the remaining cell suspension and subsequent removal of supernatant, the cell pellet was stored at −20 °C or on dry ice (during shipping to Dauphin Island) prior to toxin analyses.

4.3.2. *Gambierdiscus* Cell Enumeration

Preserved samples were gently shaken and 0.5–1.0 mL was loaded in a Sedgewick Rafter slide. *Gambierdiscus* cells were identified to genus based on cell size and shape using photomicrographs and line drawings, e.g., [73]. *Gambierdiscus* abundance was enumerated using a Zeiss Axioskop microscope at 100× magnification. Sample cell densities were determined by multiplying the summed cell counts by a subsample proportion factor, and then dividing this value by the *Dictyota* wet weight to express *Gambierdiscus* cell concentrations as cells g ww^{-1}. At the time this study was conducted, methods for discriminating *Gambierdiscus* species had not yet been developed, so cell counts are given for total *Gambierdiscus* spp.

4.4. Toxin Extraction and Analyses

4.4.1. Cell Pellet Extraction

Pellet material representing the 20–200 μm fraction of epiphytic material collected from *Dictyota* spp. (approx. 5 g per tube) were initially extracted in 10 mL of 100% methanol (MeOH) with 2 min. vortex mixing and 2 min. probe sonication on ice (5 s pulses, 20% power). The extract was centrifuged (3000× *g* for 5 min. at 20 °C) and the supernatant was collected. The sample pellet was then extracted two more times as before, but without additional probe sonication. Supernatants were pooled (30 mL total), diluted with water to

60% aqueous MeOH, and then partitioned three times with 25 mL dichloromethane (DCM). The recovered DCM fractions were pooled and dried by rotary evaporation at 30 °C. The sample residue was then quantitatively transferred from the evaporation flask with washes of MeOH and DCM, added to a 13 × 100 mm glass vial, and dried under high-purity nitrogen gas at 30 °C. Sample CTX residue was then redissolved in 100% MeOH (5 mL) with 2 min. vortex mixing and 2 min. bath sonication and stored at −20 °C until analysis. All extractions were performed with HPLC-MS grade solvents (Sigma) and ultra-pure (18 MΩ) water.

4.4.2. Quantitation of CTX by In Vitro N2a Cytotoxicity Assay

The ciguatoxin content of each sample was measured as composite toxicity using an ouabain-veratridine (O/V) dependent in vitro neuroblastoma cytotoxicity assay (N2a assay) [74]. These assays utilized mouse Neuro-2a cells (ATCC, CL131; N2a), which were propagated and maintained under continuous growth as previously described [27,75]. Cells were harvested at 85–90% confluency and seeded to sterile 96-well polystyrene plates at a density of 4×10^4 cells well^{-1}. The N2a assay measures sample toxicity as a loss in viability of N2a cells that have been sensitized with O/V, making these cell responses highly specific to sodium channel toxins (e.g., CTX) and thus adds a line of evidence for CTX (or a composite of CTXs) being present in samples when loss in viability is observed. Within each assay, the response of untreated N2a cells (serving as negative control) is assessed at the same sample doses provided to O/V-treated cells to determine if the sample contains other toxic substances that are not sodium channel toxins and could affect viability of O/V-treated cells.

For quantitative assays of CTX, triplicate dose-response curves were determined for both O/V-treated and untreated N2a cells exposed to eight concentrations of sample CTX residues redissolved by high-speed vortex in 100 µL of 5%-FBS-RPMI media spanning a 128-fold range. After 24 h of exposure to sample extracts, N2a cell viability is assessed as the reduction of 3-(4,5- dimethylthiazol-2-yl)-2,5-diphenyltetrazolium bromide (MTT) by metabolically active cells to a purple formazan product that is measured by absorbance at 570 nm. The concentration of sample extract at which 50% of N2a cells lost viability (IC_{50}) was compared to the IC_{50} of a purified C-CTX-1 standard (50 pg starting dose) that was measured in a concurrent N2a assay seeded with the same batch of N2a cells seeded to sample assays. These analyses were possible due to an aliquot of purified C-CTX-1 stock that was purified from toxic *Sphyraena barracuda* harvested from the Virgin Islands and is the same FDA stock reported in several prior studies [e.g., 27, 75, and others]. Impurities were assessed by LC-MS/MS analyses prior to use and original stocks quantified via NMR and gravimetric analysis (data not available). The toxin content of samples is expressed as the mass of C-CTX-1 equivalents in *Gambierdiscus* cells (pg C-CTX-1 eq. cell^{-1}) based on the toxin sample cell counts described above. Samples in which the amount of extract required to cause a 50% loss in viability of O/V-treated N2a cells, and also caused significant loss in viability in untreated N2a cells, were considered below the limit of detection. Samples like these, in which there is clear CTX-specific activity, but quantitation criteria are not met, were considered positive detections of CTX, but their CTX content is described as "trace".

4.4.3. Sample Screening and Dose Determination

To determine which samples contained sufficient CTX-specific toxicity to be quantitated using the procedure described above, sample extracts were initially screened using eight sample concentrations along a two-fold dilution series that were assayed in triplicate. These sample concentrations ranged from 0.0078–1.0% of the total extract, corresponding to doses of ~0.7–1000 *Gambierdiscus* cells. The extract dissolution series was prepared in 100% MeOH, dried under high-purity N_2 gas, redissolved in a minimum 100 µL of assay growth media, and 10 µL was added to assay well. Since a minimum of 100 µL was required to redissolve dried extracts, but only 10 µL of this could be used as a dose, a dosing range of 0.008–1.0% required using at least 10% of total sample extract. Due to the

nature of determining IC_{50} values from sigmoidal dose-response curves that meet quality control criteria, full quantitative N2a assays require the highest doses to result in <20% N2a cell viability and be 8 to 16-fold higher than the IC_{50} and at least 32-fold higher than doses that show no CTX-specific toxicity. Thus, samples in which a dosing of 1% of the total extract (requiring 10% of the extract to be used) demonstrated CTX-specific toxicity, but failed to cause <20% N2a cell viability, would not contain sufficient sample material for a quantitative assay result requiring a higher dosage. These low-CTX samples were considered to be positive detections of CTX, but their CTX content is described was "trace" rather than a numerical value. Samples for which the maximum dose of 1% sample extract or subsequent dilutions caused CTX-specific toxicity resulting in <20% N2a viability were analyzed by full quantitative assays. The dose for these quantitative assays was adjusted to achieve the maximum concentration at which non-O/V-treated N2a cells maintain >90% viability and O/V-treated cells have <20% N2a viability and generate a dose response curve meeting quality criteria. Quantitation was based on the mean sample IC_{50} values of six replicate dose response curves (measured in two assay plates, each containing triplicate dose response curves) that showed less than 15% variation.

4.4.4. Tests of Matrix Effects and Sample Purification

In many samples, the doses that could be used for quantitation were limited by their level of non CTX-specific toxicity in N2a cells, i.e., the doses required to produce a toxin response in O/V-treated N2a cells also caused a significant toxic response in untreated N2a cells. This reflects our use of MeOH extracts that received no purification beyond partitioning with DCM and thus would contain a variety of cell metabolites, such as free fatty acids, that could be toxic to N2a cells at high doses. Possible interference of matrix compounds and additional sample clean-up were tested on four quantifiable samples representing the range of toxin concentrations across extracts in this study. Analyses of a dilution series for each of these four samples showed a linear, proportional response to dilution in quantifiable concentrations and only 7–16% variation in determined CTX concentration, indicating a lack of matrix effects on measured CTX-specific toxicity. Solid-phase extraction (SPE) was performed on these samples using silica (Bond Elut Si; 100 mg; Agilent, Santa Clara, CA, USA). In all four samples, Si SPE purification caused a >40% reduction in toxicity to both O/V-treated and untreated N2a cells, indicating that CTX was being removed along with cytotoxic matrix compounds and that SPE clean-up would greatly affect accuracy of CTX measurement. Hence, further purification was not performed on any quantified samples to ensure accuracy rather than sensitivity. This decision was supported by C-CTX-1 spike recovery trials (below). The lowest concentration that could be quantified with confirmed CTX-specific toxicity was 0.28 ng C-CTX-1 eq. mL^{-1} (in extract), which represents the effective limit of quantitation for the samples in this study.

To better determine the limits of detection and possibility of matrix interference for N2a analyses of natural epiphyte assemblages, a sample containing no detectable CTX activity (as determined by the screening procedure described above) was spiked with C-CTX-1 standard at 8 concentrations ranging from 0.01–0.5 ng C-CTX-1 mL^{-1} (in extract) and the same range of concentrations were also produced in a dilution series (i.e., matrix concentration declined with CTX concentration). These tests indicated a limit of quantitation of 0.08 ng C-CTX-1 mL^{-1} in unpurified algal extracts and that CTX quantitation was not affected by dilution of sample matrix. However, this limit is not directly comparable to the detection limit of non-spiked samples since C-CTX-1 is a major component of bioaccumulated CTXs in fish, but has not yet been attributed as a major component in the toxin profiles of *Gambierdiscus* or *Fukoyoa* [76].

4.5. Statistical Analyses

Gambierdiscus abundance and toxicity data were tested for normality and homoscedasticity using a Shapiro–Wilk test and a Brown–Forsythe test, respectively. Log-transformed abundance data was parametric and mean abundance between sites and years were com-

pared with one-way ANOVA followed by Tukey's post hoc test for multiple comparisons. Toxicity data was highly skewed and non-parametric. A Box–Cox test was used to determine a transformation for toxicity data and all toxicity data was raised to the –2 power and mean values for sites and years were compared using a Welch's ANOVA and a Games–Howell test for multiple comparisons. All univariate statistical analyses were performed in R. Benthic community composition across sites and years were compared using a cluster analysis and non-metric multidimensional scaling and their multivariate similarity was measured with an ANOSIM test, all performed using Primer-E. Multivariate correlations between benthic community composition or environmental conditions and *Gambierdiscus* abundance or toxicity were examined in Primer-E using the BEST routine. All reported multivariate results had a significance level of 0.1% ($p < 0.001$). Significance in the PCA analyses were based on the broken stick criterion of Peres-Neto et al. [77]. Graphs were created using GraphPad Prism version 9.0.0 for macOS (GraphPad Software, San Diego, California USA, www.graphpad.com, accessed on 9 June 2021).

Supplementary Materials: The following are available online at https://www.mdpi.com/article/10.3390/toxins13060413/s1. Table S1: Pearson's correlations for environmental variables and the first two principal components from a principal components analysis of environmental data collected in this study. Table S2: Results of an ANOSIM test conducted in Primer-E, comparing macroalgal composition at Black Point, Coculus Rock, Flat Cay, and Seahorse Shoal in the U.S. Virgin Islands. Figure S1: A non-metric multidimensional scaling plot and results of ANOSIM test for benthic macroalgal composition at Black Point, Coculus Rock, Flat Cay, and Seahorse Shoal in the U.S. Virgin Islands. Figure S2: Examples of N2a assay dose-response curves for purified C-CTX-1 standards and corresponding representative field epiphyte samples.

Author Contributions: Conceptualization, A.R., T.B.S., M.L.R., D.M.A.; methodology, A.R., J.D.L., M.L.R., T.B.S., Y.X.; validation, J.D.L., A.R.; formal analysis, J.D.L., A.R., J.L.D.; investigation, J.D.L., M.L.R., T.B.S., Y.X., A.R.; resources, A.R., T.B.S., D.M.A.; data curation, J.D.L., T.B.S., J.L.D., A.R.; writing—original draft preparation, J.D.L., A.R., M.L.R., T.B.S., J.L.D.; writing—review and editing, T.B.S., D.M.A., Y.X.; visualization, J.D.L., J.L.D., A.R.; interpretation, J.D.L., M.L.R., T.B.S., J.L.D., A.R.; supervision, A.R., T.B.S., M.L.R., D.M.A.; project administration, A.R.; funding acquisition, A.R., T.B.S., M.L.R., D.M.A. All authors have read and agreed to the published version of the manuscript.

Funding: This work was funded in part by the National Oceanic and Atmospheric Administration, Ecology and Oceanography of Harmful Algal Blooms Program (ECOHAB publication number 984) through the CiguaHAB project (NA11NOS4780028), and also contributes to CIGUATOX (NA17NOS4780181) granted to coauthors AR, TBS, DMA, and MLR. Additional support was provided by NSF Partnerships in International Research and Education (1743802), and the Greater Caribbean Center for Ciguatera Research (NIH 1P01ES028949-01 and NSF 1841811). Financial support of YX was from the National Natural Science Foundation of China (41976155), the Natural Science Foundation of Guangxi Province (2020GXNSFDA297001).

Institutional Review Board Statement: Not applicable.

Informed Consent Statement: Not applicable.

Data Availability Statement: Complete environmental and physical data associated with this work is provided for open access as a downloadable file. Complete toxin and *Gambierdiscus* abundance data is presented in this manuscript but is also available on request to the corresponding author.

Acknowledgments: We greatly appreciate the extensive team of UVI graduate students and divers that contributed to the USVI coral reef monitoring program data and sample collection during the period of this study. Thanks to Robert Brewer, Sarah Heidmann, and Jonathan Jossart who analyzed benthic composition during this period. We also appreciate the efforts of Ana Garcia early in this project who assisted with sample extractions and preliminary toxicity analyses, and to Christopher Loeffler for early discussion on the cytotoxicity methodology employed.

Conflicts of Interest: The authors declare no conflict of interest.

References

1. Friedman, M.A.; Fernandez, M.; Backer, L.C.; Dickey, R.W.; Bernstein, J.; Schrank, K.; Kibler, S.; Stephan, W.; Gribble, M.O.; Bienfang, P. An updated review of ciguatera fish poisoning: Clinical, epidemiological, environmental, and public health management. *Mar. Drugs* **2017**, *15*, 72. [CrossRef]
2. Parsons, M.L.; Aligizaki, K.; Bottein, M.Y.D.; Fraga, S.; Morton, S.L.; Penna, A.; Rhodes, L. *Gambierdiscus* and *Ostreopsis*: Reassessment of the state of knowledge of their taxonomy, geography, ecophysiology, and toxicology. *Harmful Algae* **2012**, *14*, 107–129. [CrossRef]
3. Cruz-Rivera, E.; Villareal, T.A. Macroalgal palatability and the flux of ciguatera toxins through marine food webs. *Harmful Algae* **2006**, *5*, 497–525. [CrossRef]
4. Kohler, S.T.; Kohler, C.C. Dead bleached coral provides new surfaces for dinoflagellates implicated in ciguatera fish poisonings. *Environ. Biol. Fishes* **1992**, *35*, 413–416. [CrossRef]
5. Legrand, A.; Fukui, M.; Cruchet, P.; Yasumoto, T. Progress on chemical knowledge of ciguatoxins. *Bull. Soc. Pathol. Exot.* **1992**, *85*, 467–469. [CrossRef] [PubMed]
6. Pottier, I.; Vernoux, J.-P.; Jones, A.; Lewis, R.J. Characterisation of multiple Caribbean ciguatoxins and congeners in individual specimens of horse-eye jack (*Caranx latus*) by high-performance liquid chromatography/mass spectrometry. *Toxicon* **2002**, *40*, 929–939. [CrossRef]
7. Chinain, M.; Darius, H.T.; Ung, A.; Cruchet, P.; Wang, Z.H.; Ponton, D.; Laurent, D.; Pauillac, S. Growth and toxin production in the ciguatera-causing dinoflagellate *Gambierdiscus polynesiensis* (Dinophyceae) in culture. *Toxicon* **2010**, *56*, 739–750. [CrossRef]
8. Chinain, M.; Gatti, C.; Darius, H.; Quod, J.-P.; Tester, P. Ciguatera poisonings: A global review of occurrences and trends. *Harmful Algae* **2021**, *102*, 101873. [CrossRef]
9. Rodríguez, F.; Fraga, S.; Ramilo, I.; Rial, P.; Figueroa, R.I.; Riobó, P.; Bravo, I. Canary Islands (NE Atlantic) as a biodiversity 'hotspot'of *Gambierdiscus*: Implications for future trends of ciguatera in the area. *Harmful Algae* **2017**, *67*, 131–143. [CrossRef]
10. Rhodes, L.L.; Smith, K.F.; Murray, J.S.; Nishimura, T.; Finch, S.C. Ciguatera fish poisoning: The risk from an Aotearoa/New Zealand perspective. *Toxins* **2020**, *12*, 50. [CrossRef] [PubMed]
11. Nishimura, T.; Sato, S.; Tawong, W.; Sakanari, H.; Uehara, K.; Shah, M.M.R.; Suda, S.; Yasumoto, T.; Taira, Y.; Yamaguchi, H. Genetic diversity and distribution of the ciguatera-causing dinoflagellate *Gambierdiscus* spp. (Dinophyceae) in coastal areas of Japan. *PLoS ONE* **2013**, *8*, e60882. [CrossRef] [PubMed]
12. Tester, P.A.; Vandersea, M.W.; Buckel, C.A.; Kibler, S.R.; Holland, W.C.; Davenport, E.D.; Clark, R.D.; Edwards, K.F.; Taylor, J.C.; Vander Pluym, J.L. *Gambierdiscus* (Dinophyceae) species diversity in the Flower Garden Banks National Marine Sanctuary, Northern Gulf of Mexico, USA. *Harmful Algae* **2013**, *29*, 1–9. [CrossRef]
13. Fleming, L.E.; Baden, D.G.; Bean, J.A.; Weisman, R.; Blythe, D.G. Seafood toxin diseases: Issues in epidemiology & community outreach. In Proceedings of the VIII International Conference on Harmful Algae, Vigo, Spain, 25–29 June 1997; Reguera, B., Blanco, J., Fernández, M., Wyatt, T., Eds.; Xunta de Galicia and Intergovernmental Oceanographic Commission of UNESCO: Galicia, Spain, 1998; pp. 245–248.
14. Ting, J.; Brown, A. Ciguatera poisoning: A global issue with common management problems. *Eur. J. Emerg. Med.* **2001**, *8*, 295–300. [CrossRef]
15. Litaker, R.W.; Vandersea, M.W.; Faust, M.A.; Kibler, S.R.; Nau, A.W.; Holland, W.C.; Chinain, M.; Holmes, M.J.; Tester, P.A. Global distribution of ciguatera causing dinoflagellates in the genus *Gambierdiscus*. *Toxicon* **2010**, *56*, 711–730. [CrossRef] [PubMed]
16. Chinain, M.; Faust, M.A.; Pauillac, S. Morphology and molecular analyses of three toxic species of *Gambierdiscus* (Dinophyceae): *G. pacificus*, sp. nov., *G. australes*, sp. nov., and *G. polynesiensis*, sp. nov. *J. Phycol.* **1999**, *35*, 1282–1296. [CrossRef]
17. Litaker, R.W.; Holland, W.C.; Hardison, D.R.; Pisapia, F.; Hess, P.; Kibler, S.R.; Tester, P.A. Ciguatoxicity of *Gambierdiscus* and *Fukuyoa* species from the Caribbean and Gulf of Mexico. *PLoS ONE* **2017**, *12*, e0185776. [CrossRef] [PubMed]
18. Rhodes, L.; Harwood, T.; Smith, K.; Argyle, P.; Munday, R. Production of ciguatoxin and maitotoxin by strains of *Gambierdiscus australes, G. pacificus* and *G. polynesiensis* (Dinophyceae) isolated from Rarotonga, Cook Islands. *Harmful Algae* **2014**, *39*, 185–190. [CrossRef]
19. Pisapia, F.; Holland, W.C.; Hardison, D.R.; Litaker, R.W.; Fraga, S.; Nishimura, T.; Adachi, M.; Nguyen-Ngoc, L.; Séchet, V.; Amzil, Z. Toxicity screening of 13 *Gambierdiscus* strains using neuro-2a and erythrocyte lysis bioassays. *Harmful Algae* **2017**, *63*, 173–183. [CrossRef]
20. Xu, Y.; Richlen, M.L.; Liefer, J.D.; Robertson, A.; Kulis, D.; Smith, T.B.; Parsons, M.L.; Anderson, D.M. Influence of Environmental Variables on *Gambierdiscus* spp. (Dinophyceae) Growth and Distribution. *PLoS ONE* **2016**, *11*, e0153197. [CrossRef]
21. Kibler, S.R.; Litaker, R.W.; Holland, W.C.; Vandersea, M.W.; Tester, P.A. Growth of eight *Gambierdiscus* (Dinophyceae) species: Effects of temperature, salinity and irradiance. *Harmful Algae* **2012**, *19*, 1–14. [CrossRef]
22. Tosteson, T. Caribbean ciguatera: A changing paradigm. *Rev. Biol. Trop.* **2004**, *52*, 109–113.
23. Chinain, M.; Germain, M.; Deparis, X.; Pauillac, S.; Legrand, A.M. Seasonal abundance and toxicity of the dinoflagellate *Gambierdiscus* spp. (Dinophyceae), the causative agent of ciguatera in Tahiti, French Polynesia. *Mar. Biol.* **1999**, *135*, 259–267. [CrossRef]
24. Chateau-Degat, M.-L.; Chinain, M.; Cerf, N.; Gingras, S.; Hubert, B.; Dewailly, E. Seawater temperature, *Gambierdiscus* spp. variability and incidence of ciguatera poisoning in French Polynesia. *Harmful Algae* **2005**, *4*, 1053–1062. [CrossRef]

25. Chinain, M.; Darius, H.T.; Ung, A.; Fouc, M.T.; Revel, T.; Cruchet, P.; Pauillac, S.; Laurent, D. Ciguatera risk management in French Polynesia: The case study of Raivavae Island (Australes Archipelago). *Toxicon* **2010**, *56*, 674–690. [CrossRef] [PubMed]
26. Díaz-Asencio, L.; Clausing, R.J.; Vandersea, M.; Chamero-Lago, D.; Gómez-Batista, M.; Hernández-Albernas, J.I.; Chomérat, N.; Rojas-Abrahantes, G.; Litaker, R.W.; Tester, P. Ciguatoxin occurrence in food-web components of a Cuban coral reef ecosystem: Risk-assessment implications. *Toxins* **2019**, *11*, 722. [CrossRef]
27. Loeffler, C.R.; Robertson, A.; Flores Quintana, H.A.; Silander, M.C.; Smith, T.B.; Olsen, D. Ciguatoxin prevalence in 4 commercial fish species along an oceanic exposure gradient in the US Virgin Islands. *Environ. Toxicol. Chem.* **2018**, *37*, 1852–1863. [CrossRef]
28. Randall, J.E. A review of ciguatera, tropical fish poisoning, with a tentative explanation of its cause. *Bull. Mar. Sci.* **1958**, *8*, 236–267.
29. Longo, S.; Sibat, M.; Viallon, J.; Darius, H.T.; Hess, P.; Chinain, M. Intraspecific variability in the toxin production and toxin profiles of in vitro cultures of *Gambierdiscus polynesiensis* (Dinophyceae) from French Polynesia. *Toxins* **2019**, *11*, 735. [CrossRef] [PubMed]
30. Tudó, À.; Toldrà, A.; Rey, M.; Todolí, I.; Andree, K.B.; Fernández-Tejedor, M.; Campàs, M.; Sureda, F.X.; Diogène, J. *Gambierdiscus* and *Fukuyoa* as potential indicators of ciguatera risk in the Balearic Islands. *Harmful Algae* **2020**, *99*, 101913. [CrossRef] [PubMed]
31. Robertson, A.; Richlen, M.L.; Erdner, D.; Smith, T.B.; Anderson, D.M.; Liefer, J.D.; Xu, Y.; McCarron, P.; Miles, C.O.; Parsons, M.L. Toxicity, chemistry, and implications of *Gamberdiscus silvae*: A ciguatoxin superbug in the Greater Caribbean Region. In Proceedings of the 18th International Conference for Harmful Algae, Nantes, France, 21–26 October 2018.
32. Rossignoli, A.E.; Tudó, A.; Bravo, I.; Díaz, P.A.; Diogène, J.; Riobó, P. Toxicity characterisation of *Gambierdiscus* species from the Canary Islands. *Toxins* **2020**, *12*, 134. [CrossRef]
33. Radke, E.G.; Grattan, L.M.; Cook, R.L.; Smith, T.B.; Anderson, D.M.; Morris, J.G., Jr. Ciguatera incidence in the US Virgin Islands has not increased over a 30-year time period despite rising seawater temperatures. *Am. J. Trop. Med. Hygeine* **2013**, *88*, 908–913. [CrossRef]
34. Lyu, Y.; Richlen, M.L.; Sehein, T.R.; Chinain, M.; Adachi, M.; Nishimura, T.; Xu, Y.; Parsons, M.L.; Smith, T.B.; Zheng, T. LSU rDNA based RFLP assays for the routine identification of *Gambierdiscus* species. *Harmful Algae* **2017**, *66*, 20–28. [CrossRef] [PubMed]
35. NOAA. Environmental Sensitivity Index (ESI) and Geographical Information System (GIS) Mapping. Virgin Islands: U.S. and British Virgin Islands. 2000. Available online: https://response.restoration.noaa.gov/oil-and-chemical-spills/oil-spills/download-esi-maps-and-gis-data#VirginIslands (accessed on 19 March 2021).
36. Kendall, M. Benthic Habitat Mapping in Puerto Rico and the U.S. Virgin Islands for a Baseline Inventory. Benthic Habitat Map of St. Thomas and St. John, USVI in GIS Format. 2000. Available online: https://coastalscience.noaa.gov/project/benthic-habitat-mapping-puerto-rico-virgin-islands/ (accessed on 19 March 2021).
37. Yogi, K.; Oshiro, N.; Inafuku, Y.; Hirama, M.; Yasumoto, T. Detailed LC-MS/MS Analysis of Ciguatoxins Revealing Distinct Regional and Species Characteristics in Fish and Causative Alga from the Pacific. *Anal. Chem.* **2011**, *83*, 8886–8891. [CrossRef]
38. Kryuchkov, F.; Robertson, A.; Miles, C.O.; Mudge, E.M.; Uhlig, S. LC–HRMS and Chemical Derivatization Strategies for the Structure Elucidation of Caribbean Ciguatoxins: Identification of C-CTX-3 and -4. *Mar. Drugs* **2020**, *18*, 182. [CrossRef]
39. Pottier, I.; Hamilton, B.; Jones, A.; Lewis, R.J.; Vernoux, J.P. Identification of slow and fast-acting toxins in a highly ciguatoxic barracuda (*Sphyraena barracuda*) by HPLC/MS and radiolabelled ligand binding. *Toxicon* **2003**, *42*, 663–672. [CrossRef] [PubMed]
40. Caillaud, A.; De la Iglesia, P.; Darius, H.T.; Pauillac, S.; Aligizaki, K.; Fraga, S.; Chinain, M.; Diogène, J. Update on methodologies available for ciguatoxin determination: Perspectives to confront the onset of ciguatera fish poisoning in Europe. *Mar. Drugs* **2010**, *8*, 1838–1907. [CrossRef]
41. Lartigue, J.; Jester, E.L.E.; Dickey, R.W.; Villareal, T.A. Nitrogen source effects on the growth and toxicity of two strains of the ciguatera-causing dinoflagellate *Gambierdiscus toxicus*. *Harmful Algae* **2009**, *8*, 781–791. [CrossRef]
42. EFSA Panel on Contaminants in the Food Chain. Scientific Opinion on marine biotoxins in shellfish–Emerging toxins: Ciguatoxin group. *EFSA J.* **2010**, *8*, 1627. [CrossRef]
43. Withers, N.W. Ciguatera research in the northwestern Hawaiian Islands: Laboratory and field studies on ciguatoxigenic dinoflagellates in the Hawaiian Archipelago. In Proceedings of the Second Symposium on Resource Investigations in the Northwestern Hawaiian Islands, Honolulu, HI, USA, 25–27 May 1983; pp. 144–156.
44. Chinain, M.; Ung, A.; Cruchet, P.; Revel, T.; Viallon, J.; Sibat, M.; Varney, P.; Laurent, V.; Hess, P.; Darius, H.T. Evidence for the Range Expansion of Ciguatera in French Polynesia: A Revisit of the 2009 Mass-Poisoning Outbreak in Rapa Island (Australes Archipelago). *Toxins* **2020**, *12*, 759. [CrossRef]
45. Bagnis, R.; Chanteau, S.; Chungue, E.; Hurtel, J.; Yasumoto, T.; Inoue, A. Origins of ciguatera fish poisoning: A new dinoflagellate, *Gambierdiscus toxicus* Adachi and Fukuyo, definitively involved as a causal agent. *Toxicon* **1980**, *18*, 199–208. [CrossRef]
46. Bagnis, R.; Legrand, A.-M.; Inoue, A. Follow-up of a bloom of the toxic dinoflagellate *Gambierdiscus toxicus* on a fringing reef of Tahiti. In *Toxic Marine Phytoplankton*; Graneli, E., Sundstrom, B., Edler, L., Anderson, D.M., Eds.; Elsevier: New York, NY, USA, 1990; pp. 98–103.
47. Yasumoto, T.; Nakajima, I.; Oshima, Y.; Bagnis, R. A new toxic dinoflagellate [Algae, Gambier Islands] found in association with ciguatera [Ciguatoxin, maitotoxin, French Polynesia]. In *Toxic Dinoflagellate Blooms*; Taylor, L., Seliger, H.H., Eds.; Elsevier: New York, NY, USA, 1979; pp. 65–70.
48. Holmes, M.J.; Lewis, R.J.; Sellin, M.; Street, R. The origin of ciguatera in Platypus Bay, Australia. *Mem. Qld. Mus.* **1994**, *34*, 505–512.

49. Darius, H.; Ponton, D.; Revel, T.; Cruchet, P.; Ung, A.; Fouc, M.T.; Chinain, M. Ciguatera risk assessment in two toxic sites of French Polynesia using the receptor-binding assay. *Toxicon* **2007**, *50*, 612–626. [CrossRef]
50. Pawlowiez, R.; Darius, H.T.; Cruchet, P.; Rossi, F.; Caillaud, A.; Laurent, D.; Chinain, M. Evaluation of seafood toxicity in the Australes archipelago (French Polynesia) using the neuroblastoma cell-based assay. *Food Addit. Contam. Part A Chem.* **2013**, *30*, 567–586. [CrossRef]
51. McMillan, J.P.; Hoffman, P.A.; Granade, H. *Gambierdiscus toxicus* from the Caribbean: A source of toxins involved in ciguatera. *Mar. Fish. Rev.* **1986**, *48*, 48–52.
52. Durand-Clement, M. Study of production and toxicity of cultured *Gambierdiscus toxicus*. *Biol. Bull.* **1987**, *172*, 108–121. [CrossRef]
53. Bomber, J.W.; Guillard, R.R.; Nelson, W.G. Roles of temperature, salinity, and light in seasonality, growth, and toxicity of ciguatera-causing *Gambierdiscus toxicus* Adachi et *Fukuyo* (Dinophyceae). *J. Exp. Mar. Biol. Ecol.* **1988**, *115*, 53–65. [CrossRef]
54. Fraga, S.; Rodriguez, F.; Caillaud, A.; Diogene, J.; Raho, N.; Zapata, M. Gambierdiscus excentricus sp. nov. (Dinophyceae), a benthic toxic dinoflagellate from the Canary Islands (NE Atlantic Ocean). *Harmful Algae* **2011**, *11*, 10–22. [CrossRef]
55. Loeffler, C.R.; Richlen, M.L.; Brandt, M.E.; Smith, T.B. Effects of grazing, nutrients, and depth on the ciguatera-causing dinoflagellate *Gambierdiscus* in the US Virgin Islands. *Mar. Ecol. Prog. Ser.* **2015**, *531*, 91–104. [CrossRef]
56. Richlen, M.L.; Lobel, P.S. Effects of depth, habitat, and water motion on the abundance and distribution of ciguatera dinoflagellates at Johnston Atoll, Pacific Ocean. *Mar. Ecol. Prog. Ser.* **2011**, *421*, 51–66. [CrossRef]
57. Morton, S.; Bomber, J.; Tindall, D.; Aikman, K. Response of *Gambierdiscus toxicus* to light: Cell physiology and toxicity. In *Toxic Phytoplankton Blooms in the Sea*; Smayda, T., Shimizu, Y., Eds.; Elsevier: New York, NY, USA, 1993; pp. 541–546.
58. Parsons, M.L.; Settlemier, C.J.; Ballauer, J.M. An examination of the epiphytic nature of *Gambierdiscus toxicus*, a dinoflagellate involved in ciguatera fish poisoning. *Harmful Algae* **2011**, *10*, 598–605. [CrossRef]
59. Rains, L.K.; Parsons, M.L. *Gambierdiscus* species exhibit different epiphytic behaviors toward a variety of macroalgal hosts. *Harmful Algae* **2015**, *49*, 29–39. [CrossRef]
60. Mustapa, N.I.; Yong, H.L.; Lee, L.K.; Lim, Z.F.; Lim, H.C.; Teng, S.T.; Luo, Z.; Gu, H.; Leaw, C.P.; Lim, P.T. Growth and epiphytic behavior of three *Gambierdiscus* species (Dinophyceae) associated with various macroalgal substrates. *Harmful Algae* **2019**, *89*, 101671. [CrossRef]
61. Parsons, M.L.; Settlemier, C.J.; Bienfang, P.K. A simple model capable of simulating the population dynamics of *Gambierdiscus*, the benthic dinoflagellate responsible for ciguatera fish poisoning. *Harmful Algae* **2010**, *10*, 71–80. [CrossRef]
62. Tester, P.A.; Feldman, R.L.; Nau, A.W.; Kibler, S.R.; Litaker, R.W. Ciguatera fish poisoning and sea surface temperatures in the Caribbean Sea and the West Indies. *Toxicon* **2010**, *56*, 698–710. [CrossRef] [PubMed]
63. Kibler, S.R.; Davenport, E.D.; Tester, P.A.; Hardison, D.R.; Holland, W.C.; Litaker, R.W. *Gambierdiscus* and *Fukuyoa* species in the greater Caribbean: Regional growth projections for ciguatera-associated dinoflagellates. *Ecol. Model.* **2017**, *360*, 204–218. [CrossRef]
64. Pitz, K.J.; Richlen, M.L.; Fachon, E.; Smith, T.B.; Parsons, M.L.; Anderson, D.M. Development of fluorescence in situ hybridization (FISH) probes to detect and enumerate *Gambierdiscus* species. *Harmful Algae* **2021**, *101*, 101914. [CrossRef]
65. Vandersea, M.W.; Kibler, S.R.; Holland, W.C.; Tester, P.A.; Schultz, T.F.; Faust, M.A.; Holmes, M.J.; Chinain, M.; Wayne Litaker, R. Development of semi-quantitative pcr assays for the detection and enumeration of *Gambierdiscus* species (gonyaulacales, dinophyceae) 1. *J. Phycol.* **2012**, *48*, 902–915. [CrossRef]
66. Tester, P.A.; Litaker, R.W.; Berdalet, E. Climate change and harmful benthic microalgae. *Harmful Algae* **2020**, *91*, 101655. [CrossRef]
67. Food and Agriculture Organization of the United Nations and World Health Organization. Report of the Expert Meeting on Ciguatera Poisoning. In *Food Safety and Quality Series*; Food and Agriculture Organization of the United Nations: Rome, Italy, 2020; Volume 9, p. 133.
68. Ennis, R.; Kadison, E.; Heidmann, S.; Brandt, M.; Henderson, L.; Smith, T. *The United States Virgin Islands Territorial Coral Reef Monitoring Program: 2019 Annual Report*; University of the Virgin Islands: St Thomas, VI, USA, 2019; p. 295.
69. Smith, T.B.; Gyory, J.; Brandt, M.E.; Miller, W.J.; Jossart, J.; Nemeth, R.S. Caribbean mesophotic coral ecosystems are unlikely climate change refugia. *Glob. Chang. Biol.* **2016**, *22*, 2756–2765. [CrossRef]
70. Smith, T.; Kadison, E.; Ennis, R.; Gyory, J.; Brandt, M.; Wright, V.; Nemeth, R.; Henderson, L. *The United States Virgin Islands Territorial Coral Reef Monitoring Program*; University of the Virgin Islands: St Thomas, VI, USA, 2014; p. 273.
71. Smith, T.; Brandt, M.; Calnan, J.; Nemeth, R.; Blondeau, J.; Kadison, E.; Taylor, M.; Rothenberger, P. Convergent mortality responses of Caribbean coral species to seawater warming. *Ecosphere* **2013**, *4*, 1–40. [CrossRef]
72. Kohler, K.E.; Gill, S.M. Coral Point Count with Excel extensions (CPCe): A Visual Basic program for the determination of coral and substrate coverage using random point count methodology. *Comput. Geosci.* **2006**, *32*, 1259–1269. [CrossRef]
73. Faust, M.A.; Gulledge, R.A. Identifying harmful marine dinoflagellates. In *Contributions from the United States National Herbarium*; National Museum of Natural History: Washington, DC, USA, 2002; Volume 42, pp. 1–144.
74. Manger, R.L.; Leja, L.S.; Lee, S.Y.; Hungerford, J.M.; Hokama, Y.; Dickey, R.W.; Granade, H.R.; Lewis, R.; Yasumoto, T.; Wekell, M.M. Detection of sodium-channel toxins—Directed cytotoxicity assays of purified ciguatoxins, brevetoxins, saxitoxins, and seafood extracts. *J. AOAC Int.* **1995**, *78*, 521–527. [CrossRef] [PubMed]
75. Robertson, A.; Garcia, A.C.; Quintana, H.A.F.; Smith, T.B.; Castillo, B.F.; Reale-Munroe, K.; Gulli, J.A.; Olsen, D.A.; Hooe-Rollman, J.I.; Jester, E.L. Invasive lionfish (*Pterois volitans*): A potential human health threat for ciguatera fish poisoning in tropical waters. *Mar. Drugs* **2014**, *12*, 88–97. [CrossRef] [PubMed]

76. Chinain, M.; Gatti, C.M.; Roué, M.; Darius, H.T.; Subba Rao, D. Ciguatera-causing dinoflagellates in the genera *Gambierdiscus* and *Fukuyoa*: Distribution, ecophysiology and toxicology. In *Dinoflagellates: Morphology, Life History and Ecological Significance*; Subba Rao, D., Ed.; Nova Science: New York, NY, USA, 2020; pp. 405–457.
77. Peres-Neto, P.R.; Jackson, D.A.; Somers, K.M. Giving meaningful interpretation to ordination axes: Assessing loading significance in Principal Component Analysis. *Ecology* **2003**, *84*, 2347–2363. [CrossRef]

toxins

MDPI

Article

Experimental Evidence of Ciguatoxin Accumulation and Depuration in Carnivorous Lionfish

Isabel do Prado Leite [1,*], Khalil Sdiri [2], Angus Taylor [3], Jérôme Viallon [4], Hela Ben Gharbia [5], Luiz Laureno Mafra Júnior [1,6], Peter Swarzenski [3], François Oberhaensli [3], Hélène Taiana Darius [4], Mireille Chinain [4] and Marie-Yasmine Dechraoui Bottein [2,*]

1 Center for Marine Studies, Federal University of Paraná. Av. Beira-mar, s/n, Pontal do Paraná P.O. Box 61, Brazil; luiz.mafra@ufpr.br
2 Université Côte d'Azur, CNRS, ECOSEAS, UMR7035, Parc Valrose, CEDEX 2, 06103 Nice, France; sdiri.khalil06@gmail.com
3 Environment Laboratories, Department of Nuclear Science and Application, International Atomic Energy Agency, 4 Quai Antoine 1er, 98000 Monaco, Monaco; angustaylor93@gmail.com (A.T.); P.Swarzenski@iaea.org (P.S.); F.R.Oberhaensli@iaea.org (F.O.)
4 Laboratory of Marine Biotoxins, Institut Louis Malardé, UMR EIO (IFREMER, IRD, ILM, UPF), P.O. Box 30 Papeete, Tahiti, French Polynesia; jviallon@ilm.pf (J.V.); tdarius@ilm.pf (H.T.D.); mchinain@ilm.pf (M.C.)
5 MMS Laboratory (EA 2160), Sciences and Techniques Faculty, Le Mans University, Avenue Olivier Messiaen, 72085 Le Mans, France; Hela.Ben_Gharbia@univ-lemans.fr
6 Visiting Scientist Ifremer, Laboratoire Phycotoxines, Rue de l'Ile d'Yeu, 44311 Nantes, France
* Correspondence: isabel.oceano@gmail.com (I.d.P.L.); y.bottein@gmail.com (M.-Y.D.B.)

Abstract: Ciguatera poisoning is a food intoxication associated with the consumption of fish or shellfish contaminated, through trophic transfer, with ciguatoxins (CTXs). In this study, we developed an experimental model to assess the trophic transfer of CTXs from herbivorous parrotfish, *Chlorurus microrhinos*, to carnivorous lionfish, *Pterois volitans*. During a 6-week period, juvenile lionfish were fed naturally contaminated parrotfish fillets at a daily dose of 0.11 or 0.035 ng CTX3C equiv. g^{-1}, as measured by the radioligand-receptor binding assay (r-RBA) or neuroblastoma cell-based assay (CBA-N2a), respectively. During an additional 6-week depuration period, the remaining fish were fed a CTX-free diet. Using r-RBA, no CTXs were detectable in muscular tissues, whereas CTXs were measured in the livers of two out of nine fish sampled during exposure, and in four out of eight fish sampled during depuration. Timepoint pooled liver samples, as analyzed by CBA-N2a, confirmed the accumulation of CTXs in liver tissues, reaching 0.89 ng CTX3C equiv. g^{-1} after 41 days of exposure, followed by slow toxin elimination, with 0.37 ng CTX3C equiv. g^{-1} measured after the 6-week depuration. These preliminary results, which need to be pursued in adult lionfish, strengthen our knowledge on CTX transfer and kinetics along the food web.

Keywords: ciguatoxins; experimental exposure; lionfish; trophic transfer; toxin accumulation; ciguatera poisoning

Key Contribution: In this study; ciguatoxins (CTXs) were detected in the liver of juvenile lionfish *Pterois volitans* fed naturally CTX-contaminated parrotfish *Chlorurus microrhinos* fillets. CTX remained in the livers of lionfish 43 days after the last exposure. Toxin levels in the muscular tissues were below the limits of detection of the receptor binding assay.

Citation: Leite, I.d.P.; Sdiri, K.; Taylor, A.; Viallon, J.; Gharbia, H.B.; Mafra Júnior, L.L.; Swarzenski, P.; Oberhaensli, F.; Darius, H.T.; Chinain, M.; et al. Experimental Evidence of Ciguatoxin Accumulation and Depuration in Carnivorous Lionfish. *Toxins* **2021**, *13*, 564. https://doi.org/10.3390/toxins13080564

Received: 23 June 2021
Accepted: 3 August 2021
Published: 11 August 2021

1. Introduction

Gambierdiscus spp. are benthic dinoflagellates that may produce lipophilic ciguatoxins (CTXs), as well as other bioactive compounds, including maitotoxins (MTXs), gambierone, gambieroxides, gambierol, and gambieric acid [1–6]. Ciguatoxins are considered the

primary cause of Ciguatera poisoning (CP) in humans, affecting up to 500,000 fish consumers every year, including rare lethal cases [7–10]. Affected people may experience temporary and/or persistent/recurrent neurological effects resulting from CTXs binding to voltage-gated sodium channels in excitable tissues [11–15]. Ciguatera symptoms include the tingling of body extremities and/or cold allodynia and, in more severe cases, cardiovascular and respiratory insufficiency leading to coma and death [12]. Chronic neurological manifestations may persist for weeks, months, and in severe cases, years after the first exposure to CTXs [8,16,17]. Symptoms may vary geographically according to the dominant toxin profile in each region. Gastrointestinal disorders such as nausea, vomiting, abdominal pain, and diarrhea are predominantly manifested in the Caribbean region, where fish are contaminated by the so-called Caribbean ciguatoxins (C-CTXs). In contrast, in the Pacific and Indian Oceans, neurotoxic symptoms may predominate following the consumption of fish containing P-CTXs and I-CTXs, respectively. Neurotoxic symptoms may include hallucinations mostly among victims from the Indian Ocean [8].

The effects of CTXs on marine fauna are less documented. In fish, adverse effects from exposure to CTX have been observed in fresh/brackish water species such as blueheads, *Thalassoma bifasciatum* [18], juveniles of *Oreochromis* sp. [19], larvae and embryos of the genus *Oryzias* [20–24], and adult *Mugil cephalus* [25]. Ciguatoxins found in the brain, liver, and muscles of stranded *Monachus schauinslandi* monk seals [26] suggest that marine mammals may also suffer from CTX exposure, and that these compounds persist within the complex marine food webs. However, marine species experimentally fed with CTX (*Naso brevirostris* [27] and *Epinephelus coioides* [28]) did not seem sensitive to the effects of CTX. The fish resistance mechanism to CTX is still unknown.

Following the ingestion of *Gambierdiscus* cells by herbivorous and omnivorous organisms, CTX-like toxins are biotransformed and transmitted along the trophic food webs to top-chain carnivores, including fish, such as groupers and snappers, and marine mammals [28–31]. More than 400 species of fish are suspected as potential vectors of CP to humans [32]. Coral reef fish known to accumulate CTXs include barracuda, grouper, snapper, moray eel, parrotfish, trevally, and wrasse [33,34]. In general, higher-level carnivorous fish exhibit greater toxin concentrations than smaller fish and herbivores [35–37], but this is not always the case [38–42]. The complex processes and kinetics involving CTX accumulation, elimination, and trophic transfer to carnivores are still poorly understood and limited to field observations [42] and scarce laboratory studies [28].

Lionfish, *Pterois volitans* (Scorpaenidae), are carnivorous fish with venom-containing spines [43]. They are native to the Indo-Pacific region and were mostly likely introduced through aquarium releases into the Atlantic Ocean, becoming invasive to the Caribbean Sea and the Gulf of Mexico [44,45]. Due to the absence of natural predators for lionfish in reef ecosystems where they have been recently introduced, their use as a fishery resource has been stimulated to reduce the adverse ecological impacts on reef communities [46,47]. However, as with many other species, lionfish may accumulate CTXs and reach toxin concentrations above safety levels for human consumption as recommended by the U.S. Food and Drug Administration (0.1 ng C-CTX1 equiv. g^{-1}, or 0.01 ng CTX1B equiv. g^{-1}) [48]. Concentrations of CTXs in lionfish vary geographically, primarily depending on the local abundance and composition/dominance of *Gambierdiscus* species. In the Caribbean Ciguatera-endemic region, for instance, CTX accumulation in lionfish muscles can be highly frequent ($\geq$40–50%), and reach levels up to 0.3 ng C-CTX1 equiv. g^{-1} [46,49]. This suggests that *P. volitans* could become a common vector for CP in that region, where other top predators (e.g., snapper, barracuda, and grouper) can accumulate even higher CTX levels, posing a risk to human health [46,49]. Those toxin-equivalent concentrations must be considered carefully, however, because the venoms produced by lionfish itself can potentially interfere with the toxicity bioassays commonly used to quantify CTX. To avoid false-positive results on CTX tests, cooking the fillets of lionfish is recommended before testing for the presence of ciguatoxin. This procedure denatures the scorpaenitoxins, leav-

ing only CTX-related toxicity if present [50]. Regardless, at least one case of CP following the consumption of lionfish has been already confirmed [51].

Considering the ecological relevance of *P. volitans* associated with its potential threats as an invasive species and emerging CP vector, this species was selected in the present study to study the transfer of CTX from a prey to a carnivorous reef fish predator. The potential effects of CTXs, as well as their transfer, accumulation, and elimination were investigated during a long-term (12-week) laboratory feeding experiment using naturally CTX-contaminated steephead parrotfish, *Chlorurus microrhinos* (formerly *Scarus gibbus*), fillets as source of toxins. The presence and concentration of CTXs were evaluated in liver and muscle tissues of juvenile *P. volitans* during both toxin uptake and depuration phases, using distinct analytical methods such as radioligand-receptor binding assay (r-RBA), neuroblastoma cell-based assay (CBA-N2a), and liquid chromatography coupled to tandem mass spectrometry (LC-MS/MS).

2. Results and Discussion

2.1. Experimental Setting and Fish Behavior

The experimental feeding encompassed a 12-week period, including 6 weeks of exposure to CTX and 6 weeks of depuration. A gradual decrease in feeding activity was observed over the course of the experiment in both CTX exposed and control fish, although the propensity was greater among exposed fish (Figure 1). Increased food rejection episodes were indeed registered, mainly after the fifth week of experiment, during the late exposure period. The proportion of non-eating fish was 62% in the group exposed to CTX and 32% in the control group at late exposure phase (Figure 1). Such changes in feeding behavior were not observed in previous experiments using herbivorous fish (*Naso brevirostris*) or carnivorous groupers (*Epinephelus coioides*) exposed to diets containing 0.4 ng CTX3C equiv. g^{-1} over 16 weeks and ~1.0 ng CTXs equiv. g^{-1} day^{-1} (mean of CTX1B, 52-*epi*-54-deoxyCTX1B, 54-deoxyCTX1B quantifications) over 30 days of exposure, respectively [27,28]. However, the food rejection episodes observed during the present experiment did not seem to affect the CTX uptake and accumulation, since toxin levels were, in fact, detected in fish liver at the final exposure stage due to prolonged feeding (4–5 weeks) on CTX-containing parrotfish flesh (Table 1).

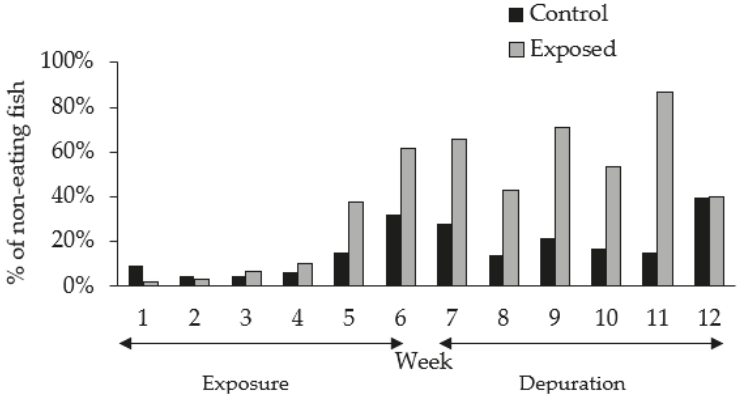

Figure 1. Proportion of control and CTX-exposed lionfish rejecting the food in relation to the number of remaining individuals at a given time during both the exposure and depuration periods.

Table 1. Detection and quantification of ciguatoxins in individual lionfish livers during the experimental exposure and depuration periods by r-RBA analysis.

Periods of Experiment	Fish Individual	Days of Exposure/ Depuration	Fish Total Weight (g)	Liver Wet Weight (g) (% Contribution)	Toxin Concentration (ng CTX3C Equiv. g^{-1})
Exposure	1	30	20.3	0.53 (3%)	<LOD **
	2	30	16.9	0.45 (3%)	7.08
	3	30	10.0	0.30 (3%)	<LOD **
	4	30	5.56	0.08 (1.5%)	<LOD **
	5	41	21.0	0.74 (3.5%)	<LOD **
	6	41	14.4	0.33 (2%)	<LOD **
	7	41	17.6	0.39 (2%)	9.43
	8	41	14.4	0.40 (3%)	<LOD **
	9	41	9.08	0.22 (2%)	<LOD **
Depuration	10	8	19.4	0.65 (3%)	9.30
	11	8	15.0	0.61 (4%)	9.42
	12	29	16.7	0.55 (3%)	8.93
	13	29	8.72	0.02 (0.2%)	<LOD **
	14	29	9.81	0.11(1.1%)	<LOD **
	15	43	21.2	0.34 (2%)	9.77
	16	43	10.3	0.18 (2%)	<LOD **

** LOD = the limit of detection of the r-RBA was 0.75 ng CTX3C equiv. g^{-1}.

Although laboratory conditions appeared to be optimal and constant throughout the experiment, unexpected deaths were registered among both control and exposed lionfish (15 out of 48 individuals in total). Mortality also affected individuals belonging to a separate batch received after the beginning of the experiment, maintained under similar conditions in the facility for future experiments. The specimens used in this study may have become more sensitive and prone to diseases such as bacterial infections when transferred to a laboratory setting. Consequently, these unexpected fish mortalities led to the loss of experimental replicates. Despite the reduction of replicates and considering that (i) fish showed no signs of suffering during the experiment, (ii) CTX-contaminated matrices were difficult to obtain, and (iii) published information of CTX trophic transfer under controlled conditions are still very limited, we decided to maintain the experimental protocol. Diet comparisons (i.e., exposed vs. control group) were thus achieved using randomly sampled individual fish as replicates.

Increased food rejection episodes may have contributed to the fish deaths observed during our experiment, although this could not be confirmed. Indiscriminate, sporadic mortality episodes registered during the experiment seemed unrelated to the exposure to CTX. Out of the 32 CTX-dosed fish, 11 fish died, mostly on week 7 (after 1 week of depuration). Similarly, 4 out of 16 control fish died, but in this case, most deaths were registered on week 12, at the end of the experiment. The cumulative proportion of fish mortalities in the exposed group (36%) was similar to that of the control (28%).

During the entire experiment, exposed lionfish exhibited no clear signs of acute intoxication, such as erratic swimming, rapid gill movement, loss of equilibrium, and fin paralysis, as described in CTX-exposed mullet *Mugil cephalus* [25]. Likewise, in natural environments, CTX-contaminated fishes, including lionfish in the Caribbean region [49], as well as snapper and grouper on Pacific coral reefs [42], have been found to exhibit no signs of intoxication. Thus, coral reef fish species facing repeated exposure to CTXs in the natural environment may have developed resistance mechanisms to these compounds, perhaps binding them to particular soluble proteins in the skeletal muscle [52,53], or storing them in compartments where they would be biologically unavailable.

2.2. Toxin Levels in the Food and Fish Dosing

The average CTX content in the naturally contaminated parrotfish (*Chlorurus microrhinos*) fillet homogenate (toxic food) was estimated as 2.27 ± 0.4 ng CTX3C equiv. g^{-1} (coefficient of variation, CV = 17.6%) by r-RBA, with no significant difference ($p < 0.05$) among the eight subsamples tested. Analysis by CBA-N2a confirmed the presence of CTXs in the CTX-contaminated food, estimated at a concentration of 0.70 ± 0.02 ng CTX3C equiv. g^{-1} ($n = 3$) with CV of 2.8% (Supplementary Materials, Figure S1). Unfortunately, the toxin levels in parrotfish flesh were too close to the LOD and LOQ values by LC-MS/MS (up to 1.5 ng CTX3C equiv. g^{-1} and 4.7 ng CTX3C equiv. g^{-1} of flesh, respectively), to allow unambiguous determination of CTXs using this technique. As expected, the CTX-free food (control) exhibited no activity by r-RBA analysis in our experimental conditions.

Given the toxin content in the CTX-contaminated food and the daily ration of 0.05 g food per g of fish, individuals from the CTX-exposed group received a dose equivalent to 0.11 ng CTX3C equiv. g^{-1} d^{-1} according to r-RBA estimations, or 0.035 ng CTX3C equiv. g^{-1} d^{-1} by CBA-N2a quantification. The dose administrated herein can be representative of an exposure that can eventually occur in the reef environment (i.e., environmentally relevant dose), as high levels of CTXs (up to 10.7 ng CTX3C equiv. g^{-1}) have been reported in parrotfish (*C. microrhinos*) sampled from French Polynesia islands [39].

Considering the average amount of food supplied and the toxin content in the experimental diet, the total toxin ingested per lionfish (initial body weight: 15.8 ± 9.6 g; $n = 32$) was estimated by r-RBA as 1.74 ng CTX3C equiv. day^{-1}, totalizing 52.2 ng CTX3C equiv. and 71.3 ng CTX3C equiv. over 30 and 41 days, respectively, assuming that the fish accept all food portions offered. Based on the CBA-N2a analysis, each exposed lionfish may have ingested, on average, a 3.2-fold lower dose.

2.3. Toxin Levels in Fish Tissues

CTX were detectable by r-RBA in the liver of fish, yet not consistently. When quantified by this assay, toxin concentrations in the livers of exposed lionfish reached 9.4 ng CTX3C equiv. g^{-1} at day 41 of exposure to CTX-contaminated food. The highest toxin concentration (9.77 ng CTX3C equiv. g^{-1}) was measured at late depuration phase (Table 1). As expected, CTX was not detected in the livers of control fish using either r-RBA (LOD: 0.75 ng CTX3C equiv. g^{-1}) or LC-MS/MS (LOD: up to 1.14 CTX3C equiv. g^{-1} of liver). In fact, this latter analytical method proved to be the least sensitive one. Unfortunately, the limited sample volumes remaining from other technique, as well as the relatively low concentrations of individual CTX compounds present in our samples, together with the matrix effect, did not allow us to make any further clarification on the toxin profile of CTX-exposed fish. In French Polynesia, CTX composition of steephead parrotfish *C. microrhinos* typically includes CTX3C type compounds (71.1% as CTX3C and its M-seco form) and, to a lesser extent, CTX4A type (28.8% as CTX4A and its M-seco form) [33,54]. However, CTX profiles in fish are species-specific and can differ from regional variations [55,56]. The typical toxin profile reported in *Gambierdiscus* species found in Pacific coral reef is also mostly composed of the less polar CTXs (48% CTX3C, 34% 49-epiCTX3C and 13% CTX4A) [33].

Following CTX absorption, toxin metabolization in fish may affect the depuration and elimination process [37,55]. Of note, as suggested in the present study for lionfish, low CTX depuration rates were also reported in other carnivorous fishes, including experimentally exposed orange-spotted grouper (*Epinephelus coioides*) [28], as well as wild-caught moray eels *Gymnothorax javanicus* (*Lycodontis javanicus*) [57] and red snapper (*Lutjanus bohar*) [58]. For the latter species, the fish would require up to 30 months to completely eliminate the acquired toxin load. Moreover, the livers of contaminated orange-spotted groupers showed faster elimination rates for CTX1B, 52-*epi*-54-deoxyCTX1B, and 54-deoxyCTX1B, which are already highly metabolized toxins, compared to other tissues such as skin, gills, and muscles, indicating different CTX elimination rates among tissues of exposed fish over 30 days [28].

Pooled liver extracts from control fish caused no cytotoxic effects on N2a cells in either OV^- or OV^+ conditions throughout the experiment. Conversely, sigmoidal dose-response curves with a negative slope were obtained under the OV^+ condition for liver extracts from fish sampled after 30 and 41 days of exposure to toxic food (Figure 2), and from those sampled after a depuration period of 8, 29, and 43 days (Figure 3). Based on the CTX-like composite toxicity using the CBA-N2a results, toxin concentrations in pooled lionfish livers were estimated as 1.36 ng CTX3C equiv. g^{-1} and 0.89 ng CTX3C equiv. g^{-1} after 30 and 41 days of exposure to toxin-containing food (herbivore *C. microrhinos* parrotfish fillets). Toxin concentration values decreased gradually over the depuration period, reaching 0.81 ng CTX3C equiv. g^{-1}, 0.52 ng CTX3C equiv. g^{-1}, and 0.37 ng CTX3C equiv. g^{-1} in pooled extracts from 8, 29, and 43 days of depuration on non-toxic food, respectively (Table 2). Considering the decrease in CTX-like cytotoxicity corresponding to a 0.44 ng CTX3C equiv. g^{-1} difference between days 8 and 43 of depuration (see Table 2), it would take an additional 35-day depuration period for lionfish livers to reach the CBA-N2a LOD of 0.06 ng CTX3C equiv. g^{-1}. The kinetics of CTX elimination in lionfish liver, however, should be examined with caution, considering: (i) the limited number of time points for sampling during depuration stage (8, 23, and 43 days after last exposure), (ii) the use of pooled samples in CBA-N2a due to an insufficient amount of remaining individual tissues, and (iii) the limited amount of pooled tissues available, which did not allow for replication of the quantification of CTX in livers by CBA-N2a.

Livers of lionfish belonging to the CTX-exposed group weighed, on average, 0.64 g (3.4% of the total fish body weight), resulting in a toxin burden of up to 4.53 ng CTX3C equiv. and 6.04 ng CTX3C equiv. in this organ after 30 and 41 days of exposure, respectively (based on the r-RBA results). When referring to the CBA-N2a results, the average toxin burden in pooled livers ranged from 0.87 ng CTX3C equiv. to 1.90 ng CTX3C equiv. after 30 and 41 days of exposure, respectively. This represents a retention of 8.6% (r-RBA) or 6.8% (CBA-N2a) of the ingested toxin burden at the end of the exposure period. Recent studies have reported that carnivorous grouper (*Epinephelus coioides*) fish, fed over 30 days, demonstrated a toxin burden of ~1 ng CTX1B g^{-1} d^{-1}—a greater toxin dose than that used in our experiment (0.11 ng CTX3C equiv. g^{-1} d^{-1} or 0.035 ng CTX3C equiv. g^{-1} d^{-1} from r-RBA or CBA-N2a analysis)—and accumulated up to 25% of the ingested toxin load in the livers and 10% in muscles [28]. In contrast, after 16 weeks of dietary exposure to 0.4 ng CTX3C equiv. g^{-1} d^{-1}, juvenile *Naso brevirostris* accumulated ~2% of the exposed CTX3C amounts in muscular tissue [27].

In the present study, toxin concentrations in the muscles of lionfish belonging to the dosed group were always below the limit of detection, as determined by r-RBA. The sample amounts remaining from this first analysis were deemed insufficient for a supplementary evaluation by CBA-N2a. In natural environments, lionfish muscles were found to contain relatively high CTX levels ($\geq$0.24 ng C-CTX1 equiv. g^{-1}), indicating the potential of this species to cause human poisoning events [46,51]. When experimentally exposed to four-fold higher weight-specific daily doses of CTXs than those administered in our experiment, the herbivorous coral reef fish *Naso brevirostris* accumulated up to 3.24 $\pm$ 0.59 ng CTX3C equiv. g^{-1} in muscular tissues [27]. This value is within the range usually found among naturally contaminated fish in French Polynesia [41]. Moreover, in CTX-exposed *N. brevirostris*, the total amount of toxins in muscles increased linearly over 16 weeks of toxin exposure [27]. The muscles of *N. brevirostris* quickly eliminated the incorporated ciguatoxins, contrary to what has been observed for mullets (*Mugil cephalus*) after nine toxic feedings with gel food containing *Gambierdiscus* cells [25,27]. Finally, muscular tissues of groupers (*Epinephelus coioides*) incorporated the equivalent of 0.34 ng CTX1B g^{-1} d^{-1} after 30 days of exposure to 1 ng CTX1B g^{-1} d^{-1} [28]. In the Caribbean region, the highest C-CTX1 levels detected in the muscles of wild-caught fish were 0.24 ng g^{-1} in grey snapper (*Lutjanus griseus*), 0.3 ng g^{-1} C-CTX1 equivalents in lionfish (*P. volitans*), 0.9 ng g^{-1} in grouper (Serranidae), 13.8 ng g^{-1} in black jack (*Caranx lugubris*), and 49 ng g^{-1} in barracuda (*Sphyraena barracuda*) [49,59–61].

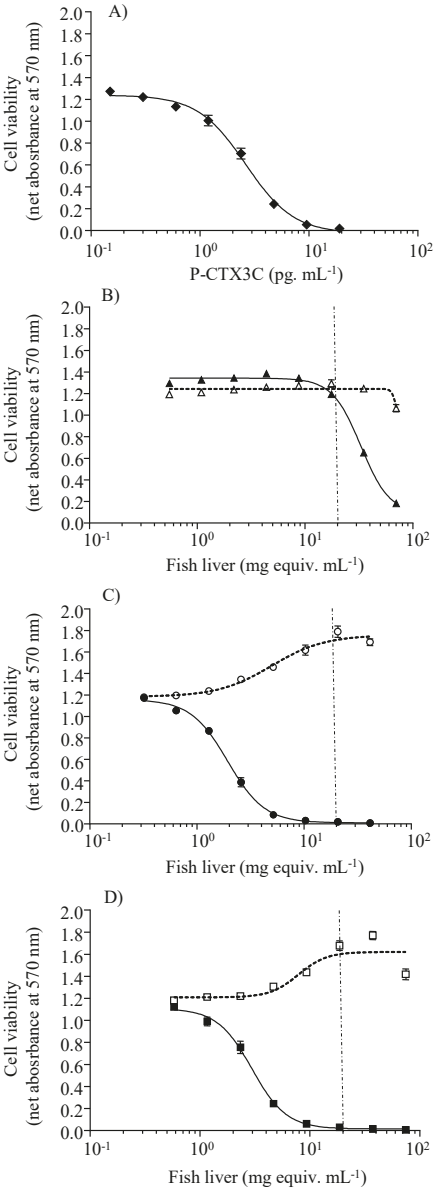

Figure 2. Quantification of CTX in fish liver during the exposure phase of the experiment. Dose-response curves of N2a cells when exposed to increasing concentrations of fish liver extracts, obtained from the exposure phase of the experiment, in OV^{-} (open symbols) and OV^{+} (solid symbols) conditions; (**A**) CTX3C (◆), (**B**) non-exposed control fish at day 42 (pool of 3 specimens) (Δ/▲), (**C**) exposed fish at day 30 (pool of 4 specimens) (○/●), and (**D**) exposed fish at day 41 (pool of 5 specimens) (□/■). Data represent the mean ± SD of 1 assay, with each point run in triplicate. The dotted vertical line corresponds to the maximum concentration of liver tissue (MCE) that does not induce a matrix effect on the assay, which was estimated at 20 mg mL^{-1} of fish liver extracts.

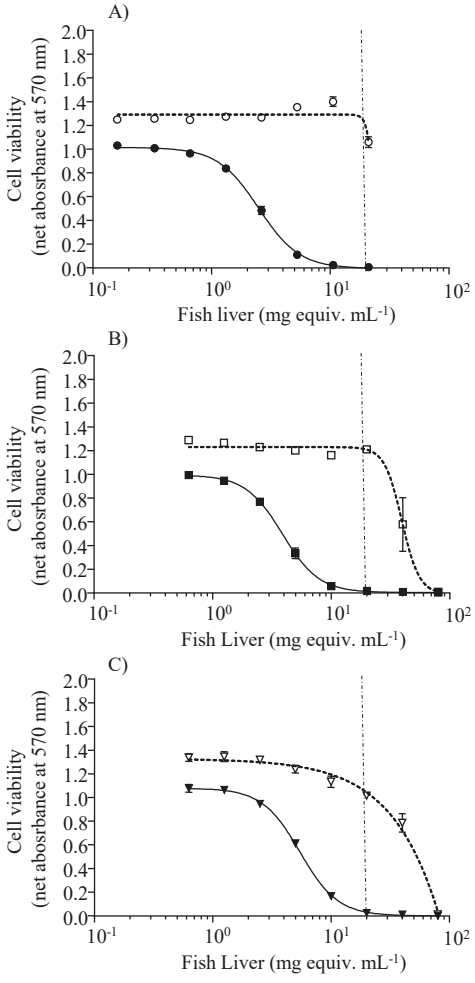

Figure 3. Quantification of CTX in fish liver during the depuration phase of the experiment. Dose-response curves of N2a cells when exposed to increasing concentrations of pooled fish liver extracts, obtained from the depuration stage of the experiment, in OV^{-} (open symbols) and OV^{+} (solid symbols); (**A**) 8 days of depuration (pool of 3 specimens) (○/●), (**B**) 29 days of depuration (pool of three specimens) (□/■), and (**C**) 43 days of depuration (pool of two specimens) (Δ/▲). Data represent the mean ± SD of one assay, with each point run in triplicate. The dotted vertical line corresponds to the maximum concentration of liver tissue (MCE) that does not induce the matrix effect, which was established at 20 mg mL^{-1} of fish liver extracts.

Despite the loss of replication and the need for a longer period of experimentation, our results indicate CTX transfer from contaminated prey to carnivorous *P. volitans*. Toxins concentrated into lionfish livers, while their transport to the muscles could not be reliably assessed. In other fish species, CTXs appear to be primarily accumulated in the liver, being secondarily distributed to the muscles and other tissues as the concentrations increase [28].

Table 2. Estimation of the EC_{50} values and the CTX-like concentration of the pooled lionfish liver samples, as determined by the CBA-N2a analysis of the control (CTX-free food) and during exposure (CTX-contaminated food) and depuration (CTX-free food) periods of the experiment.

Periods of Experiment	Days of Exposure/ Depuration	Pooled Samples (*n*)	Fish Liver Weight Per Pool (g)	EC_{50} (mg Equiv. mL^{-1})	Toxin Concentration (ng CTX3C equiv. g^{-1})
Exposure	30	4	0.47	1.93	1.36
	41	5	0.19	2.97	0.89
Control	42	2	0.50	ND *	<LOD **
	8	1	0.51	ND *	<LOD **
Depuration	8	2	0.23	2.49	0.81
	29	3	0.13	3.88	0.52
	43	2	0.11	5.46	0.37

f* ND = not determined as control samples gave no cytotoxicity at the MCE in both OV conditions. ** LOD = limit of detection of the CBA-N2a (0.06 ± 0.01 ng CTX3C equiv. g^{-1}).

3. Conclusions

The accumulation of CTX in the livers of juvenile lionfish *Pterois volitans* became evident after 5 weeks of feeding toxin-contained parrotfish *Chlorurus microrhinos* fillets. The toxin levels in the muscles of lionfish were always below the limits of detection, as determined by r-RBA, suggesting potential differential tissue distribution over the experiment. However, this could not be confirmed by a more sensitive method, such as CBA-N2a due to the insufficient amount of flesh. Lionfish retained detectable toxin levels in their livers at 43 days after the last exposure, indicating a slow elimination process. No acute intoxication signs were observed throughout the experiment, suggesting the resistance of *P. volitans* to CTXs.

4. Materials and Methods

4.1. Fish Acclimation and Maintenance

Juvenile lionfish, *Pterois volitans* (Scorpaenidae), originating from Bali, Indonesia, were acquired from a supplier (Tropic Nguyen, France). The juvenile lionfish were selected based on maintenance and individual replication needs considering the laboratory setting and aquarium size. Upon reception, the lionfish were acclimated for approximately 2 weeks in a 2000 L open-circuit tank. The thank was filled with flowing 1 µm filtered seawater at 400 L h^{-1}, 25 ± 0.5 °C, pH 8.1 ± 0.1, and a salinity of 39, and maintained under a 12:12 h (light:dark) cycle and permanent aeration. Fish were fed once a day during acclimation in amounts higher than needed for maintenance (equivalent to 5% of their body weight). The food consisted initially of living prey (guppy or seabream). Then, inert frozen food (*Antherina boyeri* and krill) was gradually incorporated into the diet before the final transition to the frozen, CTX-containing parrotfish (*Chlorurus microrhinos*) fillet.

4.2. Preparation of the Experimental Diets

The toxic material used for the feeding experiments consisted of naturally CTX-contaminated fillets of the steephead parrotfish *Chlorurus microrhinos* collected from Moruroa Atoll (Tuamotu Archipelago, French Polynesia). Parrotfish were selected based on the CTX levels in their fillets. Then, 7.8 kg (wet weight) of selected fillet were homogenized using an industrial mixer to obtain a toxic, homogenous fish fillet matrix. Toxicity of the prepared food was evaluated by means of cytotoxicity using CBA-N2a and binding affinity using r-RBA composed of 3 × 10 g and 8 × 5 g aliquots of the dried homogenate, respectively.

Different food preparations using Gelly Belly™ (Gel Food, Florida Aqua Farms, Inc., Dade City, FL, USA) and frozen food were tested. Gelly Belly™ consists of a gelatin-based food mixed with microalgae, seaweeds, fish, and krill meal, with added vitamins and minerals. The most appropriate food presentation for lionfish proved to be homogenized

cube-shaped frozen fillets. Frozen food dices were individually offered to lionfish using forceps, which were instantaneously caught and ingested without significant particle loss.

The food provided to the individuals in the control group—and to all remaining lionfish during the depuration phase—was composed of homogenized fillet of farmed seabream (*Sparus auratus*; ~120–140 g total body weight), originated from Turkey and supplied by Relais d'Or (France). After homogenization, seabream fillets were fashioned into cubes, placed in plastic bags, and kept at −18 °C until being offered to the carnivorous fish as frozen cubes. A sample of seabream fillets was collected and further tested for CTX presence.

4.3. Experimental Design

After acclimation, *P. volitans* individuals (n = 48; 5.05–34.0 g initial wet weight) were distributed among seven aquaria, allocating six fish per tank, except in two tanks where ten and eight fish were placed due to the smaller size of some individuals (~5 g) (Figure 4). This step aimed at obtaining similar fish sizes and total living biomass (15.2 g ± 9.52, mean ± SE) across the experimental tanks. Tanks were randomly assigned to either toxin-containing (5 tanks) or control diet (2 tanks), each containing 100 L of filtered seawater maintained under constant aeration and flow (100 L h^{-1}), at the same conditions of temperature, salinity, and pH used during the acclimation phase. To reduce animal stress, three tubes of 10 cm × 20 cm (D × L), assembled as a pyramidal structure, were placed inside the aquaria to provide shelter for the fish (Figure 4). Finally, the aquarium walls were covered with opaque plastic coating to limit potential stress caused by the human presence in the laboratory. Standards of animal welfare were rigorously maintained throughout the experiment. All procedures were carefully conducted to minimize handling and reduce physiological stress.

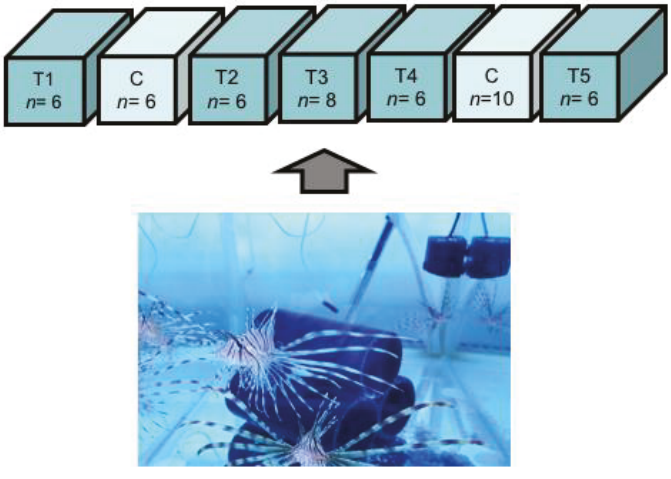

Figure 4. Design of the experiment, with 5 tanks initially containing 6 or 8 fish (n) assigned to the CTX-exposed treatment (T) and 2 tanks for control (C) containing 6 fish and 10 fish (n). The image represents a picture of the juvenile lionfish (*Pterois volitans*) individuals and their shelters made of dark tubes in one of the experimental tanks.

After 6 weeks of exposure to either the toxin-containing or control diet, fish entered the depuration stage, during which they received non-contaminated frozen food (homogenized seabream fillets) for an additional 6-week period. Fish feedings were carefully conducted throughout the experiment, assuring quick capture (usually <5 min) and no significant particle rejection. Some individuals in the control group were maintained over the entire duration of the experiment (12 weeks) and served as reference for possible visual

behavior alterations and/or intoxication symptoms relative to dosed fish. The behavioral pattern was observed daily in all tanks during the feeding period throughout the 12-week experiment. During the exposure and depuration phases, the number of deaths was computed in relation to the total number of fishes at the beginning of the experiment, while the percentage of fish rejecting the toxic food considered the average number of individuals remaining in each experimental condition.

Feeding Experiment

During the experiment, all lionfish individuals were fed in a constant proportion to 4–5% of their body weight per day, as recommended for juvenile fish. The amount of food supplied was adjusted weekly based on the average fish weight for each tank. The lionfish were individually fed, always in the afternoon (2:00 p.m.), 5 days a week. Individuals were observed over 30 min to assure complete food ingestion after every feeding procedure. At the end of this time interval, any rejected food was removed from the tank during the daily cleaning procedure. Lionfish usually consumed the entire portion of toxic food offered in less than 15 min. In addition, the tanks were connected to an open system under a constant seawater flow. Thus, any residual toxin eventually released from the food—or excreted by the fish—was quickly eliminated from the tanks. Therefore, the source of CTX to the exposed fish was considered limited to the food pathway.

After 30 days of exposure, four CTX-exposed and three control lionfish were randomly collected from the control tanks. Likewise, between two and five individuals from the exposed group were sampled each time, at the end of the exposure period (41 days) and after 8, 29, and 43 days of the following depuration stage. Finally, three additional control individuals were collected after 8, 29, and 43 days of the depuration stage (Table 3). Fish euthanasia was achieved using an overdose of eugenol, and the death was confirmed by the absence of respiratory movements [62]. Lionfish were dissected immediately following death to ensure the integrity of collected tissues. For toxin analysis, muscle and liver samples were individually weighed (wet weight) and stored in plastic tubes at −18 °C.

Table 3. Number of CTX-exposed juvenile *Pterois volitans* individuals (*n*) sampled after a given exposure or depuration period. In addition, fish fed non-toxic food (control) were sacrificed after 30 days of exposure and after 8, 29, and 43 days of depuration period (3 individuals at each time).

Periods of Experiment	Cumulative Number of Experimental Weeks	Days of Exposure/ Depuration	Cumulative Number of Feeding Episodes Toxic/Control Food	*n*
Exposure	5	30 days of exposure	22/0	4
	6	41 days of exposure	29/0	5
Depuration	7	8 days of depuration	29/6	3
	10	29 days of depuration	29/20	3
	12	43 days of depuration	29/30	2

4.4. Toxin Determination in Food and Exposed Fish

4.4.1. Sample Extraction

The extraction of CTXs from the muscle and liver samples followed the procedures described in previous studies [27,63,64]. Briefly, each tissue sample from individual lionfish was extracted as a whole when the tissues weighed <4 g, or partially, in 4 g aliquots after homogenization with T-25 digital Ultra Turrax (IKA Works, Staufen, Germany). Tissue samples were then cooked in Falcon tubes in a water bath at 70 °C for 15 min, homogenized in acetone (3 mL g^{-1} tissue) using a sonication probe (Branson digital probe cell breaker) for 2 min at 30% duty, and centrifuged for 3 min at 1400× *g*. The supernatant was recovered from the tubes, and the tissue pellet was homogenized twice again in acetone, as previously described. After three successive extraction steps, the supernatant fractions were combined and evaporated under nitrogen gas flow (Turbovap) in a water bath at 60 °C. Dried

extracts were resuspended in 5 mL of aqueous methanol (MeOH/H_2O 90:10), and the lipids were removed by solvent–solvent separation (three times) after the addition of an equal volume of *n*-hexane. The 1:1 solvent–solvent fraction was separated (3×) into an aqueous phase (MeOH/H_2O 60:40) and dichloromethane (DCM). Finally, the organic phase (DCM), containing the CTXs, was evaporated with nitrogen, resuspended in pure MeOH to 10 g tissue equivalent (TE) mL^{-1}, and stored at −18 °C until further analysis. Frozen homogenized fillet cubes of parrotfish *Chlorurus microrhinos* (toxic food) and seabream (control food) were extracted following the same procedure described for lionfish tissues, adjusting the sonication time to 20 min to ensure complete fish cell lysis.

4.4.2. Toxin Analysis

Radioligand-Receptor Binding Assay (r-RBA)

The presence and quantification of CTXs in parrotfish (*C. microrhinos*) fillet homogenates (toxic food) and in selected extracts of fish muscle and liver were first determined using the r-RBA [65]. This detection method is based on the binding competition between CTXs from the sample and a radiolabeled brevetoxin (tritiated PbTx-3) for their common receptor—on the voltage gated sodium channel (Na_v)—using a porcine brain homogenate (Sigma Aldrich, St. Louis, MO, USA) membrane preparation [11,65].

The assay was performed on a microplate according to the method reported by the authors of [63], modified according to previous studies [27,64,65]. First, 35 µL of phosphate-buffered saline (PBS-Tween®) with bovine serum albumin (BSA) (1 g L^{-1}) was added to each well of a 96-well filtration microplate (MultiScreen HTS FB Filter Plate MSFBN6B50, Millipore) to moisturize the membrane filter. Subsequently, 35 µL of either the standard CTX3C provided in dried form by Wako-Pure Chemicals, Osaka, Japan (2.85×10^{-9} to 1.92×10^{-12} M), a solution of PbTx-3 (Latoxan, Rosam, France) (1.8×10^{-8} M) used as an internal assay Quality Control (QC) (3×10^{-9} M in assay), or the diluted samples were added to each corresponding well, after vortex-mixing and sonication. Likewise, only one concentration of fish sample was tested, i.e., 0.6 g tissue equiv. mL^{-1} for the parrotfish toxic food, and 0.6 g tissue equiv. mL^{-1} and 0.12 g tissue equiv. mL^{-1} for lionfish muscle and liver, respectively. Each sample was tested in duplicate wells in one experiment. Then, 35 µL of the working solution of [^{3}H] PbTx-3 (1 nM assay concentration) and 195 µL of the diluted brain membrane homogenate (0.8 mg protein mL^{-1}) were sequentially added to all wells. After incubation for 1 h at 4 °C, each well was washed (3×) with 200 µL of ice-cold phosphate-buffered saline solution (PBST) and filtered using a MultiScreen HTS vacuum collector system (Milipore, Billerica, Massachusetts, USA) to remove the excess radiotracer [^{3}H] PbTx-3. Only the membrane receptor-bound toxin molecules were retained in the filter at this stage. After filtration, the microplate was placed on a counting cassette (Perkin-Elmer rigid 96 plate 14105), with 50 µL of liquid scintillant (Optiphase, Perkin-Elmer, USA) per well. Finally, the plate was incubated in the dark at room temperature for 2 h prior to quantification of the radioactivity in a beta-microplate counter (MicroBeta^2, Perkin-Elmer, Waltham, MA, USA).

Liquid Chromatography Coupled with Tandem Mass Spectrometry (LC-MS/MS)

Analysis by LC-MS/MS was performed on liver samples of lionfish and in CTX-contaminated parrotfish *Chlorurus microrhinos* homogenates to confirm the presence of CTXs in the extracts. Aliquots of the extracts remaining from the r-RBA analysis (10–100 µL) were dried off with nitrogen gas and resuspended with the following volume of 90% aqueous MeOH: 200 µL for lionfish liver samples and 500 µL for parrotfish homogenate, yielding a final concentration of 0.5–2.6 g liver equiv. mL^{-1} and 0.4–1.1 g flesh equiv. mL^{-1}, respectively. Different dilutions reflected the amount of matrix available in each case. Toxin determination was performed on a UHPLC system (UFLC Nexera, SHIMADZU, Japan) coupled to a hybrid triple quadrupole-linear ion-trap API4000 Qtrap mass spectrometer (ABSciex®, Framingham, MA, USA), equipped with a TurboV® electrospray ionization source.

Eluents consisted of deionized water (A) and 95% acetonitrile (B), both containing 2 mM ammonium formate and 50 mM formic acid. The following linear elution gradient was run at 0.4 mL min^{-1} through a Zorbax Eclipse Plus C18 column (50 × 2.1 mm, 1.8 µm, 95 Å; Agilent Technologies, Santa Clara, CA, USA), maintained at 40 °C: 78 to 88% B in 10 min, held at 88% B for 4 min, decreased back to 78% in 1 min, and held during 5 min to equilibrate. Samples were kept at 4 °C during the analysis, and 5 µL aliquots were injected into the system. Scheduled MRM scanning (90 s detection window; 2 s target scan time) was applied in positive electron spray ionization (ESI+) mode, using the following optimized parameters: curtain gas at 25 psi; ion spray at 5500 V; turbo gas temperature at 300 °C; gas 1 and 2 at 40 and 60 psi, respectively; declustering potential at 105 V; and entrance potential at 10 V. A list of MRM transitions (*m*/*z*) scanned in ESI+ for the detection of CTX-like compounds is given in Table 4, along with the respective collision energy (CE) and targeted retention time values. Instrument control, data processing, and analysis were conducted using Analyst software 1.6.2 (SCIEX, CA, USA). Due to the lack of standards, calibration curves of CTX3C (Wako, Japan) were applied to calculate the concentration of every compound detected, assuming an equivalent molar response for the other analogs.

Table 4. List of MRM transitions (*m*/*z*) used in ESI+ to detect CTXs by LC-MS/MS.

Compound	MRM Transitions (*m*/*z*) Precursor Ion (Q1)	MRM Transitions (*m*/*z*) Product Ion (Q3)	Precursor Ion Species	Targeted Time (min)	CE (eV)
CTX3C or CTX3B	1040.6	1005.6	$[M + NH4]^+$	11.2	30
	1023.6	1005.6	$[M + H]^+$		20
	1023.6	125.1			50
M-*seco*-CTX3C	1041.6	1023.6	$[M + H]^+$	4.7	20
	1041.6	1005.6			30
	1041.6	125.1			50
2-hydroxyCTX3C	1058.6	1005.6	$[M + NH4]^+$	5.0	30
	1058.6	1023.6			20
	1058.6	125.1			50
51-hydroxyCTX3C	1056.6	1021.6	$[M + NH4]^+$	6.3	30
	1039.6	1021.6	$[M + H]^+$		20
	1039.6	1003.6			20
CTX4A or CTX4B	1078.6	1043.6	$[M + NH4]^+$	12.8	30
	1061.6	1043.6	$[M + H]^+$		20
	1061.6	125.1			50
54-deoxyCTX1B or 52-*epi*-54-deoxyCTX1B	1112.6	1077.6	$[M + NH4]^+$	6.8	20
	1112.6	1059.6			30
	1112.6	95.1			90
CTX1B	1128.6	1093.6	$[M + NH4]^+$	3.2	20
	1128.6	1075.6			30
	1128.6	95.1			90
C-CTX1 or C-CTX2	1141.4	1123.4	$[M + H]^+$	4.4	30
	1123.4	1105.6	$[M + H–H2O]^+$		30
	1123.4	1087.6			30
2,3-dihydro-2,3-dihydroxyCTX3C	1074.6	1039.6	$[M + NH4]^+$	6.0	30
	1057.6	1039.6	$[M + H]^+$		20
	1057.6	125.1			50
CTX3C analog 1	1040.6	1005.6	$[M + NH4]^+$	10.0	30
	1023.6	1005.6	$[M + H]^+$		20
	1023.5	125.1			50
CTX3C analog 2	1040.6	1005.6	$[M + NH4]^+$	8.5	30
	1023.6	1005.6	$[M + H]^+$		20
	1023.5	125.1			50
CTX3C analog 3	1040.6	1005.6	$[M + NH4]^+$	7.5	30
	1023.6	1005.6	$[M + H]^+$		20
	1023.5	125.1			50

Cell Based Assay on Neuroblastoma (CBA-N2a)

The neuroblastoma (N2a) CCL 131 cell line (ATCC) was used in this study, and the CBA-N2a was performed following the protocol described by the authors of [66]. Briefly, the 60 inner wells of several 96-well microplates were seeded with 200 µL of a 5% FBS culture medium at an initial cell density of 50,000 ± 10,000 cells well^{-1} (exponential growth phase) and left to grow for 26 h in an incubator at 37 °C and 5% CO_2. Among the several microplates run in parallel, one microplate served as the Reference Cell Viability (RCV) control to establish the initial cell viability of N2a cells using an MTT assay [66]. For each microplate, the mean absorbance of DMSO control (12 outer wells filled with DMSO only) was subtracted from each raw absorbance value (60 inner wells containing N2a cells), and all viability data were expressed in net absorbance data.

The remaining microplates were treated as follows. The growth medium was renewed by the addition of 200 µL of 2% FBS culture medium with 90 µM of ouabain (O) and 9 µM of veratridine (V) for non-destructive treatment in the OV$^+$ condition (bottom half of the microplate). In the OV$^-$ condition, the growth medium was renewed by the addition of 200 µL of 2% FBS culture medium (upper half of the microplate). Appropriate controls in both OV conditions, namely COV$^-$ and COV$^+$, were established by adding 10 µL of 2% FBS culture medium to verify the final cell viability and the non-cytotoxicity of the OV treatment, respectively, in the absence of CTXs. The implementation of additional quality check controls (QC) to both OV$^-$ and OV$^+$ conditions, namely QCOV$^-$ and QCOV$^+$, was also undertaken to check for the specific effect of voltage gated sodium channel (VGSC) activators. Basically, 10 µL of PbTx3 (Latoxan, France) at 0.1 µg mL^{-1} were added in triplicate wells in both OV conditions to reach a final concentration of 4760 pg PbTx3 mL^{-1} in the wells. As CTX3C was tested in parallel with the fish samples, eight-point 1:2 serial dilutions of the CTX3C standard (Institut Louis Malardé) and sample stock solutions were prepared (100 µL per concentration) using a U-bottom 96-well microtiter. Then, 10 µL of CTX3C concentrations were directly added in triplicate wells under the non-destructive OV$^+$ condition (85.7/8.57 µM final concentrations) and not under OV- condition, since no cytotoxicity occurs in the absence of the O/V treatment [66]. The final concentrations of CTX3C tested ranged from 0.15 to 19.05 pg mL^{-1}. The three parrotfish (toxic food) aliquots were tested with final concentrations ranging from 74 to 9524 ng mL^{-1} of dry extract (corresponding to 0.23–29.76 mg flesh equiv. mL^{-1}). Each concentration was tested in triplicate wells in both OV conditions, in three independent microplates run the same day.

Liver extracts were further analyzed by CBA-N2a. To this end, all liver extracts prepared from individual fish collected from a single tank at the same sampling interval (days 30, 41 of the exposure phase and days 8, 29, and 43 of the depuration phase). Pooled samples ranged from 0.11–0.51 g fresh weight equivalent of fish liver. These samples were resuspended in a solution of 5 µL MeOH, 15 µL dimethyl sulfoxide (DMSO), and 2% fetal bovine serum (FBS) RPMI medium, providing concentrations of sample stock solutions ranging from 0.442 g fresh liver equiv. mL^{-1} to 1.567 g fresh liver equiv. mL^{-1}, with no more than 10% of solvent used during the serially two-fold dilution procedure. As dry extract weights were not available for lionfish livers, fresh fish liver equivalents could only be considered to estimate the concentration ranges tested. Pools of lionfish liver from the exposure experiment were tested together in one CBA-N2a experiment. In the same way, pooled liver from the depuration phase were also tested together in another CBA-N2a experiment. For each CBA-N2a experiment, CTX3C was tested in parallel with the lionfish liver samples, each concentration tested in triplicate wells in both OV conditions. Full dose-response curves were used for accurate CTX quantification. These two CBA-N2a experiments could not be repeated due to the very small amount of extract available. In all microplates, peripheral wells received 200 µL of sterile distilled water, and microplates were left to incubate overnight for about 19 h prior to the determination of the final cell viability using the MTT assay with an incubation time of 45 min.

4.5. Data Analysis

4.5.1. r-RBA

The r-RBA result of each extract was determined after the assay performance was confirmed by the Quality Control (QC), together with the additional parameters of the CTX3C standard curve (Supplementary Materials, Figure S2), such as the effective concentration inducing a 50% values effect (EC_{50}), and the slope of the linear portion of the standard curve. Sample CTX quantification was only completed when the CPM measurement of a sample dilution fell on the linear part of the CTX3C standard curve and the relative standard deviation (rSD) of the triplicate CPM values was verified to be less than 30%. The Hill equation was used to convert CPM values into CTX concentrations.

Data analysis was performed in GraphPad Prism version 6.0 (San Diego, CA, USA), allowing the determination of the parameters of each CTX3C competition sigmoidal curve (using 4 parameters). The detection limit (LOD) and the limit of quantification (LOQ) of the CTX-like composite in fish muscle and liver samples were determined based on the relative standard deviation (rSD) of the top plateau (Bmax) of the dose-response curve according the method described by the authors of [64], following the equations: LOD = Bmax–3 * rSD; and LOQ = Bmax–10 * rSD. The values of LOD and LOQ were not estimated in this study. However, previous publications have reported LOQ values corresponding to 0.32 ng CTX3C equiv. g^{-1} [27] and 1.5 ng CTX3C equiv. g^{-1} [36] and LOD values of 0.75 ng CTX3C equiv. g^{-1} [64].

4.5.2. LC-MS/MS

A calibration curve was calculated from the successive dilutions of a CTX3C standard solution (Wako, Tokyo, Japan) in MeOH at concentrations ranging from 12.5 ng mL^{-1} to 200 ng mL^{-1}. The limit of detection (LOD) and limit of quantification (LOQ) were calculated statistically based on the following formulae: LOD = 3.3 * std/S; and LOQ = 10 * std/S, where "std" is the standard deviation and "S" the slope of the calibration curve composed of successive dilutions of the CTX3C reference material. The calculated values for LOD and LOQ corresponded to 0.57 ng CTX3C mL^{-1} and 1.74 ng CTX3C mL^{-1}, respectively. This was equivalent, respectively, to 0.22–1.14 ng CTX3C mL^{-1}, and 0.67–3.48 ng CTX3C g^{-1} of lionfish liver, and to 0.54–1.54 and 1.64–4.71 ng CTX3C g^{-1} of parrotfish *Chlorurus microrhinos* flesh.

4.5.3. CBA-N2a

Net absorbance data were used to establish the full sigmoidal dose-response curves for CTX3C, lionfish liver extracts, and parrotfish *Chlorurus microrhinos* toxic food. The CTX3C and fish samples were tested in parallel in the same assay. The maximum concentration of the liver tissue (MCE) that did not induce unspecific mortality on N2a cells was determined in OV^{-} and OV^{+} conditions using the fish control sample from the exposure phase of the experiment. This concentration was further used to establish the concentration range of the fish liver samples to use for the assay in the depuration experiment. The maximum concentration of dry extract (MCE) was defined as 20 mg mL^{-1} from the fish liver control at 42 days. The limit of detection (LOD) and the limit of quantification (LOQ) of the CTX-like toxicity in the fish liver samples, expressed in ng CTX3C equiv. g^{-1} of fish liver, were determined according to the following equations: LOD = (EC_{80}/MCE) and LOQ = (EC_{50}/MCE), where EC_{80} and EC_{50} are the values obtained for CTX3C toxin standard, and were determined at 0.06 ± 0.01 and 0.12 ± 0.02 ng CTX3C equiv. g^{-1}, respectively. The composite cytotoxicity in the fish liver samples, expressed in ng CTX3C equiv. g^{-1} of fish liver, was then estimated based on the (EC_{50} of CTX3C/EC_{50} of fish liver) equation.

Supplementary Materials: The following are available online at https://www.mdpi.com/article/10.3390/toxins13080564/s1, Figure S1: Dose-response curves of N2a cells when exposed to increasing concentrations of parrotfish flesh extracts (toxic food) in OV^{-} (open symbols) and OV^{+} (solid symbols) conditions at 85.7/8.75 μM (final concentrations). Data represent the mean ± SD of each

aliquot tested, with each point run in triplicate. Absorbance values were measured at 570 nm via the MTT assay, after a 45 min MTT incubation time. The initial cell viability was 1.054 ± 0.020 in the RCV control. The mean final cell viability was 0.927 ± 0.023 in the absence of O/V treatment (COV−), and 1.031 ± 0.029 in the presence of non-destructive O/V treatment (COV+), respectively. The dotted vertical line corresponds to the MCE established at 10,000 mg mL^{-1} of fish flesh extracts, avoiding non-specific cy-totoxicity in both conditions of OV treatments. The LOD and LOQ values in fish flesh were 0.03 ± 0.01 and 0.06 ± 0.02 ng CTX3C equiv. g^{-1} [66], Figure S2. The sigmoidal dose-response curve of r-RBA was used to quantify the concentration of the CTX in the fish liver and muscle during the experiment (GraphPad Software, Inc., La Jolla, CA, USA).

Author Contributions: Conceptualization, M.-Y.D.B., L.L.M.J., I.d.P.L. Methodology, M.-Y.D.B., I.d.P.L., K.S., A.T., H.B.G., F.O., J.V., H.T.D., M.C., L.L.M.J. Formal Analysis, I.d.P.L., J.V., H.T.D., M.C., L.L.M.J., M.-Y.D.B. Funding acquisition, M.-Y.D.B., M.C. Project administration, M.-Y.D.B., Supervision, M.-Y.D.B., L.L.M.J. Investigation, M.-Y.D.B., I.d.P.L., K.S., A.T., H.B.G., F.O., P.S., J.V., H.T.D., M.C., L.L.M.J.; Writing—Original Draft Preparation, I.d.P.L.; Writing—Review & Editing, I.d.P.L., M.-Y.D.B., L.L.M.J., J.V., H.T.D., M.C., A.T., K.S., H.B.G., F.O., P.S. All authors have read and agreed to the published version of the manuscript.

Funding: The research was funded by the countries of France and French Polynesia in the framework of the CARISTO-Pf" (no. 7937/MSR/REC of 4 December 2015 and Arrêté no. HC/491/DIE/BPT of 30 March 2016) research program. This study was also partially supported by the International Atomic Energy Agency (IAEA) through the Coordinated Research Project (CRPK41014), contract #18827 ("Bentox" Project) and the Coordenação de Aperfeiçoamento de Pessoal de Nível Superior (CAPES, Brazil) for the Ph.D. scholarship awarded to I.d.P.L. at Federal University of Paraná, and for the PVEX (n. 88881.172853/2018-01) and PDSE-2018 (n. 7338918) grants awarded to L.L.M.J. and I.d.P.L., respectively.

Institutional Review Board Statement: Not applicable.

Informed Consent Statement: Not applicable.

Data Availability Statement: The data presented in this study are available in this article and Supplementary Materials.

Acknowledgments: The IAEA is grateful to the Government of the Principality of Monaco for the support provided to Environment Laboratories. Our sincere gratitude to Philipp Hess for hosting L.L.M.J. in the Laboratoire Phycotoxines (ODE\DYNECO) at IFREMER (Nantes, France) and providing the instruments and materials for the LC-MS/MS analysis.

Conflicts of Interest: The authors declare no conflict of interest.

References

1. Cuypers, E.; Abdel-Mottaleb, Y.; Kopljar, I.; Rainier, J.D.; Raes, A.L.; Snyders, D.J.; Tytgat, J. Gambierol, a toxin produced by the dinoflagellate *Gambierdiscus toxicus*, is a potent blocker of voltage-gated potassium channels. *Toxicon* **2008**, *51*, 974–983. [CrossRef] [PubMed]
2. Hoppenrath, M.; Murray, S.A.; Chomérat, N.; Horiguchi, T. *Marine Benthic Dinoflagellates—Unveiling Their Worldwide Biodiversity*; Senckenberg-Reihe: Frankfurt, Germany, 2014.
3. Morohashi, A.; Satake, M.; Nagai, H.; Oshima, Y.; Yasumoto, T. The absolute configuration of gambieric acids A-D, potent antifungal polyethers, isolated from the marine dinoflagellate *Gambierdiscus toxicus*. *Tetrahedron* **2000**, *56*, 8995–9001. [CrossRef]
4. Murray, J.S.; Selwood, A.I.; Harwood, D.T.; van Ginkel, R.; Puddick, J.; Rhodes, L.L.; Rise, F.; Wilkins, A.L. 44-Methylgambierone, a new gambierone analogue isolated from *Gambierdiscus australes*. *Tetrahedron Lett.* **2019**, *60*, 621–625. [CrossRef]
5. Soliño, L.; Costa, P.R. Differential toxin profiles of ciguatoxins in marine organisms: Chemistry, fate and global distribution. *Toxicon* **2018**, *150*, 1–70. [CrossRef] [PubMed]
6. Watanabe, R.; Uchida, H.; Suzuki, T.; Matsushima, R.; Nagae, M.; Toyohara, Y.; Satake, M.; Oshima, Y.; Inoue, A.; Yasumoto, T. Gambieroxide, a novel epoxy polyether compound from the dinoflagellate *Gambierdiscus toxicus* GTP2 strain. *Tetrahedron* **2013**, *69*, 10299–10303. [CrossRef]
7. EFSA Panel on Contaminants in the Food Chain. Scientific opinion on marine biotoxins in shellfish—Emerging toxins: Ciguatoxin group. *EFSA J.* **2010**, *8*, 1–38. [CrossRef]
8. Friedman, M.A.; Fernandez, M.; Backer, L.C.; Dickey, R.W.; Bernstein, J.; Schrank, K.; Kibler, S.; Stephan, W.; Gribble, M.O.; Bienfang, P.; et al. An updated review of ciguatera fish poisoning: Clinical, epidemiological, environmental, and public health management. *Mar. Drugs* **2017**, *15*, 72. [CrossRef]

9. Parsons, M.L.; Aligizaki, K.; Bottein, M.Y.D.; Fraga, S.; Morton, S.L.; Penna, A.; Rhodes, L. *Gambierdiscus* and *Ostreopsis*: Reassessment of the state of knowledge of their taxonomy, geography, ecophysiology, and toxicology. *Harmful Algae* **2012**, *14*, 107–129. [CrossRef]
10. Yasumoto, T.; Seino, N.; Murakami, Y.; Murata, M. Toxins produced by benthic dinoflagellates. *Biol. Bull.* **1987**, *172*, 128–131. [CrossRef]
11. Dechraoui, M.-Y.; Naar, J.; Pauillac, S.; Legrand, A.M. Ciguatoxins and brevetoxins, neurotoxic polyether compounds active on sodium channels. *Toxicon* **1999**, *37*, 125–143. [CrossRef]
12. Kumar-Roiné, S.; Darius, H.T.; Matsui, M.; Fabre, N.; Haddad, M.; Chinain, M.; Pauillac, S.; Laurent, D. A review of traditional remedies of ciguatera fish poisoning in the Pacific. *Phytother. Res.* **2011**, *25*, 947–958. [CrossRef] [PubMed]
13. Lombet, A.; Bidard, J.-N.; Lazdunski, M. Ciguatoxins and brevetoxins share a common receptor site on the neuronal voltage-dependent Na^+ channel. *FEBS Lett.* **1987**, *219*, 355–359. [CrossRef]
14. Poli, M.A.; Mende, T.J.; Baden, D.G. Brevetoxins, unique activators of voltage-sensitive sodium channels, bind to specific sites in rat brain synaptosomes. *Mol. Pharmacol.* **1986**, *30*, 129–135.
15. Au, N.P.B.; Kumar, G.; Asthana, P.; Tin, C.; Mak, Y.L.; Chan, L.L.; Lam, P.K.S.; Ma, C.H.E. Ciguatoxin reduces regenerative capacity of axotomized peripheral neurons and delays functional recovery in pre-exposed mice after peripheral nerve injury. *Sci. Rep.* **2016**, *6*, 1–13. [CrossRef] [PubMed]
16. Chinain, M.; Gatti, C.M.; Roué, M.; Darius, H.T. Ciguatera poisoning in French Polynesia: Insights into the novel trends of an ancient disease. *New Microbes New Infect.* **2019**, *31*, 100565. [CrossRef]
17. Dickey, R.W.; Plakas, S.M. Ciguatera: A public health perspective. *Toxicon* **2010**, *56*, 123–136. [CrossRef] [PubMed]
18. Davin, W.T.; Kohler, C.C.; Tindall, D.R. Effects of ciguatera toxins on the bluehead. *Trans. Am. Fish. Soc.* **1986**, *115*, 908–912. [CrossRef]
19. Kelly, A.M.; Kohler, C.C.; Tindall, D.R. Are crustaceans linked to the ciguatera food chain? *Environ. Biol. Fishes* **1992**, *33*, 275–286. [CrossRef]
20. Colman, J.R.; Dechraoui, M.Y.B.; Dickey, R.W.; Ramsdell, J.S. Characterization of the developmental toxicity of Caribbean ciguatoxins in finfish embryos. *Toxicon* **2004**, *44*, 59–66. [CrossRef]
21. Edmunds, J.S.G.; McCarthy, R.A.; Ramsdell, J.S. Ciguatoxin reduces larval survivability in finfish. *Toxicon* **1999**, *37*, 1827–1832. [CrossRef]
22. Mak, Y.L.; Li, J.; Liu, C.N.; Cheng, S.H.; Lam, P.K.S.; Cheng, J.; Chan, L.L. Physiological and behavioural impacts of Pacific ciguatoxin-1 (P-CTX-1) on marine medaka (*Oryzias melastigma*). *J. Hazard. Mater.* **2017**, *321*, 782–790. [CrossRef]
23. Yan, M.; Leung, P.T.Y.; Ip, J.C.H.; Cheng, J.; Wu, J.-J.; Gu, J.R.; Lam, P.K.S. Developmental toxicity and molecular responses of marine medaka (*Oryzias melastigma*) embryos to ciguatoxin P-CTX-1 exposure. *Aquat. Toxicol.* **2017**, *185*, 149–159. [CrossRef]
24. Yan, M.; Mak, M.Y.L.; Cheng, J.; Li, J.; Gu, J.R.; Leung, P.T.Y.; Lam, P.K.S. Effects of dietary exposure to ciguatoxin P-CTX-1 on the reproductive performance in marine medaka (*Oryzias melastigma*). *Mar. Pollut. Bull.* **2020**, *152*, 110–837. [CrossRef] [PubMed]
25. Ledreux, A.; Brand, H.; Chinain, M.; Bottein, M.Y.D.; Ramsdell, J.S. Dynamics of ciguatoxins from *Gambierdiscus polynesiensis* in the benthic herbivore *Mugil cephalus*: Trophic transfer implications. *Harmful Algae* **2014**, *39*, 165–174. [CrossRef]
26. Bottein, M.Y.D.; Kashinsky, L.; Wang, Z.; Littnan, C.; Ramsdell, J.S. Identification of ciguatoxins in hawaiian monk seals *Monachus schauinslandi* from the northwestern and main hawaiian Islands. *Environ. Sci. Technol.* **2011**, *45*, 5403–5409. [CrossRef] [PubMed]
27. Clausing, R.J.; Losen, B.; Oberhaensli, F.R.; Darius, H.T.; Sibat, M.; Hess, P.; Swarzenski, P.W.; Chinain, M.; Dechraoui Bottein, M.Y. Experimental evidence of dietary ciguatoxin accumulation in an herbivorous coral reef fish. *Aquat. Toxicol.* **2018**, *200*, 257–265. [CrossRef]
28. Li, J.; Mak, Y.L.; Chang, Y.H.; Xiao, C.; Chen, Y.M.; Shen, J.; Wang, Q.; Ruan, Y.; Lam, P.K.S. Uptake and depuration kinetics of Pacific Ciguatoxins in orange-spotted grouper (*Epinephelus coioides*). *Environ. Sci. Technol.* **2020**, *54*, 4475–4483. [CrossRef]
29. Dechraoui-Bottein, M.-Y.; Tiedeken, J.A.; Persad, R.; Wang, Z.; Granade, H.R.; Dickey, R.W.; Ramsdell, J.S. Use of two detection methods to discriminate ciguatoxins from brevetoxins: Application to great barracuda from Florida Keys. *Toxicon* **2005**, *46*, 261–270. [CrossRef]
30. Sanchez-Henao, A.; García-Álvarez, N.; Sergent, F.S.; Estévez, P.; Gabo-Martínez, A.; Martín, F.; Ramos-Sosa, M.; Fernández, A.; Diogène, J.; Real, F. Presence of CTXs in moray eels and dusky groupers in the marine environment of the Canary Islands. *Aquat. Toxicol.* **2020**, *221*, 105427. [CrossRef] [PubMed]
31. Yogi, K.; Oshiro, N.; Inafuku, Y.; Hirama, M.; Yasumoto, T. Detailed LC-MS/MS analysis of ciguatoxins revealing distinct regional and species characteristics in fish and causative alga from the Pacific. *Anal. Chem.* **2011**, *83*, 8886–8891. [CrossRef]
32. Halstead, B.W. *Poisonous and Venomous Marine Animals of the World*; The Darwin Press: Princeton, NJ, USA, 1978.
33. WHO. *Report of the Expert Meeting on Ciguatera Poisoning*; Food Safety and Quality: Rome, Italy, 2020; Volume 9, pp. 19–23. [CrossRef]
34. Clausing, R.J.; Chinain, M.; Dechraoui-Bottein, M.Y. Practical sampling guidance for determination of ciguatoxin. In *Guide for Designing and Implementing a Plan to Monitor Toxin-Producing Microalgae*; Reguera, B., Alonso, R., Moreira, A., Mendez, S., Dechraoui Bottein, M.Y., Eds.; IOC-UNESCO: Paris, France, 2016; pp. 51–63.
35. Chan, W.H.; Mak, Y.L.; Wu, J.J.; Jin, L.; Sit, W.H.; Lam, J.C.W.; Mitcheson, Y.S.; Chan, L.L.; Lam, P.K.S.; Murphy, M.B. Spatial distribution of ciguateric fish in the Republic of Kiribati. *Chemosphere* **2011**, *84*, 117–123. [CrossRef]

36. Díaz-Asencio, L.; Clausing, R.J.; Vandersea, M.; Chamero-Lago, D.; Gómez-Batiste, M.; Hernández-Albernas, J.I.; Chomérat, N.; Rojas-Abrahantes, G.; Litaker, R.W.; Tester, P.; et al. Ciguatoxin occurrence in food-web components of a cuban coral reef ecosystem: Risk-assessment implications. *Toxins* **2019**, *11*, 722. [CrossRef] [PubMed]
37. Lewis, R.J.; Holmes, M.J. Mini review origin and transfer of toxins involved in Ciguatera. *Biochem. Physiol* **1993**, *106*, 615–628.
38. Chinain, M.; Darius, H.T.; Ung, A.; Tchou Fouc, M.; Revel, T.; Cruchet, P.; Pauillac, S.; Laurent, D. Ciguatera risk management in French Polynesia: The case study of Raivavae Island (Australes Archipelago). *Toxicon* **2010**, *56*, 674–690. [CrossRef]
39. Chinain, M.; Gatti, C.M.; Ung, A.; Cruchet, P.; Revel, T.; Viallon, J.; Sibat, M.; Varney, P.; Laurent, V.; Hess, P.; et al. Evidence for the range expansion of Ciguatera in French Polynesia: A revisit of the 2009 mass-poisoning outbreak in Rapa Island (Australes Archipelago). *Toxins* **2020**, *12*, 759. [CrossRef]
40. Darius, H.T.; Ponton, D.; Revel, T.; Cruchet, P.; Ung, A.; Tchou Fouc, M.; Chinain, M. Ciguatera risk assessment in two toxic sites of French Polynesia using the receptor-binding assay. *Toxicon* **2007**, *50*, 612–626. [CrossRef]
41. Gaboriau, M.; Ponton, D.; Darius, H.T.; Chinain, M. Ciguatera fish toxicity in French Polynesia: Size does not always matter. *Toxicon* **2014**, *84*, 41–50. [CrossRef]
42. Mak, Y.L.; Wai, T.C.; Murphy, M.B.; Chan, W.H.; Wu, J.J.; Lam, J.C.W.; Chan, L.L.; Lam, P.K.S. Pacific ciguatoxins in food web components of coral reef systems in the Republic of Kiribati. *Environ. Sci. Technol.* **2013**, *47*, 14070–14079. [CrossRef] [PubMed]
43. Saunders, P.R.; Taylor, P.B. Venom of the lionfish *Pterois volitans*. *Am. J. Physiol.* **1959**, *197*, 437–440. [CrossRef]
44. Snyder, D.B.; Burgess, G.H. The Indo-Pacific red lionfish, *Pterois volitans* (Pisces: Scorpaenidae), new to Bahamian ichthyofauna. *Coral Reefs* **2007**, *26*, 175. [CrossRef]
45. Whitfield, P.E.; Gardner, T.; Vives, S.P.; Gilligan, M.R.; Courtenay, W.R.; Ray, G.C.; Hare, J.A. Biological invasion of the Indo-Pacific lionfish *Pterois volitans* along the Atlantic coast of North America. *Mar. Ecol. Prog. Ser.* **2002**, *235*, 289–297. [CrossRef]
46. Hardison, D.R.; Holland, W.C.; Darius, H.T.; Chinain, M.; Tester, P.A.; Shea, D.; Bogdanoff, A.K.; Morris, J.A.J.; Quintana, H.A.F.; Loeffler, C.R.; et al. Investigation of ciguatoxins in invasive lionfish from the greater caribbean region: Implications for fishery development. *PLoS ONE* **2018**, *13*, e0198358. [CrossRef] [PubMed]
47. Morris, J.A.J.; Whitfield, P.E. Biology, ecology, control and management of the invasive Indo-Pacific Lionfish: An updated integrated assessment. In *NOAA Technical Memorandum NOS NCCOS, 99*; NOAA: Washington, DC, USA, 2009; p. 57.
48. FDA. Fish and fishery products hazards and controls guidance. *Fish. Prod. Hazard. Control. Guide* **2011**, *4*, 1–401.
49. Robertson, A.; Garcia, A.C.; Flores Quintana, H.A.; Smith, T.B.; Castillo, B.F.; Reale-Munroe, K.; Gulli, J.A.; Olsen, D.A.; Hooe-Rollman, J.I.; Jester, E.L.E.; et al. Invasive lionfish (*Pterois volitans*): A potential human health threat for ciguatera fish poisoning in tropical waters. *Mar. Drugs* **2014**, *12*, 88. [CrossRef]
50. Wilcox, C.L.; Hixon, M.A. False positive tests for ciguatera may derail efforts to control invasive lionfish. *Environ. Biol. Fishes* **2014**, *98*, 961–969. [CrossRef]
51. Boucaud-Maitre, D.; Vernoux, J.P.; Pelczar, S.; Daudens-Vaysse, E.; Aubert, L.; Boa, S.; Ferracci, S.; Garnier, R. Incidence and clinical characteristics of ciguatera fish poisoning in Guadeloupe (French West Indies) between 2013 and 2016: A retrospective cases-series. *Sci. Rep.* **2018**, *8*, 1–7. [CrossRef] [PubMed]
52. Banner, A.; Helfrich, P.; Yoshida, T. Research on ciguatera in the tropical Pacific. *Proc. Gulf Caribb. Fish. Inst.* **1963**, *16*, 84–98.
53. Hahn, S.T.; Capra, M.F.; Walsh, T.P. Ciguatoxin-protein association in skeletal muscle of spanish mackerel (*Scomberomorus commersoni*). *Toxicon* **1992**, *30*, 843–852. [CrossRef]
54. Chinain, M.; Gatti, C.M.; Martin-Yken, H.; Roué, M.; Darius, H.T. Ciguatera poisoning: An increasing burden for Pacific Islands communities in light of climate change? In *Climate Change and Marine and Freshwater Toxins*, 2nd ed.; Botana, L.M., Louzao, M.C., Vilariño, N., Eds.; De Gruyter: Berlin, Germany; Boston, MA, USA, 2021; pp. 369–428. [CrossRef]
55. Ikehara, T.; Kuniyoshi, K.; Oshiro, N.; Yasumoto, T. Biooxidation of ciguatoxins leads to species-specific toxin profiles. *Toxins* **2017**, *9*, 205. [CrossRef] [PubMed]
56. Yogi, K.; Sakugawa, S.; Oshiro, N.; Ikehara, T.; Sugiyama, K.; Yasumoto, T. Determination of toxins involved in ciguatera fish poisoning in the Pacific by LC/MS. *J. AOAC Int.* **2014**, *97*, 398–402. [CrossRef] [PubMed]
57. Lewis, R.J.; Sellin, M.; Poli, M.A.; Norton, R.S.; MacLeod, J.K.; Sheil, M.M. Purification and characterization of ciguatoxins from moray eel (*Lycodontis javanicus*, Muraenidae). *Toxicon* **1991**, *29*, 1115–1127. [CrossRef]
58. Banner, A.H.; Helfrich, P.; Piyakarnchana, T. Retention of Ciguatera toxin by the red snapper, *Lutjanus bohar*. *Copeia* **1966**, *2*, 297–301. [CrossRef]
59. Pottier, I.; Vernoux, J.P.; Jones, A.; Lewis, R.J. Analysis of toxin profiles in three different fish species causing ciguatera fish poisoning in Guadeloupe, French West Indies. *Food Addit. Contam.* **2002**, *19*, 1034–1042. [CrossRef]
60. Pottier, I.; Hamilton, B.; Jones, A.; Lewis, R.J.; Vernoux, J.P. Identification of slow and fast-acting toxins in a highly ciguatoxic barracuda (*Sphyraena barracuda*) by HPLC/MS and radiolabelled ligand binding. *Toxicon* **2003**, *42*, 663–672. [CrossRef]
61. Soliño, L.; Widgy, S.; Pautonnier, A.; Turquet, J.; Loeffler, C.R.; Flores Quintana, H.A.; Diogène, J. Prevalence of ciguatoxins in lionfish (*Pterois* spp.) from Guadeloupe, Saint Martin, and Saint Barthélmy Islands (Caribbean). *Toxicon* **2015**, *102*, 62–68. [CrossRef] [PubMed]
62. Green, S.J.; Akins, J.L.; Morris, J. Lionfish dissection: Techniques and applications. *NOAA Tech. Memo.* **2012**, *139*, 1–24.
63. *Detection of Harmful Algal Toxins Using the Radioligand Receptor Binding Assay: A Manual of Methods*; IAEA-TECDOC-1729; IAEA: Vienna, Austria, 2013. [CrossRef]

64. Díaz-Asencio, L.; Clausing, R.J.; Rañada, M.L.; Alonso-Hernández, C.M.; Dechraoui Bottein, M.-Y. A radioligand receptor binding assay for ciguatoxin monitoring in environmental samples: Method development and determination of quality control criteria. *J. Environ. Radioact.* **2018**, *192*, 289–294. [CrossRef]
65. Dechraoui Bottein, M.-Y.; Clausing, R.J. Receptor binding assay for the analysis of marine toxins: Detection and mode of action. In *Recent Advances in the Analysis of Marine Toxins*; Diogène, J., Campàs, M., Eds.; Elsevier: Amsterdam, The Netherlands, 2017; pp. 277–301.
66. Viallon, J.; Chinain, M.; Darius, H.T. Revisiting the neuroblastoma cell-based assay (CBA-N2a) for the improved detection of marine toxins active on voltage gated sodium channels (VGSCs). *Toxins* **2020**, *12*, 281. [CrossRef] [PubMed]

toxins

MDPI

Article

An Update on Ciguatoxins and CTX-like Toxicity in Fish from Different Trophic Levels of the Selvagens Islands (NE Atlantic, Madeira, Portugal)

Pedro Reis Costa [1,2,*], Pablo Estévez [3], Lucía Soliño [1,2], David Castro [3], Susana Margarida Rodrigues [1], Viriato Timoteo [4], José Manuel Leao-Martins [3], Carolina Santos [5], Neide Gouveia [4,†], Jorge Diogène [6,*] and Ana Gago-Martínez [3,*]

1 IPMA—Portuguese Institute of the Sea and Atmosphere, Av. Brasília, 1449-006 Lisbon, Portugal; luciasolino@gmail.com (L.S.); srodrigues@ipma.pt (S.M.R.)
2 CCMAR—Centre of Marine Sciences, Campus of Gambelas, University of Algarve, 8005-139 Faro, Portugal
3 Biomedical Research Center (CINBIO), Department of Analytical and Food Chemistry, Campus Universitario de Vigo, University of Vigo, 36310 Vigo, Spain; paestevez@uvigo.es (P.E.); dcastro@uvigo.es (D.C.); leao@uvigo.es (J.M.L.-M.)
4 Regional Fisheries Management—Madeira Government, DSI-DRP, Estrada da Pontinha, 9004-562 Funchal, Madeira, Portugal; viriato.timoteo@madeira.gov.pt (V.T.); neide.gouveia@madeira.gov.pt (N.G.)
5 Instituto das Florestas e Conservação da Natureza, IP-RAM, Secretaria Regional do Ambiente, e Recursos Naturais e Alterações Climáticas, Regional Government of Madeira, Rua João de Deus, n.º 12 E/F, R/C-C, 9050-027 Funchal, Madeira, Portugal; carolina.santos@madeira.gov.pt
6 IRTA, Ctra Poble Nou km 5.5, 43540 Sant Carles de la Ràpita, Spain
* Correspondence: prcosta@ipma.pt (P.R.C.); jorge.diogene@irta.cat (J.D.); anagago@uvigo.es (A.G.-M.)
† Present address: Direção Regional de Agricultura e Desenvolvimento Rural, 9000-254 Funchal, Madeira, Portugal.

Citation: Costa, P.R.; Estévez, P.; Soliño, L.; Castro, D.; Rodrigues, S.M.; Timoteo, V.; Leao-Martins, J.M.; Santos, C.; Gouveia, N.; Diogène, J.; et al. An Update on Ciguatoxins and CTX-like Toxicity in Fish from Different Trophic Levels of the Selvagens Islands (NE Atlantic, Madeira, Portugal). *Toxins* **2021**, *13*, 580. https://doi.org/10.3390/toxins13080580

Received: 10 July 2021
Accepted: 17 August 2021
Published: 20 August 2021

Abstract: The Selvagens Islands, which are a marine protected area located at the southernmost point of the Portuguese maritime zone, have been associated with fish harboring ciguatoxins (CTX) and linked to ciguatera fish poisonings. This study reports the results of a field sampling campaign carried out in September 2018 in these remote and rarely surveyed islands. Fifty-six fish specimens from different trophic levels were caught for CTX-like toxicity determination by cell-based assay (CBA) and toxin content analysis by liquid chromatography with tandem mass spectrometry (LC-MS/MS). Notably, high toxicity levels were found in fish with an intermediate position in the food web, such as zebra seabream (*Diplodus cervinus*) and barred hogfish (*Bodianus scrofa*), reaching levels up to 0.75 µg CTX1B equivalent kg^{-1}. The LC-MS/MS analysis confirmed that C-CTX1 was the main toxin, but discrepancies between CBA and LC-MS/MS in *D. cervinus* and top predator species, such as the yellowmouth barracuda (*Sphyraena viridis*) and amberjacks (*Seriola* spp.), suggest the presence of fish metabolic products, which need to be further elucidated. This study confirms that fish from coastal food webs of the Selvagens Islands represent a high risk of ciguatera, raising important issues for fisheries and environmental management of the Selvagens Islands.

Keywords: ciguatoxins; Selvagens Islands; seafood safety; *Gambierdiscus*; ciguatera

Key Contribution: This article reports the first comprehensive evaluation of CTX in fish (n = 56) from the Selvagens Islands (Madeira, Portugal).

1. Introduction

Ciguatera poisoning (CP) is one of the most common nonbacterial illnesses associated with fish and other seafood consumption worldwide. The illness has been known since the 16th century when ciguateric-like poisonings affected classic sea explorers, such as captains of the Spanish navy in the Gulf of Guinea in 1521 or the crew of captain James Cook in his

second voyage to the South Pacific in 1772–1775 [1,2]. CP is widespread in the tropical and subtropical regions and particularly associated with the consumption of reef fish species that have bioaccumulated ciguatoxins (CTXs). These compounds are potent neurotoxins that act at the voltage-gated sodium channels (VGSC) increasing ion permeability and cell disruption leading to persistent neurological impairment [3]. The neurological symptoms include paraesthesia, dysesthesia, vertigo, and sensory abnormalities such as metallic taste, pruritus, arthralgia, myalgia, dental pain, and cold allodynia, a pathognomonic CP symptom that is characterized by burning pain in response to a cold stimulus [4–6]. Additionally, a variety of gastrointestinal symptoms including abdominal pain, nausea and vomiting, and cardiovascular symptoms, such as heart rhythm disturbances, may also affect poisoned patients. Some symptoms may become chronic and in extreme cases of severity CP may cause the death of patients [7].

The source of CTXs was linked to benthic dinoflagellates of the genus *Gambierdiscus* in the late 1970s [8,9]. *Gambierdiscus toxicus* was the first species described in the genus and, for a certain period, the only species known of this genus. Although the *Gambierdiscus* genus remains largely understudied, so far, at least 21 species have been described. *Gambierdiscus* and *Fukuyoa* are epibenthic dinoflagellates, which can be ingested by herbivorous fish. Some CTXs are produced by these dinoflagellates, but toxin congeners are products of fish metabolism. *Gambierdiscus* and *Fukuyoa* dinoflagellates are endemic to tropical and subtropical regions which are coincident with the world's highest incidence areas of ciguatera, namely the South Pacific, the Indian Ocean, and the Caribbean Sea [10]. Nevertheless, increasing occurrence and spread of *Gambierdiscus* to temperate regions has been reported and seems to be favored by the climate warming trends [11,12]. Coincident with CP outbreaks, *Gambierdiscus* have been detected in NE Atlantic subtropical-temperate regions, such as the Canary and Madeira Islands, and even in the Mediterranean Sea [13–17].

The first human poisonings in Europe due to the consumption of autochthonous fish occurred in 2004, in the Canary Islands, Spain [18]. Since then, several outbreaks have been reported in the Canary Islands and also in the nearby Portuguese islands, i.e., Madeira and Selvagens [19]. The first reported outbreak in Portugal dates from 2008 when 11 persons reported CP symptoms after consuming a 30 kg amberjack (*Seriola* sp) caught around the Selvagens Islands [20,21]. The symptoms reported by the crew members matched with symptoms previously reported by nature wardens of the natural park of the Selvagens Islands. CP was retrospectively diagnosed in the six wardens who had consumed fish caught locally [20]. In the following year, CP symptoms were observed in 20–30 people that ingested amberjack purchased in the Canary Islands but caught in the Selvagens Islands [22].

The Selvagens Islands are at the southernmost point of the Portuguese maritime area, located in the temperate-subtropical northeast Atlantic, closer to the Spanish Tenerife Island than to the Madeira Island, and 600 km from the African continental coast of Morocco (Figure 1). These small islands have a high fish species diversity and abundance, including important commercial species [23,24]. The total fish biomass has been estimated to be 3.2 times higher in the Selvagens Islands than in the Madeira habitat, and 10 times higher, when only top predators' biomass were considered [24]. The Selvagens Islands are a unique ecosystem, considered to be one of the last remaining intact ecosystems of the eastern Atlantic Ocean [25].

Despite several human poisonings associated with fish caught in waters surrounding the Selvagens Islands, only a limited number of studies have tried to assess and investigate the presence of CTX in fish from this potential ciguateric hotspot. Following the first human poisoning, in 2008, Otero and colleagues [21] analyzed by liquid chromatography coupled with tandem mass spectrometry (LC-MS/MS) two amberjacks (*S. dumerili* and *S. fasciata*) caught in the Selvagens Islands and described a suite of toxins composed of several CTX, including CTX1B, CTX3C, and C-CTX1. At the same time, Boada et al. [22] reported the presence of C-CTX1 in amberjack specimens associated with human poisonings in Tenerife but that had been caught in the Selvagens Islands. A retrospective analysis carried out by

state-of-the-art LC-MS/MS instruments to these specimens confirmed that C-CTX1 was the main toxin analogue but also suggested the presence of several metabolites of this compound [26]. More recently, LC-MS/MS analyses have been performed to assess CTX in fish opportunistically obtained from the Selvagens and Madeira Islands [27]. The results suggested a higher risk of ciguatera for fish caught in the Selvagens Islands and raised the need to better understand the natural contamination of CTX in the coastal food web of this marine protected area. Therefore, a campaign was carried out, in September 2018, on these remote and rarely surveyed islands to collect fish specimens that were representative of several trophic levels to assess CTX-like toxicity by cell-based assay (CBA) and to identify the CTXs by LC-MS/MS.

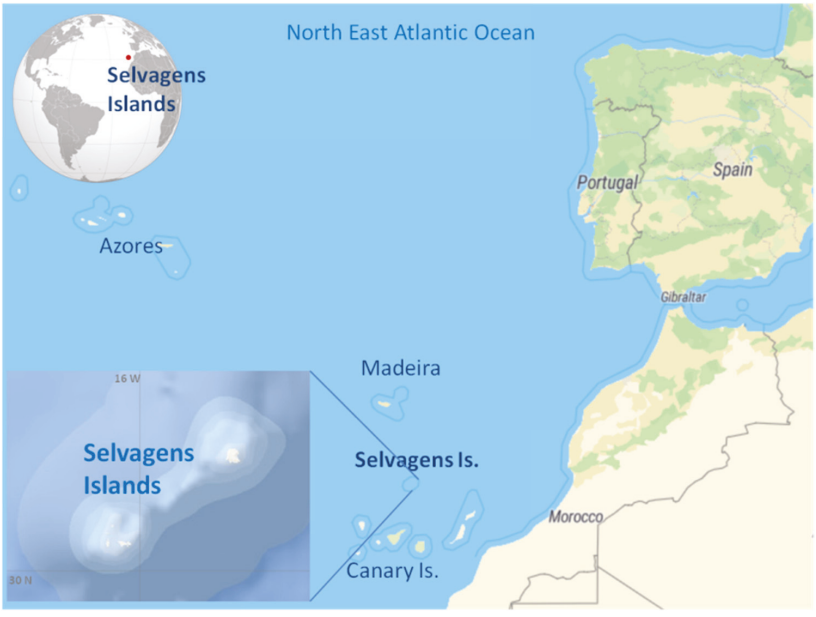

Figure 1. Location of the Selvagens Islands, NE Atlantic, Madeira, Portugal.

2. Results

2.1. Fish Toxicity by CBA

CTX-like toxicity was not detected in specimens at the lowest trophic level, representative of primary consumers of the marine food web, namely Bermuda sea chub *Kyphosus sectatrix* and scribbled leatherjacket filefish *Aluterus scriptus*. However, toxicity was particularly found in fish species with an intermediate position in the food web, such as the parrotfish *Sparisoma cretense*, zebra seabream *Diplodus cervinus,* and barred hogfish *Bodianus scrofa* (Figure 2). From the 14 parrotfish *S. cretense* caught, CTX-like activity was detected in eight specimens ranging from 0.006 to 0.04 µg CTX1B equivalent kg^{-1}. The single specimen of zebra seabream *D. cervinus* caught during the field campaign, revealed the second highest level determined, reaching 0.37 µg CTX1B equivalent kg^{-1}, highlighting this trophic level of key importance to the CTX dynamics in the Selvagens marine environment. This finding is further supported by the high levels of CTX toxicity found in the 17 barred hogfish *B. scrofa* collected, which varied from 0.04 to 0.75 µg CTX1B equivalent kg^{-1}. Although consistently found in each *B. scrofa* analyzed, CTX-like toxicity was not easily correlated with their size or weight ($p > 0.05$).

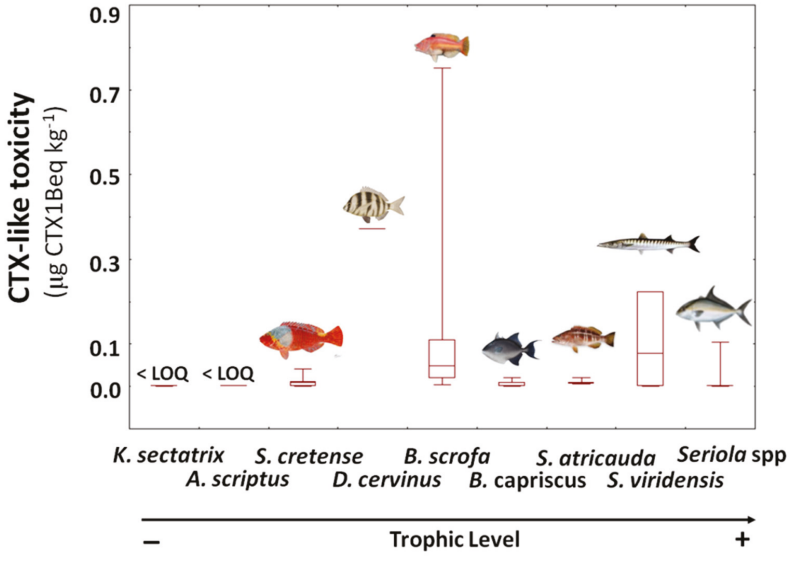

Figure 2. CTX-like toxicity (µg CTX1B equivalent kg^{-1}) determined by CBA in fish species collected from the marine food web of the Selvagens Islands during 5–7 September 2018 (median, 25 and 75 quartiles, minimum and maximum, total $n = 55$). See Materials and Methods section for details on samples.

With a higher position in the food web, grey triggerfish *Balistes capriscus* showed a reduced CTX-like activity in CBA, but toxicity in blacktail comber *Serranus atricauda* was consistently determined in each sample, ranging from 0.006 to 0.02 µg CTX1B equivalent kg^{-1}. Highly variable results were observed among the apex predators, the yellowmouth barracuda *Sphyraena viridensis*, and the amberjacks *Seriola* spp, ranging from not detected to considerably high levels (0.22 and 0.10 µg CTX1B equivalent kg^{-1} for *S. viridensis* and *Seriola rivoliana*, respectively).

2.2. Toxins Identification and Quantification by LC-MS/MS

With the aim of confirming previous results and characterizing the profile of CTX in fish from the Selvagens Islands, selected samples were analyzed by LC-MS/MS taking into consideration the CTX-like activity measured with the CBA and species trophic level. The presence of Caribbean-CTX1 was identified in the analyzed samples with the highest concentration. The highest level, reaching 0.48 µg kg^{-1}, was determined in a 3.0 kg barred hogfish *B. scrofa* specimen (Table 1). Quantification was performed, following the first detection method described in Section 4.3.3, which was based on the selection of the CTXs $[M+Na]^+$ as precursor and product ion. On the one hand, C-CTX1 was consistently detected in all specimens of this species. On the other hand, C-CTX1 or any other CTX analogue was not found in any sample of *Seriola* spp. by LC-MS/MS under the applied conditions. C-CTX1 was also not found in *D. cervinus* and only one of the two barracuda specimens analyzed showed the presence of this toxin and at low levels.

A C-CTX1 methylated congener and additional C-CTX congeners previously detected in a sample of *Seriola fasciata* from the same region and related to a CP case were also monitored by LC-MS/MS [28,29]. The presence of these C-CTX congeners was assessed by monitoring water losses and C-CTX1 specific fragments *m/z* 191.1 and *m/z* 108.9 (Figure 3A). C-CTX1 and a compound at a retention time 4.94 min showing C-CTX1 water losses but not C-CTX1 specific fragments were detected in some *B. scrofa* samples (Figure 3B). Furthermore, a compound matching C-CTX-1157 was detected at a retention time of 7.64 min in the *D. cervinus* in which C-CTX1 was absent (Figure 3C). This compound was

detected in one of the fractions obtained after HPLC fractionation, which showed CTX-like activity as indicated in a previous study [29]. Further work is needed to characterize all these congeners, being necessary to obtain the adequate reference materials to be able to accomplish their full characterization.

Table 1. Concentration of Caribbean Ciguatoxin-1 (C-CTX1) determined by LC-MS/MS in selected fish species caught in the Selvagens Islands (NE Atlantic, Portugal) in September 2018.

Species	*n*	C-CTX1 (μg kg^{-1})
Bodianus scrofa	10	0.08–0.48
Balistes capriscus	2	<LOQ–0.09
Diplodus cervinus	1	<LOQ
Seriola spp.	5	<LOQ
Sphyraena viridensis	2	<LOQ–0.14

LOQ, limit of quantification (0.015 μg kg^{-1}).

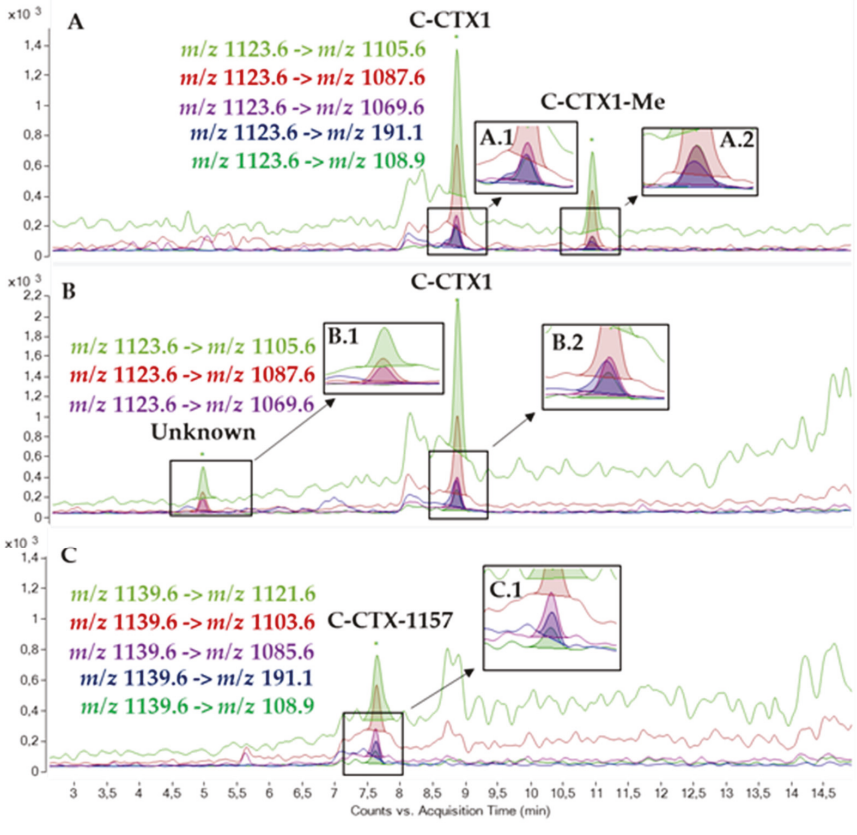

Figure 3. LC-MS/MS chromatogram in MRM mode of: (**A**) Laboratory reference material containing C-CTX1 (8.79 min) and C-CTX1-Me (10.84 min), (A.1) Zoom of C-CTX1 less intense ion transitions: *m/z* 1123.6 $[M+H-H_2O]^+$ -> *m/z* 1069.6 $[M+H-3H_2O]^+$ (purple line), *m/z* 1123.6 $[M+H-H_2O]^+$ -> *m/z* 191.1 (blue line), *m/z* 1123.6 $[M+H-H_2O]^+$ -> *m/z* 108.9 (green line), (A.2) Zoom of C-CTX1-Me less intense ion transitions: *m/z* 1123.6 $[M+H-CH_3-H_2O]^+$ -> *m/z* 1069.6 $[M+H-CH_3-3H_2O]^+$ (purple line), *m/z* 1123.6 $[M+H-CH_3-H_2O]^+$ -> *m/z* 191.1 (blue line), *m/z* 1123.6 $[M+H-CH_3-H_2O]^+$ -> *m/z* 108.9 (green line); (**B**) C-CTX1 (8.79 min) and an unknown compound (4.94 min) detected in a *Bodianus scrofa*; (**C**) C-CTX-1157 (7.64 min) detected in the *Diplodus cervinus*.

3. Discussion

The Selvagens Islands are a unique ecosystem, listed among the least disturbed islands in the Atlantic Ocean. Despite their small size that implies a small coastal area and their distance to the continental mainland, these islands show high species richness in terms of ichthyofauna, as described by [23]. CTX-like toxicity, as measured by CBA in fish species representative of the several trophic levels, highlighted the presence of toxins in fish at intermediate levels as well as in the top predators. Toxicity was not detected in the two species with the lowest position in the food web, but herbivorous fish, such as the parrotfish *Sparisoma cretense*, and omnivorous species, such as *Diplodus cervinus* and *Bodianus scrofa*, showed notable high toxicity levels. These species commonly show positive relationships in fish assemblage structures and environmental variables, such as seaweed cover and productivity [30]. Further investigation on the presence and abundance of ciguatera-causing dinoflagellates will be presented elsewhere, pointing out the Selvagens Islands as an archipelago with high abundances and biodiversity of marine life playing an important role on the growth and proliferation of *Gambierdiscus* in NE Atlantic (Godinho et al. in prep). The toxicity levels reported in the present study are similar or higher than that observed for groupers and moray eels in the nearby islands of the Canary archipelago [31], raising risks for their consumption.

Although the Selvagens Islands are a marine protected area where fisheries are interdicted, fish inhabiting these islands can migrate and spread CTX to regions in close proximity to the islands. In addition, some fisherman disrespecting fisheries interdictions are occasionally attracted by the abundance and high size fish inhabiting the Selvagens Islands. This was the case of a 4 kg red porgy (*Pagrus pagrus*), a fish species with an intermediate position in the food web, captured by Christmas 2016 that caused CP and was recently reported to contain levels of C-CTX1 as high as 0.76 μg kg^{-1}, as determined by LC-MS/MS [26]. In the present study, higher levels of C-CTX1 were found in *Bodianus scrofa* ranging from 0.08 to 0.48 μg kg^{-1}. These levels are among the highest determined in Macaronesia and exceeds the U.S. Food and Drugs Administration (FDA) guidance level of 0.1 μg C-CTX1 kg^{-1}. Such high levels have been of key importance to fully characterize and confirm fragmentation pathways of C-CTX1 by high resolution mass spectrometry [32].

The present study suggests a higher prevalence and incidence of CTX in fish from the Selvagens Islands than that initially reported by [27]. In this study, two detection methods were used. CBA is a functional assay that provides a toxicological response and LC-MS/MS is a highly selective chemical method that can be used to identify the compounds in the fish matrices. Although a comparison of the advantages and specific issues of these methods is not within the scope of this study, it is important to pay attention to discrepancies regarding CTX toxicity found in the fish top predators, namely the yellow mouth barracuda and the amberjacks, and the results obtained by LC-MS/MS below the detection limit. These contrasting results indicate that CTX toxicity of top predators may derive from metabolic fish products of C-CTX1 that have not been elucidated yet. Furthermore, the absence of C-CTX1 and the detection of C-CTX-1157 in a toxic *D. cervinus* showed a possible new toxic profile in which C-CTX1 is not the major contributor to the toxicity. Again, it is important to remember that differences were obtained by these two methods Therefore, further investigations are needed to better understand CTX biotransformation processes, to assess the full suite of toxins in the fish top predators, which are key target species for fisheries in NE Atlantic, and to accurately assess the risk of ciguatera poisoning. This study provides a quite complete evaluation of CTXs in fish (n = 56). Nonetheless, for each species or trophic level, the number of fish may be modest and further work increasing number of fish may provide a better estimation of the incidence of CTXs in the different groups.

The Selvagens Islands that are characterized by high abundances and biodiversity of marine life seem to play a role in incubation and proliferation of *Gambierdiscus* (Godinho et al. in prep) and ciguateric fish. Since fisheries, whether commercial or recreational, are forbidden, fish can grow and reach a greater size and can live longer. With a higher lifespan, fish have time to increasingly accumulate and metabolize ciguatoxins. The occurrence

of ciguatera in Europe may now pose a new challenge to the management of the marine protected area of the Selvagens Islands.

4. Materials and Methods

4.1. Fish Sampling

Fifty-six fish specimens belonging to 12 species within different trophic levels were caught between 5 and 7 September 2018 in Selvagem Grande and Selvagem Pequena (Table 2). Estimates of trophic levels were obtained from Fishbase that calculates trophic level from stomach contents data [33]. Fish were caught by means of spearfishing, performed by technicians of the Fisheries Department of Madeira Government, and after the required legal permission of the Madeira Natural Park.

Table 2. Length and weight of fish specimens caught in the coastal food web of the Selvagens Islands habitat.

Trophic Level *	Species	Common Name	*n*	Length Range (mm)	Weight Range (g)
2.0	*Kyphosus sectatrix*	Bermuda sea chub	5	420–530	1178–2387
2.8	*Aluterus scriptus*	Scribbled leatherjacket filefish	1	640	2417
2.9	*Sparisoma cretense*	Parrotfish	14	280–350	409–849
3.0	*Diplodus cervinus*	Zebra seabream	1	520	2840
3.5	*Bodianus scrofa*	Barred hogfish	16	390–530	1122–3010
4.1	*Balistes capriscus*	Grey triggerfish	4	350–490	585–2640
4.3	*Serranus atricauda*	Blacktail comber	5	250–300	193–336
4.3	*Sphyraena viridensis*	Yellowmouth barracuda	3	850–1170	2246–5955
4.5	*Seriola dumerili*	Greater amberjack	1	850	5656
4.5	*Seriola fasciata*	Lesser amberjack	2	490–620	1602–2795
4.5	*Seriola rivoliana*	Longfin yellowtail	2	600–1060	12,308–2536
4.5	*Seriola* spp	Amberjack	1	460	1163

* Estimated trophic level (TL) as expressed in Fishbase (2021). TL = 2.0 is at the base of the consumers food web, with their diet composed mainly of detritus and plants, and TL = 5.0 is a top predator fish.

4.2. CTX-like Toxicity Measured by Neuroblastoma (Neuro-2a) Cell-Based Assay (CBA)

4.2.1. CTX Extraction for CBA

Fish samples for CBA screening assays were extracted at IPMA, according tothe protocol described elsewhere [34] and with some modifications. A 10 g portion of fish flesh was minced and boiled at 70 °C for 15 min. Once cooled, samples were homogenized with 20 mL of acetone in a Polytron® homogenizer (Fisher Scientific, Porto Salvo, Portugal) at approximately 18,000× *g* for 2 min. Samples were centrifuged for 15 min at 3000× *g* and the pellets extracted again with acetone. Then, the combined supernatants were filtered through a 0.2 µm pore PTFE filter (Whatman, Lisbon, Portugal) with a syringe and evaporated at 60 °C, under vacuum in a rotary evaporator (Fisher Scientific, Porto Salvo, Portugal). The resulting aqueous residue was transferred into a tube and partitioned twice with diethyl ether keeping the ratio 8:2 relative to the amount of residual water. The diethyl ether phases were pooled and evaporated. The dry residue was partitioned with 4 mL of n-hexane and 2 mL of aqueous methanol/H_2O (4:1, *v*/*v*). The upper phase (hexane) was removed, and the partition repeated twice by adding 4 mL of hexane to the methanolic fraction. The methanolic phase was collected, evaporated, and stored at −20 °C until analysis.

4.2.2. CBA Screening Assay

For cell maintenance, neuro-2a (N2a) cells (ATCC, CCL131) were cultured in 10% fetal bovine serum (FBS) RPMI medium with 1% sodium pyruvate solution (100 mM), 1% l-glutamine solution (200 mM), and 0.5% antibiotic solution (10 mg/mL streptomycin and 1000 U/mL penicillin) (Sigma-Aldrich, St. Louis, MO, USA). Cultures were maintained at 37 °C and 5% CO_2 in a humid atmosphere incubator (Binder, Tuttlingen, Germany). The day prior to the assay, cells were seeded in a 96-well microplate in 200 µL of 5% FBS-

RPMI medium at a density of 35,000 cells per well. Cells were incubated under the same conditions as described for cell maintenance. Every standard (CTX-1B) and sample extract were assayed in triplicate. Half the wells of each microplate were pretreated with ouabain and veratridine corresponding to a final concentration of 1 and 0.1 mM, respectively. Standard solutions and sample extracts were reconstituted in RPMI 5%. Then, samples were serially diluted, and 10 µL added to each well, with (O/V+) and without (O/V-) ouabain and veratridine pretreatment. According to matrix effects estimated without (O/V-), concentrations for the different fish extracts were adjusted to avoid matrix effects. On the next day, cell viability was measured, by means of the MTT test [3-(4,5-dimethylthiadol-2-yl)-2,5-diphenyltetrazolium] (500 µg/mL) [35] and absorbance measured at 570 nm using an automated multi-well scanning. Samples were considered to be positive when cell viability was inhibited in O/V+ wells and unaffected in O/V- wells.

4.3. Determination of CTX by Liquid Chromatography with Tandem Mass Spectrometry (LC-MS/MS) Analysis

Sample pretreatment and LC-MS/MS analyses were carried out following the conditions described by [34] and modification performed by [26], and are briefly described below.

4.3.1. Reference Materials

C-CTX1 pure standard (5 ng mL^{-1}) was kindly provided by Dr. Robert Dickey (University of Texas, Austin, TX, USA) via Dr. Ronald Manger (Fred Hutchinson Cancer Research Center, Seattle, WA, USA).

The laboratory reference material (C-CTX1 and C-CTX1-Me) extracts from contaminated fish tissue were obtained after HPLC fractionation.

CTX1B (4466 ng mL^{-1}) and a qualitative mixture of P-CTXs (CTX1B, 2,3-dihydroxy CTX3C, 51-hydroxyCTX3C, 52-epi-54-deoxyCTX1B/54-deoxyCTX1B, 49-epiCTX3C/CTX3C, and CTX4A/CTX4B) were kindly provided by Prof. Takeshi Yasumoto (Japan Food Research Laboratories, Tokio, Japan).

Calibration was performed by dilution of the stock solution of CTX1B (4466 ng mL^{-1}) in methanol. The calibration range selected was from 0.45 to 27.88 ng mL^{-1} (n = 5).

C-CTX1 in samples was quantified as CTX1B in the calibration curve and transformed to C-CTX1 eq. with a correction factor previously obtained with C-CTX1 pure standard in the calibration curve.

4.3.2. Sample Pretreatment

First, 15 g of homogenized raw fish muscle was extracted with acetone (2 × 45 mL) using an UltraTurrax®. Acetone extracts were combined and evaporated to an aqueous residue which was partitioned with diethyl ether (2 × 15 mL). Diethyl ether layers were combined and evaporated to dryness. The solid residue was dissolved in 90% methanol (4.5 mL) and defatted with hexane (9 mL). The resulting methanolic fraction was dried and resuspended in ethyl acetate (2 mL) for clean-up procedures. A Florisil cartridge (J. T. Baker, 500 mg, Center Valley, PA, USA) was conditioned with ethyl acetate (3 mL) and the sample loaded into the cartridge. The cartridge was washed with ethyl acetate (3 mL) and C-CTXs eluted with ethyl acetate/methanol (9:1, *v:v*) (5 mL) and ethyl acetate/methanol (3:1, *v:v*) (5 mL). The second fraction, containing most of the toxins was further dried under nitrogen at 50 °C, and then dissolved in 60% methanol (2 mL) for a second clean-up step. Sample was loaded into a C18 cartridge (SUPELCLEAN, Supelco, 500 mg, Bellefonte, PA, USA) previously conditioned with 60% methanol (3 mL). The cartridge was washed with 60% methanol (3 mL) and CTXs were eluted with 90% methanol (5 mL). The final eluate was dried under nitrogen at 50 °C and dissolved in 0.5 mL of MeOH LC-MS grade filtering (Syringe Driver filter Unit, Millex®-CV 0.22 µm, 13 mm, Millipore, Billerica, MA, USA) prior to LC-MS/MS analysis.

4.3.3. LC-MS/MS Analysis

An Agilent 1290 Infinity LC system coupled to an Agilent 6495 iFunnel Triple Quadrupole LC-MS (Agilent Technologies, Waldbronn, Germany) were used for the LC-MS/MS analyses. Two different methods of analysis were used in order to obtain the confident identification, quantification, and confirmation of the toxins responsible for the contamination:

The first method was used for the sensitive identification and quantification of the CTXs. The chromatographic separation was performed in a Poroshell 120 EC-C18 (3.0 × 50 mm, 2.7 µm, Agilent, Santa Clara, CA, USA) column set at 40 °C. The mobile phases were: (A) 0.1% formic acid and 5 mM ammonium formate in water (J. T. Baker, Center Valley, PA, USA) and (B) methanol (Merck KGaA, Darmstadt, Germany). The gradient of mobile phase started at 78% of B increasing to 88% of B in 10 min, and holding for 5 min to finally increase to the 100% of B at 15.01 min washing the column for 3 min before reducing to the initial conditions at 18 min equilibration for 4 min before the following injection. The injection volume was set at 1 µL and the flow rate 0.4 mL/min.

The MS instrument operated in ESI^+ in multiple reaction monitoring (MRM) mode monitoring as precursor and product ion at 40 eV the sodium adduct $[M+Na]^+$ of the different CTXs with reference material available: CTX1B (*m/z* 1133.6 $[M+Na]^+$ -> *m/z* 1133.6 $[M+Na]^+$), C-CTX1 (*m/z* 1163.7 $[M+Na]^+$ -> *m/z* 1163.7 $[M+Na]^+$), C-CTX1-Me (*m/z* 1177.6 $[M+Na]^+$ -> *m/z* 1177.6 $[M+Na]^+$), 2,3-dihydroxyCTX3C (*m/z* 1079.6 $[M+Na]^+$ -> *m/z* 1079.6 $[M+Na]^+$), 51-hydroxyCTX3C (*m/z* 1061.6 $[M+Na]^+$ -> *m/z* 1061.6 $[M+Na]^+$), 52-epi-54-deoxyCTX1B/54-deoxyCTX1B (*m/z* 1117.6 $[M+Na]^+$ -> *m/z* 1117.6 $[M+Na]^+$), 49-epiCTX3C/CTX3C (*m/z* 1045.6 $[M+Na]^+$ -> *m/z* 1045.6 $[M+Na]^+$), and CTX4A/CTX4B (*m/z* 1083.6 $[M+Na]^+$ -> *m/z* 1083.6 $[M+Na]^+$).

Source and interface settings were: Drying gas 15 L/min of N_2 at 290 °C; sheath gas 12 L/min of N_2 at 400 °C; nebulizer gas, N_2 at 50 psi; capillary voltage, 5000 V; nozzle voltage: 300 V; fragmentor potential 380 V.

The second method was used to confirm the presence of C-CTX1 and specific C-CTX congeners. The chromatographic separation was performed in a Poroshell 120 EC-C18 (2.1 × 100 mm, 2.7 µm, Agilent USA) column set at 40 °C. The mobile phases were: (A) 0.1% formic acid and 5 mM ammonium formate in water (J. T. Baker, Center Valley, PA, USA); (B) acetonitrile (Merck KGaA, Darmstadt, Germany). The gradient of mobile phase started at 35% of B for 1 min increasing to 80% of B in 15 min, increasing in 1 min to a 95% of B and holding for 5 min to finally return to the initial conditions at 24 min equilibrating for 4 min before the following injection. The injection volume was set at 5 µL and the flow rate 0.4 mL/min.

The MS instrument operated in ESI^+ in MRM mode monitoring C-CTX1 water losses ($[M+H-nH_2O]^+$) and specific fragments *m/z* 191.1 and *m/z* 108.9. The MS/MS ion transitions for the C-CTXs detected are summarized in Table 3. Source and interface settings were: Drying gas 16 L/min of N_2 at 250 °C; sheath gas 12 L/min of N_2 at 400 °C; nebulizer gas, N_2 at 15 psi; capillary voltage, 5000 V; nozzle voltage 1000 V; fragmentor potential 380 V.

Table 3. MS/MS conditions for the confirmation of specific C-CTXs.

Compound	Precursor Ion (Q1)	Product Ion (Q3)	CE (eV)
C-CTX-1157	$[M+H-H_2O]^+$ *m/z* 1139.6	$[M+H-2H_2O]^+$ *m/z* 1121.6	15
	$[M+H-H_2O]^+$ *m/z* 1139.6	$[M+H-3H_2O]^+$ *m/z* 1103.6	30
	$[M+H-H_2O]^+$ *m/z* 1139.6	$[M+H-4H_2O]^+$ *m/z* 1085.6	30
	$[M+H-H_2O]^+$ *m/z* 1139.6	*m/z* 191.1	41
	$[M+H-H_2O]^+$ *m/z* 1139.6	*m/z* 108.9	52
C-CTX1 and isomers	$[M+H-H_2O]^+$ *m/z* 1123.6	$[M+H-2H_2O]^+$ *m/z* 1105.6	25
	$[M+H-H_2O]^+$ *m/z* 1123.6	$[M+H-3H_2O]^+$ *m/z* 1087.6	29
	$[M+H-H_2O]^+$ *m/z* 1123.6	$[M+H-4H_2O]^+$ *m/z* 1069.6	37
	$[M+H-H_2O]^+$ *m/z* 1123.6	*m/z* 191.1	41
	$[M+H-H_2O]^+$ *m/z* 1123.6	*m/z* 108.9	52

Table 3. *Cont.*

Compound	Precursor Ion (Q1)	Product Ion (Q3)	CE (eV)
C-CTX1-Me	$[M+H-CH_3-H_2O]^+$ *m/z* 1123.6	$[M+H-CH_3-2H_2O]^+$ *m/z* 1105.6	25
	$[M+H-CH_3-H_2O]^+$ *m/z* 1123.6	$[M+H-CH_3-3H_2O]^+$ *m/z* 1087.6	29
	$[M+H-CH_3-H_2O]^+$ *m/z* 1123.6	$[M+H-CH_3-4H_2O]^+$ *m/z* 1069.6	37
	$[M+H-CH_3-H_2O]^+$ *m/z* 1123.6	*m/z* 191.1	41
	$[M+H-CH_3-H_2O]^+$ *m/z* 1123.6	*m/z* 108.9	52

Author Contributions: Conceptualization, P.R.C., J.D. and A.G.-M.; methodology, L.S., S.M.R., P.E., D.C., J.D. and J.M.L.-M.; sampling P.R.C., L.S., N.G., V.T. and C.S.; formal analysis, L.S., J.D. and P.E.; resources, P.R.C., J.D. and A.G.-M.; data curation L.S., J.D., P.E., D.C. and J.M.L.-M.; writing—original draft preparation, P.R.C., L.S., S.M.R. and P.E.; writing—review and editing, P.R.C., J.D. and A.G.-M.; funding acquisition, P.R.C., J.D. and A.G.-M. All authors have read and agreed to the published version of the manuscript.

Funding: This research was funded by the project EUROCIGUA, "Risk Characterization of Ciguatera Fish Poisoning in Europe" GP/EFSA/AFSCO/2015/03, co-funded by the European Food Safety Authority (EFSA), the project Cigua (PTDC/CTA-AMB/30557/2017) supported by the Portuguese Foundation for Science and Technology (FCT) and FEDER, and through FCT project (UID/Multi/04326/2020). Pablo Estevez (P.E.) acknowledges financial support from the Xunta de Galicia (Regional Government, Spain) under grant ED481A-2018/207. David Castro (D.C.) received financial support for PhD studies, obtained through EUROCIGUA project, Risk characterization of Ciguatera Fish Poisoning in Europe, framework partnership agreement GP/EFSA/AFSCO/2015/03, co-funded by the EFSA. The authors also acknowledge the CERCA Programme/Generalitat de Catalunya.

Institutional Review Board Statement: Not applicable.

Informed Consent Statement: Not applicable.

Acknowledgments: Thanks are due to all technicians of Regional Fisheries Management—Madeira Government, Divisão de Serviços de Investigação—Direção Regional de Pescas (DSI-DRP), to the Natural Park of Madeira, and to the Nature's Wardens of Selvagens Islands for their efforts and contribution obtaining samples in the Selvagens Islands. The authors are also in debt to Takeshi Yasumoto (Japan Food Research Laboratories) who kindly provided the standards of Pacific ciguatoxins and Robert W. Dickey (University of Texas at Austin Marine Science Institute, Port Aransas, TX, USA) via Ronald Manger (Fred Hutchinson Cancer Research Center, Seattle, WA, USA) who kindly provided the standard of C-CTX1.

Conflicts of Interest: The authors declare no conflict of interest.

References

1. Fraga, S.; Rodríguez, F. Genus Gambierdiscus in the Canary Islands (NE Atlantic Ocean) with description of *Gambierdiscus silvae* sp. nov., a new potentially toxic epiphytic benthic dinoflagellate. *Protist* **2014**, *165*, 839–853. [CrossRef]
2. Doherty, M.J. Captain Cook on poison Fish. *Neurology* **2005**, *65*, 1788–1791. [CrossRef]
3. Schlumberger, S.; Mattei, C.; Molgó, J.; Benoit, E. Dual action of a dinoflagellate-derived precursor of Pacific ciguatoxins (P-CTX-4B) on voltage-dependent K(+) and Na(+) channels of single myelinated axons. *Toxicon* **2010**, *56*, 768–775. [CrossRef]
4. Bagnis, R.; Kuberski, T.; Laugier, S. Clinical Observations on 3,009 Cases of Ciguatera (Fish Poisoning) in the South Pacific. *Am. J. Trop. Med. Hyg.* **1979**, *28*, 1067–1073. [CrossRef] [PubMed]
5. Pearn, J. Neurology of Ciguatera. *J. Neurol. Neurosurg. Psychiatry* **2001**, *70*, 4–8. [CrossRef]
6. Vetter, I.; Touska, F.; Hess, A.; Hinsbey, R.; Sattler, S.; Lampert, A.; Sergejeva, M.; Sharov, A.; Collins, L.S.; Eberhardt, M.; et al. Ciguatoxins Activate Specific Cold Pain Pathways to Elicit Burning Pain from Cooling. *EMBO J.* **2012**, *31*, 3795–3808. [CrossRef]
7. Hamilton, B.; Whittle, N.; Shaw, G.; Eaglesham, G.; Moore, M.R.; Lewis, R.J. Human Fatality Associated with Pacific Ciguatoxin Contaminated Fish. *Toxicon* **2010**, *56*, 668–673. [CrossRef] [PubMed]
8. Yasumoto, T.; Nakajima, I.; Bagnis, R.; Adachi, R. Finding of a Dinoflagellate as a Likely Culprit of Ciguatera. *Nippon Suisan Gakkaishi* **1977**, *43*, 1021–1026. [CrossRef]
9. Adachi, R.; Fukuyo, Y. The Thecal Structure of a Marine Toxic Dinoflagellate *Gambierdiscus toxicus* Gen. et Sp. Nov. Collected in a Ciguatera-Endemic Area. *Nippon Suisan Gakkaishi* **1979**, *45*, 67–71. [CrossRef]

10. Soliño, L.; Costa, P.R. Global Impact of Ciguatoxins and Ciguatera Fish Poisoning on Fish, Fisheries and Consumers. *Environ. Res.* **2020**, *182*, 109111. [CrossRef]
11. Tosteson, T.R. Caribbean Ciguatera: A Changing Paradigm. *Rev. Biol. Trop.* **2004**, *52*, 109–113. [CrossRef] [PubMed]
12. Kibler, S.R.; Tester, P.A.; Kunkel, K.E.; Moore, S.K.; Litaker, R.W. Effects of Ocean Warming on Growth and Distribution of Dinoflagellates Associated with Ciguatera Fish Poisoning in the Caribbean. *Ecol. Modell.* **2015**, *316*, 194–210. [CrossRef]
13. Aligizaki, K.; Nikolaidis, G. Morphological identification of two tropical dinoflagellates of the genera *Gambierdiscus* and *Sinophysis* in the Mediterranean Sea. *J. Biol. Res. Thessalon.* **2008**, *9*, 75–82.
14. Fraga, S.; Rodríguez, F.; Caillaud, A.; Diogène, J.; Raho, N.; Zapata, M. *Gambierdiscus excentricus* Sp. Nov. (Dinophyceae), a Benthic Toxic Dinoflagellate from the Canary Islands (NE Atlantic Ocean). *Harmful Algae* **2011**, *11*, 10–22. [CrossRef]
15. Reverté, L.; Toldrà, A.; Andree, K.B.; Fraga, S.; de Falco, G.; Campàs, M.; Diogène, J. Assessment of Cytotoxicity in Ten Strains of *Gambierdiscus australes* from Macaronesian Islands by Neuro-2a Cell-Based Assays. *J. Appl. Phycol.* **2018**, *30*, 2447–2461. [CrossRef]
16. Hoppenrath, M.; Kretzschmar, A.L.; Kaufmann, M.J.; Murray, S.A. Morphological and Molecular Phylogenetic Identification and Record Verification of *Gambierdiscus excentricus* (Dinophyceae) from Madeira Island (NE Atlantic Ocean). *Mar. Biodivers. Rec.* **2019**, *12*, 16. [CrossRef]
17. Tudó, À.; Toldrà, A.; Rey, M.; Todolí, I.; Andree, K.B.; Fernández-Tejedor, M.; Campàs, M.; Sureda, F.X.; Diogène, J. *Gambierdiscus* and *Fukuyoa* as Potential Indicators of Ciguatera Risk in the Balearic Islands. *Harmful Algae* **2020**, *99*, 101913. [CrossRef] [PubMed]
18. Perez-Arellano, J.L.; Luzardo, O.P.; Brito, A.P.; Cabrera, M.H.; Zumbado, M.; Carranza, C.; Angel-Moreno, A.; Dickey, R.W.; Boada, L.D. Ciguatera fish poisoning, Canary Islands. *Emerg. Infect. Dis.* **2005**, *11*, 1981–1982. [CrossRef]
19. Varela Martínez, C.; León Gómez, I.; Martínez Sánchez, E.V.; Carmona Alférez, R.; Nuñez Gallo, D.; Friedemann, M.; Oleastro, M.; Boziaris, I. Incidence and Epidemiological Characteristics of Ciguatera Cases in Europe. *EFSA Support. Publ.* **2021**, *18*, 6650E. [CrossRef]
20. Gouveia, N.N.; Vale, P.; Gouveia, N.; Delgado, J. Primeiro registo da ocorrência de episódios do tipo ciguatérico no arquipélago da Madeira. In *Algas Tóxicas e Biotoxinas nas Águas da Península Ibérica-2009*; Costa, P.R., Botelho, M.J., Rodrigues, S.M., Palma, A.S., Moita, M.T., Eds.; IPIMAR: Lisboa, Potugal, 2009; pp. 152–157.
21. Otero, P.; Pérez, S.; Alfonso, A.; Vale, C.; Rodríguez, P.; Gouveia, N.N.; Gouveia, N.; Delgado, J.; Vale, P.; Hirama, M.; et al. First toxin profile of ciguateric fish in Madeira Arquipelago (Europe). *Anal. Chem.* **2010**, *82*, 6032–6039. [CrossRef]
22. Boada, L.D.; Zumbado, M.; Luzardo, O.R.; Almeida-Gonzalez, M.; Plakas, S.M.; Granade, H.R.; Abraham, A.; Jester, E.L.E.; Dickey, R.W. Ciguatera fish poisoning on the West Africa Coast: An emerging risk in the Canary Islands (Spain). *Toxicon* **2010**, *56*, 1516–1519. [CrossRef] [PubMed]
23. Almada, F.; Abecasis, D.; Villegas-Ríos, D.; Henriques, S.; Pais, M.P.; Batista, M.; Costa, B.H.e.; Martins, J.; Tojeira, I.; Rodrigues, N.V.; et al. Ichthyofauna of the Selvagens Islands. Do Small Coastal Areas Show High Species Richness in the Northeastern Atlantic? *Mar. Biol. Res.* **2015**, *11*, 49–61. [CrossRef]
24. Friedlander, A.M.; Ballesteros, E.; Clemente, S.; Gonçalves, E.J.; Estep, A.; Rose, P.; Sala, E. Contrasts in the Marine Ecosystem of Two Macaronesian Islands: A Comparison between the Remote Selvagens Reserve and Madeira Island. *PLoS ONE* **2017**, *12*, e0187935. [CrossRef] [PubMed]
25. Friedlander, A.M.; Ballesteros, E.; Clemente, S.; Estep, A.; Gonçalves, E.J.; Rose, P.; Shepard, M.; Thompson, C.; Meeuwig, J.J.; Sala, E. *Marine Biodiversity and Ecosystem Health of Ilhas Selvagens, Portugal; Scientific Report to the Government of Portugal and the Regional Government of Madeira*; National Geographic Pristine Seas: Washington, DC, USA, 2016; pp. 1–64.
26. Estevez, P.; Castro, D.; Manuel Leao, J.; Yasumoto, T.; Dickey, R.; Gago-Martinez, A. Implementation of Liquid Chromatography Tandem Mass Spectrometry for the Analysis of Ciguatera Fish Poisoning in Contaminated Fish Samples from Atlantic Coasts. *Food Chem.* **2019**, *280*, 8–14. [CrossRef] [PubMed]
27. Costa, P.; Estevez, P.; Castro, D.; Soliño, L.; Gouveia, N.; Santos, C.; Rodrigues, S.; Leao, J.; Gago-Martínez, A. New Insights into the Occurrence and Toxin Profile of Ciguatoxins in Selvagens Islands (Madeira, Portugal). *Toxins* **2018**, *10*, 524. [CrossRef]
28. Estevez, P.; Leao, J.M.; Yasumoto, T.; Dickey, R.W.; Gago-Martinez, A. Caribbean Ciguatoxin-1 stability under strongly acidic conditions: Characterisation of a new C-CTX1 methoxy congener. *Food Addit. Contam. Part. A* **2020**, *37*, 519–529. [CrossRef]
29. Estevez, P.; Castro, D.; Pequeño-Valtierra, A.; Leao, J.M.; Vilariño, O.; Diogène, J.; Gago-Martínez, A. An Attempt to Characterize the Ciguatoxin Profile in Seriola fasciata Causing Ciguatera Fish Poisoning in Macaronesia. *Toxins* **2019**, *11*, 221. [CrossRef]
30. Sangil, C.; Martín-García, L.; Hernández, J.C.; Concepción, L.; Fernández, R.; Clemente, S. Impacts of Fishing and Environmental Factors Driving Changes on Littoral Fish Assemblages in a Subtropical Oceanic Island. *Estuar. Coast. Shelf Sci.* **2013**, *128*, 22–32. [CrossRef]
31. Sanchez-Henao, A.; García-Álvarez, N.; Silva Sergent, F.; Estevez, P.; Gago-Martínez, A.; Martín, F.; Ramos-Sosa, M.; Fernández, A.; Diogène, J.; Real, F. Presence of CTXs in Moray Eels and Dusky Groupers in the Marine Environment of the Canary Islands. *Aquat. Toxicol.* **2020**, *221*, 105427. [CrossRef]
32. Estevez, P.; Sibat, M.; Leão-Martins, J.M.; Reis Costa, P.; Gago-Martínez, A.; Hess, P. Liquid Chromatography Coupled to High-Resolution Mass Spectrometry for the Confirmation of Caribbean Ciguatoxin-1 as the Main Toxin Responsible for Ciguatera Poisoning Caused by Fish from European Atlantic Coasts. *Toxins* **2020**, *12*, 267. [CrossRef]
33. Fishbase 2019. World Wide Web Electronic Publication. Froese, R., Pauly, D., Eds.; Available online: www.fishbase.org (accessed on 21 May 2019).

34. Yogi, K.; Oshiro, N.; Inafuku, Y.; Hirama, M.; Yasumoto, T. Detailed LC-MS/MS Analysis of Ciguatoxins Revealing Distinct Regional and Species Characteristics in Fish and Causative Alga from the Pacific. *Anal. Chem.* **2011**, *83*, 8886–8891. [CrossRef] [PubMed]
35. Manger, R.; Leja, L.; Lee, S.; Hungerford, J.; Wekell, M. Tetrazolium-Based Cell Bioassay for Neurotoxins Active on Voltage-Sensitive Sodium Channels: Semiautomated Assay for Saxitoxins, Brevetoxins, and Ciguatoxins. *Anal. Biochem.* **1993**, *214*, 190–194. [CrossRef]

toxins

MDPI

Article

Ciguatoxin-Producing Dinoflagellate *Gambierdiscus* in the Beibu Gulf: First Report of Toxic *Gambierdiscus* in Chinese Waters

Yixiao Xu [1,2,3], Xilin He [1,2], Wai Hin Lee [4,5], Leo Lai Chan [4,5], Douding Lu [6,7], Pengbin Wang [6,7], Xiaoping Tao [1,2], Huiling Li [1,2] and Kefu Yu [3,*]

1 Key Laboratory of Environment Change and Resources Use in Beibu Gulf, Ministry of Education, Nanning Normal University, Nanning 530001, China; xuyixiao_77@163.com (Y.X.); hexilin18177140136@163.com (X.H.); taoxiaoping0613@163.com (X.T.); huiling18307713906@163.com (H.L.)
2 Guangxi Key Laboratory of Earth Surface Processes and Intelligent Simulation, Nanning Normal University, Nanning 530001, China
3 Guangxi Laboratory on the Study of Coral Reefs in the South China Sea, Guangxi University, Nanning 530004, China
4 The State Key Laboratory of Marine Pollution, Department of Biomedical Sciences, City University of Hong Kong, Hong Kong, China; waihlee-c@my.cityu.edu.hk (W.H.L.); leochan@cityu.edu.hk (L.L.C.)
5 Shenzhen Key Laboratory for the Sustainable Use of Marine Biodiversity, Research Centre for the Oceans and Human Health, City University of Hong Kong Shenzhen Research Institute, Shenzhen 518057, China
6 Key Laboratory of Marine Ecosystem Dynamics, Second Institute of Oceanography, Ministry of Natural Resources, Hangzhou 310012, China; doudinglu@sio.org.cn (D.L.); algae@sio.org.cn (P.W.)
7 The Fourth Institute of Oceanography, Ministry of Natural Resources, Beihai 536000, China
* Correspondence: kefuyu@gxu.edu.cn

Abstract: Ciguatera poisoning is mainly caused by the consumption of reef fish that have accumulated ciguatoxins (CTXs) produced by the benthic dinoflagellates *Gambierdiscus* and *Fukuyoa*. China has a long history of problems with ciguatera, but research on ciguatera causative organisms is very limited, especially in the Beibu Gulf, where coral reefs have been degraded significantly and CTXs in reef fish have exceeded food safety guidelines. Here, five strains of *Gambierdiscus* spp. were collected from Weizhou Island, a ciguatera hotspot in the Beibu Gulf, and identified by light and scanning electron microscopy and phylogenetic analyses based on large and small subunit rDNA sequences. Strains showed typical morphological characteristics of *Gambierdiscus caribaeus*, exhibiting a smooth thecal surface, rectangular-shaped 2′, almost symmetric 4″, and a large and broad posterior intercalary plate. They clustered in the phylogenetic tree with *G. caribaeus* from other locations. Therefore, these five strains belonged to *G. caribaeus*, a globally distributed *Gambierdiscus* species. Toxicity was determined through the mouse neuroblastoma assay and ranged from 0 to 5.40 fg CTX3C eq cell^{-1}. The low level of toxicity of *G. caribaeus* in Weizhou Island, with CTX-contaminated fish above the regulatory level in the previous study, suggests that the long-term presence of low toxicity *G. caribaeus* might lead to the bioaccumulation of CTXs in fish, which can reach dangerous CTX levels. Alternatively, other highly-toxic, non-sampled strains could be present in these waters. This is the first report on toxic *Gambierdiscus* from the Beibu Gulf and Chinese waters and will provide a basis for further research determining effective strategies for ciguatera management in the area.

Keywords: *Gambierdiscus*; morphology; phylogeny; ciguatoxin; benthic dinoflagellate; Beibu Gulf; Chinese waters

Key Contribution: The first description of the morphology, phylogeny, and toxicity of *G. caribaeus* from the Beibu Gulf, as well as the first report of toxic *Gambierdiscus* spp. in Chinese coastal waters.

Citation: Xu, Y.; He, X.; Lee, W.H.; Chan, L.L.; Lu, D.; Wang, P.; Tao, X.; Li, H.; Yu, K. Ciguatoxin-Producing Dinoflagellate *Gambierdiscus* in the Beibu Gulf: First Report of Toxic *Gambierdiscus* in Chinese Waters. *Toxins* **2021**, *13*, 643. https://doi.org/10.3390/toxins13090643

Received: 28 July 2021
Accepted: 7 September 2021
Published: 10 September 2021

1. Introduction

Ciguatoxins (CTXs) are a group of polyether compounds mainly present in coral reef fish and rarely in invertebrates, which can cause ciguatera poisoning due to human consumption of CTX-contaminated seafood. CTXs are very potent and comprise one of the most significant marine biotoxin families, with 10,000–50,000 people affected worldwide annually [1]. CTX intoxication causes neurological abnormalities and gastrointestinal and cardiovascular dysfunction, with "paradoxical" sensory disturbance or "reversal" of temperature perception being the most characteristic symptoms [2]. In severe cases, intoxication symptoms can last for months or even years, and death is occasionally reported [3].

CTXs and its precursors are produced by epibenthic dinoflagellates of the genera *Gambierdiscus* and *Fukuyoa*. In the 1950s, Randall [4] proposed the famous food chain hypothesis, suggesting that CTXs originate from benthic microalgae in tropical seawater and are transferred to reef fish through the food chain. It was not until 1977 that the presence of *Diplopsalis* sp., the organism responsible for CTXs, was first confirmed in the Pacific Ocean on the Gambier Islands, French Polynesia, via a joint effort between Japan and France [5]. It was subsequently identified as a new genus and renamed *Gambierdiscus toxicus* [6]. Recently, globular *Gambierdiscus* was separated from anterior-posteriorly compressed *Gambierdiscus* based on morphology and defined independently as a new genus named *Fukuyoa* [7]. Unlike planktonic dinoflagellates that can produce blooms in surface waters, the genera *Gambierdiscus* and *Fukuyoa* mainly attach to macroalgae, dead corals, or rubble in benthic ecosystems exhibiting a patchy distribution and do not cause blooms visible to the naked eye.

Ciguatera, a human poisoning caused by the consumption of seafood [2], is predominantly endemic in tropical and subtropical Pacific, Atlantic, Caribbean, and Indian Ocean waters from 35° N to 37° S [8,9]. With increasing global warming and coastal disturbance caused by human activities, benthic dinoflagellates, including those of the genera *Gambierdiscus* and *Fukuyoa*, are experiencing geographic expansion or range shifts. As a result of expanding tourism and the global trade of reef fish, ciguatera incidents have increased significantly in recent years [10–12]. Owing to the difficulty in sampling benthic habitats, the study of CTXs and their toxin-producing organisms has been limited compared to that of planktonic microalgae [13,14]. This is particularly true in China, which has tropical and subtropical waters and has long been known to be a ciguatoxin-prone region [15–17] but with little history of CTX research.

As early as the 1970s, more than 20 species of carnivorous fish from the South China Sea islands, Guangdong coast, southern East China Sea, and Taiwan were reported to contain CTXs, although the toxicity was not determined [18]. In the 1980s and the 1990s, ciguatera incidents were first reported in Hong Kong and mainland China [19,20], but in 2007, CTX-contaminated fish were detected on the southern coast of China, including Weizhou Island and the Beibu Gulf [21]. Potential CTX-producing *Gambierdiscus* cells have been recorded in tropical and subtropical waters near the Xisha Islands, Hong Kong, Daya Bay, Hainan Island [22–26] and even in the temperate waters of Dayao Bay and Zhangzi Island in Dalian at 38°–39° N [27,28]. In addition, dormant cysts of the genus *Gambierdiscus* were found in Daya Bay and Dapeng Bay, Guangdong [29]. Recently, the potential CTX organisms *Fukuyoa ruetzleri* and *Fukuyoa* sp. HK Type 1 were recorded for the first time in the eastern waters of Hong Kong [30].

As reviewed by Chinain et al. [1], there are currently 18 species of *Gambierdiscus*, and the Pacific region has the highest species diversity and geographic distribution. Ciguatera poisoning has been widely reported in the central and southern Pacific, but is less frequently reported in the northern Pacific/Asia. In east and southeast Asia, the incidence of ciguatera is higher in coastal cities in southern China (Hong Kong, Foshan, Zhongshan) than in Japan (Okinawa Prefecture), whereas in other countries in the region, only isolated cases or small case series have been reported [17,31]. Unfortunately, fish exports from China have triggered ciguatera poisoning events in other countries; for example, between 2017–2019, Chinese exports of *Lutjanidae* led to at least two ciguatera outbreaks in Malaysia [1]. This

is closely related to the fact that China, geographically a CTX-prone country, straddles tropical and subtropical sea areas, and has a diet that favors large banquets and large carnivorous fish [16]. However, it has been previously assumed that ciguatera events in China are caused by imported fish from Pacific island countries [32,33], and thus, research on Chinese ciguatoxic fish and potentially toxic dinoflagellates of the genera *Gambierdiscus* and *Fukuyoa* is limited. For decades, CTX-producing microalgae in Chinese waters have been named monotypic *Gambierdiscus toxicus* based on light microscopy [22–25,27,28], and precise species identification and toxicity determinations have not been conducted.

Until 2016, three precise *Gambierdiscus* species, *G. australes*, *G. caribaeus*, and *G. pacificus*, were first reported in China (Hainan Island) using light and scanning electron microscopy and phylogenetic trees based on D1–D3 and D8–D10 regions of the large subunit (LSU) rDNA [26]. This was the first accurate identification of *Gambierdiscus* in Chinese waters, but no toxicity measurements were conducted on these species. In 2018, Leung et al. [30] also identified *F. ruetzleri* and *Fukuyoa* sp. HK Type 1 for the first time in Chinese waters (Hong Kong) using similar morphological and molecular taxonomic methods and determined that *F. ruetzleri* and *Fukuyoa* sp. HK Type 1 were toxic and lethal to brine shrimp larvae using a bioassay methodology. Consequently, toxin characteristics of species-level well-defined *Gambierdiscus* in Chinese waters remain unknown to date. Given the presence of CTX-contaminated fish along the Chinese coast, there is an urgent need to conduct studies on species identification and toxicity, as well as on the physiological and ecological characteristics of the genera *Gambierdiscus* and *Fukuyoa*, in the region.

Weizhou Island (20°54′–21°10′ N, 109°00′–109°15′ E), located in the northwestern part of the South China Sea, is the largest island of the coast of the Guangxi province and in the Beibu Gulf, China. It is also the largest and youngest island formed by submarine volcanic eruptions in China and belongs to one of the most northerly distributed tropical coral reef ecosystems in the world [34,35]. In the past 20 years, coral reefs of Weizhou Island have continuously been degraded by human activities and extreme climates, such as the El Niño phenomenon in 1998 and extremely low temperatures in January–February, 2008 [36,37]. Corals that once covered the substrate are replaced by rubble, turf algae, an epilithic algae matrix, and macroalgae [36], all of which provide a suitable environment for the growth of epibenthic dinoflagellates, including CTX-producing *Gambierdiscus* and *Fukuyoa* and the transfer of CTXs along the food chain [38]. In 2007, researchers found CTX detection rates of 37.5% using the Cigua-Check® kit and mouse bioassay in eight coral reef fish samples from Weizhou Island, and one *Epinephelus tauvina* sample among them exhibited the highest level of 135 ng P-CTX-1/kg meat, exceeding the safe threshold (100 ng P-CTX-1/kg meat) for consumption [21]. However, at that time, the origin and source of the CTXs in Weizhou Island were not studied.

In this study, five strains of *Gambierdiscus* spp. were isolated from dead coral and rubble on Weizhou Island in 2015–2017 in an effort to uncover the toxicity of ciguatoxin-producing microalgae in southern Chinese waters, to check whether *Gambierdiscus* produces CTXs and their potency, and to analyze their species composition and toxicity, highlighting a possible relationship with CTX-infected fish from Weizhou Island.

2. Results

2.1. Morphological Analysis

Gambierdiscus spp. belong to Dinophyta, Dinophyceae, Desmokontae, Gonyaulacales, Ostreopsidaceae, and *Gambierdiscus*. When observed under a light microscope, living cells were dark yellow and yellowish-brown, round or elliptical in the apical/antapical view, and lenticular in the lateral view. They had transverse and longitudinal grooves, and two flagella were found to arise from the cingulum and sulcus, respectively. The cells consisted of epithecae and hypothecae; however, they were mostly observed in the apical or antapical view under a light microscope. The average depth of living cells was 103.9 μm (76.1–132.6 μm) and the average width was 99.6 μm (70.8–123.8 μm).

The toxic strain GCBG01 from Station S3 and the non-toxic GCBG02 from Station S4 were chosen as representative strains and observed by scanning electron microscopy. They were found to be nearly circular in both apical and antapical views, with a plate tabulation formula of Po, 3′, 7″, 5‴, 1p, and 2⁗ (cingular and sulcus plates were not measured; Figures 1 and 2). The cell depth visualized through scanning electron microscopy averaged 77.0 μm (70.1–81.2 μm), and the cell width averaged 84.2 μm (73.4–93.6 μm). The cell surface was smooth and ornamented with many small, reticulated pores, and plates were separated by ridges. In the epithecae, an oval-shaped apical pore plate (Po) with a fishhook-like opening was observed near the center of the cell (Figures 1–3), and three apical plates (′) were attached around Po, specifically 1′, 2′, and 3′, of which 1′ had a smaller area and was nearly pentagonally distributed on the side from the Po plate to the ventral edge, whereas 2′ had the largest area among the three apical plates and was rectangular. The precingular plates 2″, 3″, 4″, 5″, and 6″ could be clearly seen, with 3″ and 4″ being larger and occupying most of the left and dorsal sides of the cell, respectively, and 4″ being nearly symmetric (Figures 1 and 2). No dorsal rostrum was found in either strain GCBG01 or GCBG02 (Figures 1 and 2).

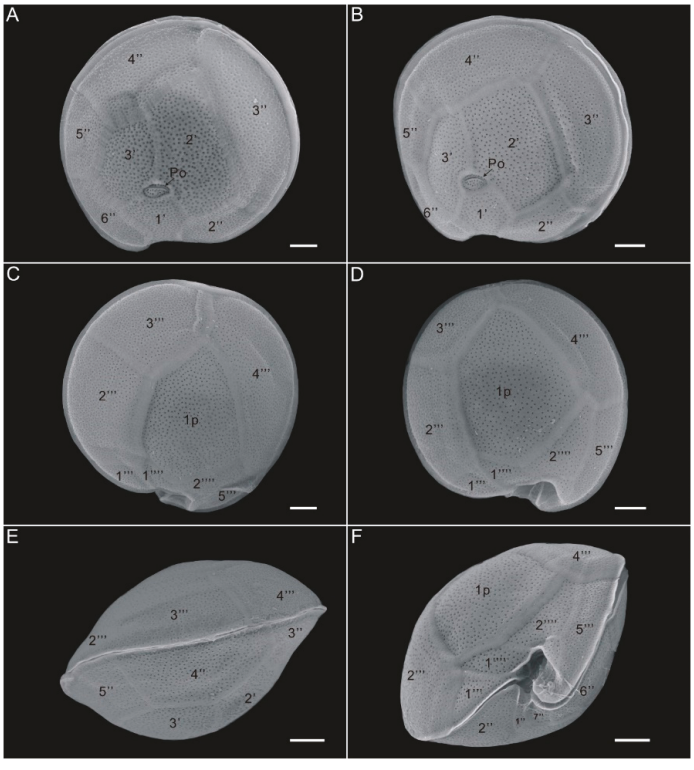

Figure 1. Scanning electron microscope images of *Gambierdiscus caribaeus* GCBG01 strain from Weizhou Island, Beibu Gulf of China. (**A**,**B**): apical view, (**C**,**D**): antapical view, (**E**): dorsal view, (**F**): ventral view. Scale bars: 10 μm.

Figure 2. Scanning electron microscope images of *Gambierdiscus caribaeus* GCBG02 strain from Weizhou Island, Beibu Gulf of China. (**A**,**B**): apical view, (**C**,**D**): antapical view, (**E**): apical–lateral view, (**F**): ventral view. Scale bars: 10 μm.

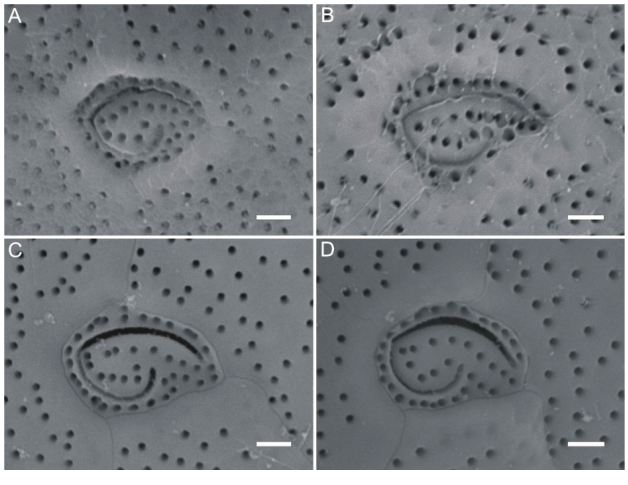

Figure 3. Scanning electron microscope images of fish-hook apical pore plates (Po) for *Gambierdiscus caribaeus* strains GCBG01 and GCBG02 from Weizhou Island, Beibu Gulf of China. (**A**,**B**): GCBG01, (**C**,**D**): GCBG02. Scale bars: 2 μm.

In the hypothecae, the postcingular plates 1‴, 2‴, 3‴, 4‴, and 5‴ could be clearly seen from the antapical view, with 4‴ and 2‴ being the largest (Figures 1 and 2). The cell had a broad pentagonal posterior intercalary plate (1p) and two antapical plates 1⁗ and 2⁗. The 1p was connected to 2‴, 3‴, 4‴, 1⁗, and 2⁗ (Figures 1 and 2). Among them, 1⁗ and 2⁗ were irregularly polygonal in shape and relatively small in area and were positioned close to the ventral side of the cell (Figures 1 and 2). From the lateral view, the cingulum of the cell was narrow and slightly protruded in a beak-like shape, and at the ventral convergence, the cingulum met the sulcus to form a swirling deep groove (Figure 1E,F and Figure 2E,F). Thus, the morphological characteristics of strains GCBG01 and GCBG02 were consistent with those of *G. caribaeus*, which have been previously described [39–44].

2.2. Sequence Analysis

The average lengths of the D1–D3 LSU rDNA, D8–D10 LSU rDNA, and small subunit (SSU) rDNA sequences obtained from the five strains of *Gambierdiscus* from the Beibu Gulf were 1390, 908, and 1743 bp, respectively. Their sequence composition characteristics were similar to those of 50, 65, and 50 *Gambierdiscus* sequences that were used to construct a phylogenetic tree (Table 1). Among the three sequence types, the D8–D10 LSU rDNA sequence had the highest and lowest proportions of conserved (58.2%) and variable (40.4%) sites, respectively, which was similar to the composition of SSU rDNA sequences of conserved (57.4%) and variable (41.1%) sites but greater than that of the D1–D3 LSU rDNA sequences of conserved (30.4%) and variable (68.0%) sites.

Table 1. Sequence composition used in *Gambierdiscus* phylogenetic tree.

Gene	Analysis Length	Average Content (%)				Conserved Site	Variable Site	Parsimonious Information Site	Monomorphic Site	Conversion/ Transversion Ratio
		A	T	G	C					
D1–D3 LSU rDNA	1035	25.3	25.1	30.8	18.8	323	696	661	35	0.9
D8–D10 LSU rDNA	914	26.1	25.8	27.8	20.3	532	369	281	87	1.5
SSU rDNA	1774	24.9	27.1	28.1	19.9	1016	728	578	149	1.6

2.3. Phylogenetic Tree Analysis

Phylogenetic trees of the D1–D3 LSU rDNA, D8–D10 LSU rDNA, and SSU rDNA were inferred using *Pyrodinium bahamense* and *Alexandrium minutum*, *Prorocentrum micans* and *A. minutum*, *P. micans* and *A. minutum*, respectively, as outgroups (Figures 4–6). Sequences from 1–3 strains per species/ribotype were used for phylogenetic tree construction based on sequence availability. Except for *Gambierdiscus belizeanus* and *Gambierdiscus honu* on the D1–D3 LSU rDNA phylogenetic tree, *Gambierdiscus cheloniae* and *Gambierdiscus lapillus*, and *Fukuyoa paulensis* and *Fukuyoa* sp. HK Type 1 on the D8–D10 LSU rDNA phylogenetic tree, the topological structures of the trees using the maximum likelihood (ML) and Bayesian inference (BI) were largely consistent. Therefore, only ML trees are shown here.

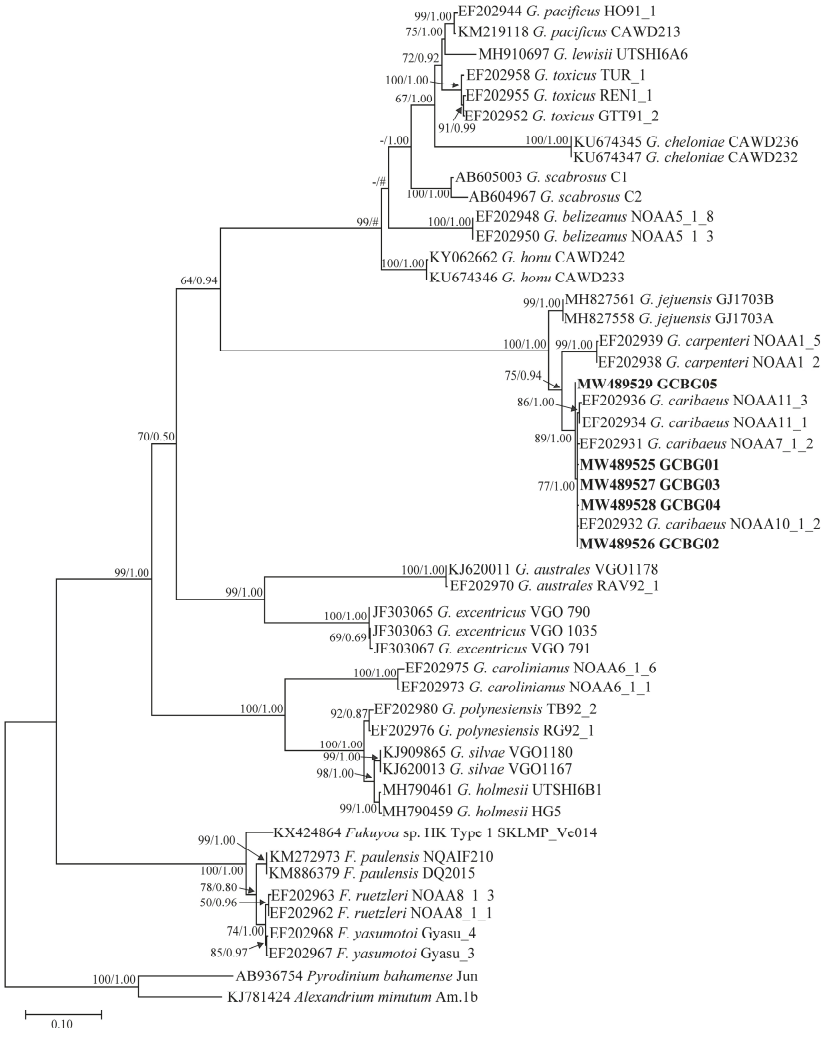

Figure 4. Phylogenetic tree constructed based on *Gambierdiscus* D1–D3 large subunit ribosomal DNA (D1–D3 LSU rDNA) sequences. Values at nodes indicate bootstrap values from the maximum likelihood method and posterior probabilities from the Bayesian inference method. Bootstrap values <50 and posterior probabilities <0.50 are not shown. # Indicates the topology; here, the maximum-likelihood tree differs from the Bayesian tree.

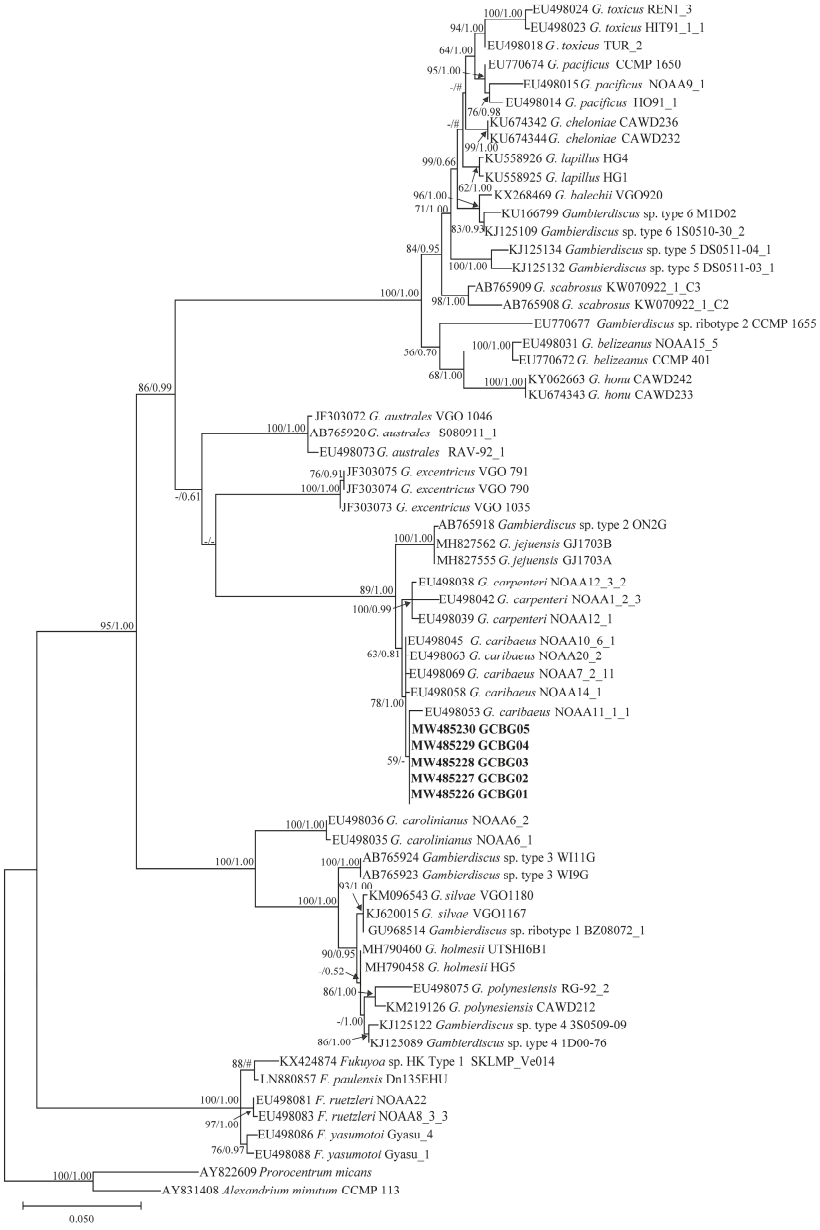

Figure 5. Phylogenetic tree constructed based on *Gambierdiscus* D8–D10 large subunit ribosomal DNA (D8–D10 LSU rDNA) sequences. Values at nodes indicate bootstrap values from the maximum likelihood method and posterior probabilities from the Bayesian inference method. Bootstrap values <50 and posterior probabilities <0.50 are not shown. # Indicates the topology; here, the maximum-likelihood tree differs from the Bayesian tree.

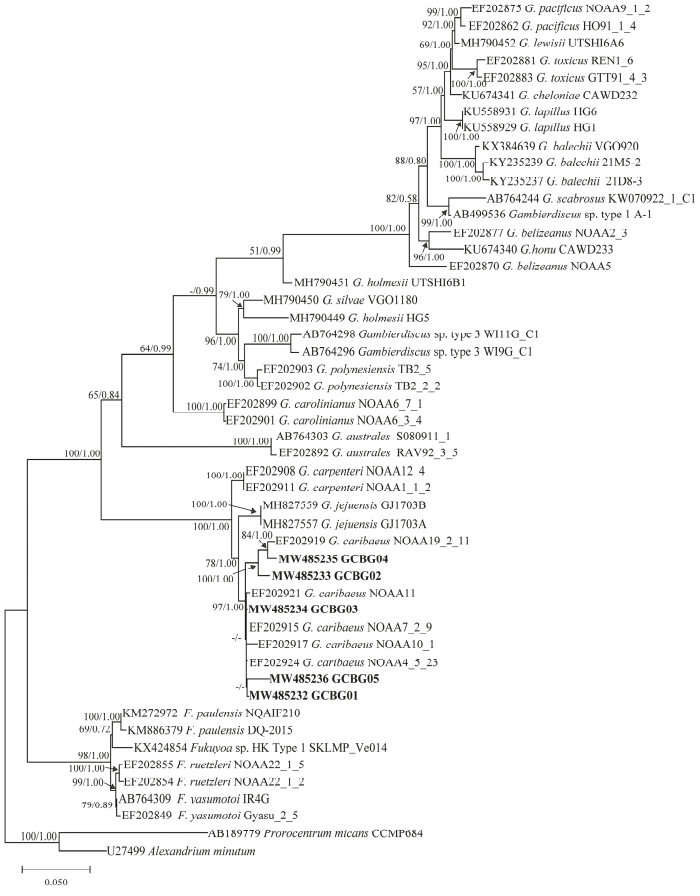

Figure 6. Phylogenetic tree constructed based on *Gambierdiscus* small subunit ribosomal DNA (SSU rDNA). Values at nodes indicate bootstrap values from the maximum likelihood method and posterior probabilities from the Bayesian inference method. Bootstrap values <50 and posterior probabilities <0.50 are not shown.

Various species and genotypes in the genera *Fukuyoa* and *Gambierdiscus* were all independently branched and had good bootstrap and Bayesian posterior probability values, varying in 50–100/0.87–1.00, 62–100/0.93–1.00, and 79–100/0.89–1.00 for D1–D3 LSU rDNA, D8–D10 LSU rDNA, and SSU rDNA, respectively (Figures 4–6). The five *Gambierdiscus* strains from Weizhou Island clustered with *G. caribaeus* from different marine areas in the world, exhibiting good support values of 89/0.94, 78/1.00, 94/0.98, respectively (Figures 4–6). Combined with morphological characteristics described previously herein, these five sample strains were thus identified as *G. caribaeus*, a worldwide distributed species of Gambierdiscus. In agreement with the results of other studies [40,41], the result from our study highlighted that *G. caribaeus* constituted a clear large clade with *Gambierdiscus jejuensis* and *Gambierdiscus carpenteri* in support of 100/1.00, 89/1.00, 100/1.00 values. On D1–D3 and D8–D10 LSU rDNA trees, *G. jejuensis* was a basal species, whereas *G. caribaeus* and *G. carpenteri* formed a sister branch (Figures 4 and 5). In SSU rDNA tree, *G. carpenteri* was a basal species and *G. caribaeus* and *G. jejuensis* formed a sister branch (Figure 6).

Genetic *distances* of D1–D3 LSU rDNA, D8–D10 LSU rDNA, and SSU rDNA sequences were calculated using the *p* distance (uncorrected genetic distance). A detailed comparison of genetic distances is shown in Table S1. In brief, the intraspecific genetic distances of D1–D3 LSU rDNA, D8–D10 LSU rDNA, and SSU rDNA sequences for *G. caribaeus* (including Weizhou Island strains) were 0.010 ± 0.005 (0.002–0.022), 0.008 ± 0.004 (0.000–0.013), and 0.014 ± 0.009 (0.001–0.035), respectively, and they were significantly smaller than the interspecific distances between *G. caribaeus* and other *Gambierdiscus* species, that is, 0.334 ± 0.109 (0.052–0.418), 0.155 ± 0.058 (0.016–0.234), and 0.143 ± 0.045 (0.017–0.187), respectively. The genetic distance data confirmed that the five *Gambierdiscus* strains from Weizhou Island, Beibu Gulf belonged to *G. caribaeus*.

2.4. Toxin Analysis

Among the five strains of *G. caribaeus* tested, only GCBG01 isolated from the northeast side of Weizhou Island (S3) produced CTX-like toxicity with a low value of 0.54 fg CTX3C eq cell^{-1}, whereas no toxicity was detected in the remaining four strains (Table 2).

Table 2. Ciguatoxin (CTX)-like toxicity of *Gambierdiscus caribaeus* isolates from Weizhou Island, Beibu Gulf of China (fg CTX3C eq cell^{-1}).

Strains	Species	Toxicity
GCBG01	*G. caribaeus*	5.4
GCBG02	*G. caribaeus*	ND
GCBG03	*G. caribaeus*	ND
GCBG04	*G. caribaeus*	ND
GCBG05	*G. caribaeus*	ND

ND: Toxicity not detected.

3. Discussion

To date, eighteen species and five ribotypes have been described within the genus *Gambierdiscus*. It is not surprising to find *G. caribaeus* in Weizhou Island, as this species is one of the most widely distributed *Gambierdiscus* species [45], recorded in many waters, including the Caribbean, North Atlantic, and Pacific (Figure S1). Moreover, it has also been found in the waters of Hainan Island, China, which is adjacent to the Weizhou Island [26].

All available *G. caribaeus* D1–D3 LSU rDNA and D8–D10 LSU rDNA sequences in the National Center for Biotechnology Information (NCBI) database were downloaded, and the genetic distance matrix was calculated through MEGA-X v10.1.8 and analyzed with principal coordinate analysis (PCoA) in RStudio (Figure S2). In the D1–D3 LSU rDNA PCoA plot, although *G. caribaeus* strains GCBG02-05, HF2, and 64B3 seemed to be separated, the explanatory degree of the X-axis and Y-axis together was only 34.16% of the total variation, whereas in the D8–D10 LSU rDNA PCoA plot, the explanatory degree of the X-axis and Y-axis together was 10.03% of the total variation (Figure S2). Therefore, sequence differences between different geographical sources of *G. caribaeus* were very small, and there was no obvious clustering pattern based on geographical location. Referring to D8–D10 LSU rDNA for *G. caribaeus*, which had more sequences than D1–D3 rDNA and SSU rDNA sequences in NCBI, the genetic distance for D8–D10 LSU rDNA among the five strains of *G. caribaeus* in this study and strains NOAA11_1_1 from Carrie Bow Cay, Belize (Caribbean), NOAA20_5 from Grand Cayman Island (Caribbean), and TF9G and TF26G from Koh Wai, Thailand was closest, with a value of 0.016 ± 0.006 (0.001–0.024).

In this study, five strains of *G. caribaeus* were isolated from Weizhou Island, and only one strain (GCBG01) had detectable toxicity at 0.54 fg P-CTX-1 eq cell^{-1}. This represents the first report of toxic *Gambierdiscus* not only from Beibu Gulf, but also from Chinese waters. The toxicity magnitude of *G. caribaeus* strains from Weizhou falls within the *G. caribaeus* toxicity range (i.e., <the limit of detection to 903.70 fg CTX3C eq. cell^{-1}) has been reported in previous studies (Table 3). *G. caribaeus* has been thought to be a low and slow toxin-producing species [44,46,47]; to date, all documented toxicity for this

species from the Caribbean and Pacific regions is less than 5.40 fg P-CTX-1 eq cell^{-1} (Table 3). However, several other strains recently isolated from the Canary Islands exhibit surprisingly high toxicity; in particular, strain VGO1367 shows an extremely high CTX-like toxicity of 903.70 fg CTX3C eq. cell^{-1}, which is comparable to that in the most highly toxic species, including *Gambierdiscus excentricus* in the Atlantic and *Gambierdiscus polynesiensis* in the Pacific [1,46,48]. In this regard, it should be attributed to the association between the toxicity and the geographical origin of the strain. Rossignoli et al. [47] have suggested that some species in the genus *Gambierdiscus*, like *G. australes* and *G. silvae*, have a similar CTX-like toxicity for strains from different locations, but *G. caribaeus* and *G. excentricus* differ considerably due to the origin of the strain. The toxicity of *G. caribaeus* from Weizhou Island here seemed to reinforce the fact that the *G. caribaeus* in the Pacific Ocean has low toxicity. The mechanism underlying for the toxicity of some *Gambierdiscus* species is unrelated to the geographical origin, whereas other species is related. Therefore, this uncertainty remains a challenge that needs to be unraveled.

Table 3. Summary on *Gambierdiscus caribaeus* ciguatoxin (CTX)-like toxicity in different strains.

Strain	Locality	Toxicity	Methodology	References
NOAA 7 (CCMP 1652)	Mataiva, Tahiti, South Pacific	2,3-dihydroxy CTX3C *	LC-MS/MS	[49]
NOAA 20 (CCMP 1651)	Grand Cayman Island, Caribbean	2,3-dihydroxy CTX3C *	LC-MS/MS	[49]
CCMP 401	St. Barthelmy Island, Caribbean	2,3-dihydroxy CTX3C *	LC-MS/MS	[49]
CCMP 1733	Carry Bow Cay, Belize, Caribbean	2,3-dihydroxy CTX3C *	LC-MS/MS	[49]
TF9G	Koh Wai, Trat, Thailand	$\geq 100 \times 10^{-4}$ MU/1000 cells	MBA	[43,50]
Gam 19	Carrie Bowe Caye Belize, Caribbean	<LOD	CBA	[51]
Pat HI Jar 2 Gam 2	Big Island, Hawaii, USA, Pacific	<LOD	CBA	[51]
CCMP1733	Carrie Bow Cay, Belize, Caribbean	0.80 ± 0.43 fg CTX3C eq cell^{-1}	CBA	[46]
CCMP 1651	Grand Cayman Island, Caribbean	0.48 ± 0.04 fg CTX3C eq cell^{-1}	CBA	[46]
SW gam 5	Southwater Cay, Belize, Caribbean	1.52 ± 0.26 fg CTX3C eq cell^{-1}	CBA	[46]
CBC gam1	Carrie Bow Cay, Belize, Caribbean	0.62 ± 0.12 fg CTX3C eq cell^{-1}	CBA	[46]
Mexico Algae 1	Cancun, Mexico	1.29 ± 0.40 fg CTX3C eq cell^{-1}	CBA	[46]
Dive 1 FA	Carrie Bow Cay, Belize, Caribbean	0.69 ± 0.19 fg CTX3C eq cell^{-1}	CBA	[46]
Keys Jar 7	Florida Keys, USA	0.19 ± 0.03 fg CTX3C eq cell^{-1}	CBA	[46]
Bill Hi Gam8	Waikiki Beach, Honolulu, Hawaii	1.60 ± 1.00 fg CTX3C eq cell^{-1}	CBA	[52]
CUB4A5	Cienfuegos coast, south-central Cuba	<LOD	RBA	[53]
VGO1362	La Gomera Porto-Playa Santiago, Canary Islands	6.00 fg CTX3C eq cell^{-1}	CBA	[47]
VGO1364	La Gomera Porto-Playa Santiago, Canary Islands	25.9 ± 5.0 fg CTX3C eq cell^{-1}	CBA	[47]
VGO1365	La Gomera Porto-Playa Santiago, Canary Islands	<LOD	CBA	[47]

Table 3. *Cont.*

Strain	Locality	Toxicity	Methodology	References
VGO1366	La Gomera Porto-Playa Santiago, Canary Islands	5.00 fg CTX3C eq cell^{-1}	CBA	[47]
VGO1367	La Gomera, San Sebastián-Playa la Cueva, Canary Islands	903.7 ± 158.9 fg CTX3C eq cell^{-1}	CBA	[47]
IRTA-SMM-17-03	Tamaduste, El Hierro, Canary Islands	<LOD	CBA	[44]
IRTA-SMM-17_03	Tamaduste, El Hierro, Canary Islands	0.13–0.21 fg 51-hydroxy CTX3C eq cell^{-1}	Immunoassay	[54]
IRTA-SMM-17_03	Tamaduste, El Hierro, Canary Islands	1.3–2.4 fg CTX3C eq cell^{-1}	Immunoassay	[54]
GCBG01	Weizhou Island, Beibu Gulf, China	5.40 fg CTX3C eq cell^{-1}	CBA	This study
GCBG02	Weizhou Island, Beibu Gulf, China	<LOD	CBA	This study
GCBG03	Weizhou Island, Beibu Gulf, China	<LOD	CBA	This study
GCBG04	Weizhou Island, Beibu Gulf, China	<LOD	CBA	This study
GCBG05	Weizhou Island, Beibu Gulf, China	<LOD	CBA	This study

*, Qualitative results; LOD, limit of detection; MBA, mouse bioassay; RBA, receptor binding assay; CBA, cell-based assay; the toxicity of VGO1362 and VGO1366 was roughly determined from Figure 3 in [47].

Production of CTX or CTX-like compounds is more dependent on intrinsic genetic factors (species/strain) than on extrinsic environmental conditions (temperature, pH, light, salinity, nutrients, and growth stage) [9,45,55,56]. In the Caribbean and Gulf of Mexico, a 1740-fold interspecies variations in *Gambierdiscus* and *Fukuyoa* toxicity were observed [46]. Here, for *G. caribaeus*, the most toxic strainVGO1367 from Canary Islands was 4755-fold more toxic than the less toxic strain Keys Jar 7 from Florida Keys (Table 3). In comparison, combined effects of light, salinity and temperature on *Gambierdiscus* culture can lead to a maximum 200-fold difference in toxicity [57]. It has also been reported that *Gambierdiscus* spp. under extreme conditions such as low temperature/increased depth, low light, and stationary and decline phase produce more CTXs than under optimal growth conditions and in the exponential phase. Therefore, if the optimal batch cultivation conditions are changed, the CTX-like toxicity of *G. caribaeus* strains in this study might increase, and it could also be detected in GCBG02–GCBG05 strains currently below the detection limit. Unfortunately, this study focused on *Gambierdiscus* species identification and preliminary toxicity analysis in Weizhou Island and did not test their toxicity associated with different growth phases and growth conditions, which to some extent, limits the comprehensive understanding of the toxin-producing characteristics of *G. caribaeus* and ciguatoxic fish in the region.

The non-toxic and low-level toxicity of *G. caribaeus* in this study seems to contradict the 37.5% CTX detection rate and 12.5% CTX exceedance rate of Weizhou Island coral reef fish. In addition to the environmental factors mentioned previously herein that might lead to a higher CTXs production in natural water bodies compared to that in the current strains GCBG01–GCBG05, the following reasons are also possible:

(1) Collection dates for fish samples in the study of Xu et al. [21] and those of CTX-producing microalgae collection in this study were different. As a result, *Gambierdiscus* species and their corresponding toxicity might differ between the two time periods. Further, even at the same sampling time, asynchrony of *Gambierdiscus* spp. abundance and toxicity have been documented in both the Pacific and Caribbean regions [56,58].

(2) Additionally, other more toxic *Gambierdiscus*/*Fukuyoa* species are present on Weizhou Island but have not been recognized because of their low abundance. Scientists have recently identified *G. pacificus*, *G. australes*, and *G. caribaeus* in the Hainan Island [26] and *F. ruetzleri* in Hong Kong waters [30], not far from Weizhou Island. According to other studies, all of these species are generally more toxic than *G. caribaeus* [44,52,59]. If the sampling intensity and frequency are enhanced in Weizhou Island, other *Gambierdiscus*/*Fukuyoa* spp. with medium- or high-level toxicity, such as *G. polynesiensis*, which has proven to be the most toxic and major toxin producer in the Pacific Ocean with a wide geographic distribution, are likely to be found [1]. The average toxicity of *G. polynesiensis* from French Polynesia calculated by Longo et al. [48] is 3285 fg CTX3C eq cell^{-1}, a 75.8-fold increase compared to the average *G. caribaeus* toxicity, specifically 43.33 ± 192.25 fg CTX3C eq cell^{-1} (Table 3).

(3) It cannot be ruled out that it was indeed the low toxicity of *G. caribaeus* that resulted in ciguatoxic fish in Weizhou Island, because this species has a wider range of tolerance to environmental conditions of temperature, salinity, and light than most other species of the genus *Gambierdiscus*, consistent with their broad geographic distribution [9,50,60]. The long-term presence of *G. caribaeus* with low toxicity in the water column will result in bioaccumulation in fish and will lead to dangerous CTX levels. Litaker et al. [46] have analyzed 33 strains representing seven *Gambierdiscus* and one *Fukuyoa* species from the Caribbean and Gulf of Mexico and have found that all except *G. excentricus* can induce high CTX-like toxicity, at 469 fg CTX3C eq cell^{-1}, comparable with the highly toxic isolates from the Pacific [1,61]. All other six species were low toxin-producers, varying from 0.27–19.6 fg CTX3C eq cell^{-1} [46], but that does not change the fact that the Caribbean and Gulf of Mexico remain among the most CTX-prone areas in the world. Our speculation needs to be verified through the long-term tracking of the abundance and species composition of *Gambierdiscus*/*Fukuyoa* spp. in Weizhou Island in the future.

4. Conclusions

In this study, species identification and toxicity analyses of CTX-producing microalgae in Weizhou Island were conducted for the first time, and five strains of *G. caribaeus* were identified based on thecal morphology and a molecular characterization. The toxicity was determined to be 0–5.40 fg CTX3C eq cell^{-1}, which represents the first report of toxic *Gambierdiscus* in Chinese waters. Further studies are strongly recommended to better explain the correlation between the causative organism abundance, species composition, species/strain-specific toxicity, and the risk of CTX-contaminated fish in Weizhou Island waters and to develop better strategies for ciguatera management in China.

5. Materials and Methods

5.1. Study Area and Sample Collection

Eight sites were sampled on Weizhou Island in October–2014–2016 (Figure 7). Benthic macroalgae and hard dead coral reef rubble were collected by diving. Cells of benthic dinoflagellates including *Gambierdiscus* attached to the macroalgae and hard dead coral were released by vigorous shaking, and 20–200 μm particles were collected through filtration for further cell isolation and monoclonal strain establishment, adding the 20 μm-filtered seawater and 1 mL of reduced enriched K medium (removing Si and Tris) [62] to the samples to keep *Gambierdiscus* cells alive but prevent fast reproduction.

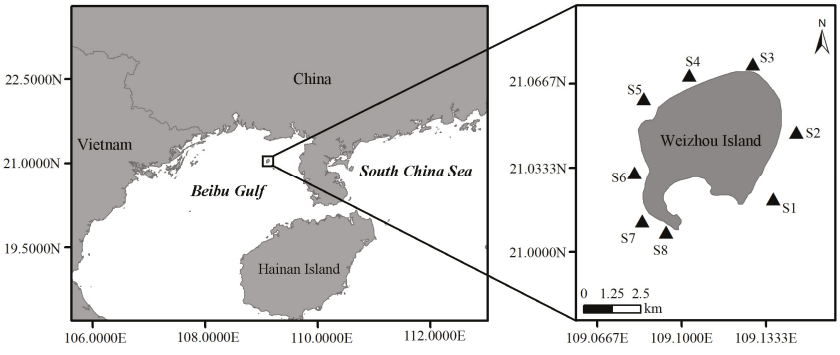

Figure 7. Sampling sites.

5.2. Culture Establishment

Field samples were transported to the laboratory and observed using an inverted microscope (TS100, Nikon, Tokyo, Japan). The cell size and shape of *Gambierdiscus* sp. were observed and photographed (NIS-Elements D 4.50.00), and these were then isolated with a capillary tube under an inverted microscope. The cells were aspirated and placed onto a glass plate with K medium, washed repeatedly 3–4 times, and then single cells were cultured in a 96-well plate in a light incubator (GHP-9270N, Ningbo Laifu Technology Co., Ningbo, China) at 23 °C, 150 μE·m^{-2} s^{-1}, with a 14 h:10 h light:dark cycle. After 4–6 weeks of culture, well-grown cells were selected and transferred to a 24-well plate for further growth, and 2–3 weeks later, cells were transferred to cell culture flasks (25 cm^2, Fisher Scientific Co., Waltham, MA, USA) and maintained as a monostrain culture of *Gambierdiscus* sp. (Table S2).

5.3. Scanning Electron Microscopy

Glutaraldehyde solution was added to the *Gambierdiscus* culture growing in exponential growth phase for 35 h for cell fixation, at a final solution concentration of 2.5%. Fixed samples (5 mL) were filtered and collected through a 3 μm polycarbonate membrane (Merck Millipore Ltd., Burlington, MA, USA) and then desalted in a salinity gradient. Using sterile seawater at a concentration of 100%, desalination was performed with a concentration gradient of 90%, 70%, 50%, 30%, 0%, and 0% (ultrapure water), with each iteration lasting for 30 min. The filter membrane was then dewatered in different concentrations of ethanol with a concentration gradient of 30%, 50%, 70%, 90%, 100%, and 100%, with each iteration conducted for 30 min, dried with a critical point drier (Joel Hi-Tech, Dalian Co., Dalian, China), and gold-coated in a sputter coater. Lastly, the *Gambierdiscus* cells were observed and photographed under a scanning electron microscope (TM-1000 Tabletop Microscope, Hitachi High-Technologies Corporation, Tokyo, Japan). The plate formula for the morphology description was the same as that described in previous publications [39,63,64].

5.4. DNA Extraction and PCR Amplification

DNA was extracted from *Gambierdiscus* cells growing in exponential phase using the BioFastSpin Plant Genomic DNA Extraction Kits (Bioer, Hangzhou, China) following the manufacturer's instructions. DNA extraction was confirmed through electrophoresis. Characteristic D1–D3 LSU rDNA, D8–D10 LSU rDNA, and SSU rDNA fragments were amplified through PCR using the primers listed in Table S3. The PCR reaction included 20 μL 2 × Es Taq Master Mix (CoWin Biosciences, Cambridge, MA, USA), forward and reverse primers (1 μL each), DNA template (1 μL), and ddH_2O (17 μL). The PCR program was run on a Biometra EasyCycler Gradient, and comprised pre-denaturation at 94 °C for 5 min, 35 cycles of 94 °C for 30 s, 56 °C for 30 s, and 72 °C for 30 s, and elongation at 72

°C for 5 min. The D1–D3 LSU rDNA and D8–D10 LSU rDNA PCR products were directly Sanger sequenced at the TsingKe Biological Technology Company (Beijing, China).

Direct SSU rDNA Sanger sequencing failed, and these samples were further cloned before sequencing. Therefore, SSU rDNA was extracted from PCR agarose gels, purified using the Universal DNA Purification Kit (Tiangen, DP214, Beijing, China), and then ligated with the pMD19-T vector overnight at 16 °C. Receptor cells (*Escherichia coli* DH5α) were removed from the −80 °C storage freezer and thawed on ice. DH5α was added to the ligation product, mixed well, incubated in an ice bath for 30 min, and heat shocked at 42 °C for 60–90 s, which was followed by rapid transfer to an ice bath for 2–3 min. Then, 500 µL of Luria-Bertani medium (without antibiotics) was added to the mixture, mixed well, and incubated at 37 °C for 45 min (150 rpm) in a shaker. The mixture (200 µL) was pipetted into a Luria-Bertani plate (containing ampicillin, Isopropyl β-d-1-thiogalactopyranoside, and X-Gal) and evenly spread. The plate was incubated a 37 °C overnight. Single colonies were picked for PCR confirmation, and the positive ones were chosen for Sanger sequencing. All sequences were deposited in GenBank (Table S2).

5.5. Phylogeny and Sequence Analysis

The D1–D3 LSU rDNA, D8–D10 LSU rDNA, and SSU rDNA sequences of the five *Gambierdiscus* isolates (GCBG01, GCBG02, GCBG03, GCBG04, and GCBG05) were searched in the NCBI website (http://www.ncbi.nih.gov) using BLAST, and sequences related to these strains with high similarity and coverage were downloaded. Totals of 44, 60, and 44 sequences were obtained, respectively. Sequences were subjected to multiple sequence alignment using ClustalW in MEGA-X v10.1.8, and redundant bases were sorted and truncated to 1035 bp, 914 bp, and 1788 bp for the D1–D3 LSU rDNA, D8–D10 LSU rDNA, and SSU rDNA, respectively. Base composition, conserved sites, variant sites, parsimony informative sites, monomorphic sites, and conversion/inversion ratios were also calculated using MEGA-X v10.1.8. The substitution model and rates among sites were determined by running the software Modeltest 3.7, showing the best selection as GTR + G, which was used in the construction of the ML and BI trees.

ML trees were constructed using software MEGA-X v10.1.8, with 1000 bootstrap replications, partial deletion of gaps/missing data treatment, and a site coverage 95% cutoff. BI trees were inferred using the Bayesian algorithm in MrBayes v3.1.2, and 1×10^6 runs of three hot chains and one cold chain were performed independently under four Markov chains, with sampling performed every 500 generations. The analysis was thought to reach stability, that is, a standard error <0.01, when the program ended. Phylogenetic trees were viewed with the software FigTree v1.4.0 and saved in PDF format. The GenBank accession number, species and strain names, bootstrap values, and posterior probability values were added to the major branch node using Adobe Acrobat Pro v11.0.5.

5.6. CTX-Like Toxicity Analysis

The 10^6–10^7 *Gambierdiscus* cells in the early stationary phase were collected by centrifugation at 2000× *g* at 4 °C and stored at −20 °C by adding methanol. CTX-like toxins were released from cells using a sonicator probe (Branson Digital Sonifier, Branson Ultrosonics Corporation, Brookfield, CT, USA) for 5 s on, 1 s off, and 80% amp. After sonication, a drop of each extract was placed on a microscope slide to verify cell disruption. The primary extract was centrifuged at 2000× *g* for 5 min at 4 °C, and the supernatant was collected. Residual cells were extracted for 2 min using a vortex mixer (Vortex-6, Qilinbeier, Jiangsu, China), and the supernatant was combined with the primary extracted supernatant. CTX-like toxins in the supernatant were then extracted using a 3:2:2 volume ratio of methanol:MilliQ water:dichloromethane and dried in a rotary evaporator; then, methanol was added, and the extract was stored at −20 °C for final toxicity measurements. Toxicity was determined using mouse neuroblastoma (Neuro-2a cells; ATCC, CCL131; ATCC, Manassas, VA, USA) according to the mouse neuroblastoma assay described by Xu et al. [64].

Supplementary Materials: The following is available online at https://www.mdpi.com/article/10.3390/toxins13090643/s1, Figure S1: global distribution map of *Gambierdiscus caribaeus*, Figure S2: principal coordinate analysis (PCoA) based on the *p* distance matrices of *Gambierdiscus caribaeus* D1–D3 LSU rDNA and D8–D10 LSU rDNA sequences downloaded from the NCBI database, Table S1: the *p* distance (uncorrected genetic distance) comparison of D1–D3 LSU rDNA, D8–D10 LSU rDNA, and SSU rDNA sequences, Table S2: sample information, Table S3: primers and PCR product information.

Author Contributions: Conceptualization, Y.X. and K.Y.; methodology, Y.X., X.H., W.H.L., L.L.C., D.L. and P.W.; software, X.H. and Y.X.; validation, Y.X. and K.Y.; formal analysis, Y.X., X.H., W.H.L., L.L.C., X.T. and H.L.; investigation, Y.X.; resources, Y.X., X.T. and H.L.; data curation, Y.X. and X.H.; writing—original draft preparation, Y.X. and X.H.; writing—review and editing, Y.X., D.L. and K.Y.; visualization, X.H. and Y.X.; supervision, Y.X.; project administration, Y.X. and K.Y.; funding acquisition, Y.X. and K.Y. All authors have read and agreed to the published version of the manuscript.

Funding: This research was funded by the National Natural Science Foundation of China (41976155, 41506137, 41676111, 41876139), the Natural Science Foundation of Guangxi Province (2020GXNSFDA297001), the Opening Project of Guangxi Laboratory on the Study of Coral Reefs in the South China Sea (GXLSCRSCS2019002), and Research Grants Council of Hong Kong (CityU 11104821 and C7013-19G).

Institutional Review Board Statement: Not applicable.

Informed Consent Statement: Not applicable.

Data Availability Statement: Data are available upon request, please contact the first author Yixiao Xu.

Acknowledgments: We are very grateful to Shauna Murray and Arjun Verma of University of Technology Sydney for kindly sharing the PCR amplification technique, and to Donald M. Anderson of Woods Hole Oceanographic Institution for nicely reviewing this manuscript.

Conflicts of Interest: The authors declare no conflict of interest.

References

1. Chinain, M.; Gatti, C.M.I.; Darius, H.T.; Quod, J.P.; Tester, P.A. Ciguatera poisonings: A global review of occurrences and trends. *Harmful Algae* **2021**, *102*, 101873. [CrossRef] [PubMed]
2. Lehane, L.; Lewis, R.J. Ciguatera: Recent advances but the risk remains. *Int. J. Food Microbiol.* **2000**, *61*, 91–125. [CrossRef]
3. Chan, T.Y.K. Characteristic features and contributory factors in fatal Ciguatera Fish Poisoning—Implications for prevention and public education. *Am. J. Trop. Med. Hyg.* **2016**, *94*, 704–709. [CrossRef]
4. Randall, J.E. A review of ciguatera, tropical fish poisoning, with a tentative explanation of its cause. *Bull. Mar. Sci.* **1958**, *8*, 236–267.
5. Yasumoto, T.; Nakajima, I.; Bagnis, R.; Adachi, R. Finding of a dinoflagellate as a likely culprit of ciguatera. *Bull. Jpn. Soc. Sci. Fish.* **1977**, *43*, 1021–1026. [CrossRef]
6. Adachi, R.; Fukuyo, Y. The thecal structure of a marine toxic dinoflagellate *Gambierdiscus toxicus* gen. et sp. nov. collected in a ciguatera-endemic area. *Bull. Jpn. Soc. Sci. Fish.* **1979**, *45*, 67–71. [CrossRef]
7. Gómez, F.; Qiu, D.J.; Lopes, R.M.; Lin, S.J. *Fukuyoa paulensis* gen. et sp nov., a new genus for the globular species of the dinoflagellate *Gambierdiscus* (Dinophyceae). *PLoS ONE* **2015**, *10*, e0119676.
8. Parsons, M.L.; Aligizaki, K.; Bottein, M.Y.D.; Fraga, S.; Morton, S.L.; Penna, A.; Rhodes, L. *Gambierdiscus* and *Ostreopsis*: Reassessment of the state of knowledge of their taxonomy, geography, ecophysiology, and toxicology. *Harmful Algae* **2012**, *14*, 107–129. [CrossRef]
9. Xu, Y.; Richlen, M.L.; Liefer, J.D.; Robertson, A.; Kulis, D.; Smith, T.B.; Parsons, M.L.; Anderson, D.M. Influence of environmental variables on *Gambierdiscus* spp. (Dinophyceae) growth and distribution. *PLoS ONE* **2016**, *11*, e0153197. [CrossRef]
10. Tester, P.A.; Litaker, R.W.; Berdalet, E. Climate change and harmful benthic microalgae. *Harmful Algae* **2020**, *91*, 101655. [CrossRef]
11. Friedman, M.A.; Fernandez, M.; Backer, L.C.; Dickey, R.W.; Bernstein, J.; Schrank, K.; Kibler, S.; Stephan, W.; Gribble, M.O.; Bienfang, P. An updated review of ciguatera fish poisoning: Clinical, epidemiological, environmental, and public health management. *Mar. Drugs* **2017**, *15*, 72. [CrossRef] [PubMed]
12. Núñez-Vázquez, E.J.; Almazán-Becerril, A.; López-Cortés, D.J.; Heredia-Tapia, A.; Hernández-Sandoval, F.E.; Band-Schmidt, C.J.; Bustillos-Guzmán, J.J.; Gárate-Lizárraga, I.; García-Mendoza, E.; Salinas-Zavala, C.A.; et al. Ciguatera in Mexico (1984–2013). *Mar. Drugs* **2019**, *17*, 13. [CrossRef] [PubMed]

13. Berdalet, E.; Bravo, I.; Evans, J.; Fraga, S.; Kibler, S.; Kudela, M.; Larsen, J.; Litaker, W.; Penna, A.; Tester, P.; et al. *Global Ecology and Oceanography of Harmful Algal Blooms, GEOHAB Core Research Project: HABs in Benthic Systems*; Intergovernmental Oceanographic Commission: Lausanne, Switzerland, 2012.
14. Berdalet, E.; Tester, P.A. Key Questions and Recent Research Advances on Harmful Algal Blooms in Benthic Systems. In *Global Ecology and Oceanography of Harmful Algal Blooms*; Glibert, P.M., Berdalet, E., Burford, M.A., Pitcher, G.C., Zhou, M., Eds.; Springer: Cham, Switzerland, 2018; Volume 232, pp. 261–286.
15. Hua, Z. Overview of studies on ciguatoxin. *Mar. Environ. Sci.* **1994**, *13*, 57–63.
16. Chan, T.Y.K. Emergence and epidemiology of ciguatera in the coastal cities of southern China. *Mar. Drugs* **2015**, *13*, 1175–1184. [CrossRef] [PubMed]
17. Chan, T.Y.K. Ciguatera fish poisoning in east Asia and southeast Asia. *Mar. Drugs* **2015**, *13*, 3466–3478. [CrossRef]
18. Wu, H.; Jin, X. Toxic fish in China. *Chin. J. Zool.* **1977**, 38–40.
19. Chan, T.Y.K.; Wang, A.Y.M. Life-threatening bradycardia and hypotension in a patient with ciguatera fish poisoning. *Trans. R. Soc. Trop. Med. Hyg.* **1993**, *87*, 71. [CrossRef]
20. Zhong, W.; Wu, G. Clinical manifestations of cardiovascular system in patients with ciguatoxin poisoning. *J. New Med.* **2006**, *37*, 316–317.
21. Xu, Y.; Wang, A.; Hu, R.; Jiang, T.; Jiang, T. Ciguatera toxins in coral fishes along the southern coast of China. *China Environ. Sci.* **2012**, *32*, 330–336.
22. Chen, G. Studies on the dinoflagellata in adjacent waters of the Xisha Islands III. some rare tropical ocean species. *Oceanol. Limnol. Sin.* **1989**, *20*, 230–237.
23. Lu, S.H.; Hodgkiss, I.J. An unusual year for the occurrence of harmful algae. *Harmful Algal News* **1999**, *18*, 1–3.
24. Lu, S.H.; Hodgkiss, I.J. Harmful algal bloom causative collected from Hong Kong waters. *Hydrobiologia* **2004**, *512*, 231–238. [CrossRef]
25. Lei, A.; Chen, H.; Chen, J.; Hu, Z. Research on species composition and biomass of Phytoplankton in Daya Bay artificial reef area. *J. Ocean Technol.* **2009**, *28*, 83–88.
26. Zhang, H.; Wu, Z.; Cen, J.; Li, Y.; Wang, H.; Lu, S. First report of three benthic dinoflagellates, *Gambierdiscus pacificus*, *G. australes* and *G. caribaeus* (Dinophyceae), from Hainan Island, South China Sea. *Phycol. Res.* **2016**, *64*, 259–273. [CrossRef]
27. Zhao, W.; Wei, H.; Guo, K. The community structure and the seasonal changes of phytoplankton in Dayao Bay in Dalian Coast from 2006 to 2007. *J. Dalian Ocean Univ.* **2011**, *26*, 291–298.
28. Wu, H.; Luan, Q.; Guo, M.; Gu, H.; Zhai, Y.; Tan, Z. Phycotoxins in scallops (*Patinopecten yessoensis*) in relation to source, composition and temporal variation of phytoplankton and cysts in North Yellow Sea, China. *Mar. Pollut. Bull.* **2018**, *135*, 1198–1204. [CrossRef]
29. Wang, Z.; Fu, Y.; Kang, W.; Liang, J.; Gu, Y.; Jiang, X. Germination of phytoplankton resting cells from surface sediments in two areas of the Southern Chinese coastal waters. *Mar. Ecol.* **2013**, *34*, 218–232. [CrossRef]
30. Leung, P.T.Y.; Yan, M.; Lam, V.; Yiu, S.K.F.; Chen, C.Y.; Murray, J.S.; Harwood, D.T.; Rhodes, L.L.; Lam, P.K.S.; Wai, T.C. Phylogeny, morphology and toxicity of benthic dinoflagellates of the genus *Fukuyoa* (Goniodomataceae, Dinophyceae) from a subtropical reef ecosystem in the South China Sea. *Harmful Algae* **2018**, *74*, 78–97. [CrossRef]
31. Ho, T.V.; Bing, H.Y.N. First report of *Gambierdiscus caribaeus* and *G. carpenteri* (Dinophyceae) from Nha Trang Bay, South Central Vietnam. *J. Mar. Biol. Ass. India* **2018**, *60*, 5–11. [CrossRef]
32. Wong, C.K.; Hung, P.; Lo, J.Y. Ciguatera fish poisoning in Hong Kong-A 10-year perspective on the class of ciguatoxins. *Toxicon* **2014**, *86*, 96–106. [CrossRef]
33. Lv, S.; Li, Y. Research on the prevalence of ciguatera fish poisoning in China. *China J. Public Health* **2006**, *22*, 226–227.
34. Wang, X.; Li, G. The status and prospect of researches on coral reef in Weizhou Island. *J. Guangxi Acad. Sci.* **2009**, *25*, 72–75.
35. Wang, W.; Yu, K.; Wang, Y. A review on the research of coral reefs in the Weizhou Island, Beibu Gulf. *Trop. Geogr.* **2016**, *36*, 72–79.
36. Zhou, H.; Wang, X.; Liang, W. Reflections on the characteristics, evolution and protection and rehabilitation strategies of the coral reefs at Weizhou Island. *J. Guangxi Acad. Sci.* **2020**, *36*, 228–236.
37. Wang, Y. Assessment of Coral Reef Ecosystem Health and Ecological Assets in Past Three Decades at Weizhou Island Reef, Beibu Gulf. Master's Thesis, Guangxi University, Guangxi, China, 2020.
38. Mustapa, N.I.; Yong, H.L.; Lee, L.K.; Lim, Z.F.; Lim, H.C.; Teng, S.T.; Luo, Z.; Gu, H.; Leaw, C.P.; Lim, P.T. Growth and epiphytic behavior of three *Gambierdiscus* species (Dinophyceae) associated with various macroalgal substrates. *Harmful Algae* **2019**, *89*, 101671. [CrossRef]
39. Litaker, R.W.; Vandersea, M.W.; Faust, M.A.; Kibler, S.R.; Chinain, M.; Holmes, M.J.; Holland, W.C.; Tester, P.A. Taxonomy of *Gambierdiscus* including four new species, *Gambierdiscus caribaeus*, *Gambierdiscus carolinianus*, *Gambierdiscus carpenteri* and *Gambierdiscus ruetzleri* (Gonyaulacales, Dinophyceae). *Phycologia* **2009**, *48*, 344–390. [CrossRef]
40. Kretzschmar, A.L.; Larsson, M.E.; Hoppenrath, M.; Doblin, M.A.; Murray, S.A. Characterisation of two toxic *Gambierdiscus* spp. (Gonyaulacales, Dinophyceae) from the great barrier reef (Australia): *G. lewisii* sp. nov. and *G. holmesii* sp. nov. *Protist* **2019**, *170*, 125699. [CrossRef] [PubMed]
41. Jang, S.H.; Jeong, H.J.; Du, Y.Y. *Gambierdiscus jejuensis* sp. nov., an epiphytic dinoflagellate from the waters of Jeju Island, Korea, effect of temperature on the growth, and its global distribution. *Harmful Algae* **2018**, *80*, 149–157. [CrossRef] [PubMed]

42. Vacarizas, J.; Benico, G.; Austero, N.; Azanza, R. Taxonomy and toxin production of *Gambierdiscus carpenteri* (Dinophyceae) in a tropical marine ecosystem: The first record from the Philippines. *Mar. Pollut. Bull.* **2018**, *137*, 430–443. [CrossRef] [PubMed]
43. Tawong, W.; Nishimura, T.; Sakanari, H.; Sato, S.; Yamaguchi, H.; Adachi, M. Characterization of *Gambierdiscus* and *Coolia* (Dinophyceae) isolates from Thailand based on morphology and phylogeny. *Phycol. Res.* **2015**, *63*, 125–133. [CrossRef]
44. Tudó, À.; Gaiani, G.; Rey Varela, M.; Tsumuraya, T.; Andree, K.B.; Fernández-Tejedor, M.; Campàs, M.; Diogène, J. Further advance of *Gambierdiscus* species in the Canary Islands, with the first report of *Gambierdiscus belizeanus*. *Toxins* **2020**, *12*, 692. [CrossRef]
45. Litaker, R.W.; Vandersea, M.W.; Faust, M.A.; Kibler, S.R.; Nau, A.W.; Holland, W.C.; Chinain, M.; Holmes, M.J.; Tester, P.A. Global distribution of ciguatera causing dinoflagellates in the genus *Gambierdiscus*. *Toxicon* **2010**, *56*, 711–730. [CrossRef] [PubMed]
46. Litaker, R.W.; Holland, W.C.; Hardison, D.R.; Pisapia, F.; Hess, P.; Kibler, S.R.; Tester, P.A. Ciguatoxicity of *Gambierdiscus* and *Fukuyoa* species from the Caribbean and Gulf of Mexico. *PLoS ONE* **2017**, *12*, e0185776. [CrossRef] [PubMed]
47. Rossignoli, A.E.; Tudó, A.; Bravo, I.; Díaz, P.A.; Diogène, J.; Riobó, P. Toxicity characterisation of *Gambierdiscus* species from the Canary Islands. *Toxins* **2020**, *12*, 134. [CrossRef]
48. Longo, S.; Sibat, M.; Viallon, J.; Darius, H.T.; Hess, P.; Chinain, M. Intraspecific variability in the toxin production and toxin profiles of In vitro cultures of *Gambierdiscus polynesiensis* (Dinophyceae) from French Polynesia. *Toxins* **2019**, *11*, 735. [CrossRef] [PubMed]
49. Roeder, K.; Erler, K.; Kibler, S.; Tester, P.; Nguyen-Ngoc, L.; Gerdts, G.; Luckas, B. Characteristic profiles of ciguatera toxins in different strains of *Gambierdiscus* spp. *Toxicon* **2010**, *56*, 731–738. [CrossRef]
50. Tawong, W.; Yoshimatsu, T.; Yamaguchi, H.; Adachi, M. Temperature and salinity effects and toxicity of *Gambierdiscus caribaeus* (Dinophyceae) from Thailand. *Phycologia* **2016**, *55*, 274–278. [CrossRef]
51. Lewis, R.J.; Inserra, M.; Vetter, I.; Holland, W.C.; Hardison, D.R.; Tester, P.A.; Litaker, R.W. Rapid extraction and identification of maitotoxin and ciguatoxin-like toxins from Caribbean and Pacific *Gambierdiscus* using a new functional bioassay. *PLoS ONE* **2016**, *11*, e0160006. [CrossRef]
52. Pisapia, F.; Holland, W.C.; Hardison, D.R.; Litaker, R.W.; Fraga, S.; Nishimura, T.; Adachi, M.; Nguyen-Ngoc, L.; Séchet, V.; Amzil, Z.; et al. Toxicity screening of 13 *Gambierdiscus* strains using neuro-2a and erythrocyte lysis bioassays. *Harmful Algae* **2017**, *63*, 173–183. [CrossRef]
53. Díaz-Asencio, L.; Clausing, R.J.; Vandersea, M.; Chamero-Lago, D.; Gómez-Batista, M.; Hernández-Albernas, J.I.; Chomérat, N.; Rojas-Abrahantes, G.; Litaker, R.W.; Tester, P.; et al. Ciguatoxin occurrence in food-web components of a Cuban coral reef ecosystem: Risk-assessment implications. *Toxins* **2019**, *11*, 722. [CrossRef]
54. Gaiani, G.; Leonardo, S.; Tudó, À.; Toldrà, A.; Rey, M.; Andree, K.B.; Tsumuraya, T.; Hirama, M.; Diogène, J.; O'Sullivan, C.K.; et al. Rapid detection of ciguatoxins in *Gambierdiscus* and *Fukuyoa* with immunosensing tools. *Ecotoxicol. Environ. Saf.* **2020**, *204*, 111004. [CrossRef] [PubMed]
55. Lartigue, J.; Jester, E.L.E.; Dickey, R.W.; Villareal, T.A. Nitrogen source effects on the growth and toxicity of two strains of the ciguatera-causing dinoflagellate *Gambierdiscus toxicus*. *Harmful Algae* **2009**, *8*, 781–791. [CrossRef]
56. Liefer, J.D.; Richlen, M.L.; Smith, T.B.; DeBose, J.L.; Xu, Y.; Anderson, D.M.; Robertson, A. Asynchrony of *Gambierdiscus* spp. Abundance and Toxicity in the U.S. Virgin Islands: Implications for Monitoring and Management of Ciguatera. *Toxins* **2021**, *13*, 413. [CrossRef] [PubMed]
57. Morton, S.; Bomber, J.; Tindall, D.; Aikman, K. Response of *Gambierdiscus toxicus* to light: Cell physiology and toxicity. In *Toxic Phytoplankton Blooms in the Sea*; Smayda, T., Shimizu, Y., Eds.; Elsevier: New York, NY, USA, 1993; pp. 541–546.
58. Chinain, M.; Germain, M.; Deparis, X.; Pauillac, S.; Legrand, A.M. Seasonal abundance and toxicity of the dinoflagellate *Gambierdiscus* spp. (Dinophyceae), the causative agent of ciguatera in Tahiti, French Polynesia. *Mar. Biol.* **1999**, *135*, 259–267. [CrossRef]
59. Reverté, L.; Toldrà, A.; Andree, K.B.; Fraga, S.; De Falco, G.; Campàs, M.; Diogène, J. Assessment of cytotoxicity in ten strains of *Gambierdiscus australes* from Macaronesian Islands by neuro-2a cell-based assays. *J. Appl. Phycol.* **2018**, *30*, 2447–2461. [CrossRef]
60. Kibler, S.R.; Litaker, R.W.; Holland, W.C.; Vandersea, M.W.; Tester, P.A. Growth of eight *Gambierdiscus* (Dinophyceae) species: Effects of temperature, salinity and irradiance. *Harmful Algae* **2012**, *19*, 1–14. [CrossRef]
61. Chinain, M.; Darius, H.T.; Ung, A.; Cruchet, P.; Wang, Z.; Ponton, D.; Laurent, D.; Pauillac, S. Growth and toxin production in the ciguatera-causing dinoflagellate *Gambierdiscus polynesiensis* (Dinophyceae) in culture. *Toxicon* **2010**, *56*, 739–750. [CrossRef]
62. Morton, S.; Norris, D. The role of temperature, salinity, and light on the seasonality of *Prorocentrum lima*. In *Toxic Marine Phytoplankton*; Graneli, E., Ed.; Elsevier: New York, NY, USA, 1990; pp. 201–205.
63. Chinain, M.; Faust, M.A.; Pauillac, S. Morphology and molecular analyses of three toxic species of *Gambierdiscus* (Dinophyceae): *G. pacificus*, sp. nov., *G. australes*, sp. nov., and *G. polynesiensis*, sp. nov. *J. Phycol.* **1999**, *35*, 1282–1296. [CrossRef]
64. Xu, Y.; Richlen, M.L.; Morton, S.L.; Mak, Y.L.; Chan, L.L.; Tekiau, A.; Anderson, D.M. Distribution, abundance and diversity of *Gambierdiscus* spp. from a ciguatera-endemic area in Marakei, Republic of Kiribati. *Harmful Algae* **2014**, *34*, 56–68. [CrossRef]

toxins

MDPI

Article

Screening for Predictors of Chronic Ciguatera Poisoning: An Exploratory Analysis among Hospitalized Cases from French Polynesia

Clémence Mahana iti Gatti [1,*], Kiyojiken Chung [1], Erwan Oehler [2], T. J. Pierce [3], Matthew O. Gribble [4] and Mireille Chinain [1]

[1] Laboratory of Marine Biotoxins, Institut Louis Malardé (ILM), UMR 241-EIO (IFREMER, ILM, IRD, Univ. Polynésie Française), Papeete, Tahiti 98713, French Polynesia; kiyo.chung@outlook.com (K.C.); mchinain@ilm.pf (M.C.)
[2] Centre Hospitalier de Polynésie française, Papeete, Tahiti 98713, French Polynesia; erwan.oehler@cht.pf
[3] Gangarosa Department of Environmental Health, Department of Epidemiology, Emory University Rollins School of Public Health, Atlanta, GA 30322, USA; tjpierce223@gmail.com
[4] Department of Epidemiology, University of Alabama at Birmingham, Birmingham, AL 35233, USA; mgribble@uab.edu
* Correspondence: cgatti@ilm.pf

Abstract: Ciguatera poisoning is a globally occurring seafood disease caused by the ingestion of marine products contaminated with dinoflagellate produced neurotoxins. Persistent forms of ciguatera, which prove to be highly debilitating, are poorly studied and represent a significant medical issue. The present study aims to better understand chronic ciguatera manifestations and identify potential predictive factors for their duration. Medical files of 49 patients were analyzed, and the post-hospitalization evolution of the disease assessed through a follow-up questionnaire. A rigorous logistic lasso regression model was applied to select significant predictors from a list of 37 patient characteristics potentially predictive of having chronic symptoms. Missing data were handled by complete case analysis, and a survival analysis was implemented. All models used standardized variables, and multiple comparisons in the survival analyses were handled by Bonferroni correction. Among all studied variables, five significant predictors of having symptoms lasting $\geq$3 months were identified: age, tobacco consumption, acute bradycardia, laboratory measures of urea, and neutrophils. This exploratory, hypothesis-generating study contributes to the development of ciguatera epidemiology by narrowing the list from 37 possible predictors to a list of five predictors that seem worth further investigation as candidate risk factors in more targeted studies of ciguatera symptom duration.

Keywords: ciguatera poisoning; epidemiology; least absolute shrinkage and selection operator; machine learning; data science; medical informatics; survival analysis; foodborne diseases

Key Contribution: This study is the first exploration of predictors of chronic ciguatera among severe ciguatera cases that required hospitalization.

Citation: Gatti, C.M.i.; Chung, K.; Oehler, E.; Pierce, T.J.; Gribble, M.O.; Chinain, M. Screening for Predictors of Chronic Ciguatera Poisoning: An Exploratory Analysis among Hospitalized Cases from French Polynesia. *Toxins* **2021**, *13*, 646. https://doi.org/10.3390/toxins13090646

Received: 23 August 2021
Accepted: 8 September 2021
Published: 12 September 2021

1. Introduction

Ciguatera poisoning (CP) is a non-infectious food poisoning resulting from the consumption of marine organisms contaminated by ciguatoxins (CTXs), neurotoxins produced by microalgae in the genera *Gambierdiscus* and *Fukuyoa*, that preferentially proliferate in tropical and subtropical ecosystems [1,2]. According to current figures, this would affect 10,000 to 50,000 persons every year [3], nevertheless, it is likely that these numbers only represent 20% of the true situation due to the absence of diagnostic tools, and a strong under reporting of the disease at a global scale [4]. Due to the nature and the large distribution of CTXs' biological targets (e.g., voltage-gated sodium channels, potassium

channels, and calcium channels) and the variety of cells affected [5–8], CP results in a variable and highly subjective syndrome. Indeed, symptom expression and severity may vary [9] under the combined influence of the amount, and likely, the family of CTXs ingested, as well as individual susceptibility. CP diagnosis is solely based on the history of poisoning and symptoms' description, and must be considered in a non-febrile patient presenting with a combination of gastrointestinal, cardiovascular, musculoskeletal and/or neurological disorders (especially cold allodynia, unsustainable itching and heightened nociperception), which appear within 48 h after the ingestion of "at-risk" marine organisms [9]. Gastrointestinal manifestations (i.e., diarrhea, vomiting, nausea, and abdominal pain) usually occur first, sometimes accompanied by cardiovascular disorders, mostly bradycardia and hypotension. These manifestations generally disappear within 48–72 h, either spontaneously or under adapted medication, while neurological and other systemic manifestations (e.g., cold allodynia, itching, paraesthesia, myalgia, arthralgia) appear during subsequent days [10–13].

Chronic forms of CP with symptoms lasting $\geq$3 months are a real clinical challenge. Even though chronic CP cases are regularly reported, studies dedicated to the understanding of this phenomenon are scarce, especially due to the lack of a clear consensus regarding its clinical definition. Indeed, some CP manifestations may persist for months or even years after the initial poisoning, mostly under the traits of neurological and psychiatric disorders (i.e., tenacious fatigue, paraesthesia, dysesthesia, pruritus, attention deficit disorder, anxiety, depression) [14–17]. These manifestations can be expressed continuously or through transient reactivation peaks, triggered by multiple factors (e.g., consumption of marine/fresh water-related products, even from non-endemic region, alcohol, nuts, and red meat. Stress and contrasted ambient temperature may also impact [9,17]. Diagnosing a chronic CP, with a time lag from the initial poisoning, represents a real struggle for both patients and clinicians, as it often required costly and unsatisfactory biological tests. To date, no treatment has proven effective in CP medical management. Treatment essentially relies on supportive care, with variable results [9,18]. Considering that at least 20% of the persons affected by CP are likely to develop a persistent form [19], this health issue deserves an increased attention and dedicated studies.

The present study aims at better characterizing CP chronic forms among a cohort of individuals that have been hospitalized for CP motive at the main hospital of French Polynesia (FP), a territory with a high CP endemicity, and assessing a statistical predictive model for symptoms' duration.

2. Results

2.1. Participants' Description

Among the n = 49 participants, n = 26 were identified as acute CP cases (with symptoms that fully improved in less than 3 months) and n = 23 as chronic CP cases. As shown in Table 1, the median age was 50 years (47 years old in acute cases vs. 52 years old in chronic cases); and males were predominant ($SR_{n=49}$: 1.882; SR_{acute}: 1.364; SR_{chonic}: 2.833). The cohort was composed of 65% (n = 32) Polynesian, 26% (n = 13) mixed-race and 8% (n = 4) non-Polynesians. A total of 52% (n = 12) of chronic patients had one or more comorbidities such as chronic hypertension and type 2 diabetes vs. 11% (n = 3) among the acute CP cases; and 65% (n = 15) of chronic CP cases declared weekly tobacco consumption at the time of the poisoning vs. 23% (n = 6) among acute CP cases.

Table 1. Participant's characteristics.

	All Participants% (n = 49)	Acute CP Cases (n = 26)	Chronic CP Cases (n = 23)
Median age	50	47	52
Sex ratio (M/F)	1.882	1.364	2.833
Ethnicity:			
Polynesian	65% (n = 32)	58% (n = 15)	74% (n = 17)
Mixed-race	26% (n = 13)	31% (n = 8)	22% (n = 5)
Non-Polynesian	8% (n = 4)	11% (n = 3)	4% (n = 1)
Tobacco consumption	43% (n = 21)	23% (n = 6)	65% (n = 15)
Comorbidities:	31% (n = 15)	11% (n = 3)	52% (n = 12)
Chronic hypertension	16% (n = 8)	11% (n = 3)	22% (n = 5)
Type 2 Diabetes	16% (n = 8)	4% (n = 1)	30% (n = 7)

Italics are used to better distinguish the subpopulations in the different groups (Ethnicity and Comorbidities).

2.2. Acute Symptoms and Biological Variables

In Table 2 we reported the acute symptoms and biological characteristics of the n = 49 participants (or the subset of participants with complete data on that variable) vs. the n = 38 participants included in the rigorous logistic lasso regression (RLLR model). For binary variables, the percent reporting "yes" is reported; for continuous variables, the median (25th percentile, 75th percentile) is reported. The symptoms incubation time was once recorded as ">3 h", and once as "<24 h"; for data analysis, these were assumed to fall into the categories of <12 h and $\geq$12 h, respectively.

Table 2. Characteristics of the full n = 49 participants vs. the n = 38 participants included in the RLLR model.

Variable	All Participants with Data (n = 49)	RLLR Model Sample (n = 38)
Age	50 (45, 60)	49.5 (45, 56)
Male sex	65%	71%
Ate non-herbivorous fish	89% *	89%
Ate head and/or viscera	79% **	82%
Prior ciguatera	57%	63%
Tobacco consumption	43%	45%
Chronic hypertension	16%	16%
Type 2 diabetes	16%	13%
Symptoms incubation time $\geq$12 h	10%	11%
Acute Digestive disorders		
Diarrhea	90%	92%
Vomiting	71%	74%
Abdominal pain	69%	66%
Nausea	53%	50%
Acute Cardiovascular disorders		
Hypotension	80%	82%
Bradycardia	55%	58%
Heart rhythm disorder	16%	18%
Tachycardia	4%	3%

Table 2. *Cont.*

Variable	All Participants with Data (n = 49)	RLLR Model Sample (n = 38)
Acute Neurological and Other Disorders		
Asthenia	88%	87%
Paraesthesia	84%	79%
Itching	71%	66%
Cold allodynia	69%	71%
Dizziness	59%	63%
Migraine	53%	47%
Dysesthesia	51%	45%
Gait disorder	51%	50%
Chill	45%	42%
Muscle disorder	43%	37%
Joint pain	39%	34%
Blurred vision	39%	34%
Hypothermia	35%	37%
Balance disorder	35%	32%
Oral/peri-oral burning sensation	24%	21%
Urogenital pain/itching or discomfort	22%	18%
Dysgeusia	20%	24%
Language disorder	18%	18%
Coordination disorder	14%	11%
Heat allodynia	6%	8%
Dysuria	4%	0%
Depression	2%	0%
Biological Tests		
Urea (g/L) [0.13–0.43] ***	0.48 (0.41, 0.56)	0.50 (0.41, 0.57)
Creatinine (mg/L) [6–12]	12 (10, 15)	12.5 (10, 15)
Sodium (mEq/L) [136–145]	140 (138, 141)	140 (138, 141)
Potassium (mEq/L) [3.4–4.4]	4.1 (3.7, 4.4)	4.1 (3.9, 4.4)
Chloride (mEq/L) [98–107]	105 (103, 108)	106 (103, 109)
Leukocytes (g/L) [4.0–10.7]	9.7 (7.4, 11.7)	9.75 (7.7, 11.9)
Neutrophils (g/L) [1.8–7.3]	7.1 (4.4, 8.8)	7.3 (4.8, 8.8)
Eosinophils (g/L) [0.0–0.6]	0.2 (0.1, 0.2)	0.15 (0.1, 0.2)
Basophils (g/L) [0.0–0.2]	0 (0, 0.1)	0 (0, 0.1)
Lymphocytes (g/L) [1.0–3.4]	2 (1.4, 2.6)	1.9 (1.4, 2.6)

* n = 46. ** n = 48. *** normal ranges.

2.3. Chronic Symptoms and Triggering Factors

As shown in Table 3, the most prevalent chronic symptoms were neurological (i.e., itching (65%), asthenia (61%), paraesthesia (56%), cold allodynia (39%), dysesthesia (26%), muscular disorders (26%) and blurred vision (26%)), whereas digestive and cardiovascular manifestations were less present (diarrhea (17%) and peak of hypotension (13%)). As to neuropsychiatric manifestations such as sleep disorder, irritability, depression, and attention disorders, they were expressed with a respective prevalence of 22%, 17%, 9%, and 4%.

Those manifestations were reported to be triggered or worsened by factors that mainly belong to food products category, such as fish (56%), chicken (30%), beef (26%), nuts (22%), pork (17%), soy related products (17%), canned food (17%), dairy products (17%), alcohol (13%), coffee/tea (9%), chocolate (9%) and spices (4%) (Table 4). Note that the prevalence for fish, meat, and alcohol may be lowered by the fact that some of the participants avoided them following their hospital discharge, under the recommendation of their physician, and still did not reintroduce them in their diet when the interview was realized. Non-food factors were also reported to influence chronic symptoms' expression, such as cold/hot ambient air contrast (n = 4), rapid weight loss (n = 4), physical activity (n = 3), and sun exposure (n = 4).

Table 3. Frequency of chronic symptoms in the sample of chronic CP cases (n = 23).

Chronic Symptoms	Category	% (n = 23)
Itching	N	65 (n = 15)
Asthenia	N	61 (n = 14)
Paraesthesia	N	56 (n = 13)
Cold allodynia	N	39 (n = 9)
Dysesthesia	N	26 (n = 6)
Muscle disorder	N	26 (n = 6)
Blurred vision	N	26 (n = 6)
Sleep disorder	Np	22 (n = 5)
Diarrhea	D	17 (n = 4)
Joint pain	O	17 (n = 4)
Irritability	Np	17 (n = 4)
Gait disorder	N	17 (n = 4)
Headache/Migraine	N	13 (n = 3)
Hypothermia	N	13 (n = 3)
Chill	N	13 (n = 3)
Peak of hypotension	Cv	13 (n = 3)
Vomiting	D	13 (n = 3)
Urogenital discomfort/pain/burning	O	13 (n = 3)
Abdominal pain	D	9 (n = 2)
Nausea	D	9 (n = 2)
Heart rhythm disorder	Cv	9 (n = 2)
Language disorder	N	9 (n = 2)
Balance disorder	N	9 (n = 2)
Depression	Np	9 (n = 2)
Bradycardia	Cv	4 (n = 1)
Dizziness	N	4 (n = 1)
Coordination disorder	N	4 (n = 1)
Dysgeusia	O	4 (n = 1)
Oral/peri-oral burning sensation	N	4 (n = 1)
Attention disorder	Np	4 (n = 1)

N: neurologic; Np: neuropsychiatric; D: digestive; Cv: cardiovascular; O: other.

Table 4. Chronic CP manifestations triggering/worsening factors.

Triggering Factors	% (n = 23)
Food Origin	
Fish	56
Chicken	30
Beef	26
Nuts	22
Pork	17
Soy related products	17
Canned products	17
Dairy products	17
Alcohol	13
Coffee/Tea	9
Chocolate	9
Spices	4
Non-Food Origin	
Cold/hot air contrast	17
Rapid weight loss	17
Physical activity	13
Sun exposure	13

2.4. Chronic CP Predictors

Table 5 provides the p value from either a Fisher's exact test for categorical predictors (e.g., tobacco consumption, acute bradycardia symptoms) or a t-test for continuous predictors (e.g., age, urea, neutrophils) comparing cases to non-cases of chronic CP. There were n = 49 included in tests of the binary predictors, and n = 45 participants with complete data on laboratory biomarkers for two sample equal-variance t-tests. Only the comparison of tobacco consumption between the cases and non-cases of chronic CP was Bonferroni-significant ($p < 0.01$) considering the 5 hypothesis tests. Unlike the RLLR analysis, these hypothesis tests did not use standardized variables.

Table 5. Significant variables for chronic CP predictors.

Chronic CP Predictors	N	p Value (Fisher's Exact or t Test)
Age	49	0.10
Tobacco consumption	49	0.004
Bradycardia	49	0.25
Urea	45	0.03
Neutrophils	45	0.12

A two-by-two table of the observed chronic case status vs. the predicted chronic case status given the RLLR model, with model predictions calculated for all n = 49 participants is presented in Table 6. There were n = 35 patients for whom the model prediction matched the observed chronic case status vs. n = 14 for whom the model prediction did not match. The sensitivity of this prediction model was 92% (95% confidence interval: 75%, 99%) and the specificity of this prediction model was 48% (95% confidence interval: 27%, 69%). The positive predictive value of this model was 67% (95% confidence interval: 57%, 75%), and the negative predictive value of this model was 85% (95% confidence interval: 58%, 96%). The model accuracy was 71% (57%, 83%).

Table 6. Two-by-two table of the observed chronic case status vs. the predicted chronic case status from the RLLR model.

	Observed Chronic	Observed Non-Chronic
Predicted Chronic	n = 24	n = 12
Predicted Non-Chronic	n = 2	n = 11

2.5. Time until Cessation of Symptoms among Chronic Cases

The smallest sample-size survival model had 20 participants, 13 with observed cessation of symptoms during follow-up, and 450 total months of follow-up.

The results of the parametric survival analyses of time until cessation of symptoms among chronic cases, considering only the variables suggested as predictive of being a chronic case in the RLLR model, are presented in Table 7. There were 16 chronic cases with recorded cessation of symptoms and 7 who had not yet experienced a cessation of symptoms at the end of the study follow-up period (total n = 23). The maximum analysis time at risk in this survival analysis was 535 person-months (n = 23 participants, n = 16 events) and the minimum was 450 person-months (n = 20 participants, n = 13 events). Note that standardized variables were used for this predictive analysis. One of the bootstrap estimates for the lognormal survival-time model with bradycardia as the predictor failed to converge so the confidence interval was based on 499 bootstrap replicates.

Table 7. Parametric survival analyses of time until cessation of symptoms among chronic cases.

Standardized Predictor	n of Participants, n of Events, Person-Months at Risk	Weibull Assumption Time Ratio (Bootstrap 95% CI)	Lognormal Assumption Time Ratio (Bootstrap 95% CI)
Age	23, 16, 535	1.39 (0.65, 3.02)	1.51 (0.55, 2.67)
Tobacco consumption	23, 16, 535	1.19 (0.79, 2.62)	1.38 (0.70, 2.48)
Bradycardia	23, 16, 535	1.31 (0.82, 2.81)	1.60 (0.81, 2.76)
Urea	20, 13, 450	0.71 (0.33, 0.95)	0.72 (0.30, 1.11)
Neutrophils	21, 15, 528	0.94 (0.49, 1.53)	0.88 (0.54, 2.03)

3. Discussion

Among the n = 49 participants, 47% (n = 23) kept suffering from persisting symptoms at least 3 months after the initial poisoning. However, this number may be biased as it can be hypothesized that candidates who developed chronic manifestations were more inclined to contribute to the study. As comparison, Pearn [19] and Baumann et al. [20] have respectively estimated this prevalence at 20% and 34%.

The acute clinical picture of our cohort is comparable with the one described by Gatti et al. [21]. Indeed, among the n = 129 hospitalizations for ciguatera registered at the same hospital between 1999 and 2005, the most prevalent symptoms were identical, i.e., diarrhea, vomiting and abdominal pain regarding gastrointestinal symptoms; hypotension and bradycardia, as cardiovascular symptoms; and paraesthesia, asthenia and pruritus among neurological symptoms.

Moreover, 43% of the participants in the present study declared smoking tobacco (vs. 41% of the population of French Polynesia in 2010 [22]), suffering from chronic hypertension for 16% of them (vs. 26.7% [22]) and type 2 diabetes for 16% of them (vs. 19% in 2012 [23]). In addition, the prevalence of participants with antecedent of ciguatera (57%) is in accordance with the estimations observed among ambulatory cases recorded through the surveillance program of FP (51.6% in 2016 [24], 56% in 2020 [25]). This information suggests that the study cohort does not present higher risk or fragility than the general population.

3.1. Chronic Manifestations and Triggering Factors

Chronic manifestations, that are mainly dominated by neurological symptoms, are also consistent with observations made in a 20 months' follow-up of 9 tourists contaminated with trochus shell, *Tectus niloticus* (whose specimens from the same site were showed to contain high amounts of CTXs) [17,26]. Indeed, itching, asthenia, paranesthesia and cold allodynia were also the most prevalent persisting symptoms which gives CP its status as mixed sensory neuropathy that predominantly affects the lemniscal system [12,27], while cardiovascular and digestive manifestations were absent or anecdotal. Note that in both studies, neuropsychiatric manifestations essentially made their appearance during the chronic stage.

There are several mechanisms that were given as explanations for the persistence of CP symptoms. It has been hypothesized that it could result from prolonged activation of voltage-gated sodium channels by CTXs, fixed in deep tissues and occasionally released into the bloodstream following lipid metabolism activation [28], and/or a possible immune imbalance common to several chronic auto-inflammatory and auto-immune diseases [29–33]. In the present study, the first theory is supported by the declaration of symptoms worsening after non-rapid weight loss in 4 participants. Concerning neuropsychiatric manifestations such as depression, anxiety, memory loss or attention disorder [11,34–36], they could be attributable to (i) a pre-existing non-CP related psychiatric illness, (ii) a secondary consequence of a certain lassitude linked to persistent invalidating manifestations that could not be mitigated or removed by effective treatments, and a lack of recognition by medical professionals, (iii) to direct physiological damages caused by CTXs on the central nervous system, or (iv) to a synergistic effect of CTXs biological impacts combined with

functional/psychiatric disorders. As also observed in the Gatti et al. 20 month's follow-up study [17], except for psychiatric-related symptoms that can make their appearance weeks or months after the initial poisoning, no new symptoms other than the ones expressed during the acute phase made their appearance.

As also observed in the present study, characteristic of CP is that its symptoms, especially neurological ones, may be modulated by external factors contributing to transient relapse or intensification. [9]. Although many symptom-triggering factors reported by the ciguatera cases in this study (Table 4) have a food-based origin, others are related to the environment (e.g., contrasted ambient air temperature, sun exposure) or linked to patients' physical condition (e.g., rapid weight loss, intense physical activity). Assembling a list of potentially modifiable triggering factors would be helpful to assist CP patients in their recovery process by adapting their diet and behavior. It is possible that mechanism for symptom triggering might be related to histamine metabolism, due to the similarities that can be observed in CP patients and certain histamine-related disorders, although this has not been assessed in this study.

Finally, in this study as also observed in Chateau-Degat et al. [16] and Gatti et al. [17], CP usually showed a positive evolution, with symptoms that progressively and spontaneously regressed in frequency and intensity over time.

3.2. Chronic CP Predictive Factors

In this exploratory study, our RLLR model identified five potentially predictive variables of developing a chronic ciguatera form that would merit further investigation: age, tobacco consumption, acute bradycardia, laboratory measures of urea and neutrophils. This predictor-screening RLLR model used a standardized version of each predictor variable rather than the real-world untransformed observed values of each variable. When we considered untransformed variables, only tobacco consumption was Bonferroni-significant when considered in relation to observed chronic case status. In secondary survival analyses for duration of symptoms among chronic cases, the point estimates for tobacco consumption were consistent with an extended duration of symptoms among tobacco consumers, but these model estimates were imprecise and not statistically significant. Nevertheless, this finding is consistent with the observation of Chateau-Degat et al. [16] who identified a clear association between tobacco consumption and CP symptoms persistence on mild CP cases. Further toxicological research on tobacco implication (through a co-modulation of cholinergic receptors by CTXs and nicotine), as a potential obstacle in the healing process, is warranted.

Acute hypotension and bradycardia were respectively expressed in 80% and 55% of participants, which reinforces the idea that our study population suffers from a severe form of CP. Indeed, according to Geller and Benowitz [37], these manifestations would result from an autonomic dysfunction (combination of parasympathetic excess and sympathetic failure), considered one of the most serious CP complications, also used as determining factor for patient's hospitalization. By comparison, hypotension and bradycardia prevalence among CP ambulatory cases reported in French Polynesia were respectively 19.7% and 24.3% in 2018 [38]. Bradycardia as predictive factors for chronic cases could mean that the severity of the poisoning would have an influence on patients' recovery capacity. At this stage, a prospective comparative study between ambulatory and hospitalized cases, with the support of a severity index, may be able to answer this question.

Our study also suggested that age may be a predictive factor. Such observation is consistent with the result of Katz et al. [39] who found a correlation between age and increasing duration of CP symptoms while describing an outbreak in Hawaii. This finding has biologically plausible mechanisms relating to the decreasing capacity of neuronal repair and/or a slower sodium channel regeneration with age, accentuated by the ability of some CTX to reduce the intrinsic growth capacity of peripheral neurons as observed on animal model [40].

Known to be a significant actor of the innate immune response, neutrophils are also implicated in several other processes, such as acute cell injury and repair, cancer, autoimmunity or chronic inflammation [41]. Even though the innate immune response to non-protein toxins is poorly documented, there is some evidence that CTXs are involved in both immune and inflammatory dysregulation [7,31]. As mentioned by Pierre et al. [42], available data suggest that the systemic immune response following acute CTX exposure is rather an anti-inflammatory Th2 response that may result in a possible genetic predisposition associated with MHC variants conferring susceptibility to develop a persistent syndrome. As these processes are not clearly established yet, we are unsure about the mechanism by which neutrophil regulation is related to CP symptoms duration. These findings merit further dedicated studies.

Urea, a nitrogenous metabolite resulting from the catabolism of proteins, is mainly measured to assess kidney function, even though its production may be easily influenced by several unconnected medical causes [43]. At this stage, suggesting a significant biological explanation for its role as a potential predictive factor for symptoms duration remains nebulous and needs further research.

It is possible that some of these factors, although they did not show detectable associations in this sample, could have a causal relationship that might be detectable in a larger sample; for example, it is possible that diabetes may contribute to more sensitive nerve cells to the variations of osmolarity induced by CTXs, and consequently to more substantial neurological disturbances.

3.3. Limitations of the Study

As in any study based on the recall of past events, recall bias represents a significant weakness, which, however, was partially controlled by comparing data collected through questionnaires with data from hospital medical records. Yet, and above all, the main weakness resides in the small sample size of the cohort, especially given the population initially targeted (n = 254 potential candidates). Another limitation of this study resides in the fact that it was focused on screening individual predictors and did not allow for possible interactions between predictors. This screen suggested that tobacco consumption may be of particular interest for follow-up research as a potentially modifiable, significant predictor of being a chronic case; we do not evaluate in this study possible heterogeneity in the association of tobacco with ciguatera duration according to sex or any other participant characteristics.

Overall, there was a good agreement of our RLLR model prediction of the most likely outcome per participant vis-à-vis the observed outcomes. The overall model accuracy was 71%, which can likely be improved if additional predictive variables are identified in the future, but suggests that these five variables may be informative for risk stratification of new ciguatera patients as having elevated risk of becoming a chronic case. The negative predictive value of this model was better than the positive predictive value, and the sensitivity was better than the specificity.

The survival analysis examining the associations of these five variables to the duration of symptoms is conditional on the results of the original RLLR model with a somewhat related outcome variable, as well as having five separate hypothesis tests, and so would be expected to also have an inflated Type I error rate. We find a nominally significant ($p < 0.05$), but not Bonferroni-significant, association of higher levels of (standardized) urea with shorter duration of symptoms, assuming a Weibull distribution for survival times. However, this is no longer nominally significant when we consider a lognormal distributional assumption for the survival-time distribution. Thus, our inferences about statistical significance or lack thereof are sensitive to our parametric model assumptions, although we obtained similar point estimates for each predictor variable regardless of distributional assumptions. Our subjective impression is that both urea and bradycardia merit further investigation as potential predictors of the timing of cessation of symptoms in a future study. We intentionally limited our number of hypothesis tests due to our very

limited sample size for the survival analyses. Since we used RLLR for chronic ciguatera as a screening tool to reduce the number of modeled covariates, we cannot preclude the possibility that another variable that was not identified in the RLLR model as significantly predictive would nevertheless be predictive of the duration of symptoms conditional on being a chronic case.

Despite the lack of knowledge about the mechanisms underlying CP, it appears important to bring to the attention of healthcare workers the existence of CP chronic manifestations, especially in a context of globalization of this affliction [44]. Moreover, collaborative international efforts must be encouraged in order to (i) increase CP awareness, especially in non-endemic regions, (ii) define a "Medical Consensus Guideline" to come in support of the medical community, (iii) develop diagnosis tools and effective treatments. Although the conclusions of the present study are very preliminary, based on a limited sample size and mixed findings, it may be of valuable interest in order to narrow the search space for future investigations from an agnostic set of 37 potential predictors to a more feasible study set of 5 candidate predictors with suggestive but not conclusive prior evidence for association.

4. Materials and Methods

4.1. Cohort Recruitment and Data Collection

Candidates to the study were selected from the medical records register of patients hospitalized for ciguatera motive (coded T61.0 according to the International Classification of Diseases), between 1 January 2010 and 31 December 2015, at the Centre Hospitalier de Polynésie Française. All T61.0-corresponding files were then verified by the CP referent physician of the hospital for a posteriori diagnosis confirmation. After excluding (i) incorrectly coded cases, (ii) persons that have left the territory, (iii) deceased persons, (iv) people with serious physical or mental condition incompatible with the holding of an interview, (v) and people who could not be contacted due to false or no contact information; n = 100 potential candidates were identified to be included in the study and met the investigators for a follow-up interview. Among them, n = 13 refused to participate and n = 38 never showed up to the follow-up interview despite giving their consent. The study was finally conducted on 49 participants for whom we disposed of acute ciguatera hospitalization medical records (which dates back to 3 months at the earliest) and chronic symptom's evolution collected through a dedicated questionnaire carried out in face-to-face or remotely with the assistance of the investigators when needed. In detail, medical records gathered information about patients' characteristics (age, sex, medical history, tobacco consumption, comorbidities), the context of poisoning, the acute clinical description and biological test results (carried out systematically for all incoming patients regardless of the reason for their hospitalization). The follow-up questionnaire included questions related to the participant medical history, the initial poisoning context, the acute symptoms during the hospitalization (in order to assess the level of reliability of their memories, by comparing this information with that contained in the hospital medical records), the chronic evolution of symptoms, and the factors likely to influence their expression.

4.2. Statistical Analysis and Predictive Model

Lasso regression [45] is a well-established machine learning approach that uses regularization to stabilize model estimation by solving for optimal regression coefficients $\hat{\beta}$ to minimize a loss function $-\frac{2}{n}\mathrm{LL}(\beta) + \lambda \sum_j |\beta_j|$, where LL represents the log-likelihood of the model for coefficient set β, n is the sample size, λ is a model tuning parameter that determines how much penalty to attach to extra model complexity (i.e., inclusion of nonzero coefficients), and β_j is each regression parameter. The lasso regression approach lacks a formal causal interpretation but can be useful for discerning predictive variables in situations where there is data sparsity (e.g., a large number of candidate predictors compared to the number of observations, with the number of predictors potentially exceeding the number of observations). The primary goal of lasso regression is prediction rather than

causal inference; it is possible that a variable that is retained in the model as predictive is correlated with a causal variable but is not a causal variable.

Rigorous logistic lasso regression [46], is an extension of the lasso modeling framework developed to handle binary outcome variables with potentially heteroskedastic errors or clustering of observations and a limited sample size relative to the number of observations. The penalty in RLLR is defined by the equation $\lambda = \frac{c}{2}\sqrt{n}\Phi^{-1}(1-\gamma)$, where c is a slack parameter (we constrained to $c = 0.1$), Φ is the Gaussian cumulative distribution function, and γ is the significance level (we constrained to $\gamma = \frac{0.05}{\max(p*\log(n),n)}$). Thus, using this constrained approach there was only a single λ possible and no grid search was needed for an optimal λ.

For the RLLR model, we included biological test that had been realized in ≥90% of participants (for urea, creatinine, sodium, potassium, chloride, leukocytes, neutrophils, eosinophils, basophils and lymphocytes measures); whether the patient had consumed herbivorous fish or a different kind of seafood; and whether or not the patient had consumed a part of the seafood more likely to be high in CTXs (i.e., head or viscera). We excluded participants missing data on any of these variables, leading to a reduced sample size of $n = 38$, and considered acute symptoms that were observed in >10% ($n \geq 4$) and <90% ($n \leq 34$) of the $n = 38$ patients with complete data on the included biological tests and fish-related variables. We also considered participant age, sex, ciguatera incubation time (dichotomized at ≥12 h, with the assumption that a recorded ">3 h" meant <12 h, and a recorded "<24 h" meant ≥12 h), previous ciguatera, chronic hypertension, diabetes status, and tobacco consumption.

Thus, there were a total of $n = 38$, $p = 44$ included in the RLLR. All these candidate predictors were standardized prior to the RLLR to allow for comparable-magnitude regression coefficients. The RLLR models were implemented in Stata version 16.1 M/P software using the <lassopack> contributed by Ahrens, Hansen, and Schaffer [47]. We subsequently evaluated the predictive ability of the RLLR model by calculating the most likely outcome (i.e., chronic ciguatera case or not) model predictions in Stata for all n = 49 participants. All predictors were included in one model.

We then considered whether the significant candidate predictors of being a CP chronic case in the RLLR model were individually associated with being a chronic case in the larger patient sample with complete data on the candidate predictor (i.e., missing data were handled by pairwise deletion). We used Fisher's exact test for binary variables and two-sample equal-variance *t*-tests for the continuous variables (i.e., laboratory measures) differing according to chronic case status; we report two-tail hypothesis test *p* values. The Fisher's exact test and *t*-tests were implemented using Stata version 16.1 M/P software. Because there are likely to be an inflated Type I error rate when separately considering *p* values from multiple hypothesis tests [48,49], we therefore considered whether the post-hoc test results were Bonferroni-significant accounting for the number of hypothesis tests, assuming these predictors were independent hypothesis tests, by dividing the original significance threshold "$p < 0.05$" by the number of hypothesis tests. We deliberately chose a conservative method for dealing with multiple comparisons because we were aware of a second reason our results in the post-hoc test may be prone to elevated Type I error rates: these post hoc tests were selected conditional an already-fitted model applied to almost the same dataset [50]. These tests assumed independent and identically distributed observations which may be an unrealistic simplifying assumption.

We contrasted the most likely outcome for each participant predicted by the RLLR model against the observed chronic case status of each participant using MedCalc Statistical Software version 19.5.2. We report the model sensitivity, specificity, positive predictive value, negative predictive value, and accuracy [sensitivity * prevalence + specificity * (1-prevalence). We report exact confidence intervals [51] for the sensitivity, specificity, and accuracy, and standard logit confidence intervals [52] for the positive and negative predictive values. We assumed that the prevalence observed in this sample is representative

of the prevalence in the general population; similar assumptions about representativeness of our sample also apply to the other analyses reported in this paper.

We then considered the relationships of the variables suggested as predictive of being a chronic by the rigorous logistic lasso to another outcome: the time until cessation of symptoms among chronic ciguatera cases. For this analysis, we implemented a parametric survival analysis using accelerated failure-time regression models [53] assuming proportionate survival times. We conducted sensitivity analyses assuming a lognormal distribution of survival times vs. assuming a Weibull distribution of survival times. The predictors in the survival analysis models were standardized. Results are presented as survival time ratios per one unit change in predictor, with bootstrap percentile 95% confidence intervals [54], with 500 bootstrap replicates. These confidence intervals were selected due to their often-good performance at small sample sizes but ignore possible clustering of participants. These survival analyses were implemented using Stata version 16.1 M/P software.

Author Contributions: Conceptualization, C.M.i.G., K.C., E.O., M.O.G., and M.C.; Methodology, C.M.i.G., K.C., and E.O.; Formal analysis, T.J.P. and M.O.G.; Investigation, C.M.i.G. and K.C.; Data curation, C.M.i.G., K.C., and E.O.; Writing—original draft, C.M.i.G. and M.O.G.; Writing—review & editing, C.M.i.G., K.C., E.O., T.J.P., and M.C.; Supervision, C.M.i.G., E.O., and M.C.; Project administration, C.M.i.G.; Funding acquisition, M.O.G. All authors have read and agreed to the published version of the manuscript.

Funding: This study did not receive specific grants and was mainly performed as part of the professional activities of the authors whose employers are the Institut Louis Malardé and the Centre Hospitalier de la Polynésie française. Nevertheless, data statistical analysis received some funds from the United States National Institute for Environmental Health Sciences (NIEHS) and the National Institute on Aging (NIA): The Stata software license used in this paper was sponsored by NIA U54AG062334, and Dr. Gribble's effort was supported in part by NIEHS P30ES019776.

Institutional Review Board Statement: This study was conducted with the approval of the Direction of the Centre Hospitalier de Polynésie française, the ethic committee of French Polynesia). Data were processed in compliance with the European General Data Protection Regulation.

Informed Consent Statement: Informed consent was obtained from all subjects involved in the study.

Acknowledgments: The authors thank all the participants for their contribution to this study.

Conflicts of Interest: The authors declare no conflict of interest.

References

1. Lewis, R.J.; Holmes, M.J. Origin and transfer of toxins involved in ciguatera. *Comp. Biochem. Physiol. Part C Pharmacol. Toxicol. Endocrinol.* **1993**, *106*, 615–628. [CrossRef]
2. Litaker, R.W.; Holland, W.C.; Hardison, D.R.; Pisapia, F.; Hess, P.; Kibler, S.R.; Tester, P.A. Ciguatoxicity of Gambierdiscus and Fukuyoa species from the Caribbean and Gulf of Mexico. *PLoS ONE* **2017**, *12*, e0185776. [CrossRef]
3. Friedman, M.A.; Fleming, L.E.; Fernández, M.; Bienfang, P.; Schrank, K.; Dickey, R.; Bottein, M.-Y.; Backer, L.; Ayyar, R.; Weisman, R.; et al. Ciguatera Fish Poisoning: Treatment, Prevention and Management. *Mar. Drugs* **2008**, *6*, 456–479. [CrossRef] [PubMed]
4. Skinner, M.P.; Brewer, T.D.; Johnstone, R.; Fleming, L.E.; Lewis, R.J. Ciguatera Fish Poisoning in the Pacific Islands (1998 to 2008). *PLoS Negl. Trop. Dis.* **2011**, *5*, e1416. [CrossRef]
5. Benoit, E.; Juzans, P.; Legrand, A.-M.; Molgo, J. Nodal swelling produced by ciguatoxin-induced selective activation of sodium channels in myelinated nerve fibers. *Neuroscience* **1996**, *71*, 1121–1131. [CrossRef]
6. Hidalgo, J.; Liberona, J.L.; Molgó, J.; Jaimovich, E. Pacific ciguatoxin-1b effect over Na^+ and K^+ currents, inositol 1,4,5-triphosphate content and intracellular Ca^{2+} signals in cultured rat myotubes. *Br. J. Pharmacol.* **2002**, *137*, 1055–1062. [CrossRef]
7. Matsui, M.; Kumar-Roiné, S.; Darius, H.T.; Chinain, M.; Laurent, D.; Pauillac, S. Pacific ciguatoxin 1B-induced modulation of inflammatory mediators in a murine macrophage cell line. *Toxicon* **2010**, *56*, 776–784. [CrossRef] [PubMed]
8. Inserra, M.C.; Israel, M.R.; Caldwell, A.; Castro, J.; Deuis, J.R.; Harrington, A.J.; Keramidas, A.; Garcia-Caraballo, S.; Maddern, J.; Erickson, A.; et al. Multiple sodium channel isoforms mediate the pathological effects of Pacific ciguatoxin-1. *Sci. Rep.* **2017**, *7*, 42810. [CrossRef] [PubMed]

9. Friedman, M.A.; Fernandez, M.; Backer, L.C.; Dickey, R.W.; Bernstein, J.; Schrank, K.; Kibler, S.; Stephan, W.; Gribble, M.O.; Bienfang, P.; et al. An Updated Review of Ciguatera Fish Poisoning: Clinical, Epidemiological, Environmental, and Public Health Management. *Mar. Drugs* **2017**, *15*, 72. [CrossRef] [PubMed]
10. Cameron, J.; Capra, M.F. The Basis of the Paradoxical Disturbance of Temperature Perception in Ciguatera Poisoning. *J. Toxicol. Clin. Toxicol.* **1993**, *31*, 571–579. [CrossRef]
11. Pearn, J. Neurology of ciguatera. *J. Neurol. Neurosurg. Psychiatry* **2001**, *70*, 4–8. [CrossRef]
12. Chateau-Degat, M.L.; Beuter, A.; Vauterin, G.; Nguyen, N.L.; Chinain, M.; Darius, T.; Legrand, A.M.; Chansin, R.; Dewailly, E. Neurologic Signs of Ciguatera Disease: Evidence of their Persistence. *Am. J. Trop. Med. Hyg.* **2007**, *77*, 1170–1175. [CrossRef]
13. Vetter, I.; Touska, F.; Hess, A.; Hinsbey, R.; Sattler, S.; Lampert, A.; Sergejeva, M.; Sharov, A.; Collins, L.S.; Eberhardt, M.; et al. Ciguatoxins activate specific cold pain pathways to elicit burning pain from cooling. *EMBO J.* **2012**, *31*, 3795–3808. [CrossRef] [PubMed]
14. Pearn, J.H. Chronic fatigue syndrome: Chronic ciguatera poisoning as a differential diagnosis. *Med. J. Aust.* **1997**, *166*, 309–310. [CrossRef] [PubMed]
15. Chan, T.Y. Lengthy persistence of ciguatoxin in the body. *Trans. R. Soc. Trop. Med. Hyg.* **1998**, *92*, 662. [CrossRef]
16. Chateau-Degat, M.L.; Huin-Blondey, M.O.; Chinain, M.; Darius, T.; Legrand, A.M.; Nguyen, N.L.; Laudon, F.; Chansin, R.; Dewailly, E. Prevalence of Chronic Symptoms of Ciguatera Disease in French Polynesian Adults. *Am. J. Trop. Med. Hyg.* **2007**, *77*, 842–846. [CrossRef] [PubMed]
17. Gatti, C.M.I.; Lonati, D.; Darius, H.T.; Zancan, A.; Roué, M.; Schicchi, A.; Locatelli, C.A.; Chinain, M. Tectus niloticus (Tegulidae, Gastropod) as a Novel Vector of Ciguatera Poisoning: Clinical Characterization and Follow-Up of a Mass Poisoning Event in Nuku Hiva Island (French Polynesia). *Toxins* **2018**, *10*, 102. [CrossRef] [PubMed]
18. Mullins, M.E.; Hoffman, R.S. Is mannitol the treatment of choice for patients with ciguatera fish poisoning? *Clin. Toxicol.* **2017**, *55*, 947–955. [CrossRef] [PubMed]
19. Pearn, J. Chronic Ciguatera. *J. Chronic Fatigue Syndr.* **1996**, *2*, 29–34. [CrossRef]
20. Baumann, F.; Bourrat, M.-B.; Pauillac, S. Prevalence, symptoms and chronicity of ciguatera in New Caledonia: Results from an adult population survey conducted in Noumea during 2005. *Toxicon* **2010**, *56*, 662–667. [CrossRef]
21. Gatti, C.; Oelher, E.; Legrand, A.M. Severe seafood poisoning in French Polynesia: A retrospective analysis of 129 medical files. *Toxicon* **2008**, *51*, 746–753. [CrossRef]
22. Bertrand, S.; Berry, A.L. Enquête santé 2010 en polynésie française: Surveillance des facteurs de risque des maladies non transmissibles. *Bull. Épidémiol. Hebd.* **2013**, *28–29*, 326–332.
23. CPS. Le Diabète en Polynésie Française. Available online: http://www.cps.pf/espace-assure/promotion-de-la-sante/le-diabete-en-polynesie-francaise-0#2-quel-est-le-nombre-de-patients-diabtiques-en-lon (accessed on 1 July 2021).
24. Gatti, C.; Chinain, M.; Giard, M. *Situation de la Ciguatéra en Polynésie Française. Bilan 2016*; Institut Louis Malardé: Pape'ete, French Polynesia, 2017.
25. Gatti, C.; Chinain, M.; Henry, S. *Surveillance de la Ciguatéra en Polynésie Française. Bilan 2020*; Institut Louis Malardé: Pape'ete, French Polynesia, 2021.
26. Darius, H.T.; Roué, M.; Sibat, M.; Viallon, J.; Vandersea, M.W.; Tester, P.A.; Litaker, R.W.; Amzil, Z.; Hess, P.; Chinain, M. *Tectus niloticus* (Tegulidae, Gastropod) as a Novel Vector of Ciguatera Poisoning: Detection of Pacific Ciguatoxins in Toxic Samples from Nuku Hiva Island (French Polynesia). *Toxins* **2018**, *10*, 2. [CrossRef]
27. Schnorf, H.; Taurarii, M.; Cundy, T. Ciguatera fish poisoning: A double-blind randomized trial of mannitol therapy. *Neurology* **2002**, *58*, 873–880. [CrossRef]
28. Nicholson, G.M.; Lewis, R.J. Ciguatoxins: Cyclic Polyether Modulators of Voltage-gated Iion Channel Function. *Mar. Drugs* **2006**, *4*, 82–118. [CrossRef]
29. Shoemaker, R.C.; House, D.; Ryan, J.C. Defining the neurotoxin derived illness chronic ciguatera using markers of chronic systemic inflammatory disturbances: A case/control study. *Neurotoxicol. Teratol.* **2010**, *32*, 633–639. [CrossRef] [PubMed]
30. Lonati, D.; Martinetti, M.; Pasi, A.; Gatti, A.; Buonocore, M.; Locatelli, C.A. Clinical findings and genomic biomarkers in three cases of chronic ciguatera poisoning. *Clin. Toxicol.* **2014**, *52*, 395.
31. Ryan, J.C.; Wu, Q.; Shoemaker, R.C. Transcriptomic signatures in whole blood of patients who acquire a chronic inflammatory response syndrome (CIRS) following an exposure to the marine toxin ciguatoxin. *BMC Med. Genom.* **2015**, *8*, 1–12. [CrossRef]
32. Lopez, M.-C.; Ungaro, R.F.; Baker, H.V.; Moldawer, L.L.; Robertson, A.; Abbott, M.; Roberts, S.M.; Grattan, L.M.; Morris, J.G., Jr. Gene expression patterns in peripheral blood leukocytes in patients with recurrent ciguatera fish poisoning: Preliminary studies. *Harmful Algae* **2016**, *57*, 35–38. [CrossRef]
33. Schicchi, A.; Pasi, A.; Lonati, D.; Coccini, T.; Locatelli, C.A.; Martinetti, M. Ciguatoxin-induced chronic disease unmasks people carrying human leukocyte antigen (hla) epitopes peculiar to celiac disease and rheumatoid arthritis. *Clin. Toxicol.* **2017**, *55*, 469.
34. Blythe, D.; De Sylva, D.P.; Cramer-Castro, S. Ciguatera fish poisoning-the name may be difficult to remember. But if you get this disease, you'll never forget it. *Aqua Int.* **1992**, *13*, 26.
35. Arena, P.; Levin, B.; Fleming, L.; Friedman, M.A.; Blythe, D. A pilot study of the cognitive and psychological correlates of chronic ciguatera poisoning. *Harmful Algae* **2004**, *3*, 51–60. [CrossRef]

36. Friedman, M.A.; Arena, P.; Levin, B.; Fleming, L.; Fernandez, M.; Weisman, R.; Bernstein, J.; Schrank, K.; Blythe, D.; Backer, L.; et al. Neuropsychological study of ciguatera fish poisoning: A longitudinal case-control study. *Arch. Clin. Neuropsychol.* **2007**, *22*, 545–553. [CrossRef]
37. Geller, R.J.; Benowitz, N.L. Orthostatic Hypotension in Ciguatera Fish Poisoning. *Arch. Intern. Med.* **1992**, *152*, 2131–2133. [CrossRef] [PubMed]
38. Gatti, C.; Chinain, M.; Giard, M. *La Ciguatéra en Polynésie Française. Bilan 2018*; Institut Louis Malardé: Pape'ete, French Polynesia, 2019.
39. Katz, A.R.; Terrell-Perica, S.; Sasaki, D.M. Ciguatera on Kauai: Investigation of Factors Associated with Severity of Illness. *Am. J. Trop. Med. Hyg.* **1993**, *49*, 448–454. [CrossRef]
40. Au, N.P.B.; Kumar, G.; Asthana, P.; Tin, C.; Mak, Y.L.; Chan, L.L.; Lam, P.K.S.; Ma, C.H.E. Ciguatoxin reduces regenerative capacity of axotomized peripheral neurons and delays functional recovery in pre-exposed mice after peripheral nerve injury. *Sci. Rep.* **2016**, *6*, 26809. [CrossRef] [PubMed]
41. Liew, P.X.; Kubes, P. The Neutrophil's Role during Health and Disease. *Physiol. Rev.* **2019**, *99*, 1223–1248. [CrossRef] [PubMed]
42. Pierre, O.; Misery, L.; Talagas, M.; Le Garrec, R. Immune effects of the neurotoxins ciguatoxins and brevetoxins. *Toxicon* **2018**, *149*, 6–19. [CrossRef] [PubMed]
43. Wang, H.; Ran, J.; Jiang, T. Urea. *Subcell. Biochem.* **2014**, *73*, 7–29. [PubMed]
44. Chinain, M.; Gatti, C.M.I.; Darius, H.T.; Quod, J.-P.; Tester, P.A. Ciguatera poisonings: A global review of occurrences and trends. *Harmful Algae* **2021**, *102*, 101873. [CrossRef]
45. Tibshirani, R. Regression Shrinkage and Selection via the Lasso. *J. R. Stat. Soc. Ser. B* **1996**, *58*, 267–288. [CrossRef]
46. Belloni, A.; Chernozhukov, V.; Wei, Y. Post-Selection Inference for Generalized Linear Models with Many Controls. *J. Bus. Econ. Stat.* **2016**, *34*, 606–619. [CrossRef]
47. Ahrens, A.; Hansen, C.B.; Schaffer, M.E. lassopack: Model selection and prediction with regularized regression in Stata. *Stata J. Promot. Commun. Stat. Stata* **2020**, *20*, 176–235. [CrossRef]
48. Benjamini, Y.; Hochberg, Y. Controlling the False Discovery Rate: A Practical and Powerful Approach to Multiple Testing. *J. R. Stat. Soc. Ser. B* **1995**, *57*, 289–300. [CrossRef]
49. Benjamini, Y. Simultaneous and selective inference: Current successes and future challenges. *Biom. J.* **2010**, *52*, 708–721. [CrossRef] [PubMed]
50. Lee, J.D.; Sun, D.L.; Sun, Y.; Taylor, J.E. Exact post-selection inference, with application to the lasso. *Ann. Stat.* **2016**, *44*, 907–927. [CrossRef]
51. Clopper, C.J.; Pearson, E.S. The use of confidence or fiducial limits illustrated in the case of the binomial. *Biometrika* **1934**, *26*, 404–413. [CrossRef]
52. Mercaldo, N.D.; Lau, K.F.; Zhou, X.H. Confidence intervals for predictive values with an emphasis to case–control studies. *Stat. Med.* **2007**, *26*, 2170–2183. [CrossRef]
53. Cox, C.; Chu, H.; Schneider, M.F.; Muñoz, A. Parametric survival analysis and taxonomy of hazard functions for the generalized gamma distribution. *Stat. Med.* **2007**, *26*, 4352–4374. [CrossRef]
54. DiCiccio, T.J.; Efron, B. Bootstrap confidence intervals. *Stat. Sci.* **1996**, *11*, 189–228. [CrossRef]

toxins

MDPI

Article

Depuration Kinetics and Growth Dilution of Caribbean Ciguatoxin in the Omnivore *Lagodon rhomboides:* Implications for Trophic Transfer and Ciguatera Risk

Clayton T. Bennett [1,2] and Alison Robertson [1,2,*]

[1] School of Marine and Environmental Sciences, University of South Alabama, Mobile, AL 36688, USA; claybennett08@gmail.com
[2] Dauphin Island Sea Lab, Dauphin Island, AL 36528, USA
* Correspondence: arobertson@disl.org; Tel.: +1-(251)-414-8163

Abstract: Modeling ciguatoxin (CTX) trophic transfer in marine food webs has significant implications for the management of ciguatera poisoning, a circumtropical disease caused by human consumption of CTX-contaminated seafood. Current models associated with CP risk rely on modeling abundance/presence of CTX-producing epi-benthic dinoflagellates, e.g., *Gambierdiscus* spp., and are based on studies showing that toxin production is site specific and occurs in pulses driven by environmental factors. However, food web models are not yet developed and require parameterizing the CTX exposure cascade in fish which has been traditionally approached through top-down assessment of CTX loads in wild-caught fish. The primary goal of this study was to provide critical knowledge on the kinetics of C-CTX-1 bioaccumulation and depuration in the marine omnivore *Lagodon rhomboides*. We performed a two-phase, 17 week CTX feeding trial in *L. rhomboides* where fish were given either a formulated C-CTX-1 (n = 40) or control feed (n = 37) for 20 days, and then switched to a non-toxic diet for up to 14 weeks. Fish were randomly sampled through time with whole muscle, liver, and other pooled viscera dissected for toxin analysis by a sodium channel-dependent MTT-based mouse neuroblastoma (N2a) assay. The CTX levels measured in all tissues increased with time during the exposure period (days 1 to 20), but a decrease in CTX-specific toxicity with depuration time only occurred in viscera extracts. By the end of the depuration, muscle, liver, and viscera samples had mean toxin concentrations of 189%, 128%, and 42%, respectively, compared to fish sampled at the start of the depuration phase. However, a one-compartment model analysis of combined tissues showed total concentration declined to 56%, resulting in an approximate half-life of 97 d (R^2 = 0.43). Further, applying growth dilution correction models to the overall concentration found that growth was a major factor reducing C-CTX concentrations, and that the body burden was largely unchanged, causing pseudo-elimination and a half-life of 143–148 days (R^2 = 0.36). These data have important implications for food web CTX models and management of ciguatera poisoning in endemic regions where the frequency of environmental algal toxin pulses may be greater than the growth-corrected half-life of C-CTX in intermediate-trophic-level fish with high site fidelity.

Keywords: *Lagodon rhomboides*; pinfish; bioaccumulation; depuration; ciguatoxin; Caribbean ciguatoxin; ciguatera; growth dilution; model; kinetics

Key Contribution: This study demonstrates that decreases in C-CTX concentration in fish tissues relate to organismal redistribution across tissues and are a factor of growth dilution, rather than systemic elimination. We demonstrate the importance of evaluating growth dilution during long-term studies of CTX and other natural toxins to avoid underestimates of toxin body burden and overestimates of depuration rates, which have clear implications for trophic transfer and ciguatera poisoning risk.

Citation: Bennett, C.T.; Robertson, A. Depuration Kinetics and Growth Dilution of Caribbean Ciguatoxin in the Omnivore *Lagodon rhomboides:* Implications for Trophic Transfer and Ciguatera Risk. *Toxins* **2021**, *13*, 774. https://doi.org/10.3390/toxins13110774

Received: 27 September 2021
Accepted: 29 October 2021
Published: 1 November 2021

1. Introduction

Benthic dinoflagellates have the capacity to produce a diverse suite of bioactive secondary metabolites that have been linked with seafood safety and human health concerns globally. One such group includes the neurotoxic ciguatoxins (CTXs) that have been linked to ciguatera poisoning and have been associated with some species and strains of epibenthic dinoflagellates from the genus *Gambierdiscus* and *Fukuyoa* [1–5]. Several studies have reported that the in situ dinoflagellate community assemblage can change with environmental factors (e.g., temperature) and that species and strains may have physiological niches [6–8]. Likewise, long-term field studies have demonstrated that the CTX load of field-collected benthic microalgae is: (1) asynchronous with *Gambierdiscus* abundance; (2) site specific; (3) seasonal; and (4) occurring in pulses in tropical reef ecosystems [6,9]. It has also been proposed that CTX environmental pulses are linked to the presence of highly toxic *Gambierdiscus* strains rather than high overall algal biomass [5,6,9,10] potentially reducing the effectiveness of genus-level monitoring for these benthic HABs in terms of risk reduction. This presents some questions on the subsequent CTX load and CTX pulses that may occur in other demersal marine biota feeding on potentially toxicogenic epiphytic algae, aquatic invertebrates (e.g., amphipods), and other small grazers.

While still a working hypothesis in the field, the bioaccumulated CTX load in fish collected from ciguatera poisoning hotspots (and therefore ciguatera risk) is a function of the rate of toxin production by epi-benthic dinoflagellates (conceptual model in Lewis et al. [11] and revisited in Lewis and Holmes [12]). However, there remains a gap in understanding the timing between these processes. Field-based studies have provided evidence of a temporal lag of months to years occurring between the environmental triggers that increase toxin production, toxicity in upper-trophic-level fish, and increasing ciguatera cases [13,14]. Further, high fish toxicity (and resulting ciguatera prevalence) has been observed in high-site-fidelity fish when toxigenic dinoflagellate abundance and toxicity are low (or absent), suggesting a shift towards a non-toxic area [15,16], which leads to an assumption that bioaccumulated CTX is persistent in fish after the dinoflagellate source declines. However, field studies lack the ability to properly investigate ecologically relevant exposure routes (e.g., dietary, respiration, dermal) or the rates of uptake and depuration once a CTX source is removed, because total source removal can only be assumed.

Early studies attempted to investigate the retention of CTX-like toxicity (as a proxy for CTX, which was yet to be structurally elucidated) in a laboratory setting using fish that had naturally incurred toxin. For example, in Hawaii, Takata and colleagues (reported by [17]) allowed wild-caught Lutjanids (*Lutjanus bohar*, *L. gibbus*) and a Serranid (*Variola louti*) to depurate in aquariums at various intervals up to 14 months, while Banner et al. [17] kept wild *L. bohar* in holding ponds up to 30 months. In both studies, fish at the end remained toxic when fed to cats and mongoose. Davin et al. [18] fed several species of marine and freshwater fish the ground flesh or extracts of barracuda (*Sphyraena*) or whole *Gambierdiscus* cells (both sourced near the Caribbean Antilles Islands), followed by depuration time up to 81 d. Many of the fish died or were intoxicated. Largemouth bass (*Micropterus salmoides*) fed a high dose of cells recovered behaviorally but remained moderately toxic by intraperitoneal injection to mice after 81 days of clean feed, but fish fed lower doses were non-toxic after depuration. Recently, more laboratory studies have focused on CTX elimination using several exposure methods and in a variety of organisms. For instance, Ledreux et al. [19] performed single-oral dose-recovery experiments with mullet (*Mugil cephalus*) fed *G. polynesiensis* cells and reported only 5% of the CTX activity occurred in tissues after 24 h when analyzed by the mouse neuroblastoma assay (N2a). Li et al. [20] described multiple tissue kinetics of three Pacific CTX congeners, namely P-CTX-1 (CTX1B), P-CTX-2 (52-epi-54-deoxyCTX1B), and P-CTX-3 (54 deoxyCTX1B) extracted from eel (*Lycodontis javanicus*). Toxins were added to a pelleted feed and given to juvenile orange-spotted grouper (*Epinephilus coioides*) for 30 d and subsequently depurated for 30 d. The authors reported that CTX declined exponentially in depuration in some tissues (including muscle); however, CTX burden by the end of the study was not significantly different from

the levels measured prior to depuration [20]. In another recent report, Caribbean CTX (C-CTX-1) depuration was investigated in the muscle of the freshwater goldfish (*Carassius auratus*) following a 43 d daily feeding of naturally C-CTX incurred amberjack (*Seriola* sp.) flesh prepared in agarose [21]. Estimated CTX toxicity (concentration) in muscle was reported to decline by approximately 86% out to 60 d post-exposure, but other tissues were not analyzed. Most recently, a depuration experiment using juvenile lionfish (*Pterois volitans*) was reported after 30–41 d experimental feeding on the flesh of the naturally P-CTX-contaminated parrotfish (*Chlorurus microrhinos*) [22]. Extracts from pooled liver showed a gradual decline in CTX concentration in fish harvested during a 43 d depuration, where fish were switched to a non-toxic diet of farmed sea bream (*Sparus auratus*). These two latter studies report depuration in single tissues (muscle and liver, respectively) and provide informative data on trends in bioaccumulation and depuration following oral exposure but were unable to capture cross-tissue distribution and did not examine fish growth that may contribute to the change in CTX tissue concentrations, but not body burden, as suggested by Holmes et al. [23] in a recent field-based study and review. We propose that estimates of toxicokinetic rates that also incorporate growth dilution may be more valuable than CTX concentrations in tissues in studies aiming to predict or model CP risk in the food web across species.

In this study, we provide data on the kinetic rate of C-CTX-1 bioaccumulation and depuration in the ecologically relevant marine omnivore *Lagodon rhomboides* (pinfish). Replicate fish were either fed a C-CTX-1 (n = 40) formulated diet or matrix matched control (n = 37) for 20 d, and then placed into depuration for up to 99 d. CTX toxicity in the major tissue compartments of *L. rhomboides* were quantified and compared through time and across replicates compared to control fish using an in vitro mouse neuroblastoma (N2a-MTT) assay.

Sampling and CTX analysis of whole muscle, liver, and other pooled visceral contents (heart, spleen, gall bladder, intestine) throughout the time course revealed dynamic trends in tissue burden and kinetics. Further, modeling concentrations corrected for fish growth dilution revealed an increase in the estimated half-life of C-CTX-1 in *L. rhomboides*, highlighting growth as a major source of pseudo-elimination of accumulated CTX. This correction reveals that C-CTX (measured here as a CTX3C equivalents) can be retained for several months following removal from the toxin source and if not accounted for could result in error during CP risk assessment and analysis of food web transfer potential. This work should be considered when sampling mid-trophic-level fish with high site fidelity and in the development of temporal models of CTX cascades where the frequency of toxin pulses may be shorter than the CTX half-life in fish. These data have implications for CP risk analysis in fish and may help to explain high toxin loads in highly migratory species collected in non-endemic regions for ciguatera (e.g., barracuda, mackerel, amberjack).

2. Results

2.1. Experimental Design, Diet Formulation and Consistency

Two dual-phase experimental trials were conducted to assess the depuration of Caribbean CTX-1 (C-CTX-1) that had bioaccumulated in *Lagodon rhomboides* fed a control or low-dose CTX diet through time and were sampled according to Table 1. A laboratory formulated diet was prepared and analyzed for procedural consistency (Table 2). Parameters including water content, pellet weight, whole-food CTX concentration, and pellet CTX concentration were quantified in all three batches of CTX pellets and four batches of control food for each trial. Slight differences were recorded in the water content of pellets after drying; however, food preparation was identical and resulted in the equivalent pellet weights. See methods for full details on the preparation of the control and CTX formulated diet.

Table 1. Number of replicates (*n*) Control and ciguatoxin (CTX)-exposed *Lagodon rhomboides* sampled during two trials where CTX-exposed individuals were fed pelleted Caribbean CTX-1 at 0.02 ng CTX3C eq. g^{-1} fish (initial weight) day^{-1}. Days in parentheses are number of days in the depuration phase while non-parentheses numbers are total days in the experiment.

Phase of Experiment	Experiment Day	Trial 1 (N)		Trial 2 (N)	
		Control	CTX	Control	CTX
Bioaccumulation	0	4	-	3	-
	6	4	4	-	-
	10	4	4	-	-
	20	4	4	2	4
Depuration	25 (5)	4	4	-	-
	30 (10)	4	4	-	-
	40 (20)	4	4	-	-
	60 (40)	-	-	2	4
	90 (70)	-	-	-	4
	119 (99)	-	-	2	4
Total		28	24	9	16

Table 2. Quality control of experimental treatments using the formulated pellet diet. Values are provided as the mean ± standard deviation (s.d.) of subsamples from each batch (per trial, control = 4, CTX = 3).

Quality Control Parameter	Trial 1		Trial 2	
	Treatment			
	Control	CTX	Control	CTX
Pellet Water Content (%) [a]	35.8 ± 0.5	27.0 ± 4.0	37.3 ± 1.5	33.7 ± 2.9
Pellet Weight (g) [b]	0.10 ± 0.00	0.09 ± 0.01	0.09 ± 0.01	0.09 ± 0.01
Food CTX Concentration (ng g^{-1}) [c]	0	1.06 ± 0.06	0	0.96 ± 0.04
Pellet CTX Concentration (ng $pellet^{-1}$) [c]	0	0.096 ± 0.020	0	0.091 ± 0.019
% of Initial Weight Fed Daily (whole) [d]	1.9 ± 0.2	1.8 ± 0.2	1.7 ± 0.1	1.8 ± 0.1
% of Initial Weight Fed Daily (dry) [e]	1.2 ± 0.1	1.3 ± 0.1	1.1 ± 0.1	1.2 ± 0.0
Consumption Rate (ng g^{-1} fish day^{-1}) [f]	0	0.019 ± 0.002	0	0.017 ± 0.001

[a] Calculated from the weight of dry ingredients in the whole food after drying. [b] Calculated from the mean weight of 40 pellet subsamples per batch. [c] Calculated using the CTX3C eq. concentration of dried toxic barracuda powder and amount of powder in the mixture. [d] Calculated from the average weight of pellets provided daily and weight of fish on day 0. [e] Calculated using pellet water content and percentage of initial weight fed daily (whole). [f] Calculated from total weight of pellets provided daily, pellet CTX3C eq. concentration, and initial weight of fish.

2.2. Fish Growth

The mean initial weight of fish in the first trial (24.4 ± 9.4 g) was smaller than the second (36.4 ± 5.9 g; $p < 0.0001$); however, feeding rate was normalized to each fish at the start of trials so that fish consumed proportionally similar food and CTX relative to their mass (Table 2). At initial, fish were fed approximately 1.8% by weight equaling an exposure rate of around 0.018 ng CTX3C eq. g^{-1} fish day^{-1} that declined to 0.015 ng CTX3C eq. g^{-1} fish day^{-1} due to fish growth by day 20 when CTX feeding was stopped. The growth rate constants (k_g) of control and CTX-treated fish collected at the same time point were similar except on experimental day 20 in both trials (see Supplementary Table S1). This effect was resolved when CTX-fed fish were swapped to the non-toxic diet for depuration.

Raw k_g determined for the combined experiment between treatments were non-parametric according to statistical comparisons and visual inspection of the residual plots highlighted that the variability on day 6 and 10 d were responsible. Growth rates between replicate fish stabilized from day 10 to 20 (bioaccumulation) as fish stabilized to their control and experimental feeding regime. Exclusion of the data points in the early portion of the trial (day 1–10) restored normality and homoscedasticity. An ANOVA and post hoc analysis showed that the k_g on days 20 and 25 were significantly different than days 90 and

119 in the CTX fish (Supplementary Figure S2B). The k_g at day 40 was a transition period and was not significantly different than other time points. Non-linear regression using a one-phase exponential decay model to the k_g of fish against time ($R^2 = 0.70$) showed k_g neared a plateau around experimental day 55 at approximately 4.07×10^{-3} day^{-1} (see Figure 1). The mean weight of CTX and control fish on the last day were 78 ± 13% and 65 ± 17% larger than at the beginning of the study which caused the daily feeding rate to decrease from around 1.8% to 1.0% of fish biomass by the end of the experiment.

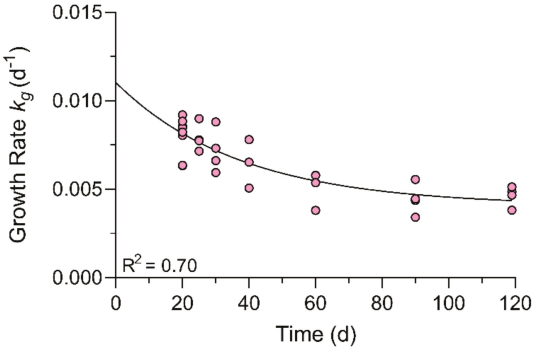

Figure 1. Non-linear regression of growth rate (k_g) and time course in days of CTX fish in depuration.

2.3. Toxin Distribution in the Bioaccumulation Phase

Maximum concentrations of extracts used for CTX quantification were 50, 10, and 2.5 mg tissue equivalents (TE) $well^{-1}$ (217.4, 43.5, and 10.9 mg TE mL^{-1}) for muscle, liver, and viscera samples, respectively, and the mean value of the 75% maximal effective concentration (EC_{75}) from CTX3C dose–response curves was 0.452 ± 0.151 pg $well^{-1}$ (1.965 ± 0.657 pg mL^{-1}). Based on these data the limit of quantification (LOQ) for each tissue was 0.009 ± 0.003 (muscle), 0.045 ± 0.015 (liver), and 0.181 ± 0.060 (viscera) ng CTX3C eq. g^{-1} tissue (Supplementary Figure S1). Brain was extracted and analyzed on a screening basis up to a 30 mg TE dose (130.4 mg TE mL^{-1}) on the N2a-MTT, but all were non-toxic. Likewise, only 9 fish had gonads that were mature while all others were immature and unrecognizable. Mature gonads were extracted and assayed up to a 10 mg TE (43.5 mg TE mL^{-1}) and were also non-toxic, therefore brain and gonads were excluded from further study. Quantifiable CTX3C eq. concentrations were possible in viscera across all sampling points, whereas the CTX toxicities in other tissues were detectable but not quantifiable (based on our QAQC criteria) until later time points.

For instance, CTX was detected on the first sampled time point (day 6) in all muscle extracts, but only one fish reached levels exceeding the LOQ. Likewise, CTX was not detected in 3 of the 4 fish livers from day 6 due to non-specific matrix effects on the N2a-MTT but were quantifiable from one replicate fish. After 10 d of CTX meals, 2 of 4 fish had CTX detectable in muscle and 2 of 4 fish sampled could be quantified. After 20 d of CTX feeding, all tissue extracts of sampled fish had toxicity above the determined LOQ and were the highest measured during the CTX feeding phase.

Mean CTX3C eq. concentrations in all tissues of fish harvested on day 20 were not different between trials based on a *t*-test (Table 3). Mean CTX3C eq. concentrations were significantly different in muscle on day 20 of trial 1 and trial 2 compared to day 6 ($p < 0.05$ and $p < 0.001$, respectively) and on day 20 (trial 2) compared to day 10 ($p < 0.01$; $\alpha = 0.05$; Supplementary Figure S3A), but no statistical difference was found in liver or viscera of fish sampled during the bioaccumulation phase (day 6–20) based on ANOVA (Supplementary Figure S3B,C). A steady state of CTX concentration was not reached by day 20 based on the continued upward trend in CTX through the feeding period (Figure 2). Since this was not the goal of the present study, this was an acceptable outcome.

Table 3. Between-trial reproducibility of CTX-1 concentrations measured as CTX3C eq. by mouse neuroblastoma assay (N2a-MTT) in fish tissues collected at day 20. Data for each trial are the mean ± s.d. (n = 4). All controls were negative and are not shown. A two-tailed t-test was performed to test for significant differences (α 0.05; df = 6).

Tissue	CTX3C Eq.		Statistics	
	Trial 1	Trial 2	t	p-Value
Muscle	0.04 ± 0.02	0.06 ± 0.01	1.39	0.214
Liver	1.01 ± 0.99	0.91 ± 0.48	0.165	0.875
Viscera	4.40 ± 1.17	3.80 ± 0.37	0.971	0.369

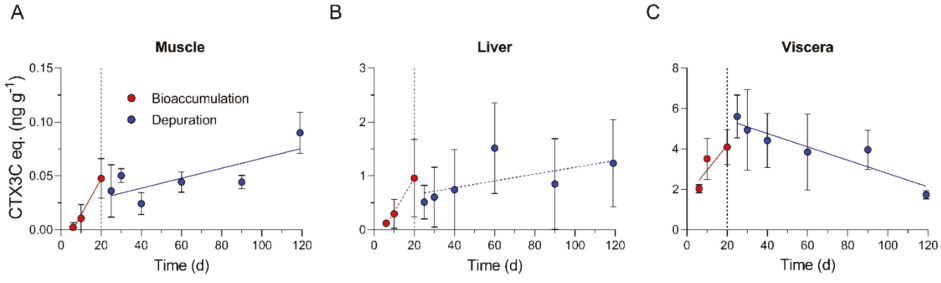

Figure 2. Linear regression of CTX-1 measured as a CTX3C eq. concentration (mean ± s.d.) in sampled (**A**) muscle, (**B**) liver, and (**C**) viscera through bioaccumulation (red) and depuration (blue). Solid regression lines denote a significant correlation while dashed lines were not significant due to high variability between individual fish within a tissue type. Control fish were negative for CTX in all cases and are not plotted. Data points represent the mean ± s.d. of replicate fish (n = 4 except on day 20 where n = 8 across two trials).

2.4. Toxin Distribution in the Depuration Phase

The primary goal of this study was to estimate depuration and based on the consistency of CTX3C eq. concentrations in fish analyzed at day 20 (see Table 3), we had confidence in combining sample data from the two identical trials for an extended depuration phase analysis (details in methods; summary in Table 1).

Mean CTX3C eq. concentration in muscle extracts were not significantly different between 0 and 70 d into the depuration period (Supplementary Figure S3A). The highest mean muscle CTX concentrations were measured in fish 99 d into depuration (day 119 of the complete study) and was 0.09 ng CTX3C eq. g^{-1} TE (Figure 2A). The mean concentration in muscle on the last day of depuration was significantly higher than those measured at all prior time points based on ANOVA, except for the day 20 fish from trial 2 which only marginally fell outside the criteria for significance (α = 0.05; p = 0.054; Supplementary Figure S3A). Consistent with these results were lower extract doses on the N2a-MTT needed for fish sampled on day 119 (5–20 mg TE) versus fish sampled earlier in the depuration phase (30–50 mg TE).

Liver extract CTX3C eq. concentrations from replicate fish in the depuration phase were the most variable of the tissues analyzed with relative standard deviation for trials 1 and 2 between 60 and 100% and 52 and 99%, respectively. This variability was consistent during both trials and through each sampling point with no significant trends (R^2 = 0.09; p = 0.152; Figure 2B). Concentrations in liver of fish from trials 1 and 2 during depuration ranged from 0.12 to 1.77 and 0.23 to 2.52 ng CTX3C eq. g^{-1} TE, respectively, and no statistical differences were found between days 20 and 119 (α = 0.05; Supplementary Figure S3B).

Mean toxicity of viscera extracts were highest in fish sampled 5 d into the depuration phase (5.61 ± 1.06 ng CTX3C eq. g^{-1} TE; Figure 2C). No significant loss of CTX from viscera was measured by the end of trial 1 (day 20 = 4.40 ± 1.17 vs. day 40 = 4.43 ± 1.34 ng CTX3C eq. g^{-1} TE; Supplementary Figure S3C). When depuration time was extended in

trial 2, a significantly lower concentration was measured on day 119 (1.73 ± 0.21 ng CTX3C eq. g^{-1} TE) than was measured 5 d and 10 d into depuration (day 25 vs. 119 $p < 0.01$; day 30 vs. 119 $p = 0.018$; Supplementary Figure S3C).

2.5. Muscle, Liver, and Viscera CTX Kinetics

Linear regression of the bioaccumulation phase data showed a positive correlation between the number of exposure days and CTX3C eq. concentration for muscle and viscera ($R^2 = 0.70$, $p = 0.0001$; $R^2 = 0.47$, $p < 0.01$, respectively; Figure 2A, and 2C; Table 4). The best fit models for bioaccumulation in both cases were simple straight-line equations (muscle and viscera AICc = 100 and 99.4%, respectively) in the form of $y = k_{uptake} * x + b$, where k_{uptake} is uptake rate (ng CTX3C eq. g^{-1} fish day^{-1}) equal to 3.37×10^{-3} for muscle and 0.124 for viscera (Table 4). Some liver samples on days 6 ($n = 3$) and 10 ($n = 2$) were excluded from the regression analyses due to significant non-specific matrix issues on the N2a-MTT assay because a value of zero could not be assumed. Liver concentrations during accumulation followed a non-significant increase ($R^2 = 0.24$, $p = 0.129$; Table 4), so an uptake rate is not reported.

Table 4. Results of linear regression analysis for CTX3C eq. concentrations in fish samples during the experimental bioaccumulation and depuration phases.

Tissue	Statistical Parameters	Bioaccumulation	Depuration
Muscle	Linear equation	y = 0.0034x − 0.0200	y = 0.0005x + 0.0201
	R^2	0.70	0.43
	p-value	0.0001	0.0005
Liver	Linear equation	y = 0.0630x − 0.3024	y = 0.0063x + 0.5277
	R^2	0.24	0.09
	p-value	0.1291	0.1518
Viscera	Linear equation	y = 0.1239x + 1.704	y = −0.0331x + 6.093
	R^2	0.47	0.43
	p-value	0.0034	0.0005

Straight line and one-phase exponential decay models were chosen for comparison of depuration kinetics of individual tissues. Depuration resulted in a linear decrease in viscera CTX3C eq. concentration ($R^2 = 0.44$; $p = 0.0005$; Figure 2C), but an unexpected linear increase occurred with depuration time for muscle ($R^2 = 0.43$; $p = 0.0005$; Figure 2A). The regression was likely skewed because of the weight of day 119 on the end of the regression line. Model comparison to describe depuration kinetics of tissues also showed simple linear models were the most probable in each case and depuration rates for muscle and viscera were -4.62×10^{-4} and 3.31×10^{-2}, respectively (Table 4). However, liver CTX concentrations did not follow any pattern of depuration ($R^2 = 0.09$; $p = 0.152$), so a depuration rate is not reported here.

2.6. Muscle, Liver, and Viscera CTX Burdens

Tissue burden, i.e., the amount of contaminant per tissue (ng CTX $tissue^{-1}$) was calculated by multiplying the CTX concentration in each tissue by the whole tissue wet weight determined at the time of dissection. The concentrations of CTX (ng CTX g^{-1} TE) within *L. rhomboides* tissues were present at levels of descending concentration as follows: viscera > liver > muscle. However, the tissue CTX burden (that incorporates total tissue mass) showed some variability between individuals. For instance, viscera carried the highest toxin burden in all fish fed CTX throughout the entire experiment followed by muscle in 28 individuals. In the other 12 CTX-exposed individuals, liver CTX burden was slightly higher (1.4 ± 0.3 fold) than in muscle for 10 fish. CTX was not detected in muscle and liver of two fish at day 6 which prevented a comparison.

Total CTX body burdens in fish were not directly compared across days because fish were fed different amounts of CTX based on individual starting body weight. Instead,

toxin burdens of replicate fish were compared by the relative distribution of CTX as a percent of the sum of toxin burden measurements in tissue compartments (Figure 3). Up to day 40, viscera contained most of the total measured toxicity (89 ± 9%) followed by muscle (7 ± 4%) and liver (3 ± 2%). From day 40 to 119, the relative distribution of toxicity began to shift. While relative viscera burden declined to 44% the relative muscle burden increased to 41% on the last day.

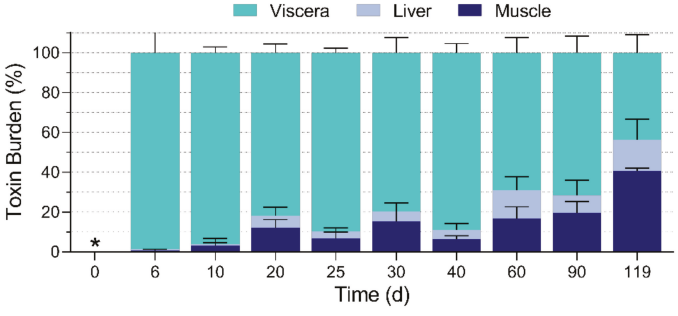

Figure 3. Distribution of the C-CTX-1 burden in tissues of *L. rhomboides* expressed as a percent of the whole burden measured in CTX3C eq. Note that fish were placed into depuration after day 20. Bars represent the mean ± s.d. of replicate fish (n = 4 except on day 20 where n = 8 across two trials). * CTX was below detectable levels on day 0.

2.7. One-Compartment Model Kinetics and Growth Correction

For the one-compartment model, the total concentration (C_{fish}) represents the sum of CTX burdens in muscle, liver, and viscera divided by the combined mass of those tissues. The one-compartment model showed CTX bioaccumulation in *L. rhomboides* followed a linear increase from day 0 to 20 at an overall k_{uptake} of 8.80 × 10^{-3} ng g^{-1} day^{-1} (R^2 = 0.67, p = 0.0001; Figure 4).

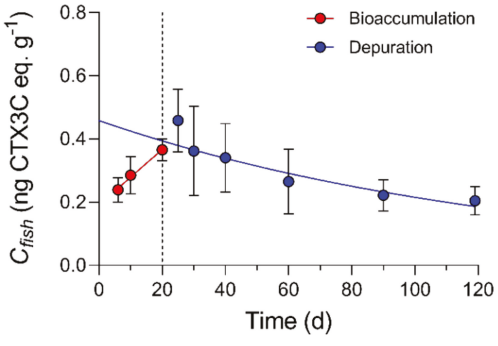

Figure 4. One compartment analysis of accumulated C-CTX-1 quantified by N2a-MTT as a PCTX3C eq. showed bioaccumulation (red) followed a linear pattern, while depuration (blue) followed exponential decay. The uptake rate (k_{uptake}) calculated by linear regression was equal to 8.80 × 10^{-3} ng CTX3C eq. g^{-1} day^{-1} (R^2 = 0.67, p = 0.0001) and logarithmic transformation of depuration data resulted in a first-order relationship (R^2 = 0.43). The overall elimination rate constant (k_2) was 7.161 × 10^{-3} day^{-1} based on the slope of the linear plot. Vertical dashed lines indicate the point where fish were swapped from CTX feed to a non-toxic food for the depuration phase. Data points represent the mean ± s.d. of replicate fish (n = 4 except on day 20 where n = 8 across two trials).

The straight-line plot of the transformed total concentration data (Ln [C_{fish}]) against time confirmed depuration approximately followed first-order kinetics (R^2 = 0.43) and the overall k_2 (linear slope) was equal to 7.161 × 10^{-3} with an estimated half-life of 97 d. Significant fish growth that was measured during the depuration phase meant the kinetic rate of elimination needed to be normalized to the CTX dilution rate due to increasing fish mass, a source of pseudo-elimination. Growth correction of k_2 was investigated through multiple exponential decay simulations of the depuration phase data, where measured k_2 is adjusted using measured fish growth rates ($k_2 - k_g = k_{2\ growth\text{-}corrected}$) and based on estimates of initial CTX3C eq. concentrations ($C_{fish(i)}$) immediately prior to depuration. The combined mass of whole muscle, liver, and viscera tissues (∑ [muscle + liver + viscera] g) had a strong linear correlation with whole body mass (R^2 = 0.95; Figure 5) during the study, as did total accumulated burdens with cumulative doses at the end of the bioaccumulation phase (day 20) (R^2 = 0.95; Figure 6) and provided a good estimate of initial CTX3C eq. concentrations (estimated $C_{fish(i)}$ = total CTX3C eq. burden/sum mass of whole muscle, liver, and viscera) in each fish that entered depuration.

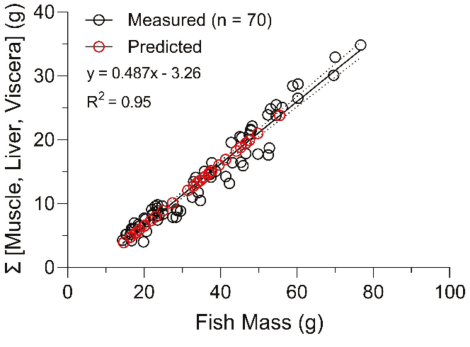

Figure 5. Combined sum of measured tissue masses (∑ [muscle + liver + viscera]) (black) of all *L. rhomboides* sampled in this study as a function of total fish mass. Total body masses at the start of depuration were estimated using an exponential growth formula (see Methods) and were used to estimate the ∑ [muscle + liver + viscera] (red) for each fish at experiment day 20 which entered the depuration phase (n = 24). Dashed lines are 95% confidence intervals.

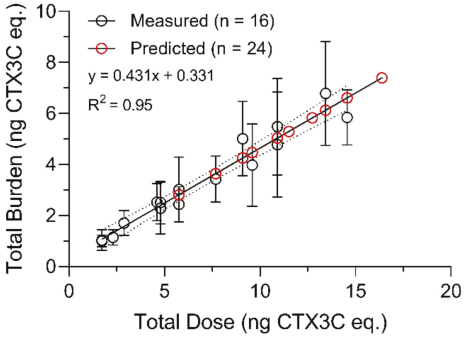

Figure 6. Linear correlation of cumulative CTX burden with total dose in *L. rhomboides* sampled during the bioaccumulation phase (black; n = 16; R^2 = 0.95). The relationship was used to estimate the CTX burden at the start of the depuration phase (i.e., after day 20) for fish remaining after the bioaccumulation period that entered depuration (red; n = 24). Dashed lines are 95% confidence intervals. Error bars are standard deviation of the CTX burdens (measured concentration ± s.d. × tissue mass). Some points overlap.

In the Simulation Model (Figure 7A), regression analysis with logarithmic transformation of the predicted $C_{fish(t)}$ values for each depuration time point (Ln [$C_{fish(t)}$] = $-k_2 * t$ + Ln [$C_{fish(i)}$]) resulted in a predicted half-life of 75 d (R^2 = 0.70; compared to 97 d from measured $C_{fish(t)}$) and a correlation showed the Simulation Model fit closely to the measured $C_{fish(t)}$ (R^2 = 0.68; p = 0.02). The Simulation Model was used as a starting point whereby several models were compared to assess the effect of growth. In Model 1, growth correction of the Simulation Model using the replicate average k_g at each sampled time point (Figure 1; Table 5) increased the half-life to approximately 143 d based on model fitting parameters (Model 1: $k_{2\ growth\text{-}corrected}$ = 4.84 × 10^{-3}; R^2 = 0.364; Figure 7B). Growth correction for Model 2 was performed using three growth rates based on the ANOVA and Tukey's test (Table 6; Supplementary Figure S1B) and produced a similar half-life at 148 d (Model 2: $k_{2\ growth\text{-}corrected}$ = 4.68 × 10^{-3}; R^2 = 0.345; Figure 7C). Likewise, growth correction using the k_g measured for each individual fish resulted in a half-life of approximately 143 d (Model 3: $k_{2\ growth\text{-}corrected}$ = 4.83 × 10^{-3}; R^2 = 0.360; Figure 7D). Lastly, a common approach to growth correction was performed by multiplying the measured concentrations by a correction factor (1 + k_g * time). The correction factor method resulted in a half-life of approximately 157 d, although the uncertainty was greater in this model shown by the lower coefficient of determination (correction factor method: $k_{2\ growth\text{-}corrected}$ = 4.41 × 10^{-3}; R^2 = 0.22; Figure 7).

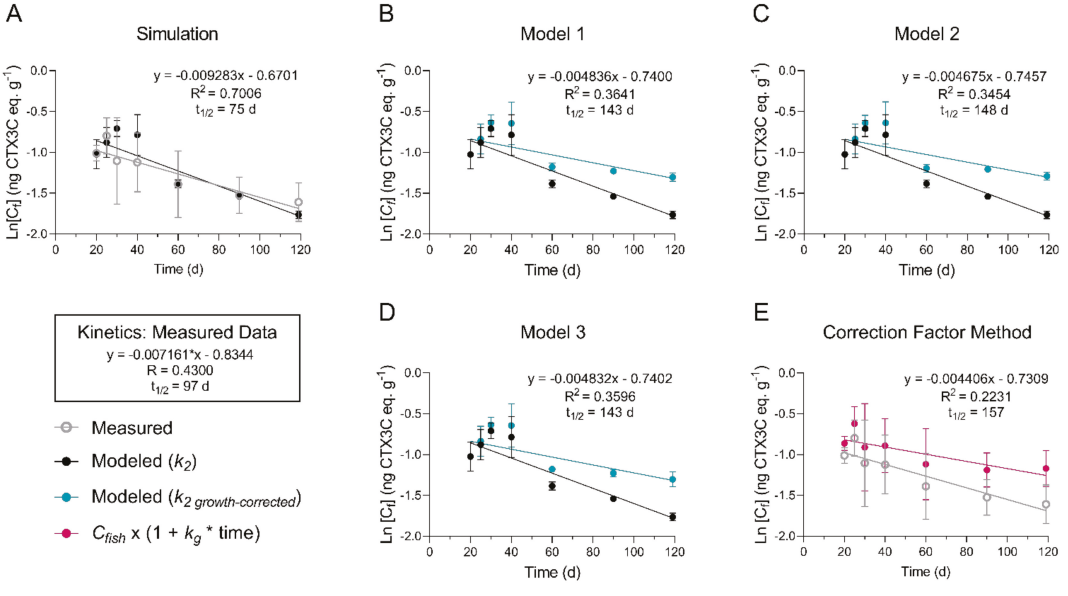

Figure 7. Modeled C-CTX-1 concentrations (based on CTX3C equiv.) compared to measured and growth-dilution-corrected models. Complete details on the (**A**) simulation model; (**B**) Model 1; (**C**) Model 2; (**D**) Model 3; are provided in the methods. (**E**) In the correction factor method, measured concentrations were adjusted using a simplistic approach where measured data were multiplied by a growth correction factor (i.e., $C_{fish} * (1 + k_g * t_{\Delta\ total})$). Plotted symbols represent the mean ± s.d. (n = 4 except on day 20 where n = 8).

Table 5. Growth-corrected depuration rate constants ($k_{2\ growth\text{-}corrected}$) that were used in growth-dilution correction Model 1 of this study. The mean k_g (n = 4) of replicate fish at each time point were used for the correction in this model.

Experiment Day	Trial	Average $k_g \times 10^{-3}$ (d^{-1})	$k_{2\ growth\text{-}corrected} \times 10^{-3}$ (d^{-1}) [a]
20	1	7.615 ± 1.492	−0.454
20	2	8.402 ± 0.345	−1.241
25	1	7.747 ± 0.676	−0.586
30	1	7.037 ± 1.132	0.124
40	1	6.489 ± 1.270	0.672
60	2	5.187 ± 0.943	1.975
90	2	4.447 ± 0.878	2.714
119	2	4.619 ± 0.567	2.542

[a] Calculated by subtracting average k_g from the overall k_2 value of 7.16×10^{-3}.

Table 6. The $k_{2\ growth\text{-}corrected}$ that were used in the growth-dilution correction Model 2 of this study. Time intervals where significant differences were detected by ANOVA and a Tukey's test (See Supplementary Figure S2B) were used for correction in this model.

Experiment Day	Trial	Average $k_g \times 10^{-3}$ (d^{-1})	$k_{2\ growth\text{-}corrected} \times 10^{-3}$ (d^{-1}) [a]
20–25	1, 2	7.921	−0.760
30–40	1	6.763	0.398
60–119	2	4.785	2.410

[a] Calculated by subtracting average k_g from the overall k_2 value of 7.161×10^{-3}.

3. Discussion

This study is the first multi-tissue report on the dynamics of C-CTX elimination in an ecologically relevant intermediate consumer from the greater Caribbean region. This also represents the longest experimental C-CTX fish depuration in an important and rapidly expanding area of research. Since the initiation of these experiments in 2019, at least three similar experiments have been undertaken [20–22] and recently a conceptual model based on field-collected fish, focused on the contribution of growth in lowering CTXs was released [23]. Clearly, the knowledge gaps on CTX bioaccumulation and depuration kinetics have been acknowledged, and several groups are working to fill these. Modeling the disposition of CTX in wild reef fish is a next step for the development of predictive models on the time course of environmental changes, dinoflagellate proliferation and/ or toxification, and CP outbreaks.

3.1. Experimental Considerations and Outcomes

Pinfish (*L. rhomboides*) are omnivorous and undergo transitional feeding behavior during their life cycle. For instance, juvenile pinfish have a wide-ranging diet (small crustaceans, fish, polychaetes, tunicates, hydroids, seagrasses, epiphytes), while adults are reported to feed predominantly on epiphytes and macrophytes but continue to supplement their diet with many small invertebrates throughout their life [24–27]. As such, a generic trophic-level analysis can be difficult to determine based on the wide dietary range and multiple ontogenetic transitions during the lifecycle [25]. Pinfish are found from the coasts of New England to Brazil, and are widely distributed throughout the Gulf of Mexico, Florida Keys, and Yucatan [28], where CP also occurs. Pinfish also represent a substantial portion of the biomass in seagrass meadows and other structurally complex habitats (e.g., mangrove propagules, reefs, docks) and are a major source of organic matter exported to reef fish during seasonal migrations towards offshore reefs (20–100 m deep) in the Florida Big Bend area [29,30]. The stomach contents of gag grouper, a commercially important species from offshore reefs, contained 47% pinfish during migration periods [31], highlighting this species as a key prey item for higher-trophic-level fishes that have been implicated in ciguatera. Pinfish have also been used to study brevetoxin accumulation and

exposure of many other natural and human contaminants [32]. Wild-collected fish used in this study were collected from an area with low prevalence of CTX and in the absence of brevetoxin-producing *K. brevis* blooms; however, to ensure no naturally incurred levels of CTX or brevetoxin that may skew our results, fish were acclimated, and subsamples of the population were tested for CTX and brevetoxins immediately following collection and the beginning of our experimental trials to ensure no detectable levels.

Some of the differences in our experimental design and the design of prior studies were important for the study goals. There is a trade-off to consider for experiments where it is necessary to maintain equal treatment conditions including the exposure rate (feeding) across large groups of experimental replicates. Since space was limited, alternatives such as grouping animals together in exposure tanks or pooling samples for analytical purposes, were considered, but risked the loss of statistical power and would introduce pseudo-replication. One of our goals were to capture the variability of CTX uptake and depuration in this species, so while fish had some minor size variability at the start of the trials, feed rations based on individual fish mass were prepared and maintained to ensure a consistent daily intake. Now that we have characterized the variability in these fish, we may be able to reconsider these alternatives in future studies to include changes in CTX metabolite formation and distribution via LC-MS/MS strategies (that require greater biomass for the CTX doses used here). The commercial omnivorous fish food that was mixed to create the pellets provided supplemental nutrition and acted as a binding agent which prevented fragmentation and loss of the powderized barracuda during feeding. In other studies, control and treated diets were either not matrix matched [33] or controls were not used [19]. In this case we were able to track similar growth rates between control and treated fish across trials since both of these aspects were controlled. The regulated feeding rate also led to a strong correlation (day 0–20; $R^2 = 0.95$) between cumulative burdens and the ingested dose in fish sampled during the CTX feeding phase as reported by others [33]. This correlation was used to estimate the accumulated CTX burden in fish prior to their depuration and allowed the analysis of the change in total body concentration of individuals over time under multiple projections using growth correction which was also attempted in one prior experimental study [20]. The isolation of fish, controlled feeding rate, and sufficient replication also are important to capture the individual physiological variability in CTX toxicokinetics, but these have not always been met in other CTX studies [21]. Parallel controls at each sampling time point (except experimental day 90) provided both growth and behavioral assessment (no behavioral issues observed) and analytical controls for the tissue analyses by the N2a-MTT assay.

The procedural consistency across trials was crucial for us to consider CTX distribution data through time as a single set in the analyses. Several points of data support our consistency in approach. Quality control data shows reproducible pellet toxicity and feeding rates across both trials which was supported by the cumulative burden measurements in fish related to the total dose (Figure 6). Further, four fish were analyzed in both trials on the last day of the bioaccumulation phase (day 20) and the toxicity of all tissues sampled were not significantly different (see Table 3). The controlled formulation of the experimental pellet diet also showed that pellet weight and proportional amount of food provided to each fish between control and treated groups was consistent. Based on the supporting evidence collected, we deemed it acceptable to combine datasets from the two experimental trials for analyses of the extended depuration kinetics.

Use of the N2a-MTT assay to determine tissue CTX concentrations has been widely accepted by the CP research community and seafood management agencies alike for several decades [34]. This methodology has been used in prior CTX exposure studies of various organisms to analyze CTX activity over time [19,21,35,36] and provides a measure of the composite toxicity of sodium channel activating metabolites that have implications for human health. In selecting N2a-MTT for our measurements we gained the sensitivity that we needed to evaluate toxicokinetics across individuals through time in this small species but lost the ability to evaluate trends in CTX profiles throughout the experiment. Unfortunately,

we had insufficient tissue to support LC-MS/MS analyses without combining replicates (as in other studies) and we wanted to maintain and evaluate the variability between fish so that trends in depuration among tissues would be more robust. As LC-MS/MS methods for CTXs become more sensitive (or with the use of a larger species) we hope to revisit the change in toxin profiles (if any) through these processes in future work.

3.2. Muscle, Liver, and Viscera CTX Kinetics: Bioaccumulation

Prior to the study, fish were acclimated to the feeding schedule using cooked shrimp and transitioned to gel pellets (no barracuda added) over the 2-week period. By the start of experiments fish were consuming pellets immediately when added to the tanks and continued to do so throughout the entire study. Rapid consumption during the experiment likely limited leaching of toxin from the CTX-pellets into the aquarium water. Additionally, 35% water changes were performed weekly on all aquarium systems to maintain water quality and prevent accumulation of possible residual toxins in the tank water. Although tank water was not analyzed for CTX, the tanks of control and CTX-dosed fish shared the same recirculating artificial seawater by randomized design and none of the control fish tissue extracts or control feed exhibited CTX activity by the N2a-MTT. Additionally, tank substrate was regularly vacuumed by siphoning to prevent the re-uptake of any CTX in fish excrement. Therefore, we assumed with confidence that measured CTX activity was dominated via the dietary exposure route.

During the uptake phase (day 1–20), measured CTX concentrations in muscle and viscera of pinfish were positively correlated with number of CTX exposure days and followed linear trends (Figure 2). Toxin uptake rate estimated in pinfish muscle (0.003 ng CTX3C eq. g^{-1} TE day^{-1}) by N2a-MTT was in the range of uptake rates reported for P-CTX-2 and -3 in juvenile grouper (*Epinephelus coioides*) measured by LC-MS/MS (0.001–0.005 ng g^{-1} day^{-1}) but was 10-fold lower than P-CTX-1 (0.033 ng g^{-1} day^{-1}) [20]. Toxin uptake rate in pinfish viscera (0.123 ng CTX3C eq. g^{-1} TE day^{-1}) was not comparable to other studies due to sample preparation of this compartment; however, CTX bioaccumulation in viscera was >41 times the rate in pinfish muscle which led to extremely high visceral concentrations (4.40 ng CTX3C eq. g^{-1}) versus muscle (0.04 ng CT3C eq. g^{-1}) by the end of the bioaccumulation phase.

Between days 6 and 20, CTX concentrations in viscera were 42–330 fold (except 1 fish on day 6) and in liver, 3–69 fold higher than the concentration in muscle. The range of concentration ratios for liver to muscle are similar to what has been reported from fish collected in CP endemic waters [37]. However, as noted by Vernoux et al. [37], we did not detect any pattern in the concentration ratios (data not shown), and therefore support their recommendation to avoid using liver or viscera results to extrapolate flesh toxicity. These compartments may confirm CTX exposure in fish but would not reliably estimate risk of consuming fish fillets.

In some cases, the variability observed in CTX tissue concentration between individual fish replicates in this study was high. This variability was important to capture if we are to extrapolate future field studies where intraspecies variability will be even greater. The strength of the correlation between cumulative CTX burden and total ingested dose supports that fish were provided a normalized amount of CTX and nutritional food, as does our quality assurance/quality control data (Tables 2 and 3). Our time until detection in the muscle and liver using the N2a-MTT assay was much longer than found for mullet, which occurred 3 hrs post-exposure to a single dose of *G. polynesiensis* cells [19] which could relate to species differences or the increased toxicity of P-CTXs produced by *G. polynesiensis* compared to C-CTX-1 that was used in this exposure study. Additionally, our CTX dose was approximately 15-fold lower (0.02 vs. 0.3 ng CTX3C eq. per g of body weight) to ensure that no behavioral disturbances were detected and supports an ecologically relevant range. Intraspecific variability in assimilating and compartmentalizing CTX also could have contributed to the limited detectability of CTXs in the muscle and liver during the first 10 days of the bioaccumulation phase. Omnivorous goldfish fed C-CTX-1 from *Seriola* sp.

flesh at a rate of 0.014 ng CTX1B eq g^{-1} TE also had undetectable CTX in muscle after the first CTX dose but CTX was measurable (n = 2) by day 8 [21]. The dose and physiological differences between herbivorous and omnivorous fish may explain the observed lag time between the CTX activity of benthic dinoflagellates and herbivores compared to upper-trophic-level fish [6,13].

Through this work, we estimated an average net CTX assimilation of 43% in pinfish from the ingested dose throughout the bioaccumulation phase of this study (days 1–20; see Figure 6). The bioavailable amount of the CTX dose, which is the total CTX absorbed into systemic circulation, was not quantified here, but our estimate of net assimilation (bioavailable amount—first pass metabolism elimination) in pinfish was much higher than reported for C-CTX-1 in freshwater goldfish [21], P-CTX-1, -2, and -3 in juvenile grouper [20], and CTX3C in naso [33], which were all less than ~10%. In contrast, mullet assimilated 42% of ciguatoxicity from a single dose of *G. polynesiensis* [19] and orally bioavailable CTX in rats was calculated around 39% [35] which are congruent with measured levels in this study. The CTX burden in mullet declined to 5% of the single dose administered by 24 h, but repeated exposure was not evaluated [19]. It is also possible that C-CTX-1 investigated in this study has a higher assimilation compared to other CTX congeners, among other factors.

Considering the continued linearly increasing trend of CTX in each tissue during the exposure and bioaccumulation phase, we do not assume a steady state was reached during the CTX feeding phase. Clausing et al. [33] determined in herbivorous naso fed *G. polynesiensis* cells, that muscle CTX concentration stabilized somewhere between 8 and 16 weeks of exposure at bioaccumulated levels of approximately 3 ng CTX3C eq. g^{-1} TE. However, the CTX concentration in muscle of goldfish stabilized by day 29 at 0.03 ng CTX1B eq. g^{-1} TE [21]. This dissimilarity could be due in part to different physiology of freshwater and marine fish, but the possibility that the low sample size (n = 2) combined with biological variability prevented detectable trends in the goldfish study cannot be dismissed. Goldfish were reportedly not growing during the study whereas biomass of juvenile naso increased approximately four times compared with initial, therefore, the possibility that there may be differences in the steady-state concentrations reached between growing and non-growing fish cannot be ruled out.

3.3. Muscle, Liver, and Viscera CTX Kinetics: Depuration

Depuration resulted in an expected decrease in viscera CTX3C eq. concentration with time that followed a simple linear relationship (Figure 2C). Initially, however, the C-CTX-1 (measured as CTX3C eq.) concentrations in viscera continued increasing into the depuration phase and were at the highest measured levels five days after depuration was initiated (day 25 = 5.61 ng CTX3C eq. g^{-1}). A similar trend was reported in a depuration study of juvenile grouper (*Epinephelus coioides*) where P-CTX- 1, -2, -3 concentrations in the skin and intestine were higher 4 days after depuration was started and then followed an exponential decline through the next 30 days [20]. One factor mentioned by the authors was that they observed some undigested material in stomachs when dissected, so this could have had an effect. In this study, we excluded stomachs to avoid possible crossover between assimilated and non-assimilated CTX. We did not measure fecal pellets or the tank water during the trials, so we were unable to capture the CTX levels eliminated from the organism directly; however, controls shared circulating tank water with CTX fish and no controls had detectable CTX levels supporting that dietary uptake was the only relevant exposure route.

Further explanation of the lag of CTX seen in the viscera compartment during this study could be attributed to the amount and quality of protein and the presence of carbohydrates and fiber in the pelleted food. Food quality has been well established as a factor that may increase gut retention and modify absorption kinetics for other toxicants in humans and mammals (see [38–40]), which could be examined in future studies for CTX. Variability of CTX kinetics, particularly from visceral organs, that has been reported between studies may be a function of dietary differences, in addition to species and experimental factors

already described. Persistent viscera contamination could also be influenced by enterohepatic recirculation as seen for anthropogenic contaminants where a xenobiotic is re-absorbed by the intestine after first pass metabolism and returned to systemic circulation [41,42]. Cycling the toxin back through the system would redispose it in tissues, altering toxin compartmentalization dynamics.

CTX depuration in muscle tissue was reported to be rapid in recent studies of juvenile grouper, with half-lives for P-CTX-1, -2 and -3 reported as 28, 26 and 33 days, respectively [20]. Our data on C-CTX-1 depuration in pinfish muscle contrast with these results with C-CTX (as CTX3C eq.) concentrations being significantly higher on the last day than at the start of depuration (Figure 2A), highlighting possible species-level differences. Our data from day 119 likely pull the regression analyses towards a positive slope, but the low variability between replicate fish and significant differences measured between days 20 and 119 showed that an increase in CTX tissue concentration in muscle was real. Further supporting this phenomenon, it should be noted that during long-term studies such as ours, fish are growing, and if CTX levels in muscle were growth-corrected a further increase would be expected. These effects and models were comprehensively explored in this study. Decreasing trends in viscera were paralleled by the increasing CTX levels observed in muscle tissue, suggesting that CTX may be redistributed and/ or compartmentalized into muscle from other tissues through time. A biphasic change in the location of the cyanotoxin cylindrospermopsin was also reported in mussels and attributed to a re-distribution of the toxin within tissues [43]. This may explain the persistent high levels of CTX found in the upper-trophic-level fish in regions with frequent CTX exposure. Analysis of CTX levels in blood between days 90 and 119 may have determined if enterohepatic recirculation of CTX was occurring but was not performed in this study. These data remind us that toxicokinetic models of CTX should consider organ compartments as dynamic places where the toxins have the potential to be in flux and influenced by many environmental and physiological mechanisms, yet to be elucidated. Hopefully, these data will press further studies to investigate the CTX dynamics between tissues, since this may aid in fisheries management and future dockside testing once rapid field assays become available (i.e., knowing which tissues will provide a reliable assessment of CTX risk).

There were no significant trends observed in the liver over time, except for highly variable CTX concentrations throughout the depuration phase. This variability could be attributed to metabolic process regulating elimination from liver. For instance, novel glucuronide metabolites of C-CTX were recently identified in hepatic microsomes indicating that C-CTX glucuronidation may be a prevalent biotransformation pathway in fish [44]. In contrast, grouper efficiently eliminated 90% of the P-CTX from liver by the end 30 days [20]. Additionally, under controlled exposure conditions, pooled lionfish liver samples (n = 1 of pooled fish) analyzed by N2a-MTT gradually became less toxic over a 43 d depuration.

3.4. CTX Tissue Distribution

The relative CTX distribution in *L. rhomboides* tissues allowed us to compare the disposition of CTX burden across fish of different sizes through time (Figure 3). The order of highest to lowest CTX burden during the entire study was viscera > muscle > liver, but prior studies have reported a similar analysis with variable findings. The highest percentage of total CTX was in the muscle of grouper fed 1 ng P-CTX g^{-1} fish day^{-1} (approximately 50-fold higher dose than the present study) followed by other visceral tissues (intestine and liver combined) for the entire experiment (except day 2 where skin CTX burden was highest) [20]. Our visceral extract contained several tissues not analyzed in the grouper (heart, spleen, gall bladder) which have been shown containing high CTX concentrations in some fish and could explain the differences reported between studies [19]. The CTX burden reported in the muscle of mullet also contained the highest toxin load when fewer than nine CTX meals had been given [19]. However, similar to our findings, data extending beyond nine CTX feedings on dinoflagellate cells by mullet, saw most of the CTX activity detected in the intestine and gall bladder (~50%) followed by muscle (22%) and a small

amount in liver (2%) [19]. Likewise, giant clams also contained most of the CTX in the viscera following exposure [36].

3.5. One-Compartment Model Kinetics and Growth Correction

The C-CTX-1 uptake rate calculated for the combined tissue compartments in *L. rhomboides* was 8.80×10^{-3} ng CTX3C eq. g^{-1} TE day^{-1}. For comparison, the estimates for P-CTX-1 and -2 uptake rates in whole body of juvenile grouper were 25.2 and 3.51×10^{-3} ng g^{-1} day^{-1} by LC-MS analysis [20]. While our analyses do not account for CTX in some organismal compartments (e.g., kidney, carcass), the included tissues likely contained the large majority of CTX that was bioaccumulated. Toxin accumulation was lower in muscle tissue, which was exhaustively removed from fish during dissection, except for muscle tissue surrounding the head, which was difficult to reliably remove from the small fish and minor in mass. Bioaccumulation in hard parts such as bone and fin are possible but are likely minor contributors to storage and not evaluated in this study. CTX activity was below detection in the brain and gonads so these were excluded from whole body concentrations reported in this study. There is still a lot of room for future studies that will better inform organismal models of CTX bioaccumulation, and these should include longer period of bioaccumulation, different fish species, life stages, and varied CTX congeners, for a more comprehensive analysis of bioaccumulation rates.

Fish growth which contributes to lowered concentration of contaminants, can be a difficult effect to control when investigating depuration, and complicates analyses in exposures when significant [45]. Clausing et al. [33] found that naso growth masked CTX accumulation, causing an apparent steady state in muscle at 8 weeks with similar CTX concentrations occurring at 16 weeks of exposure and significant growth. In that example, growth dilution kept CTX concentrations stable between weeks 8 and 16 while the muscle CTX burden continued to increase. This effect cannot be ignored in the present study which covered a 4 month timeframe. Quantifying the growth-dilution effect has been handled in several ways when studying elimination of contaminants, including adjusting measured concentrations by a growth correction factor as performed by Li et al. [20]. However, these growth adjustment strategies have been critiqued by others and alternative strategies suggested [45,46]. In our study, we applied several growth models and corrections including the one reported by Li et al. [20] to determine the best approach for this and future investigations for C-CTX depuration and growth. We first evaluated the rate constant subtraction method outlined by Brooke and Crookes [45], which eliminates the change in concentration due to growth from the other first-order depuration process (i.e., elimination by respiration, feces, and metabolic transformation). Essential to our rate constant growth correction analyses were the predicted concentrations ($C_{fish(i)}$) from body CTX burden and weight estimates at the start of depuration. In our case, knowing the feeding rate, dose, and growth rates of all fish (i.e., for n= 40 C-CTX treated; and n= 37 control) in the study allowed us to perform model analyses that have not been used in past CTX exposure studies. While first order kinetics were assumed based on regression of the transformed concentration data (Figure 4), we acknowledge that a first order relationship is approximate, and is a potential source of uncertainty in the model. However, this method did provide evidence that fish growth was the major contributor to declining CTX concentrations through time in this study.

The growth-corrected half-life for P-CTX-1, -2 and -3 (e.g., 21, 21, and 38 d, and R^2 equal to 0.97, 0.84, and 0.37, respectively) in the whole body of the juvenile grouper *E. coioides* [20] were much shorter than reported by us and others [11,17]. This anomaly could be attributed to unequal toxicokinetics between *E. coioides* and other fish, the use of juvenile specimens, differences between CTX variants, or the statistical power or models applied in that study. Our growth correction modeling technique increased the estimated CTX depuration half-life from approximately 80 d in the raw data simulation to approximately 146 d (Figure 7A–D). Compared to other studies, our growth-corrected half-lives of total ciguatoxicity are more similar to estimates in naturally incurred ciguatoxic Pacific

moray eels (*L. javanicus*) and red snapper (*L. bohar*) where half-lives of 264 and 900 d were reported, respectively [11,17]. Comparison to these data would depend on whether the fish grew significantly, but if growth was positive (as would be expected), growth correction would increase the reported half-life. From this study and others, we might expect a half-life of several months or longer which would be in line with long-term patterns of persistent ciguatoxicity in fish from regions with CTX-producing benthic dinoflagellates. Additionally, brevetoxins which are also Na_V activators produced by the pelagic dinoflagellate *Karenia brevis*, have been detected in fish livers more than a year after algal blooms subside [32]. The CTX binding affinity for the primary Na_V receptor was also shown to outcompete brevetoxin for the site [47]. Therefore, it is not unreasonable to consider CTXs have extremely long biological half-lives that are likely to vary based on the physicochemical properties of each toxin variant.

In this study of *L. rhomboides*, the calculated CTX burdens for each fish at the end of the depuration period were not measurably different than burdens measured (or estimated using the correlation between cumulative dose and total CTX burden) for day 20 (see Supplementary Figure S4). Although the level of uncertainty in the kinetic rate measurement limits the precision of our half-life estimate, the remaining high CTX burden after depuration suggests that the models presented here are valid and show that pseudo-elimination via growth was a primary factor in lowering concentration in *L. rhomboides*. The growth correction Model 1, Model 2, and Model 3 (Figure 7B–D) showed that the use of mean and individual measured growth rate constants agreed, suggesting that this method is robust enough for use in food web modeling if accurate estimates of growth rates are available for wild-fish. Age and growth studies are available for numerous reef fish species globally and a thorough example of how these data could be useful was recently provided in a critical review on conceptual models for ciguatera risk assessment [23].

3.6. Conclusions and Implications for Trophic Transfer

In this study we report that C-CTX-1 was bioaccumulated in *L. rhomboides* from low environmentally relevant doses (0.02 ng CTX3C eq. g^{-1} day^{-1}), and present that total ciguatoxicity was retained for at least 3.3 months and depuration was mostly a function of fish growth, a pseudo-elimination factor. These data highlight that field determined concentrations of C-CTX may not reflect the mass balance of CTX that is bioavailable in food webs. Increased elimination may be expected in wild-caught fish that have varied diets and expend more energy, thus augmenting metabolic rates and lowering CTX levels. However, the retention of C-CTX-1 in *L. rhomboides* at a basal level is remarkable. This long-term CTX retention in fish helps to explain how regions with no recent sign of *Gambierdiscus* sp. blooms can produce toxic fish that cause CP outbreaks, whether by fish migration or after a period of low CTX production [12,48]. This study also suggests that field data may need to be staggered if *Gambierdiscus* abundance and toxicity are collected as a baseline in parallel with fish samples for food web toxin analysis, as is the traditional framework for field studies. Future studies could include repeated exposures with intermittent depuration periods to understand CTX kinetics once fish are re-exposed to the toxins while still depurating, which likely occurs in migratory fish and in areas with regular temporal swings in toxicity [6,9]. Quantifying the kinetics of elimination via respiration, feces, and metabolic transformations, as well as sequestration in reproductive tissues, may also be useful for future food web models of CTX exposure.

Improving our understanding of CTX kinetics has clear advantages to our interpretation of CTX dynamics in the field, and in developing improved risk models to prevent CP. Our prior efforts have shown clear pulses of C-CTX in the benthic algal community [9] in hyperendemic regions that may be dictated by lower temperature tolerance of toxigenic *Gambierdiscus* species [8,49]. If the timing of the CTX source pulses occur in higher frequency than the depuration of CTXs at higher trophic levels, we may expect increasing prevalence of toxic fishes once CTX-producing algae are established in a region. While more evidence on these dynamic cascades and factors that might influence them is needed,

experimental studies such as these help to parameterize the capacity of toxin removal from the organism. From a resource management perspective, understanding periods of high and low risk, even if only possible for fish with high site fidelity, would be a great advantage to the fishery, especially when coupled to spatial resolution of CTX.

4. Materials and Methods

4.1. Reagents and Chemicals

All solvents were HPLC grade obtained from Fisher Scientific (Waltham, MA, USA) and were acetone, MeOH, *n*-hexanes, $CHCl_3$, and dimethyl sulfoxide (DMSO). Bond Elut silica solid-phase extraction (SPE) cartridges (100 mg and 500 mg) were from Agilent Technologies (Santa Clara, CA, USA). Ouabain octahydrate (O) and veratrine hydrochloride (V) used for in vitro assays were from Sigma (St. Louis, MO, USA). The 3-[4,5-dimethylthiazol-2-yl]-2,5-diphenyl- tetrazolium (MTT) was sourced from Alfa Aesar (Haverhill, MA, USA) and was prepared in sterile phosphate buffered saline (PBS) from Medicago (Quebec City, QC, Canada). Ciguatoxin 3C (CTX3C) was purchased from Wako Chemicals (Osaka, Japan) and a 50 ng mL^{-1} stock was prepared in LCMS grade MeOH and aliquoted in sealed amber vials maintained at -20 °C until use.

Adherent murine neuroblastoma cells (Neuro-2a; ATCC CCL-131) were originally purchased from the American Tissue Culture Collection (Manassas, VA, USA) and modified (i.e., OV desensitized) lines generated and maintained to ensure maximal and stable cell response to CTX in MTT-based assays prior to use (available on request). Powdered Roswell Park Memorial Institute (RPMI) 1640 medium (Millipore Sigma, Burlington, MA, USA) was prepared in 10 L batches with sterile ultrapure water (18 mΩ) and 1L aliquots filtered (polyethersulfone 0.2 μM Supor membrane; Pall Corp; Port Washington, NY, USA) into sterile bottles. Supplements included sterile L-glutamine (200 mM stock), sodium pyruvate (100 mM stock), and fetal bovine serum (all from Gibco; Grand Island, NY, USA). Trypsin-EDTA (0.025% stock) used in cell detachment and harvest was from Corning (Corning, NY, USA). Cell culture consumables including serological pipettes, tubes, flasks, and micro-well plates were from CellTreat (Shirley, MA, USA). Trypan blue (Fisher Scientific, Waltham, MA, USA) was prepared to 0.2% in sterile PBS (pH 7.4) and used in cell enumeration and viability assessment.

4.2. Controlled Exposure

4.2.1. Fish Collection and Acclimation

Wild pinfish, *Lagodon rhomboides* (Sparidae), were collected from Mississippi Sound (Dauphin Island, AL, USA) and Perdido Bay (Orange Beach, AL, USA) using hook-and-line with sabiki rigs. To reduce stress from handling, fish were directly transferred to an aerated, seawater-filled cooler using a specialized dehooking tool which does not require fish handling. Fish were transported in aerated, temperature and salinity-controlled tanks to the experimental wet-lab facility at the Dauphin Island Sea Lab (DISL) within one hour. Prior to transfer to a primary acclimation tank, a five-minute freshwater dip was performed to remove marine ectoparasites. This step was important to reduce the chance of disease in the closed system. The recirculating aquarium system was composed of a 450 L sump, 375 L head tank, and 120 L enclosure tank and filled with artificial seawater (Crystal Sea Marine mix; Mount Dora, FL, USA). To limit stress, environmental enrichment provided to each tank habitat included a two-inch bed of pool filter grade silica sand, 12 cm diameter $\times$ 12 cm length PVC tubes for structure, and artificial submerged aquatic vegetation. Fish were collectively monitored in the acclimation tanks in groups of 25 for three weeks for signs of parasitic diseases and behavioral abnormalities prior to transfer into individual tanks for experimental treatment. Two fish collections were performed to supply fish for the exposure study, once in January 2019 and again in May 2020. The water conditions across all systems were maintained on a 12 h light: 12 h dark cycle with weekly water changes (artificial seawater: 15–17 psu; 24 $\pm$ 2 °C; ammonia $\leq$ 0.1 ppm, nitrite $\leq$ 0.1 ppm, nitrate $\leq$ 40 ppm, pH = 8.1 $\pm$ 0.1).

4.2.2. Feed Formulation

Experimental (CTX feed) and control diets (no CTX) were created from a blend of fish meal, Mazuri Aquatic Gel Diet for Omnivorous Fish (sku: 1815252-409; Mazuri Exotic Animal Nutrition, St. Louis, MO, USA), and water. The fish meal consisted of white muscle tissue from either non-toxic great barracuda, *Sphyraena barracuda*, collected from the northern Gulf of Mexico, Alabama (control) or *S. barracuda* with naturally incurred C-CTX that were collected from the U.S. Virgin Islands during concurrent efforts. Fillets with skin, scales, and bones removed, were cut into small chunks and subsequently homogenized in an industrial food-grade stainless steel grinder (STX Turboforce 3000; Lincoln, NE, USA). From each fish, at least five replicate subsamples of minced *S. barracuda* tissue were extracted and analyzed for the presence of CTX-like activity using N2a-MTT, and C-CTX-1 confirmed by liquid chromatography-mass spectrometry as previously reported [50]. After verifying control and CTX fish, batches were pooled and mixed three times, then frozen in stainless steel trays and freeze dried. Dehydrated tissue (300 g) was powdered using a grain mill (HC-300; C-Goldenwall, Amazon, Seattle, WA, USA) at 28,000 rpm for 1 min and sieved to $\leq$500 µm to create a fine and uniform product. All fish powder was thoroughly mixed and kept in 500 g aliquots at −20 °C in airtight containers until use. Subsamples of the homogenized freeze-dried fish powder were taken for analysis by the N2a-MTT for final quantification of toxicity of the pelleted diet prior to further preparation. The control and CTX diets for *L. rhomboides* were created by combining equal parts Mazuri gel powder and fish powder, then homogenized and combined with 60% water (by weight) that was warmed to 65 °C. The homogenized feed was transferred to a pastry piping bag with a round tip (Wilton size 10), then dispensed in even rows onto pre-weighed parchment paper. After fully dispensing the gel, wet weight was recorded, and the gel was cut into 5 mm pellets. The tray was then placed in a drying oven at 65 °C for approximately 1 h to remove approximately 2/3 water so that pellets retained a uniform shape. To maintain a consistent product across batches, the water content (as a percent of the final product) was calculated by subtracting the weight of solid ingredients in the mixture from the weight of the formulated food after drying, then dividing by the whole-food dry weight. Subsamples of pellets were weighed on an analytical balance to collect an average pellet weight.

4.2.3. Experimental Design

To accomplish optimal control and observation of fish, *L. rhomboides* were individually transferred to 12 L tanks attached to a closed recirculating aquarium system. Four recirculating aquarium systems with 10 to 15 tanks per system were used in this study. Fish were acclimated to the individual tanks (one fish per tank) for at least 2 weeks prior to the beginning of experimental treatment to ensure water quality parameters and fish health were stable. This acclimation period was in addition to the post-collection acclimation.

The experiments were designed to provide control over dietary intake of C-CTX-1 in individual fish so that the toxicokinetics of bioaccumulation and depuration could be analyzed across multiple tissues with sufficient replication for the subsequent statistical analyses. Tanks designated to receive control or CTX pellets were assigned a sampling day on the day prior to the start of experiments using a random number generator. Control fish received control pellets throughout trials while CTX fish received CTX pellets for up to 20 days (bioaccumulation phase) and then transitioned to the control feed for the depuration phase (see Table 1 for sampling scheme). Both control and CTX pellets contained powderized *S. barracuda* flesh (non-toxic or toxic, respectively) to match the nutritional intake across groups and maintain consistency (minus CTX) when fish were transitioned from the bioaccumulation to the depuration phase. Fish fed only the control pellets were designated for each sampling point to be used as matrix controls in assays, and to compare differences in behavior, and growth rate compared to the CTX treatment groups.

Data were collected from two feeding experiments (trial 1 and 2, hereafter) to allow adequate replication. The first experiment had maximum bioaccumulation and depuration phases of 20 days each with a total of 52 fish and was performed 5 March–13 April 2019.

Fish were sampled as baseline controls prior to feeding on the first experimental day and on days 6, 10, and 20 of bioaccumulation and days 5, 10, and 20 of depuration. In the second experiment performed 30 July–25 November 2020, the bioaccumulation phase was replicated identical to trial 1, and depuration was extended out to a maximum of 99 days to increase the depuration course. Fish were collected on day 20 of the bioaccumulation phase to compare to trial 1 for reproducibility, and then on days 40, 70, and 99 of the depuration phase. Based on the lack of overt signs of intoxication during the first experiment and ample analytical controls, during the second experiment, remaining *L. rhomboides* were allocated towards maintaining experimental replication in the CTX treatment group (CTX fish, $n = 4$) and control replicates were reduced to $n = 2$ per time point (except day 0, $n = 3$) (Table 1).

Daily feed requirements were calculated based on initial weights (g) of fish which were recorded using a water displacement method one or two days prior to the beginning of exposure trials. All fish were fed either control or CTX pellet food at the same time daily, normalized to body mass (approximately 1.8% of initial body weight day^{-1}). Fish were fed the same amount of food daily relative to the initial whole wet weight for the entire experiment. Individuals were closely observed to ensure all food was eaten during feeding times, and after acclimation *L. rhomboides* were consistently consuming the pellets within seconds of entering the tank. Fish were also re-weighed at multiple points (at minimum initial and at time of sampling) throughout the study to track growth rate and to determine if somatic growth influenced C-CTX concentration as previously expected by others in P-CTX fish studies [20,33,51].

4.2.4. Fish Sampling, Dissection, and Extraction

On a designated day and time of sampling, fish were fed and left undisturbed for 7 h. Fish were euthanized according to approved IACUC protocols by iced seawater immersion and mortality was confirmed by cessation for at least 10 min. A secondary spinal transection was performed to ensure mortality, and fish were then dissected. Dissected tissues were weighed whole including muscle, brain, liver, gonads (when present), and additional visceral organs combined (heart, spleen, pancreas, gall bladder, intestine). Swim bladder was discarded and not analyzed in this study. Stomach was removed from the viscera samples to limit residual CTX signal from undigested food in downstream toxicity assays; however, given reported gut clearance rates <24 h, the amount of residual CTX in the intestinal tract was expected to be below the limit of quantification (LOQ; described in Section 4.3 Data Analysis) in the viscera on our assays.

Muscle subsamples (5–7 g) were extracted twice in acetone (2 mL g^{-1} tissue weight) by bead disruption (2.6 mm diameter; ceramic) using a Bead Ruptor 24 (Omni International; Kennesaw, GA) at a speed of 5 m/s for two cycles of 30 s duration each. Resultant homogenates were centrifuged at 2465× *g* for 5 min at room temperature (approximately 21 °C) between extractions to obtain the supernatant. Combined supernatants were placed at −20 °C for 18 h, then centrifuged (4 °C, 2465× *g*, 10 min), and supernatants dried under a gentle nitrogen stream (45 °C). Dried residues were reconstituted in 90% aq. MeOH (1 mL g^{-1} original weight) and partitioned twice using *n*-hexane (2 mL g^{-1} original weight) to remove non-polar lipids. The aq. MeOH phase was dried under nitrogen, and the resultant residue was partitioned with $CHCl_3$: H_2O (50:50, v:v). The $CHCl_3$ layer containing CTX was collected, then water phase partitioned again with the same volume of $CHCl_3$. Pooled $CHCl_3$ fractions were dried, reconstituted in 500 µL $CHCl_3$, and further cleaned by silica SPE. Powderized fish tissue (CTX and control) was extracted in a similar manner using a 5:1 solvent (mL) to tissue (g) weight ratio. Non-muscular tissues were extracted whole due to their small size and solvent ratios adjusted accordingly. Final tissue extracts were dissolved in 1 mL 100% MeOH and stored at −20 °C until analysis.

4.3. Toxin Analysis

4.3.1. Maintenance of Neuroblastoma Cells

Cells were maintained in vented 175 cm^2 sterile culture flasks with RPMI medium supplemented with 5% heat-inactivated FBS, 1 mM sodium pyruvate, and 2 mM L-glutamine (complete media) and maintained in a humidified water jacketed incubator at 37 °C with 5% CO_2: 95% atmospheric air. Cells were passaged every 48 h and maintained in exponential growth. During passaging and in preparation for seeding 96-well plates, cells were harvested with 0.025% trypsin-EDTA for <2 min, trypsin deactivated with 10% FBS-RPMI complete medium, centrifuged, supernatant discarded and cells washed two times in PBS. Duplicate aliquots of cells resuspended in 5% FBS-RPMI medium were enumerated on a hemocytometer to calculate growth rates, and passage % viability via trypan blue staining.

4.3.2. Neuroblastoma MTT Assay (N2a-MTT)

Sample extracts were tested for composite voltage-gated sodium channel (Na_V) response using a standardized in vitro mouse neuroblastoma assay (N2a-MTT) as previously described [50] with toxin quantification of serially diluted samples evaluated and compared to a 9-point 2-fold serial dilution of CTX3C (initial dose equal to 20 pg $well^{-1}$ or 86.96 pg mL^{-1}). The European Food Safety Authority (EFSA) has developed guidelines outlining toxic equivalency factors for the various CTX-group toxins [52]. CTX3C has been reported to be two-fold more toxic than C-CTX-1 based on intraperitoneal toxicity and was accepted here as the better certified reference standard compared to P-CTX1 which was reportedly ten-fold more toxic than C-CTX-1. The difference in CTX3C standard toxicity could cause lower estimates of C-CTX-1 content. For better understanding of toxin content, conversion from CTX3C eq. to C-CTX-1 can be done by multiplying CTX3C eq. concentrations by a factor of 2.

Due to the sample size of subsampled fish tissues, we were unable to perform additional LC-MS/MS analysis which requires much higher CTX concentrations compared to N2a-MTT. These analyses could have been accomplished by pooling tissues and/or extracts from replicate fish for each sampling point as described by others [20] but this would have lost the experimental replication that we deemed critical to the validity of this study, so was delayed to a future study with larger fish specimens.

N2a cells from established OV adapted lines, were seeded into 96-well plates at a density of 3×10^5 cells per well, in complete RPMI media (200 µL). After 20 h, cells were dosed in triplicate with standards, controls, and sample extracts; all with and without OV. To prepare fish extracts for dosing, an extract aliquot dissolved in MeOH was transferred to a 1.5 mL microcentrifuge tube, dried under ultrapure $N_{2(g)}$, and redissolved in 5% FBS-RPMI complete media by vortex (30 s, room temperature). Cells in assay wells were carefully inspected by light microscopy prior to dosing and development. Positive controls (CTX-positive reference material), negative controls (containing PBS and medium), and assay controls with (sensitized) and without (non-sensitized) O/V (final well concentration: 0.22 mM ouabain/0.022 mM veratrine) were used to ensure quality assurance and control throughout the several hundred assays performed during this study. Sample wells were dosed with 10 µL of the fish extract solubilized in culture media or PBS (final well volume 230 µL). After a 20 h incubation, well contents were removed and MTT (1 mg/mL) diluted in 5% FBS-RPMI-1640 complete medium was added for 30 min. The resultant insoluble formazan product produced by mitochondrial activity of remaining live cells was solubilized in 100% DMSO (100 µL) with the colorimetric change measured within 5 min on a spectrophotometric microplate reader (µQuant; Biotek Instruments; Winooski, VT, USA) at 570 nm. Cells sensitized with O/V were used to assess CTX-like activity, while non-O/V-sensitized cells were used to monitor non-specific activity induced by sample extracts. When O/V-dependent toxicity was detected by at least a 20% difference between controls and wells dosed with fish extracts, a two-fold serial dilution of extract was prepared and assayed parallel to a CTX3C standard dilution series on the same day.

4.3.3. N2a-MTT Data Analysis

Raw data were analyzed using Microsoft Excel version 2013 (Microsoft Corporation, Redmond, WA, USA). Normalized data were analyzed with GraphPad Prism version 9.0.0 (GraphPad Software, San Diego, CA, USA).

Raw absorbance values for wells dosed with standards and fish extracts were normalized to the OV control wells (20 µL O/V + 10 µL PBS, or 30 µL PBS), to account for minor OV N2a mortality established during cell line adaptation as described by others [53]. Triplicate absorbance responses within a single assay plate were deemed acceptable when the relative standard deviation was below 20%. To produce standard curves for quantification on the day of each assay, CTX3C standard doses (x-values) were logarithm transformed and fit by non-linear regression against the normalized response (y-values) in wells at each dose using a four-parameter logistic equation with variable slope ($Y = Bottom + (Top/Bottom)/(1 + 10\hat{}((LogIC_{50} - X) * HillSlope)$). Toxicity of tissue extracts were estimated by interpolating the normalized responses (y-value) in wells onto the standard curve to estimate the dose (unknown x-value) in pg CTX3C equivalence. Values that fell between the effect concentration 20–80 (EC_{20} to EC_{80}) which is the linear portion of the standard curve are acceptable, but we chose to use more strict parameters for quantification by accepting only values between EC_{30} and EC_{75} because full curves with a top and bottom plateau were not always possible based on the CTX concentrations in tissues. Interpolated results (pg CTX3C eq.) were divided by the tissue equivalence (mg TE) of the dose to calculate the concentration in ng CTX3C eq. g^{-1} TE. The LOQ for CTX in each tissue type was determined by dividing the mean value of the EC_{75} from the CTX3C dose–response curve and the maximum TE dosed in wells without a matrix induced effect defined as either growth enhancement >20% of the control wells or cell death associated with non-Na_v mechanisms (evaluated in sample wells without OV). All samples were analyzed in triplicate across 2–4 independent assays performed on separate days with a CTX3C standard curve prepared on the day of each assay.

4.4. Ciguatoxin Kinetics

4.4.1. Muscle, Liver, and Viscera Ciguatoxin Kinetics

Kinetics of CTX uptake and depuration in separate tissues were investigated through non-linear regression analysis of the experimentally determined CTX concentration in sample extracts against time for both phases using GraphPad Prism version 9.0.0 (model comparison function). When CTX was below detection levels due to a non-specific matrix effect, those replicates were excluded from analyses (see Results Section 2.5). Normality of toxin data was evaluated using a Shapiro–Wilk test and models were fit using a least squares regression with no weighting and compared by an iterative process. Best fit models were compared based on the Akaike's Information Criterion (AICc) which balances the goodness of fit using sum-of-squares and the simplicity (number of degrees of freedom) of the two models.

4.4.2. One-Compartment Model Kinetics

The combined CTX concentrations (C_{fish}) for the measured tissues were calculated for each fish by multiplying the quantified concentration for each tissue (muscle, liver, and viscera) by the whole tissue mass (conc. x mass = tissue burden), summing the tissue CTX burdens, and dividing by the total sum of the whole muscle, liver, and viscera mass. The C_{fish} was used to investigate a one-compartment model of CTX kinetics which assumes a homogenous concentration in the fish. While our analyses do not account for CTX in some compartments (kidney, stomach, and carcass), the included tissues (muscle, liver, viscera) contained the majority portion of CTX in the major tissue compartments in the fish. No CTX activity was detectable in brain or gonads, so these were excluded.

The uptake rate was calculated by linear regression of the measured C_{fish} (ng g^{-1}) during the bioaccumulation phase against time (d = 0 to 20)

$$C_{fish} = k_{uptake} \times t + a \quad (1)$$

where the slope of regression is equal to the rate of increasing CTX concentration (k_{uptake}; ng g^{-1} day^{-1}), t is time (d), and a is a constant which in this case is the y-intercept (ng g^{-1}).

The first-order depuration rate constant (k_2) was calculated using the methods outlined by Brooke and Crookes [45]. A one-compartment model of exponential decay was fitted to the measured C_{fish} during the depuration phase

$$C_{fish(t)} = C_{fish(i)}\ e^{-k_2 t} \quad (2)$$

where $C_{fish(t)}$ is the concentration (ng g^{-1}) measured at the time of sampling, $C_{fish(i)}$ is the initial concentration (ng g^{-1}) at the start of the depuration phase (day 20), t is time (d), and k_2 is the overall depuration rate constant (day^{-1}). For curve fitting, the measured C_{fish} in the depuration phase were natural Log transformed, i.e., Ln [C_{fish}], to allow linear regression of Log-concentrations versus time in which the slope of regression is the k_2, and the coefficient of determination is used to confirm first-order kinetics. The k_2 calculated by these methods is the overall elimination rate constant including the sum of four first-order kinetic processes

$$k_2 = k_r + k_m + k_e + k_g \quad (3)$$

where k_r, k_m, and k_e (all in units day^{-1}) are the rate constant for elimination via respiration, metabolic transformation, and feces, respectively, and k_g is the rate constant for the change in concentration due to fish growth, a pseudo-elimination process. For an in-depth summary on each of the rate constants and application to overall k_2, see Gobas [54] (pp. 4–9).

To correct the overall k_2 for growth of the fish, k_g was calculated using the growth rate data collected for each fish. Fish masses were applied to an exponential growth model

$$W_{fish(t)} = W_{fish(i)}\ e^{k_g t} \quad (4)$$

where $W_{fish(t)}$ is the wet weight (g) of the fish at any point, $W_{fish(i)}$ is the initial wet weight at the start of the experiment, and k_g is the growth rate constant (day^{-1}). To allow a linear fit, the inverse of measured weights was natural Log transformed, i.e., Ln ($1/W_{fish}$), and plotted against time where the slope is equal to k_g (day^{-1}). The effect of growth, which results in diluted concentrations over time, was factored out of the depuration rate constant by subtracting the k_g from the overall k_2 to give the growth-corrected depuration rate constant ($k_{2\ growth\text{-}corrected}$; day^{-1})

$$k_{2\ growth-corrected} = k_2 - k_g \quad (5)$$

and describes the rate constant for elimination processes that result in removal of CTX from the fish ($k_r + k_m + k_e$) [45].

4.4.3. Kinetic Modeling and Correction of Growth Dilution

The exponential growth Equation (4) was used to estimate the mass of each fish on day 20 (end of bioaccumulation phase) that entered the depuration phase using measured growth rate constants (k_g) and solving for $W_{f(t)}$. For trials 1 and 2, respectively, values of t were set to 20 and 22 days, because initial weights were collected on day 0 (trial 1) and two days prior to start (trial 2), while depuration was initiated on day 20 for both trials. The sum of muscle, liver, and viscera mass was estimated at day 20 using a linear correlation between whole fish mass (g) and the sum of tissue masses, i.e., Σ (whole muscle + liver + viscera; g), that were dissected from sampled fish for CTX analysis. The combined CTX burden in

the whole muscle, liver, and viscera at day 20 was estimated from the linear relationship between the cumulative dose administered (total ng CTX3C eq. consumed = number of pellets fed daily × number of days in bioaccumulation phase × pellet CTX3C eq. conc.) and the combined CTX burden measured in fish that were sampled between 0 and 20 d. Estimates of total CTX burden and combined tissue mass at the end of the bioaccumulation phase (day 20) were divided for an estimate of an overall CTX concentration in the fish at the start of depuration ($C_{fish(i)}$).

A simulation model of our data was created using the estimated $C_{fish(i)}$ to study the effect of fish growth on elimination of CTX. Final concentrations were simulated for each fish in the depuration phase at all time points using the one-phase exponential decay model (Equation (2)) where $C_{fish(i)}$ is an estimate on day 20, time is delta time in depuration depending on when the fish was sampled, and overall k_2 was measured from the linear plot depuration data. The resulting simulated concentrations were natural Log transformed (as previously described for the measured C_{fish}) and plotted against time (d) to compare the regression slope (k_2) with the slope from the measured data. A correlation was then performed to check how well the simulated data fit the measured concentrations.

Simulated concentration data served as the baseline for growth-corrected models to compare the change in half-life (Ln [2]/ k) under different conditions of $k_{2\ growth\text{-}corrected}$. The growth-corrected models were produced by adjusting the depuration rate constant (k_2) in the simulation exponential decay model. Three growth-corrected models were produced using different values of $k_{2\ growth\text{-}corrected}$ that were calculated based on fish growth rates in the depuration phase, i.e., average growth rates at each sampled time point (Model 1), average growth rate based on ANOVA grouping (Model 2), and the individually measured growth rate (Model 3). Results of each model compared to the simulation are presented using the linear version of the exponential decay model where concentrations are natural Log transformed and plotted against time. The growth-corrected half-lives of the models were finally compared to the half-life calculated from growth correction by a simpler approach reported by others [20,55] that uses a growth correction factor, where measured concentrations in fish during the depuration phase are multiplied by ($1 + k_g \times$ time).

4.5. Statistical Analyses

Fish size (mass in g) at the initial time point across studies was analyzed using a non-parametric two-tailed Mann–Whitney U test since trial 1 weights were not normally distributed. Growth rate constants (k_g) of control and treatment groups collected at the same time point were tested for normality using a Shapiro–Wilk test and compared for differences using a two-tailed *t*-test, respectively. Growth rate and toxicity data between control and exposure treatments were tested for normality and homoscedasticity using a Shapiro–Wilk test and Brown-Forsythe test, respectively, and residual plots were visually inspected as a parallel method prior to one-way ANOVA with Tukey's multiple comparisons test. Growth trends were investigated by a linear regression plot of k_g against time. A simple correlation was used to analyze the fit of the measured and model simulated $C_{fish(t)}$ in the depuration phase prior to investigating growth correction of the model.

Supplementary Materials: The following are available online at https://www.mdpi.com/article/10.3390/toxins13110774/s1; Supplementary Figure S1: Representative in vitro dose–response curves from the neuroblastoma-MTT assay in this study. Supplementary Table S1: Results of a *t*-test on the first order growth rate constants (k_g) between Control and CTX-treated *L. rhomboides* at each sampled time point. Supplementary Figure S2: Results of ANOVA with Tukey's test on k_g of Control and CTX feeding treatments across time. Supplementary Figure S3: Results of ANOVA with Tukey's test for C-CTX-1 measured in CTX3C eq. concentrations (mean ± s.d.) in muscle, liver, and pooled viscera of *L. rhomboides* in this study. Supplementary Figure S4: Sum of total C-CTX burdens (measured as CTX3C eq.) in the tissues of *L. rhomboides* sampled in this study.

Author Contributions: Conceptualization, C.T.B. and A.R.; Investigation, C.T.B.; Methodology, C.T.B. and A.R.; Analysis and Visualization, C.T.B. and A.R.; Writing—original draft, C.T.B.; Writing—

review and editing, A.R.; Funding acquisition, A.R.; project administration, A.R.; supervision, A.R.; and resources, A.R. All authors have read and agreed to the published version of the manuscript.

Funding: This work was funded by the National Oceanic and Atmospheric Administration (NOAA NOS NCCOS) Ecology and Oceanography of Harmful Algal Blooms (ECOHAB) program (CiguaTOX: NA11NOS4780028) and is publication 985. Research and graduate student funding were also supported through the National Science Foundation (NSF) Partnerships in International Research and Education Program (CiguaPIRE; 1743802) and contributes to the NSF and NIEHS Center for Oceans and Human Health: Greater Caribbean Center for Ciguatera Research (NSF: 1841811; and NIH: 1P01ES028949-01). C.T.B. was supported by a graduate research assistantship funded by NOAA and NSF and received additional internal research support from the Bullard Fund (Marine Sciences, University of South Alabama).

Institutional Review Board Statement: The study was approved by the Institutional Animal Care and Use Committee (IACUC) Review Board of the University of South Alabama (protocol number 1105747-2 approved 24 August 2017, and 1640293-2 approved 27 August 2020).

Informed Consent Statement: Not applicable.

Data Availability Statement: The data in this study are available in this article and Supplementary Materials.

Acknowledgments: We are thankful to Matthew Boehm, Diana Marchant, and Jonathan Wittmann from the Dauphin Island Sea Lab (DISL) for additional support of aquarium and fish maintenance during this extended study. We also appreciate the aquarist expertise of Brian Jones (DISL Estuarium). Special thanks to Tony Dovi (Dovi Design & Illustration) for assistance with original preparation of graphical art used in the graphical abstract.

Conflicts of Interest: The authors declare no conflict of interest. The funders had no role in the design of the study; in the collection, analyses, or interpretation of data; in the writing of the manuscript, or in the decision to publish the results.

References

1. Adachi, R.; Fukuyo, Y. The thecal structure of a marine toxic dinoflagellate *Gambierdiscus toxicus gen. et sp. nov*. collected in a ciguatera-endemic area. *Bull. Jpn. Soc. Sci. Fish* **1979**, *45*, 67–71. [CrossRef]
2. Bagnis, R.; Chanteau, S.; Chungue, E.; Hurtel, J.; Yasumoto, T.; Inoue, A. Origins of ciguatera fish poisoning: A new dinoflagellate, *Gambierdiscus toxicus Adachi and Fukuyo*, definitively involved as a causal agent. *Toxicon* **1980**, *18*, 199–208. [CrossRef]
3. Laza-Martínez, A.; David, H.; Riobó, P.; Miguel, I.; Orive, E. Characterization of a strain of *Fukuyoa paulensis* (Dinophyceae) from the Western Mediterranean Sea. *J. Eukaryot. Microbiol.* **2016**, *63*, 481–497. [CrossRef]
4. Litaker, R.W.; Holland, W.C.; Hardison, D.R.; Pisapia, F.; Hess, P.; Kibler, S.R.; Tester, P.A. Ciguatoxicity of *Gambierdiscus* and *Fukuyoa* species from the Caribbean and Gulf of Mexico. *PLoS ONE* **2017**, *12*, e0185776. [CrossRef]
5. Rhodes, L.; Harwood, T.; Smith, K.; Argyle, P.; Munday, R. Production of ciguatoxin and maitotoxin by strains of *Gambierdiscus australes*, *G. pacificus* and *G. polynesiensis* (Dinophyceae) isolated from Rarotonga, Cook Islands. *Harmful Algae* **2014**, *39*, 185–190. [CrossRef]
6. Chinain, M.; Germain, M.; Deparis, X.; Pauillac, S.; Legrand, A.-M. Seasonal abundance and toxicity of the dinoflagellate *Gambierdiscus* spp. (Dinophyceae), the causative agent of ciguatera in Tahiti, French Polynesia. *Mar. Biol.* **1999**, *135*, 259–267. [CrossRef]
7. Parsons, M.L.; Settlemier, C.J.; Bienfang, P.K. A simple model capable of simulating the population dynamics of *Gambierdiscus*, the benthic dinoflagellate responsible for ciguatera fish poisoning. *Harmful Algae* **2010**, *10*, 71–80. [CrossRef]
8. Xu, Y.; Richlen, M.L.; Liefer, J.D.; Robertson, A.; Kulis, D.; Smith, T.B.; Parsons, M.L.; Anderson, D.M. Influence of environmental variables on *Gambierdiscus* spp.(Dinophyceae) growth and distribution. *PLoS ONE* **2016**, *11*, e0153197. [CrossRef] [PubMed]
9. Liefer, J.D.; Richlen, M.L.; Smith, T.B.; DeBose, J.L.; Xu, Y.; Anderson, D.M.; Robertson, A. Asynchrony of *Gambierdiscus* spp. Abundance and Toxicity in the US Virgin Islands: Implications for Monitoring and Management of Ciguatera. *Toxins* **2021**, *13*, 413. [CrossRef] [PubMed]
10. Holmes, M.J.; Lewis, R.J.; Poli, M.A.; Gillespie, N.C. Strain dependent production of ciguatoxin precursors (gambiertoxins) by *Gambierdiscus toxicus* (Dinophyceae) in culture. *Toxicon* **1991**, *29*, 761–775. [CrossRef]
11. Lewis, R.; Sellin, M.; Street, R.; Holmes, M.; Gillespie, N. Excretion of ciguatoxin from moray eels (Muraenidae) of the central Pacific. In Proceedings of the Third International Conference on Ciguatera Fish Poisoning, La Parguera, Puerto Rico, 30 April–5 May 1990; Tosteson, T.R., Ed.; Polyscience Publications: Morin Heights, QC, Canada, 1992; pp. 131–143.
12. Lewis, R.J.; Holmes, M.J. Origin and transfer of toxins involved in ciguatera. *Comp. Biochem. Physiol. Part C Pharmacol. Toxicol. Endocrinol.* **1993**, *106*, 615–628. [CrossRef]

13. Chateau-Degat, M.-L.; Chinain, M.; Cerf, N.; Gingras, S.; Hubert, B.; Dewailly, E. Seawater temperature, *Gambierdiscus* spp. variability and incidence of ciguatera poisoning in French Polynesia. *Harmful Algae* **2005**, *4*, 1053–1062. [CrossRef]
14. Llewellyn, L.E. Revisiting the association between sea surface temperature and the epidemiology of fish poisoning in the South Pacific: Reassessing the link between ciguatera and climate change. *Toxicon* **2010**, *56*, 691–697. [CrossRef]
15. Darius, H.; Ponton, D.; Revel, T.; Cruchet, P.; Ung, A.; Fouc, M.T.; Chinain, M. Ciguatera risk assessment in two toxic sites of French Polynesia using the receptor-binding assay. *Toxicon* **2007**, *50*, 612–626. [CrossRef] [PubMed]
16. Chinain, M.; Darius, H.T.; Ung, A.; Fouc, M.T.; Revel, T.; Cruchet, P.; Pauillac, S.; Laurent, D. Ciguatera risk management in French Polynesia: The case study of Raivavae Island (Australes Archipelago). *Toxicon* **2010**, *56*, 674–690. [CrossRef] [PubMed]
17. Banner, A.H.; Helfrich, P.; Piyakarnchana, T. Retention of ciguatera toxin by the red snapper, *Lutjanus bohar*. *Copeia* **1966**, *2*, 297–301. [CrossRef]
18. Davin, W.T.; Kohler, C.C.; Tindall, D.R. Ciguatera toxins adversely affect piscivorous fishes. *Trans. Am. Fish. Soc.* **1988**, *117*, 374–384. [CrossRef]
19. Ledreux, A.; Brand, H.; Chinain, M.; Bottein, M.-Y.D.; Ramsdell, J.S. Dynamics of ciguatoxins from *Gambierdiscus polynesiensis* in the benthic herbivore *Mugil cephalus*: Trophic transfer implications. *Harmful Algae* **2014**, *39*, 165–174. [CrossRef]
20. Li, J.; Mak, Y.L.; Chang, Y.-H.; Xiao, C.; Chen, Y.-M.; Shen, J.; Wang, Q.; Ruan, Y.; Lam, P.K. Uptake and Depuration Kinetics of Pacific Ciguatoxins (P-CTXs) in Orange-spotted Grouper (*Epinephelus coioides*). *Environ. Sci. Technol.* **2020**, *54*, 4475–4483. [CrossRef] [PubMed]
21. Sanchez-Henao, A.; García-Álvarez, N.; Padilla, D.; Ramos-Sosa, M.; Silva Sergent, F.; Fernández, A.; Estévez, P.; Gago-Martínez, A.; Diogène, J.; Real, F. Accumulation of C-CTX1 in Muscle Tissue of Goldfish (*Carassius auratus*) by Dietary Experience. *Animals* **2021**, *11*, 242. [CrossRef]
22. Leite, I.d.P.; Sdiri, K.; Taylor, A.; Viallon, J.; Gharbia, H.B.; Mafra Júnior, L.L.; Swarzenski, P.; Oberhaensli, F.; Darius, H.T.; Chinain, M. Experimental Evidence of Ciguatoxin Accumulation and Depuration in Carnivorous Lionfish. *Toxins* **2021**, *13*, 564. [CrossRef]
23. Holmes, M.J.; Venables, B.; Lewis, R.J. Critical Review and Conceptual and Quantitative Models for the Transfer and Depuration of Ciguatoxins in Fishes. *Toxins* **2021**, *13*, 515. [CrossRef] [PubMed]
24. Hansen, D.J. Food, growth, migration, reproduction, and abundance of pinfish, Lagodon rhomboides, and Atlantic croaker, *Micropogon undulatus*, near Pensacola, Florida, 1963–1965. *Fish. Bull.* **1969**, *68*, 135–146.
25. Stoner, A.W. Feeding ecology of *Lagodon rhomboides* (Pisces: Sparidae): Variation and functional responses. *Fish. Bull.* **1980**, *78*, 337–352.
26. Luczkovich, J.J.; Norton, S.R.; Gilmore, R.G. The influence of oral anatomy on prey selection during the ontogeny of two percoid fishes, *Lagodon rhomboides* and *Centropomus undecimalis*. *Environ. Biol. Fishes* **1995**, *44*, 79–95. [CrossRef]
27. Luczkovich, J.J. *The Patterns and Mechanisms of Selective Feeding on Seagrass-Meadow Epifauna by Juvenile Pinfish, Lagodon Rhomboides (Linnaeus)*; The Florida State University: Tallahassee, FL, USA, 1987.
28. Hoese, H.D.; Moore, R.H. *Fishes of the Gulf of Mexico, Texas, Louisiana, and Adjacent Waters*, 2nd ed.; Texas A&M University: College Station, TX, USA, 1977.
29. Nelson, J.; Wilson, R.; Coleman, F.; Koenig, C.; DeVries, D.; Gardner, C.; Chanton, J. Flux by fin: Fish-mediated carbon and nutrient flux in the northeastern Gulf of Mexico. *Mar. Biol.* **2012**, *159*, 365–372. [CrossRef]
30. Nelson, J.A.; Stallings, C.D.; Landing, W.M.; Chanton, J. Biomass transfer subsidizes nitrogen to offshore food webs. *Ecosystems* **2013**, *16*, 1130–1138. [CrossRef]
31. Naughton, S.P.; Saloman, C.H. *Food of Gag (Mycteroperca microlepis) from North Carolina and Three Areas of Florida*; US Department of Commerce, National Oceanic and Atmospheric Administration: Panama City, FL, USA, 1985; Volume 160.
32. Naar, J.P.; Flewelling, L.J.; Lenzi, A.; Abbott, J.P.; Granholm, A.; Jacocks, H.M.; Gannon, D.; Henry, M.; Pierce, R.; Baden, D.G. Brevetoxins, like ciguatoxins, are potent ichthyotoxic neurotoxins that accumulate in fish. *Toxicon* **2007**, *50*, 707–723. [CrossRef]
33. Clausing, R.J.; Losen, B.; Oberhaensli, F.R.; Darius, H.T.; Sibat, M.; Hess, P.; Swarzenski, P.W.; Chinain, M.; Bottein, M.-Y.D. Experimental evidence of dietary ciguatoxin accumulation in an herbivorous coral reef fish. *Aquat. Toxicol.* **2018**, *200*, 257–265. [CrossRef]
34. Friedman, M.A.; Fleming, L.E.; Fernandez, M.; Bienfang, P.; Schrank, K.; Dickey, R.; Bottein, M.-Y.; Backer, L.; Ayyar, R.; Weisman, R.; et al. Ciguatera Fish Poisoning: Treatment, Prevention and Management. *Mar. Drugs* **2008**, *6*, 456–479. [CrossRef]
35. Ledreux, A.; Ramsdell, J.S. Bioavailability and intravenous toxicokinetic parameters for Pacific ciguatoxin P-CTX-1 in rats. *Toxicon* **2013**, *64*, 81–86. [CrossRef]
36. Roué, M.; Darius, H.T.; Picot, S.; Ung, A.; Viallon, J.; Gaertner-Mazouni, N.; Sibat, M.; Amzil, Z.; Chinain, M. Evidence of the bioaccumulation of ciguatoxins in giant clams (*Tridacna maxima*) exposed to *Gambierdiscus* spp. cells. *Harmful Algae* **2016**, *57*, 78–87. [CrossRef]
37. Vernoux, J.P.; Lahlou, N.; Abbad El Andaloussi, S.; Riyeche, N.; Magras, L. A study of the distribution of ciguatoxin in individual Caribbean fish. *Acta Tropica* **1985**, *42*, 225–233. [CrossRef]
38. Welling, P.G. Influence of food and diet on gastrointestinal drug absorption: A review. *J. Pharmacokinet. Biopharm.* **1977**, *5*, 291–334. [CrossRef]
39. Takagaki, R.; Ishida, Y.; Sadakiyo, T.; Taniguchi, Y.; Sakurai, T.; Mitsuzumi, H.; Watanabe, H.; Fukuda, S.; Ushio, S. Effects of isomaltodextrin in postprandial lipid kinetics: Rat study and human randomized crossover study. *PLoS ONE* **2018**, *13*, e0196802. [CrossRef] [PubMed]

40. Have, G.A.M.T.; Engelen, M.P.K.J.; Luiking, Y.C.; Deutz, N.E.P. Absorption Kinetics of Amino Acids, Peptides, and Intact Proteins. *Int. J. Sport Nutr. Exerc. Metab.* **2007**, *17*, S23–S36. [CrossRef]
41. Marier, J.-F.; Vachon, P.; Gritsas, A.; Zhang, J.; Moreau, J.-P.; Ducharme, M.P. Metabolism and disposition of resveratrol in rats: Extent of absorption, glucuronidation, and enterohepatic recirculation evidenced by a linked-rat model. *J. Pharmacol. Exp. Ther.* **2002**, *302*, 369–373. [CrossRef] [PubMed]
42. Herman, R.J.; Van Pham, J.D.; Szakacs, C.B. Disposition of lorazepam in human beings: Enterohepatic recirculation and first-pass effect. *Clin. Pharmacol. Ther.* **1989**, *46*, 18–25. [CrossRef] [PubMed]
43. Saker, M.L.; Metcalf, J.S.; Codd, G.A.; Vasconcelos, V.M. Accumulation and depuration of the cyanobacterial toxin cylindrospermopsin in the freshwater mussel *Anodonta cygnea*. *Toxicon* **2004**, *43*, 185–194. [CrossRef]
44. Gwinn, J.K.; Uhlig, S.; Ivanova, L.; Fæste, C.K.; Kryuchkov, F.; Robertson, A. *In Vitro* Glucuronidation of Caribbean Ciguatoxins in Fish: First Report of Conjugative Ciguatoxin Metabolites. *Chem. Res. Toxicol.* **2021**, *34*, 1910–1925. [CrossRef]
45. Brooke, D.; Crookes, M. *Depuration Rate Constant: Growth Correction and Use as an Indicator of Bioaccumulation Potential*; Environment Agency: Bristol, UK, 2012; Volume 7371.
46. Brooke, D.; Crookes, M.; Gray, D.; Robertson, S. *Environmental Risk Assessment Report: Octamethylcyclotetrasiloxane*; Environment Agency of England and Wales: Bristol, UK, 2009.
47. Dechraoui, M.-Y.B.; Wacksman, J.J.; Ramsdell, J.S. Species selective resistance of cardiac muscle voltage gated sodium channels: Characterization of brevetoxin and ciguatoxin binding sites in rats and fish. *Toxicon* **2006**, *48*, 702–712. [CrossRef] [PubMed]
48. Randall, J.E. A review of ciguatera, tropical fish poisoning, with a tentative explanation of its cause. *Bull. Mar. Sci.* **1958**, *8*, 236–267.
49. Robertson, A.; Richlen, M.L.; Erdner, D.; Smith, T.B.; Anderson, D.M.; Liefer, J.D.; Xu, Y.; McCarron, P.; Miles, C.O.; Parsons, M.L. Toxicity, Chemistry, and Implications of *Gamberdiscus silvae*: A Ciguatoxin Superbug in the Greater Caribbean Region. In Proceedings of the 18th International Conference for Harmful Algae, Nantes, France, 21–26 October 2018; p. 115.
50. Kryuchkov, F.; Robertson, A.; Miles, C.O.; Mudge, E.M.; Uhlig, S. LC–HRMS and Chemical Derivatization Strategies for the Structure Elucidation of Caribbean Ciguatoxins: Identification of C-CTX-3 and-4. *Mar. Drugs* **2020**, *18*, 182. [CrossRef]
51. Ward, D.M.; Nislow, K.H.; Chen, C.Y.; Folt, C.L. Rapid, efficient growth reduces mercury concentrations in stream-dwelling Atlantic salmon. *Trans. Am. Fish. Soc.* **2010**, *139*, 1–10. [CrossRef]
52. EFSA Panel on Contaminants in the Food Chain. Scientific Opinion on marine biotoxins in shellfish–Emerging toxins: Ciguatoxin group. *EFSA J.* **2010**, *8*, 1627.
53. Viallon, J.; Chinain, M.; Darius, H.T. Revisiting the neuroblastoma cell-based assay (CBA-N2a) for the improved detection of marine toxins active on voltage gated sodium channels (VGSCs). *Toxins* **2020**, *12*, 281. [CrossRef]
54. Gobas, F.A. A model for predicting the bioaccumulation of hydrophobic organic chemicals in aquatic food-webs: Application to Lake Ontario. *Ecol. Model.* **1993**, *69*, 1–17. [CrossRef]
55. Munschy, C.; Héas-Moisan, K.; Tixier, C.; Olivier, N.; Gastineau, O.; Le Bayon, N.; Buchet, V. Dietary exposure of juvenile common sole (*Solea solea L.*) to polybrominated diphenyl ethers (PBDEs): Part 1. Bioaccumulation and elimination kinetics of individual congeners and their debrominated metabolites. *Environ. Pollut.* **2011**, *159*, 229–237. [CrossRef] [PubMed]

toxins

MDPI

Review

Advances in Detecting Ciguatoxins in Fish

Tibor Pasinszki [1,*], Jimaima Lako [2] and Todd E. Dennis [3]

[1] Department of Chemistry, School of Pure Sciences, College of Engineering, Science and Technology, Fiji National University, P.O. Box 3722 Samabula, Suva, Fiji

[2] Department of Food Technology and Home Economics, School of Applied Sciences, College of Engineering, Science and Technology, Fiji National University, P.O. Box 3722 Samabula, Suva, Fiji; jimaima.lako@fnu.ac.fj

[3] Department of Biology, School of Pure Sciences, College of Engineering, Science and Technology, Fiji National University, P.O. Box 5529 Lautoka, Fiji; todd.dennis@fnu.ac.fj

* Correspondence: tibor.pasinszki@fnu.ac.fj; Tel.: +679-298-4306

Received: 28 June 2020; Accepted: 26 July 2020; Published: 31 July 2020

Abstract: Ciguatera fish poisoning (CFP) is currently the most common marine biotoxin food poisoning worldwide, associated with human consumption of circumtropical fish and marine invertebrates that are contaminated with ciguatoxins. Ciguatoxins are very potent sodium-channel activator neurotoxins, that pose risks to human health at very low concentrations (>0.01 ng per g of fish flesh in the case of the most potent Pacific ciguatoxin). Symptoms of CFP are nonspecific and intoxication in humans is often misdiagnosed. Presently, there is no medically approved treatment of ciguatera. Therefore, to mitigate the risks of CFP, reliable detection of ciguatoxins prior to consumption of fish tissue is acutely needed, which requires application of highly sensitive and quantitative analytical tests. During the last century a number of methods have been developed to identify and quantify the concentration of ciguatoxins, including in vivo animal assays, cell-based assays, receptor binding assays, antibody-based immunoassays, electrochemical methods, and analytical techniques based on coupling of liquid chromatography with mass spectrometry. Development of these methods, their various advantages and limitations, as well as future challenges are discussed in this review.

Keywords: ciguatera; ciguatoxin; cytotoxicity assay; ELISA; HPLC; immunoassay; LC-MS/MS; mouse bioassay; receptor-binding assay

Key Contribution: Methods to detect and quantify ciguatoxins in fish tissue are critically reviewed.

1. Introduction

Ciguatera fish poisoning (CFP), currently the most common marine biotoxin food poisoning worldwide, is a non-bacterial foodborne disease associated with consumption of circumtropical fish and marine invertebrates that are contaminated with polyether sodium channel activator neurotoxins (ciguatoxins, CTXs) [1–12]. CTXs are a family of heat-stable and lipid-soluble compounds that cannot be degraded by normal cooking. CTXs are colorless and odorless, therefore cannot be detected by smell or visual inspection of fish flesh. Ciguatoxins are produced by certain benthic dinoflagellate species from the *Gambierdiscus* and *Fukuyoa* genera and enter the marine food chain via herbivorous fish and invertebrates [2,5,9,13]. These toxins are subsequently biotransformed in herbivorous, omnivorous, and carnivorous fishes to more oxidized and more potent forms of CTXs and accumulate to toxic levels in edible fish. During the biotransformation of P-CTX-4B to P-CTX-1 (see below) there is a ten-fold increase in potency [8]. The structure of CTXs varies according to geographic distribution; therefore, they are classified as Pacific Ocean (P-CTX), Caribbean Sea (C-CTX) and Indian Ocean (I-CTX) ciguatoxins. P-CTX-1 is regarded as the most potent toxin, and the recommended safety limit for CTXs in fish for human consumption has been set at 0.01 ng P-CTX-1 toxin equivalent/g fish tissue (0.01 ppb

P-CTX-1 equivalent) by both the European Food Safety Authority (EFSA) and United States Food and Drug Administration (US FDA) [1,14]. The recommended safety level for C-CTX-1 equivalent toxicity is 0.10 ppb [1,9,14]. Although the safety limit for I-CTXs has not been published yet, based on experiments indicating that the toxicity of I-CTX-1 is 60% of that of P-CTX-1 potency [15], a safety level of 0.017 ppb for I-CTX-1 equivalent toxicity may be considered. CFP is known in tropical regions for centuries, and it is an increasing risk of food poisoning worldwide; it occurs now in non-endemic areas due to international trade of fish and fish products and the expansion of the geographic ranges of dinoflagellates as a likely result of global warming [12,16,17]. Intoxication by CTXs may cause neurological, gastrointestinal, and cardiovascular symptoms depending on the amount and type of the toxin ingested [1–7,18], and occasionally in severe cases, CFP can be fatal [19,20]. P-CTX-1 possesses risk to human health at concentrations higher than 0.022–0.1 ng g^{-1} in fish flesh [8,21]. About 10,000 to 50,000 people suffer from the illness annually [1]; however, this is likely a substantial underestimate considering the incidence of non-reported cases from remote areas and non-diagnosis. Only 2–10% of CFP cases are estimated to be reported to health authorities [4]. Currently, there is no routine, rapid, reliable, and cost-effective point-of-care (POC) test that can detect ciguatoxins on-site or prior to consumption. Identification and quantification of CTXs is challenging even for laboratories due to the low CTX concentrations in fish flesh, the low recommended limit of 0.01 ng g^{-1}, and the lack of reference materials and standards for all CTXs. The concentration of toxins in fish liver is about 10–50 times higher than in muscle tissue [22,23], thereby CFP becomes more problematic in communities consuming fish viscera. In extreme cases, such as for the liver of a large moray eel caught in Kiribati, toxicity can be as high as 539 ng g^{-1}, 50,000 times higher than the accepted safety level of 0.01 ng g^{-1} [23]. The symptoms of CFP were first described by Captain James Cook and Don Antonio Parra in the 17th century during their exploration of the Pacific Ocean and Caribbean Sea, respectively [3,24]. CFP was finally linked to dinoflagellates in 1977 [25]. Several methods have been developed to test for CTX presence in fish, ranging from indigenous observations and animal mortality tests to modern analytical techniques. The present review aims to summarize such methods and identify future challenges in CFP testing. *Gambierdiscus* strains, from which *G. polynesiensis* in the Pacific Ocean and *G. excentricus* in the Atlantic Ocean represent the major threat to human health [26,27], are known to produce not only CTXs but other toxins, such as the water-soluble and structurally related maitotoxins [28,29] and gambierones [30,31]. However, the contributions of these latter toxins to CFP is insignificant compared to that of CTXs, due to their high water solubility and low oral potency [8,9]; therefore, these toxins are beyond the scope of this review.

2. Ciguatoxins

The metabolic modification of dinoflagellate toxins in fish produces a large number of structurally related CTX congeners. Multiple CTX congeners exist in fishes, and each may contribute to CFP. To date, 47 CTXs have been identified but less than half are structurally characterized due to the insufficient amounts of pure toxin available for analysis. Legrand et al. isolated 0.35 mg of pure P-CTX-1 from 125 kg of fish viscera, including 43 kg of liver, from 4150 kg of moray eels, *Gymnothorax javanicus* [32]. The specific chemical structures of major CTXs, however, were elucidated using NMR and mass spectrometry [33–42]. CTXs are composed of contiguous cyclic ether rings aligned in a ladder-like fashion, and the two termini of the rigid ladder are varied in congeners. Most of the CTX congeners possess a primary hydroxyl group that may allow selective derivatization. The toxicity of various CTX congeners are different. On the basis on their acute intraperitonial median lethal dose (LD_{50}) in mice, EFSA has adopted the following toxicity equivalency factors (TEFs) for CTXs: P-CTX-1 = 1, P-CTX-2 = 0.3, P-CTX-3 = 0.3, P-CTX-3C = 0.2, 2,3-dihydroxy-P-CTX-3C = 0.1, 51-hydroxy-P-CTX-3C = 1, P-CTX-4A = 0.1, P-CTX-4B = 0.05, C-CTX-1 = 0.1 and C-CTX-2 = 0.3 [1].

To date twenty-two CTXs have been identified from Pacific fish samples (Table 1). The skeletal structures of the 22 structurally characterized toxins can be separated into two groups, the P-CTX-1 (or CTX-1B) type and the P-CTX-3C type. P-CTX-1 (mass 1110.6 Da, $C_{60}H_{86}O_{19}$) exhibits the highest

toxicity against mice [33]. Molecular masses of P-CTXs are summarized in Table 1, and structures of CTXs are shown in Figure 1.

Table 1. Molecular formula and mass (in Da) of identified ciguatoxins [1].

Pacific CTXs			**Caribbean CTXs**		
P-CTX-1	$C_{60}H_{86}O_{19}$	1110.6 [37]	C-CTX-1 [5]	$C_{62}H_{92}O_{19}$	1140.6 [35]
52-*epi*-P-CTX-1	$C_{60}H_{86}O_{19}$	1110.6 [38]	C-CTX-2 [5]	$C_{62}H_{92}O_{19}$	1140.6 [35]
54-*epi*-P-CTX-1	$C_{60}H_{86}O_{19}$	1110.6 [38]	C-CTX-1141a	n.a.	1140.6 [34]
54-*epi*-52-*epi*-P-CTX-1	$C_{60}H_{86}O_{19}$	1110.6 [38]	C-CTX-1141b	n.a.	1140.6 [34]
P-CTX-2 [2]	$C_{60}H_{86}O_{18}$	1094.6 [33]	C-CTX-1141c	n.a.	1140.6 [34]
P-CTX-3 [2]	$C_{60}H_{86}O_{18}$	1094.6 [33]	C-CTX-1127	n.a.	1126.6 [34]
7-oxo-P-CTX-1	$C_{60}H_{86}O_{20}$	1126.6 [38]	C-CTX-1143	n.a.	1142.6 [34]
6,7-diH-7-OH-P-CTX-1	$C_{60}H_{88}O_{20}$	1128.6 [38]	C-CTX-1143a	n.a.	1142.6 [34]
3,4-diH-4-OH-7-oxo-P-CTX-1	$C_{60}H_{88}O_{21}$	1144.6 [38]	C-CTX-1157	n.a.	1156.6 [34]
54-deoxy-50-OH-P-CTX-1	$C_{60}H_{86}O_{19}$	1110.6 [38]	C-CTX-1157a	n.a.	1156.6 [34]
P-CTX-3C [3]	$C_{57}H_{82}O_{16}$	1022.6 [39]	C-CTX-1157b	n.a.	1156.6 [34]
P-CTX-3B [3]	$C_{57}H_{82}O_{16}$	1022.6 [38]	C-CTX-1159	n.a.	1158.6 [34]
51-OH-P-CTX-3C	$C_{57}H_{82}O_{17}$	1038.6 [40]			
2,3-diH-2-OH-P-CTX-3C	$C_{57}H_{84}O_{17}$	1040.6 [38]	**Indian CTXs**		
2,3-diH-2,3-diOH-P-CTX-3C	$C_{57}H_{84}O_{18}$	1056.6 [40]	I-CTX-1	$C_{62}H_{92}O_{19}$	1140.6 [15]
M-*seco*-P-CTX-3C	$C_{57}H_{84}O_{17}$	1040.6 [41]	I-CTX-2	$C_{62}H_{92}O_{19}$	1140.6 [15]
P-CTX-4A [4]	$C_{60}H_{84}O_{16}$	1060.6 [42]	I-CTX-3	$C_{62}H_{92}O_{20}$	1156.6 [15]
P-CTX-4B [4]	$C_{60}H_{84}O_{16}$	1060.6 [37]	I-CTX-4	$C_{62}H_{92}O_{20}$	1156.6 [15]
M-*seco*-P-CTX-4A/B	$C_{60}H_{86}O_{17}$	1078.6 [41]	I-CTX-5	$C_{62}H_{90}O_{19}$	1138.6 [19]
51-OH-2-oxo-CTX-3C	$C_{57}H_{82}O_{18}$	1054.6 [38]	I-CTX-6	$C_{62}H_{90}O_{20}$	1154.6 [19]
2,3-diH-2,3,51-triOH-P-CTX3C	$C_{57}H_{84}O_{19}$	1072.6 [38]			
A-*seco*-2,3-diH-51-OH-P-CTX-3C	$C_{57}H_{86}O_{18}$	1058.6 [38]			

[1] OH = hydroxy, H = hydro, n.a. = not available; [2] Epimers; [3] Epimers; [4] Epimers; [5] Epimers. Alternative or old names: P-CTX-1 = CTX-1B and CTX; P-CTX-2 = 52-*epi*-54-deoxy-CTX-1B; P-CTX-3 = 54-deoxy-CTX-1B; P-CTX-3B = 49-*epi*-P-CTX-3C; P-CTX-4B = 52-*epi*-P-CTX-4A, GTX-4B, GT-4B or gambiertoxin-4B; 49-*epi*-P-CTX-3C = P-CTX-3B; 56-*epi*-C-CTX-1 = C-CTX-2; 2,3-dihydro-2,3-dihydroxy-P-CTX-3C = 2,3-dihydroxy-P-CTX-3C = CTX-2A1.

Twelve Caribbean CTXs have been identified thus far [34], and the structures of the two major toxins (epimers C-CTX-1 and C-CTX-2, mass 1040.6 Da, $C_{62}H_{92}O_{19}$, see Figure 2) have been determined [35]. The molecular structure of C-CTX-1 has been recently revised [36] (Figure 2). Based on molecular fragmentation in a mass spectrometer at high collision energies, the N-ring of C-CTX-1 is more likely to be a seven-membered ring [36] than a six-membered [35]. Structure and toxicity of the other 10 CTXs have not been established yet. C-CTX-1 is considered to be 10-times less toxic than P-CTX-1 [8].

Six CTXs have been identified to date from fishes and sharks of the Indian Ocean [15,19,43], two isomer pairs with masses of 1140.6 Da (I-CTX-1 and -2, $C_{62}H_{92}O_{19}$) and 1156.6 Da (I-CTX-3 and -4, $C_{62}H_{92}O_{20}$) [15], as well as two congeners with only 2H less, 1138.6 Da (I-CTX-5, $C_{62}H_{90}O_{19}$) and 1154.6 Da (I-CTX-6, $C_{62}H_{90}O_{20}$), which corresponds to the formation of a double bond [19]. The exact structure of these toxins has not been determined as yet. Various experiments have indicated that the toxicity of both I-CTX-1 and -2 is 60% and both I-CTX-3 and -4 is 20% of the P-CTX-1 potency [15].

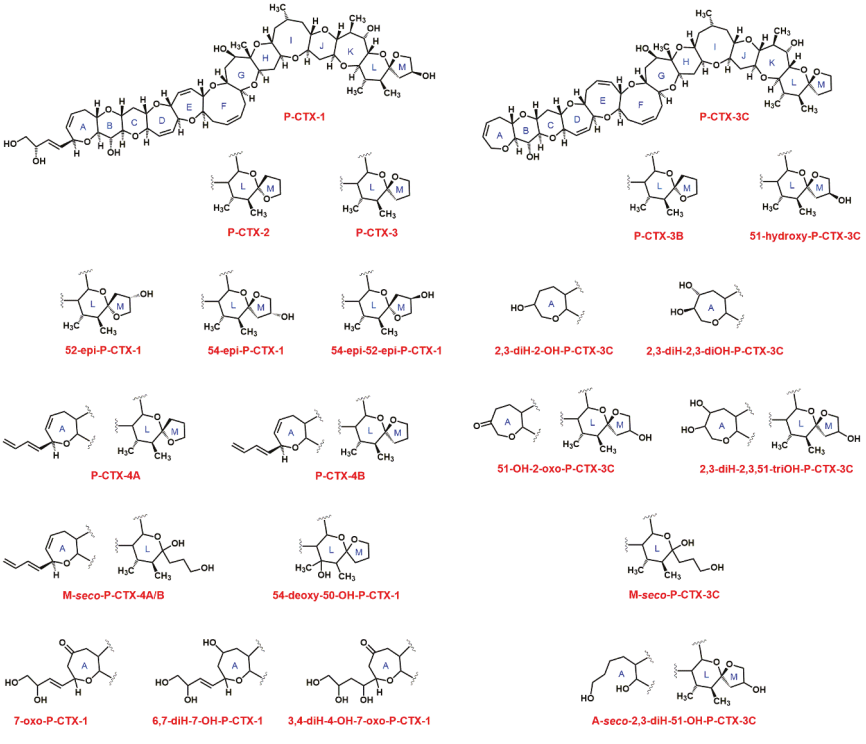

Figure 1. Structure of Pacific CTXs (alternative or old names are given in Table 1).

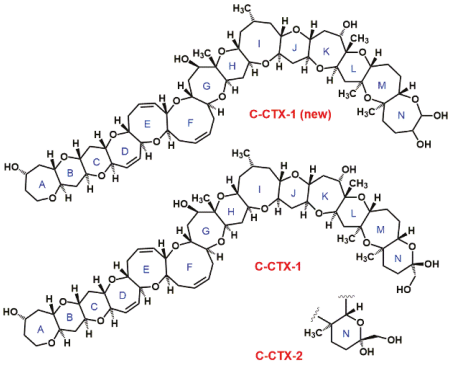

Figure 2. Structure of C-CTX-1 and C-CTX-2, according to Lewis et al. [35], and the suggested new structure, C-CTX-1(new) [36].

3. Extraction of Ciguatoxins from Fish Tissue

Extracting CTXs from fish tissue is a critical step in CTX quantification and strongly influences analyte recovery and thus analytical reliability. This purification step is also important to efficiently remove matrix-derived interfering compounds that negatively affect sample analysis, such as lipids. Extraction methods involve multiple steps, and are time consuming; they include, in general, the following major steps: (1) extraction of raw, freeze-dried or cooked muscle tissue with a polar organic solvent (typically acetone or methanol); (2) purification of the extract by liquid-liquid partitioning

(using diethyl ether, chloroform, or dichloromethane); (3) defeating the extract by liquid-liquid partitioning using hexane or cyclohexane; and (4) purification of the crude extract by solid-phase extraction (SPE), in one step using normal-phase or reverse-phase SPE, or more typically in two steps using consecutive orthogonal SPE phases. Several modified versions of the original extraction method of Lewis et al. [44] have been published during the last three decades, e.g., [12,43,45–49]; two currently used methods are summarized in Figure 3 as examples [41,45,50,51]. Varying the solvent used for extraction, the sample-to-solvent ratio, the number of extraction cycles used to extract fish tissue, and the number of SPE steps can influence the extraction efficiency of CTXs and extract purity, and determine time for extract preparation. A further complicating factor is that extraction efficiency depends also on the CTX analogue; for example, methanol is a good extraction solvent for various CTXs, but produces high levels of co-extractives. Using more polar solvent such as aqueous methanol limits the amount of co-extractives in the extract, is effective for the more polar CTX analogues, but much less effective for less polar CTX analogues [49]. Application of consecutive purification steps varies considerably among sample preparation protocols that exist in the literature. Most of the existing protocols are reviewed by Harwood et al. in 2017 [49]. Selection of the extraction protocol is not unambiguous, and unsurprisingly no validated extraction method exists to date. Current extraction protocols are complicated and not efficient enough.

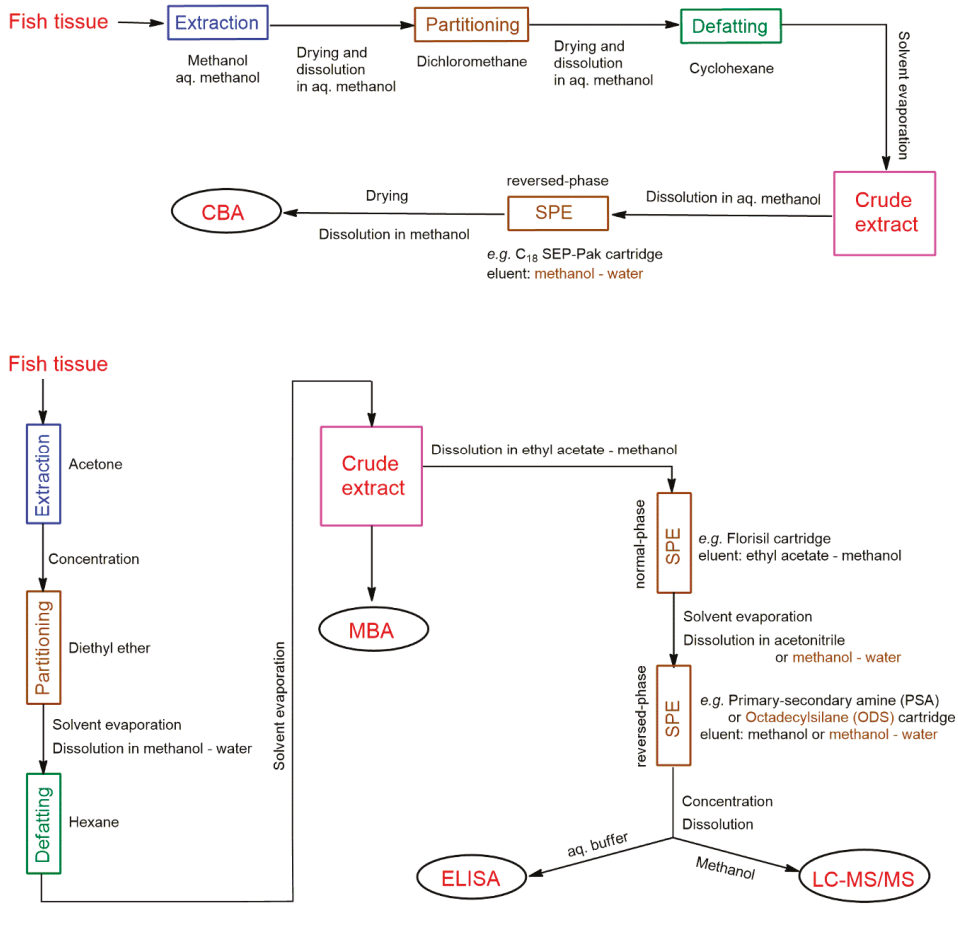

Figure 3. Examples of extraction of CTXs from fish tissue for various CTX tests [41,45,50,51].

The fish tissue extraction process due to several purification steps is slow compared to the time frame of modern analytical techniques (e.g., liquid chromatography-tandem mass spectrometry, LC-MS/MS, see below), therefore it is the rate-determining step for testing a fish sample. To decrease extraction time, a ciguatoxin rapid-extraction method (CREM), which uses only 2 g of fish tissue and combines the first three extraction steps mentioned above by applying a methanol-hexane mixture, has also been developed by Lewis et al. [52]. The method was updated and modified later by Stewart et al. [53] and Meyer at al. [54]. The rapid extraction method was estimated to be two-to-three times faster than the standard method for extraction and clean-up of CTXs [53]. It is, however, less effective than 'normal' protocols in terms of efficiency and toxin yield [54], and therefore not widely used by all specialized laboratories. Although, in principle, higher extract purity is better for all CTX detection techniques, it is worth considering minimum extract purity requirements for various analytical techniques, regarding time and cost. The crude extract is sufficient for mouse bioassay (MBA), the SPE provides sufficiently pure extract for Cell-based Assay (CBA), Receptor-binding Assays (RBA), Enzyme-Linked ImmunoSorbent Assay (ELISA) and LC-MS/MS. Further high-performance liquid chromatography (HPLC) separation produces purer fractions which can be useful for specific investigations, such as for example the determination of toxicity profile using CBA-N2a (see Section 4.4 below).

4. Detection and Quantification of Ciguatoxins

Due to the serious threat to human health caused by CFP, to date a wide variety of methods have been developed to detect CTXs in fish, including native tests, animal mortality tests, biological methods (cytotoxicity assays, receptor-binding assays and immunoassays), and chemical methods (HPLC with fluorescence detection, LC-MS/MS) (Figure 4). Many of these methods are not specific to CTXs, inadequate for quantification, or allow quantification of CTXs only with results expressed in "equivalent of a CTX standard". Currently, the most advanced methods for monitoring CTXs are based on combination of biological and chemical methods into two steps by screening fish extract toxicity with sensitive functional assays first, followed by confirmation of the presence of CTXs via LC-MS/MS.

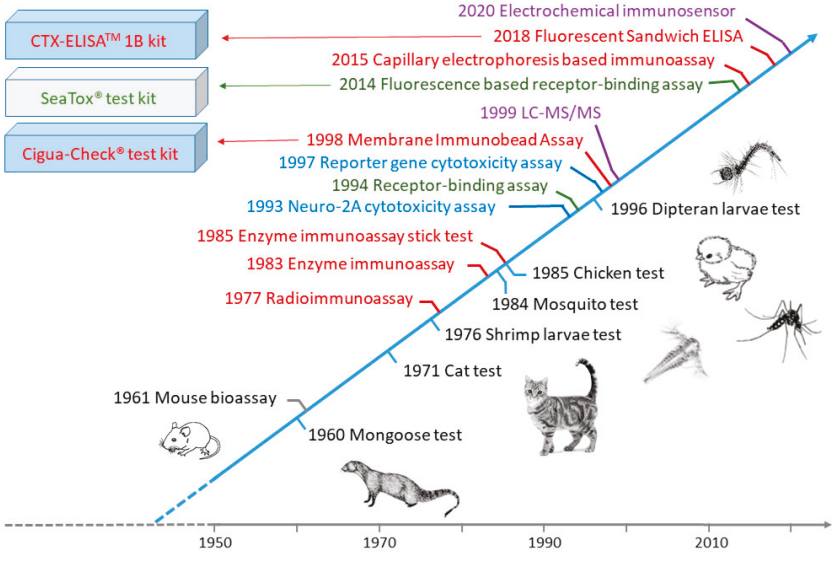

Figure 4. Timelines of CTX detection methods.

4.1. Indigenous Tests

Island communities that are strongly dependent on fish for food resources have developed various means over centuries to decrease the risk of CFP [10,11,55,56]; these include rubbing a small piece of liver on the mouth or skin and then testing for itchiness, cooking fish with a silver coin or copper wire and assessing discoloration, observing the color of fish gallbladder, examining food avoidance by ants and flies, feeding dogs, cats or pigs with suspected fish and observing sickness or fatality of animals, and bleeding and *rigor mortis* tests [10,11,55,56]. A fish is considered to be toxic in the bleeding test if haemorrhagic signs are visible at an incision on the tail of the dead fish. In the *rigor mortis* test, a fish is considered to be toxic if its flesh is flaccid an hour after death. All of these native and traditional test methods are now discredited due to their lack of specificity and the regular occurrence of both false negative and positive results. Darius et al. investigated the accuracy of the bleeding and *rigor mortis* tests by comparing test results with laboratory toxicity data obtained via the RBA and CBA on neuroblastoma cells [56], and concluded that intoxication in communities where CFP is highly prevalent may be reduced on the basis of traditional knowledge and a good understanding of high-risk versus relatively safe fishing areas.

4.2. Animal-Feeding Bioassay Tests

CTXs are toxic to a wide range of animal species [57]. Animal bioassay tests were developed during the 20th century. These tests were based on feeding cats [58], mongooses [59], chickens [60], or Dipteran larvae [61] with the flesh or viscera of suspected fish, or treating mosquitoes [62] or brine shrimp larvae [63] with fish extracts, and observing signs of intoxication and death of animals over time. Symptoms of cats and mongooses after being fed with toxic fish have been found to be similar in some respects to those of humans [59]. These reactions after a single test feeding, within 48 h, have been classified in five stages based on the maximal response of the test animal and numbered as: 0 = no symptoms; 1 = slight weakness and flexion of the forelimbs; 2 = slight motor ataxia, more pronounced flexion of the forelimbs, and weakness of the hind limbs; 3 = moderate motor ataxia with weakness and partial paralysis of limbs and body musculature; 4 = acute motor ataxia and extreme weakness or coma; and 5 = death. Stages 3–5 are indicative of high toxicity, 1–2 moderate toxicity, and 0 non-toxicity in fish. However, neither cats nor mongooses are satisfactory test animals to establish an LD_{50} because cats often regurgitate the test meal and mongooses commonly consume too much fish to permit the necessary replicate testing [59]. The chicken-feeding test is based on force feeding 8–10 days old chicks with cooked fish tissue (10% of body weight) and assessing the change in body weight of the study animals over a 48-h period [60]. The response of chickens to being fed contaminated fish liver has been found to be roughly quantitative. The mosquito bioassay test, where mosquitoes (*Aedes aegypti*) are intrathoracically injected, requires much smaller amounts of fish samples (8 g) than the tests discussed above, is much cheaper due to the low cost of mosquitoes, and is able to provide a LD_{50} value in 2 h [62]. This test requires, however, a fish extract, therefore use of laboratory, as it is not practical to conduct the extraction procedure under field conditions. Based on the mosquito bioassay and human symptomatology, the minimum lethal dose of P-CTX-1 in humans has been estimated to be 0.02 ng g^{-1} [64]. Although brine shrimp are seemingly unaffected by consuming finely ground ciguateric fish, their larvae have been found to be sensitive to fish extract. The brine shrimp larvae bioassay was based on treating approximately 100 freshly hatched larvae in artificial sea water with fish extract and observing the proportion of larvae that died over a 24-h period [63]. The Dipteran larvae-feeding test is extremely simple, does not require cooking or any pretreatment of fish samples, and can be evaluated visually; therefore, this test has been suggested to be appropriate for use in communities inhabiting remote islands that have no laboratory facilities [61]. The larvae, however, are sensitive to other toxic substances. In the Dipteran larvae test, ten larvae are placed on ca. 5 g of fish sample and the inhibition of larval growth is followed for 3−24 h. Fish samples containing more than 1 ng CTXs in 1 g of flesh kill the larvae in about 3 h. By weighing the larvae and comparing them to healthy reference samples, a limit of detection (LOD) of 0.15 ng g^{-1} can be achieved [61].

Although animal feeding tests, in general, are simple, easy to implement and do not require complex analytical equipment, such tests are insufficiently sensitive, incapable of providing specific information on individual toxins, time consuming, cannot be automated, and are expensive due to the required animal facilities and expertise. Further, there are serious ethical concerns about the application of these tests. Unsurprisingly, none of these tests currently are used in modern laboratories.

4.3. Mouse Bioassay (MBA)

The mouse bioassay [65,66] is the only animal test today that remains in use, e.g., [67], despite its disadvantages and ethical concerns. The MBA is simple and does not require complex analytical equipment, but it is expensive due to the need for animal facilities, is time consuming, and cannot be automated. The MBA provides information only about the total toxicity of a sample, therefore lacks specificity, and CFP caused by CTXs may be overestimated. The limit of quantitation (LOQ) of MBA is approximately 0.56 ng g^{-1} for P-CTX-1 [1], therefore the bioassay is insufficiently sensitive to cover the suggested tolerance limit of 0.01 ng g^{-1} in fish. CTXs are highly potent toxins in mice by either the intraperitoneal (i.p.) or oral route [33]. Injecting fish extract intraperitoneally into mice is the generally applied method in MBA [1,3]. Raw extracts are usually suspended in 1% Tween 60, 0.9% saline solution prior to injection. The test is administered either by establishing dose/survival-time relationships or by observing mice for motor ataxia or other bodily dysfunction for 24 h after injecting serial dilutions of CTX extracts. The end point in the assay is the death of the test animal. The dose-vs-time-to-death relationships for CTXs (Figure 5) are found to be as follows: log(dose) = c log(1 + t^{-1}), where dose is in mouse units (MU), time (t) to death is in hours, and constants c is 3.3, 2.4, 3.9, and 2.3 for pure P-CTX-1, pure P-CTX-2, pure P-CTX-3, and partially purified P-CTX, respectively. One MU is defined as the i.p. LD_{50} dose for a 20 g mouse, equal to 5.0, 46 and 18 ng P-CTX-1, PCTX-2, and P-CTX-3, respectively [33].

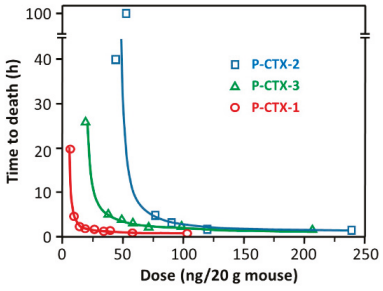

Figure 5. Relationship between intraperitoneal dose in mice and time to death for Pacific CTXs, reproduced with permission from [33]. Copyright Elsevier Ltd., 1991. The equation of the fitted curves is shown in the main text.

4.4. Cell-Based Assay (Cytotoxicity Assay)

Cell-based assays are dependent on the toxic activity of fish extracts on cultured cells and reflect the combined potency of related toxins in the mixture. The overall toxicological effects of CTXs are caused by the action of CTXs on neuronal potassium and voltage-gated sodium channels [2]. CTXs bind quasi-irreversibly to voltage-sensitive sodium channels, enhancing sodium influx into cells, causing them to open at the normal cell-resting membrane potential, thereby impeding normal function. In addition, CTXs also inhibit neuronal potassium channels, which is likely to act in concert with effects on voltage-gated sodium channels to increase neuronal excitability [2,3]. Evaluation of cell viability forms the basis of CTX determination in CBAs [1].

Several cell and tissue-based assays were developed previously, namely the guinea pig ileum [68], guinea pig atrium [69,70], isolated frog nerve fiber [71], crayfish nerve cord [72], and blood cell hemolytic [73] tests. These tests, however, are outperformed by the mouse neuroblastoma cell assay

(CBA-N2a) and thus are no longer employed. The CBA-N2a is widely used today, and its development by Manger et al. [74] is one of the most important milestones of replacing MBA in modern laboratories. The assay is based on the colorimetric detection of metabolically active N2a cells treated with CTX extract in the presence of ouabain/veratridine [74–76]; it expresses negatively the concentration of various voltage-gated sodium channel toxins and assesses cell death [3]. CTXs have no cytotoxic effect on N2a cells, therefore their detection requires addition of veratridine (a sodium-channel-activator that have a different binding site than CTXs) and ouabain (a sodium/potassium ion ATPase inhibitor). The combined effect of CTXs together with ouabain and veratridine causes an elevation of intracellular sodium ions to toxic levels in cells and a resultant decrease in cell viability that can be measured as a function of CTX concentration. Toxins are detected as a dose-dependent loss of cell viability, based on an end-point determination of mitochondrial dehydrogenase activity, due to the synergistic effect of ouabain/veratridine-induced cytotoxicity by CTXs (Figure 6a). Color development is based on the ability of active cells to reduce 3-[4,5-dimethylthiazol-2-yl]-2,5-diphenyltetrazolium (MTT) to a blue-colored formazan product. The advantage of this MTT-based bioassay is that it is more sensitive for CTXs (at ng/g fish level) than the mouse bioassay, and suits to automation due to color reading [1]. Results obtained from CBA-N2a bioassays of fish extracts have correlated well with those obtained from MBA [1,74]. Although CBA-N2a have been widely used in the last three decades and the protocol has undergone numerous changes [77], a consensus assay protocol is still lacking. To this end, research to standardize this CBA [77,78] and to avoid matrix effects [79] also have been conducted. Viallon et al. revisited recently the CBA-N2a assay by investigating six key parameters, namely cell seeding densities, cell layer viability after 26 h growth, MTT incubation time, veratridine and ouabain treatment, and solvent and matrix effects [77]. A step-by-step protocol was defined by identifying five viability controls for the validation of CBA-N2a results, therefore, the improved method is an important step towards implementation of a reference detection test.

An advantage of the CBA-N2a assay is that necessary materials and reagents, as well as basic laboratory equipment are commercially available. A major disadvantage of CBA-N2a, however, is that it is time consuming, including, in general, 24 h incubation of neuro-2a cells, 24 h exposure of the neuro-2a cells to fish extracts, and a 4–6 h cell viability assessment. Achieved LOD and LOQ using this assay depends also on assay protocol. Nonetheless, CBA-N2a is able to provide LOD below the clinically relevant toxin levels in fish tissue. Selected examples for CBA application are summarized in Table 2 (more data are provided in the cited articles).

Fairey et al. modified the cell-based directed cytotoxicity assay and developed a reporter-gene modification by using CBA-N2a clones expressing c-*fos*–Luciferase; the assay was thereby utilizing a luciferase-catalyzed light generation as an endpoint and a microplate luminometer for quantification [81,82]. c-*fos* is an immediate response gene and a sensitive biomarker to localize the effects of toxins. This assay, however, is not commonly used possibly due to the problematic interpretation of the bell-shaped dose–response curve and the cost of fluorescent dye.

N2a cell lines are widely and routinely used in cell-based assays. However, other cell lines have also been tested for potential application in CBA. Zimmermann et al. [83] and Lewis et al. [84] developed fluorescent CTX assays using the human neuroblastoma cell line SH-SY5Y, expressing a range of voltage-gated sodium channel subtypes. SH-SY5Y cells were loaded with Calcium-4 No-Wash dye absorbed into the cells' cytoplasm. Cells were incubated for 5 min with CTXs prior to addition of veratridine. Fluorescence responses to CTXs, arising due to calcium ion influx into cells, were recorded using a Fluorescent Imaging Plate Reader. The performance of the SH-SY5Y assay was comparable to a N2a-based cytotoxicity assay [84]. The assay, however, is currently not widely used because it requires specialized equipment, the fluorescent dyes are expensive, and a small carryover of maitotoxins into the CTX fraction during purification steps could potentially obscure CTX responses due to saturation of fluorescence by maitotoxin-induced increase of intracellular calcium ions [3].

CTXs accumulate in fish tissue due to their lipophilic character, however, they also circulate in blood for some time. Bottein Dechraoui et al. were able to detect CTX in blood of mice after 12 h

post-exposure of sublethal dose of Caribbean ciguatoxic extract (0.59 ng g^{-1} C-CTX-1 equivalents), and pointed out that neuroblastoma assay (LOD 0.006 ng ml^{-1} C-CTX-1) is suitable to monitor CTX in blood at sublethal doses in mice and argued that CTX monitoring in blood could be a useful procedure for fish screening [91]. Blood is a much simpler matrix than fish tissue, and CTX recovery from fresh blood is close to 100% due to lack of matrix effects [92]. Taking blood samples is a non-lethal sampling method for detection of CTXs in wild fish. O'Toole et al. studied the toxin level in tissue, blood and liver of the great barracuda (*Sphyraena barracuda*) [88] and observed a correlation between blood and liver toxin concentrations.

Although cytotoxicity assays are simple and provide an alternative to the MBA, they are currently not time- and cost-effective for mass screening, reflect only the combined potency of all-sodium-channel blocking toxins in an extract, and thus fail to provide any information about the toxin profile. Considering this latter point, however, limited information can be obtained by fractionating an extract using HPLC and then testing the toxicity of these fractions. Estevez et al. fractionated an amberjack sample, and CBA-N2a toxicity profile indicated the presence of at least four toxins (Figure 6b), which was confirmed by LC-MS/MS [51].

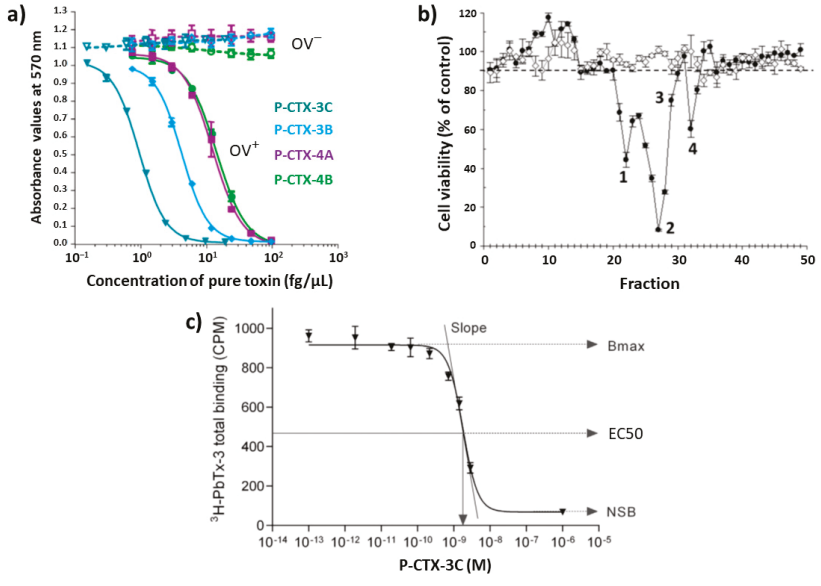

Figure 6. (**a**) Dose-response curve for N2a cells under OV^+ (cells treated with ouabain and veratridine mixture) conditions and under OV^- (untreated cells without ouabain and veratridine added) conditions, exposed to increasing concentrations of four P-CTX standards, reproduced with permission from ref. [45]. Copyright MDPI AG, 2018; (**b**) CBA-N2a cytotoxicity profile of an HPLC fractionated sample, reproduced with permission from ref. [51]. Copyright MDPI AG, 2019; (**c**) Typical sigmoidal dose response curve of R-RBA. Bmax is the maximum binding of the bound radioligand (in counts per minute, CPM) in the absence of competing CTXs. Non-specific binding (NSB) represents the minimum total radioligand binding in the presence of saturating concentrations of CTXs, the EC50 is the effective concentration at 50%, reproduced with permission from [80]. Copyright Elsevier Ltd., 2018.

Table 2. Examples for the application of cytotoxicity and receptor-binding assays [1].

Assay [1]	Fish Species (Family)	Equiv. [2]	Mass [3] (g)	Conc. [2] (ng g^{-1})	LOQ [4,5] (ng g^{-1})	Ref.
CBA-N2a	*Carcharhinus leucas* (Carcharhinidae)	P-CTX-1	10 [6]	92.78	0.13	[19]
CBA-N2a	*Lutjanus sp.* (Lutjanidae)	P-CTX-1	5	0.4708	0.032	[21]
CBA-N2a	*Gymnothorax spp.* (Muraenidae)	P-CTX-1	20 [7]	539	0.0016	[23]
CBA-N2a	*Seriola fasciata* (Carangidae)	C-CTX-1	15	1.4	n.a.	[51]
CBA-N2a	*Chlorurus microrhinos* (Parrotfish)	P-CTX-3C	10	6.66	0.064	[77]
CBA-N2a	*Epinephelus merra* (Serranidae)	P-CTX-3C	10	3.31	0.064	[77]
CBA-N2a	*Seriola fasciata* (Carangidae)	P-CTX-1	10	6.231	0.0096	[78]
CBA-N2a	*Balistes vetula* (Balistidae)	C-CTX-1	n.a.	0–0.11	0.006	[85]
CBA-N2a	*Sphyraena barracuda* (Sphyraenidae)	C-CTX-1	10 [7]	2.1	0.039	[86]
CBA-N2a	*Balistapus undulatus* (Balistidae)	P-CTX-1	5	4.64	0.00195	[87]
CBA-N2a	*Epinephelus multinotatus* (Serranidae)	P-CTX-1	5	6.49	0.00195	[87]
CBA-N2a	*Sphyraena barracuda* (Sphyraenidae)	C-CTX-1	n.a.	0.099	0.001	[88]
R-RBA	*Scarus altipinnis* (Scaridae)	P-CTX-3C	5	0.36–4.52	0.155	[89]
R-RBA	*Kyphosus cinerascens* (Kyphosidae)	P-CTX-3C	5	0.46–4.25	0.155	[89]
R-RBA	*Plectropomus leopardus* (Serranidae)	P-CTX-3C	5	0.36–3.29	0.155	[89]
R-RBA	*Liza vaigiensis* (Mugilidae)	P-CTX-3C	5	16.23	0.155	[89]
F-RBA	*Pterois volitans* (Scorpaenidae)	C-CTX-1	5	0.1–0.2	0.23	[90]

[1] CBA-N2a = mouse neuroblastoma cell assay; RBA = receptor binding assay (R-radioligand-based, F-fluorescence-based); n.a. = not available; [2] Composite toxicity (ng C-CTX-1 (TEF = 0.1), P-CTX-3C (TEF = 0.2) or P-CTX-1 toxin equivalent/g fish tissue); [3] Mass of fish tissue used for the analysis; [4] LOQ for CBA-N2a: (EC_{50} of P-CTX-3C/maximum concentration of dry extract)×(dry extract weight/fresh weight of flesh tissue extracted); [5] LOQ determination for RBA: LOQ = IC_{50} of P-CTX-3C/quantity maximum of a sample that does not cause matrix interferences; [6] Shark stomach sample; [7] Liver.

4.5. Receptor-Binding Assays (RBA)

CTXs compete with brevetoxin for the same neurotoxin receptor sites at sodium channels, having at least 20–50-times higher affinity [81], therefore CTXs are competitive inhibitors of brevetoxin binding [7,33,93,94]. Measuring the inhibition of radioactively labeled [3H]-brevetoxin-3 binding to rat brain membrane can be used to detect CTXs in fish extracts using either test tube [89,95] or microplate format [96]. Radioligand RBA (R-RBA) is based on competitive binding between CTXs and a radioactively labeled brevetoxin for a given number of available receptor sites in a membrane preparation. When the concentrations of the radioactively labeled brevetoxin and the receptor are kept constant and the concentration of CTXs increases, the binding of the radioactively labeled brevetoxin to the receptor sites is proportionally reduced. A competition dose-response curve can be constructed by measuring the concentration of the radioligand-receptor complex across a range of concentrations of CTX standard (Figure 6c), and the amount of CTXs in an unknown sample can be quantified [80]. RBA and CBA-N2a are more specific to CTXs than the MBA due to receptor binding, but RBA and CBA-N2a, like the MBA, do not provide any information on the toxin profile. The sensitivity of RBA is highly dependent on the receptor source. Bottein Dechraoui et al. compared the performance of the R-RBA and the CBA-N2a cytotoxicity assay, and the RBA was found to be 12-fold less sensitive than CBA-N2a for Caribbean ciguatoxin analysis [86]. It was also noted that R-RBA provided systematically higher estimates of CTX concentration than CBA-N2a [86,97]. Although R-RBA have been widely used, screening methods have not been standardized. Díaz-Asencio et al. recently published a methodological development and also determined criteria for quality control [80]. The developed microplate format was able to detect 0.75 ng g^{-1} P-CTX-3C equivalent in fish tissue in only 3 h (process for full plate, not considering up to 2 d extraction time for 10 samples). An analyst could run an estimated 32 samples per day (with up to eight samples per plate run in triplicate at two dilutions) [80].

Large-scale field screening using R-RBA was performed by Darius et al. while evaluating toxic versus safe areas at two sites in French Polynesia, using the R-RBA test-tube format and rat brain synaptosomes as receptors [89]. Results indicated significant disagreement with the knowledge of local people regarding toxicity in several cases and findings were congruent only for fish species with high risk of CTX accumulation, indicating the need of close monitoring to prevent epidemiological outbreaks of CFP (see examples in Table 2, and more data in the original reference).

A disadvantage in the original radioligand format, and a constraint to application, is that R-RBA requires application of radioactive [3H]-brevetoxin compounds. To overcome this problem, McCall et al. recently developed a fluorescence-based RBA method (F-RBA) [98], which assesses competitive binding between CTXs and fluorescently labeled brevetoxin-2. Several fluorescent compounds, including BODIPY, 6-TAMRA, Texas Red, Alexa Fluor 350, Fluorescein, Coumarin, and Dansyl hydrazine, were conjugated to polyether brevetoxin-2, from which the BODIPY-brevetoxin-2 exhibited the best performance in terms of lowest nonspecific binding. The constructed F-RBA was faster (with an assay and analysis time of less than 3 h versus overnight), less expensive and safer than R-RBA, and generated binding constants comparable to the radioligand assay. As a continuation of this work, Hardison et al. developed a F-RBA using fluorescently labeled BODIPY®-brevetoxin-2 [97]. The method was relatively fast and took approximately 2 h to perform and exhibited a LOD and LOQ of 0.075 and 0.1 ng g^{-1} P-CTX-3C equivalent, respectively. Based on this principle, a commercial test kit for detecting CTXs was developed by SeaTox Research Inc. (Wilmington, NC, USA; https://www.seatoxresearch.com/testing-kits/) and currently distributed by MARBIONC® Development Group LLC (Wilmington, NC, USA; http://www.marbionc.org/gallery/detail.aspx?id=2274946). The SeaTox kit can be used as a screening or quantitative tool, and CTX analyses can be completed in less than two hours after fish tissue extraction.

4.6. Immunoassays

Immunoassays are dependent on the application of a high-affinity antibody that is selective and specific for CTXs, therefore, CTX detection and quantification with immunoassays are based on the structure of CTXs, not on their toxicity. In principle, a 100%-specific antibody could capture only one target, therefore detection of all toxins and toxin profile determination of a mixture of different toxins would require application of the same number of specific antibodies than the number of targets. If the antibody is less specific and selective only for a common structural motive of target molecules, it can capture several targets, but cross-reactivity with non-target compounds having the same structural element cannot be avoided. Production of antibodies is one of the key issues and constraints of immunoassays. In all cases, a label is attached to the antibody to detect target-antibody interaction; this label can be a radioisotope, enzyme, or fluorescent probe. Immunoassay methods, in general, are fast and easy to use, the sole exception being the radioimmunoassay (RIA). Unless several antibodies are used, they do not provide information on the toxin profile. Selecting antibodies only against the major toxin might also be problematic; P-CTX-1 in carrier fish, for example, represents in many cases greater than 90% of the toxins, but C-CTX-1 in fish represents only about 50% of total toxins [8]. Another problem that may rise with immunoassays is the possible cross-reaction of low-potency CTXs with antibodies, which increases the possibility of obtaining false-positive results. Antibodies developed for Pacific CTXs may not be suitable for testing Caribic CTXs, and *vice versa*.

The first immunoassay test, RIA, was developed by Hokama et al. in 1977 to assess fish tissues directly [99]. Labeled CTX antibodies were prepared by: (1) coupling purified CTX, isolated from toxic eel tissues, to human serum albumin; (2) injecting the CTX-human serum albumin conjugate into sheep for generating the anti-CTX-human serum albumin; (3) bleeding animals and collecting serum after 8 weeks; and (4) iodinating sheep anti-CTX-human serum albumin with ^{125}I. This method was successfully used in the following years to test and reject toxic fish on the Hawaiian market [100], but it was time-consuming, expensive, and required special radioisotopic facilities, therefore it was impractical for routine screening of fish samples. The same sheep anti-CTX serum synthesized for

RIA was used by Hokama et al. to develop an enzyme-immunoassay (EIA) by coupling horseradish peroxidase (HRP) to sheep anti-CTX-human serum albumin instead of ^{125}I [101]. 4-chloro-l-naphthol was used as substrate for the enzymatic reaction with spectrophotometric reading. EIA exhibited similar sensitivity and specificity to that of the RIA, yet, it was easier to run and economically feasible for screening fishes. However, this test remained labor intensive, and cross-reactions occurred with other polyether compounds. As a further development, Hokama constructed the first POC test utilizing the same sheep-anti-CTX antiserum [102,103]. The simplified enzyme immunoassay stick test (S-EIA) was rapid and did not require any instrumentation. The reagents for S-EIA were similar to those of EIA, and the salient feature of S-EIA was use of a coating (Liquid Paper, Liquid Paper Corp., Rockville, MD, USA) applied to a bamboo stick to adsorb the lipid CTX and its related polyether toxins onto the stick. Fish samples were poked with the stick and after fixation, the stick was immersed consecutively into sheep-anti-CTX-HRP solution and substrate solution. The substrate color change was read after 10 min, which provided a fast estimation of toxin content as being negative, borderline, or positive. All of these methods – RIA, EIA, and S-EIA—used fish flesh directly without extraction, but the antibody was not sufficiently selective, as the polyclonal sheep-anti-CTX detected not only CTXs but also structurally-related polyether toxins, including okadaic acid and brevetoxin [104,105]. This attribute resulted in false-positive tests [8,10]. Lack of sufficient sensitivity for S-EIA was also noted [106]. Due to these drawbacks, Hokama et al. prepared and used monoclonal antibodies, MAb, to CTXs in immunoassays [105]. Monoclonal antibodies are more selective to CTXs than are polyclonal variants, having some cross-reactivity with okadaic acid (16%), but little or none with polyethers (e.g., ionomycin). Using MAbs, Y. Hokama developed a simplified solid-phase colored latex immunobead assay (SPIA) for the field detection of CTXs and related polyethers (Figure 7) [107,108]. MAb-CTX was labeled with colored latex. In the simplified procedure, a paddle end of the stick coated with correction fluid (organic base solvent) is inserted into an incision in the fish so that the fish tissue is touched, then removed; the paddle end of the stick is then dried, fixed with methanol, and immersed into MAb-CTX-latex suspension. Visually detectable coloration of the stick is considered to be a positive test result. Hawaii Chemtect International (Pasadena, CA, USA) purchased the patents covering the S-EIA and SPIA tests and commercialized a rapid solid-phase immunobead assay (Ciguatect™) for the detection of ciguatera toxins [109]. The Ciguatect™ test kit could determine the ciguatera potential directly in the fish flesh or after toxin extraction. Toxin extraction increased the sensitivity and decreased the limit of detection [109]. The Ciguatect™ test was more sensitive than S-EIA and better suited to field applications [110]. (Note that the test is no longer used.) The S-EIA test required application of six assay sticks per fish [102,111].

Based on the same immunological principles as the SPIA, Hokama et al. developed a Membrane Immunobead Assay (MIA) using a polyvinylidene fluoride hydrophobic membrane laminated onto a solid plastic support to collect CTXs and a MAb to purified moray eel (*Muraenidae*) ciguatoxin attached to colored polystyrene beads [112]. Application of the hydrophobic membrane was an advantage in reducing non-specific binding of the immunobeads. The test procedure involved placing about 5 mg of fish tissue sample, 0.5 mL methanol, and the membrane stick into a test tube for 20 min, then removing, drying, and immersing this into 0.5 mL immunobead suspension (Figure 7). The intensity of the color on the membrane related to the concentration of the CTX. MIA exhibited much higher specificity than RIA, S-EIA, and SPIA [112]. Oceanit Test Systems, Inc. (Honolulu, HI, USA) marketed a POC test kit, Cigua-Check® test kit, what was based on MIA for P-CTX-1, and developed to test rice-grain-size amounts of fish flesh and to detect CTX higher than 0.05 ng g^{-1} flesh [8]. In principle, this method was able to detect ciguatoxin at concentrations that induce clinical symptoms in humans (above 0.08 ng P-CTX-1/g fish flesh [8]). Concerns were, however, raised against the method's sensitivity and specificity, as well as the interpretation of the test-strip results [113], and possibly due to these and marketing issues, this method is currently not commercially available.

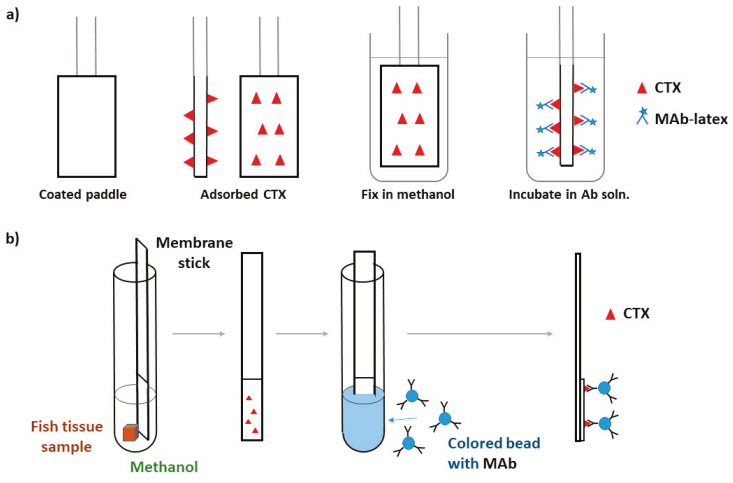

Figure 7. (**a**) Working principle of the simplified solid-phase colored latex immunobead assay (SPIA) test, adapted from ref. [107]; (**b**) Working principle of Membrane Immunobead Assay (MIA) test, adapted from [112].

Antibodies for antibody-based immunoassays are typically produced using scarce natural toxins. This limitation, in principle, could be overcome by replacing natural toxins with synthesized toxins, or with fragments of CTXs. The synthesis of fragments is more simple and cost-effective than that of the whole CTX molecule. These fragments, typically haptens, can be used to generate monoclonal antibodies against CTXs. Sandwich-type ELISA is very promising for increasing selectivity of assays by using two antibodies for the recognition of CTX, where one recognizes the left and the other the right wing of CTX. One of the MAb is conjugated with the enzyme label, typically HRP (Figure 8). To improve performance of immunoassays, Campora et al. constructed a sandwich-type ELISA, utilizing two antibodies, a chicken immunoglobulin Y specific to the ABCD domain of P-CTX-1 and a mouse monoclonal immunoglobulin G-HRP conjugate label specific to the JKLM domain of P-CTX-1 produced by injecting chicken and mouse with synthesized CTX fragments [114]. Significant cross reactivity was not observed for brevetoxin-3, okadaic acid, or domoic acid. Good correlation was observed between this ELISA and CBA-N2a assays by screening three fish species commonly implicated in ciguatera fish poisoning in Hawaii [115]. Tsumuraya et al. developed sandwich-type ELISA detection protocols for the four principal congeners of Pacific ciguatoxins, P-CTX-1, P-CTX-3, P-CTX-3C, and 51-hydroxy-P-CTX-3C, using MAbs produced by immunizing mice with the corresponding left and right wing haptens [116–119]. P-CTX-1 could be detected specifically as low as 0.28 ng mL^{-1} without cross-reactivity with other related marine toxins; this concentration was still higher than the regulatory limit of 0.01 ppb [117]. As a further development, Tsumuraya et al. combined these MAbs into a single sandwich ELISA assay to detect any of these four CTX congeners [50,120]. Detection of the immunoreaction was changed to a fluorescent method using alkaline phosphatase(ALP)-linked MAb and a fluorescent substrate system, 2′-(2-benzothiazoyl)-6′-hyrodxybenzothiazole phosphate (BBTP). The fluorescent ELISA was highly sensitive, having a detection limit of less than 1 pg mL^{-1}. P-CTX-1 spiked into fish at the recommended safety level of 0.01 ppb P-CTX-1 equivalent was reliably detected by this ELISA. The ELISA assay was shown to be very sensitive to CTXs, but required fish extract and laboratory conditions. Based on this ELISA, a fluorescent sandwich ELISA kit "CTX-ELISATM 1B" developed for detection of the P-CTX-1 series (P-CTX-1 and P-CTX-3) was commercialized and could be purchased from Fujifilm Wako Corporation (Osaka, Japan; cat. 382-14341) [120].

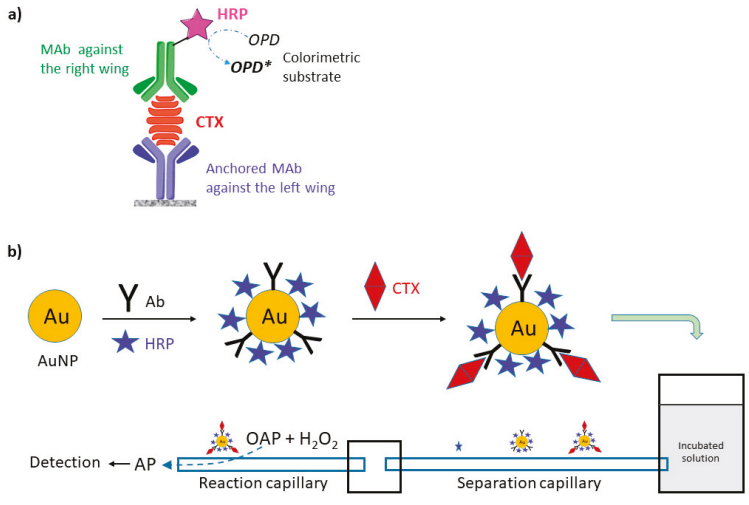

Figure 8. (**a**) Schematic of the sandwich ELISA detection of CTXs (*OPD* = *o*-phenylenediamine); (**b**) Illustration of the preparation of noncompetitive immunoassay with CE separation, adapted from [121].

Zhang et al. developed a capillary electrophoresis (CE)-based immunoassay for detection of P-CTX-1, applying electrochemical detection and gold nanoparticles (AuNPs) as carriers of HRP and CTX antibodies (Ab-AuNP-HRP) as target-capture elements [121]. Crude fish extract was sufficient for detection, which involved mixing the extract with Ab-AuNP-HRP probe solution, dilution, incubation, and analysis by CE separation and electrochemical detection. The unbound HRP, Ab-AuNP-HRP probe and the formed CTX-Ab-AuNP-HRP immunocomplex were separated according to the velocity difference in the separation capillary, and catalyzed the o-aminophenol (OAP) and hydrogen peroxide reaction to 2-aminophenoxazine-3-one (AP) (Figure 8). This latter was electrochemically detected. Due to the high separation power of CE and the high target specificity of the immunoassay, a LOD of 0.045 ng mL^{-1} was achieved. As a further development, Zhang et al. fabricated an ultrasensitive immunoassay for P-CTX-3C detection exhibiting a LOD of 0.09 pg mL^{-1}, based on CE separation and on-line sandwich immunoassay with rotating magnetic field [122]. The sandwich system utilized rabbit anti-P-CTX-3C-functionalized magnetite NP beads as immunosensing probes, and HRP and monoclonal sheep anti-P-CTX-3C-functionalized AuNPs as recognition elements. The rotating magnetic field enhanced the mixing efficiency and molecular binding rates, and the immunoreaction time of the assay was decreased to 15 min. The latter was much faster than normal ELISA.

The first electrochemical immunosensor for CTX detection was constructed by Leonardo et al. this year, 2020 [67]. Capture antibodies were prepared by immobilizing two different mouse MAbs on magnetic beads; these MAbs were able to bind to the left wing of P-CTX-1/P-CTX-3 and P-CTX-3C/51-hydroxy-P-CTX-3C, respectively. A mouse MAb, which was able to bind to the right wing of P-CTX-1, P-CTX-3, P-CTX-3C, or 51-hydroxy-P-CTX-3C, was biotinylated, linked to polyHRP-streptavidin signal reporter, and used as a detector antibody.

To develop the biosensor, the magnetic immunocomplexes were deposited on eight-electrode arrays, and the assay was performed by successively incubating the magnetic immunocomplexes with the CTX analyte and detector antibody. Although LOD and LOQ values of this CTX biosensor were higher than those of fluorescence ELISA, the electrochemical biosensor had an advantage of lower cost, the possibility to be integrated into compact analytical devices, and portability. The immunosensor was successfully applied to the analysis of fish samples and was able to detect P-CTX-1 at 0.01 ng g^{-1} toxin level, as well as exhibited a good correlation with CTX levels determined by the CBA-N2a.

4.7. HPLC, LC-MS/MS and LC-HRMS

CFP is a complex disease in which several different compounds contribute to the toxicity of a fish sample. Current CBA-N2a, F-RBA, and immunoassays are very sensitive, but do not provide information about the toxin profile. Unfortunately, CTXs do not have characteristic functional groups for spectroscopic detection, therefore separating and separately identifying toxins is the only viable route for toxin profiles, and HPLC is the key method for separating CTX congeners. Classical HPLC methods using UV detectors, however, are not sensitive enough to detect very small concentrations of CTXs at clinically relevant levels, and CTXs cannot be distinguished using UV detection due to the lack of useful UV chromophores [12,33,123,124]. At a terminus of the molecule, however, most of the CTX congeners have a primary hydroxyl group (see Figures 1 and 2) that is available for fluorescence labelling. HPLC with fluorescence detection using 1-anthrylcarbocyanide and carbonyl azides or carbonyl nitriles of coumarin derivatives as labels was found to be more sensitive for CTX detection than HPLC-UV, however, still could not reach the recommended tolerance level of 0.01 ng g^{-1} for P-CTX-1 [12,125,126]. The main limitation of this technique was that it could not detect CTXs without a primary hydroxyl group (e.g., P-CTX-3C; see Figure 1), what is especially problematic for herbivores where CTXs without primary hydroxyl group are more abundant [127].

To utilize the separating power of HPLC, a sensitive detector is required. HPLC coupled with tandem mass spectrometry (HPLC-MS/MS) were applied for CTX detection the first time by Lewis and Jones in 1994 [128], and the first successful application of the combined HPLC-MS/MS technique for CTX detection at clinically relevant levels, with detection limits of at least 0.04 ppb for P-CTX-1 and 0.1 ppb for C-CTX-1, was reported by Lewis et al. in 1999 using gradient reversed-phase HPLC and an electrospray triple quadrupole mass spectrometer [129]. The method was significantly more sensitive than fluorometric HPLC. In the following decades LC-MS/MS became one of the leading and indispensable techniques of modern CFP laboratories due to the method's ability to separate and identify toxins, and its uniqueness in providing toxin profiles. Both the identification and quantitation of CTXs, however, require reference toxin molecules. Although the molecular peak and fragmentation pattern in MS can provide valuable information for CTX identification, a diagnostic fragmentation pattern is not always achieved (water losses are often the most abundant fragment ions and depending on the MS instrument used, results may be different). LC-MS/MS must be used in combination to biological assay as a confirmation. In general, raw fish extract could be used for LC-MS/MS, but to decrease possible interference of lipids and fatty acids in fish tissue, the raw extract is usually purified using SPE in one or two steps (Figure 3). The presence of matrix co-extractives significantly interferes with ionization and causes severe signal suppression [49]. To reach very low detection limits, both HPLC and MS conditions must be optimized for sensitivity and selectivity, namely: LC conditions, ionization sources, ion choices and acquisition modes [41,46,130,131]; a comparison of analytical protocols to find the best conditions for sensitivity and/or selectivity for LC-MS/MS has been published recently [130].

LC separation is most frequently performed with acetonitrile-water or methanol-water linear gradients; the methanol-based mobile phases have been found to be more advantageous. Electrospray ionization and positive ion detection mode, using either Single Ion Monitoring (SIM), Multiple Reaction Monitoring (MRM) or Enhanced Product Ion (EPI) scanning, are typically used in MS. Applying MRM is advantageous for increasing specificity. The mobile phase composition, solvents and additives, and flow rate of the mobile phase affect ionization efficiency and ion abundance, therefore they have to be optimized. Monitoring ammonium or sodium adduct as the parent ion often exhibited higher signal-to-noise ratios than protonated parent ion; however, this depends not only on LC and MS conditions, but also on the analyzed CTX (Figure 9a). With formic acid, as a mobile phase additive, the sodium adduct was favored using either acetonitrile/water or methanol/water linear gradients in LC. The sodium adduct, however, has been found to be relatively stable, therefore to obtain MS/MS fragmentation its generation should be avoided by proper selection of eluent and additives, e.g., ammonium formate [130]. The ammoniated adduct ion, as a precursor ion, showed an

advantage for selectivity through confirmatory transitions [130]. Figure 9b shows an example for the LC separation and detection of a mixture of CTX standards. The technique using triple quadrupole detectors (low resolution, LC-MS/MS) is significantly more sensitive than high-resolution MS coupled to HPLC (LC-HRMS, time-of-flight and orbitrap based spectrometers). An important advantage of HRMS, however, is that HRMS provides molecular formula and isotopic patterns of molecules (Figure 9c), therefore providing improved identification of CTX analogues [130,132]. LC-HRMS together with reference material may be the best choice for accurate identification of CTXs. The two techniques may be considered complementary, as LC-MS/MS is more adequate for quantitation and LC-HRMS performs better for identification of toxins. Selected examples for the application of LC-MS for CTX quantification in fish tissue, including fish species, toxin content and LOQ, are shown in Table 3 (more data are provided in the cited articles). Fish blood for determining the CTX content was studied recently by Mak et al. [133], and the matrix effect was found to be smaller than that of using fish muscle tissue. The main advantage of LC-MS is that it is very specific and adequately sensitive to detect CTXs at the clinically relevant toxin levels, and superior to any other techniques as the toxin confirmatory method.

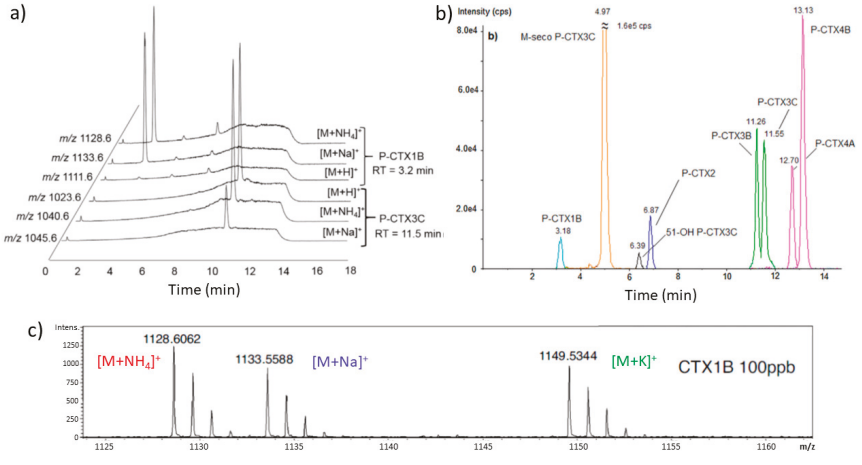

Figure 9. (**a**) LC-MS/MS chromatogram of standard CTX solutions showing that the $[M + Na]^+$ and $[M + NH_4]^+$ ions were favored for P-CTX1B (P-CTX-1), while the $[M + NH_4]^+$ and $[M + H]^+$ ions were dominant with similar intensities for P-CTX3C (P-CTX-3C) at identical conditions. A linear gradient of water-methanol solvent mixture, containing ammonium formate and formic acid, was used for chromatographic separation. SIM was performed in positive mode for ions at *m/z* $[M + Na]^+$, $[M + H]^+$ and $[M + NH_4]^+$. Reproduced with permission from ref. [130]; (**b**) LC-MS/MS chromatogram and retention time of P-CTXs standards using a Zorbax C18 column, water and methanol as eluents, and a linear gradient. The separation of various CTX congeners is shown. Reproduced with permission from [130]. Copyright Elsevier Ltd., 2018; (**c**) LC-HRMS high resolution mass spectra of CTX1B (P-CTX-1) obtained from CTX standard, showing adduct peaks and isotopic patterns, reproduced with permission from [132]. Copyright Elsevier Ltd., 2017.

Table 3. Examples of the application of LC-MS for CTX detection.

Method	Fish Species (Family)	Toxin Detected	Mass [1] (g)	Conc. [2] (ng g^{-1})	LOQ [3] (ng g^{-1})	Ref.
LC-MS/MS	*Lutjanus bohar* (Lutjanidae)	P-CTX-1 P-CTX-2 P-CTX-3	5	3.7 0.74 0.36	0.32	[134]
LC-MS/MS	*Sphyraena putnamae* (Sphyraenidae)	P-CTX-1	2	11.4	0.07	[53]
LC-MS/MS	*Sphyraena putnamae* (Sphyraenidae)	P-CTX-1 P-CTX-2 P-CTX-3	2	5.6 7.9 1.4	n.a.	[20]
LC-MS/MS	*Epinephelus spilotoceps* (Serranidae)	P-CTX-1	5	2.73	0.01	[48]
LC-MS/MS	*Variola louti* (Serranidae)	P-CTX-1 P-CTX-2 P-CTX-3	5	2.0 [4]	<0.01	[41]
LC-MS/MS	*Cephalopholis argus* (Serranidae)	P-CTX-1 P-CTX-2 P-CTX-3	5	1.710 0.555 0.711	0.0005 0.0050 0.0050	[87]
LC-MS/MS	*Gymnothorax flavimarginatus* (Muraenidae)	P-CTX-1 P-CTX-2 P-CTX-3	5	39.20 24.40 5.940	0.0005 0.0050 0.0050	[87]
LC-MS/MS	*Scomberomorus commerson* (Scombridae)	P-CTX-1	5	0.13	n.a.	[135]
LC-HRMS	*Variola louti* (Serranidae)	P-CTX-1	10	1.609	~0.4	[67]
LC-MS/MS	*Pagrus Pagrus* (Sparidae)	C-CTX-1	15	0.76	0.0045	[36]
LC-MS/MS	*Lutjanus cyanopterus* (Lutjanidae)	C-CTX-1	15	0.49	0.0045	[36]
LC-MS/MS	*Seriola fasciata* (Carangidae)	C-CTX-1	15	0.84	n.a.	[51]
LC-MS/MS	*Mycteroperca fusca* (Serranidae)	C-CTX-1	15	0.25	0.0150	[136]
LC-MS/MS	*Caranx lugubris* (Carangidae)	C-CTX-1	100	13.79	n.a.	[137]
LC-HRMS	*Bodianus scrofa* (Wrasse)	C-CTX-1	15	n.a.	n.a.	[138]
LC-HRMS	*Carcharhinus leucas* (Carcharhinidae)	I-CTX-1,2 I-CTX-3,4	10 [5]	6.54 9.74	1.67 [6]	[19]

[1] Mass of fish tissue used for the analysis; [2] Concentration of toxin (ng toxin/g fish tissue); n.a. = not available; [3] Due to the relationship between the limit of detection, LOD (S/N > 3), and limit of quantitation, LOQ (S/N > 10), only LOQ is shown in table (ng toxin/g fish tissue); [4] total toxicity; [5] Shark stomach; [6] in P-CTX-1 equivalent.

5. Outlook and Conclusions

CFP is an old problem for communities in tropical regions that rely on seafood for survival, and CFP has now become a global issue due to the worldwide seafood trade, international travel, and ongoing expansion of the geographic ranges of fish contaminated with ciguatoxins. There is, therefore, high demand to test fish for CTXs prior to human consumption, both for mitigation of the health risks of CFP and for clinical identification of toxins in cases of intoxication. Currently, however, reliable biomarkers that can confirm exposure to CTXs and accepted diagnostic tests for direct detection of CTXs in humans are not available; therefore, diagnosis of ciguatera relies on clinical observations of its overt symptoms and/or testing remnants of consumed fish, if available. Several methods have been developed to screen for the presence of CTXs in fish tissue prior to consumption. In vivo whole-animal detection methods are now superseded by in vitro assays that have greater sensitivity, including receptor-binding assays (RBAs), cell-based assays (CBAs), Enzyme-Linked Immunosorbent Assays (ELISA), capillary electrophoresis (CE)-based immunoassays, electrochemical immunosensors (ECS), and liquid chromatography tandem mass spectrometry (LC-MS/MS). Currently employed methods are compared in Table 4. Present methods for CTX analysis, in general, are labor-intensive, time-consuming, and require laboratory facilities with well-trained technicians. To date, these methods have not been properly validated. At present it is difficult to obtain sufficient standard CTXs as reference calibrants, impeding corroboration and widespread application of these analytical techniques.

Table 4. Comparison of methods for CTX detection.

Method	Extract Preparation [1]	Assay Duration	Parallel Samples [2]	Sensitivity [3] (ng g^{-1})	Specificity	Toxin Profile
MBA	5–6 h	24 h	1–10	0.56	No	No
R-RBA	5–6 h	3–4 h	96	0.03–0.15	No	No
F-RBA	5–6 h	2–3 h	96	0.02–0.023	No	No
CBA	5–6 h [4]	53 h [4]	96	0.001–0.13	No	No
ELISA	7–8 h	2–4 h	96	<0.01 [5]	Yes	No
CE	5–6 h	1 h	1	<0.01 [5]	Yes	No
ECS	5–6 h	2 h	1	0.01	Yes	No
LC-MS/MS	5–8 h	5–15 min [6]	1	0.0005–0.32	Yes	Yes

[1] Depends on purity requirements. Parallel samples can be prepared simultaneously depending on lab conditions and operator. Extraction time is different depending on the protocol used. See also Figure 3. As an example, the estimated time for preparing the raw extract is 5–6 h, and for the two SPE purification step is 2 h; [2] 96-well microtiter plate is typically used for RBA, CBA and ELISA; however, sample throughput can be 96–1436; [3] LOQ for P-CTX-1 equivalent toxin in fish tissue (protocol dependent), note that the suggested tolerance limit for P-CTX-1 in fish tissue is 0.01 ng g^{-1}, respectively; [4] Includes 24-h incubation and 24-h exposure of the neuro-2a cells to fish extracts, and 4–6 h assay time; extract preparation can be undertaken during incubation time; [5] LOD, no specific measurement for LOQ was done; [6] This estimation considers only the time of a single injection of a sample into the LC-MS system, and does not includes calibration and quality controls.

Detection of CTXs in fish tissue is not simple, due to their generally low concentrations, the presence of multiple CTX congeners, the limited amount or lack of CTX reference materials for many derivatives, the difficult synthesis or lack of CTX antibodies, the co-occurrence of interfering molecules in fish tissue, and the typically unpredictable incidence of CTXs. Not all of the currently used methods for quantification of CTXs offer sufficient sensitivity, specificity and selectivity. The mouse bioassay (MBA) and radioligand receptor-binding assays (R-RBA) are expected in the near future to be replaced in laboratories due to their low sensitivity, lack of specificity, and high cost, as well as ethical and safety concerns. The fluorescence-based receptor-binding assay (F-RBA) eliminates safety issues associated with radioactive compounds, and its wider application is expected in the future, especially due to the commercial availability of SeaTox® F-RBA test kit. One of the most successful screening methods seems to be the cell-based assay (CBA) using mouse neuroblastoma cells (N2a). This method is simple and sufficiently sensitive, but is time consuming and reflects only the combined effect of the various CTXs present in fish extract. Further, other toxins can also block sodium channels, therefore, the method fails to provide information on toxin profiles. Immunosensors and immunoassays in the form of ELISA or CE-based tests are sensitive and selective tools for ciguatoxin detection, however, they are limited to the availability of CTX-antibodies. Although, in principle, several toxins can be targeted simultaneously, assays typically contain one or a very limited number of antibodies, therefore these methods do not provide information about toxin profiles. Detecting specific toxins can be misleading because toxin profiles can vary considerably among fish. Interestingly, electrochemical biosensors, except for CE and the recently constructed electrode array ECS, have not been developed for CTX detection in fish tissue, possibly due to the lack of sufficient amounts and types of CTX antibodies. Solving the antibody problem in the future may stimulate large-scale development in this field, especially since antibody-based methods offer the potential for miniaturization and development of portable devices and POC tests [139–141]. The application of LC-MS/MS for CTXs detection was an important break-through in CTX screening, because this method is sufficiently sensitive, selective, and unique in providing toxin profiles. The major obstacle of its wide-scale application is the lack of widely available reference toxins for quantification. Currently, state-of-the-art CTX detection involves a combination of CBA-N2a assay and LC-MS/MS, where CBA-N2a assay is used for screening the total toxicity of the sample, and LC-MS/MS to confirm the toxins and for providing toxin profiles [19,45,51,87]. LC-MS/MS together with reference materials can fulfill the role of the sensitive and specific CTX detection method, however, it requires highly trained operator and laboratory facilities. Further the method cannot be miniaturized and field application is not possible.

Testing fish tissue for CTXs is of crucial importance because typically muscle tissue is consumed by humans. Such testing, however, requires a highly invasive sampling method, therefore it is not suitable for testing protected fish species, environmental risk assessment, or clinical diagnosis of human ciguatera fish poisoning. Collecting blood samples is not particularly invasive, and has an added advantage that blood is a much less complicated matrix for analysis than muscle tissue. Unfortunately, few studies have been conducted for testing CTXs in fish blood samples, and the possible relationship between the concentrations of CTXs in muscle tissue and blood, if one indeed exists, is not yet known—elucidation of the functional association between these two parameters though statistical modelling would be highly beneficial towards effective screening of the toxin. It is, however, expected that circulating CTX content in blood is higher after a meal of ciguateric fish. Future research will likely focus in this area because it is especially important for identifying CTXs in humans following its intoxication.

Presently, there is great demand for a portable, fast, reliable, easy-to-use, and cheap CTX screening assay for private customers, fishermen, and fish vendors to test their food or catch before consuming or selling it. These point-of-care tests, however, currently do not exist, notwithstanding that performance requirements may be lower than for those methods used in laboratories. CTX testing is still in the hand of specialists, and specialized laboratories are now able to provide sufficiently accurate information about toxin profile and toxin concentration in fish. Although significant advances have been made to develop and improve the performance of ciguatera assays, the ideal assay, one that is simple, rapid, reliable, robust, highly sensitive, quantitative, provides specific toxin profiles, cheap and does not require trained operators and specialized equipment, does not exist to date; developing one is the key challenge for future research on this field.

Funding: This research received no external funding.

Conflicts of Interest: The authors declare no conflict of interest.

References

1. EFSA Panel on Contaminants in the Food Chain. Scientific Opinion on marine biotoxins in shellfish—Emerging toxins: Ciguatoxin group. *EFSA J.* **2010**, *8*, 1627. [CrossRef]
2. Lewis, R.J.; Vetter, I. Ciguatoxin and Ciguatera. In *Marine and Freshwater Toxins, Toxinology*; Gopalakrishnakone, P., Haddad, V., Jr., Tubaro, A., Kim, E., Kem, W.R., Eds.; Springer Science+Business Media: Dordrecht, The Natherlands, 2016; pp. 71–92. [CrossRef]
3. Inserra, M.; Lavrukhina, Y.; Jones, A.; Lewis, R.J.; Vetter, I. Ciguatoxin Detection Methods and High-Throughput Assays. In *Analysis of Food Toxins and Toxicants*, 1st ed.; Wong, Y.-C., Lewis, R.J., Eds.; John Wiley & Sons Ltd: New Jersey, USA, 2017; Volume 2, pp. 469–487.
4. Friedman, M.A.; Fleming, L.E.; Fernandez, M.; Bienfang, P.; Schrank, K.; Dickey, R.; Bottein, M.-Y.; Backer, L.; Ayyar, R.; Weisman, R.; et al. Ciguatera Fish Poisoning: Treatment, Prevention and Management. *Mar. Drugs* **2008**, *6*, 456–479. [CrossRef] [PubMed]
5. Lewis, R.J. The changing face of ciguatera. *Toxicon* **2001**, *39*, 97–106. [CrossRef]
6. Friedman, M.A.; Fernandez, M.; Backer, L.C.; Dickey, R.W.; Bernstein, J.; Schrank, K.; Bernstein, J.; Stephan, W.; Weisman, R.; Kibler, S.; et al. An Updated Review of Ciguatera Fish Poisoning: Clinical, Epidemiological, Environmental, and Public Health Management. *Mar. Drugs* **2017**, *15*, 72. [CrossRef]
7. Nicholson, G.M.; Lewis, R.J. Ciguatoxins: Cyclic Polyether Modulators of Voltage-gated Ion Channel Function. *Mar. Drugs* **2006**, *4*, 82–118. [CrossRef]
8. Lehane, L.; Lewis, R.J. Ciguatera: Recent advances but the risk remains. *Int. J. Food Microbiol.* **2000**, *61*, 91–125. [CrossRef]
9. Dickey, R.W.; Plakas, S.M. Ciguatera: A public health perspective. *Toxicon* **2010**, *56*, 123–136. [CrossRef]
10. Juranovic, L.R.; Park, D.L. Foodborne Toxins of Marine Origin: Ciguatera. In *Reviews of Environmental Contamination and Toxicology*; Ware, G.W., Ed.; Springer: New York, NY, USA, 1991; Volume 117, pp. 51–94.

11. Chinain, M.; Darius, H.T.; Ung, A.; Fouc, M.T.; Revel, T.; Cruchet, P.; Pauillac, S.; Laurent, D. Ciguatera risk management in French Polynesia: The case study of Raivavae Island (Australes Archipelago). *Toxicon* **2010**, *56*, 674–690. [CrossRef]
12. Caillaud, A.; de la Iglesia, P.; Darius, H.T.; Pauillac, S.; Aligizaki, K.; Fraga, S.; Chinain, M.; Diogene, J. Update on Methodologies Available for Ciguatoxin Determination: Perspectives to Confront the Onset of Ciguatera Fish Poisoning in Europe. *Mar. Drugs* **2010**, *8*, 1838–1907. [CrossRef]
13. Clausing, R.J.; Losen, B.; Oberhaensli, F.R.; Darius, H.T.; Sibat, M.; Hess, P.; Swarzenski, P.W.; Chinain, M.; Dechraoui Bottein, M.-Y. Experimental evidence of dietary ciguatoxin accumulation in an herbivorous coral reef fish. *Aqua. Toxicol.* **2018**, *200*, 257–265. [CrossRef]
14. U.S. Department of Health and Human Services Food and Drug Administration Center for Food Safety and Applied Nutrition: Fish and Fishery Products Hazards and Controls Guidance, Fourth Edition—March 2020. Available online: https://www.fda.gov/media/80637/download (accessed on 25 June 2020).
15. Hamilton, B.; Hurbungs, M.; Jones, A.; Lewis, R.J. Multiple ciguatoxins present in Indian Ocean reef fish. *Toxicon* **2002**, *40*, 1347–1353. [CrossRef]
16. Rhodes, L.L.; Smith, K.F.; Murray, J.S.; Nishimura, T.; Finch, S.C. Ciguatera Fish Poisoning: The Risk from an Aotearoa/New Zealand Perspective. *Toxins* **2020**, *12*, 50. [CrossRef]
17. Bravo, J.; Suarez, F.C.; Ramirez, A.S.; Acosta, F. Ciguatera, an Emerging Human Poisoning in Europe. *J. Aquac. Mar. Biol.* **2015**, *3*, 00053. [CrossRef]
18. Pearn, J. Neurology of ciguatera. *J. Neurol. Neurosurg. Psychiatry* **2001**, *70*, 4–84. [CrossRef] [PubMed]
19. Diogène, J.; Reverté, L.; Rambla-Alegre, M.; del Río, V.; de la Iglesia, P.; Camps, M.; Palacios, O.; Flores, C.; Caixach, J.; Ralijaona, C.; et al. Identification of ciguatoxins in a shark involved in a fatal food poisoning in the Indian Ocean. *Sci. Rep.* **2017**, *7*, 8240. [CrossRef]
20. Hamilton, B.; Whittle, N.; Shaw, G.; Eaglesham, G.; Moore, M.R.; Lewis, R.J. Human fatality associated with Pacific ciguatoxin contaminated fish. *Toxicon* **2010**, *56*, 668–673. [CrossRef]
21. Hossen, V.; Solino, L.; Leroy, P.; David, E.; Velge, P.; Dragacci, S.; Krys, S.; Flores Quintana, H.; Diogene, J. Contribution to the risk characterization of ciguatoxins: LOAEL estimated from eight ciguatera fish poisoning events in Guadeloupe (French West Indies). *Environ. Res.* **2015**, *143*, 100–108. [CrossRef] [PubMed]
22. Yasumoto, Y.; Scheuer, P.J. Marine Toxins of the Pacific-VIII Ciguatoxin from Moray Eel Livers. *Toxicon* **1969**, *7*, 273–276. [CrossRef]
23. Chan, W.H.; Mak, Y.l.; Wu, J.J.; Jin, L.; Sit, W.H.; Lam, J.C.W.; Sadovy de Mitcheson, Y.; Chan, L.L.; Lam, P.K.S.; Murphy, M.B. Spatial distribution of ciguateric fish in the Republic of Kiribati. *Chemosphere* **2011**, *84*, 117–123. [CrossRef]
24. Campora, C.E.; Hokama, Y. Marine Toxins. In *Handbook of Seafood and Seafood Products Analysis*; Nollet, L.M.L., Toldra, F., Eds.; Taylor and Francis Group, LLC: Boca Raton, FL, USA, 2010; pp. 649–674. [CrossRef]
25. Yasumoto, T.; Nakajima, I.; Bagnis, R.; Adachi, R. Finding of a dinoflagellate as a likely culprit of ciguatera. *Bull. Jap. Soc. Sci. Fisheries* **1977**, *43*, 1021–1026. [CrossRef]
26. Longo, S.; Sibat, M.; Viallon, J.; Darius, H.T.; Hess, P.; Chinain, M. Intraspecific Variability in the Toxin Production and Toxin Profiles of In Vitro Cultures of Gambierdiscus polynesiensis (Dinophyceae) from French Polynesia. *Toxins* **2019**, *11*, 735. [CrossRef] [PubMed]
27. Hoppenrath, M.; Kretzschmar, A.L.; Kaufmann, M.J.; Murray, S.A. Morphological and molecular phylogenetic identification and record verification of Gambierdiscus excentricus (Dinophyceae) from Madeira Island (NE Atlantic Ocean). *Mar. Biodivers. Rec.* **2019**, *12*, 16. [CrossRef]
28. Holmes, M.; Lewis, R.J. Purification and Characterisation of Large and Small Maitotoxins From Cultured Gambierdiscus toxicus. *Nat. Toxins* **1994**, *2*, 64–72. [CrossRef] [PubMed]
29. Pisapia, F.; Sibat, M.; Herrenknecht, C.; Lhaute, K.; Gaiani, G.; Ferron, P.-J.; Fessard, V.; Fraga, S.; Nascimento, S.M.; Litaker, R.W.; et al. Maitotoxin-4, a Novel MTX Analog Produced by *Gambierdiscus excentricus*. *Mar. Drugs* **2017**, *15*, 220. [CrossRef]
30. Boente-Juncal, A.; Alvarez, M.; Antelo, A.; Rodriguez, I.; Calabro, K.; Vale, C.; Thomas, O.P.; Botana, L.M. Structure elucidation and biological evaluation of maitotoxin-3, a homologue of gambierone, from *Gambierdiscus belizeanus*. *Toxins* **2019**, *11*, 79. [CrossRef]
31. Rodríguez, I.; Genta-Jouve, G.; Alfonso, C.; Calabro, K.; Alonso, E.; Sánchez, J.A.; Alfonso, A.; Thomas, O.P.; Botana, L.M. Gambierone, a Ladder-Shaped Polyether from the Dinoflagellate Gambierdiscus belizeanus. *Org. Lett.* **2015**, *17*, 2392–2395. [CrossRef]

32. Legrand, A.M.; Litaudon, M.; Genthon, J.N.; Bagnis, R.; Yasumoto, T. Isolation and some properties of ciguatoxin. *J. Appl. Phycol.* **1989**, *1*, 183–188. [CrossRef]
33. Lewis, R.J.; Sellin, M.; Poli, M.A.; Norton, R.S.; MacLeod, J.K.; Sheil, M.M. Purification and characterization of ciguatoxins from moray eel (*Lycodontis javanicus*, *Muraenidae*). *Toxicon* **1991**, *29*, 1115–1127. [CrossRef]
34. Pottier, I.; Vernoux, J.-P.; Jones, A.; Lewis, R.J. Characterization of multiple Caribbean ciguatoxins and congeners in individual specimens of horse-eye jack (Caranx latus) by high-performance liquid chromatography/mass spectrometry. *Toxicon* **2002**, *40*, 929–939. [CrossRef]
35. Lewis, R.J.; Vernoux, J.-P.; Brereton, I.M. Structure of Caribbean Ciguatoxin Isolated from *Caranx latus*. *J. Am. Chem. Soc.* **1998**, *120*, 5914–5920. [CrossRef]
36. Estevez, P.; Castro, D.; Manuel Leao, J.; Yasumoto, T.; Dickey, R.; Gago-Martinez, A. Implementation of liquid chromatography tandem mass spectrometry for the analysis of ciguatera fish poisoning in contaminated fish samples from Atlantic coasts. *Food Chem.* **2019**, *280*, 8–14. [CrossRef] [PubMed]
37. Murata, M.; Legrand, A.M.; Ishibashi, Y.; Fukui, M.; Yasumoto, T. Structures and Configurations of Ciguatoxin from the Moray Eel *Gymnothorax javanicus* and Its Likely Precursor from the Dinoflagellate *Gambierdiscus toxicus*. *J. Am. Chem. Soc.* **1990**, *112*, 4380–4386. [CrossRef]
38. Yasumoto, T.; Igarashi, T.; Legrand, A.-M.; Cruchet, P.; Chinain, M.; Fujita, T.; Naoki, H. Structural Elucidation of Ciguatoxin Congeners by Fast-Atom Bombardment Tandem Mass Spectroscopy. *J. Am. Chem. Soc.* **2000**, *122*, 4988–4989. [CrossRef]
39. Satake, M.; Murata, M.; Yasumoto, T. The Structure of CTX3C, a Ciguatoxin Congener Isolated from Cultured *Gambierdiscus Toxicus*. *Tetrahedron Lett.* **1993**, *34*, 1975–1978. [CrossRef]
40. Satake, M.; Fukui, M.; Legrand, A.-M.; Cruchet, P.; Yasumoto, T. Isolation and Structures of New Ciguatoxin Analogs, 2,3-DihydroxyCTX3C and 51-HydroxyCTX3C, Accumulated in Tropical Reef Fish. *Tetrahedron Lett.* **1998**, *39*, 1197–1198. [CrossRef]
41. Yogi, K.; Oshiro, N.; Inafuku, Y.; Hirama, M.; Yasumoto, T. Detailed LC-MS/MS Analysis of Ciguatoxins Revealing Distinct Regional and Species Characteristics in Fish and Causative Alga from the Pacific. *Anal. Chem.* **2011**, *83*, 8886–8891. [CrossRef]
42. Satake, M.; Ishibashi, Y.; Legrand, A.-M.; Yasumoto, T. Isolation and Structure of ciguatoxin-4A, a New Ciguatoxin Precursor, from Cultures of Dinoflagellate *Gambierdiscus toxicus* and Parrotfish *Scarus Gibbus*. *Biosci. Biotech. Biochem.* **1997**, *60*, 2103–2105. [CrossRef]
43. Hamilton, B.; Hurbungs, M.; Vernoux, J.-P.; Jones, A.; Lewis, R.J. Isolation and characterization of Indian Ocean ciguatoxin. *Toxicon* **2002**, *40*, 685–693. [CrossRef]
44. Lewis, R.J.; Endean, R. Purification of ciguatoxin-like material from Scomberomorus commersoni, and its effect on the rat phrenic nerve-diaphragm. *Toxicon* **1983**, *3*, 249–252. [CrossRef]
45. Darius, H.T.; Roué, M.; Sibat, M.; Viallon, J.; iti Gatti, C.M.; Vandersea, M.W.; Tester, P.A.; Litaker, R.W.; Amzil, Z.; Hess, P.; et al. *Tectus niloticus* (Tegulidae, Gastropod) as a Novel Vector of Ciguatera Poisoning: Detection of Pacific Ciguatoxins in Toxic Samples from Nuku Hiva Island (French Polynesia). *Toxins* **2018**, *10*, 2. [CrossRef]
46. Murray, J.S.; Boundy, M.J.; Selwood, A.I.; Harwood, D.T. Development of an LC–MS/MS method to simultaneously monitor maitotoxins and selected ciguatoxins in algal cultures and P-CTX-1B in fish. *Harmful Algae* **2018**, *80*, 80–87. [CrossRef] [PubMed]
47. Pottier, I.; Hamilton, B.; Jones, A.; Lewis, R.J.; Vernoux, J.P. Identification of slow and fast-acting toxins in a highly ciguatoxic barracuda (*Sphyraena barracuda*) by HPLC/MS and radiolabelled ligand binding. *Toxicon* **2003**, *42*, 663–672. [CrossRef] [PubMed]
48. Wu, J.J.; Mak, Y.L.; Murphy, M.B.; Lam, J.C.W.; Chan, W.H.; Wang, M.; Chan, L.L.; Lam, P.K.S. Validation of an accelerated solvent extraction liquid chromatography-tandem mass spectrometry method for Pacific ciguatoxin-1 in fish flesh and comparison with the mouse neuroblastoma assay. *Anal. Bioanal. Chem.* **2011**, *400*, 3165–3175. [CrossRef] [PubMed]
49. Harwood, D.T.; Murray, S.; Boundy, M.J. Sample Preparation Prior to Marine Toxin Analysis. *Compr. Anal. Chem.* **2017**, *78*, 89–136. [CrossRef]
50. Tsumuraya, T.; Sato, T.; Hirama, M.; Fujii, I. Highly Sensitive and Practical Fluorescent Sandwich ELISA for Ciguatoxins. *Anal. Chem.* **2018**, *90*, 7318–7324. [CrossRef]

51. Estevez, P.; Castro, D.; Pequeño-Valtierra, A.; Leao, J.M.; Vilariño, O.; Diogène, J.; Gago-Martínez, A. An Attempt to Characterize the Ciguatoxin Profile in *Seriola fasciata* Causing Ciguatera Fish Poisoning in Macaronesia. *Toxins* **2019**, *11*, 221. [CrossRef]
52. Lewis, R.J.; Yang, A.; Jones, A. Rapid extraction combined with LC-tandem mass spectrometry (CREM-LC/MS/MS) for the determination of ciguatoxins in ciguateric fish flesh. *Toxicon* **2009**, *54*, 62–66. [CrossRef]
53. Stewart, I.; Eaglesham, G.K.; Poole, S.; Graham, G.; Paulo, C.; Wickramasinghe, W.; Sadler, R.; Shaw, G.R. Establishing a public health analytical service based on chemical methods for detecting and quantifying Pacific ciguatoxin in fish samples. *Toxicon* **2010**, *56*, 804–812. [CrossRef]
54. Meyer, L.; Carter, S.; Capper, A. An updated ciguatoxin extraction method and silica cleanup for use with HPLC-MS/MS for the analysis of PCTX-1, PCTX-2 and P-CTX-3. *Toxicon* **2015**, *108*, 249–256. [CrossRef]
55. Lewis, N.D. Disease and Development: Ciguatera Fish Poisoning. *Soc. Sci. Med.* **1986**, *23*, 983–993. [CrossRef]
56. Darius, H.T.; Drescher, O.; Ponton, D.; Pawlowiez, R.; Laurent, D.; Dewailly, E.; Chinain, M. Use of folk tests to detect ciguateric fish: A scientific evaluation of their effectiveness in Raivavae Island (Australes, French Polynesia). *Food Additiv. Contam. Part A* **2013**, *30*, 550–566. [CrossRef]
57. Gillespie, N.C.; Lewis, R.J.; Pearn, J.; Burke, A.T.C.; Holmes, M.J.; Bourke, J.B.; Shields, W.J. Ciguatera in Australia: Occurrence, clinical features, pathophysiology and management. *Med. J. Aust.* **1986**, *145*, 584–590. [CrossRef]
58. Bagnis, R.; Fevai, G. La ciguatera feline experimentale a Tahiti. *Rev. Med. Vet.* **1971**, *122*, 629–638.
59. Banner, A.H.; Scheuer, P.J.; Sasaki, S.; Helfrich, P.; Alendert, C.B. Observations on Ciguatera-type Toxin in Fish. *Ann. N. Y. Acad. Sci.* **1960**, *90*, 770–787. [CrossRef] [PubMed]
60. Vernoux, J.P.; Lahlou, N.; Magras, L.P.; Greaux, J.B. Chick feeding test: A simple system to detect ciguatoxin. *Acta Trop.* **1985**, *42*, 235–240. [CrossRef] [PubMed]
61. Labrousse, H.; Matile, L. Toxicological biotest on Diptera larvae to detect ciguatoxins and various other toxic substances. *Toxicon* **1996**, *34*, 881–891. [CrossRef]
62. Chungue, E.; Bagnis, R.; Parc, F. The use of mosquitoes (*Aedes aegypti*) to detect ciguatoxin in surgeon fishes (*Ctenochaetus striatus*). *Toxicon* **1984**, *22*, 161–164. [CrossRef]
63. Granade, H.R.; Cheng, P.C.; Doorenbos, N.J. Ciguatera I: Brine Shrimp (*Artemia salina L.*) Larval Assay for Ciguatera Toxins. *J. Pharm. Sci.* **1976**, *65*, 1414–1415. [CrossRef]
64. Bagnis, R.; Barsinas, M.; Prieur, C.; Pompon, A.; Chungue, E.; Legrand, A.M. The use of the mosquito bioassay for determining the toxicity to man of ciguateric fish. *Biol. Bull.* **1987**, *172*, 137–143. [CrossRef]
65. Banner, A.; Sasaki, S.; Helfrich, P.; Alender, C.B.; Scheuer, P.J. Bioassay of Ciguatera Toxin. *Nature* **1961**, *189*, 229–230. [CrossRef]
66. Hoffman, P.A.; Granade, H.R.; McMillan, J.P. The mouse ciguatoxin bioassay: A dose-response curve and symptomatology analysis. *Toxicon* **1983**, *21*, 363–369. [CrossRef]
67. Leonardo, S.; Gaiani, G.; Tsumuraya, T.; Hirama, M.; Turquet, J.; Sagristà, N.; Rambla-Alegre, M.; Flores, C.; Caixach, J.; Diogène, J.; et al. Addressing the Analytical Challenges for the Detection of Ciguatoxins Using an Electrochemical Biosensor. *Anal. Chem.* **2020**, *92*, 4858–4865. [CrossRef] [PubMed]
68. Endean, R.; Griffith, J.K.; Robins, J.J.; Monks, S.A. Multiple toxins in a specimen of the narrow-barred spanish mackerel, *Scomberomorus commersoni*. *Toxicon* **1993**, *31*, 195–204. [CrossRef]
69. Hokama, Y.; Asahina, A.Y.; Titus, E.; Ichinotsubo, D.; Chun, S.; Hong, T.L.W.P.; Shirai, J.L.; Asuncion, D.A.; Miyahara, J.T. Assessment of ciguateric fish in Hawaii by immunological mouse toxicity and guinea pig atrial assay. *Mem. Qld. Mus.* **1994**, *34*, 489–496.
70. Miyahara, J.; Akau, C.; Yasumoto, T. Effects of ciguatoxin and maitotoxin on the isolated guinea pig atria. *Res. Comm. Chem. Pathol. Pharmacol.* **1979**, *25*, 177–180.
71. Benoit, E.; Legrand, A.M.; Dubois, J.M. Effects of ciguatoxin on current and voltage clamped frog myelinated nerve fibre. *Toxicon* **1986**, *24*, 357–364. [CrossRef]
72. Miller, D.M.; Tindall, D.R.; Tibbs, B. Ciguatera-type toxins: Bioassay using crayfish nerve cord (Abstract 1103). *Fed. Proc. Abstr.* **1986**, *45*, 344.
73. Shimojo, R.Y.; Iwaoka, W.T. A rapid hemolysis assay for the detection of sodium channel-specific marine toxins. *Toxicology* **2000**, *154*, 1–7. [CrossRef]
74. Manger, R.L.; Leja, L.S.; Lee, S.Y.; Hungerford, J.M.; Wekell, M.M. Tetrazolium-based cell bioassay for neurotoxins active on voltage-sensitive sodium channels: Semiautomated assay for saxitoxins, brevetoxins, and ciguatoxins. *Anal. Biochem.* **1993**, *214*, 190–194. [CrossRef]

75. Manger, R.L.; Leja, L.S.; Lee, S.Y.; Hungerford, J.M.; Hokama, Y.; Dickey, R.W.; Granade, H.R.; Lewis, R.; Yasumoto, T.; Wekell, M.M. Detection of sodium channel toxins: Directed cytotoxicity assays of purified ciguatoxins, brevetoxins, saxitoxins, and seafood extracts. *J. AOAC Intern.* **1995**, *78*, 521–527. [CrossRef]
76. Manger, R.L.; Leja, L.S.; Lee, S.Y.; Hungerford, J.M.; Wekell, M.M. Cell bioassay for the detection of ciguatoxins, brevetoxins. and saxitoxins. *Mem. Qld. Mus.* **1994**, *34*, 571–575.
77. Viallon, J.; Chinain, M.; Darius, H.T. Revisiting the Neuroblastoma Cell-Based Assay (CBA-N2a) for the Improved Detection of Marine Toxins Active on Voltage Gated Sodium Channels (VGSCs). *Toxins* **2020**, *12*, 281. [CrossRef] [PubMed]
78. Caillaud, A.; Eixarch, H.; de la Iglesia, P.; Rodriguez, M.; Dominguez, L.; Andree, K.B.; Diogene, J. Towards the standardisation of the neuroblastoma (neuro-2a) cell-based assay for ciguatoxin-like toxicity detection in fish: Application to fish caught in the Canary Islands. *Food Add. Contam. Part A* **2012**, *29*, 1000–1010. [CrossRef] [PubMed]
79. Castro, D.; Manger, R.; Vilariño, O.; Gago-Martínez, A. Evaluation of Matrix Issues in the Applicability of the Neuro-2a Cell Based Assay on the Detection of CTX in Fish Samples. *Toxins* **2020**, *12*, 308. [CrossRef]
80. Diaz-Asencio, L.; Clausing, R.J.; Ranada, M.L.; Alonso-Hernandez, C.M.; Dechraoui Bottein, M.-Y. A radioligand receptor binding assay for ciguatoxin monitoring in environmental samples: Method development and determination of quality control criteria. *J. Environ. Rad.* **2018**, *192*, 289–294. [CrossRef]
81. Fairey, E.R.; Edmunds, J.S.G.; Ramsdell, J.S. A Cell-Based Assay for Brevetoxins, Saxitoxins, and Ciguatoxins Using a Stably Expressed c-fos–Luciferase Reporter Gene. *Anal. Biochem.* **1997**, *251*, 129–132. [CrossRef]
82. Fairey, E.R.; Ramsdell, J.S. Reporter Gene Assays for Algal-derived Toxins. *Nat. Toxins* **1999**, *7*, 415–421. [CrossRef]
83. Zimmermann, K.; Deuis, J.R.; Inserra, M.C.; Collins, L.S.; Namer, B.; Cabot, P.J.; Reeh, P.W.; Lewis, R.J.; Vetter, I. Analgesic treatment of ciguatoxin-induced cold allodynia. *Pain* **2013**, *154*, 1999–2006. [CrossRef]
84. Lewis, R.J.; Inserra, M.; Vetter, I.; Holland, W.C.; Hardison, R.D.; Tester, P.A.; Litaker, R.W. Rapid Extraction and Identification of Maitotoxin and Ciguatoxin-Like Toxins from Caribbean and Pacific Gambierdiscus Using a New Functional Bioassay. *PLoS ONE* **2016**, *11*, e0160006. [CrossRef]
85. Loeffler, C.R.; Robertson, A.; Flores Quintana, H.A.; Silander, M.C.; Smith, T.B.; Olsen, D. Ciguatoxin prevalence in 4 commercial fish species along an oceanic exposure gradient in the US Virgin Islands. *Environ. Toxicol. Chem.* **2018**, *37*, 1852–1863. [CrossRef]
86. Bottein Dechraoui, M.-Y.; Tiedeken, J.A.; Persad, R.; Wang, Z.; Granade, H.R.; Dickey, R.W.; Ramsdell, J.S. Use of two detection methods to discriminate ciguatoxins from brevetoxins: Application to great barracuda from Florida Keys. *Toxicon* **2005**, *46*, 261–270. [CrossRef] [PubMed]
87. Mak, Y.L.; Wai, T.-C.; Murphy, M.B.; Chan, W.H.; Wu, J.J.; Lam, J.C.W.; Chan, L.L.; Lam, P.K.S. Pacific Ciguatoxins in Food Web Components of Coral Reef Systems in the Republic of Kiribati. *Environ. Sci. Technol.* **2013**, *47*, 14070–14079. [CrossRef] [PubMed]
88. O'Toole, A.C.; Dechraoui Bottein, M.-Y.; Danylchuk, A.J.; Ramsdell, J.S.; Cooke, S.J. Linking ciguatera poisoning to spatial ecology of fish: A novel approach to examining the distribution of biotoxin levels in the great barracuda by combining non-lethal blood sampling and biotelemetry. *Sci. Total Environ.* **2012**, *427–428*, 98–105. [CrossRef]
89. Darius, H.T.; Ponton, D.; Revel, T.; Cruchet, P.; Ung, A.; Tchou Fouc, M.; Chinain, M. Ciguatera risk assessment in two toxic sites of French Polynesia using the receptor-binding assay. *Toxicon* **2007**, *50*, 612–626. [CrossRef] [PubMed]
90. Litaker, R.W.; Hardison, D.R.; Holland, W.C.; Bourdelais, A.J.; McCall, J.R.; Baden, D.G.; Morris, J.A., Jr.; Bogdanoff, A.K.; Tester, P.A. Ciguatoxin concentrations in invasive lionfish estimated using a fluorescent receptor binding assay. In *Marine and Freshwater Harmful Algae 2014, Proceedings of the 16th International Conference on Harmful Algae, Cawthorn Institute, Nelson, New Zealand, 27–31 October 2014*; MacKenzie, A.L., Ed.; The International Society for the Study of Harmful Algae (ISSHA): Helsinki, Finland, 2014; pp. 184–187.
91. Bottein Dechraoui, M.-Y.; Wang, Z.; Turquet, J.; Chinain, M.; Darius, T.; Cruchet, P.; Radwan, F.F.Y.; Dickey, R.W.; Ramsdell, J.S. Biomonitoring of ciguatoxin exposure in mice using blood collection cards. *Toxicon* **2005**, *46*, 243–251. [CrossRef]
92. Bottein Dechraoui, M.-Y.; Wang, Z.; Ramsdell, J.S. Optimization of ciguatoxin extraction method from blood for Pacific ciguatoxin (P-CTX-1). *Toxicon* **2007**, *49*, 100–105. [CrossRef]
93. Lombet, A.; Bidard, J.-N.; Lazdunski, M. Ciguatoxin and brevetoxins share a common receptor site on the neuronal voltage-dependent Na^+ channel. *FEBS Lett.* **1987**, *219*, 355–359. [CrossRef]

94. Perez, S.; Vale, C.; Alonso, E.; Alfonso, C.; Rodríguez, P.; Otero, P.; Alfonso, A.; Vale, P.; Hirama, M.; Vieytes, M.R.; et al. A Comparative Study of the Effect of Ciguatoxins on Voltage-Dependent Na^+ and K^+ Channels in Cerebellar Neurons. *Chem. Res. Toxicol.* **2011**, *24*, 587–596. [CrossRef]
95. Dechraoui, M.Y.; Naar, J.; Pauillac, S.; Legrand, A.-M. Ciguatoxins and brevetoxins, neurotoxic polyether compounds active on sodium channels. *Toxicon* **1999**, *37*, 125–143. [CrossRef]
96. Van Dolah, F.M.; Finley, E.L.; Haynes, B.L.; Doucette, G.J.; Moeller, P.D.; Ramsdell, J.S. Development of rapid and sensitive high throughput pharmacologic assays for marine phycotoxins. *Nat. Toxins* **1994**, *2*, 189–196. [CrossRef]
97. Hardison, D.R.; Holland, W.C.; McCall, J.R.; Bourdelais, A.J.; Baden, D.G.; Darius, H.T.; Chinain, M.; Tester, P.A.; Shea, D.; Quintana, H.A.F.; et al. Fluorescent Receptor Binding Assay for Detecting Ciguatoxins in Fish. *PLoS ONE* **2016**, *11*, e0153348. [CrossRef]
98. McCall, J.R.; Jacocks, H.M.; Niven, S.C.; Poli, M.A.; Baden, D.G.; Bourdelais, A.J. Development and utilization of a fluorescence-based receptor-binding assay for the site 5 voltage-sensitive sodium channel ligands brevetoxin and ciguatoxin. *J. AOAC Int.* **2014**, *97*, 307–315. [CrossRef]
99. Hokama, Y.; Banner, A.H.; Boylan, D.B. A radioimmunoassay for the detection of ciguatoxin. *Toxicon* **1977**, *15*, 317–325. [CrossRef]
100. Kimura, L.H.; Abad, M.A.; Hokama, Y. Evaluation of the radioimmunoassay (RIA) for detection of ciguatoxin (CTX) in fish tissues. *J. Fish Biol.* **1982**, *21*, 671–680. [CrossRef]
101. Hokama, Y.; Abad, M.A.; Kimura, L.H. A rapid enzyme-immunoassay for the detection of ciguatoxin in contaminated fish tissues. *Toxicon* **1983**, *21*, 817–824. [CrossRef]
102. Hokama, Y. A rapid, simplified enzyme immunoassay stick test for the detection of ciguatoxin and related polyethers from fish tissues. *Toxicon* **1985**, *23*, 939–946. [CrossRef]
103. Hokama, Y. Immunological studies using monoclonal antibodies for detection of low dalton marine toxins. *Food Add. Contam.* **1993**, *10*, 83–95. [CrossRef]
104. Hokama, Y.; Shirai, L.K.; Iwamoto, L.M.; Kobayashi, M.N.; Goto, C.S.; Nakagawa, L.K. Assessment of a rapid enzyme immunoassay stick test for the detection of ciguatoxin and related polyether toxins in fish tissues. *Biol. Bull.* **1987**, *172*, 144–153. [CrossRef]
105. Hokama, Y.; Honda, S.A.A.; Asahina, A.Y.; Fong, J.M.L.; Matsumoto, C.M.; Gallacher, T.S. Cross-reactivity of ciguatoxin, okadaic acid, and polyethers with monoclonal antibodies. *Food Agricult. Immunol.* **1989**, *1*, 29–35. [CrossRef]
106. Iwaoka, W.; Horita, J.; Shimojo, R.; Tran, T. Analysis of *Acanthurus triostegus* for marine toxins by the stick enzyme immunoassay and mouse bioassay. *Toxicon* **1992**, *30*, 1575–1581. [CrossRef]
107. Hokama, Y. Simplified solid-phase immunobead assay for detection of ciguatoxin and related polyethers. *J. Clin. Lab. Anal.* **1990**, *4*, 213–217. [CrossRef]
108. Hokama, Y. Recent methods for detection of seafood toxins: Recent immunological methods for ciguatoxin and related polyethers. *Food Add. Contam.* **1993**, *10*, 71–82. [CrossRef]
109. Park, D.L. Evolution of methods for assessing ciguatera toxins in fish. In *Reviews of Environmental Contamination and Toxicology*; de Voogt, P., Ed.; Springer-Verlag, New York, Inc.: New York, NY, USA, 1994; Volume 136, pp. 1–20.
110. Park, D.L.; Gamboa, P.M.; Goldsmith, C.H. Rapid facile solid-phase immunobead assay for screening ciguatoxic fish in the market place. *Bull. Soc. Pathol. Exot.* **1992**, *85*, 504–507.
111. Lewis, R.J. Immunological, biochemical and chemical features of ciguatoxins: Implications for the detection of ciguateric fish. *Mem. Qld. Mus.* **1994**, *34*, 541–548.
112. Hokama, Y.; Takenaka, W.E.; Nishimura, K.L.; Ebesu, J.S.; Bourke, R.; Sullivan, P.K. A Simple Membrane Immunobead Assay for Detecting Ciguatoxin and Related Polyethers from Human Ciguatera Intoxication and Natural Reef Fishes. *J. AOAC Int.* **1998**, *81*, 727–735. [CrossRef]
113. Bienfang, P.; DeFelice, S.; Dowling, A. Quantitative Evaluation of Commercially Available Test Kit for Ciguatera in Fish. *Food Nutr. Sci.* **2011**, *2*, 594–598. [CrossRef]
114. Campora, C.E.; Hokama, Y.; Yabusaki, K.; Isobe, M. Development of an enzyme-linked immunosorbent assay for the detection of Ciguatoxin in fish tissue using chicken immunoglobulin. *J. Clin. Lab. Anal.* **2008**, *22*, 239–245. [CrossRef]
115. Campora, C.E.; Dierking, J.; Tamaru, C.S.; Hokama, Y.; Vincent, D. Detection of ciguatoxin in fish tissue using sandwich ELISA and neuroblastoma cell bioassay. *J. Clin. Lab. Anal.* **2008**, *22*, 246–253. [CrossRef]

116. Tsumuraya, T.; Fujii, I.; Hirama, M. Preparation of anti-ciguatoxin monoclonal antibodies using synthetic haptens: Sandwich ELISA detection of ciguatoxins. *J. AOAC Int.* **2014**, *97*, 373–379. [CrossRef]
117. Tsumuraya, T.; Takeuchi, K.; Yamashita, S.; Fujii, I.; Hirama, M. Development of a monoclonal antibody against the left wing of ciguatoxin CTX1B: Thiol strategy and detection using a sandwich ELISA. *Toxicon* **2012**, *60*, 348–357. [CrossRef]
118. Tsumuraya, T.; Fujii, I.; Hirama, M. Production of monoclonal antibodies for sandwich immunoassay detection of Pacific ciguatoxins. *Toxicon* **2010**, *56*, 797–803. [CrossRef]
119. Tsumuraya, T.; Fujii, I.; Inoue, M.; Tatami, A.; Miyazaki, K.; Hirama, M. Production of monoclonal antibodies for sandwich immunoassay detection of ciguatoxin 51-hydroxyCTX3C. *Toxicon* **2006**, *48*, 287–294. [CrossRef]
120. Tsumuraya, T.; Hirama, M. Rationally Designed Synthetic Haptens to Generate Anti-Ciguatoxin Monoclonal Antibodies, and Development of a Practical Sandwich ELISA to Detect Ciguatoxins. *Toxins* **2019**, *11*, 533. [CrossRef]
121. Zhang, Z.; Liu, Y.; Zhang, C.; Luan, W. Horseradish peroxidase and antibody labeled gold nanoparticle probe for amplified immunoassay of ciguatoxin in fish samples based on capillary electrophoresis with electrochemical detection. *Toxicon* **2015**, *96*, 89–95. [CrossRef]
122. Zhang, Z.; Zhang, C.; Luan, W.; Li, X.; Liu, Y.; Luo, X. Ultrasensitive and accelerated detection of ciguatoxin by capillary electrophoresis via on-line sandwich immunoassay with rotating magnetic field and nanoparticles signal enhancement. *Anal. Chim. Acta* **2015**, *888*, 27–35. [CrossRef]
123. Vernoux, J.-P.; Lewis, R.J. Isolation and characterization of Caribbean ciguatoxins from the horse-eye jack (*Caranx latus*). *Toxicon* **1997**, *35*, 889–900. [CrossRef]
124. Lewis, R.J.; Sellin, M. Multiple ciguatoxins in the flesh of fish. *Toxicon* **1992**, *30*, 915–919. [CrossRef]
125. Yasumoto, T.; Satake, M. Chemistry, Etiology and Determination Methods of Ciguatera Toxins. *J. Toxicol. Toxin Rev.* **1996**, *15*, 91–107. [CrossRef]
126. Yasumoto, T.; Fukui, M.; Sasaki, K.; Sugiyama, K. Determinations of marine toxins in foods. *J. AOAC Int.* **1995**, *78*, 574–582. [CrossRef]
127. Legrand, A.-M.; Fukui, M.; Cruchet, P.; Yasumoto, T. Progress on Chemical Knowledge of Ciguatoxins. *Bull. Soc. Path. Ex.* **1992**, *85*, 467–469.
128. Lewis, R.J.; Jones, A. Characterization of ciguatoxins and ciguatoxin congeners present in ciguateric fish by gradient reversephase high-performance liquid chromatography/mass spectrometry. *Toxicon* **1997**, *35*, 159–168. [CrossRef]
129. Lewis, R.J.; Jones, A.; Vernoux, J.-P. HPLC/Tandem Electrospray Mass Spectrometry for the Determination of Sub-ppb Levels of Pacific and Caribbean Ciguatoxins in Crude Extracts of Fish. *Anal. Chem.* **1999**, *71*, 247–250. [CrossRef] [PubMed]
130. Sibat, M.; Herrenknecht, C.; Darius, H.T.; Roué, M.; Chinain, M.; Hess, P. Detection of pacific ciguatoxins using liquid chromatography coupled to either low or high resolution mass spectrometry (LC-MS/MS). *J. Chromat. A* **2018**, *1571*, 16–28. [CrossRef] [PubMed]
131. Moreiras, G.; Leao, J.M.; Gago-Martinez, A. Design of experiments for the optimization of electrospray ionization in the LC-MS/MS analysis of ciguatoxins. *J. Mass Spectrom.* **2018**, *53*, 1059–1069. [CrossRef] [PubMed]
132. Toshiyuki, S.; Ha, D.V.; Uesugi, A.; Uchida, H. Analytical challenges to ciguatoxins. *Curr. Opin. Food Sci.* **2017**, *18*, 37–42. [CrossRef]
133. Mak, Y.L.; Wu, J.J.; Chan, W.H.; Murphy, M.B.; Lam, J.C.W.; Chan, L.L.; Lam, P.K.S. Simultaneous quantification of Pacific ciguatoxins in fish blood using liquid chromatography-tandem mass spectrometry. *Anal. Bioanal. Chem.* **2013**, *405*, 3331–3340. [CrossRef] [PubMed]
134. Ha, D.V.; Uesugi, A.; Uchida, H.; Ky, P.X.; Minh, D.Q.; Watanabe, R.; Matsushima, R.; Oikawa, H.; Nagai, S.; Iwataki, M.; et al. Identification of Causative Ciguatoxins in Red Snappers *Lutjanus bohar* Implicated in Ciguatera Fish Poisonings in Vietnam. *Toxins* **2018**, *10*, 420. [CrossRef]

135. Kohli, G.S.; Haslauer, K.; Sarowar, C.; Kretzschmar, A.L.; Boulter, M.; Harwood, D.T.; Laczka, O.; Murray, S.A. Qualitative and quantitative assessment of the presence of ciguatoxin, P-CTX-1B, in Spanish Mackerel (*Scomberomorus commerson*) from waters in New South Wales (Australia). *Toxicol. Rep.* **2017**, *4*, 328–334. [CrossRef]
136. Costa, P.R.; Estevez, P.; Castro, D.; Solino, L.; Gouveia, N.; Santos, C.; Rodrigues, S.M.; Leao, J.M.; Gago-Martinez, A. New insights into the occurrence and toxin profile of ciguatoxins in Selvagens Islands (Madeira, Portugal). *Toxins* **2018**, *10*, 524. [CrossRef]
137. Pottier, I.; Vernoux, J.P.; Jones, A.; Lewis, R.J. Analysis of toxin profiles in three different fish species causing ciguatera fish poisoning in Guadeloupe, French West Indies. *Food Add. Contam.* **2002**, *19*, 1034–1042. [CrossRef]
138. Estevez, P.; Sibat, M.; Leão-Martins, J.M.; Costa, P.R.; Gago-Martínez, A.; Hess, P. Liquid Chromatography Coupled to High-Resolution Mass Spectrometry for the Confirmation of Caribbean Ciguatoxin-1 as the Main Toxin Responsible for Ciguatera Poisoning Caused by Fish from European Atlantic Coasts. *Toxins* **2020**, *12*, 267. [CrossRef] [PubMed]
139. Pasinszki, T.; Krebsz, M.; Tung, T.T.; Losic, D. Carbon Nanomaterial Based Biosensors for Non-Invasive Detection of Cancer and Disease Biomarkers for Clinical Diagnosis. *Sensors* **2017**, *17*, 1919. [CrossRef]
140. Pasinszki, T.; Krebsz, M. Biosensors for Non-Invasive Detection of Celiac Disease Biomarkers in Body Fluids. *Biosensors* **2018**, *8*, 55. [CrossRef] [PubMed]
141. Pasinszki, T.; Krebsz, M. Advances in Celiac Disease Testing. *Adv. Clin. Chem.* **2019**, *91*, 1–29. [CrossRef]

toxins

MDPI

Review

Ciguatera in the Indian Ocean with Special Insights on the Arabian Sea and Adjacent Gulf and Seas: A Review

Nazima Habibi [1], Saif Uddin [1,*], Marie-Yasmine Dechraoui Bottein [2] and Mohd Faizuddin [3]

[1] Environment and Life Sciences Research Center, Kuwait Institute for Scientific Research, Safat 13109, Kuwait; nhabibi@kisr.edu.kw
[2] Université Côte d'Azur, CNRS, ECOSEAS, UMR7035, Parc Valrose, 06108 Nice, France; y.bottein@gmail.com
[3] Gulf Geoinformation Solutions, Sharjah, United Arab Emirates; faiz_ud_din@yahoo.com
* Correspondence: sdin@kisr.edu.kw; Tel.: +965-24989224

Abstract: The dinoflagellates of the genus *Gambierdiscus* are found in almost all oceans and seas between the coordinates 35° N and 35° S. *Gambierdiscus* and *Fukuyoa* are producers of ciguatoxins (CTXs), which are known to cause foodborne disease associated with contaminated seafood. The occurrence and effects of CTXs are well described in the Pacific and the Caribbean. However, historically, their properties and presence have been poorly documented in the Indian Ocean (including the Bay of Bengal, Andaman Sea, and the Gulf). A higher occurrence of these microorganisms will proportionately increase the likelihood of CTXs entering the food chain, posing a severe threat to human seafood consumers. Therefore, comprehensive research strategies are critically important for developing effective monitoring and risk assessments of this emerging threat in the Indian Ocean. This review presents the available literature on ciguatera occurrence in the region and its adjacent marginal waters: aiming to identify the data gaps and vectors.

Keywords: the Indian Ocean; Arabian sea; Kuwait bay; Aden Gulf; Red Sea; Gulf of Aqaba; Andaman Sea; Bay of Bengal; seafood safety; foodborne disease

Key Contribution: This review highlights the paucity of data on ciguatoxins from the vast Indian Ocean region, which is home to an enormous mass of seafood-consuming populations. Furthermore, it exports fisheries to Europe and North America, which resulted in toxic fish being found during 2012, 2015, and 2016. The monitoring of *Gambierdiscus* and *Fukuyoa* is not taken up regularly despite their recorded presence all over the Indian Ocean.

Citation: Habibi, N.; Uddin, S.; Bottein, M.-Y.D.; Faizuddin, M. Ciguatera in the Indian Ocean with Special Insights on the Arabian Sea and Adjacent Gulf and Seas: A Review. *Toxins* **2021**, *13*, 525. https://doi.org/10.3390/toxins13080525

Received: 2 July 2021
Accepted: 22 July 2021
Published: 27 July 2021

1. Introduction

Ciguatera poisoning (CP) is a syndrome caused by ingestion of coral reef fish and shellfish of tropical and subtropical regions, which has caused global concern. Some dinoflagellate species of the genera *Gambierdiscus* and *Fukuyoa* are known to produce ciguatoxins (CTXs); the organisms that consume these toxic algae accumulate CTXs that are transferred and biotransformed along the marine and human food chain. These lipid-soluble and heat-resistant toxins cause gastrointestinal, cardiovascular, and neurological disorders among humans consuming the CTX-contaminated seafood [1–5]. According to a study published in 2008, CP disease estimations are uncertain and often misdiagnosed [6]. However, few reports predict 2–10 million people are annually affected by CP [7,8].

Ciguatera poisoning is regarded globally as the most significant non-bacterial poisoning associated with fish consumption. It is usually limited to the consumption of toxic fish from regions between the latitudes 35° N and 35° S [9–17]. Studies have shown a strong positive correlation between *Gambierdiscus* abundance and algal macrophytes [18]. Some earlier studies proposed a standardized methodology for estimating *Gambierdiscus* abundance based on sampling macroalgae [19–21]. More recent studies brought to light the significant biases in *Gambierdiscus* cell distribution within the macrophytes. A 33–150%

variation was reported among replicates [22–24]. Despite these limitations, some first-order estimates on *Gambierdiscus* distributions for large geographic regions have been attempted using the average abundances [11,25]. These have shown a global distribution spreading across oceans with 85% of *Gambierdiscus* density estimates <1000 cells g^{-1} wet weight algae, with <10% occurrence with 10–10,000 cells g^{-1} wet weight algae and <5% incidences where the concentration was >100,000 cells g^{-1} wet weight algae. With the growing global demands for seafood and international trade ease, CP concerns the population beyond the endemic regions and is increasingly becoming a global issue. Moreover, a greater threat is posed as there are no current antidotes for CP [26].

Historically, poisoning associated with seafood consumption was reported in different parts of the globe. It was first recounted in the West Indies as early as 1511 [27] and in the Gulf of Guinea in 1521, killing the Captains of the Spanish army [28]. It was also reported in the islands of the Indian Ocean in 1601 and various archipelagos of the Pacific Ocean in 1606 [27]. Additionally, in 1786, the surgeon of HMS Endeavour, en route to Australia, New Zealand, and the Pacific Islands, reported that the ship's Captain was poisoned by ciguatoxins [29]. A year later, the ingestion of a local gastropod (*Livonia* sp.) was discovered to induce neurological symptoms in the Antilles of the Caribbean Sea [30]. In 1948, the organism *Gambierdiscus* (originally referred to as *Goniodoma* sp.) was described for the first time in Cabo Verde [31]. The term "ciguatera poisoning" was coined in Cuba (Caribbean Sea) after the ingestion of a marine snail (*Turbo pica*) locally known as cigua [32]. The historical facts suggested the tropical and subtropical Pacific and Indian Ocean insular regions, the tropical Caribbean region, and the continental reefs to be endemic to ciguatera [27].

In recent years, there has been an increase in the frequency of reports of toxic and harmful benthic algal blooms, predominantly *Gambierdiscus* with the presence of *Fukuyoa* and *Ostreopsis* blooms, throughout the world [33,34]. The interest in *Gambierdiscus* blooms has been heightened because of increased awareness of the effects of CP on human health. A growth in species abundance has already been observed in subtropical and temperate regions with the threat of global warming expected to further exacerbate the situation [35–38]. However, a recent article by Hallegraeff et al. [39] suggested that intensified monitoring efforts and heightened aquaculture activities are responsible for these perceived increases in HABs events that are not underpinned to be expanded as an empirical assumption. Ciguatoxins are reported globally, being described from new sites in the Canary Islands, Indian Ocean, Japan, and Western Gulf of Mexico [8,40–45]. Until recently, the records of *Gambierdiscus* in the Indian Ocean were scarce and restricted to the western tropical region, whereas now its presence has been found in the Northern part of the ocean [42]. There is paucity of information on ciguatera phenomena, including the occurrence of human poisonings, of toxins in seafood, and of the causative organisms, in the Indian Ocean in general, and the northern part in particular. In the present review, we gathered the published information on reported occurrences of *Gambierdiscus* and identified the research gaps related to its monitoring as a tool to manage this emerging hazard.

2. Results

2.1. Environmental and Global Pressures in the Northern Part of the Indian Ocean

The Indian Ocean is the third largest ocean enclosing densely populated landmasses: In the North, India, Bangladesh, Burma, Thailand, Pakistan, Iran, and Oman among others. It also includes regional seas in the North such as the Arabian Sea and the adjacent Lakshadweep Sea, Aden Gulf in the Red Sea, the Gulf of Aqaba and Suez, the Bay of Bengal and the Andaman Sea, as well as the Gulf of Oman and the Persian Gulf further north. Countries from the Indian Ocean region have experienced unusual climatological conditions such as cyclones, El Niño-Southern Oscillation events, and coral reef bleaching during the past two decades [46–48]. Benthic microalgae are particularly influenced by these disturbances especially the coral mortality, which provides a good substrate for the formation of algal turfs and associated epiphytes [49]. The study conducted by

Quod et al. [46] reported a significant increase in the CP causative organisms in comparison to those reported in 1980 [47], following the coral bleaching event in 1998, thus posing an incremental risk of HABs in the region and drawing detrimental consequences to the marine biodiversity and human health [50].

The unfavorable effects of increasing atmospheric levels of carbon dioxide (CO_2) and other greenhouse gases in the Indian Ocean and its marginal seas are leading towards acidification of the marine environment [48,51–53]. Supporting evidence for increased CO_2 sequestration was drawn from increased marine primary productivity over the past decade [51,54]. The eutrophication of Kuwait bay and the nearby water bodies due to upwelling events is considered to be a predominant factor influencing the onset of algal blooms due to enriched nutrient conditions [54]. Other potential factors that have influenced the onset of blooms consist of coral bleaching, unusual variances in temperature, and calm conditions. Additional factors such as dust storms that carry micronutrients, domestic and industrial inputs, natural meteorological and oceanographic forcings, and the introduction of invasive species from ballast water discharge may all play a major role in the onset and expansion of HABs [41,45,55–58].

2.2. Ciguatera Causative Organisms Occurrence

The dinoflagellates *Gambierdiscus* and *Fukuyoa* are the causative organisms of CP worldwide [5]. The genus *Gambierdiscus* has a pantropic distribution with about 18 known species while *Fukuyoa* has 3 known species. Within the Indian Ocean, *Gambierdiscus* are more dominant in the western part. Of the several known *Gambierdiscus* sp., initially only *Gambierdiscus toxicus* was reported in Mayotte since *G. toxicus* was the first species that was described [50,59–61]. Later it was reported in La Reunion and Mauritius [62–65] as well (Figure 1). *Gambierdiscus toxicus* was also found in Mbudya Island, Oysterbay, Bawe Island, and Makoba Islands in Tanzania at depths of 5–10 m and temperatures ranging from 25 to 32 °C [66] (Figure 2). Thereafter, *Gambierdiscus yasumotoi* (now *Fukuyoa yasumotoi* (M.J. Holmes) [67]) and *Gambierdiscus belizeanus* were confirmed to occur in Mayotte in the Comoros archipelago [50] (Figure 3).

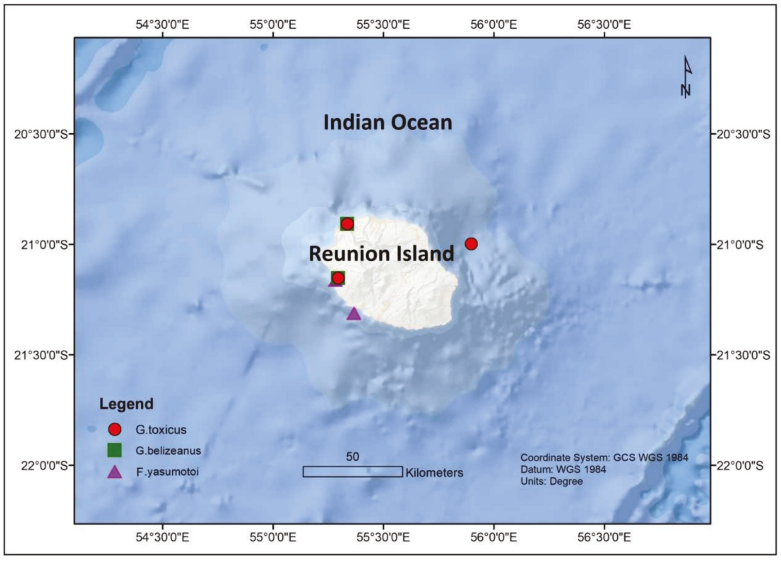

Figure 1. Spatial distribution of *Gambierdiscus* and *Fukuyoa* sp. from Reunion Island.

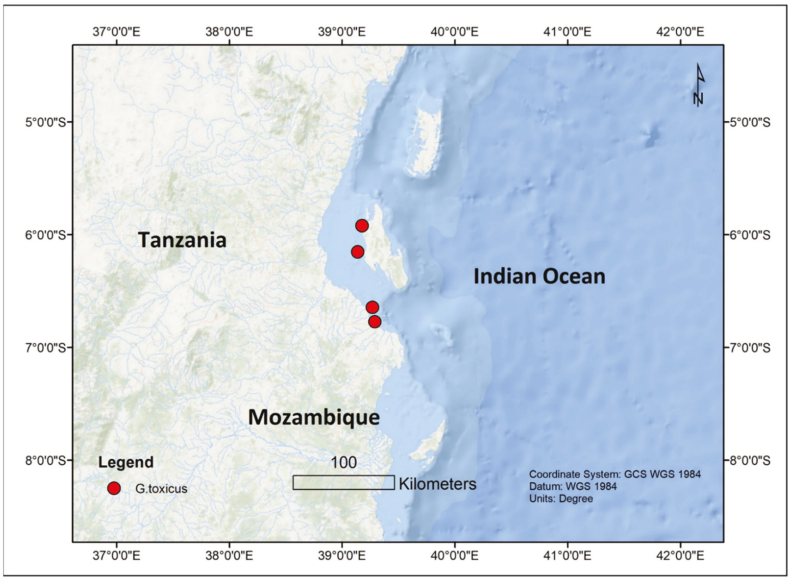

Figure 2. The occurrence of *Gambierdiscus* sp. from Tanzanian coastal area.

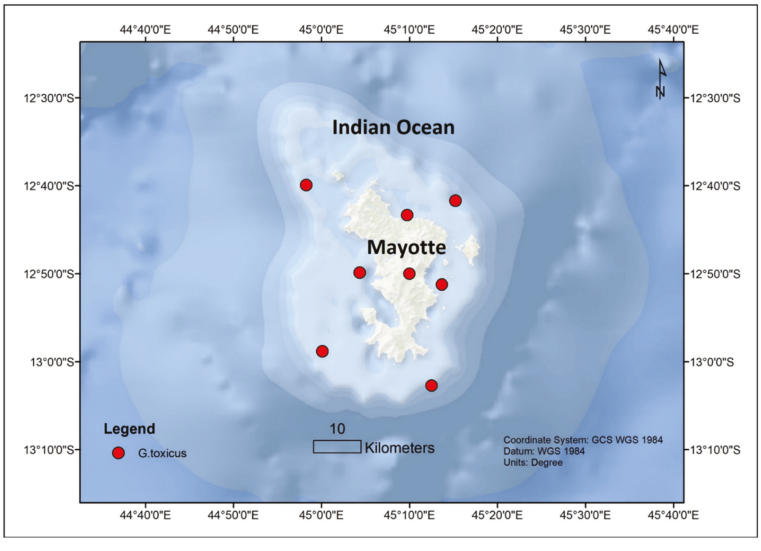

Figure 3. *Gambierdiscus* sp. reported from Mayotte Island, Indian Ocean.

In the northern part of the Indian Ocean, *Gambierdiscus* species have been noticed in the marginal seas of the Indian Ocean, such as the Arabian Sea [41,42,45,68]; Red Sea [41–45]; Gulf of Aqaba [42]; and Manora Channel, Pakistan [69]. An assessment carried out in Kuwait (Persian Gulf) from November 2012 to March 2013 showed the presence of *G. yasumotoi* in the shallow lagoons of Qit'at Julai'ah and southern coastal waters of Kuwait at 1–3 m depth [68,70] (Figure 4). The average seawater temperatures and salinity during this time were between 23.5–25 °C and 41.2–42.4 ppt, respectively. In another study, *G. toxicus* was also identified in Kuwait's territorial water [41,45] (Figure 4).

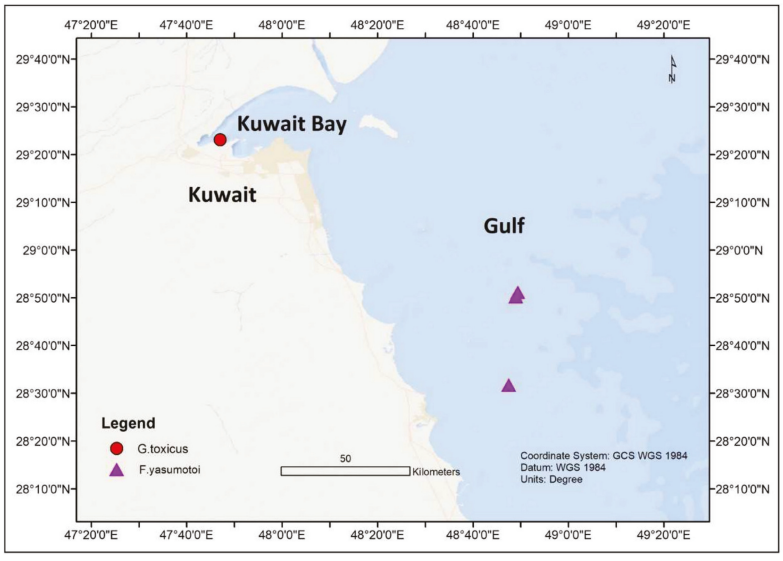

Figure 4. *Gambierdiscus toxicus* and *Fukuyoa yasumotoi* occurances in Kuwait Coastal waters.

In an investigation from the Gulf of Aqaba, Jordan during October 2010, with a seawater temperature range of 24–25 °C and salinity of 40 ppt, *G. belizeanus* was reported from a depth of 1.5–2.0 m (Figure 5). The toxigenic *G. belizeanus* was reported from the Red Sea, Saudi Arabian coast during February 2012 and May 2013 [43,44] at a sampling depth between 0.4–0.8 m, with seawater temperatures and salinity range of 28.9–38.4 °C and 36.1–38.4 ppt respectively. The oxygen saturation during this period was very variable between 1.73–32.1%.

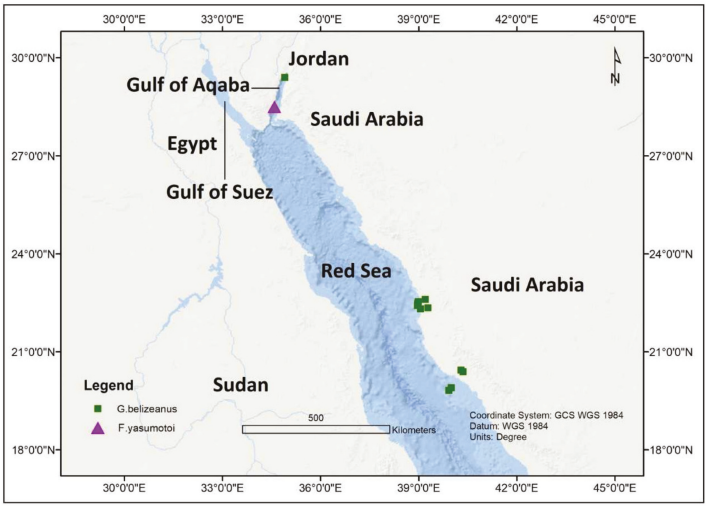

Figure 5. The Spatial distribution of *Gambierdiscus belizeanus* and *Fukuyoa yasumotoi* occurances in Red Sea and adjacent areas.

In 2011, four *Gambierdiscus* species including *G. toxicus*, *G. belizeanus*, *G. polynesiensis*, *G. australes*, and *Fukuyoa yasumotoi* were also reported from the coastal waters of Pakistan in the northern Indian Ocean [69] (Figure 6). An unidentified *Gambierdiscus* sp.

was also discovered in middle of the Bay of Bengal [71] (Figure 7). In Mangalore at the southwest coast of India, CP was first described during June 2015 outbreak involving red snapper(*Lutjanus bohar*) [72,73], and a second outbreak during September 2016 involving red snapper again [74]. In another incidence, CP was also reported from Trivandrum, India [75].

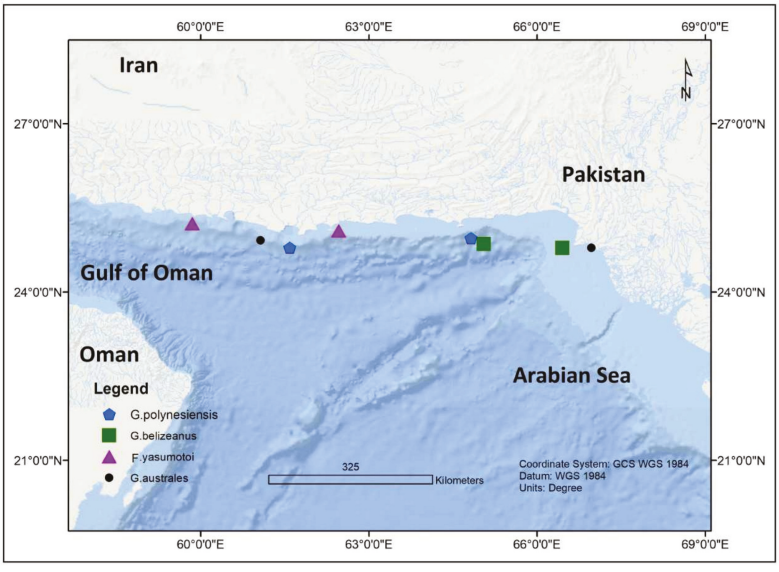

Figure 6. Occurrences of *Gambierdiscus* in Gulf of Oman and Pakistan's coastal regions.

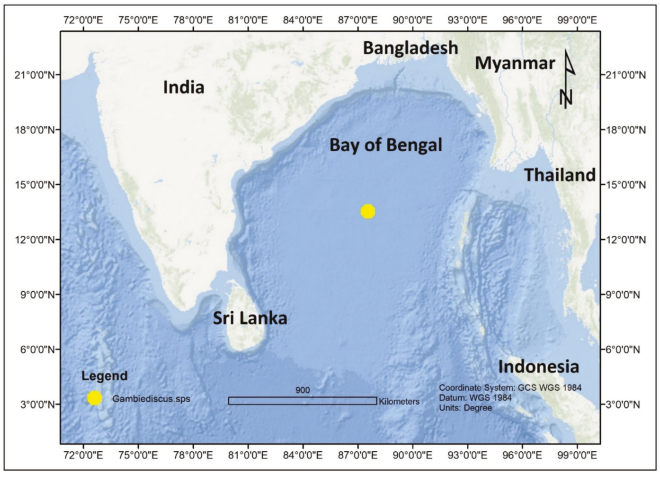

Figure 7. *Gambierdiscus* sp. reported from the Bay of Bengal, Indian Ocean.

3. Discussion

3.1. Toxin Production by Ciguatera in Indian Ocean Region and Adjoining Marginal Seas

Ciguatoxins form a large group of toxins of 40 confirmed or suspected chemical analogs. They are classified into four types, according to both their geographical origin

and chemical structure: The Pacific CTXs (P-CTX) of the type CTX3C and CTX4A, the Caribbean CTXs (C-CTX type), and the Indian CTXs (I-CTX type) [8,27]. The existence of the I-CTX type is still speculative and may be similar to that of the C-CTX. Their structural characteristic has not yet been elucidated. Six derivatives I-CTX 1–6 were identified with a molecular weight in Dalton of 1140.6, 1156.6, 1138.6, and 1154.6, however, their chemical structure is still unknown. Four of them were retrieved from a highly toxic *Lutjanus sebae* (Red Emperor) from the coast of the Republic of Mauritius through optimized gradient reversed-phase high-performance liquid chromatography-electrospray ionization mass spectrometry (LC/MS) methods, in combination with a radioligand receptor binding assay (r-RBA) [76,77], and two from in a bull shark (*Carcharhinus leucas*) implied in a fatal intoxication in Madagascar [76–78]. The lipid-soluble extracts retrieved from the edible fishes were reported to possess CTX activity and induced lethal symptoms in mice [77] and responded to the cell bioassay [78].

The toxicity of these *Gambierdiscus* species collected in the Pacific and/or the Caribbean was found to vary by over 2 orders of magnitude [11,79,80]. It remains to be confirmed that the same ranges are observed in the Indian ocean where only a few species have been analyzed for their toxin contents. Using in vitro cytotoxicity cell-based assays (CBA with neuroblastoma with N2a cells), the toxicity of two isolates of *G. belizeanus* from the Red Sea was estimated at 6.50×10^{-5} pg P-CTX-1 eq. cell^{-1} for RS2-B6 and 1.02×10^{-5} pg P-CTX-1 eq. cell^{-1} for RS3-B8. Toxin production was slightly higher in *G. belizeanus* strains from Tahiti (0.0246 fg P-CTX-3C eq. cell^{-1}) [4,43,44]. As compared to *G. belizeanus*, the species of *G. polynesiensis*—0.017–4.4 pg P-CTX-3C eq. cell^{-1}; *G. toxicus*—0.028 pg P-CTX-3C eq. cell^{-1} [4]; and *G. australes*—0.04 pg CTX-1 eq cell^{-1} [40] are more toxigenic.

More recently, Gambieric acid D was identified for the first time in the flesh of a bull shark (*Carcharhinus leucas*) employing the technique of liquid chromatography coupled with high-resolution mass spectrometry (HRMS). The toxicity was confirmed through mouse bioassays (Lowest dose = 72 mg equiv. stomach per mouse of 20–22 g) and neuro-2a cell-based assays (flesh—0.06 µg P-CTX-1 equiv./kg; stomach—92.78 µg P-CTX-1 equiv./kg; fins 1—0.12 µg P-CTX-1 equiv./kg; and fin 3—µg P-CTX-1 equiv./kg) [78]. Ciguatoxins were identified as CTX1B and 2,3-dihydroxy CTX3C; 51-hydroxy CTX3C; or positive by cell assay in Snapper fish (Lutjanidae) caught in the Indian Ocean and involved in 5 CP outbreak [81]. Fish samples from Sri Lanka were analyzed by the European Union Reference Laboratory for Marine Biotoxins (EURLMB) in Vigo, Spain, and the putatively contaminated fish samples were analyzed by liquid chromatography-tandem mass spectrometry (LC-MS/MS) according to a method published by [82] with slight modifications. The only available analytical standard was P-CTX-1B. Seven out of 11 samples tested positive for P-CTX-1B. In addition, other putative CTX variants were detected across most samples, however, they could not be confirmed as CTXs due to the lack of reference compounds. There are incidences of ciguatera poisoning due to the import of contaminated fish from the Indian ocean region, mainly India and Sri Lanka.

It is important to note that the investigations conducted so far have been limited in spatial coverage. Additional research is, therefore, required at a broader spatial scale to make meaningful conclusions regarding the occurrence, abundance, and temporal variability of ciguatoxins in the region.

3.2. Ciguatera Causative Organism's Abundance

Globally, ciguatera causative organisms' densities have been found to vary from few cells to thousands of cells per gr of substrate. *Gambierdiscus* is known as a slow-growing species compared to many other dinoflagellates; it takes about 5 months to increase its abundance. Chinain et al., [4] found a mean growth rate in *G. polynesiensis* as 0.13 ± 0.03 div d^{-1} at exponential phase in batch culture condition [4]. In the field, a 17 months lag time is estimated between a major environmental event (such as hurricane) and before it blooms and releases toxins into the environment and gets into the food chain [83]. During October 1998, a remarkably higher concentration of *G. toxicus* equivalent to 60,463 cells per gram of algae was

recorded in Mayotte Islands (Comoros, southwest Indian Ocean) following a bloom event. This density is the highest ever recorded in the region and also the highest globally [50]. In a non-bloom event, the cell densities of *Gambierdiscus* were far less and often non-detectable.

In the western Indian Ocean region, the cell densities of *G. toxicus* were variable and affected by spatial and temporal variations. In Tanzania, it ranged from 0.0 to 879.5 (Bawe station) cells g^{-1} wet weight (ww) algae and 0 to 92.6 cells g^{-1} ww seagrass (Mbudya) [66]. The abundances on macroalgae in the Mayotte coral reef complex were reported to range from 0.0 to 2800 cells g^{-1} [60]. Monitoring of *G. toxicus* in the locality of Saint Leu (Reunion) since 1993 revealed high variability in population density with an average value of 122 $\pm$ 24 cells g^{-1} of algal turf [64]. In the coral reef complex of Mayotte Island (SW Indian ocean), the concentrations of *G. toxicus* ranged from 800–5400 dinoflagellates g^{-1} of biodeposits in the northeast lagoon. Up to 6000 dinoflagellates g^{-1} were recorded at Bambo islet in the southeast lagoon. Lower abundances up to 400 g^{-1} were recorded near the main island shore; seawards on the outer side of the barrier reef; and in luxurious coral areas more exposed to humans. At stations near the main island coast, abundance of *G. toxicus* was less than 100 cells g^{-1} [60]. The density of *G. toxicus* was as low as 0–4 cells g^{-1} of macrolagae in the lagoons of Trou Aux Biches, Mauritius [84].

In the northern part of the Indian ocean, the cell numbers of *Gambierdiscus* from the central Red Sea, Saudi Arabian coast were <40 cells g^{-1} ww of algae [43,44]. Similarly, *F. yasumotoi* in Kuwaiti shores had an average cell density of 116.7 $\pm$ 47.5 cells g^{-1} of ww algae. The high biomass algae (HABs) were estimated through the Ocean Color Modis Algorithm (OC3M), Garver-Siegel-Maritorena Algorithm (GSM), Generalized Inherent Optical Property (GIOP) model [41,45]; these areas when sampled showed the presence of *G. toxicus* in a concentration of ~1000 cells per liter of seawater [41].

3.3. Ciguatera Causative Organisms' Substrates and Co-Occurring Species

Gambierdiscus is an epiphytic benthic dinoflagellate, commonly found on algal turfs, coral rubble, and macroalgae. A study from the Coastal region of Tanzania reported the *G. toxicus* strains along with unknown brown algae mixed with filamentous cyanobacteria species and the red alga *Gracillaris* sps. [66]. The dinoflagellate was also separated from two species of seagrass namely *Thalassia hemprichii* and *Thalasodendron ciliatum* in the same study [66]. The dinoflagellate assemblage observed in coral reefs revealed toxic species including *G. toxicus*, *Prorocentrum* spp., and *Ostreopsis* spp [85]. The co-occurrence of *Prorocentrum* sps. and *Ostreospis* sps. with *G. toxicus* were reported by Grzebyk and his group. In the same study, it was also demonstrated that some microalga stimulated whereas the others subsided the growth of *G. toxicus* [60]. Benthic thecate dinoflagellates in the sandy ecosystem of La Possession bay (Reunion Islands) were isolated as a complex of five toxic species namely *G. yasumotoi*, *G. toxicus*, *P. arenarium*, *P. concavum,* and *P. lima*. At St. Leu and Saline reef, 25 benthic thecate dinoflagellate species coexisted out of which 15 were harmful and are presented in Table 1 [65]. The benthic dinoflagellate of *G. toxicus* was reported to coexist with *Ostreopsis* spp., *Prorocentrum* spp., *Coolia monotis,* and *Amphidinium* sp. in the lagoon of Trou Aux Biches, Mauritius [84]. In Mayotte islands, South west of Indian Ocean, *G. toxicus* were reported along with *Prorocentrum* spp., *Ostreopsis* sp., and *Amphidinium* spp. [50,59].

Table 1. Occurrence of *Gambierdiscus* species in the Indian Ocean region.

Species	Location	Marginal Seas	GPS Coordinates	Sampling Depth	Temperature	Associated Species	Salinities	Reference
G. toxicus	Kuwait	Persian Gulf	29.3860° N, 47.7830° E		17.59 °C	*Karenia selliformis*, *Karenia brevis*, *Prorocentrum lima*, *Phalacroma rotundatum*, *Tripos muelleri* and *Mesodinium rubrum*		[41,45]
F. yasumotoi	Qit'at Julai'ah, Kuwait	Persian Gulf	28.8370° N, 48.8160° E	1–3 m	21–22.3 °C	*Padina tetrastomatica*, *Sargassum oligocystum*, *Chaetomorpha* sp., *Amphidinium carterae*, *Coolia monotis*, *Ostreopsis* sps., *Prorocentrum formosum*, *P. tsawwassenense*, *Blixaea quinquecornis*, *Adenoides eludens* and *Cabra matta*	41.2–42.4	[42]
F. yasumotoi	Semi protected shallow lagoons, Kuwait	Persian Gulf	28.8530° N, 48.8230° E	1–3 m	23.5–25 °C		41.2–42.4	[42]
F. yasumotoi	Southern coast, Kuwait	Persian Gulf	28.8530° N, 48.8230° E	1–3 m	23.5–25 °C		42.1–42.8	[42]
F. yasumotoi	Jordan	Gulf of Aqaba	29.8250° N,34.8580° E	1.5–2 m	24–25 °C	NA	40.0	[42]
G. belizeanus	Jordan	Gulf of Aqaba	29.8250° N, 34.8580° E	1.5–2 m	24–25 °C	NA	40.0	[42]
G. belizeanus	Qita Al Kirsh, Saudi Arabia	Red Sea	22.6058° N, 39.1980° E	0.5–0.6 m	29.3 °C	*Turbinaria decurrens* and *Halimeda* sp.	38.4	[43,44]
G. belizeanus	Sh'ib Nazar, Saudi Arabia	Red Sea	22.4916° N, 38.9722° E	0.4 m	30.1 °C	*Turbinaria decurrens*	28.9	[43,44]
G. belizeanus	Malathu Reef, Saudi Arabia	Red Sea	19.8194° N, 39.9194° E	0.5–0.7 m	NA	*Turbinaria decurrens*	NA	[43,44]
G. belizeanus	Marmar Reef, Saudi Arabia	Red Sea	19.9038° N, 39.9947° E	0.8 m	NA	*Turbinaria decurrens*	NA	[43,44]
G. belizeanus	Al Fahal, Saudi Arabia	Red Sea	22.5386° N, 38.9813° E	0.6–0.8 m	30.4 °C	*Turbinaria decurrens* and *Halimeda* sp.	36.0	[43,44]
G. belizeanus	Abu Shosha, Saudi Arabia	Red Sea	22.3505° N, 39.2811° E	0.5 m	29.6 °C	*Turbinaria decurrens* and *Halimeda* sp.	38.3	[43,44]
G. belizeanus	Um Al Balam, Saudi Arabia	Red Sea	22.4277° N, 38.9652° E	0.4–0.6 m	29.3 °C	*Turbinaria decurrens* and *Halimeda* sp.	36.1	[43,44]
G. belizeanus	Um Al Kiethl, Saudi Arabia	Red Sea,	22.3197° N, 39.0541° E	0.5 m	29.5 °C	*Turbinaria decurrens* and *Halimeda* sp.	28.9	[43,44]
G. belizeanus	Coast Guard Reef, Saudi Arabia	Red Sea	20.3950° N, 40.3580° E	0.5 m	NA	*Turbinaria decurrens* and *Halimeda* sp.	NA	[43,44]
G. belizeanus	Mangrove Reef, Saudi Arabia	Red Sea	20.4400° N, 40.2911° E	0.4 m	NA	*Turbinaria decurrens*	NA	[43,44]
G. toxicus	Sindh Coast, Pakistan	Manora Channel; Chuma Island	24.8091° N, 66.9908° E	1.0 m	32 °C			[69]
G. toxicus	Balochistan Coast, Pakistan	Manora Channel; Chuma Island	24.7861° N, 66.4516° E	1.0 m	28 °C			[69]

Table 1. *Cont.*

Species	Location	Marginal Seas	GPS Coordinates	Sampling Depth	Temperature	Associated Species	Salinities	Reference
G. belizeanus	Sindh Coast, Pakistan	Manora Channel; Chuma Island	24.8091° N, 66.9908° E	1.0 m	32 °C			[69]
G. belizeanus	Balochistan Coast	Manora Channel; Chuma Island, Pakistan	24.7861° N, 66.4516° E	1.0 m	28 °C			[69]
G. australes	Sindh Coast	Manora Channel; Chuma Island, Pakistan	24.8091° N, 66.9908° E	1.0 m	32 °C			[69]
G. australes	Balochistan Coast	Manora Channel; Chuma Island, Pakistan	24.7861° N, 66.4516° E	1.0 m	28 °C			[69]
G. polynesiensis	Sindh Coast	Manora Channel; Chuma Island, Pakistan	24.8091° N, 66.9908° E	1.0 m	32 °C			[69]
G. polynesiensis	Balochistan Coast	Manora Channel; Chuma Island, Pakistan	24.7861° N, 66.4516° E	1.0 m	28 °C			[69]
F. yasumotoi	Sindh Coast	Manora Channel; Chuma Island, Pakistan	24.8091° N, 66.9908° E	1.0 m	32 °C			[69]
F. yasumotoi	Balochistan Coast	Manora Channel; Chuma Island, Pakistan	24.7861° N, 66.4516° E	1.0 m	28 °C			[69]
Gambierdiscus sp.	Bay of Bengal	India						[71]
G. toxicus	Mbudya Island, Dar es Salaam	Tanzania		5.0 m	25.5–31.0 °C	Seagrass—*Thalassodendron ciliatum*	35–37	[66]
G. toxicus	Bawe Island, Zanzibar	Tanzania		10.0 m	26.0–29.0 °C	Unknown brown algae mixed with Filamentous cyanobacteria	34–36	[66]
G. toxicus	Makoba, Zanzibar	Tanzania		10.0 m	26.0 °C	*Gracilaria* sp.	35–43	[66]
G. toxicus	Longoni Bay (Stations 1 and 2)	Mayotte, Mozambique	12.8333° N, 45.1666° E	Between the depth of the lower intertidal level and 30 m	26–31 °C	*Ostreopsis lenticularis*; *O. lenticularis*; *Prorocentrum lima* and 4 new species of *Prorocentrum*	35–37	[60]
G. toxicus	Surprise Reef (Station 3)	Mayotte, Mozambique	12.8333° N, 45.1666° E					[60]

Table 1. *Cont.*

Species	Location	Marginal Seas	GPS Coordinates	Sampling Depth	Temperature	Associated Species	Salinities	Reference
G. toxicus	Prevoyante Reef (Station 5)	Mayotte, Mozambique	12.8333° N, 45.1666° E					[60]
G. toxicus	Great Barrier Reef (Station 4A–C)	Mayotte, Mozambique	12.8333° N, 45.1666° E					[60]
G. toxicus	Cape Andrema Station 6)	Mayotte, Mozambique	12.8333° N, 45.1666° E					[60]
G. toxicus	M'Songoma (Station 7)	Mayotte, Mozambique	12.8333° N, 45.1666° E					[60]
G. toxicus	M'Sanga Tsohole Reef (Station 8A,B)	Mayotte, Mozambique	12.8333° N, 45.1666° E					[60]
G. toxicus	Bambo Reef (Station 9A,B)	Mayotte, Mozambique	12.8333° N, 45.1666° E					[60]
G. toxicus	Mayotte	South West Indian Ocean				*Prorocentrum* spp., *Ostreopsis* sp., *Amphidinium* spp		[59]
G. toxicus	Mayotte	South West Indian Ocean						[86]
G. belizeanus	St-Leu and Saline reef	Reunion Island	21.1533° N, 55.2944° E	1–5 m		*P. arenarium*; *P. belizeanum*; *P. concavum*; *P. elegans*; *P. emarginatum*; *P. hoffmannianum*; *P. lima*; *P. mexicanum*; *P sculptile*; *P. borbonicum*; *O. heptagona*; *O. labens*; *O. lenticularis*; *O. mascarensis*; *O. ovata*; *O. siamensis*; *C. monotis*; *C. tropicalis*; *Sinophysis microcephalis*; *S. canaliculate*; *Amphidiniopsis* sp.; *Bysmatrum* sps.		[65]
G. belizeanus	Possession Bay	La Reunion	20.9347° N, 55.3491° E	10–12 m		*P. arenarium*; *P. emarginatum*; *P. concavum*; *P. lima*; *P panamensis*; *Coolia* sps.		[65]
G. toxicus	St-Leu and Saline reef	La Reunion	21.1533° N, 55.2944° E	1–5 m		*P. arenarium*; *P. belizeanum*; *P. concavum*; *P. elegans*; *P. emarginatum*; *P. hoffmannianum*; *P. lima*; *P. mexicanum*; *P sculptile*; *P. borbonicum*; *O. heptagona*; *O. labens*; *O. lenticularis*; *O. mascarensis*; *O. ovata*; *O. siamensis*; *C. monotis*; *C. tropicalis*; *Sinophysis microcephalis*; *S. canaliculate*; *Amphidiniopsis* sp.; *Bysmatrum* sps.		[65]
G. toxicus	Possession Bay	La Reunion	20.9347° N, 55.3491° E	10–12 m		*P. arenarium*; *P. emarginatum*; *P. concavum*; *P. lima*; *P panamensis*; *Coolia* sp.		[65]

Table 1. *Cont.*

Species	Location	Marginal Seas	GPS Coordinates	Sampling Depth	Temperature	Associated Species	Salinities	Reference
F. yasumotoi	St-Leu and Saline reef	La Reunion	21.1533° N, 55.2944° E	1–5 m		*P. arenarium*; *P. belizeanum*; *P. concavum*; *P. elegans*; *P. emarginatum*; *P. hoffmannianum*; *P. lima*; *P. mexicanum*; *P sculptile*; *P. borbonicum*; *O. heptagona*; *O. labens*; *O. lenticularis*; *O. mascarensis*; *O. ovata*; *O. siamensis*; *C. monotis*; *C. tropicalis*; *Sinophysis microcephalis*; *S. canaliculate*; *Amphidiniopsis* sp.; *Bysmatrum* sp.		[65]
F. yasumotoi	Possession Bay	La Reunioin	20.9347° N, 55.3491° E	10–12 m		*P. arenarium*; *P. emarginatum*; *P. concavum*; *P. lima*; *P panamensis*; *Coolia* sp.		[65]
G. toxicus	Reunioin Islands	Mauritius				*Prorocentrum* sp.; *Ostreopsis* sp.		[64]
Gambierdiscus	Mangalore	India	12.91777° N, 74.79162° E					[72–74]

NA-Not available.

In the reports of Catania and her team [43,44], the Red Sea strains of *G. belizeanus* were associated with the macroalgae species of *Turbinaria decurrens* and *Halimeda* sps. Information on macroalgal species associated with *G. belizeanus* isolated from the Gulf of Aqaba is unavailable [42]. In the case of *G. yasumotoi*, the macroalgal substrates were identified as *Padina tetrastomatica* and *Sargassum oligocystum* in winter (November 2012) collections whereas in summers (March 2013) they occurred along with *Chaetomorpha* sp. The group also reported the co-occurrence of macroalgal species of *Amphidinium carterae*, *Coolia monotis*, *Ostreopsis* sps., *Prorocentrum formosum*, *P. tsawwassenense*, *Peridinium quinquecorne*, *Adenoides eludens*, and *Cabra matta* [42]. Moderate Resolution Imaging Spectroradiometer (MODIS) and Medium Resolution Imaging Spectrometer (MERIS) data and its various operational algorithms such as OC3M-547, GSM, GIOP, and other bio-optical methods developed by Uddin and coworkers [41,45,54], revealed algal blooms; during field verification, it was observed that *G. toxicus* was also part of the algal bloom on 21 December 2009. Samples collected from location 29.38694° N, 47.78389° E had over 1000 cells/L. Other algae identified in the field samples were *G. toxicus*, *Karenia selliformii*, *K. brevis*, *P. lima*, *Dinophysis rotundata*, *Ceratium tripos*, and *Myrionecta rubrum*.

Recent deliberations by the experts in an international meeting in Rome on ciguatera poisoning recommended the next generation sequencing (NGS) to mass-amplify specific gene sequences from sediment samples to characterize all species or specific taxa present in the sample [8]. This approach allows better identification and resolution of microbial community composition than the conventional morphological and molecular methodologies. The information on ciguatera from the Indian Ocean region is still in its initial phase. This approach would provide comprehensive information on ciguatera diversity and its interaction with associated communities as reported elsewhere [87–91].

3.4. Ciguatera Causative Organism's Morphology and Phylogeny

A variety of techniques are known to be used for ciguatera identification at a particular site. These include light microscopy (LM), scanning electron microscopy (SEM), DNA sequencing, restriction fragment length polymorphism (RFLP), quantitative polymerase chain reaction (qPCR), and metabarcoding [8,87]. While performing the morphological identification, the taxonomic key reported earlier [25] was followed by the research groups

to confirm the species of *Gambierdiscus* found in the region. Earlier in the 1990s, SEM was used for the identification of *G. toxicus* from Reunion Islands [64]. SEM was also used recently to identify the species of *G. toxicus*; *G. belizeanus*; *G. polynesiensis*; *G. australes;* and *F. yasumotoi* [69]. The morphological identification of Gulf strains of *G. yasumotoi and G. belizeanus* was based on both LM and SEM [42–44]. A description of morphological parameters of strains present in the Indian Ocean region is given in Table 2.

Table 2. Morphological features of *Gambierdiscus* species found in the Indian Ocean region.

	***F. yasumotoi* [12]**	***G. belizeanus* [92]**	***G. toxicus* [93]**	***G. polynesiensis* [94]**	***G. australes* [94]**
Cell depth	54 to 73 µm	59 to 73 µm	71 to 96 µm	65 to 87 µm	60 to 82 µm
Cell width	46 to 61 µm	60 to 73 µm	45 to 140 µm	64 to 75 µm	65 to 85 µm
Cell length	49 to 70 µm	47 to 51 µm	50 to 150 µm	57 to 75 µm	76 to 93 µm
Cell shape	Globular	Round	Rounded/ellipsoid	Rounded/ellipsoid	Rounded/ellipsoid
Apical pore	Fish hook-shaped	Fish hook-shaped	Fish hook shaped	Fish hook shaped	Fish hook shaped
Thecal surface		Moderately aerated		Smooth	Smooth
Apical plate	elongated and teardrop-shaped	Ellipsoid	Ellipsoid	large triangular apical pore plate	broad ellipsoid apical pore plate
Hypotheca		Truncate-conical			Eight hypothecal plates
Epitheca		dome-shaped	Ellipsoid		Eleven plates
Sulcus			Short		
Chloroplast	elongated golden-brown chloroplasts were peripherally arranged	golden-brown drop-shaped chloroplasts radiating from the cell centre			
Nucleus	large, oblong and located in the right posterior	large, oblong and crescent-shaped, and located in the right posterior cell part			Posteriorly situated nucleus
Cingulum		deeply excavated, descending,	Ascending narrow cingulum		Narrow and deep
Plate Formulae			Po, 3′, 7″, 6C, 8S, 5‴, 1p, 2‴	Po, 3′, 7″, 6C, 8S, 5‴, 1p et 2‴	Po, 3′, 7″, 6C, 8S, 5‴, 1p et 2‴
Studied by	[42,69]	[42–44,69]	[66,69]	[69]	[69]

Owing to the plasticity of morphological characteristics of some species of *Gambierdiscus*, the identification can be ambiguous if only morphology is used. Currently, molecular techniques are gaining popularity for the confirmation of species identified through microscopic methods. The only report on molecular identification of *Gambierdiscus* in the Arabian Gulf was by Catania [43] and her team [44]. The group amplified an 850 bp hypervariable (D8-D10) region of the larger subunit (LSU) of rRNA using primers FD8 and RB [11,25] through Sanger sequencing. A query of assembled nucleotides on the National Centre for Biotechnology and Informatics (NCBI) through the basic local alignment search tool (BLAST) resulted in a 100% match with *G. belizeanus*. Their (KY782637–KY782645) strains depicted a close resemblance with the Caribbean strain of *G. belizeanus*. The group also reported a 116 bp deletion at 493–609 position in one of the isolates, probably imparting the distinctiveness from other species of *Gambierdiscus* [95,96].

Phylogenetic analysis (methodology described in the Supplementary file) based on multiple alignments (Clustal2.1) of all the available DNA sequences (n = 345) of the D8–D10 region of the large sub unit (LSU) of ribosomal RNA (rRNA) [9,11,14,15,25,26,40,43,44,89,96–114] distributes the *Gambierdiscus* genus into five major clades (clade I–V) as seen in Figure 8. Clade II and III exclusively contain the species *G. australes* (Atlantic and Pacific strains) and *G. excentricus* (Atlantic strains), respectively. Clade I encompass all of the *G. carribaeus* (Atlantic and Pacific

strains) and newly discovered *G. carpenteri* (Atlantic and Pacific strains) as well as *G. jejuensis* (Pacific strains). Clade IV and V are more diverse. Of this, *G. belizeanus* (Red Sea, Saudi Arabia; Charco Azul, El Hierro, Spain; St. Barthelemy Island, Caribbean Sea) appears as a distinct branch in Clade V with the closest genetic relationship with *G. honu* (Kermadec Islands, Australia). The yet unclassified *Gambierdiscus* ribotype 1 follows the same lineage as of *G. belizeanus*. Other species in close proximity were *G. balechii* (Celebes Sea, Pacific Ocean; Phuket Islands, Indonesia, North Pacific), *G. lapillus* (Great Barrier Reef, Australia, Pacific Ocean; Cook Islands, Rarotonga, North Atlantic), *G. cheloniae* (Rarotonga, Cook Islands, North Atlantic), *G. scabrous* (Japan, South China Sea, North Pacific), and *G. pacificus* (Balearic Islands, Spain, North Atlantic; Cook Islands, Rarotonga, North Atlantic; Marshall Islands, Micronesia, South Pacific). The *G. toxicus* (Indian Ocean) strains are also in the same clade.

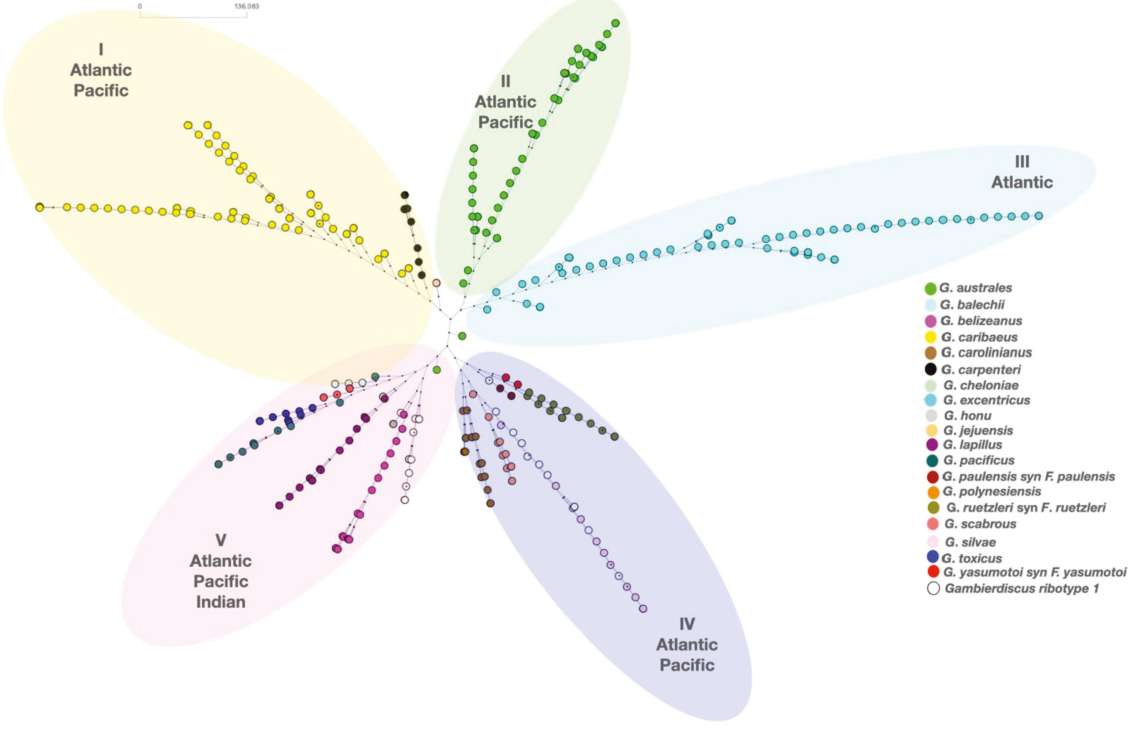

Figure 8. Phylogenetic associations of globally distributed *Gambierdiscus* and *Fukuyoa* species. A split decomposition algorithm was applied on multiple aligned D8-D10 sequences of LSU of available *Gambierdiscus* species (downloaded from NCBI) and aligned through ClustalW2.

Molecular identification of *F. yasumotoi* on the Kuwaiti shore waters and Gulf of Aqaba have not yet been performed. Similarly, *G. australes*, *G. toxicus,* and *G. polynesiensis* from Manora Channel, Indian Ocean region are pending molecular identification. *F. yasumotoi* isolated from the Pacific [11] and Atlantic region fall in the same branch as that of *F. reutzleri* (North Atlantic and North Pacific Ocean) and *F. paulensis* (North Atlantic and South Pacific Oceans). All the *F. yasumotoi* strains discovered so far showed a similarity of ~80% with the unique ribotype A213 [11,97]. Other species in the same clade are that of *G. carolinianus* (Bermuda, North Atlantic; Bahamas, North Atlantic; Cancun, Mexico, North Atlantic; Caribbean Sea, North Atlantic), *G. silvae* (Canary Island, North Atlantic), *G. polynesiensis* (Cook Islands, Rarotonga, North Atlantic; Pacific Ocean), and unclassified *Gambierdiscus* ribotypes (Curlew Cay, Belize, North Atlantic).

More diversity in clade IV and V including the species discovered from Indian Ocean may be due to a smaller number of samples owing to the recent discovery of these species. The presence of unclassified *Fukuyoa* sps. and *Gambierdiscus* ribotypes in these clades is suggestive of unexplored novel species. In 2016, at the 32nd session of the Codex Committee on Fisheries and Fishery Products, the Pacific Nations raised CP as an issue that is increasingly affecting the tropical and subtropical regions of the Pacific Ocean, Indian Ocean and the Caribbean Sea between the latitudes of 35° N and 35° S [8]. The strains found in the Indian Ocean and their adjoining seas lie near the strains commonly found in these high-risk regions. Probably, the interconnection between the water bodies and the ballast water is the major source of ciguatera infiltration in the Indian Ocean waters. Given this, extensive monitoring and risk management program should be developed for the unexplored regions and specifically in the Middle East region.

3.5. Vectors of Ciguatera in Indian Ocean Region

The CP is recognized as a tropical disease but the existence of ciguatoxic fishes is reported globally due to international seafood trade and shipment [115]. According to a recent FAO/WHO report, globally 425 species of fish, especially those inhabiting the coral reefs, have been associated with CP [8]. The most significant toxic fish have been made by barracuda (Sphyraenidae), amberjack (*Seriola*), grouper (Serranidae), snapper (Lutjanidae), po'ou (*Labridae* spp.), jack (*Carangidae* spp.), trevally (*Caranx* spp.), wrasse (*Labridae* spp.), surgeonfish (*Acanthuridae* spp.), moray eel (*Muraenidae* spp.), roi (*Cephalopholis* spp.), parrotfish (*Scaridae* spp.), etc.

The CP cases have mainly been reported in the southwestern region encompassing Comoros, Mayotte, La Reunion, Mauritius, Rodrigues, and Seychelles. The reports from the Northern part of the Indian ocean have been scarce and involve cases in Mangalore and Trivandrum on the southern Indian coast and an outbreak resulting in one fatality from Pakistan, but the fish species involved and their origin could not be confirmed [74,75,116,117]. Few cases of CFP were also reported in Thailand after eating ocean fish particularly sea bass and red snapper [118,119]. One CP record from Egypt exists [120]. There has been no event recorded in the Northern part of the Arabian sea, in countries bordering the Gulf region or the Red Sea. The very first incidence of ciguatera poisoning in the Indian Ocean region was reported in 1993 from Manakara and Madagascar where about 500 persons were infected after consuming ciguatoxic shark. The fatality rate of this outbreak was 20% [121]. In Trivandrum, India, an autochthonous outbreak was reported in 2015 and 2016, due to which nearly 200 workers of a fish factory contracted CFP after eating heads of Red Snappers [75]. In 2013, also severe food poisoning events were witnessed after consuming a bull shark (*Carcharhinus leucas*), resulting in the deaths of 11 people in Madagascar in 2013 [78]. Fish originating from the Indian ocean region were implicated in ciguatera poisoning in other part of the world. The rapid alert system for food and feed (RASFF) created in 1979 by the European Union (EU) successively warned in 2012, 2015, and 2016 about ciguatoxic fishes originating from India and Sri Lanka (RASFF No. 2012-1602, 2015-0088, 2016-0932, 2016-1152, 2016-1155, 2017-1112). In 2016, scientists and regional public health authorities warned the population in Southwest India about the CFP risk caused by the consumption of Red Snappers [122], yet snappers from India were imported by France and distributed to Germany (RASFF No. 2016-0932). The French Poison Control center network reported from 2012 to 2019, 17 events with fish caught from the Indian Ocean. In a recent report from Germany, the rarely occurring CP outbreaks were reported between 2012–2017, the main reason identified as imports of snappers (Lutjanidae) from the Indian Ocean region mainly from countries like India, Indonesia, and Vietnam. The author emphasized that fishes from the Indian Ocean can cause ciguatera, which has been poorly documented [81].

Although incidences of CP have not been reported from the Arabian Gulf yet, however, the fishes such as grouper, snapper, emperors, barracuda, jacks, trevallies, kingfish, and tuna form the part of common catch by local fishermen in Arabian Gulf [123]. The database search in Fish base returned a minimum of 13 (Iraq) to a maximum of 60 (Oman) fishes

associated with CP elsewhere in the world [124] (Figure 9). An increase in ciguatera causative organism could have a major impact on food safety and food security given that those species are highly consumed in the region. The suspicion of a high number of unreported cases is warranted given that ciguatera is difficult to diagnose and not subject to mandatory reporting [125].

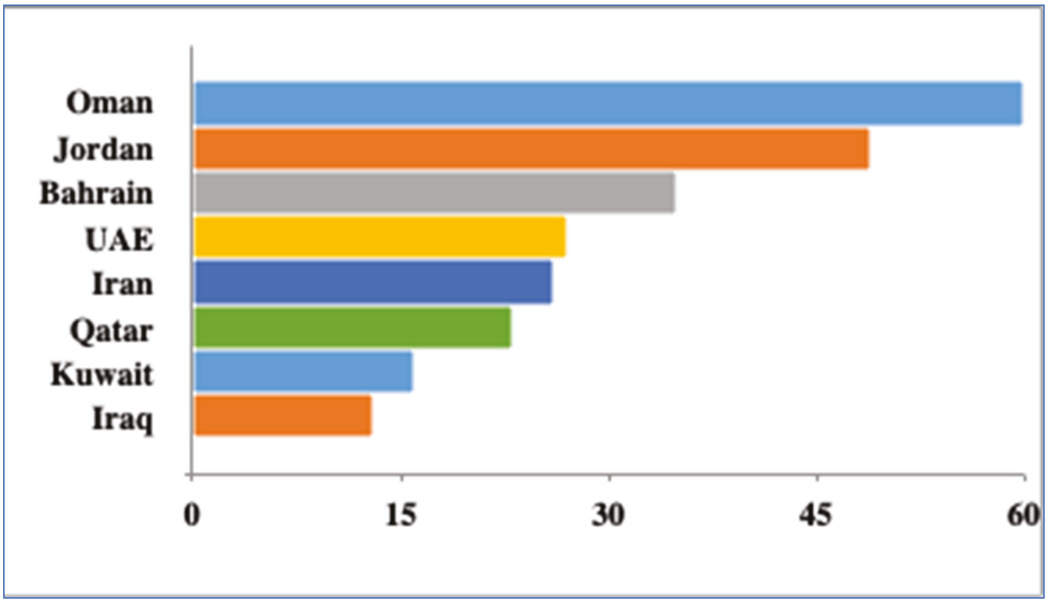

Figure 9. Number of Fishes associated with CP in Persian Gulf Countries as per the records of Fish Base (accessed on 1 June 2021).

The Persian Gulf water is the only source of freshwater through seawater desalination to most Gulf countries and an important source of seafood for the region. Previous reports on incidences of harmful algal blooms on drinking water and food safety and of massive fish kills in the region further creates awareness and interest to investigate the occurrence of ciguatera causative organisms and associated toxins, as well as their health implications in the Gulf countries [58].

3.6. Ciguatera Monitoring in Indian Ocean Region

Risk assessment and monitoring of Ciguatera in the Indian Ocean region is largely lacking with only a couple of previous attempts from la Reunion [47] and Mayotte Island [61]. In 2014, an algal bloom monitoring system was developed for Kuwait's coastal waters. The OC3M (Aqua-MODIS) and OC4E (ENVISAT-MERIS) algorithms most accurately measured chlorophyll-a concentrations in Kuwait bay. Due to the poor temporal resolution and the decommissioning of ENVISAT-MERIS, Aqua-MODIS data was used for continuous observation. Additionally, algorithms such as Generalized Inherent Optical Properties (GIOP), Garver, Siegel, Maritorena Model, OC2, MODIS fluorescence line height, and the MERIS-based NIR-Red algorithms were attempted, which have a lower accuracy when compared to the OC3M algorithm. The OC3M detected the most reported in-situ algal bloom events (19/50) and most accurately measured chlorophyll-a concentration (RMS: 2.42, RMSE: 4.11, Mean Bias: 54.2%). The Aqua-MODIS OC3M was selected as the preferred algorithm to monitor chlorophyll-a concentration and to detect algal blooms in Kuwait bay and surrounding waters [41,45]. Data variables such as sea surface temperature, OC3M, distance to aquaculture, Garver-Siegel-Maritorena (GSM), generalized

inherent optical properties (GIOP), euphotic depth, Secchi disk depth, distance to shore, precipitation, photosynthetically active radiation (PAR), distance to the river, bathymetry, colored dissolved organic matter, wind direction, speed, and precipitation, etc. were also estimated through a multivariate regression model, a hybrid multivariate regression model, an artificial neural network model, and a hybrid artificial neural network model by Uddin and his group [41,45].

A synergistic model was created that combines the GIS-imaging, the different estimates of environmental parameters, and in situ monitoring with traditional toxin analytical methods [41,54]. Sampling epiphytic substrates and analyzing samples using traditional optical microscopy will provide very useful and immediate information and developing ciguatera early warning systems in the region. The molecular methods of qPCR and metabarcoding can be useful but only as a complement not as the basic methodology to estimate *Gambierdiscus* abundance.

4. Conclusions

Ciguatera research in the Indian Ocean region is limited and fragmented. Although, there are reported cases of CP in the region. The most significant toxic fish in the region were barracuda (Sphyraenidae), amberjack (*Seriola*), grouper (Serranidae), snapper (Lutjanidae), po'ou (*Labridae* spp.), jack (*Carangidae* spp.), trevally (*Caranx* spp.), wrasse (*Labridae* spp.), surgeonfish (*Acanthuridae* spp.), moray eel (*Muraenidae* spp.), roi (*Cephalopholis* spp.), parrotfish (*Scaridae* spp.), seabass, shark, and red snapper to name a few. Since the region exports fisheries, some of the fish originating from India and Sri Lanka in 2012, 2015, and 2016 were implicated in ciguatera poisoning in Europe.

A comprehensive survey of algal substrates in the region complemented with high throughput metabarcoding would provide insights into novel and undiscovered contributors of ciguatera. Although less in numbers, the presence of ciguatera causative organisms in the region cannot be ignored and their interaction with substrate and other microbial species is worthy of further investigation. The development of an early warning system for HABs is very much the need of the hour.

Supplementary Materials: The following are available online at https://www.mdpi.com/article/10.3390/toxins13080525/s1, Metadata and percent identity matrix of 345 Gambierdiscus sequences downloaded from NCBI and aligned using Clustal W2.1.

Author Contributions: Conceptualization, S.U., N.H.; methodology, N.H., S.U.; software, N.H., M.F.; resources, S.U., N.H., M.-Y.D.B., M.F.; data curation, S.U., M.F.; writing—original draft preparation, N.H., S.U.; writing—review and editing, N.H., S.U., M.-Y.D.B.; visualization, M.F., M.-Y.D.B. All authors have read and agreed to the published version of the manuscript.

Funding: This research received no external funding.

Institutional Review Board Statement: Not applicable, since this study does not involve humans or animals.

Informed Consent Statement: Not applicable as no human subject was involved.

Data Availability Statement: Data provided as Supplementary file and within manuscript itself.

Acknowledgments: Authors will like to thank the Kuwait Institute for Scientific Research for supporting this study.

Conflicts of Interest: The authors declare no conflict of interest. The Kuwait Institute for Scientific Research has no role in the design of the study; in the collection, analyses, or interpretation of data; in the writing of the manuscript, or in the decision to publish the results.

References

1. Senthilkumaran, S.; Meenakshisundaram, R.; Michaels, A.; Suresh, P.; Thirumalaikolundusubramanian, P. Cardiovascular complications in ciguatera fish poisoning: A wake-up call. *Heart Views Off. J. Gulf Heart Assoc.* **2011**, *12*, 166. [CrossRef] [PubMed]
2. Albinali, H. Ciguatera fish poisoning. *Heart Views* **2011**, *12*, 165. [CrossRef] [PubMed]

3. Accoroni, S.; Romagnoli, T.; Colombo, F.; Pennesi, C.; Di Camillo, C.G.; Marini, M.; Battocchi, C.; Ciminiello, P.; Dell'Aversano, C.; Dello Iacovo, E.; et al. Ostreopsis cf. ovata bloom in the northern Adriatic Sea during summer 2009: Ecology, molecular characterization and toxin profile. *Mar. Pollut. Bull.* **2011**, *62*, 2512–2519. [CrossRef] [PubMed]
4. Chinain, M.; Darius, H.; Ung, A.; Cruchet, P.; Wang, Z.; Ponton, D.; Laurent, D.; Pauillac, S. Growth and toxin production in the ciguatera-causing dinoflagellate Gambierdiscus polynesiensis (Dinophyceae) in culture. *Toxicon* **2010**, *56*, 739–750. [CrossRef]
5. Chinain, M.; Gatti, C.M.i.; Darius, H.T.; Quod, J.P.; Tester, P.A. Ciguatera poisonings: A global review of occurrences and trends. *Harmful Algae* **2021**, *102*, 101873. [CrossRef]
6. Friedman, M.; Fleming, L.; Fernandez, M.; Bienfang, P.; Schrank, K.; Dickey, R.; Bottein, M.; Backer, L.; Ayyar, R.; Weisman, R. Ciguatera fish poisoning: Treatment, prevention and management. *Mar. Drugs* **2008**, *6*, 456–479. [CrossRef]
7. Fleming, L.; Baden, D.; Bean, J.; Weisman, R.; Blythe, D. *Marine Seafood Toxin Diseases: Issues in Epidemiology & Community Outreach*; National Institute of Environmental Health Sciences: Durham, NC, USA, 1998.
8. WHO, F.A. *Report of the Expert Meeting on Ciguatera poisoning: Rome, 19–23 November 2018*; Food Safety and Quality Series; World Health Organization: Rome, Italy, 2020.
9. Parsons, M.; Richlen, M. An overview of ciguatera fish poisoning in the Bahamas. In *The 15th Symposium on the Natural History of the Bahamas*; Gerace Research Centre San Salvador Bahamas; A & A Printing Inc.: Tampa, Florida, USA, 2016.
10. Chinain, M.; Gatti, C.; Roué, M.; Darius, H. Ciguatera-causing dinoflagellates in the genera gambierdiscus and fukuyoa: Distribution, ecophysiology and toxicology. In *Dinoflagellates: Morphology, Life History and Ecological Significance*; Subba Rao, D.V., Ed.; Nova Science Publishers, Inc.: Hauppauge, NY, USA, 2020; pp. 405–457.
11. Litaker, R.W.; Vandersea, M.W.; Faust, M.A.; Kibler, S.R.; Nau, A.W.; Holland, W.C.; Chinain, M.; Holmes, M.J.; Tester, P.A. Global distribution of ciguatera causing dinoflagellates in the genus Gambierdiscus. *Toxicon* **2010**, *56*, 711–730. [CrossRef]
12. Holmes, M. Gambierdiscus yasumotoi sp. nov.(Dinophyceae), a toxic benthic dinoflagellate from southeastern Asia. *J. Phycol.* **1998**, *34*, 661–668. [CrossRef]
13. Kashiwada, S.; Ishikawa, H.; Miyamoto, N.; Ohnishi, Y.; Magara, Y. Fish test for endocrine-disruption and estimation of water quality of Japanese rivers. *Water Res.* **2002**, *36*, 2161–2166. [CrossRef]
14. Nishimura, T.; Sato, S.; Tawong, W.; Sakanari, H.; Uehara, K.; Shah, M.; Suda, S.; Yasumoto, T.; Taira, Y.; Yamaguchi, H. Genetic diversity and distribution of the ciguatera-causing dinoflagellate Gambierdiscus spp.(Dinophyceae) in coastal areas of Japan. *PLoS ONE* **2013**, *8*, e60882. [CrossRef]
15. Rhodes, L.; Gimenez, P.; Smith, K.; Harwood, T. Gambierdiscus cf. yasumotoi (Dinophyceae) isolated from New Zealand's sub-tropical northern coastal waters. *N. Z. J. Mar. Freshw. Res.* **2014**, *48*, 303–310. [CrossRef]
16. Casabianca, S.; Perini, F.; Casabianca, A.; Battocchi, C.; Giussani, V.; Chiantore, M.; Penna, A. Monitoring toxic Ostreopsis cf. ovata in recreational waters using a qPCR based assay. *Mar. Pollut. Bull.* **2014**, *88*, 102–109. [CrossRef]
17. Cohu, S.; Thibaut, T.; Mangialajo, L.; Labat, J.P.; Passafiume, O.; Blanfune, A.; Simon, N.; Cottalorda, J.M.; Lemee, R. Occurrence of the toxic dinoflagellate Ostreopsis cf. ovata in relation with environmental factors in Monaco (NW Mediterranean). *Mar. Pollut. Bull.* **2011**, *62*, 2681–2691. [CrossRef]
18. Parsons, M.L.; Brandt, A.L.; Ellsworth, A.; Leynse, A.K.; Rains, L.K.; Anderson, D.M. Assessing the use of artificial substrates to monitor Gambierdiscus populations in the Florida Keys. *Harmful Algae* **2017**, *68*, 52–66. [CrossRef]
19. Yasumoto, T.; Nakajima, I.; Bagnis, R.; Adachi, R. Finding of a dinoflagellate as a likely culprit of ciguatera. *Bull. Jpn. Soc. Sci. Fish.* **1977**, *43*, 1021–1026. [CrossRef]
20. Yasumoto, T.; Inoue, A.; Bagnis, R. Ecological survey of a toxic dinoflagellate associated with ciguatera. In *Toxic Dinoflagellate Blooms*; Taylor, D.L., Seliger, H.H., Eds.; Elsevier North Holland, Inc.: New York, NY, USA, 1979; pp. 221–224.
21. Yasumoto, T.; Inoue, A.; Ochi, T.; Fujimoto, K.; Oshima, Y.; Fukuyo, Y.; Adachi, R.; Bagnis, R. Environmental studies on a toxic dinoflagellate responsible for ciguatera. *Bull. Jpn. Soc. Sci. Fish.* **1980**, *46*, 1397–1404. [CrossRef]
22. Ballantine, D.L.; Tosteson, T.R.; Bardales, A.T. Population dynamics and toxicity of natural populations of benthic dinoflagellates in southwestern Puerto Rico. *J. Exp. Mar. Biol. Ecol.* **1988**, *119*, 201–212. [CrossRef]
23. Lobel, P.S.; Anderson, D.M.; Durand-Clement, M. Assessment of Ciguatera Dinoflagellate Populations: Sample Variability and Algal Substrate Selection. *Biol. Bull.* **1988**, *175*, 94–101. [CrossRef]
24. Bomber, J.W.; Rubio, M.G.; Norris, D.R. Epiphytism of dinoflagellates associated with the disease ciguatera: Substrate specificity and nutrition. *Phycologia* **1989**, *28*, 360–368. [CrossRef]
25. Litaker, R.; Vandersea, M.; Faust, M.; Kibler, S.; Chinain, M.; Holmes, M.; Holland, W.; Tester, P. Taxonomy of Gambierdiscus including four new species, Gambierdiscus caribaeus, Gambierdiscus carolinianus, Gambierdiscus carpenteri and Gambierdiscus ruetzleri (Gonyaulacales, Dinophyceae). *Phycologia* **2009**, *48*, 344–390. [CrossRef]
26. Rhodes, L.; Smith, K.; Murray, J.; Nishimura, T.; Finch, S. Ciguatera fish poisoning: The risk from an Aotearoa/New Zealand perspective. *Toxins* **2020**, *12*, 50. [CrossRef]
27. Biotoxins, F.M. *FAO Food and Nutrition Paper 80*; Food and Agriculture Organization of the United Nations: Rome, Italy, 2004.
28. De Rota, F. *URDANETA¿ CIENTÍFICO?* Institute de Historia and Cultura Naval: Madrid, Spain, 2009; 38p.
29. Pearn, J. Around the rim: The role of surgeons in discovery and research in the Pacific rim. Part I. Surgeons in the Pacific: Expeditioners and expedition leaders. *Aust. New Zealand J. Surg.* **1994**, *64*, 38–44. [CrossRef]
30. Lee, C. Fish poisoning with particular reference to ciguatera. *J. Trop. Med. Hyg.* **1980**, *83*, 93–97. [PubMed]

31. Silva, S. Contribution al'etude du microplankton de dakar et des regions maritimes voisines. *Bull. Inst. Fr. Afr. Noire. Ser. A. Sci. Nat.* **1956**, *18*, 335–371.
32. Guzman-Perez, S.; Park, D. Ciguatera toxins: Chemistry and detection. *Food Sci. Technol. N.Y. Marcel Dekker* **2000**, 401–418.
33. Tester, P.A.; Litaker, R.W.; Berdalet, E. Climate change and harmful benthic microalgae. *Harmful Algae* **2020**, *91*, 101655. [CrossRef]
34. Landrigan, P.J.; Stegeman, J.J.; Fleming, L.E.; Allemand, D.; Anderson, D.M.; Backer, L.C.; Brucker-Davis, F.; Chevalier, N.; Corra, L.; Czerucka, D.; et al. Human Health and Ocean Pollution. *Ann. Glob. Health* **2020**, *86*, 1–64. [CrossRef]
35. Kibler, S.; Litaker, R.; Holland, W.; Vandersea, M.; Tester, P. Growth of eight Gambierdiscus (Dinophyceae) species: Effects of temperature, salinity and irradiance. *Harmful Algae* **2012**, *19*, 1–14. [CrossRef]
36. Gingold, D.B.; Strickland, M.J.; Hess, J.J. Ciguatera fish poisoning and climate change: Analysis of National Poison Center Data in the United States, 2001–2011. *Environ. Health Perspect.* **2014**, *122*, 580–586. [CrossRef] [PubMed]
37. Kibler, S.R.; Tester, P.A.; Kunkel, K.E.; Moore, S.K.; Litaker, R.W. Effects of ocean warming on growth and distribution of dinoflagellates associated with ciguatera fish poisoning in the Caribbean. *Ecol. Model.* **2015**, *316*, 194–210. [CrossRef]
38. Yong, H.L.; Mustapa, N.I.; Lee, L.K.; Lim, Z.F.; Tan, T.H.; Usup, G.; Gu, H.; Litaker, R.W.; Tester, P.A.; Lim, P.T. Habitat complexity affects benthic harmful dinoflagellate assemblages in the fringing reef of Rawa Island, Malaysia. *Harmful Algae* **2018**, *78*, 56–68. [CrossRef]
39. Hallegraeff, G.M.; Anderson, D.M.; Belin, C.; Bottein, M.-Y.D.; Bresnan, E.; Chinain, M.; Enevoldsen, H.; Iwataki, M.; Karlson, B.; McKenzie, C.H.; et al. Perceived global increase in algal blooms is attributable to intensified monitoring and emerging bloom impacts. *Commun. Earth Environ.* **2021**, *2*, 117. [CrossRef]
40. Rhodes, L.; Smith, K.; Munday, R.; Selwood, A.; McNabb, P.; Holland, P.; Bottein, M. Toxic dinoflagellates (Dinophyceae) from Rarotonga, Cook Islands. *Toxicon* **2010**, *56*, 751–758. [CrossRef]
41. Uddin, S.; Sultan, M.; Behbehani, M.; Al-Rashed, W.; Al-Shamroukh, D.; Al-Khabbaz, A.; Al-Yaegoub, A.; Al-Bahloul, M. *A Remote Sensing-Based Early Warning System for Algal Blooms in Kuwait Bay and Coastal Waters*; Project EM033C, Final Report, KISR12320; Kuwait Institute for Scientific Research, 2014; 145p.
42. Saburova, M.; Polikarpov, I.; Al-Yamani, F. New records of the genus Gambierdiscus in marginal seas of the Indian Ocean. *Mar. Biodivers. Rec.* **2013**, *6*, e91. [CrossRef]
43. Catania, D. The Prevalence of Benthic Dinoflagellates Associated with Ciguatera in the Central Red Sea. M.Sc. Thesis, King Abdullah University of Science and Technology, Thuwal, Saudi Arabia, 2012; 40p.
44. Catania, D.; Richlen, M.; Mak, Y.; Morton, S.; Laban, E.; Xu, Y.; Anderson, D.; Chan, L.; Berumen, M. The prevalence of benthic dinoflagellates associated with ciguatera fish poisoning in the central Red Sea. *Harmful Algae* **2017**, *68*, 206–216. [CrossRef] [PubMed]
45. Manche, C. A Remote Sensing Based Early Warning System for Algal Blooms in Kuwait Bay and Coastal Waters. Master's Thesis, Western Michigan University, Kalamazoo, MI, USA, 2014. Available online: https://scholarworks.wmich.edu/masters_theses/546 (accessed on 1 June 2021).
46. Quod, J.-P.; Turquet, J.; Conejero, S.; Ralijaona, C. Ciguatera risk assessment in the Indian Ocean following the 1998 coral bleaching event. *Coral Reef Degrad. Indian Ocean. Status Rep.* **2000**, 166–168.
47. Bagnis, R. L'ichtyosarcotoxisme de type ciguatera: Phénomène complexe de biologie marine et humaine. *Oceanol. Acta* **1981**, *4*, 375–387.
48. Behbehani, M.; Uddin, S.; Dupont, S.; Sajid, S.; Al-Musalam, L.; Al-Ghadban, A. Response of corals *Acropora pharaonis* and *Porites lutea* to changes in pH and temperature in the Gulf. *Sustainability* **2019**, *11*, 3156. [CrossRef]
49. Reguera, B.; Alonso, R.; Moreira, A.; Méndez, S.; Dechraoui-Bottein, M.-Y. Guide for Designing and Implementing a Plan to Monitor Toxin-Producing Microalgae. In *Intergovermental Oceanographic Commission Manuals and Guides*, 2nd ed.; UNESCO: Paris, France; IAEA: Vienna, Austria, 2016; 66p, Available online: http://hdl.handle.net/11329/304 (accessed on 1 June 2021).
50. Jean Turquet, J.-P.Q.; Ten-Hage, L.; Dahalani, Y.; Wendling, B. Example of a Gambierdiscus toxicus flare-up following the 1998 coral bleaching event in Mayotte Island (Comoros, south-west Indian Ocean). In Proceedings of the Harmful Algal Blooms 2000: Proceedings of the Ninth International Conference on Harmful Algal Blooms, Hobart, Australia, 7–11 February 2000.
51. Uddin, S.; Gevao, B.; Al-Ghadban, A.; Nithyanandan, M.; Al-Shamroukh, D. Acidification in Arabian Gulf–Insights from pH and temperature measurements. *J. Environ. Monit.* **2012**, *14*, 1479–1482. [CrossRef]
52. Al-Musalam, L.; Uddin, S. *Effect of Ocean Acidification on Growth and Abundance of Penaeus Semisulcatus in the Northern Arabian Gulf*; Annual Progress Report No. 1(EM078C); Kuwait Insitute for Scientific Research: Kuwait City, Kuwait, 2018; 27p.
53. Al-Musallam, L.; Uddin, S.; Al-Dakkor, S.; Kumar, V. Effect of ocean acidification and ocean warming on the growth and survival of *Penaeus semisulcatus* Post-Larvae. *J Earth Env. Sci* **2019**, *3*. [CrossRef]
54. Elkadiri, R.; Manche, C.; Sultan, M.; Al-Dousari, A.; Uddin, S.; Chouinard, K.; Abotalib, A.Z. Development of a Coupled Spatiotemporal Algal Bloom Model for Coastal Areas: A Remote Sensing and Data Mining-Based Approach. *IEEE J. Sel. Top. Appl. Earth Obs. Remote Sens.* **2016**, *9*, 5159–5171. [CrossRef]
55. Heil, C.A.; Glibert, P.M.; Al-Sarawi, M.A.; Faraj, M.; Behbehani, M.; Husain, M. First record of a fish-killing Gymnodinium sp. bloom in Kuwait Bay, Arabian Sea: Chronology and potential causes. *Mar. Ecol. Prog. Ser.* **2001**, *214*, 15–23. [CrossRef]
56. Glibert, P.; Landsberg, J.; Evans, J.; Al-Sarawi, M.; Faraj, M.; Al-Jarallah, M.; Haywood, A.; Ibrahem, S.; Klesius, P.; Powell, C. A fish kill of massive proportion in Kuwait Bay, Arabian Gulf, 2001: The roles of bacterial disease, harmful algae, and eutrophication. *Harmful Algae* **2002**, *1*, 215–231. [CrossRef]

57. Walsh, J.; Steidinger, K. Saharan dust and Florida red tides: The cyanophyte connection. *J. Geophys. Res. Ocean.* **2001**, *106*, 11597–11612. [CrossRef]
58. Richlen, M.L.; Morton, S.L.; Jamali, E.A.; Rajan, A.; Anderson, D.M. The catastrophic 2008–2009 red tide in the Arabian gulf region, with observations on the identification and phylogeny of the fish-killing dinoflagellate Cochlodinium polykrikoides. *Harmful Algae* **2010**, *9*, 163–172. [CrossRef]
59. Berland, B.; Grzebyk, D.; Thomassin, B.-A. Benthic dinoflagellates from the coral reef lagoon of Mayotte Island (SW Indian Ocean); identification, toxicity and preliminary ecophysiological study. *Bull.-Soc. Pathol. Exot.* **1992**, *85*, 453. [PubMed]
60. Grzebyk, D.; Berland, B.; Thomassin, B.A.; Bosi, C.; Arnoux, A. Ecology of ciguateric dinoflagellates in the coral reef complex of Mayotte Island (SW Indian Ocean). *J. Exp. Mar. Biol. Ecol.* **1994**, *178*, 51–66. [CrossRef]
61. Thomassin, B.; ME, A.H.; Quod, J.; Maggiorani, J.; Berland, B.; Grzebyk, D.; Coqueugniot, J. Evolution of Gambierdiscus toxicus populations in the coral reef complex of Mayotte Island (SW Indian Ocean) during the 1985–1991 period. *Bull. Soc. Pathol. Exot.* **1992**, *85*, 449–452.
62. Quod, J.; Prunaux, O.; Guignard, A. Les empoisonnements par poissons tropicaux à La Réunion: Synthèse et perspectives. *Rev. Méd. Vét.* **1990**, *141*, 1005–1009.
63. Quod, J.; Bourdeau, P.; Turquet, J.; Guignard, A. La ciguatera dans les DOM-TOM: Aspects épidémiologiques et physiopathologiques. *Rev. Méd. Vét.* **1994**, *170*, 141–146.
64. Quod, J.; Turquet, J. Ciguatera in Reunion Island (SW Indian Ocean): Epidemiology and clinical patterns. *Toxicon* **1996**, *34*, 779–785. [CrossRef]
65. Ten-Hage, L.; Turquet, J.; Quod, J.-P.; Couté, A. An overview of the biodiversity of benthic diniflagellates from La Reunion Island (France, South-west Indian Ocean). In *9th Int Conference on Harmful Algal Blooms (HAB 2000)*; Hobart, Tasmania, 2000.
66. Lugomela, C. Autecology of the Toxic Dinoflagellate *Gambierdiscus toxicus* Adachi et Fukyo (Dinophyceae) in Central Coastal Areas of Tanzania. *West. Indian Ocean J. Mar. Sci.* **2006**, *5*, 213–221. [CrossRef]
67. Gómez, F.; Qiu, D.; Lopes, R.M.; Lin, S. Fukuyoa paulensis gen. et sp. nov., a New Genus for the Globular Species of the Dinoflagellate Gambierdiscus (Dinophyceae). *PLoS ONE* **2015**, *10*, e0119676. [CrossRef]
68. Saburova, M.; Igor, P.; Al-Yamani, F. Gambierdiscus in Kuwait. *Harmful Algae News* **2013**, *47*, 22–23.
69. Munir, S.; Siddiqui, P.; Morton, S.L. The occurrence of the ciguatera fish poisoning producing dinoflagellate genus Gambierdiscus in Pakistan waters. *Algae* **2011**, *26*, 317–325. [CrossRef]
70. Polikarpov, I.; Saburova, M.; Al-Yamani, F. Diversity and distribution of winter phytoplankton in the Arabian Gulf and the Sea of Oman. *Cont. Shelf Res.* **2016**, *119*, 85–99. [CrossRef]
71. Naik, R.K.; Hegde, S.; Anil, A.C. Dinoflagellate community structure from the stratified environment of the Bay of Bengal, with special emphasis on harmful algal bloom species. *Environ. Monit. Assess.* **2011**, *182*, 15–30. [CrossRef]
72. Rajeish, M.; Shekar, M.; Madhushree, H.; Venugopal, M. Presumptive case of ciguatera fish poisoning in Mangalore, India. *Curr. Sci.* **2016**, *111*, 1543–1547. [CrossRef]
73. Rajisha, R.; Kishore, P.; Panda, S.K.; Ravishankar, C.N.; Kumar, K.A. Confirmation of ciguatoxin fish poisoning in red snapper, Lutjanus bohar (Forsskål, 1775) by mouse bioassay. *Fish. Technol.* **2017**, *54*, 287–290.
74. Karunasagar, I.; Turner, A.D.; Maskrey, B.; Robertson, A.; Shivanagouda Hosagoudar, S.; Rai, P.; Adappa, S.; Hiremath, S.; Kogaluru Shivakumaraswamy, S.; Dechraoui Bottein, M.Y.; et al. Report of a major outbreak of ciguatera fish poisoning in Mangalore, India. In *Proceedings of the 18th International Conference on Harmful Algae*; Rome, Italy, 2018; p. 482.
75. Rajisha, R.; Kishore, P.; Panda, S.K.; Harikrisnan, G.; Ajitha, K.C.; Suresh, M.K.; Chowdhury, L.M.; Ravishankar, C.N.; Kumar, K.A. Incidence of ciguatoxin fish poisoning in Trivandrum, India. *Indian J. Fish.* **2017**, *64*, 129–133. [CrossRef]
76. Hamilton, B.; Hurbungs, M.; Jones, A.; Lewis, R.J. Multiple ciguatoxins present in Indian Ocean reef fish. *Toxicon* **2002**, *40*, 1347–1353. [CrossRef]
77. Hamilton, B.; Hurbungs, M.; Vernoux, J.-P.; Jones, A.; Lewis, R.J. Isolation and characterisation of Indian Ocean ciguatoxin. *Toxicon* **2002**, *40*, 685–693. [CrossRef]
78. Diogène, J.; Reverté, L.; Rambla-Alegre, M.; Del Río, V.; De La Iglesia, P.; Campàs, M.; Palacios, O.; Flores, C.; Caixach, J.; Ralijaona, C. Identification of ciguatoxins in a shark involved in a fatal food poisoning in the Indian Ocean. *Sci. Rep.* **2017**, *7*, 1–8. [CrossRef]
79. Roeder, K.; Erler, K.; Kibler, S.; Tester, P.; Van The, H.; Nguyen-Ngoc, L.; Gerdts, G.; Luckas, B. Characteristic profiles of Ciguatera toxins in different strains of Gambierdiscus spp. *Toxicon* **2010**, *56*, 731–738. [CrossRef] [PubMed]
80. Pisapia, F.; Holland, W.C.; Hardison, D.R.; Litaker, R.W.; Fraga, S.; Nishimura, T.; Adachi, M.; Nguyen-Ngoc, L.; Séchet, V.; Amzil, Z.; et al. Toxicity screening of 13 Gambierdiscus strains using neuro-2a and erythrocyte lysis bioassays. *Harmful Algae* **2017**, *63*, 173–183. [CrossRef]
81. Friedemann, M. Ciguatera fish poisoning outbreaks from 2012 to 2017 in Germany caused by snappers from India, Indonesia, and Vietnam. *J. Consum. Prot. Food Saf.* **2019**, *14*, 71–80. [CrossRef]
82. Yogi, K.; Oshiro, N.; Inafuku, Y.; Hirama, M.; Yasumoto, T. Detailed LC-MS/MS Analysis of Ciguatoxins Revealing Distinct Regional and Species Characteristics in Fish and Causative Alga from the Pacific. *Anal. Chem.* **2011**, *83*, 8886–8891. [CrossRef] [PubMed]

83. Clausing, R.; Chinain, M.; Bottein, M. Practical Sampling Guidance for Determination of Ciguatoxin in Fish. In *Guide for Designing and Implementing a Plant to Monitor Toxin-Producing Microalgae*, 2nd ed.; IOC Manuals and Guides, no. 59; Intergovernmental Oceanographic Commission (IOC) of UNESCO: Paris, France; International Atomic Energy Agency (IAEA): Vienna, Austria, 2016; pp. 51–63.
84. Hurbungs, M.D.; Jayabalanm, N.; Chineah, V. Seasonal distribution of potentially toxic benthic dinoflagellates in the lagoon of Trou aux Biches, Mauritius. In Proceedings of the 5th Annual Meeting of Agricultural Scientists, Reduit, Mauritius, 3–4 May 2001; Lalouette, J.A., Bachraz, D.Y., Eds.; The Food and Agricultural Research Council: Reduit, Mauritius, 2002; pp. 211–217.
85. Quod, J.; Turquet, J.; Diogene, G.; Fessard, V. Screening of extracts of dinoflagellates from coral reefs (Reunion Island, SW Indian Ocean), and their biological activities. *Harmful Mar. Algal Bloom.* **1995**, 815–820.
86. Turquet, J. Assemblage of benthic dinofagellates and monitoring of harmful species in Reunion Island, SW Indian Ocean, 1993–1996. *Harmful Algae* **1998**, 44–47.
87. Roué, M.; Smith, K.; Sibat, M.; Viallon, J.; Henry, K.; Ung, A.; Biessy, L.; Hess, P.; Darius, H.; Chinain, M. Assessment of Ciguatera and Other Phycotoxin-Related Risks in Anaho Bay (Nuku Hiva Island, French Polynesia): Molecular, Toxicological, and Chemical Analyses of Passive Samplers. *Toxins* **2020**, *12*, 321. [CrossRef] [PubMed]
88. Smith, K.; Kohli, G.; Murray, S.; Rhodes, L. Assessment of the metabarcoding approach for community analysis of benthic-epiphytic dinoflagellates using mock communities. *N. Z. J. Mar. Freshw. Res.* **2017**, *51*, 555–576. [CrossRef]
89. Rhodes, L.; Smith, K.; Verma, A.; Murray, S.; Harwood, D.; Trnski, T. The dinoflagellate genera Gambierdiscus and Ostreopsis from subtropical Raoul Island and North Meyer Island, Kermadec Islands. *N. Z. J. Mar. Freshw. Res.* **2017**, *51*, 490–504. [CrossRef]
90. Hoppenrath, M.; Kretzschmar, A.; Kaufmann, M.; Murray, S. Morphological and molecular phylogenetic identification and record verification of Gambierdiscus excentricus (Dinophyceae) from Madeira Island (NE Atlantic Ocean). *Mar. Biodivers. Rec.* **2019**, *12*, 1–9. [CrossRef]
91. Rhodes, L.; Smith, K. A checklist of the benthic and epiphytic marine dinoflagellates of New Zealand, including Rangitāhua/Kermadec Islands. *N. Z. J. Mar. Freshw. Res.* **2019**, *53*, 258–277. [CrossRef]
92. Faust, M. Observation of sand-dwelling toxic dinoflagellates (Dinophyceae) from widely differing sites, including two new species. *J. Phycol.* **1995**, *31*, 996–1003. [CrossRef]
93. Adachi, R.; Fukuyo, Y. The thecal structure of a marine toxic dinoflagellate Gambierdiscus toxicus gen. et sp. nov. collected in a ciguatera endemic area. *Bull. Jpn. Soc. Sci. Fish.* **1979**, *45*, 67–71. [CrossRef]
94. Chinain, M.; Faust, M.A.; Pauillac, S. Morphology and molecular analyses of three toxic species of Gambierdiscus (Dinophyceae): G. pacificus sp. nov., G. australes, sp. nov. and G. polynesiensis, sp. nov. *J. Phycol.* **1999**, *35*, 1282–1296. [CrossRef]
95. Xu, Y.; Richlen, M.L.; Morton, S.L.; Mak, Y.L.; Chan, L.L.; Tekiau, A.; Anderson, D.M. Distribution, abundance and diversity of Gambierdiscus spp. from a ciguatera-endemic area in Marakei, Republic of Kiribati. *Harmful Algae* **2014**, *34*, 56–68. [CrossRef]
96. Dai, X.; Mak, Y.; Lu, C.; Mei, H.; Wu, J.; Lee, W.; Chan, L.; Lim, P.; Mustapa, N.; Lim, H. Taxonomic assignment of the benthic toxigenic dinoflagellate Gambierdiscus sp. type 6 as Gambierdiscus balechii (Dinophyceae), including its distribution and ciguatoxicity. *Harmful Algae* **2017**, *67*, 107–118. [CrossRef]
97. Richlen, M.; Morton, S.; Barber, P.; Lobel, P. Phylogeography, morphological variation and taxonomy of the toxic dinoflagellate Gambierdiscus toxicus (Dinophyceae). *Harmful Algae* **2008**, *7*, 614–629. [CrossRef]
98. Fraga, S.; Rodríguez, F.; Caillaud, A.; Diogène, J.; Raho, N.; Zapata, M. Gambierdiscus excentricus sp. nov.(Dinophyceae), a benthic toxic dinoflagellate from the Canary Islands (NE Atlantic Ocean). *Harmful Algae* **2011**, *11*, 10–22. [CrossRef]
99. Fraga, S.; Rodríguez, F. Genus Gambierdiscus in the Canary Islands (NE Atlantic Ocean) with description of Gambierdiscus silvae sp. nov., a new potentially toxic epiphytic benthic dinoflagellate. *Protist* **2014**, *165*, 839–853. [CrossRef] [PubMed]
100. Fraga, S.; Rodríguez, F.; Riobó, P.; Bravo, I. Gambierdiscus balechii sp. nov (Dinophyceae), a new benthic toxic dinoflagellate from the Celebes Sea (SW Pacific Ocean). *Harmful Algae* **2016**, *58*, 93–105. [CrossRef] [PubMed]
101. Nascimento, S.; Melo, G.; Salgueiro, F.; Diniz, B.; Fraga, S. Morphology of Gambierdiscus excentricus (Dinophyceae) with emphasis on sulcal plates. *Phycologia* **2015**, *54*, 628–639. [CrossRef]
102. Rodríguez, F.; Fraga, S.; Ramilo, I.; Rial, P.; Figueroa, R.; Riobó, P.; Bravo, I. Canary Islands (NE Atlantic) as a biodiversity 'hotspot'of Gambierdiscus: Implications for future trends of ciguatera in the area. *Harmful Algae* **2017**, *67*, 131–143. [CrossRef] [PubMed]
103. Leung, P.; Yan, M.; Lam, V.; Yiu, S.; Chen, C.; Murray, J.; Harwood, D.; Rhodes, L.; Lam, P.; Wai, T. Phylogeny, morphology and toxicity of benthic dinoflagellates of the genus Fukuyoa (Goniodomataceae, Dinophyceae) from a subtropical reef ecosystem in the South China Sea. *Harmful Algae* **2018**, *74*, 78–97. [CrossRef]
104. Rhodes, L.; Smith, K.; Verma, A.; Curley, B.; Harwood, D.; Murray, S.; Kohli, G.; Solomona, D.; Rongo, T.; Munday, R. A new species of Gambierdiscus (Dinophyceae) from the south-west Pacific: Gambierdiscus honu sp. nov. *Harmful Algae* **2017**, *65*, 61–70. [CrossRef] [PubMed]
105. Smith, K.; Biessy, L.; Argyle, P.; Trnski, T.; Halafihi, T.; Rhodes, L. Molecular identification of Gambierdiscus and Fukuyoa (Dinophyceae) from environmental samples. *Mar. Drugs* **2017**, *15*, 243. [CrossRef]
106. Tudó, À.; Toldrà, A.; Rey, M.; Todolí, I.; Andree, K.; Fernández-Tejedor, M.; Campàs, M.; Sureda, F.; Diogène, J. Gambierdiscus and Fukuyoa as potential indicators of ciguatera risk in the Balearic Islands. *Harmful Algae* **2020**, *99*, 101913. [CrossRef]
107. Bravo, I.; Rodríguez, F.; Ramilo, I.; Afonso-Carrillo, J. Epibenthic Harmful Marine Dinoflagellates from Fuerteventura (Canary Islands), with Special Reference to the Ciguatoxin-Producing Gambierdiscus. *J. Mar. Sci. Eng.* **2020**, *8*, 909. [CrossRef]

108. Jang, S.H.; Jeong, H.J.; Yoo, Y.D. Gambierdiscus jejuensis sp. nov., an epiphytic dinoflagellate from the waters of Jeju Island, Korea, effect of temperature on the growth, and its global distribution. *Harmful Algae* **2018**, *80*, 149–157. [CrossRef]
109. Nishimura, T.; Sato, S.; Tawong, W.; Sakanari, H.; Yamaguchi, H.; Adachi, M. Morphology of G ambierdiscus scabrosus sp. nov.(G onyaulacales): A new epiphytic toxic dinoflagellate from coastal areas of Japan. *J. Phycol.* **2014**, *50*, 506–514. [CrossRef] [PubMed]
110. Tawong, W.; Nishimura, T.; Sakanari, H.; Sato, S.; Yamaguchi, H.; Adachi, M. Characterization of G ambierdiscus and C oolia (D inophyceae) isolates from T hailand based on morphology and phylogeny. *Phycol. Res.* **2015**, *63*, 125–133. [CrossRef]
111. Larsson, M.; Harwood, T.; Lewis, R.; SWA, H.; Doblin, M. Toxicological characterization of Fukuyoa paulensis (Dinophyceae) from temperate Australia. *Phycol. Res.* **2019**, *67*, 65–71. [CrossRef]
112. Zhang, H.; Wu, Z.; Cen, J.; Li, Y.; Wang, H.; Lu, S. First report of three benthic dinoflagellates, Gambierdiscus pacificus, G. australes and G. caribaeus (Dinophyceae), from Hainan Island, South China Sea. *Phycol. Res.* **2016**, *64*, 259–273. [CrossRef]
113. Kretzschmar, A.; Verma, A.; Harwood, T.; Hoppenrath, M.; Murray, S. Characterization of Gambierdiscus lapillus sp. nov.(Gonyaulacales, Dinophyceae): A new toxic dinoflagellate from the Great Barrier Reef (Australia). *J. Phycol.* **2017**, *53*, 283–297. [CrossRef] [PubMed]
114. Murray, S.; Momigliano, P.; Heimann, K.; Blair, D. Molecular phylogenetics and morphology of Gambierdiscus yasumotoi from tropical eastern Australia. *Harmful Algae* **2014**, *39*, 242–252. [CrossRef]
115. Dickey, R.; Plakas, S. Ciguatera: A public health perspective. *Toxicon* **2010**, *56*, 123–136. [CrossRef]
116. Wasay, M.; Sarangzai, A.; Siddiqi, A.; Nizami, Q. Ciguatera fish poisoning with elevated muscle enzymes and abnormal spinal MRI. *Southeast Asian J. Trop. Med. Public Health* **2008**, *39*, 307.
117. Rajisha, R.; Kishore, P.; Panda, S.; Kumar, K.A. Ciguatoxin-An Emerging Biological Hazard among Reef Fishes of India. *Fish. Tech.* **2018**, *55*, 153–167.
118. Saraya, A.; Sintunawa, C.; Wacharapluesadee, S.; Swangpun, K.; Dumrongchua, S.; Wilde, H.; Hemachudha, T. Marine Fish Toxins in Thailand: Report of 6 Suspected Ciguatera Cases. *Case Rep. Clin. Med.* **2014**, *3*, 7. [CrossRef]
119. Sozzi, G.; Marotta, P.; Aldeghi, D.; Tredici, G.; Calvi, L. Polyneuropathy Secondary to Ciguatoxin Poisoning. *Ital. J. Neurol. Sci.* **1988**, *9*, 491–495. [CrossRef] [PubMed]
120. De Haro, L.; Pommier, P.; Valli, M. Emergence of Imported Ciguatera in Europe: Report of 18 Cases at the Poison Control Centre of Marseille. *J. Toxicol. Clin. Toxicol.* **2003**, *41*, 927–930. [CrossRef]
121. Habermehl, G.G.; Krebs, H.C.; Rasoanaivo, P.; Ramialiharisoa, A. Severe ciguatera poisoning in Madagascar: A case report. *Toxicon* **1994**, *32*, 1539–1542. [CrossRef]
122. Anonymous. *Mangaluru: Khader Warns against Consumption of Red Snapper, Puffer Fish Heads*, in *Daijiworld* Published on 6 October 2016: Mangaluru, India. Available online: https://www.daijiworld.com/news/newsDisplay?newsID=417564 (accessed on 1 June 2021).
123. Jin, D.; Kite-Powell, H.; Hoagland, P.; Solow, A. A bioeconomic analysis of traditional fisheries in the Red Sea. *Mar. Resour. Econ.* **2012**, *27*, 137–148. [CrossRef]
124. Anonymous. *Fishbase*. Available online: https://www.fishbase.de (accessed on 1 June 2021).
125. Mattei, C.; Vetter, I.; Eisenblätter, A.; Krock, B.; Ebbecke, M.; Desel, H.; Zimmermann, K. Ciguatera fish poisoning: A first epidemic in Germany highlights an increasing risk for European countries. *Toxicon* **2014**, *91*, 76–83. [CrossRef] [PubMed]

toxins

MDPI

Review

Digital Technologies and Open Data Sources in Marine Biotoxins' Risk Analysis: The Case of Ciguatera Fish Poisoning

Panagiota Katikou

Ministry of Rural Development and Food, Directorate General of Rural Development, Directorate of Research, Innovation and Education, Hapsa & Karatasou 1, 54626 Thessaloniki, Greece; pkatikou@otenet.gr

Abstract: Currently, digital technologies influence information dissemination in all business sectors, with great emphasis put on exploitation strategies. Public administrations often use information systems and establish open data repositories, primarily supporting their operation but also serving as data providers, facilitating decision-making. As such, risk analysis in the public health sector, including food safety authorities, often relies on digital technologies and open data sources. Global food safety challenges include marine biotoxins (MBs), being contaminants whose mitigation largely depends on risk analysis. Ciguatera Fish Poisoning (CFP), in particular, is a MB-related seafood intoxication attributed to the consumption of fish species that are prone to accumulate ciguatoxins. Historically, CFP occurred endemically in tropical/subtropical areas, but has gradually emerged in temperate regions, including European waters, necessitating official policy adoption to manage the potential risks. Researchers and policy-makers highlight scientific data inadequacy, under-reporting of outbreaks and information source fragmentation as major obstacles in developing CFP mitigation strategies. Although digital technologies and open data sources provide exploitable scientific information for MB risk analysis, their utilization in counteracting CFP-related hazards has not been addressed to date. This work thus attempts to answer the question, "What is the current extent of digital technologies' and open data sources' utilization within risk analysis tasks in the MBs field, particularly on CFP?", by conducting a systematic literature review of the available scientific and grey literature. Results indicate that the use of digital technologies and open data sources in CFP is not negligible. However, certain gaps are identified regarding discrepancies in terminology, source fragmentation and a redundancy and downplay of social media utilization, in turn constituting a future research agenda for this under-researched topic.

Keywords: Ciguatera Fish Poisoning; digital technologies; open data; risk analysis; marine biotoxins

Key Contribution: The manuscript summarizes the utilization extent of digital technologies and open data sources with regard to risk analysis tasks related to Ciguatera Fish Poisoning and discusses future research required to approach this topic more in depth.

Citation: Katikou, P. Digital Technologies and Open Data Sources in Marine Biotoxins' Risk Analysis: The Case of Ciguatera Fish Poisoning. *Toxins* **2021**, *13*, 692. https://doi.org/10.3390/toxins13100692

Received: 20 July 2021
Accepted: 28 September 2021
Published: 30 September 2021

1. Introduction

The rapid acceleration of digital technologies, evidenced more intensely during the past decade, globally permeates every private and public organization, transforming their daily working practices, at the same time reshaping social interactions and citizens' expectations [1,2]. Digital tools, among which the Internet, social media, mobile computing, big data, data analytics, and numerous others, open up a fascinating world of innovation opportunities with a significant impact on multiple aspects of contemporary societies [1–3]. This overwhelming penetration of information and communication technologies (ICTs) in everyday life is altering the information sharing preconditions and can technically support more collaborative cultures of information production and dissemination, thus shifting the focus from technology itself to strategies for its exploitation [4].

Substantial implementation of digital technologies in government/public sector operations, commonly intersecting with the e-Government concept, entails the use of public

information systems and the creation of open data repositories, to serve as tools supporting the fundamental principles of transparency, participation and collaboration [4,5]. Efficient incorporation and interoperability of these tools can improve decision-making, by providing policy-formulators with ample data to address complex problems and to design effective public policies in various governmental disciplines [5,6]. The public health sector, and particularly food safety authorities, should be no exception. Digital technologies and open/big data can be of utmost importance in risk analysis processes, the latter considered necessary to proactively refine and optimize food safety and legislation, rather than maintaining a reactive management approach [7,8].

Emergence of new pathogenic microorganisms and the unintentional presence of chemical contaminants constitute major biological and chemical hazards, respectively, significantly challenging global food safety. Natural toxins, and marine biotoxins (MBs) in particular, comprise a distinct type of food hazard, in the sense that they are chemical toxic substances but are of biological origin [8]. MBs are synthesized by specific marine microorganisms, mainly microalgae (usually termed as phytoplankton) and a few bacterial species. Under certain favorable environmental conditions, toxic or harmful algae may proliferate and aggregate to form dense cell assemblages, commonly known as 'harmful algal blooms' (HABs), accompanied by MBs production able to contaminate seafood, resulting in a serious health threat to consumers. MBs could cause severe human intoxications, such as amnesic, diarrheic, azaspiracid, neurotoxic and paralytic shellfish poisonings and Ciguatera Fish Poisoning (CFP) [9]. MBs are in general heat-stable compounds, resistant to common food processing technologies, whereas no antidote exists to reverse their effects in humans [10]. Illness prevention is thus essential to manage MB-related public health risks, with risk analysis being an irreplaceable tool in the arsenal of public authorities pursuing mitigation of HABs' negative impacts [9,10].

Worldwide, CFP is the most prevalent biotoxin-related seafood poisoning, resulting from the consumption of seafood contaminated by its associated toxins, known as ciguatoxins (CTXs) [11]. Despite the significant under-reporting of cases due to a lack of diagnostic methods, CFP is estimated to annually affect approximately 50,000–500,000 people [12]. Historically, this syndrome is mainly encountered in tropical and subtropical areas. In the recent past, however, a geographical expansion of CFP in more temperate areas has been evidenced. Factors such as climate change, but also some anthropogenic activities, are incriminated for altering the geographical distribution of the causative organisms, which are dinoflagellates of the genera *Gambierdiscus* and *Fukuyoa*, as well as the migration patterns of ciguateric fish [13,14]. Additional factors influencing the occurrence of CFP in non-endemic areas are related to international trade and consumption of imported ciguateric fish species in non-tropical areas and/or travelers returning from CFP endemic areas [11,12]. Current reports of CFP in temperate waters of the Canary Islands (Spain) and the Madeira archipelago (Portugal), accompanied by the documented presence of *Gambierdiscus* and *Fukuyoa* spp. in the Mediterranean Sea, constitute CFP being emerging hazard in European waters, thus necessitating the adoption of official policies to manage the potential risks [12,15]. Nonetheless, the European Food Safety Authority (EFSA) highlighted scientific data inadequacy among the reasons hindering the development of appropriate human health protection strategies against CFP [16], whereas the problems of CFP cases' under-reporting and information sources' fragmentation are emphasized by both researchers and policy-makers [12,16]. Taking into account these shortcomings, in combination with the significant health, socioeconomic and socio-cultural impacts of CFP, as well as its increasing emergence in non-endemic areas, improvements in data collection and availability are evidently required at a global level, to allow for more efficient risk monitoring and mitigation [11,12]. In this context, recognizing some of the technological developments able to generate CFP data and assist their dissemination, as well as compiling a roster of openly accessible information sources for CFP, could facilitate the efforts to tackle the weaknesses identified.

Doubtlessly, developments in digital technologies and open data sources amplified the volume of potentially exploitable scientific information for MBs risk analysis purposes. However, bibliographical references on the advancements achieved with the participation of such means in counteracting CFP-related hazards are scattered, whereas, to date, no substantial summary or research study has cumulatively investigated their utilization. The problem addressed in the present work thus relates to examining digital technologies' and open data sources' utilization in CFP research associated with risk analysis tasks. The research question answered in this review, therefore, is "What is the current extent of digital technologies' and open data sources' utilization within risk analysis tasks in the MBs field, particularly on CFP?"

The absence of targeted review articles and scarcity of structured information on the topic necessitated an in-depth literature investigation, within both peer-reviewed publications and grey literature documents to accomplish this study. For the purposes of this review, grey literature is defined according to the Prague definition, "manifold document types produced on all levels of government, academics, business and industry in print and electronic formats that are protected by intellectual property rights, of sufficient quality to be collected and preserved by libraries and institutional repositories, but not controlled by commercial publishers; i.e., where publishing is not the primary activity of the producing body" [17] (p.11), typically including "conference abstracts, presentations, proceedings; regulatory data; unpublished trial data; government publications; reports (such as white papers, working papers, internal documentation); dissertations/theses; patents; and policies & procedures" [18] (para.2).

The structure of the review is as follows: the next section provides brief background knowledge on the concepts of digital technologies, open data sources and risk analysis, viewed from a public health and food safety perspective, to assist in determining the appropriate keywords for the literature investigation. The subsequent two sections describe the research methodology employed and present the bibliographical analysis results. Finally, the findings are discussed, and relevant future research is suggested.

2. Background

2.1. Digital Technologies

Digital technologies are broadly defined as "combinations of information, computing, communication, and connectivity technologies" [19]. An initial review of recent research mainly focusing on the public health and food safety contexts, but also at wider level, reveals that concepts such as 'technology', 'digital technologies', 'ICT', 'information technologies', 'digital media' and 'digital tools' are used interchangeably to refer to a broad set of digital devices and applications, such as websites, databases, blogs, online platforms, mobile/wearable devices, mobile phones, social media and the Internet [20–24]. Digital technologies/ICTs are also strongly intertwined with the 'digital transformation' and 'digitalization' concepts. Indeed, 'digital transformation' is defined as the use of digital technologies/ICTs to enable changes and improvements for achieving business and/or organizational goals [25] and 'digitalization' as the sociotechnical process of using digital infrastructures [1]. In this context, the terms 'digital transformation' and 'digitalization' may also constitute relevant keywords for investigating digital technologies utilization, as they are linkable to improvements and changes in work processes of organizations responsible for risk analyses. Digital technologies' proliferation enhances the quality and quantity of daily generated data, creating conditions of information abundance, able to significantly facilitate public authorities' decision- and policy-making processes [19,26].

2.2. Open Data Sources

Open data refer to "non-privacy-restricted and non-confidential data produced with public money by public and/or private organizations and made available without any usage or distribution restrictions" [6] (p. 258). Open data, frequently termed also as 'public data', can be enriched with data from other sources, resulting in the emergence of large

datasets, known as 'big data' [7]. The latter present specific needs for processing, curation, linking, visualization and maintenance, as their sizes overpass common software tools' abilities, whereas value is generated by the combination of different datasets [19,26].

Public policy development frequently relies on 'open data' and 'big data' availability, being indispensable tools for public organizations. Ample open data in diverse formats are stored in repositories on national or international organizations' websites and also can be exploited by other public institutions, thus counteracting unnecessary duplication and associated costs [6]. However, food safety data and information are generally scattered across the food, health and agriculture sectors, with limited interoperability. Consequently, public authorities in charge of food safety-related risk analysis tasks ordinarily resort to multiple open access scientific resources, such as research project websites, online databases, open-access journals, dissertations or other published material, to obtain up-to-date technical information. Efficient access to such sources is granted by the growth of digital technologies [27,28]. For the purposes of the present review, the 'open data sources' concept will also extend to 'big data', including those forms of 'open-source' and 'open-access' scientific data and software freely available in the public domain [7]. Consequently, the search for appropriate information based on the keywords selected, will also encompass results of common Internet search engines, besides the literature databases [29].

2.3. Risk Analysis in Food Safety

Risk analysis is a powerful science-based tool for reaching sound, consistent solutions to food safety problems. The Codex Alimentarius Commission defines risk analysis in a food safety context as "a process consisting of three components: risk assessment, risk management, and risk communication" [30] (p. 120). More precisely, risk analysis in food safety is a systematic, disciplined decision-making approach, used to estimate human health and safety risks, to identify and implement appropriate measures for risk control, and to communicate with stakeholders about the risks and measures applied [31]. 'Risk assessment' is the science-based component of risk analysis, comprising hazard identification and characterization, exposure assessment and risk characterization. 'Risk management', on the other hand, involves weighing policy alternatives in consultation with relevant stakeholders, according to the risk assessment outcomes and other factors relevant for consumers' health protection, towards selecting appropriate prevention and control options. Lastly, 'risk communication' entails an "interactive exchange of information and opinions throughout the risk analysis process concerning risk, risk-related factors and risk perceptions, among risk assessors, risk managers, consumers, industry, the academic community and other interested parties, including the explanation of risk assessment findings and the basis of risk management decisions" [30,31].

Food safety risk analyses are carried out by national, regional and international authorities, depending on the nature and localization of the specific risk examined [31]. Scientific knowledge on the food issue identified is considered a prerequisite for successful risk analysis; therefore, aggregation of the largest possible appropriate datasets is essential [28]. Strategies to obtain data on food contaminant issues, particularly MBs, require multidisciplinary approaches combining scientific information from fields such as environmental sciences, biology, chemistry, veterinary science, public administration, epidemiology, public health and toxicology. Data collection can present significant difficulties due to frequent gaps identified in information availability; in this context, the exploitation of digital technologies and open/big data sources may catalyze these efforts [10,28,31].

3. Literature Research Method

The current state of digital technologies and open data utilization in the field of CFP risk analysis was envisaged by a systematic literature review conducted according to previously established principles [29,32]. Three main steps were followed: (i) selecting appropriate keywords and combinations thereof; (ii) choosing source database(s) and running the searches; and (iii) analyzing the results.

The literature review protocol employed is detailed in Table 1. The focus period was set from 2010 to date (mid 2021). The main keywords identified within the background section were divided into five groups, namely, "Digital technologies", "Open data", "Risk analysis", "Biotoxins" and "Ciguatera", according to the concepts comprising the research topic. Each of the keywords from Groups 1–3 was combined with one or more keywords from the remaining two groups to retrieve the articles of interest, utilizing the Boolean operators "AND" and "OR" (on a case basis) to produce more focused results. Searches were performed separately for each combination of keywords and applied to the journals' abstracts, title and keywords, using the Scopus abstract and citation database of peer-reviewed literature. All subject areas were selected, due to the multidisciplinary character of this research.

Table 1. Literature review protocol (Scopus search).

Item	**Description**				
Time Period	**2010 to Date**				
Boolean Operators	**AND/OR**				
Keywords	1: Digital Technology	2: Open Data	3: Risk Analysis	4: Biotoxins	5: CFP
	Digital technolog* [1] Digital tool* Digital media Digital transformation Digitalization Information technolog* ICT(s) Social media	Open data Big data Public data Open source* Data*	Risk analysis Risk management Risk communication Risk*	Biotoxin* Marine toxin* Phycotoxin*	Ciguatera Ciguatoxin*
Language	English				
Availability	Documents available online as full text				
Research Discipline	All subject areas (indicatively: Pharmacology, Toxicology and Pharmaceutics; Agricultural and Biological Sciences; Environmental Science; Medicine; Chemistry; Immunology and Microbiology; Biochemistry, Genetics and Molecular Biology; Engineering; Veterinary; Earth and Planetary Sciences; Chemical Engineering; Health Professions; Multidisciplinary; Computer Science; Arts and Humanities; Social Sciences)				
Exclusion Criteria	Articles unrelated to intended subject (keywords with other semantic way)				
Publication type	All available types (Article, Review, Book, Book chapter, Conference paper, Conference review, Letter, Editorial, Note, Short survey, Business article or Press, Erratum, Data paper)				

[1] An asterisk was used as a wildcard symbol to retrieve all possible variations of the relevant search term.

This strategy yielded only one result when the keywords of the "Digital technologies" or "Open data" groups were combined with keywords of the "Biotoxins" or "Ciguatera" groups. A much higher total number of articles was obtained, as expected, when the "Risk analysis" group keywords were looked-up in combination to those of the "Biotoxins" and "Ciguatera" groups. Searches were merged, and after removing the duplicates, 88 articles of multiple types and subject areas remained (Figure 1). The articles' abstracts were carefully read to assess their relevance and to exclude articles containing the selected keywords in another semantic way, shortening down the list to 28 articles. After full-text examination for the presence of appropriate information, more were excluded as "out of topic", with only 11 studies remaining, a rather expectable outcome considering the narrowness of the field and the specialized nature of the research topic. An additional search in the "Pubmed" database, using the same keyword combinations, yielded five further articles. Thereafter, a thorough Google search was conducted, combining in pairs all the above keywords and some additional terms (e.g., database, smartphone, website, satellite imaging, machine learning), to obtain further material from both the scientific and grey literature, such as

press releases, health and fishery authorities' websites, local media, project documents, codes of practice, etc. Finally, reference lists of all selected documents were reviewed to find other articles of interest, whereas their citations in later publications were also evaluated for inclusion in this review [32].

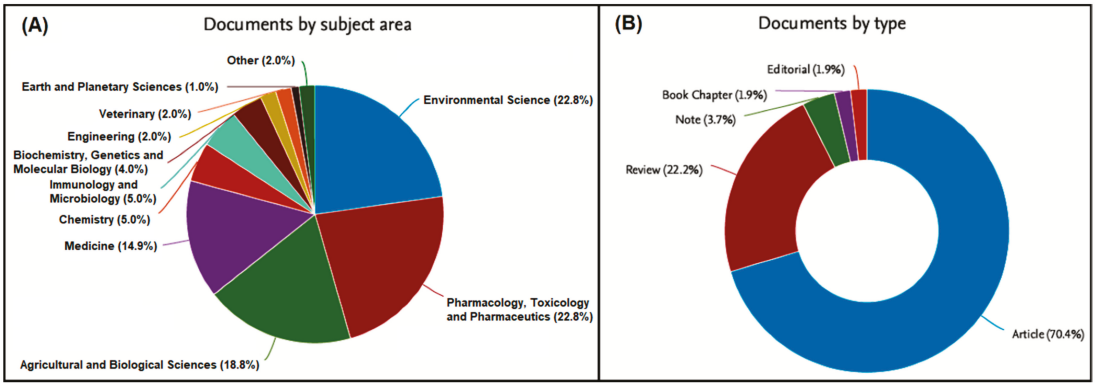

Figure 1. Combined search for the "Risk analysis". "Biotoxins" and "Ciguatera" group keywords by (**A**) subject areas and (**B**) types of retrieved documents. "Other" indicates research disciplines not individually mentioned (refer to Table 1 for details).

Articles considered relevant contained at least one reference to data input for CFP risk analysis or its individual components (assessment, management, communication) obtained by means of digital technologies and/or open data sources, such as websites, databases, software, social media, specific pieces of digital equipment, etc. It is noted that this research only considers digital equipment utilization in terms of mass-market tools, such as computers and portable digital devices (e.g., notebooks, smartphones, tablets); the use of sophisticated analytical equipment, such as liquid chromatographs and mass spectrometers, although largely incorporating digital components (computerized appliances, support PCs and processing software), is beyond the scope of this work. Similarly, statistical analysis software packages, as well as common office-computer software for word processing, spreadsheets creation, etc., are not included in this literature review, as their use is a prerequisite in CFP data generation. In this context, the above strategy resulted in a final list of 38 articles, of which only 19 were openly accessible to the regular public. In the next step, information of relevance was abstracted from the selected documents and contents were analyzed within the identified research concepts' framework, as presented in the following section.

4. Result

Keywords found in the 38 articles meeting the eligibility criteria are summarized in Table 2. Notably, references connected to digital technologies were fewer than those categorized within the open data sources concept, with 16 and 33 articles, respectively, whereas 11 articles contained keywords of both groups. 'Database' was the keyword most encountered, with 28 articles, while the highest incidence keyword combination was 'website'–'database', with five articles. Further details are provided in Supplementary Materials Table S1.

Table 2. Keywords identified in articles meeting the eligibility criteria.

Keyword Group/Keywords Found	Number of Studies *
Digital Technologies	**16**
Software	3
Smartphone	3
Website	7
Digital technologies	1
Social media	2
Open Data	**33**
Database	28
Big data	1
Dataset/data	4
Total Selected	**38**

* Number of studies containing keywords from individual groups cumulatively exceed the total number of selected articles, as some studies contain keywords of both groups.

4.1. Digital Technologies

Only three results [33–35] were finally obtained using the exact keywords indicated within the digital technologies concept, combined with those related to ciguatera and risk analysis (Table 1); on the other hand, the extended search for specific digital tools retrieved 13 studies containing the terms 'software', 'smartphone' and 'website', as semantic content relevant to the production, processing and/or communication of the data necessary for CFP risk analysis (Table 2). Interestingly, only two articles combining 'social media' and 'ciguatera' within the context of risk analysis were retrieved, despite the existence of several CFP-relevant Facebook and Twitter accounts (Supplementary Materials Table S2) and the popularity of social media [34,35]. The first one referred to social media mechanisms for food/waterborne complaints surveillance and indicated specific social media accounts serving this purpose [34]. The second one only mentioned the appearance of anecdotal reports of CFP cases on social media, such as online fishing for a, where fishers comment on their own experiences providing the opportunity for broader data collection and risk communication, but without pointing to any specific social media accounts [35].

The term 'software' in risk analysis-related CFP studies primarily concerned programs used for molecular/phylogenetic identification of ciguateric fish and CTX-producing microalgae and secondly web applications assisting record-keeping and communication regarding the presence of ciguateric fishes in trade operations [36–38]. Accurate identification of high-risk fish species implicated in CFP and the ability to prevent these from reaching the market, according to regional legislative requirements, are critical in CFP risk assessment, management and communication; therefore, software-based tools can facilitate risk analysis processes [39,40].

Generally, instances of 'website' in the selected articles referred to governmental and organizations' internet pages containing diverse scientific information, including CFP case reports, epidemiological and environmental data, outbreaks occurrence and advice to consumers, as well as other public health data, all being major inputs to CFP risk analysis components [11,39,41–45]. Nevertheless, 'website' was also used by some authors to denote any type of online-available content, such as public databases or even open data portals (Table 3) [41,44,45]. Furthermore, although fishing bans related to geographical origin (known toxic locations), high-risk fish species and fish size restrictions constitute fundamental measures in terms of CFP risk management in endemic areas [11], often communicated to relevant stakeholders through designated websites, social media or applications belonging to public agencies, no relevant articles were retrieved in the literature (scientific or grey) referring to these specific risk communication actions.

Widely marketed digital tools, such as smartphones, have recently emerged as attractive analytical platforms, which in the future may revolutionize food safety control by enabling citizens without any expertise to perform screening tests [46]. A number of

smartphone-based devices or assays have already been developed for various contaminants, including marine toxins [28,46,47] and CTXs, in particular [48]. It should be noted that, currently, smartphones cannot be used on their own to detect food contaminants, without the contribution of some auxiliary part or hand-held device, such as portable electrochemical or optical sensors [28,47–49]. However, they possess independent power sources, computing power, flash-light cameras (i.e., optical systems with constant light sources), web access and wireless data communication, being powerful alternative analytical tools, able to radically change food testing. Although smartphone apps for CTXs testing are not yet commercially available, the future ability of consumers to screen fish for CFP is expected to improve food security and increase public awareness, facilitating also risk assessment and management [47,49].

4.2. Open Data Sources

Occurrence of keywords belonging to the 'open data sources' group combined to 'ciguatera' was extensively searched, but no studies were found containing 'open data', 'public data' and 'open source', whereas only one publication (a Master's thesis) included the term 'big data' [50]. On the other hand, searching specifically for 'database', after exclusion of instances related to literature/journal databases, resulted in 28 publications containing at least one reference to a data source compliant to the 'open data sources' concept of the present work [11,14,36,37,40,41,43–45,51–66]. Another relevant term encountered in a semantic fitting the concept was 'dataset' [67,68], a term frequently used interchangeably to 'database' [69], while the more general term 'data' was the only one present in other works containing records of CFP incidents derived from public databases [39,70]. A cumulative presentation of the open data sources found in the selected studies is included in Table 3, along with the geographic coverage and an attempt to categorize source types in compliance with the concept description of the present work, using terms as 'open data portal', 'open documents repository', 'public/open source software', etc. This summary is provided in order to explicitly demonstrate the extent, diversity and fragmentation of the available sources, as well as the type of data available for risk analysis purposes, but also to facilitate future CFP research with regard to data retrieval. To our knowledge, all sources included in Table 3 are openly accessible to the regular public, although in some cases a user registration may be required.

The variety of open data source types found in the studied literature (Table 4) indicates that the data derived thereof are sufficiently exploited in the field of CFP research and risk analysis. Evidently though, the terms 'open data' 'public data', 'open source' and 'big data', commonly used in relevant social sciences' research, are practically unknown to authors involved in this field. On the other hand, 'database' was the most frequently used term to describe such information sources, with some articles specifically referring to databases as 'public' [33,55,56], 'web-based' [34], 'online' [59], 'internet' [60], 'electronic' [61] or 'open access' [65], whereas 'online data' was also used in one case [43].

Table 3. Open data sources used in CFP literature related to risk analysis (sources referred to as 'websites' are included).

Geographic Coverage	Organization/Website ID	Source Type	Nature of CFP-Related Data	Link [(1)]	Reference [(2)]
Worldwide	3i Interactive Key and Taxonomic Database Software	Public database and software	Taxonomic species identification	http://dmitriev.speciesfile.org/ http://dmitriev.speciesfile.org/key.asp?key=Bacillariales&lng=En&i=1&keyN=1	[37] and PW
Worldwide	AlgaeBase	Public database	Algal species information	https://www.algaebase.org/ http://www.algaebase.org/search/genus/detail/?genus_id=45535	[33]
Worldwide	Barcode of Life Data System (BOLD)	Public database and open data portal	DNA-based species identification	http://www.boldsystems.org/	[36,56,57]
Worldwide	Bayesian Evolutionary Analysis Sampling Trees (BEAST)—Tracer	Open-source software	Molecular sequencing/Phylogenetic analysis	http://beast.community/index.html http://beast.community/tracer	[36]
Worldwide	Bayesian Tip-association Significance testing (BaTS)	Open-source software	Phylogenetic analysis	http://evolve.zoo.ox.ac.uk/Evolve/BaTS.html	[36] and PW
Worldwide	FishBase—A Global Information System on Fishes	Public database	Ciguateric fish species	https://www.fishbase.in/search.php (Information by topic/Uses/Ciguatera) https://www.fishbase.in/Topic/List.php?group=27	[36,39,55,57,61]
Worldwide	FishSource—Sustainable Fisheries Partnership	Public database	Status of fisheries, fish stocks, and aquaculture	https://www.fishsource.org/	[70]
Worldwide	GenBank	Public database and open data portal	Genetic sequence (algal species and ciguateric fish)	https://www.ncbi.nlm.nih.gov/genbank/ https://www.ncbi.nlm.nih.gov/genbank/ftp/	[56,57,59] and PW
Worldwide	Global Biodiversity Information Facility (GBIF)—Integrated Publishing Toolkit (IPT)	Open data portal	Biodiversity (reef fish, invertebrates and algae, HABs, water quality)	https://www.gbif.org/ https://www1.usgs.gov/obis-usa/ipt/ https://www.gbif.org/dataset/search	[41,50] and PW
Worldwide	Intergovernmental Oceanographic Commission of UNESCO—Harmful Algal Bloom Programme/IOC-UNESCO Taxonomic Reference List of Harmful Micro Algae	Public database	Harmful microalgal species information	http://www.marinespecies.org/hab/	[66]

Table 3. *Cont.*

Geographic Coverage	Organization/Website ID	Source Type	Nature of CFP-Related Data	Link [(1)]	Reference [(2)]
Worldwide	MrBayes: Bayesian Inference of Phylogeny	Open-source software	Phylogenetic and evolutionary models	http://nbisweden.github.io/MrBayes/index.html http://nbisweden.github.io/MrBayes/download.html	[36] and PW
Worldwide	National Aeronautics and Space Administration (NASA)/Ocean Color & Physical Oceanography Distributed Active Archive Center (PO.DAAC)	Public database, maps and open data portal	Sea surface temperature, salinity, density	https://oceancolor.gsfc.nasa.gov/ https://oceandata.sci.gsfc.nasa.gov/ https://podaac.jpl.nasa.gov/	[45]
Worldwide	National Aeronautics and Space Administration (NASA)/Worldview EOSDIS (Worldview app) and Earth Science Data Systems (ESDS) program (Earthdata)	Public database, maps and open data portal	Satellite-derived sea surface temperature	https://worldview.earthdata.nasa.gov/ https://search.earthdata.nasa.gov/search	[33] and PW
Worldwide	National Oceanic and Atmospheric Administration (NOAA)—Coral Reef Watch (CRW)	Public database and maps	Coral Reef Satellite Monitoring	https://coralreefwatch.noaa.gov/satellite/index.php	[67]
Worldwide	NOAA—Physical Sciences Laboratory (PSL)	Open data portal	Climate, sea surface temperature	https://psl.noaa.gov/data/gridded/ https://psl.noaa.gov/data/gridded/data.noaa.oisst.v2.html	[51,67]
Worldwide	NOAA—National Centers for Environmental Information (NCEI) (formerly National Climate Data Center)	Public database, maps and open data portal	Environmental (atmospheric, coastal, geophysical & oceanic)	https://www.ncei.noaa.gov/ https://www.ncei.noaa.gov/access https://www.ncei.noaa.gov/products/world-ocean-database	[45,68] and PW
Worldwide	Ocean Biodiversity Information System (OBIS)	Open data portal and public maps	Toxic algal species occurrence	https://obis.org/ https://mapper.obis.org/ https://obis.org/manual/access/	[14,60,66]
Worldwide	The Met Office UK—Hadley Centre Sea Ice and Sea Surface Temperature data set (HadISST)	Open data portal	Climate, sea surface temperature	https://www.metoffice.gov.uk/hadobs/hadisst/ https://www.metoffice.gov.uk/hadobs/hadisst/data/download.html	[58] and PW

Table 3. *Cont.*

Geographic Coverage	Organization/Website ID	Source Type	Nature of CFP-Related Data	Link [1]	Reference [2]
Worldwide	UNESCO–IOC–ICES–PICES/Harmful Algae Event Database (HAEDAT)	Public database and maps	HAB events	http://haedat.iode.org/ http://envlit.ifremer.fr/var/envlit/storage/documents/parammaps/haedat/	[11,14,53,60,63,65,66]
Worldwide	World Register of Marine Species (WoRMS)	Public database	Marine organisms' taxonomy (algae and fish)	http://www.marinespecies.org/index.php	[52]
European Union	European Commission—Rapid Alert System for Food and Feed (RASFF)	Public database	Occurrence in foods	https://webgate.ec.europa.eu/rasff-window/portal/?event=SearchForm&cleanSearch=1 https://webgate.ec.europa.eu/rasff-window/portal/?event=SearchByKeyword&NewSearch=1&Keywords=cigua	[53,54] and PW
France, Italy, Monaco	RAMOGE/Regional workshop on monitoring and management strategies for benthic HABs	Open documents repository	Various informational	http://www.ramoge.org/fr/news.aspx?id=112	[11]
Canary Islands	Gobierno de Canarias	Open documents repository	CFP occurrence data, general information on CFP intoxication in Canary islands	https://www.gobiernodecanarias.org/agp/sgt/temas/estadistica/pesca/index.html https://www.gobiernodecanarias.org/agp/sgt/galerias/doc/estadisticas/pesca/Estadistica-ciguatera-2017_2018.ods https://www3.gobiernodecanarias.org/sanidad/scs/contenidoGenerico.jsp?idDocument=bb1799ed-b4c0-11de-ae50-15aa3b9230b7&idCarpeta=3ec36999-d4e1-11e2-8241-7543da9dbb8a	[70]
America	Pan American Health Organization/Institutional Repository for Information sharing	Open documents repository	Various informational	https://iris.paho.org/	[11,44] and PW
America (various territories)	NOAA—Environmental Sensitivity Index (ESI) and Geographical Information System (GIS) Mapping	Public database, maps	Benthic habitat data	https://response.restoration.noaa.gov/esi_download	[68]

Table 3. *Cont.*

Geographic Coverage	Organization/Website ID	Source Type	Nature of CFP-Related Data	Link [(1)]	Reference [(2)]
United States of America	Centers for Disease Control and Prevention (CDC)—National Center for Environmental Health	Open documents repository	General information, Ciguateric fish species, HAB events, statistics	https://www.cdc.gov/nceh/ciguatera/default.htm https://www.cdc.gov/nceh/ciguatera/fish.htm https://www.cdc.gov/habs/index.html	[11,34,43] and PW
United States of America	Centers for Disease Control and Prevention (CDC)—Foodborne Disease Outbreak Surveillance System	Open documents repository	Foodborne outbreaks' occurrence	https://www.cdc.gov/fdoss/annual-reports/index.html	
United States of America	CDC—National Outbreak Reporting System (NORS)	Public database, maps and statistics, open data portal	Outbreaks' occurrence by etiology, year, state, primary mode, setting	https://wwwn.cdc.gov/norsdashboard/ (select Etiology → Ciguatoxin)	
United States of America	CDC—One Health Harmful Algal Bloom System (OHHABS)	Open documents repository	HABs-related human and animal illnesses & environmental data	https://www.cdc.gov/habs/ohhabs.html https://www.cdc.gov/habs/ohhabs_tables_and_figures.html	[62]
United States of America	Food and Drug Administration (FDA)	Open documents repository	Public policies, Ciguateric fish species, Fish and Fishery Products Hazards and Controls Guidance (CFP included)	www.fda.gov/Food/GuidanceRegulation/GuidanceDocumentsRegulatoryInformation/Seafood/ucm2018426.htm https://www.fda.gov/media/80748/download https://www.federalregister.gov/documents/2013/11/22/2013-27913/guidance-for-industry-on-purchasing-reef-fish-species-associated-with-the-hazard-of-ciguatera-fish https://www.fda.gov/media/80637/download	[33,43] and PW
Florida/US	Florida Complaint & Outbreak Reporting System (FL-CORS)	Public database	Online food and waterborne illness complaint forms	https://www.flcors.com/Home.aspx https://www.flcors.com/FWSupport	[34]
Florida/US	Coral Reef Evaluation and Monitoring Project (CREMP)	Open data portal	Coral reefs	https://www1.usgs.gov/obis-usa/ipt/resource?r=coralreefevaluationandmonitoringproject-1999	[50] and PW

Table 3. *Cont.*

Geographic Coverage	Organization/Website ID	Source Type	Nature of CFP-Related Data	Link [1]	Reference [2]
Florida/US	Southeast Environmental Research Center (SERC)—Water Quality Monitoring Network	Open documents repository	Water quality monitoring	http://serc.fiu.edu/wqmnetwork/ http://serc.fiu.edu/wqmnetwork/Report%20Archive/report%20index.htm	[50] and PW
Florida/US	NOAA—National Hurricane Center (NHC)	Public database, open data portal	Tropical cyclones reporting (North Atlantic and eastern North Pacific basins)	https://www.nhc.noaa.gov/ https://www.ncei.noaa.gov/access/search/index	[68]
Hawaii	NOAA—Central Pacific Hurricane Center	Public database, open data portal	Tropical cyclones reporting (central Pacific)	https://www.nhc.noaa.gov/	[68]
Hawaii	State of Hawaii/Department of Health Disease Outbreak Control Division	Open documents repository	Case reports and statistics	https://health.hawaii.gov/docd/resources/reports/summary-of-reported-cases-of-notifiable-diseases/	[11]
Caribbean countries	Caribbean Epidemiology Center (CAREC)	Open documents repository	Epidemiology	https://iris.paho.org/handle/10665.2/2961	[14,44,60]
Caribbean countries	Caribbean Public Health Agency (CARPHA) CARPHA EvIDeNCe portal	Open documents repository	Public health data	https://carpha.org/Portals/0/Documents/CARPHA-State_of_Public_Health_Inaugural_Report_2013.pdf http://carphaevidenceportal.bvsalud.org/	[14,60] and PW
Caribbean countries	Caribbean Coastal Ocean Observing System (CARICOOS)—Part of Integrated Ocean Observing System (IOOS)	Open data portal, public database and maps	Climate, sea surface temperature, algae index, chlorophyll concentration	https://www.caricoos.org/ https://www.caricoos.org/data-download https://www.caricoos.org/ecosystem-and-water-quality https://www.caricoos.org/#!?detail=SelectOceanColor	[41,68] and PW
Caribbean + Gulf of Mexico	University of South Florida-College of Marine Science-Optical Oceanography Laboratory/Satellite-based Sargassum Watch System (SaWS)	Open data portal, public database and maps	*Sargassum* sp. seaweed presence/changes	https://optics.marine.usf.edu/projects/SaWS.html Interoperability with CARICOOS: https://www.caricoos.org/oceans/observation/modis_aqua/ECARIBE/afai	[41]
Mexico	Gobierno de México/Comisión Federal de Protección Contra Riesgos Sanitarios (COFEPRIS)	Open documents repository	HAB events	https://www.gob.mx/cofepris/acciones-y-programas/antecedentes-en-mexico-76707	[60] and PW

Table 3. *Cont.*

Geographic Coverage	Organization/Website ID	Source Type	Nature of CFP-Related Data	Link [1]	Reference [2]
Australia	Australian Government Department of Health (AGDH)/Communicable Diseases Intelligence	Scientific journal (open access)	Epidemiology, surveillance, prevention & control	https://www1.health.gov.au/internet/main/publishing.nsf/Content/cdi-search	[11,35] and PW
Australia	AGDH—OzFoodNet	Open documents repository	Foodborne diseases' surveillance	https://www1.health.gov.au/internet/main/publishing.nsf/Content/cdna-ozfoodnet-reports.htm	
Australia	Safefish—National Ciguatera Fish Poisoning Research Strategy	Open documents repository	Risk mitigation information	https://www.safefish.com.au/-/media/fish-safefish/documents/technical-reports/national-ciguatera-fish-poisoning-research-strategy-final.ashx	[11] and PW
Australia	Sydney Fish Market	Open documents repository	Seafood handling guidelines (incl. CFP)	https://www.sydneyfishmarket.com.au/Seafood-Trading/Quality/Food-Safety https://www.sydneyfishmarket.com.au/Portals/0/adam/Content/41UIctIuJECV0p4vxMVS4Q/ButtonLink/Seafood%20Handling%20Guidelines.pdf	[33]
Cook Islands	Cook Islands Ministry of Health/Te Marae Ora	Open documents repository	Cases statistics 2000–2016 (by year & month)	https://www.health.gov.ck/wp-content/uploads/2018/01/2016-National-Health-Information-Bulletin.pdf	[67] and PW
Fiji	Ministry of Health and Medical Services of Fiji	Open documents repository	Outbreak response guidelines	http://www.health.gov.fj/publications/ http://www.health.gov.fj/wp-content/uploads/2018/08/Fiji-Communicable-Disease-Surveillance-and-Outbreak-Response-Guidelines-2016-1.pdf	[11]
French Polynesia	Institut Louis Malardé—Ciguatera website	Open documents repository, public database and maps	General information, Ciguateric fish species, epidemiology mapping, surveillance and statistics, various documents	http://www.ciguatera.pf/ https://www.ciguatera.pf/images/poissons/CATALOGUE%20BR%20.pdf https://www.ciguatera.pf/index.php/fr/consultation-et-declaration https://www.ciguatera.pf/index.php/fr/la-ciguatera/surveillance-et-statistiques https://www.ciguatera.pf/index.php/fr/la-ciguatera/videos-et-medias	[11,33,39,41,51,61,64]

Table 3. *Cont.*

Geographic Coverage	Organization/Website ID	Source Type	Nature of CFP-Related Data	Link [1]	Reference [2]
New Zealand	New Zealand Ministry of Health/Institute of Environmental Science and Research Ltd. (ESR)/Public Health Surveillance	Open documents repository	Outbreaks occurrence at annual and monthly basis	https://surv.esr.cri.nz/surveillance/annual_outbreak.php https://surv.esr.cri.nz/surveillance/monthly_surveillance.php	[52] and PW
South Pacific	Pacific Community/South Pacific Epidemiological and Health Information Services (SPEHIS)	Open documents repository	Epidemiology, health data (years: 1974–1996)	https://www.spc.int/DigitalLibrary/PHD/Collection/SPEHIS_SIESPS	[11,40,44,55,58]
Hong Kong	The Government of the Hong Kong special administrative region—Center for Food Safety	Open documents repository	General information, code of practice	https://www.cfs.gov.hk/english/multimedia/multimedia_pub/multimedia_pub_fsf_69_02.html https://www.cfs.gov.hk/english/whatsnew/whatsnew_fsf/whatsnew_fsf_poison_fish.html	[11,61]
Hong Kong	The Government of the Hong Kong special administrative region—Department of Health	Open documents repository	Annual case reports, press releases	https://www.search.gov.hk/result?tpl_id=stdsearch&ui_lang=en&ui_charset=utf-8&gp1=dh_home&gp0=dh_home&site=dh_home&web=this&query=ciguatera	[11]

[1] All links accessed on 25 September 2021. [2] "PW" indicates absent/broken/obsolete links in referenced works retrieved/updated by the present work.

Table 4. Types and total instances of open data sources identified in the 33 selected articles (refer to Table 3 for details).

Open Data Source Type	Total Instances
Open documents repository	22
Public database	22
Open data portal	15
Public maps	12
Public/open source software	5
Open access journal	1

Geographical coverage of the open data sources found in the selected articles ranged from worldwide to regional, with the majority of non-global coverage sources focusing their data on areas located in the American and Oceania continents, where CFP is long encountered and considered endemic. In contrast, sources targeting for instance European countries, where CFP issue has recently emerged, are scarcer.

The nature of the CFP-related data contained within the identified open data sources varied widely, including data on taxonomy and identification of marine species (fish and microalgae) [11,14,33,36,37,39,43,52,55–57,59–61,66], epidemiology and outbreaks occurrence [11,14,33–35,39–41,43,44,51–55,58,60,61,63–65,70], HAB events [11,14,43,53,60,62–66], climate and environment (temperature, salinity, water quality monitoring, benthic habitats) [33,41,45,50,51,58,62,67,68], public policies and risk mitigation strategies [11,33,43,61] as well as general information on CFP's public health perspective to aid risk communication to the public [11,34,39,41,43,44,51,61,70].

Plurality in open data sources of a similar nature containing data on different regions is also noteworthy, indicating that efforts to collect data, especially those related to CFP surveillance, epidemiology, case reports and outbreaks incidence, are localized and fragmented, even within the same country, such as the data sources of different states within the USA. Conversely, the evident absence of instances of open data sources in certain CFP-susceptible areas of the world, such as some African and Asian countries of the West Indian Ocean, is also notable. Significant redundancies are also encountered, primarily with regard to climate data, and sea surface temperatures in particular, where at least five different sources are available at a worldwide level. Similarly, at least four different open sources exist for fish or algal species taxonomy and identification. As such, policy-makers and researchers undertaking international risk analysis tasks are commonly obliged to resort to multiple information sources and spend considerable time to obtain the required amount of data. On the other hand, discrepancies may also occur between data from different sources, the resolution of which may create an additional burden in order to obtain acceptable data quality for risk analysis purposes.

5. Discussion

5.1. Research Question Revisited

This review addressed the research question, "What is the current extent of digital technologies' and open data sources' utilization within risk analysis tasks in the MBs field, particularly on CFP?" Although the commonly expected terminology was almost absent in the relevant bibliography, modifying the search keywords revealed the existence of several CFP risk analysis-related publications, 38 in total, where the data input originated from the use of diverse digital tools and sources. As such, it appears that the current utilization of digital technologies and open data sources in the investigated field is generally not negligible, which reasonably answers the research question.

5.2. Further Remarks on the Findings

The aforementioned findings demonstrate that exploitation of digital technologies and open data sources in CFP risk analysis and policy-making studies is not negligible, with their utilization being more widespread in scientific works targeting CFP-endemic

areas [40,42,44,45,50–52,60,61,64,66–68,70]. Nevertheless, the pronounced shortage of published works on CFP referring to common social sciences terminology, such as 'digital technologies', 'digital transformation', 'open data' and 'big data', in conjunction with the use of the general terms, e.g., 'website', 'database' and 'dataset', is indicative of an unfamiliarity with these terms regarding the scientific community creating/uploading information and datasets of interest on the Internet, as well as researchers utilizing the data obtained by these sources. Lack of uniformity between the social and natural sciences' terminology is not a new issue; in fact, it forms part of a long-observed general gap between social and natural sciences, thus highlighting the necessity to adopt more transdisciplinary and collaborative approaches across research fields belonging to environmental/marine sciences, toxicology, public health and social sciences [62,71,72].

The fragmented dispersion of data related to CFP surveillance, epidemiology and outbreaks occurrence encountered in the open data sources identified in this literature review, has also been suggested in previous studies. In fact, under-reporting or inconsistent and fragmented recording of CFP cases has been attributed to the absence of formal epidemiological and surveillance methods and a lack of clinical protocols and experience, whereas the need to establish an international register for CFP intoxication cases and also consolidate monitoring of HAB events at a global level is largely emphasized [11,43,53,55,62,73].

Surprisingly only two instances of 'social media' related to CFP [34,35] were found within both peer-reviewed and grey literature publications, suggesting that these digital tools could be underexploited in CFP risk analysis. In fact, food safety agencies already use social media, such as Facebook and Twitter, for risk communication with the general public on food safety issues [26,74], and CFP is no exception. Several CFP-relevant accounts already exist in social media (Table S2), and CFP risk communications, such as notifications of fishing bans or advice to fishers on species and areas at risk, are not uncommon, especially in CFP-endemic regions. On the other hand, online reporting of CFP cases in social media accounts [34], as well as exchange of CFP-related experiences through posts on fishing forums, are also frequent. Evidently, this does not seem to be adequately reflected in the literature, indicating that the impact of social media in the CFP field may constitute a scientific knowledge gap, requiring further research to elucidate their dynamics as data-providing sources and communication tools in CFP policy-making.

6. Limitations, Conclusions and Future Research

To our knowledge, to date, no previous works have summarized the utilization of both digital technologies and open data sources in tasks relevant to risk analysis, regarding either MBs or specifically CFP. As such, this review constitutes an initial attempt towards documenting the utilization extent of these tools in CFP risk analysis, according to the currently available literature, but certainly cannot be considered an exhaustive summary of their contribution or an assessment of their effectiveness in this HAB management field. We anticipate this first theoretical approach to trigger further investigation, entailing empirical data, in order to provide concrete evidence on the extent of the interactions between developments in the digital world and their practical applications in the diverse natural sciences fields, including MBs and CFP in particular. In this context, a structured research strategy is required to thoroughly evaluate the impact level of such ICT tools in a qualitative and quantitative way. To achieve this objective, the following approaches are suggested:

(1) Interviewing relevant stakeholders, such as experts, public administrators and researchers, involved in the field of CFP risk management, in order to assess (a) their degree of familiarization with the terminology related to digital technologies and open data sources; and (b) their understanding, own use and perception of specific digital technologies and open data sources. This assessment can be accomplished by means of structured questionnaires, containing both multiple-choice/close-ended (with a rating scale) and open-ended questions, as well as free statements, subsequently followed by content and statistical analysis of the responses obtained. Participation could also be

expanded using online forms and/or email-invited questionnaires to more effectively target expert audiences.

(2) Introducing qualitative and quantitative criteria to create a framework for evaluating the impact of the given digital technologies and open data sources and subsequent application of this model to analyze the answers obtained within the context of the available literature. Unequivocally, capitalization of technological progress is the way forward to scientific progress in the modern world. On this basis, accessibility to and exploitation of digital tools and open/big data are synergistically expected to derive innovative applications and services, aiming to facilitate risk analysis and policy-making procedures in the field of food safety, similarly to the progress envisaged in the fisheries sector by the implementation of emerging data technologies, such as blockchain, data mining and artificial intelligence [75]. In the framework of the gaps identified within the present study, research towards consolidation of the currently fragmentary open data sources, such as epidemiological and HAB presence databases, at a worldwide level, can support more robust practices towards mitigation of the CFP problem. On the other hand, embracing the social media potential to strengthen data collection and enhance risk communication channels in the CFP sector is also considered crucial, and definitely requires further scientific research in order to both capture the benefits and tackle the challenges involved. Finally, and most importantly, transdisciplinary collaboration is essential to bridge the evident chasm between humanities and natural sciences, with establishing mutually accepted terminology and definitions for concepts of common interest as a starting point.

Supplementary Materials: The following are available online at https://www.mdpi.com/article/10.3390/toxins13100692/s1, Table S1: Main keywords present in the selected articles related to the present review concepts, Table S2: Indicative social media accounts potentially relevant to CFP risk analysis.

Funding: This research received no external funding.

Institutional Review Board Statement: Not applicable.

Informed Consent Statement: Not applicable.

Conflicts of Interest: The author declares no conflict of interest.

References

1. Nambisan, S.; Lyytinen, K.; Majchrzak, A.; Song, M. Digital innovation management: Reinventing innovation management research in a digital world. *MIS Quart.* **2017**, *41*, 223–238. [CrossRef]
2. Rippa, P.; Secundo, G. Digital academic entrepreneurship: The potential of digital technologies on academic entrepreneurship. *Technol. Forecast. Soc.* **2019**, *146*, 900–911. [CrossRef]
3. Nambisan, S. Digital Entrepreneurship: Toward a Digital Technology Perspective of Entrepreneurship. *Entrep. Theory Pract.* **2017**, *41*, 1029–1055. [CrossRef]
4. Hansson, K.; Belkacem, K.; Ekenberg, L. Open government and democracy: A research review. *Soc. Sci. Comput. Rev.* **2015**, *33*, 540–555. [CrossRef]
5. Sundgren, B. What is a Public Information System? *Int. J. Public Inf. Syst.* **2005**, *1*, 81–99.
6. Janssen, M.; Charalabidis, Y.; Zuiderwijk, A. Benefits, adoption barriers and myths of open data and open government. *Inform. Syst. Manag.* **2012**, *29*, 258–268. [CrossRef]
7. Laessig, M.; Jacob, B.; AbouZahr, C. Opening Data for Global Health. In *The Palgrave Handbook of Global Health Data Methods for Policy and Practice*; Macfarlane, S., AbouZahr, C., Eds.; Palgrave Macmillan: London, UK, 2019; pp. 451–468. [CrossRef]
8. King, T.; Cole, M.; Farber, J.M.; Eisenbrand, G.; Zabaras, D.; Fox, E.M.; Hill, J.P. Food safety for food security: Relationship between global megatrends and developments in food safety. *Trends Food Sci. Tech.* **2017**, *68*, 160–175. [CrossRef]
9. Morabito, S.; Silvestro, S.; Faggio, C. How the marine biotoxins affect human health. *Nat. Prod. Res.* **2017**, *32*, 621–631. [CrossRef]
10. Lawrence, J.; Loreal, H.; Toyofuku, H.; Hess, P.; Karunasagar, I.; Ababouch, L. *Assessment and Management of Biotoxin Risks in Bivalve Molluscs. FAO Fisheries and Aquaculture Technical Paper No. 551*; Food and Agriculture Organization of The United Nations: Rome, Italy, 2011; p. 337. Available online: http://www.fao.org/3/i2356e/i2356e.pdf (accessed on 25 September 2021).
11. Chinain, M.; Gatti, C.M.I.; Darius, H.T.; Quod, J.P.; Tester, P.A. Ciguatera poisonings: A global review of occurrences and trends. *Harmful Algae* **2021**, *102*, 101873. [CrossRef]
12. Bravo, J.; Suárez, F.C.; Ramírez, A.S.; Acosta, F. Ciguatera, an Emerging Human Poisoning in Europe. *J. Aquac. Mar. Biol.* **2015**, *3*, 00053. [CrossRef]

13. Tudó, À.; Gaiani, G.; Rey Varela, M.; Tsumuraya, T.; Andree, K.B.; Fernández-Tejedor, M.; Campàs, M.; Diogène, J. Further Advance of *Gambierdiscus* Species in the Canary Islands, with the First Report of *Gambierdiscus belizeanus*. *Toxins* **2020**, *12*, 692. [CrossRef]
14. Zingone, A.; Escalera, L.; Aligizaki, K.; Fernández-Tejedor, M.; Ismael, A.; Montresor, M.; Mozetič, P.; Taş, S.; Totti, C. Toxic marine microalgae and noxious blooms in the Mediterranean Sea: A contribution to the global HAB status report. *Harmful Algae* **2021**, *102*, 101843. [CrossRef]
15. Estevez, P.; Sibat, M.; Leão-Martins, J.M.; Tudó, A.; Rambla-Alegre, M.; Aligizaki, K.; Diogène, J.; Gago-Martinez, A.; Hess, P. Use of Mass Spectrometry to determine the diversity of toxins produced by *Gambierdiscus* and *Fukuyoa* species from Balearic Islands and Crete (Mediterranean Sea) and the Canary Islands (Northeast Atlantic). *Toxins* **2020**, *12*, 305. [CrossRef]
16. EFSA Panel on Contaminants in the Food Chain. Scientific Opinion on marine biotoxins in shellfish–Emerging toxins: Ciguatoxin group. *EFSA J.* **2010**, *8*, 1627. [CrossRef]
17. Schöpfel, J. Towards a Prague Definition of Grey Literature. In Proceedings of the Twelfth International Conference on Grey Literature: Transparency in Grey Literature. Grey Tech Approaches to High Tech Issues, Prague, Czech Republic, 6–7 December 2010; pp. 11–26. Available online: https://archivesic.ccsd.cnrs.fr/sic_00581570 (accessed on 25 September 2021).
18. Duke University Medical Center Library and Archives. Systematic Reviews: The Process: Grey Literature. Last Updated: 28 July 2021. Available online: https://guides.mclibrary.duke.edu/sysreview/greylit (accessed on 25 September 2021).
19. Bharadwaj, A.; El Sawy, O.A.; Pavlou, P.A.; Venkatraman, N. Digital business strategy: Toward a next generation of insights. *MIS Quart.* **2013**, *37*, 471–482. [CrossRef]
20. McMeekin, T.A.; Baranyi, J.; Bowman, J.; Dalgaard, P.; Kirk, M.; Ross, T.; Schmid, S.; Zwietering, M.H. Information systems in food safety management. *Int. J. Food Microbiol.* **2006**, *112*, 181–194. [CrossRef]
21. Safi, S.; Thiessen, T.; Schmailzl, K.J. Acceptance and Resistance of New Digital Technologies in Medicine: Qualitative Study. *JMIR Res. Protoc.* **2018**, *7*, e11072. [CrossRef] [PubMed]
22. Šmahel, D.; Macháčková, H.; Šmahelová, M.; Čevelíček, M.; Almenara, C.A.; Holubčíková, J. Digital Technology and Health: A Theoretical Framework. In *Digital Technology, Eating Behaviors, and Eating Disorders*; Springer International Publishing AG: Cham, Switzerland, 2018; pp. 21–43. [CrossRef]
23. Demartini, M.; Pinna, C.; Tonelli, F.; Terzi, S.; Sansone, C.; Testa, C. Food industry digitalization: From challenges and trends to opportunities and solutions. *IFAC-PapersOnLine* **2018**, *51*, 1371–1378. [CrossRef]
24. Dong, C.; Mertala, P. It is a tool, but not a "must": Early childhood preservice teachers' perceptions of ICT and its affordances. *Early Years* **2019**, 1–16. [CrossRef]
25. Reis, J.; Amorim, M.; Melão, N.; Matos, P. Digital Transformation: A Literature Review and Guidelines for Future Research. In *Trends and Advances in Information Systems and Technologies*; Rocha, Á., Adeli, H., Reis, L.P., Costanzo, S., Eds.; WorldCIST'18 2018 Advances in Intelligent Systems and Computing; Springer: Cham, Switzerland, 2018; Volume 745, pp. 411–421. [CrossRef]
26. Janssen, M.; Wimmer, M.A. Introduction to policy-making in the digital age. In *Policy Practice and Digital Science*; Janssen, M., Wimmer, M.A., Deljoo, A., Eds.; Springer: Cham, Switzerland, 2015; pp. 1–14. [CrossRef]
27. Gilsenan, M.B.; Abbinante, F.; O'Dea, E.; Canals, A.; Tritscher, A. Special issue: Open risk assessment: Data. *EFSA J.* **2016**, *14*, s0509. [CrossRef]
28. Marvin, H.J.P.; Janssen, E.M.; Bouzembrak, Y.; Hendriksen, P.J.M.; Staats, M. Big data in food safety: An overview. *Crit. Rev. Food Sci. Nutr.* **2016**, *57*, 2286–2295. [CrossRef]
29. Creswell, J.W. Chapter 3: Reviewing the Literature. In *Educational Research: Planning, Conducting, and Evaluating Quantitative and Qualitative Research*, 4th ed.; Creswell, J.W., Ed.; Pearson: Boston, MA, USA, 2012; pp. 79–103.
30. FAO/WHO. Working principles for risk analysis for application in the framework of the Codex Alimentarius. In *Codex Alimentarius Commission. Procedural Manual*, 24th ed.; Food and Agriculture Organization of the United Nations (FAO)/World Health Organization (WHO): Rome, Italy, 2015; pp. 113–121. Available online: http://www.fao.org/3/a-i5079e.pdf (accessed on 25 September 2021).
31. FAO/WHO. *Food Safety Risk Analysis. A Guide for National Food Safety Authorities. FAO Food and Nutrition Papers 87*; FAO/WHO: Rome, Italy, 2006; p. 119. Available online: https://apps.who.int/iris/bitstream/handle/10665/43718/9789251056042_eng.pdf (accessed on 25 September 2021).
32. Webster, J.; Watson, R.T. Analyzing the past to prepare for the future: Writing a literature review. *MIS Quart.* **2002**, *26*, 13–23. Available online: https://www.jstor.org/stable/4132319 (accessed on 25 September 2021).
33. Loeffler, C.R.; Tartaglione, L.; Friedemann, M.; Spielmeyer, A.; Kappenstein, O.; Bodi, D. Ciguatera Mini Review: 21st Century Environmental Challenges and the Interdisciplinary Research Efforts Rising to Meet Them. *Int. J. Environ. Res. Public Health* **2021**, *18*, 3027. [CrossRef]
34. Li, X.; Sapp, A.C.; Singh, N.; Matthias, L.; Bailey, C.; DeMent, J.; Havelaar, A.H. Detecting Foodborne Disease Outbreaks in Florida through Consumer Complaints. *J. Food Prot.* **2020**, *83*, 1877–1888. [CrossRef]
35. Beatty, P.; Boulter, M.; Carter, S.; Chinain, M.; Doblin, M.; Farrell, H.; Gatti, C.; Hallegraeff, G.; Harwood, T.; Sandberg, S.; et al. *National Ciguatera Research Strategy: Reducing the Incidence of Ciguatera in Australia through Improved Risk Management*; Seger, A., Dowsett, N., Turnbull, A., Eds.; South Australian Research and Development Institute: Adelaide, Australia, 2019; pp. 1–32. Available online: https://www.safefish.com.au/-/media/fish-safefish/documents/technical-reports/national-ciguatera-fish-poisoning-research-strategy-final.ashx (accessed on 25 September 2021).

36. Schoelinck, C.; Hinsinger, D.D.; Dettaï, A.; Cruaud, C.; Justine, J.-L. A Phylogenetic Re-Analysis of Groupers with Applications for Ciguatera Fish Poisoning. *PLoS ONE* **2014**, *9*, e98198. [CrossRef]
37. Mustapa, N.I.; Teng, S.T.; Tan, T.H.; Lim, H.C.; Lim, P.T.; Leaw, C.P. Character evolution of the benthic thecate dinoflagellate, *Gambierdiscus* (Dinophyceae), with an introduction of the interactive key to species. *Malays. J. Sci.* **2015**, *34*, 33–42. [CrossRef]
38. Cabrera-Suárez, F.; Bilbao-Sieyro, A.; Perez-González, Y.; Castro-Rodríguez, R.; Torres-López, C.; Sánchez-Herrera, R.; Pavón-Salas, N. A web application as a contribution to the risk analysis of the Ciguatera in the Canary Islands. In Proceedings of the Conference Abstract: XX Iberian Symposium on Marine Biology Studies (SIEBM XX), Braga, Portugal, 9–12 September 2019; Available online: https://www.frontiersin.org/Community/AbstractDetails.aspx?ABS_DOI=10.3389/conf.fmars.2019.08.00157&eid=6597&sname=XX_Iberian_Symposium_on_Marine_Biology_Studies_(SIEBM_XX)_ (accessed on 25 September 2021).
39. Clausing, R.J.; Chinain, M.; Dechraoui-Bottein, M.Y. Practical sampling guidance for determination of ciguatoxin. In *Guide for Designing and Implementing a Plan to Monitor Toxin-Producing Microalgae*; Reguera, B., Alonso, R., Moreira, A., Méndez, S., Dechraoui-Bottein, M.Y., Eds.; Manuals and Guides 59; IOC-UNESCO: Paris, France, 2016; pp. 51–63.
40. Clua, E.; Brena, P.F.; Lecasble, C.; Ghnassia, R.; Chauvet, C. Prevalence and proposal for cost-effective management of the ciguatera risk in the Noumea fish market, New Caledonia (South Pacific). *Toxicon* **2011**, *58*, 591–601. [CrossRef]
41. Anderson, C.R.; Berdalet, E.; Kudela, R.M.; Cusack, C.K.; Silke, J.; O'Rourke, E.; Dugan, D.; McCammon, M.; Newton, J.A.; Moore, S.K.; et al. Scaling Up from Regional Case Studies to a Global Harmful Algal Bloom Observing System. *Front. Mar. Sci.* **2019**, *6*, 250. [CrossRef]
42. Chan, T.Y.K. Ciguatera Fish Poisoning in East Asia and Southeast Asia. *Mar. Drugs* **2015**, *13*, 3466–3478. [CrossRef] [PubMed]
43. Friedman, M.A.; Fernandez, M.; Backer, L.C.; Dickey, R.W.; Bernstein, J.; Schrank, K.; Kibler, S.; Stephan, W.; Gribble, M.O.; Bienfang, P.; et al. An Updated Review of Ciguatera Fish Poisoning: Clinical, Epidemiological, Environmental, and Public Health Management. *Mar. Drugs* **2017**, *15*, 72. [CrossRef]
44. Tester, P.A.; Feldman, R.L.; Nau, A.W.; Kibler, S.R.; Litaker, R.W. Ciguatera fish poisoning and sea surface temperatures in the Caribbean Sea and the West Indies. *Toxicon* **2010**, *56*, 698–710. [CrossRef] [PubMed]
45. Kibler, S.R.; Davenport, E.D.; Tester, P.A.; Hardison, D.R.; Holland, W.C.; Litaker, R.W. *Gambierdiscus* and *Fukuyoa* species in the greater Caribbean: Regional growth projections for ciguatera-associated dinoflagellates. *Ecol. Model.* **2017**, *360*, 204–218. [CrossRef]
46. Nelis, J.L.D.; Tsagkaris, A.S.; Dillon, M.J.; Hajslova, J.; Elliott, C.T. Smartphone-based optical assays in the food safety field. *TrAC Trends Anal. Chem.* **2020**, *129*, 115934. [CrossRef]
47. Tsagkaris, A.S.; Nelis, J.L.D.; Ross, G.M.S.; Jafari, S.; Guercetti, J.; Kopper, K.; Zhao, Y.; Rafferty, K.; Salvador, J.P.; Migliorelli, D.; et al. Critical assessment of recent trends related to screening and confirmatory analytical methods for selected food contaminants and allergens. *TrAC Trends Anal. Chem.* **2019**, *121*, 115688. [CrossRef]
48. Leonardo, S.; Tsumuraya, T.; Oshiro, N.; Hirama, M.; Diogène, J.; Campàs, M. Smartphone-based electrochemical immunosensor for ciguatoxins detection. In Proceedings of the 1st International Electronic Conference on Toxins, online, 16–31 January 2021. [CrossRef]
49. Bano, K.; Khan, W.S.; Cao, C.; Khan, R.F.; Webster, T.J. Biosensors for Detection of Marine Toxins. In *Nanobiosensors: From Design to Applications*; Chapter 14; Wu, A., Khan, W.S., Eds.; Wiley-VCH Verlag GmbH & Co. KGaA: Weinheim, Germany, 2020; pp. 329–356. [CrossRef]
50. Hian, M.E. Ciguatera in Florida Keys patch reefs: Biogeographic indicators of *Gambierdiscus* Density and temporal abundance (CFP: Big data). Master's Thesis, Faculty of the College of Arts and Sciences, Florida Gulf Coast University, Fort Myers, FL, USA, 2018. Available online: https://fgcu.digital.flvc.org/islandora/object/fgcu%3A31535 (accessed on 25 September 2021).
51. Chinain, M.; Gatti, C.M.I.; Ung, A.; Cruchet, P.; Revel, T.; Viallon, J.; Sibat, M.; Varney, P.; Laurent, V.; Hess, P.; et al. Evidence for the Range Expansion of Ciguatera in French Polynesia: A Revisit of the 2009 Mass-Poisoning Outbreak in Rapa Island (Australes Archipelago). *Toxins* **2020**, *12*, 759. [CrossRef]
52. Cressey, P.; Bolton, A.; Pantos, O.; Nicolas, J. Risk Profile: Ciguatoxins in seafood. New Zealand Food Safety Technical Paper No: 2019/06, prepared for New Zealand Food Safety. Ministry for Primary Industries, New Zealand Government. 2019. Available online: https://www.mpi.govt.nz/dmsdocument/37859/direct (accessed on 25 September 2021).
53. FAO/WHO. Report of the Expert Meeting on Ciguatera Poisoning. Rome, 19–23 November 2018. In *Food Safety and Quality No. 9*; FAO/WHO: Rome, Italy, 2020. [CrossRef]
54. Friedemann, M. Ciguatera fish poisoning outbreaks from 2012 to 2017 in Germany caused by snappers from India, Indonesia, and Vietnam. *J. Consum. Prot. Food Saf.* **2019**, *14*, 71–80. [CrossRef]
55. Goater, S.; Derne, B.; Weinstein, P. Critical Issues in the Development of Health Information Systems in Supporting Environmental Health: A Case Study of Ciguatera. *Environ. Health Persp.* **2011**, *119*, 585–590. [CrossRef]
56. Kappel, K.; Schröder, U. Difficulties in DNA barcoding-based authentication of snapper products due to ambiguous nucleotide sequences in public databases. *Food Control* **2020**, *118*, 107348. [CrossRef]
57. Kusche, H.; Hanel, R. Consumers of mislabeled tropical fish exhibit increased risks of ciguatera intoxication: A report on substitution patterns in fish imported at Frankfurt Airport, Germany. *Food Control* **2021**, *12*, 107647. [CrossRef]
58. Llewellyn, L.E. Revisiting the association between sea surface temperature and the epidemiology of fish poisoning in the South Pacific: Reassessing the link between ciguatera and climate change. *Toxicon* **2010**, *56*, 691–697. [CrossRef]

59. Parsons, M.L.; Aligizaki, K.; Dechraoui Bottein, M.-Y.; Fraga, S.; Morton, S.L.; Penna, A.; Rhodes, L. *Gambierdiscus* and *Ostreopsis*: Reassessment of the state of knowledge of their taxonomy, geography, ecophysiology, and toxicology. *Harmful Algae* **2012**, *14*, 107–129. [CrossRef]
60. Sunesen, I.; Méndez, S.M.; Mancera-Pineda, J.E.; Dechraoui-Bottein, M.-Y.; Enevoldsen, H. The Latin America and Caribbean HAB status report based on OBIS and HAEDAT maps and databases. *Harmful Algae* **2021**, *102*, 101920. [CrossRef] [PubMed]
61. Yang, Z.; Luo, Q.; Liang, Y.; Mazumder, A. Processes and pathways of ciguatoxin in aquatic food webs and fish poisoning of seafood consumers. *Environ. Rev.* **2016**, *24*, 144–150. [CrossRef]
62. Young, N.; Sharpe, R.A.; Barciela, R.; Nichols, G.; Davidson, K.; Berdalet, E.; Fleming, L.E. Marine harmful algal blooms and human health: A systematic scoping review. *Harmful Algae* **2020**, *98*, 101901. [CrossRef] [PubMed]
63. Anderson, D.M.; Fensin, E.; Gobler, C.J.; Hoeglund, A.E.; Hubbard, K.A.; Kulis, D.M.; Landsberg, J.H.; Lefebvre, K.A.; Provoost, P.; Richlen, M.L.; et al. Marine harmful algal blooms (HABs) in the United States: History, current status and future trends. *Harmful Algae* **2021**, *102*, 101975. [CrossRef]
64. Boucaud-Maitre, D.; Vernoux, J.P.; Pelczar, S.; Daudens-Vaysse, E.; Aubert, L.; Boa, S.; Ferracci, S.; Garnier, R. Incidence and clinical characteristics of ciguatera fish poisoning in Guadeloupe (French West Indies) between 2013 and 2016: A retrospective cases-series. *Sci. Rep.* **2018**, *8*, 3095. [CrossRef]
65. Bresnan, E.; Arévalo, F.; Belin, C.; Branco, M.A.C.; Cembella, A.D.; Clarke, D.; Correa, J.; Davidson, K.; Dhanji-Rapkova, M.; Lozano, R.F.; et al. Diversity and regional distribution of harmful algal events along the Atlantic margin of Europe. *Harmful Algae* **2021**, *102*, 101976. [CrossRef]
66. Hallegraeff, G.M.; Schweibold, L.; Jaffrezic, E.; Rhodes, L.; MacKenzie, L.; Hay, B.; Farrell, H. Overview of Australian and New Zealand harmful algal species occurrences and their societal impacts in the period 1985 to 2018, including a compilation of historic records. *Harmful Algae* **2021**, *102*, 101848. [CrossRef]
67. Zheng, L.; Gatti, C.M.i.; Garrido Gamarro, E.; Suzuki, A.; Teah, H.Y. Modeling the time-lag effect of sea surface temperatures on ciguatera poisoning in the South Pacific: Implications for surveillance and response. *Toxicon* **2020**, *182*, 21–29. [CrossRef]
68. Liefer, J.D.; Richlen, M.L.; Smith, T.B.; DeBose, J.L.; Xu, Y.; Anderson, D.M.; Robertson, A. Asynchrony of *Gambierdiscus* spp. Abundance and Toxicity in the U.S. Virgin Islands: Implications for Monitoring and Management of Ciguatera. *Toxins* **2021**, *13*, 413. [CrossRef]
69. Economic Commission for Europe of the United Nations (UNECE). Glossary of Terms on Statistical Data Editing. In Proceedings of the Conference of European Statisticians Methodological Material, Geneva, Switzerland. 2000. Available online: https://stats.oecd.org/glossary (accessed on 25 September 2021).
70. Soliño, L.; Costa, P.R. Global impact of ciguatoxins and ciguatera fish poisoning on fish, fisheries and consumers. *Environ. Res.* **2020**, *182*, 109111. [CrossRef]
71. Barthel, R.; Seidl, R. Interdisciplinary Collaboration between Natural and Social Sciences-Status and Trends Exemplified in Groundwater Research. *PLoS ONE* **2017**, *12*, e0170754. [CrossRef]
72. Pohl, C. How to bridge between natural and social sciences? An analysis of three approaches to transdisciplinary from the Swiss and German field of environmental research. *Nat. Sci. Soc.* **2001**, *9*, 37–46. [CrossRef]
73. Daneshian, M.; Botana, L.M.; Dechraoui Bottein, M.-Y.; Buckland, G.; Campàs, M.; Dennison, N.; Dickey, R.W.; Diogène, J.; Fessard, V.; Hartung, T.; et al. A roadmap for hazard monitoring and risk assessment of marine biotoxins on the basis of chemical and biological test systems. *ALTEX–Altern. Anim. Ex.* **2013**, *30*, 487–545. [CrossRef]
74. Bean, H.; Sutton, J.; Liu, B.F.; Madden, S.; Wood, M.M.; Mileti, D.S. The study of mobile public warning messages: A research review and agenda. *Rev. Commun.* **2015**, *15*, 60–80. [CrossRef]
75. Probst, W.N. How emerging data technologies can increase trust and transparency in fisheries. *ICES J. Mar. Sci.* **2020**, *77*, 1286–1294. [CrossRef]

MDPI
St. Alban-Anlage 66
4052 Basel
Switzerland
Tel. +41 61 683 77 34
Fax +41 61 302 89 18
www.mdpi.com

Toxins Editorial Office
E-mail: toxins@mdpi.com
www.mdpi.com/journal/toxins

MDPI
St. Alban-Anlage 66
4052 Basel
Switzerland

Tel: +41 61 683 77 34

www.mdpi.com

ISBN 978-3-0365-6429-6